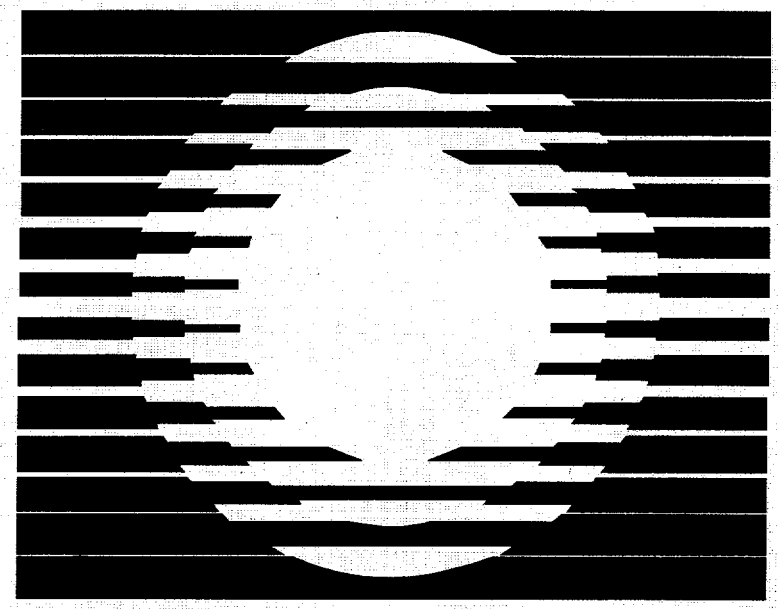
FG05-93ER75865
CONF-9504289--Vol.3



PROCEEDINGS
NINTH NATIONAL CONFERENCE ON UNDERGRADUATE RESEARCH
1995

Robert D. Yearout
Editor

Volume III

MASTER

UNCA
THE UNIVERSITY OF NORTH CAROLINA AT ASHEVILLE

NA[illegible]L EDITORIAL BOARD NCUR IX

Merritt Moseley
UNC Asheville

John Knecht
Colgate University

John Bernhardt
UNC Asheville

Gilles Einstein
Furman University

Paul Heidger
University of Iowa

Steven McLoon
University of Minnesota

Jarold Ramsey
University of Rochester

Larry Wilson
UNC Asheville

Donald Scott
Wofford College

Phyllis Betts
Memphis State University

Rex Adelberger
Guilford College

Susan Harrison
Eckerd College

Ariel Anderson
Western Michigan University

LaDelle Olion
Fayetteville State

Robert Cordero
Holy Family College

Laurie Hayes
University of Minnesota

David Kerr
Eckerd College

David Peak
Union College

John G. Stevens
UNC Asheville

Toufic Hakim
Jacksonville University

Brenda Alston-Mills
NC State University

Mary Baum
Princeton University

Dr. Patsy Reed
UNC Asheville

William Kelly
Eckerd College

UNCA EDITORIAL BOARD

Robert Yearout, Chair

Gregg Kormanik

Katherine Whatley

Pamela Laughon

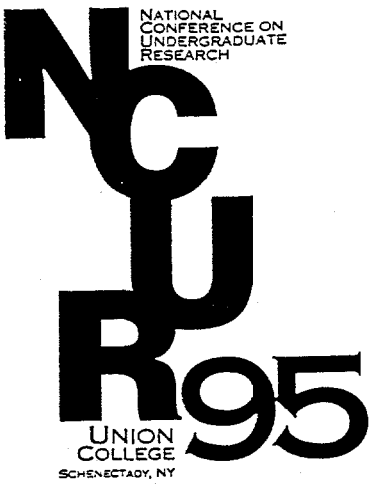
Phyllis Lang

Donald Lisnerski

William Spellman

Lisa Reeves

Robert Dunning



PROCEEDINGS

NINTH

NATIONAL CONFERENCE

ON

UNDERGRADUATE

RESEARCH

DISTRIBUTION OF THIS DOCUMENT IS UNLIMITED

VOLUME III

THE UNIVERSITY OF NORTH CAROLINA at ASHEVILLE

JULY, 1995

DISCLAIMER

This report was prepared as an account of work sponsored by an agency of the United States Government. Neither the United States Government nor any agency thereof, nor any of their employees, makes any warranty, express or implied, or assumes any legal liability or responsibility for the accuracy, completeness, or usefulness of any information, apparatus, product, or process disclosed, or represents that its use would not infringe privately owned rights. Reference herein to any specific commercial product, process, or service by trade name, trademark, manufacturer, or otherwise does not necessarily constitute or imply its endorsement, recommendation, or favoring by the United States Government or any agency thereof. The views and opinions of authors expressed herein do not necessarily state or reflect those of the United States Government or any agency thereof.

DISCLAIMER

Portions of this document may be illegible in electronic image products. Images are produced from the best available original document.

Foreword for the **Proceedings of the Ninth National Conference on Undergraduate Research**
Union College, April 20-22, 1995

The Ninth National Conference on Undergraduate Research (NCUR 95) was held at Union College in Schenectady, New York. This annual celebration of undergraduate scholarly activity continues to elicit strong nation-wide support and enthusiasm among both students and faculty. Attendance was nearly 1650, which included 1213 student oral and poster presenters. In addition, thirty faculty and administrators gave talks describing their perspectives on undergraduate scholarly activity in symposia organized by the Undergraduate Research Network. Representatives from 280 institutions in 47 states, plus Puerto Rico and Washington, D.C., attended NCUR 95.

There were three plenary speakers at NCUR 95. Dr. Baruch Blumberg, the 1976 Nobel Laureate in Physiology and Medicine and currently Fox Chase Distinguished Scientist at the Fox Chase Cancer Center in Philadelphia, talked about his important discovery of the causes of viral hepatitis and the development of a screening test for the virus in donor blood. Donna Cox, Professor and Associate Director for Technology at the School of Art & Design at the University of Illinois, presented a fascinating video lecture on her work, which is at the interface of computer art and science. Julian Bond, a longtime, articulate champion of civil rights and now Distinguished Adjunct Professor at American University, gave his perspectives on the current state of minority issues in this country.

Perhaps the high point of NCUR 95 was ARTSFEAST, the Friday evening event which featured the work of undergraduates in the performing and visual arts. Over 50 students participated in this event, which included exhibitions of student paintings, drawings, and video art, student compositions by a professional brass quintet.

For the second year in a row, many student papers had to be rejected for presentation at NCUR due to conference size limitations. Thus, submitted papers for presentation at NCUR 95 were put through a careful review process before acceptance. Those of you who have been selected to have your paper appear in these Proceedings have been through yet a second review process. As a consequence, your work has been judged to represent an impressive level of achievement at the undergraduate level. We offer you our congratulations on a job well done, and we hope your work is the precursor of many fine contributions to come from future endeavors.

Tom Werner
Helen Madden
NCUR 95 Site Co-Chairs

Dr. Larry Wilson
Vice Chancellor for Academic Affairs
The University of North Carolina at Asheville



The UNCA Editorial Board has dedicated the Proceedings of the Ninth National Conference on Undergraduate Research to Dr. Larry Wilson, former Vice Chancellor for Academic Affairs at The University of North Carolina at Asheville. In the fall of 1995, Dr. Wilson left UNCA to take on a new role as president of Marietta College in Ohio. His past support of the Proceedings and his commitment to undergraduate research has been greatly appreciated and will be missed.

Dr. Wilson received a B.S. degree in Chemistry from Baker University in Baldwin, Kansas (1958) and a Ph.D. in Chemistry from the University of Kansas (1963). From there, Dr. Wilson embarked on a teaching career at Ohio Wesleyan University where he went on to serve as Acting Provost, Dean of Academic Affairs, and Executive Assistant to the President. During the 1987-88 academic year, which coincided with the first year of the National Conference on Undergraduate Research, Dr. Wilson came to UNCA. Since then, he has served the University as Professor of Chemistry, Vice Chancellor for Academic Affairs, and as Interim Chancellor since 1994.

While a member of the National Editorial Board and a reviewer for the NCUR Proceedings, Dr. Wilson's main support came in the area of finance. By dedicating funds from the UNCA Foundation to send students to the Conference, he also made money available to send the UNCA Editorial Board to review and process papers. This on-site processing made possible the September publication of the Proceedings each year. Without Dr. Wilson's support, the Proceedings would have come out much later in the year resulting in low sales and jeopardizing the Proceedings' ability to sustain itself. With the help of Larry Wilson, the Proceedings has become self supporting through corporate donations and sales as well.

The Proceedings Board wishes Dr. Wilson well in his new position and looks forward to seeing Marietta College participants at NCUR 10!

PREFACE

The 249 papers published in these three volumes are representative of the approximately 1200 papers and posters presented at the celebration of undergraduate research that was NCUR '95'. The faculty, staff and students of Union College are to be commended for making NCUR '95' such an enriching experience. The student authors deserve recognition for their hard work and for their persistence in seeing their research through to its final publications.

Special thanks are extended to Dr. Helen Madden, Ms. Kelly Buttridge and other members of the NCUR '95' Staff. Their help during the days of the Conference was invaluable. Many thanks also to the members of the National Board, who reviewed a large number of papers submitted to the Proceedings under time constraints. Their continued efforts to standardize has raised the Proceedings quality. This project would have not been successful without their assistance.

I would also like to thank the UNCA Editorial Board, who put in many long hours reviewing, checking and organizing papers, and Lisa Reeves, Patricia Roullard and Holly Beveridge, who did all of the cutting and pasting necessary for these volumes. I owe a special debt of gratitude to Katherine Whatley and Lisa Reeves for their support, encouragement and mentorship during the entire process of organizing the Proceedings.

To all the students who submitted papers to the Proceedings go thanks for their participation and congratulations for their achievements. Your enthusiasm and achievement will serve as role models for the next group of student researchers-who we look forward to meeting at the Tenth National Conference on Undergraduate Research at the University of North Carolina Asheville.

Robert D. Yearout
UNC at Asheville
July, 1995

**PROCEEDINGS OF THE
NINTH NATIONAL CONFERENCE ON
UNDERGRADUATE RESEARCH**

Number 1 1995

CONTENTS

VOLUME I

FOREWARD iii

DEDICATION iv

PREFACE v

ARTS AND HUMANITIES

Botticelli's *Primavera* and the Role of Women in the Renaissance 1
Jennifer Houghton (Patricia Meilman)

Information and Decoration in Seventeenth century Netherlandish Maps and Views 6
Jane Elizabeth Patterson (Roger P. Hull)

The Inter-Relation of Specectacle and View Painting With Emphasis on Canaletto and Guardi 11
Sallie Sturart Shuford (Peter Schmunk)

Mantegna and the Parnassus: a Renaissance Humanist Allegory of Marriage 16
Amy R. Walston (Shirley Schwarz)

Complex Imagery Through Combination Drafting 21
Sharon A. Hilgers (Dianne DeBeixedon)

The Effects of Advancing and Retreating Colors on Objects in the Picture Plane 26
Roger Kurtenbach (Darrel Nelson and RaVae Luckhart)

Combined Aesthetics: A Case For Art School Curriculum Changes 29
Scott Capell Weiland (Robert Dunning)

Attitudes Toward the Vietnam War in the United States: Sevier County, Tennessee as a Case Study 33
Suzanne Reagan (William Spellman)

Aristocracy and Grace in Pindar's *Olympian Odes* 38
Jeffrey Kearney (Sophie J. V. Mills)

Elizabeth Murphy-Moss, The *Afro-American (Baltimore)*, and the 1963 Cambridge, Maryland Civil Rights Movement 41
Brenda Edgerton-Webster (Catherine Mitchell)

Convergence Theory and the Adoption of Health Innovations by Students from Developing Countries 46
Tanya Devadason (Rod Korba)

Predictors of Girls' Math and Science Attitudes and Aptitudes 50
Wanda J. Kilgore (Joann Keyton)

Tourism and Environmental Effects Utila, Honduras 55
Angela B. Caudle (Clifton Dixon)

Before Black was "Black": The African American Experience in the American Colonies, 1607-1700 60
Keesha R. Starks (Larry D. Eldridge)

Brevard, North Carolina as Home Front: A Study of Small Town in America During World War II 63
Jo L. Peterson (William Spellman)

Giving the Poor Access to Open Space: Frederick Law Olmsted and the Boston Park System 68
Eliot Wilczek (Vivian Conger)

Greco-Turkish Exchange of Minorities: Experience and Intellectual Response 72
Melih Karakullukcu (Patricia Herlihy)

Henry VIII: His Conscience in The Divorce From Catherine of Aragon 76
Melinda Kaye McDow (Robin Rudoff)

A Curse of Memories on the Town of Wheatland: The Hop Fields Riot of 1913 80
Oskar Scheikl (Raymond M. Hyser)

Japan and the West: A Miracle or Japanese Innovation 85
John W. N. Buell (Albert Mann)

Life in Stalin's Labor Camps: A Comparison Between the Treatment of Criminal and Political Prisoners 90
Matthew A. Zimmerman (Lawrence Buck)

A New Frontier: Contemporary Film and the American West 95
Dina Clark (David Wrobel)

Patterns of Crime and Punishment: Delaware County, Pennsylvania, 1790-1829 100
Tina Arcidiacono (Larry D. Eldridge)

A Place of Refuge: Poor Houses of Early Pennsylvania 104
Samuel E. Mormando (Larry D. Eldridge)

Sassy Brown Woman: A Collection of Poetry 108
Cheryl Bell (Sally McNall)

The Ungrateful Art of Correspondence: A Love Affair 111
Monika K. Lee (Sandra Lauderdale-Graham)

EL PROBLEMA DE LA FE EN LA OBRA DE MIGUEL DE UNAMUNO 115
Jessica A. Vasquez (Raysa Amador)

The Great Language Debate: French, English, and Indigenous Tongues in Post-Colonial African Literature 119
Jay Jordan (Dwight B. Mullen)

The Lives and Experiences of the German Children During World War II 124
Fabiola C. Plaut (Jerry Cox)

Maria Moskvina's "My Dog Loves Jazz" and the Art of Literary Translation 129
Rebecca Van Sciver (W.G. Fiedorow, D. Kirjanov, S. Bailey,R.V. Meulen)

Public vs. Private: The Success of Dolley Payne Madison and Sarah Childress Polk 133
Jennifer Stromer-Galley (Karlyn Kohrs Campbell)

The Reconciliation of Bipolarities or Conflicts in Hermann Hesse's *Glass Bead Game:* The *I Ching's* Idea of Harmonious Unity 137
Juliana Tioanda (Ross Vander Meulen)

Violence in Voltaire's Candide 142
Amy J. Partridge (Gerard Gouvernet)

Beyond the Pre-Raphaelites and Tractarians: Christina Rossetti's Own Voice 147
Virginia Gaylor (Linda Julian)

Disintegration and Unity in Faraway, So Close! 152
Charlotte M. Butzin (Suzan Harrison)

The Double Edged Blade of Adolescence in McCullers' The Member of the Wedding 157
Lucy A. Kozikowski (William B. Kelly)

Encouraging Critical Thinking and Writing Through an Exploration of Dance 160
Erin Trista Merk (Cynthia Scheinberg)

The Garden of Instability: The Interrelationships Between Relativity Theory, Quantum Mechanics, and T.S. Eliot's "Burnt Norton" 165
Clasina Leslie Smith (Jeff Rackham)

The Mother and the Motherland: An Analysis of Symbolism and Style in Jamaica Kincaid's Annie John and Lucy 170
Edward Hoffman (Elaine Ognibene)

Violence and Revelation in Eudora Welty's "Where Is the Voice Coming From?" 175
Bronson Elliott (Suzan Harrison)

The Wandering Reader in Joyce's *Ulysses* 179
Todd Alan Nicolet (Julienne Empric)

E.M. Forster's India-Colonial Construct or Anthropological Other? 184
Michael R. Klozotsky (John Haegert)

Maya Angelou's I Know Why the Caged Bird Sings and Maxine Hong Kingston's The Woman Warrior Writing Rebellion and the Telling of Self in the Autobiographies of Women of Color 189
Sarah McCarthy (Elaine Ognibene)

Mongrels, Mixed-Bloods, Hybrids & Half-Breeds: The Construction of Black/White Multiracials in America 194
Nicole Stanton (Susan Smulyan)

Objective and Progressive Allegories in Chan Kom 198
Tom Bremer (Daniel Reff)

Keyboards and Stagelights: the Life and Works of Elizabeth Billington 204
Elizabeth J. Stow (Martha S. Asti)

A Matter of Taste: Observing Baroque Performance Practices in Handel's *Water Music* in Performance and on Recording 209
Scott T. Anderson (Patricia Kazarow)

Bio-Spirituality: The Role of The Spirit In Healing 214
Jeffrey Davis Golden (Andrew Tallon)

Immanuel Kant's View of God 220
Kathryn Ryan Willeford (Edgar V. McKnight)

Locating Lydia In A "Lopsided" World 225
Hal Walter (F. Scott Spencer)

A Review of Cherokee Formularies: The Critical Foundation for Inter-Cultural Understanding 230
Courtney Caswell-Peyton (Lance Factor, Paul Christianson and Charles Kammer)

Zarathustra as Mystic Healer: Nietzsche and Asian Philosophy 234
Mark Schillinger (Ken Pahel)

SOCIAL AND BEHAVIORAL SCIENCES

Diachronic Aspects of the Human Condition of the Island of Cyprus: The Evidence of the Human Skeletal Record 239
John G. Lagamjis and Theodoulos A. Hadjipetros (Anagnosti P. Agelarakis)

The Old People Know Different: Navajo Elders in the Context of Change 244
Lori E. Dodd (Charles C. Hughes)

A Re-Evaluation Of The Methods Used In Deciphering Anthropological Information From Cremated Human Osseous Remains 249
Jeffrey M. Rosenstein and Anna Konstantatos (Anagnosti P. Agelarakis)

Resolving a Historical Byzantine Riddle Through Analysis of the Archaeological-Anthropological Record 254
Paulette Pappas (Anagnosti Agelarakis)

Application of Activity-Based Costing To A Not-For-Profit Service Organization 259
Anthony Stroupe (Linda Nelms)

An Inquiry into the Firms that Practice Income-smoothing Techniques and the Associated Ethical Implications 264
Corinne Painter (Susan Weihrich)

The Role of Accounting in Jury Decision Making 269
Sufia Babar (Ehsan Feroz)

A Comparative Study Between the Methods of Marketing Accounting Services in the United Kingdom and the United States 273
Stephen C. Leap (Michael Garner and Reed Muller)

Genes and Jeans 278
Jennifer Lugg (Michael Dietrich)

Selling Difference: Otherness as Exotic in Women's Magazine Images 283
Ananya Mukherjea (Sandra Gilchrist)

An Analysis of Political Violence in Twentieth-Century Southwestern Pennsylvania Coal Company Towns 288
Karaleah Sabina Jones (Paul F. Clark)

An Aristotelian Analysis of Communication on the Net 292
Lisa J. Nelson (James Dorris)

Group Development and Performance Among Business Students 295
Willie E. Sutton, Jr. (Mary Jones Phillips)

A Brief Discussion for those Considering Year-Round Schooling 300
Ryan E. Argot (James F. Nolan)

Gifted Students with Learning Disabilities: How Can We Help? 305
Danielle Kennington (Charlotte Lofgreen)

Is It Really Fair For Girls? Gender and Communication in Middle School Math Classes 309
Sara A. Sturm (Debra L. Peterson)

An Econometric Analysis of the Price Elasticity of Demand for Residential Electricity 314
Farzaan Nusserwanji (Gene Pollock)

Economic Development for Puerto Rico: An Economic Analysis of Two Main Strategies 317
Joselyn M. Carreras (E. Tom Dickens)

Dietary Delocalization in a Yucatecan Resort Community in Quintana Roo, Mexico: Junk Food in Paradise 322
Catherine McGarty (Dolores Shapiro, Anne Sheridan and Brooke Thomas)

The Effectiveness of Informal Health Promotion on Chronic Disease Management of Children with Insulin Dependent Diabetes 327
Jonathan C. Beach (David Bedworth)

Combating Global Warming with an International Transferable Permit System 331
Angela M. Dusenbury (John K. Stranlund)

Development of the Mafia as an Institution in Russia 334
Timothy G. Mills (Laurie Iudin-Nelson and John E. Moeller)

Nsamanfoo: The Ancestral Beliefs and Rituals of the Akan People in Nyafoma, Techiman of Ghana, West Africa 338
Regine Michaelle Zekora Romain (Abdul Karim Bangura)

The Path of Least Resistance: Fighting Environmental Racism in Alabama 342
Paige Black (Dwight Mullen)

Punctuated Pluralism: The Case of the Civil Rights Act of 1990/91 347
JoAnn R. Yamani (Paul Schulman)

A Case Study of the Baby M Trial Involving Surrogate Parenthood as a Method of Exploring the ways in which the Courts Create Social Policy 351
DeAnne C. DeFuccio (Paula Consolini)

Testing of Infant's Bodily Fluids for Controlled Substances: A Comparison of State Policies 355
Michael P. Anello (Janet Boles)

The Effects of Individualism on the Moral and Political Choices of American Lifestyles 360
Alice Freist (Erik Olsen)

Neighborhood Based Services: A Rochester Case Study 365
Cynthia A. Rapp (Bruce Jacobs and Carolyn Whitfield)

The Role of Attitudes in the Management of Diabetes in Children 370
Denise K. Gordon (Tomi-Ann Roberts)

A Study on The Value of Family Relationships 375
Nancy Wolfe Nowinski (Runi Mukherji)

The Relationship Between Homophobia, Peer Counseling Effectiveness and Peer Counseling Self-Confidence 379
Marc T. Kiviniemi (Pamela Laughon)

Wisdom-Related Judgements in College Students: an Approach to Measurement 384
Gregory Frantz Dix (Adrian Tomer)

Comparison of Political Attitudes and Voting Behavior Using the Lost Letter Technique 389
Anthony T. Rallo and Linda Santos (Susan Petry)

Correlates of Peer-Rated Aggression: Maternal Cue Detection and Disciplinary Beliefs 393
Jon Paz, Jennifer Kellenbenz, Michelle VanNess-Knolls, Theresa Davis and Allison Ward (Adeline S.C. Tryon)

The Moderating Effect of Racial Identity on the Relationship Between Ethnicity and College Satisfaction 397
Jonathan L. Iuzzini and Renee M. Tobin (Monica L. Rodriguez)

Does not thinking about food make you think about it more? An investigation of the Wegner Rebound Effect 402
Bradley S. Moorefield (Natalie A. Oransky)

American Perceptions of Japan: A Collegiate Perspective 407
Rachel Hall (Jonathan Noyes)

Stress Prediction vs. Stress Control: Same Underlying Neurobiological Substrate? 412
Adam Cohen (Robert C. Drugan)

Perceptions of the Kinship Ties of Rural and Urban Families 417
Shane J. Walker (Millicent H. Abel)

The Accuracy With Which Professional Actors Perform Different Theatrical Roles 421
Michelle Milner and Jenny Danielson (Helga Noice)

Differences Between Actors and Non-Actors: An Analysis of Cognitive Abilities 426
Bonnie McLain Allen (Arthur C. Graesser)

Priming of Homograph Meaning in Word Association 430
Christian DeBiasi (David S. Gorfein)

Testing the Capture Hypothesis through Inhibition and Priming Effects in a Variation of the Stroop Task 435
Rebecca Ledford (Tracy Brown)

The Effect of Visual Perception on Mental Imagery Processes Used in Working Spatial Problems 440
Marie Julia Maher (Sybillyn Jennings and Bronna Romanoff)

Effects of Task Quality on Mood in Depressed and Nondepressed Participants 445
Jean Jamison (Sandra T. Sigmon and Marie J. Hayes)

Chromatic Information in Human Stereoscopic Vision 448
Robin E. Rustad (Lauren V. Scharff)

Media's Effect on Female Adolescents' Ideal Body Type 452
Kristen M. Cerbone, Bridgette A. Chalila and Catherine A. Dufresne (Marie J. Hayes)

Gender, Age and Education Differences in Parenting Styles 456
Gloria Ehrenberg (B. Runi Mukherji)

Age and Sexual Experience Are Factors In Female Choice In Milkweed Bugs (Oncepeltus fasciatus) 459
Alduan Tartt (Duane Jackson)

The Cat's Orienting Response to Brief Sounds in a Natural Environment 464
Angelia J. Trivette (Mark C. Zrull)

Progressive Lesions of the Entorhinal Cortex in Rats Accelerate Hippocampal Sprouting 469
Sandra L. Castle (Julio J. Ramirez)

The Relationship between Automatic and Intentional Processing and Working Memory Span 474
Jennifer R. Mangum (Natalie A. Oransky)

Serial Position Learning in Honeybees 479
Prentiss L. McNeill, Christine V. Cowan and Randall Grisi (Gordon B. Bauer)

Self-mutilation: Symptom or Syndrome 484
Kimberlly M. Bowman (Sharon K. Calhoon)

"Goldiamond's Paradox" Responding in the presence of S-minus is sustained if it functions to protect S-plus reinforcement opportunities 489
Martha A. Shurburtt (Spencer Mathews, Janet LeFrancois and William Baker)

Clothes Preschoolers Wear 494
Petrina Simmons (Magnoria W. Lunsford)

The Influence of Race of Survivor, Status of Harasser, Intensity of Harassment, and Policy in Place on Women's Responses to Sexual Harassment 499
Ricky Bland, Fonville Day, Charlottee Hope, Deanna Powell and Anna Rodriguez (Susan H. Franzblau)

Pedagogy and Practice in Academic Sociology: A Qualitative Study 504
Jason Smith (David Brain)

Poor, Young, Black Males = Three Strikes 508
Rosanne Handford (Patricia Pearson)

Race and Identity: A Study of Biracialism 513
Aprille L. Walker (Myra George and Richard Jones)

The Realities of Occupational Gender Equality in Kibbutz Aleph-Bet 518
Daya Masada Laufer (E. Keith Bramlett)

Strategic Discourse and Social Conflict in Idaho's Anti-Gay Initiative 523
Joseph T. De Angelis (Michael Blain)

Three-tiered Structure of the Homeless Subculture 528
Carol Diane Sholander (Jacqueline Helfgott)

VOLUME II

ENGINEERING AND MATHEMATICS

Carbon Dioxide Retention in Yucca Mountain 532
Shawonda Brockington (Franklin King)

Computer Simulation of Pressure-Volume Behavior in the vicinity of the Triple Point 538
Yea-Ling Ong (Bruce D. Drake and Robert G. Root)

Enzymatic Resolution of Enantiomeric ß-Blockers in Non-Aqueous Solvents 543
Christopher J. Schult (Bruce Drake)

Gas Holdup in a Bubble Column Reactor Using a Porous Plate Distributor: Gas Density Effect 548
Jum S. Kim (Sarvani Mikkilineni)

Acceleration Feedback Control Strategies for Active Mass Drivers 553
Anmarie E. Belknap (B.F. Spencer, Jr.)

Dynamic Analysis of A Beam Supported By A Winkler Foundation Subject To A Moving Load 558
Beth T. Kueter (David J. Kirkner)

Architecture of An Operating System Specifically Designed for Research in Virtual Reality 563
Gregory Gerard (Gerald Pitts)

Feasibility of Object Oriented, Real Time Animated Rendering for Virtual Reality Applications 566
Scott McCaskill (Gerald Pitts)

Image Processing Using Fuzzy Logic 571
Nakesha L. Gully (M. Giguette, A. Lopez,Jr. and K. Henson-Mack)

An Implementation of Objects and Object-Oriented Programming Using PROLOG 576
Richard A. Butler and William J. Dean (Antonio Lopez, Jr. and Marguerite Giguette)

A Parallel Application for Delaunay Triangulation on the Intel Paragon 581
Francis Y. Fong (Fenglien Lee)

Using a Neural Network in Predicting Stock Market Return 586
Jovina Roman (Akhtar Jameel)

Quadratic Feedback Shift Register Sequences 591
Diana I. Simen (Agnes Chan)

Virtual Fire Propagation in Heterogeneous Media 595
Scott Walnum (Gerald Pitts)

Development and Fabrication of Microelectromechanical Optical Switches 599
Jack C. Barr, Westley D. Cox and John J. Wolfgang (Lawrence A. Hornak and Kolin Brown)

Development of A Metal-Semiconductor-Metal Photodiode For Use In A Microwave Phased Array Antenna System 604
Neil B. Davids (MAJ Bradford Tousley)

Negative Output Resistance Voltage Source for Device Testing 609
Chadwin D. Young (Dean P. Neikirk)

Optical-To-Optical Modulator Based on A Multiple Quantum Well Device 614
Jordan J. Fisher (Barry L. Shoop)

Radiometric Calibration of the Landsat Thematic Mapper (TM) 619
Ron Morfitt (Dennis Helder)

Selective Etching of InGaAs over InAlAs Using CH_4/Ar Reactive Ion Etching 624
Frank D. Bannon, III (Theresa S. Mayer)

Messy Data Assist 627
Renee M. Barger (Robert Yearout, George Yates and Charles Massey)

Pilot Fatigue and Instrumental Disputes 632
Dara Strickland and Maranda McBride (Barbara Pioro)

An Analysis of Silicon Based Solar Cells: The Effects of High Temperature on Power Output 636
Isaac Garaway (Donald R. Garrett)

Autoignition Characteristics of Methanol 640
Michael Bowman (Richard Wilk)

Development of A Liquid Crystal Polymer For Use As A Biological Membrane 644
Eric A. Kutcher (Christopher K. Ober)

Effect of Zirconia On Ni-Al-O Metal-Ceramic Composites 649
Yelena Shapiro (Stephen Sass and Ersan Ustundag)

Healing of Flaws During *In Situ* Formation of Metal-Ceramic Composites by Partial Reduction Reactions in the Ni-Al-O System 654
Marshall L. Stocker (Stephen Sass and Ersan Ustundag)

In Search of Stresses Due to the Volume Change Associated with Partial Reduction of $NiAl_2O_4$ 659
Jessika Trancik (Stephen L. Sass)

Testing of a Two-Axis Laser Doppler Velocimeter in the Laboratory and Under Field Conditions in the Chesapeake Bay 664
Eric L. Luft (Lawrence P. Sanford)

In Vitro Flow Experiments with the Union College Vortex Blood Pump 669
Charles B. Howarth (J.R. Shanebrook)

Wind Tunnel Investigation of Steady Flow Through Coronary Artery bypass Grafts 674
Tricia L. Nelson (J.R. Shanebrook)

Cake-Cutting, Hugo Steinhaus Style: Beyond N=3 679
Carolyn E. Custer (Alan D. Taylor)

Computer Modeling Of He II In A Microchannel Array 684
Francisco J. Diez-Garias and Atsushi Uchida (Charles E. Montfort III)

Evaluating Sums of Powers 689
Anjanette Finnegan (Peter Yang)

An Empirical Investigation of Outdoor Advertising of Alcohol and Tobacco Targeting Blacks 694
Jeff Foerster (Sharon Galbraith)

Inversion of An Integral Transform For SU (p, 1) 698
Deborah Alterman, D. Matthew Hill, Sejung Kim and Angela M. Minnick (Lisa A. Mantini)

Monitoring of Corrosion in Steel Structures Using Optical Fiber Sensors 703
L.R. McLaughlin (K.D. Bennett)

A Novel Solution of Linear Congruences 708
Jeffrey F. Gold (Don H. Tucker)

The Relative Efficiencies of One-Hot and Binary Encodings for FPGA-based Finite State Machines 713
Vladimir K. Jurista (William A. Chren, Jr.)

A.I.D.S. Cholecystopathy: A Comparison of Ultrasound vs. Computed Tomography Imaging 718
Michelle Rhodes and Colleen Ellerick (Jeff Pope)

Determining Pulmonary Capillary Wedge Pressure With Pulsed Wave Doppler Echocardiography 723
Jane M. Nova (Suzanne Adams)

PHYSICAL SCIENCE

Automated Recognition of Galaxy Morphology Using Neural Networks 728
Matthew L. Nielson (Stephen C. Odewahn and Roberta M. Humphreys)

The Disappearance of the Eclipse Minima of the Binary Star SS Lacertae 733
Tammy L. Clifton (Stephen J. Schiller)

Photoluminescence and Photoluminescence Excitation Spectroscopy of ZnTe/ZnCdTe Multiple Quantum Wells 738
Susan E. Thysell (J.J. Song and J.M. Hays)

BVRI Photometry of G Dwarf Stars Towards The North Galactic Pole 743
Robert Lanczycki (Phillip K. Lu)

Spectrophotometric Analysis of F and G-Stars At The Galactic Poles 748
Donald Platt (Phillip K. Lu)

Automatic Real-Time Phoneme Recognition 753
Zac Walton (J. Van der Spiegel)

The Measurement of Alkali Doped C_{60} Spectra in the Visible Range 757
Alfred Badowski (Laszlo Mihaly)

A Study of Leidenfrost Phenomena Using Digitized Video Image Capture and Analysis 761
Katarina Plavetic (Rexford E. Adelberger)

Transverse Relaxation Time in DMS Crystals: A Theoretical Study 766
J. Matthew Kreider (Carl S. Helrich)

Lattice Arrangements for Inert Gas Solids and Hydrogen-Argon Mixtures Using Monte Carlo Simulations 771
Bruce S. Nguyen (T.M. Hakim)

Non-degenerate Two-Photon Absorption in ZnSe 776
Todd E. Buhr and Corey S. Gerving (LTC John E. LaSala and CPT Brian Kowalski)

Photoluminescence and Low-Frequency Raman Scattering From Semiconductor Nanocrystals 781
Eric E. Pearson (John Schroeder and Joseph Haus)

Thermal Annealing of Organic Thin Films in MIS Devices 786
Benjamin A. Meier (Vijendra K. Agarwal)

Inclusions in Carbonaceous Chondrite Meteorites and the Formation of the Solar System 791
K. Amanda Leach (Steve Simon and Lawrence Grossman)

Kinetic Studies of the Ionic Current through the M_2 Channel in the Influenza A Virus 794
Yuqi Qiao (Carl S. Helrich)

Parity Dependence in Level Denisty of ^{48}Ti 799
John Quesenberry (J.F. Shriner, Jr.)

Comparison of Lyapunov Time and Crossing Times For Prediction of Orbital Instabilities 804
Mark C. Lewis (Gerald Pitts)

Steady-state Analysis of Semiconductor Laser With Feedback Loop 809
Karen Matheny (Donna Kay Bandy)

VOLUME III

BIOLOGICAL SCIENCES

Modifications in the Rate of Cellular Adhesion Associated with the Overexpression of Alzheimer ß/A^4 Amyloid 813
Ruben Amarasingham (Ronald Majocha)

Acetylcholinesterase and its High Concentration in Human Amniotic Fluid as an Indicator of Open Neural Tube Defects 818
Paul Riley (Mark Wener)

Development of A Neovascularized Bioartificial Pancreas Organoid 823
Jennifer L. Long (Ronald Fournier and Jeffrey Sarver)

Characterization and Isolation of Lectins from the Marine Bryozoan Bugula neritina 828
Fassil Mesfin and Yvonne M. Gonzalez (Rita Colon-Urban)

Effect of nutrients on glutathione catabolic enzymes in *Candida albicans* during dimorphism 832
Munyaradzi Imbayagwo, Suresh Gunasekaran and Louise McDonald (Muthukumaran Gunasekaran and Elias Manavathu)

Examination of Somatic Polyploidy in Nonsecretory Cells of Idothea wosnesenskii 837
Katie M. Headley (Daniel B. Matlock)

Genetic Variability Within and Among Local Populations of Dame's Rocket (*Hesperis matronalis*) 841
Everett Porter (Veronique Delesalle)

Isolation and Characterization of Yeast Nuclear pre-mRNA Splicing Genes and Factors in Saccharomyces cerevisiae 846
Lin Zhuo Jia (John N. Abelson)

Mechanism of the Effect of Citrulline On Valproate (VPA)-Induced Hyperammonemia 850
Elena Valcarlos (Jeffrey R. Stephens)

Messenger RNA Stability and Membrane Phospholipid Composition in Heat Stressed Barley Aleurone Cells 855
Paul A.S. Benson (Mark Brodl)

Antifungal Activity of Thiol-Blockers 860
Louise McDonald and Tyler Parker (Elias Manavathu and Muthukumaran Gunasekaran)

What is Kamboucha? 865
Tia M. Barringer (Jack Harris and Robert Gehrig)

Mechanisms of Phorbol Ester-Induced Cell Death in EL4 Cells 869
Sandra Fulwood and K. Meyer (W.W. Gearheart)

A Comparison of the Seed Banks of Adjacent Disturbed and Undisturbed North Carolina Wetlands 872
Carolyn Wells (James Perry)

Multiple Bioassay of Housatonic River Water Above and Below Two Industrial Use Sites 877
Erik Carlson, Heather Martin and Ana C. Ribeiro (Frank Dye)

Productivity of Grassland Bird Species at Iroquois National Wildlife Refuge, NY 882
Kathleen M. Hartman (Chris Norment)

The Effect of Environmental pH on the Morphology of Gill Tissue in *Carassius Auratus* (Goldfish) 886
Randy L. Durren (Gregg Kormanik)

Long-Term Nutrient Assimilation by A Diked Lake Erie Coastal Marsh 890
Michael Liptak (Johan Gottgens)

Ingestion Rates of an estuarine copepod, Acartia tonsa, in labratory mesocosms 895
B. Wysor (M. Roman)

Photoperiod and Seasonal Differences of Endophytic and Freeliving Forms of the Two Marine Green Algae, *Acrosiphonia and Monostroma* 900
Ami C. Ongstad (Margaret L. Hudson)

The Distribution and Ecology of Freshwater Sponges in Connecticut with an Emphasis on the Thames River Basin 905
Elizabeth M. De Santo (Paul E. Fell)

Immunolocalization of a Conserved Tektin Peptide Sequence 910
Aimee M. deCathelineau (Richard W. Linck)

Artisanal Trapping of Land Crabs in Puerto Rico 913
Darwin Caraballo-Burgos (Frank Barnwell)

Total Hemocy Anin Content in Response to Varying Oxygen and Salinity in the Blue Crab *Callinectes Sapidus* 918
Toren Andrew Prawdzik (Lee Ann Clements)

Beta-Hydroxybutyrate-Induced Teratogenesis in the Sea Urchin Embryo 923
Jeffrey B. King (Margaret T. Peeler)

Zebra Mussel (*Dreissena polymorpha*) Biofilter Reduction of Waterborne Microbes 928
Mary L. Seaman (Jerry L. Kaster)

Altering Serum IGF-1 Concentration and its Relationship to Reproductive Performance to Lactating Holstein Cows 933
Lance Baumgard (Brian Crooker)

The Function and Evolution of Rabbit C Repeats 938
Gabrielle A. DeVere, Jeanne L. Uy and Carri R. Eagler (Dan Krane)

Supplementation Rate of Breast Fed Babies at a Local Hospital and Possible Effects on the Duration of Breast Feeding in Infant Nutrition 943
Anne M. Delles (Christine Gruhn, Matthew Temple and Cynthia Howard)

Truncated Preprosomatostatin Targets a-Globin To Storage Granules in a Mouse Anterior Pituitary Cell Line 947
Nanditha J. Vivekananthan (Jeanne Koger and Evan Jones)

Superior Olivary Complex Inputs to the Dorsomedial Inferior Colliculus of the CBA Mouse Model of Presbycusis Remain Stable With Age 952
Jonathan D. Byrd (Robert Frisina and Joseph Walton)

The Amygdala Kindling Rat Model as a Tool for Screening Novel Anticonvulsant Compounds 957
Teresa Seo (Christine Hinko)

Juvenile Growth Rates in Six Turtle Species 961
Jeannine Mogavero and Christopher Benetatos (Scott McRobert)

A Comparison of Insecticide Susceptibility and Esterase Activity Using A Resistant Strain of the German Cockroach, *Blattella Germanica* (Dictyoptera:Blattellidae) 965
Brian R. Wamhoff and Michael S. Sabom (Bobby Jones)

The Effects of Mating on Sexual Receptivity in Drosophila Biarmipes 970
Carissa R. Adams (Scott McRobert)

Protease Activity in Developing Silkmoth Embryos 974
Yashoda Sharma (Elain Rubenstein)

Morphological Examination of Spermathecae from Three Grasshopper Species 979
Rita Michelle Roberts (Marianne Niedzlek-Feaver)

Rearing and Pathogenic Biological Control of the Citrus Leafminer, Phyllocnistis citrella Stainton 982
Dorothy Hoppe (Sandra Gilchrist)

The Effect of Thorax Temperature on Flight Speed in Honey Bee Drones *(Apis mellifera)* 987
Allan J. Ross (Joseph Coelho)

The Influence of Menstrual Cycle Phases on the Chaotic Behavior of R-R Intervals in College-Age Women 992
Allyson Rich and Stephanie Duncan (James' Watrous)

Alcohol Consumption and Its Effects on Grade Point Average and Acute Illness in College Students 996
Marlene A. Faust (Robert Byrd)

Alcohol Inhibits Tumor Necrosis Factor-alpha Production by Alveolar Macrophages during Pneumonia caused by *Streptococcus pneumoniae* 1000
Paul Nelson and Elaina Bleifield (Martha Mellencamp)

A Study of the Acceptance Rates of Prenatal Genetic Testing Among Women with High Risk Pregnancies 1005
Tara Butler (Ann McNeal and Chris Jarvis)

Microcurrent Versus a Placebo for the Control of Pain and Swelling in Acute Ankle Sprains 1010
Ann Samuelson (Richard Ray and John Shaughnessy)

The Reliability of the Biodex Stability System 1016
Stephanie Smith (John Bernhardt)

Current Science Textbooks: How Do They Rate with the Ohio Science Model? 1021
Anne Fay (Andrew Lumpe)

CHEMICAL SCIENCES

The Identification of the Kinetic Pathways in the Thermal Decomposition of Zinc (II) Acetylacetonate 1025
Jennifer Ann Condon (Thomas DeVore)

The Effects of Ion Binding on the Adenine-Thymine Base Pair 1029
Angela Felicia Chatman (Beatriz Cardelino)

The tert-Butylbenzyl Moiety, a New Protecting Group for Alcohols 1034
Jason Stamm, Ronald Aungst, Ann Bullion, Stephen Cairone, Bryan Firth and Lisa Jarrell (Chriss McDonald)

Enantioselective Addition of Metal-Based Nucleophiles to Unsaturated Aldehydes 1038
Cynthia A. Papesch (Timothy Friebe)

Production and HPLC Purification of Siderophores: Enterobactin and Ferric Eneterobactin 1041
William C. Putnam (Dick van der Helm)

Contact Angle Study of Porphyrin Monolayers on Solar Cells 1045
Thea J. Wilmarth (Carl Wamser)

Reduction and Purification of Water Soluble Porphyrins 1050
Tom Newman (Russ Selzer)

Second-Order Polarizabilities of Substituted Schiff's Bases 1053
Sonya D. McCall (Beatriz Cardelino)

Substance Isolated from the Marine Bryozoa Bugula Stolonifera 1057
Angelo Volpe (Rita Colon-Urban)

Determination of Structural Changes of Conductive Vapor Deposited Polyaniline Films 1060
Traci Simpson (Gerald Caple)

NMR and FT/IR Studies of Tryptophanase 1065
Karen N. Toppin (Herbert Ashline)

Mössbauer Analysis of Bog Soil Samples 1069
John A. Jones (Katherine Whatley)

Analytical Spectroelectrochemistry of Selected Analytes 1073
Sherry-Ann Callender (Paul Flowers)

Synthesis of the Acceptor Portion of a Molecular Triad for Artificial Photosynthesis 1078
Tavia S. Boston and Aquita C. Robinson (John Myers)

Study of Salt Effects on a Hydrophobically Accelerated Diels-Alder Reaction 1082
Jessica Speltz (Robert Whitnell)

A Qualitative Analysis of Iron Carbonyls by Mössbauer Spectroscopy 1086
Willie Randolph Hargrove Jr. (John Stevens and Katherine Whatley)

Substrate Specificity With Regards to the Inhibitory Characteristics of Carbonic Anhydrase 1091
Joseph M. Wilson (John Meany)

Thermodynamic Studies of the Enolization of Pyruvic Acid and Pyruvate Anions 1096
Anthony P. Esposito (John Meany)

Large Zeolite Crystals: Environmental Applications and Heavy Metal Recovery 1101
Richard O. Mikula (Patricia Enzel)

Evaluation of Soil-Washing Process For "Unwashable" Clays and Silts From The Palmerton Zinc Site 1105
Brian M. Snyder (Mary J.S. Roth and Ronald Dennis)

Sorption Versus Coagulation In The Treatment of Hydrocarbon Contaminated Waters 1110
James L. Eifert (Berrin Tansel)

ENVIRONMENTAL SCIENCES

Chronic and Acute Dioxin Exposures and Their Impacts on Human Populations 1115
Deborah Feder (Susan Craddock and David Lighthall)

Comparison of Endomycorrhizal Fungi of Organically and Conventionally Grown Crops 1120
Kelley McMurray Sarkis (Christine Gruhn)

Institutional Implications of Ecosystem Management: Perspectives of Innovative Natural Resource Managers 1125
Patricia Bungert (David Bengston and Vernon Ruttan)

Proposed Wilderness Areas of the Dixie National Forest Using A GIS 1130
D. Craig and Mitzi R. Nyborg (Danny Vaughn)

Soil Characteristics of McClure's Bog, Henderson County, North Carolina 1135
Rachel E. Moynihan (Kevin Moorhead)

Water Efficiency at the University of North Carolina at Asheville 1140
Wendy L. Mackin (Richard Maas)

Radial Relief Displacement in Vertical Aerial Photographs 1145
Jason D. Wolfe (Danny Vaughn)

Modifications in the Rate of Cellular Adhesion Associated with the Overexpression of Alzheimer β/A4 Amyloid

Ruben Amarasingham
Department of Neural Science
Brown University
Providence, RI

Faculty Advisor:
Ronald E. Majocha Ph.D.
Department of Psychiatry
The Miriam Hospital
164 Summit Ave.
Providence, RI 02906

Alzheimer's disease (AD), a neurodegenerative disorder that currently claims 70% of all dementia cases worldwide, is characterized pathologically by the presence of extracellular senile plaques and neurofibrillary tangles in the brain. Aggregates composed of β-Amyloid protein, neuronal and glial processes are the primary constituents of these plaques. The amyloid which accumulates in Alzheimer's Disease is a small (4.2 kD) self-aggregating peptide (β/A4) derived from a larger, membrane bound protein named amyloid precursor protein (APP). APP can bond to the extracellular matrix of the brain (ECM). It is possible that the abnormal accumulation of β-amyloid that occurs in AD may produce changes in the ECM which eventually produce or contribute to the pathogenesis of the disorder. Since laminin is a known component of the Alzheimer plaques and tangles, it is also possible that β/A4 may alter the normal adhesive activity of this ECM constituent. In this study, immortal, neuron-like pheochromocytoma rat cells (PC12) permanently transfected with DNA coding for the β/A4-C terminal region of the amyloid precursor protein were used to assess the modification of adhesion induced by β-amyloid. Using a novel cell adhesion assay, we found that overexpression of β/A4 significantly disturbs the adhesive properties of PC12 cells, especially on laminin.

BACKGROUND

Alzheimer's Disease (AD) is a debilitating neurodegenerative disorder which currently affects millions worldwide and is becoming more prevalent in an aging population. The incidence of this destructive form of dementia rises steadily with age, increasing 0.5% per year from ages 60 to 80, and 2% to 3% per year afterward. It is thought to account for 60%-80% of all cases of dementia among people over aged 65 (Yankner and Mesulam, 1989). The brain tissue of all AD patients exhibit several distinguishing morphological attributes. One of these, termed senile plaques, consists of proteinaceous, 7-10 nm extracellular amyloid fibrils surrounded by spherical clusters of dystrophic neurites and glial cells which accumulate in specific areas of the brain (Katzman and Jackson, 1991).

Senile plaques, common to all AD patients, and to a lesser extent, a normal product of aging, contain the amyloid β protein (β/A4) at their core (Weidemann, *et al.*, 1989). The specific filament sub-unit seen in AD, β-amyloid, is a hydrophobic 4 kDa protein, which self-aggregates under certain conditions and is known to principally maintain a cross β-sheet conformation. These plaques also contain significant quantities of the extracellular glycoprotein, laminin (Perlmutter et al., 1991). Alzheimer brains also contain neurofibrillary tangles that are composed of masses of both straight and helically wound, 10 - 15 nanometer filaments consisting principally of hyperphosphorylated tau protein.

Several researchers have stated that β/A4 is neurotoxic (Yankner et. al., 1990).Work by Pike et al. (1993) seems to indicate that β/A4 can induce neuron degeneration in vitro. Studies show that β/A4 may destabilize calcium homeostasis and thus leave human cortical neurons vulnerable to excitotoxicity (Mattson et. al, 1992). Davison et. al. (1994) have found that incubation of cells with β/A4 greatly changes the flux of cations across the membrane, indicating that the neurotoxic effect of β/A4 may be mediated by it ability to form cation channels or, at least, alter the activity of calcium channels already present on the membrane.

Amyloid β Protein originates from the Amyloid Protein Precursor (APP) molecule. APP is a membrane-spanning glycoprotein, defined by a locus on chromosome 21, which is

know to exist in multiple isoforms of 770, 751,714, 695, 563, and 365 amino acids (Kang, et al., 1987). APP may serve as an extracellular matrix molecule which modulates the adhesion and growth of different classes of cells (Breen et. al., 1991).

Since APP is highly associated with the extracellular matrix of the brain (Klier et. al., 1990), it is possible that the abnormal accumulation of β amyloid that occurs in AD may produce changes in the ECM which eventually produce or contribute to the pathogenesis of the disorder. Of all the extracellular matrix components, laminin has perhaps received the most attention in AD research. Laminin was first identified as a cell adhesion molecule, with such activity being demonstrated on epithelial, endothelial, and neuronal cells (Kleinman et. al., 1985). Since laminin is a known component of the Alzheimer plaques and tangles (Perlmutter et al., 1991), it is possible that β/A4-induced alterations in the activity of this ECM constituent may adversely affect cellular adhesion. Elucidation of the interaction between β/A4, ECM components, and the cellular membrane is therefore critical to our understanding of β-amyloid toxicity.

In this study, immortal, neuron-like pheochromocytoma rat cells (PC12) permanently transfected with DNA coding for the β/A4-C terminal region of the amyloid precursor protein were used to assess modification of adhesion induced by β-amyloid. These transfected cells are referred to as A7 (Marotta et al., 1989).

METHODS

CELL CULTURE

PC12 and A7 cells were grown in 75 x 75 cm. tissue culture flasks at 37°C and 0.5% CO_2 at subconfluent levels.

CELL REMOVAL AND COUNT

Cells were removed from the tissue culture flasks at subconfluent levels with 0.25% trypsin in Hank's balanced salt solution (HBSS). The trypsin was neutralized with an equivalent ratio of Dulbecco's modified eagle medium once the cells were removed. Cell and viability counts were determined using a hemocytometer in conjunction with a trypan blue stain.

APPLICATION OF EXTRACELLULAR MATRIX PROTEINS

Each well was coated with laminin (4 ug./ul.) in 300 µl (HBSS). The protein was allowed to bind for 1/2 hr. at room temperature and then removed. The wells were subsequently washed with HBSS for 10 minutes. In some cases wells were blocked for 1/2 hr. with 0.5% gelatin or 1% bovine serum albumin in HBSS.

CELL ADHESION ASSAY

All of the experiments were performed in triplicate. Approximately 1×10^5 to 1.5×10^5 cells were added per 16 mm. well in 24 well plate. After incubation at 37°C for an interval specified by the exact experiment, individual plates were removed, gently inverted and drained of media in order to remove unadherent cells. Each well was then washed once with 500 µl of HBSS. Cells were pre-fixated with 0.5% glutaraldehyde in HBSS for five minutes followed by 2% glutaraldehyde in HBSS. The cells remained in fixative overnight. Fixative was removed and replaced with 500 µl 0.1% cresyl violet dye per well. After 30 minutes, the wells were rinsed with water for 15 minutes. Non-specific staining was removed by adding 50% ethanol in water for 20 minutes. This was replaced with 1 ml. portions of 1% acetic acid in water for 1 hour. The acetic acid was then removed and the dye content was measured in the spectrophotometer for absorption at 580 nanometers.

3A3 ANTIBODY FOR INHIBITION EXPERIMENTS

3A3 is a mouse monoclonal antibody. This antibody has been shown to recognize the active site of laminin binding integrins.(Turner et. al., 1989). The 3A3 used for the experiments presented here was kindly donated by D.Turner (New York).

RESULTS

Measuring Rates of Adhesion for PC 12 and A7 cells on polystyrene and laminin

In the first experiment, PC12 and A7 cells were tested for rate of adhesion on uncoated wells in the presence of serum-containing DMEM media. As figure 1 indicates, A7 cells which overexpress the β/A4 peptide adhere less rapidly to plastic than PC12 cells. The difference between A7 and PC12 adherence is extremely significant at 1/4 hour as indicated by the p value at this point (p=.012).

This experiment was repeated under the same media conditions with laminin as a substrate in Figure 2. In this case, however, A7 cells adhered more rapidly than PC 12 cells.

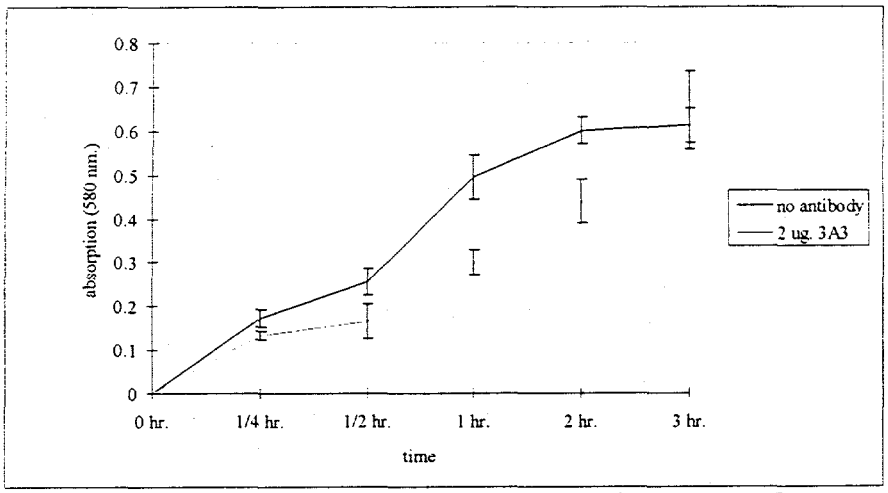


FIG. 3. ADHERENCE OF A7 CELLS ON LAMININ IN THE PRESENCE OF 3A3 ANTIBODY. CELL ADHESION ASSAY PERFORMED FOR A7 CELLS AT 1/4, 1/2, 1 AND 3 HOURS (MAXIMAL BINDING). AVERAGES AND STANDARD DEVIATIONS FOR EACH DATA POINT REPRESENT 3 DIFFERENT WELLS @ 150,000 CELLS. WELLS CONTAIN 2 µG./ML OF ANTIBODY. A TWO-TAILED T-TEST BETWEEN ANTIBODY AND NO ANTIBODY VALUES AT 1/4, 1/2, 1, 2 AND 3 HRS. YIELDED .072,.022,.008,.014 AND .599 RESPECTIVELY.

The antibody 3A3 is reported to inhibit PC12 attachment to laminin. (Turner et. al., 1990) Since A7 cells bind to laminin substrate, it was decided to test whether integrin receptors contributed to this effect. As figure 3 indicates, 3A3 does inhibit the rate of adhesion of A7 cells on a laminin substrate.

CONCLUSIONS

Transfected PC12 cells (A7) that overexpress Alzheimer's amyloid peptides show a decrease in adhesion to a plastic substrate when compared to normal cells. However, using laminin as substrate, these cells show an increase in rate of adhesion. Inhibition of adhesion with an antibody that binds to laminin receptors suggests that at least some of the modifications in the cellular membrane is specific for laminin receptors. Changes in adhesion could effect the way neurons communicate with their environment in AD.

REFERENCES

1. Breen KC, Bruce M, Anderson BH. (1991) Beta amyloid precursor protein mediates neuronal cell-cell and cell-surface adhesion. *Journal of Neuroscience Research.* 28:90-100.
2. Davidson RM, Shajenko L, and Donta TS. (1994) Amyloid beta-peptide (AβP) potentiates a nimodipine-sensitive L-type barium conductance in N1E-115 neuroblastoma cells. *Brain Research.* 643: 324-327.
3. Kang, J., Lemaire, H., Unterbeck, A. et al. (1987) The Precursor of Alzheimer's Disease Amyloid A4 Protein Resembles a Cell-Surface Receptor. *Nature.* 325: 733-736.
4. Katzman, R., Jackson, E. (1991) Alzheimer's Disease: Basic and Clinical Advances. *Journal of the American Geriatrics Society.* 39: 516-525.
5. Kleinman, HK, Cannon FB, Laurie GW, et al.. (1985). Biological activities of laminin. *Journal of Cell Biochemistry.* 27: 317-325.
6. Mattson MP, Chen G, Davis D, et al. (1992). β-amyloid peptides destabilize calcium homeostasis and render human cortical neurons vulnerable to excitotoxicity. *Journal of Neuroscience.* 12: 376-389.
7. Marotta CA, Majocha RE, Tate B. (1992) Molecular and cellular biology of Alzheimer amyloid. *Journal of Molecular Neuroscience.* 3: 111-125.
8. Marotta CA, Chou WG, Majocha RE, Watkins R, Zain SB (1989) Overexpression of amyloid precursor protein A4 (beta-amyloid) immunoreactivity in genetically transformed cells. Implications for a cellular model of Alzheimer amyloidosis. *Proceedings of the National Academy of Sciences. USA* 86: 337-341.

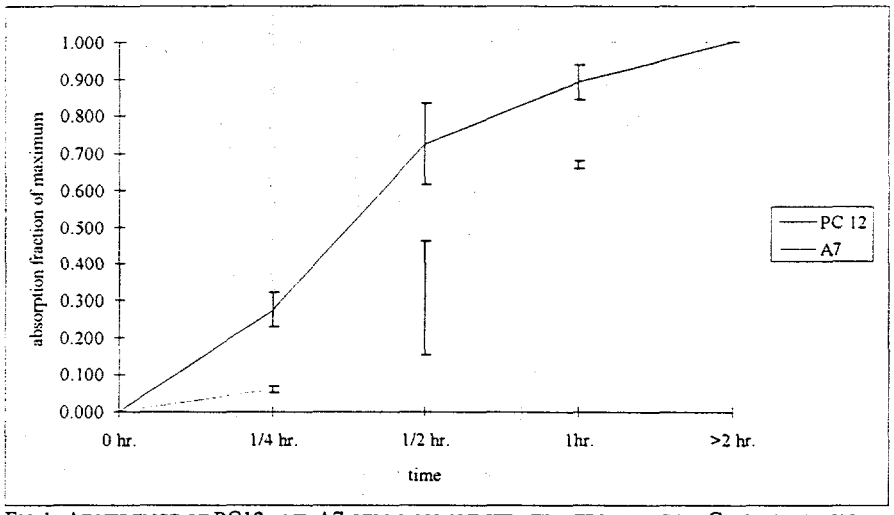


FIG 1. ADHERENCE OF PC12 AND A7 CELLS, NO SUBSTRATE, SERUM MEDIA. CELL ADHESION ASSAY PERFORMED FOR PC12 AND A7 CELLS AT 1/4, 1/2, 1 AND > 2 HOURS (MAXIMAL BINDING). THE GRAPH ABOVE IS A NORMALIZED CURVE OF THE VALUES TABULATED FOR A7 AND PC12 CELLS. FINAL VALUES ARE FRACTIONS OBTAINED BY DIVIDING INDIVIDUAL ABSORPTIONS BY THE MAXIMUM FOR EACH CELL TYPE. AVERAGES AND STANDARD ERRORS FOR EACH DATA POINT REPRESENTS 3 DIFFERENT TRIALS. A TWO-TAILED T-TEST BETWEEN A7 AND PC12 CELLS RETURNED A P VALUE OF .012 AT 1/4 HOUR, INDICATING THAT PC12 CELLS ADHERE FASTER UNDER THIS CONDITION.

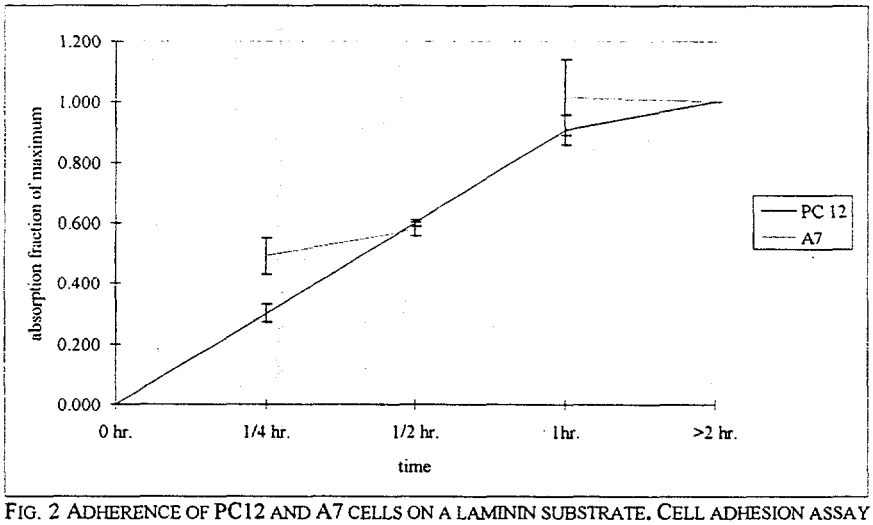


FIG. 2 ADHERENCE OF PC12 AND A7 CELLS ON A LAMININ SUBSTRATE. CELL ADHESION ASSAY PERFORMED FOR PC12 AND A7 CELLS AT 1/4, 1/2, 1 AND > 2 HOURS (MAXIMAL BINDING). THE GRAPH ABOVE IS A NORMALIZED CURVE OF THE VALUES TABULATED FOR A7 AND PC12 CELLS. A TWO-TAILED T-TEST BETWEEN A7 AND PC 12 CELLS RETURNED A P VALUE OF .0132 AT 1/4 HOUR, INDICATING THAT A7 CELLS ADHERE FASTER UNDER THIS CONDITION.

9. Perlmutter, LS, Barron E, Saperia D, and Chui HC (1991) Association between vascular basement membrane components and the lesions of Alzheimer's Disease. *Journal of Neuroscience Research.* 20: 673-681.
10. Pike CJ, Burdick D, Walencewicz AJ, Glabe CG, and Cotman CW (1993). Neurodegeneration induced by β-amyloid peptides in vitro: The role of peptide assembly state. *Journal of Neuroscience.* 13: 1676-1687.
11. Turner DC, Flier LA, and Carbonetto, SC (1989). Identification of a cell-surface protein involved in PC 12 cell-substratum adhesion and neurite outgrowth on laminin and collagen. *Journal of Neuroscience.* 9:3287-3296.
12. Yankner BA, Duffy LK, and Kirschner DA. (1990) Neurotrophic and neurotoxic effects of amyloid β-protein: reversal by tachykinin neuropeptides. *Science.* 250: 279-286.
13. Weidemann, A., König, G., Bunke, D., Fisher, P., Salbaum, J.M., Masters, C.L., Beyreuther, K. (1989) Identification, Biogenesis, and Localization of Precursors of Alzheimer's Disease A4 Amyloid Protein. *Cell.* 57: 115-126.
14. Yankner, B.A., Mesulam, M. (1989) β-amyloid and the Pathogenisis of Alzheimer's Disease. *Services in Medicine of the Beth Israel Hospital, Boston.* 325(26): 1849-1857.

Acetylcholinesterase and its High Concentration in Human Amniotic Fluid as an Indicator of Open Neural Tube Defects

Paul Riley

Department of Chemistry
Seattle University
Broadway and Madison
Seattle WA 98122

Sponsor:
Mark Wener, M.D.
Department of Laboratory Medicine
University of Washington Medical Center
Mail Stop SB-10
Seattle WA 98195

Abstract

The current project involves the development of a working method for the testing of high acetylcholinesterase (AChE) activity in human amniotic fluid using polyacrylamide slab gels. Amniotic fluid samples are run on 1.5mm acrylamide slab gels with bromphenol blue dye and sucrose solution. If two bands are present after constant current electrophoresis, possible presence of the neural enzyme AChE is demonstrated. After reaction of the components of the gel with the inhibitor BW284C51 (1,5-bis(4-allyldimethylammoniumphenyl)-pentan-3-one-dibromide), then with the substrate acetylthiocholine iodide, one band, consisting of pseudocholinesterase, or the cholinesterase enzyme non-specific for acetylcholine (ACh) remains visible on the gel, proving the presence of the enzyme specific for AChE in the sample. Initial results were promising. Band resolution was good, with expected relative concentrations and band consistencies confirmed by densitometer readings. The new method will be applied to the clinical lab setting in the hospital, where high AChE concentration in amniotic fluid indicates the presence in the developing fetus any one of several open neural tube defects. The presence of the pseudocholinesterase band is normal and must be present in each sample. Background information on the enzyme, densitometer readings, and other data will be presented in the following research paper.

Introduction

Cholinesterases are part of a large group of hydrolytic enzymes found in the human body. The specific function of cholinesterases, and AChE in particular, is to hydrolyze the neurotransmitter ACh in order to terminate the intercellular communication pathway known as cholinergic signaling. This pathway produces different responses in multiple tissues and cell types, including chromaffin and ganglion cells, nerve cells wrapped in bundles found outside the brain in the autonomic nervous system alongside the spinal chord, motor nerves, central nervous system neurons, and muscle cells (Soreq, Zakut, 1993).

ACh is a neurotransmitter, a substance that acts as a messenger between two neurons. The neurons cannot directly transmit electrical signals to each other, and so need neurotransmitters to carry the message to the receiving neuron by chemical means. AChE, by hydrolyzing the excess neurotransmitters in the synapses, prevents the electrical potential in the postsynaptic neuron from being too high and in this way, plays an integral part in maintaining homeostasis.

The chemical-electric signal conversion process is quite complex. When the electrical message is received at the end of the neuron (or synaptic knob), synaptic vesicles fuse with the plasma membrane of the cell at the synaptic knob and release the many neurotransmitter particles they hold. This fusion is caused by the sudden increase in calcium ions in the synaptic knob, caused by the depolarization of the cell membrane by the electrical signal traveling the length of the presynaptic neuron. This depolarization of the presynaptic neuron membrane causes calcium ions to rush into the cell from the outside by diffusion. The neurotransmitters travel the space across the synapse to the

membrane of the postsynaptic cell. Many neurons use a specific neurotransmitter suited only to its purposes and the purposes of surrounding neurons (Barrett, Magleby, 1976).

When proteins that function as receptors project from the membrane of the postsynaptic neuron receive the neurotransmitter, they open an ion channel protein connected to the receptor. The ion channel opens, allowing ions such as potassium, sodium, or chloride to enter into the postsynaptic neuron. The entering ions change the ionic potential of the postsynaptic neuron, making it either more or less polarized than it was before. The postysynaptic neuron may respond to this change in electric potential by initiating an electric signal in itself, which travels to an adjacent neuron. The cycle continues until reaching a cell that will produce an effect from the electrical message (Campbell, 1990).

Once the message has been transmitted, the chemical signal must be quickly muted. ACh still remaining in the synapse must be broken down by enzymes including AChE, which along with other kinds of cholinesterases fills this synaptic neurotransmitter breakdown role.

Cells that secrete, synthesize, and store the neurotransmitter ACh are referred to as cholinergic (Soreq, Zakut, 1993). AChE breaks apart ACh into acetate and choline molecules. This binding of ACh produces a signal inside the neurons known as cholinergic signaling. The functions of cholinergic signaling have been shown to include control of sperm cell motility. Rama Sastry and Sadvongvivad (1978) proved this by showing that the choline acetyltransferase inhibitor 2-benzoylethyltrimethyl ammonium, at concentrations as low as $1x10^{-6}$ moles/liter, produces loss of sperm motility.

Physical Properties and Structure of AChE

The probable molar mass of purified human cholinesterase has been found to be around 345,000 to 371,000 daltons, suggesting multiple subunits. The four subunits have an equal molecular weight of around 84,000, and are probably identical in substructure. The four subunits are split into two dimers, with one intersubunit disulfide bond holding them together. Each subunit consists of approximately 400 amino acids (Whittaker, 1986).

Ranges of half-lives, the time it takes for half of the original amount of enzyme to denature, of cholinesterase have been found from 2 to 16 days, depending on conditions under which the enzyme is kept. The enzyme may be kept frozen in plasma for several years without appreciable loss in activity, but a single freezing and thawing will produce a decrease in 30% in activity levels (Whittaker, 1986).

There are two active sites in cholinesterase - the anionic and esterative sites. The anionic site is a negatively charged region of the substrate molecule. The anionic site also contains two hydrophobic areas that produce greater specificity for the substrate by their lack of affinity for water molecules and any functional groups that may look like water to the enzyme. The esteratic site links to the carbonyl group (C=O) of the ester linkage and performs the actual hydrolysis of the ester bond. Because of this function, the esteratic site is usually referred to as the catalytic active site (Whittaker, 1986).

Laboratory Research - Purpose and Theory

Demonstrating AChE activity in amniotic fluid, a clear indicator of open neural tube defects in the developing fetus (Chubb, Springell, Pilowsky, and Pollard, 1979), is accomplished through the use of gel electrophoresis, a laboratory process used to separate large molecules on a gelatin-like medium.

Open neural tube defects occur when the neural tube, a feature of vertebrate embryonic development, is left open to the surrounding amniotic fluid for an unusually long period of time during fetal development. The neural tube develops from embryonic cells collectively known as the mesoderm, or middle layer, or epithelial, those outermost cells on the developing cells on the developing organism. The neural tube then develops into the whole central nervous system which includes both the brain and spinal cord.

When the neural tube is not sealed, proteins and enzymes normally only found in spinal fluid leak out into the surrounding amniotic fluid. When the neural tube is not sealed, the level of AChE is very high compared to this natural low concentration of AChE. Spina bifida is one abnormality that is revealed in the developing fetus when the

level of AChE is high in the amniotic fluid. Spina bifida occurs in varying degrees of severity from the neural tube staying open during gestation, then the vertebrae fail to fuse during the later stages of gestation, creating a significant neurological problem for the child. In the most severe form of the disorder, spina bifida myelomeningocele, the vertebrae fail to fuse, and the spinal cord along with other spinal tissues protrude from the body to form a sac. Spinal nerves are damaged, and the spinal cord is impaired below the level of the sac as well as above it for several segments of vertebrae.

The level of AChE activity in the amniotic fluid must be compared to the level of activity in maternal serum so the high AChE concentration may be attributed to the fetus. Usually a small concentration of AChE is found in blood serum, due to the release of AChE from non-neural cells (Chubb, Pilowsky, Springell, Pollard, 1979). In normal pregnancies, the level of AChE activity can be very high during one part of gestation then will decrease as the nervous system matures. This has been shown to be the case in bovine fetal serum, where levels of AChE are eight times the adult concentration. Lambs, by comparison, demonstrate very high levels of AChE activity early in gestation, which decrease to adult levels by a time late in pregnancy (Chubb, Comline, Silver, Smith, 1978).

Procedures for Laboratory Research

The present method for demonstrating AChE activity involves running the amniotic fluid samples on polyacrylamide using the tube gel system. Tube gels are thin glass tubes open at both ends. While the acrylamide is being poured into the tubes, one end is kept plugged. After the acrylamide polymerizes, the plug is removed and the tube is inserted into an apparatus that can hold many tubes along with the working buffer, containing glycine and Tris(hydroxymethylaminomethane) base (Sigma), and cool circulating water needed to carry away the heat produced while the electric current is running through the buffer.

The advantages of the slab gel system include having the bands for the patient, high positive, low positive, and negative controls directly adjacent to one another, making analysis easier, rather than having each of patient and control samples in separate gels as with the tube gels.

Disadvantages of the slab gel system include the greater difficulty that it takes to pour the gelling material in to the glass plates, and the trouble of setting up the apparatus. Some of these difficulties may be overcome with operator practice. Homemade gels were used even though premade gels ordered from Jule, Inc. were available because the resolution using the premade gels was very poor.

When a sample is run that contains a high concentration of AChE, two bands emerge in the gel, with usually several millimeters separation between them, depending on how long the gel was subjected to the electric current. The band that travels farthest from the point of entry of the sample into the gel is the true AChE portion of the sample. A thicker, wider band consisting of pseudo, or non-specific AChE remains closest to the sample well, where the samples are injected and enter into the gel.

The first step in running the slab gels involves equilibrating the gels with the buffer solution at a constant voltage of 350V until the current running through the gels drops to around 15mA. These values will be halved when only one gel is run. In the next step, samples and/or controls are mixed with a third of the total sample volume of bromphenol blue dye mixed into 40% sucrose solution. 30µl of each sample is inserted into the gel wells with a micropipet. The gels are run until the dye front runs off the gel, which takes about an hour and a half at a constant current of 5mA for 30 minutes, then 20mA for the remaining hour or so. The longer the gels are run without the bands running off, the better.

After the electrophoresis is completed, the identity of a true AChE band is confirmed by pouring one milliliter of a solution containing an inhibitor at a concentration of $5x10^{-5}$ moles/liter into a container with one half of the gel. The inhibitor BW284C51 [1,5-bis(4-allyldimethylammoniumphenyl) -pentan-3-one-dibromide (Sigma)], is used. This inhibitor has been shown to react specifically with the AChE band. When the true AChE band reacts with the inhibitor, the AChE molecules are prevented from reacting with the substrate in the subsequent step, and do not appear after the gel is incubated in the solution containing the substrate. The samples are always run in duplicate so one tube can be reacted with the inhibitor while the other remains unreacted. In this way, the presence of a high concentration of AChE may be confirmed.

After the gels are inhibited, the substrate acetylthiocholine iodide (Sigma) is dissolved in a solution of sodium sulfate, maleic acid, copper sulfate, glycine, and magnesium chloride and added to a container with the gel in order to saturate the enzyme and keep it in its enzymatic form. rather that letting it denature as it would over time if left unreacted.

The substrate visualizes the enzymes, which appear as a white band, so their concentration relative to one another can be found using a densitometer along with a personal computer which produces a graph of optical density vs. gel length. The test for AChE in the amniotic fluid sample is positive if and only if there are two peaks in an uninhibited sample gel densitometric analysis, and one peak in the inhibited sample gel densitometric analysis. These graphs produced by the densitometer are kept and used as proof of the positive results, the ratios of peak height calculated by the densitometer are written in a record book, and the gels stored for future analysis if necessary.

Results and Implications

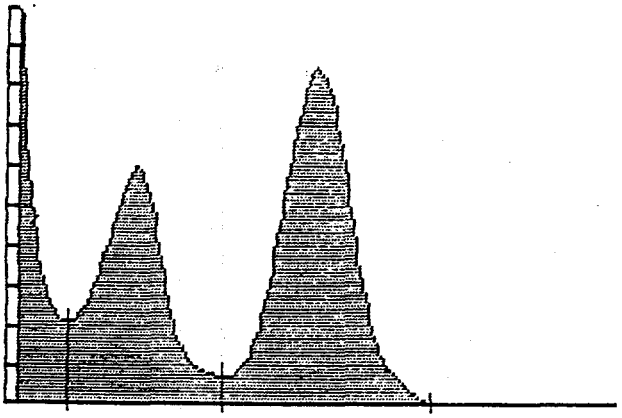
The overall result of the research was the forming of a laboratory protocol that involved all of the above steps. The procedure as written in the protocol was run repeatedly to ensure the method worked as properly and efficiently as possible. It took many unsuccessful trials using premade gels, agarose gels, and different working conditions to find the successful method described in the protocol, which may be obtained by a request in writing to the address above the abstract at the UWMC.

The protocol may be found to be more efficient and desirable over other methods when applied to different laboratory settings. Different methods for this particular prenatal test are desirable when many tests of this kind need to be accomplished in a given clinical laboratory, and this method definitely has its advantages.

References

1. Barrett, E.F., Magleby, K.L., *Physiology of Cholinergic Transmission,* edited by Goldberg, Alan M., Hanin, Israel, Biology of Cholinergic Function, Raven Press: New York, 1976
2. Campbell, Neil E., Biology, Second Edition, The Benjamin Cummings Publishing Company, Inc. , Redwood City, CA 1990
3. Chubb, I.W., Pilowsky, P.M., Springell, H.J., Pollard, A.C., *Acetylcholinesterase in Human Amniotic Fluid: An Index of Fetal Neural Development?*, The Lancet, 1979, 1: 688
4. Kelly, J.C., Petrocik, E., Wassman, E.R., *Amniotic Fluid Acetylcholinesterase Ratios in Prenatal Diagnosis of Fetal Abnormalities*, American Journal of Obstetrics and Gynecology, 1989 September, 161(3), Pages 703-5
5. Silver, Ann, The Biology of Cholinesterases, North-Holland Publishing Company: New York, 1974
6. Soreq, Hermona, Zakut, Haim, Human Cholinesterases and Anticholinesterases, Academic Press: San Diego, 1993
7. Whittaker, Mary, Cholinesterase, Basel, New York, 1986
8. Williamson, G. Gordon, Children With Spina Bifida, Paul H. Brookes Publishing Co., Baltimore, 1987

Figure 1: Densitometer Scan of Optical Density vs. Gel Length for a Positive Cerebral Spinal Fluid Control Sample Run on September 27, 1994, Showing the AChE Peak on the Far Right and the Pseudocholinesterase Band in the Middle (the Band on the Left is the Scan of the End of the Gel)

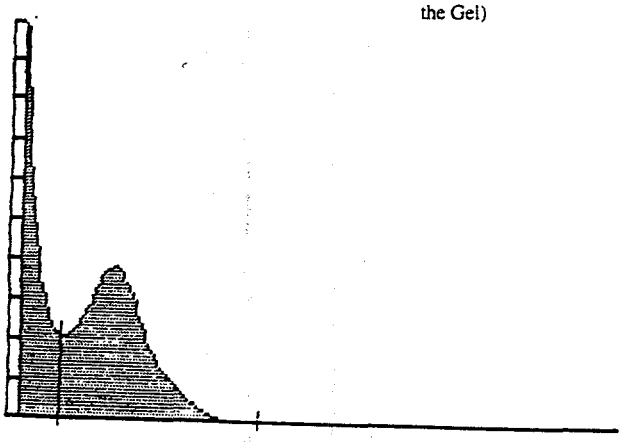


SAMPLE 1 08:57:06 September27, 1994

ACQ # : i140 NAME : pos ct
DATE DRAWN: 09-27-94

FRACTION	%
1	15.0
2	33.6
3	51.3
2/1	2.24

Figure 2: Densitometer Scan of Optical Density vs. Gel Length for a Negative Cerebral Spinal Fluid Control Sample Run on September 27, 1994, Showing the Pseudocholinesterase Band on the Right (the Band on the Left is the Scan of the End of the Gel)



SAMPLE 3 09:01:13 September27, 1994

ACQ # : i160 NAME : neg ct
DATE DRAWN: 09-27-94

FRACTION	%
PSEUDO	37.5
ACETYL	62.5
2/1	1.67

DEVELOPMENT OF A NEOVASCULARIZED BIOARTIFICIAL PANCREAS ORGANOID

Jennifer L. Long

Department of Chemical Engineering
University of Toledo
2801 W. Bancroft St.
Toledo, OH 43606

Faculty Advisors:

Dr. Ronald L. Fournier
Dr. Jeffrey G. Sarver

Bioartifical organoid devices are a possible treatment for various diseases, including diabetes mellitus. Current remedies for diabetes include a special diet, insulin therapy, and pancreas transplantation; and effective transplantable device could provide another option. We have developed such a device. This device integrates the body's own vascular system, xenographic porcine islets of Langerhans, and an immunoisolation membrane. It mimics the function of a healthy pancreas by automatically producing insulin in response to ever-changing blood glucose levels; this is an advantage over insulin injections which cause widely fluctuating glucose levels. Also, the ingrowth of the body's vascular system into a porous matrix material in the device provides a natural blood supply, preventing the clogging effect found in some artificial shunts.

The membrane is the final crucial element of the design, because it eliminates the need for immunosuppression that is normally present with a xenograft. Using the passive diffusion of a wide range of solutes, we have developed and evaluated a highly permeable membrane for use in a bioartificial organoid device such as this one. The membrane is adequately permeable to allow free passage of oxygen, glucose, and insulin while selective enough to prevent the passage of the immune system components. The membrane is also long-lived and biocompatible. This membrane and device are currently being evaluated in rodents, and could eventually provide a new treatment for sufferers of diabetes mellitus.

INTRODUCTION

Type I, or insulin-dependent diabetes mellitus, affects nearly two million Americans. For most of those patients, daily insulin and strict nutritional control are required to maintain healthy glucose concentrations in the blood. Even with insulin treatments, though, persons with diabetes are more likely to suffer blindness, stroke, heart attack, or kidney disease than other individuals.

Type I diabetes occurs when the insulin-releasing cells of the pancreas, known as the islets of Langerhans, are destroyed by an auto-immune response. For some unknown reason, the body's own immune system selectively attacks and kills the islets while leaving the rest of the pancreas unharmed. The pancreas continues its other digestive functions but can no longer produce insulin. Without insulin, other cells in the body cannot absorb enough glucose from the blood stream to continue their normal functioning. Consequently, glucose levels in the blood rise very high while the cells are unable to use any sugar for energy.

To stimulate glucose uptake by cells, patients with diabetes inject commercial insulin, which is often derived from islets of Langerhans isolated from pig pancreati. Although this treatment does allow cells to absorb the energy they need, blood glucose concentrations still vary more widely than in healthy persons. Since the glucose levels are controlled by drug rather than homeostatically, they can reach fairly high levels between doses and then drop dramatically after a dose. Those higher concentrations of glucose cause many of the long-term debilitating effects of diabetes.

Alternatives such as pancreas transplantation or implantation of encapsulated islets of Langerhans have been proposed to better regulate the use and concentration of glucose in the blood of patients with Type I diabetes. Although allographic pancreas transplants have successfully reinstated normoglycemia in diabetic patients, they are only possible in conjunction with immune system suppression. The complications that accompany immunosuppression are at least as serious as the risks from the diabetes itself, so transplants are generally only performed on patients concurrently receiving kidney transplants. In addition, nationwide shortages of organ donors limit the number of patients who can receive pancreas transplants.

Immunoisolation of Transplanted Islets

To eliminate the need for immunosuppression and a human donor, islets of Langerhans can be separated from a mammalian pancreas (usually porcine) and implanted within a semipermeable barrier. The barrier is constructed to allow free passage of insulin, glucose, and oxygen, while blocking the passage of immune system components. The smallest antibodies have molecular weights around 150,000 daltons while white blood cells are much larger; insulin, however, has a molecular weight of only 6,000 daltons. Thus, most barriers are designed to exclude macromolecules above a molecular weight of about 50,000 daltons.

Four primary types of bioartificial pancreas involve an immunoisolation membrane protecting implanted islet cells. The intravascular pancreas routes blood through an artificial, semiper-

meable vessel while the islets are enclosed in a space around the vessel. Although this method ensures adequate blood supply to the islets, swirling of the blood at the entrance and exit of the shunt causes dangerous blood clotting (11,13). In microencapsulation, single islets are enclosed in microscopic membraneous spheres for implantation. Mass transfer between the islets and their environment is fairly easy because of the small diffusion distance, but removal of the islets, if necessary, may be difficult (9,16). Macroscopic hollow fibers holding thousands of islets pose the opposite problems; removal is easier, but the thicker membrane walls reduce rates of mass transport (2,10).

An example of the fourth type of bioartificial pancreas, the organoid device, was created by Sarver et al. (15) and described here. The organoid does not rely on immunosuppression or artificial shunts and is easily reseedable with new cells. It incorporates a neovascularizing matrix material to ensure a close blood supply, a flat immunoisolation membrane with good mass transport properties, and an islet chamber with ports for cell addition or removal. This device, when charged with porcine islets of Langerhans, has produced temporary glucose control in rodents.

EXPERIMENTAL EFFORTS

The bioartificial organoid consists of a stainless steel chamber with two loading ports sealed with screws; the chamber is covered on the open side by a semipermeable polymer membrane (Fig. 1). The membrane is crucial to the pancreas device because it protects the implanted islet cells from immune system attack. Also essential to the organoid design is the vascularizing matrix material. Prior to islet implantation, the body's own vasculature infiltrates the matrix providing a reliable blood supply to the cells. Some experiments have been completed evaluating the organoid in diabetic rodents.

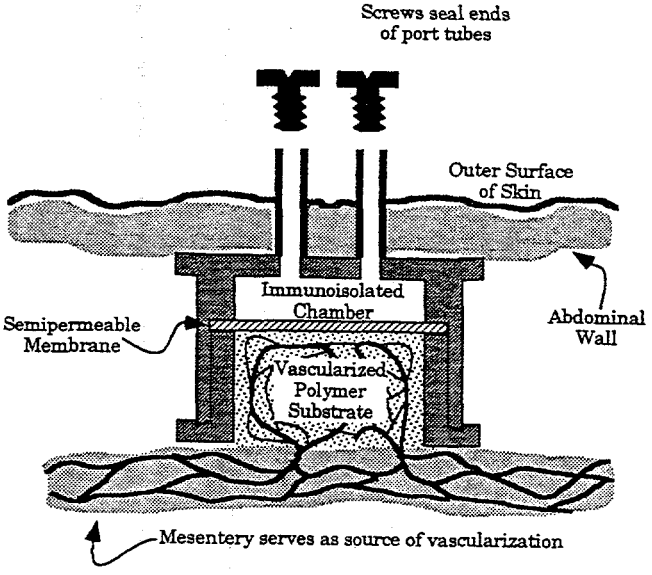


Fig. 1. Schematic diagram of neovascularized bioartificial pancreas organoid for a rodent after implantation.

Immunoisolation Membrane Evaluation

A semi-permeable membrane has been developed for use in this device; it has demonstrated acceptable characteristics for use in an immunoisolated system. Permeabilities of glucose and insulin are high yet the permeability of albumin is very low, signifying that the membrane can reject high-molecular weight components of the immune system.

Membrane permeability was determined by the passive diffusion of radiolabeled tracer solutes. Four identical membranes were mounted vertically in separate double-sided chambers, and both sides of the chambers were filled with a sterile saline solution at a pH of 7.4. The system was allowed to equilibrate overnight. After a given time period, the fluid was removed from each side of the chamber and suspended in water and Universol cocktail for counting in a gamma-ray counter.

To derive the permeability of the solute across the membrane, a mass balance was calculated for the radioactive solute. Three solutes of interest, glucose, inulin, and albumin, were considered individually in this manner. Inulin was chosen for analysis because it has a molecular weight and structure similar to those of insulin, but is more stable. Albumin, with a molecular weight of 69,000 daltons is a cut-off target for antibody exclusion from the membrane.

As seen in Fig. 2, the permeabilities determined for this membrane by Fournier, et al. (6) are acceptable for an immunoisolation device and are comparable to those reported by Dionne, et

al. (5). Permeabilities of a commercial ultrafiltration membrane with a reported molecular weight cutoff of 50,000 daltons (Amicon XM50, W.R. Grace Co.) were determined in the same manner as described above. The permeability of our polymer membrane is comparable to or higher than that of both the commercial membrane and that of Dionne for glucose and inulin yet is lower than that of Dionne and essentially equal to that of Amicon for albumin.

Matrix Vascularization

Devices with a felt matrix material coated with fibroblast growth factor were implanted in the abdominal wall of rodents for 1, 7, 14, or 28 days. After that implantation period, the devices were removed, and the matrix was sectioned and stained with hematoxylin to identify blood vessels and eosin to identify cellular invasion. Numbers of capillaries and their diameters and numbers of immune cells present were counted under a light microscope. The vascularized fraction of the matrix increased with longer implantation periods (Fig. 3). Limited numbers of immune cells were present near the device. However, some fibrosis was observed around the implanted device after removal; studies quantifying the degree of fibrotic encapsulation are underway.

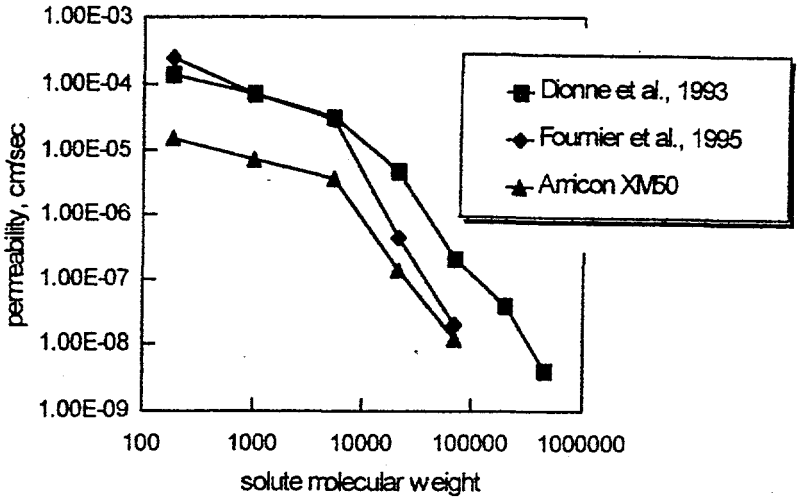


Fig. 2. Comparison of permeabilities for three different membranes.

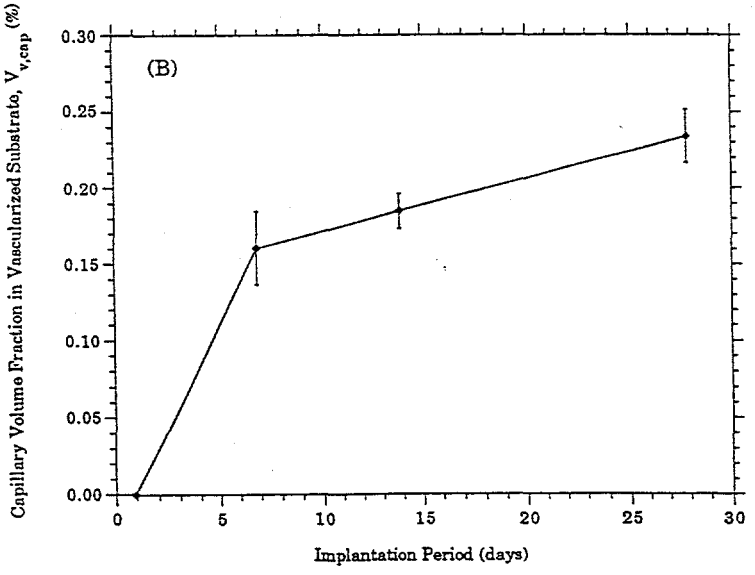


Fig. 3. Progression of matrix vascularization with time.

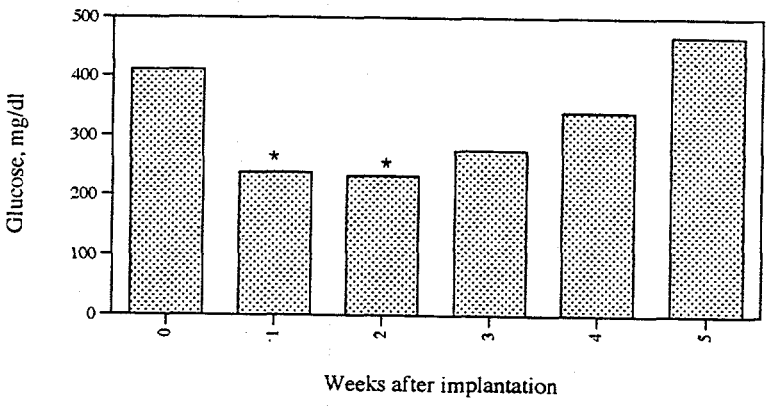
Organoid Evaluation in Diabetic Animals

To assemble the device, a circular membrane is glued to a ring around the stainless steel chamber. Prior to implantation, the entire device is sterilized by steam autoclaving while being soaked in distilled water. Separately, a single layer of a surgical support felt material is sterilized by steam autoclaving. This felt matrix is then soaked in fibroblast growth factor overnight and is attached under sterile conditions to the sides of the device adjacent to the membrane. A thin circular stainless steel ring is inserted within the walls of the device to hold the matrix in place.

After assembly, the device is implanted aseptically into the abdominal wall of an anesthetized male rat. A flap of tissue is pulled away from the abdomen; the device is then positioned matrix-side down on the abdomen. Two small holes are cut in the tissue flap for the loading ports, which extend outside the body of the rodent. The device is sutured in place with surgical silk, and the tissue flap is closed and stitched shut.

Two to four weeks after the device implantation, islets are seeded into the islet chamber. Porcine islets of Langerhans are isolated from a whole pancreas according to the method of Ricordi (14). Both of the screws closing the device ports are removed and sterile polyethylene tubing is attached to each port. Sterile saline is injected into one port and collected from the other to flush the chamber. Then, an appropriate number of purified islets suspended in a gel delivery system can be injected into the chamber aseptically. Finally, the screws are replaced on the ports to prevent contamination of the chamber.

Some short-term success has been seen in rodents with islets of Langerhans implanted into this device. Fig. 4 shows the variation in blood glucose concentration of a rat in which 1500 porcine islets had been implanted. Although the glucose concentration did not reach normal values, the relatively low number of islets implanted precludes normoglycemia. Based on models for insulin release (12) and utilization (4), about twice as many islets would be necessary to produce normoglycemia. In addition, the device implanted in that animal was constructed with the Amicon XM50 membrane, which has lower permeability characteristics than the polymer membrane developed by this laboratory. Devices with the improved membrane will be implanted later for glucose control tests.



* indicates significant difference from glucose level before islet implantation ($p<0.05$)

Fig. 4. Glucose concentrations of rat with implanted organoid.

FUTURE ISSUES IN THE DEVELOPMENT OF THIS BIOARTIFICIAL PANCREAS DEVICE

Our organoid device has been shown to provide some glucose control in rodents. Its unique matrix undergoes vascularization with little immune or inflammatory response; as a result, the device is essentially incorporated into the body. A polymer membrane, also developed by this laboratory, shows the desired permeability characteristics for an immunoisolation system. Still, issues common to most bioartificial devices include cell viability within the implantation chamber, quantification of immune response near and within the device, and long-term organoid integrity. All those issues are currently being evaluated for this device. Two issues of particular relation to this organoid include scale-up to larger mammals and humans and transport of insulin into capillaries in the matrix.

Capillary insulin transport

The rate of insulin release by isolated islets of Langerhans at various glucose concentrations has been well-characterized (1,17). In healthy humans, the insulin diffuses to capillaries within and around the islets in the pancreas; it is then transported throughout the body to virtually all cells. Hormonal receptors on the cell surface bind with the insulin to initiate its action. Many researchers have suggested that a similar receptor-mediated process governs the transport of the insulin across

the capillary walls, since the observed rate of transport seems to be greater than that expected purely based on diffusion through the narrow pores of capillaries (3,7). However, the bioartificial pancreas device presents a novel question regarding the receptor-mediated transport of insulin across the capillaries in the body. Everywhere except in the pancreas itself, insulin is expected to move from the lumen of the capillary to the interstitial space. In the vascularized region of this device, however, insulin must move in the opposite direction. Previous studies have suggested that receptor-mediated insulin transport occurs in only one direction across the capillary (8). But then, can the blood vessels which infiltrate the device area "learn" to transport insulin in the opposite direction?

Of course, the rate of insulin uptake by the capillaries is crucial to device design. If receptor-mediated transcytosis of the insulin does not occur in the young capillaries of the matrix region, greater amounts of insulin must be produced for an adequate amount to enter the capillary by diffusion. In that case, more islets and a larger chamber may be necessary. Experiments to quantify the rate of insulin uptake from the neovascularized matrix region are underway.

Human scale-up

Many design questions must be answered in the scaleup of a bioartificial pancreas from rodents to humans. An adequate number of islets to produce normoglycemia can be determined based on glucose tolerance test data. The number of islets and their oxygen requirements define the needed volume of the islet chamber. Currently, a flattened cylinder is used for the rat device; alternative geometries may be explored for the scaled-up model. Also, lighter and more flexible plastic may be used for the implant, rather than stainless steel. Of course, exposed ports for islet loading would not be ideal in a human device. Instead, the islets could be loaded through a catheter or during a simple outpatient surgery after the device had been implanted long enough for vascularization to occur.

Although limited success has been shown in controlling the diabetic state of rodents with this bioartificial pancreas device, vital issues remain. The problems of biocompatibility, adequate mass transport to support cell viability, and scale-up from small animal to human size are common to almost all bioartificial devices. The same principles described here as part of a pancreas device to cure diabetes could be used in many other applications as well, including artificial livers for sufferers of cirrhosis or liver disease, implantation of genetically engineered cells to produce a missing or deficient protein, or delivery of a therapeutic agent.

ACKNOWLEDGMENTS

This work was supported by the Juvenile Diabetes Foundation, the American Diabetes Association, SenMed Medical Ventures (Cincinnati, Ohio) and the University of Toledo Honors Program.

REFERENCES

1. Ader, M; Bergman, R.N., Am. J. Physiol., 266 (Endocrinol. Metab. 29):E17-E25. 1994.
2. Archer, J.; Kaye, R; Mutter, G., J. of Surgical Research, 28:77-85. 1980.
3. Bar, R.S.; Boes, M.; Sandra, A., J. Clin. Invest., 81:1225-1233. 1988.
4. Berger, M.; Rodbard, D, Diabetes Care, 12:725-736. 1989.
5. Dionne, KE, Insulin Dependent Diabetes, Recent Developments in Prediction, Prevention, and Treatment conference, 1994.
6. Fournier, R.L.; Sarver, J.G., et al., American Chemical Society Annual meeting, 1995.
7. Hachiya, H.L.; Halban, P.A.; King, G.L., Am. J. Physiol. 255 (Cell Physiol. 24):C459-C464. 1988.
8. King, G.L.; Johnson, S.M., Science, 227:1583-1586. 1985.
9. Lacy, P.E.; Davie J.M. Ann. Rev. Immunol., 2:183-198. 1984.
10. Lanza, R.P.; Beyer, A.M., et al., Transplantation, 56:1067-72. 1993.
11. Monaco, A.P.; Maki, T.; Ozato, H., et al. Ann. Surg., 9:339-362. 1991.
12. Nomura, N; Schihiri, M; Kawamori, R, et al., Comput. Biomed. Res., 17:570-579. 1984.
13. Petruzzo, D.; Pibiri, L.; de Giudici, M.A.; et al. Transplant. Int., 4:200-204. 1991.
14. Ricordi, C; Socci, C; Davilla, A; et al., Transplant. Proc., 22:784-785. 1990a.
15. Sarver, J.G; Fournier, R.L.; Goldblatt, P.J.; et al., Cell Transplant., 4:201-217. 1995.
16. Sharp, D.W.; Lacy, P.E.; Santiago, J.V.; et al. Diabetes, 39:515-518. 1990.
17. Yang, Y.J.; Hope, I.D.; Ader, M, J. Clin. Invest., 84:1620-1628. 1989.

Characterization and Isolation of Lectins from the Marine Bryozoan Bugula neritina

Fassil Mesfin and Yvonne M. Gonzalez

Department of Biological Sciences
SUNY College at Old Westbury
Old Westbury, NY. 11568

Faculty Advisor:

Rita Colon-Urban

Lectins or carbohydrate binding proteins have been implicated in the recognition systems of invertebrate organisms. This project has been involved in the purification and characterization of these macromolecules in the marine bryozoan, Bugula neritina. Hemagglutination and hemagglutination inhibition assays using rabbit erythrocytes and a series of simple sugars, complex carbohydrates and glycoproteins have been used to detect their activity. This investigation reports a new lectin designated BnA-III. Mannose and glucose were potent inhibitors while complex carbohydrates and glycoproteins had either no or weak inhibitory effects on this lectin. BnA-III was purified by ammonium sulfate precipitation followed by molecular sieve chromatography(G-75). The lectin obtained was stable between pH 6.0-7.0 and appeared to require Ca^{++}. Studies using SDS-PAGE gel electrophoresis showed that the active fraction exhibited a band with a molecular weight of 50Kd.

BACKGROUND

Two different lectins from Bugula neritina have been previously purified with distinct sugar specificities and seasonal expression (Colon-Urban and Oppenheim, 1990). Lectins are very common in plants and have been identified in several invertebrate phyla including sponges, molluscs and arthropods (Lis and Sharon, 1986). While these lectins are intrinsically interesting, their functions are unknown. This paper focuses on the purification and identification of an additional lectin termed BnA-III which was also purified from Bugula neritina utilizing its carbohydrate specificity and seasonal occurrence.

PROCEDURES

Crude extracts were prepared following the procedure described by Colon-Urban and Oppenheim (1990). Hemagglutination tube assays and hemagglutination inhibition assays were performed as described by Oppenheim et al. (1983). All assays were done utilizing rabbit erythrocytes purchased from Lampire, Pennsylvania. Values indicating the degree of agglutination of the test RBCs are based on the following standards: - = no agglutination; 1+ = many small clumps; 2+ = many large clumps; 3+ = few large clumps; 4+ = one single clump. Bryozoans were purchased from Cal Bio Marine Technologies, Inc., California.

Two different approaches were used in the purification of BnA-III. An affinity chromatography column (Thyroglobulin-Sepharose) was prepared, based on the hemagglutination inhibition assay, followed by SDS-PAGE electrophoresis (Colon-Urban and Oppenheim 1990). This method was used when thyroglobulin and N-acetyl glucosamine were the inhibitors. However, during late Spring collections, other potent inhibitors including glucose and mannose were found in the same crude extract. These crude extracts were precipitated with ammonium sulfate and fractions that showed biological activity were pooled, concentrated and added to a molecular Sephadex chromatography column (G-75). Blue dextran was utilized as a marker. All fractions obtained were monitored for biological activity, SDS-PAGE was performed on the active fractions and gels were stained with Coomassie blue. Known molecular weight markers were electrophoresed and used for calculating molecular mass. Proteins were determined using the Bio-Rad protein assay (Bradford, 1976).

RESULTS AND DISCUSSION

The hemagglutination and hemagglutination inhibition assays performed on crude lectins from Bugula neritina showed carbohydrate specificity to glucose, mannose and thyroglobulin as summarized in Table 1. Attempts were made to purify the lectin based on thyroglobulin specificity. When using affinity chromatography, considerable activity was lost so alternative methods were utilized. These results have been summarized in Table 2. Successful recovery was obtained when crude bryozoan extracts were precipitated with twenty percent (20%) ammonium sulfate followed by molecular sieve chromatography. Lesser activity was also recovered at forty and fifty percent while none was obtained at sixty percent (60%). The active fractions were then pooled and subjected to Sephadex G-75 column chromatography. Fractions obtained from the Sephadex column were monitored for activity using the bioassay already described and the active fractions were pooled and concentrated. The specific activity was calculated by dividing the total protein obtained as measured by the Bio Rad method (Bradford, 1976). This fraction showed a major band with a molecular weight of 50 Kd (Davis 1964). These invertebrates express seasonal variability in their ability to express hemagglutination activity as well as inhibitory activity of sugars and it can be concluded that the activity exhibited is apparent only on a small fraction of lectin it possesses. This is the third lectin isolated from this species of bryozoan. Future studies will attempt to elucidate the relatedness of this lectin to other bryozoan and invertebrate lectins in general by protein sequencing. Finally the laboratory will try to determine the function of these important glycoproteins in the organisms.

TABLE 1. Inhibitory activity of various carbohydrates and glycoproteins on the agglutination of rabbit erythrocytes by the crude bryozoan lectin, BnA-III.

INHIBITORS	CONCENTRATION	INHIBITORY ACTIVITY
CARBOHYDRATES		
Glucose	0.20M	I
Galactose	0.20M	NI
Mannose	0.20M	I
N-Acetylglucosamine	0.20M	NI
N-Acetylgalactosamine	0.20M	NI
GLYCOPROTEINS		
Thyroglobulin	0.1mg/ml	I

I = inhibitory activity expressed as the concentration of inhibiting four doses of lectin.
NI = No inhibition at the maximum concentration of inhibitor used in the assay which was 0.20M for carbohydrates and 0.10mg/ml for glycoproteins.
*** Assays performed a minimal of three times.

TABLE 2. Purification of BnA-III,(Mannose, Glucose, and Thyroglobulin specificity)

STEPS	HEMAGGLUTINATION TITER	TOTAL VOLUME OF PROTEIN (ml)	CONCENTRATION OF PROTEIN (mg/ml)	SPECIFIC ACTIVITY
Supernatant from starting extract	1:64	480	0.164	390
Precipitated with ammonium sulfate				
20%	1:512			
40%	1:128			
50%	1:32			
60%	No activity			
Active fractions pooled and subjected to G-75	1:64	2	0.013	4923

SPECIFIC ACTIVITY = hemagglutination titer divided by protein concentration (mg/ml)

ACKNOWLEDGEMENTS

This work was supported by NIH-MBRS 08183.

REFERENCES

Colon-Urban,R. and Joel D. Oppenheim (1990) Seasonally Occurring Lectins from the Bryozoan Bugula neritina. J. Exp. Zool. 254:238-243

Bradford M. M. A Rapid and Sensitive Method for the Quantitation of Microgram Quantities of Protein utilizing the Principle of Protein Dye Binding. Anal.Biochem., 72, 248 (1976).

Davis, B.J., Disc electrophoresis-II. Method and application to human serum proteins. Ann. N.Y. Acad. Sci., 121, 404-427 (1964).

Lis, H., and N. Sharon (1986) Lectins as molecules and as tools. Ann. Rev. Biochem., 55:35-67. Oppenheim, J.D., M.S. Nachbar, M.R.J. Salton, and F. Aull (1974) Purification of a hemagglutinin from Limulus polyphemus by affinity chromatography. Biochem. Biophys. Res. comm., 58:1127-1134

Oppenheim, J.D., M.S.Nachbar, and M. Blank (1983) The distribution of and biochemical serological relationships between I/i and ABH blood group antigens of the human erythrocyte membrane as determined by immunoelectrophoretic techniques. Electrophoresis, 4:53-62.

Effect of nutrients on glutathione catabolic enzymes in *Candida albicans* during dimorphism

Munyaradzi Imbayagwo[1] Suresh Gunasekaran[1] and Louise McDonald[2]

[1]Department of Biology, Fisk University, Nashville, TN 37208 and
[2]Department of Medicine, Wayne State University, Detroit, MI 48201

Advisors

Muthukumaran Gunasekaran
Department of Biology,
Fisk University, Nashville, TN 37208

Elias Manavathu
Department of Medicine,
Wayne State University, Detroit, MI 48201

ABSTRACT

Candida albicans, an opportunistic human pathogen, exhibits nutrient dependent dimorphism, which has been implicated in its pathogenic potential. Furthermore, previous study has shown that low glutathione levels have corresponded to yeast to mycelial transition. In order to further investigate this phenomenon, the influence of different carbon and nitrogen sources on the activities of glutathione metabolic enzymes has been studied. Glucose and sucrose were used as the carbon sources and ammonia, glutamate and L-citrulline served as the nitrogen sources. Yeast and mycelial cells were used for identifying the changes in the activity levels of glutathione reductase (GSSGR), glutathione transferase (GST), glutathione peroxidase (GPX) and γ-glutamyl transpeptidase (GGT). In general, the enzyme activities from the cells grown in sucrose media were lower than in glucose media regardless of the enzyme tested, morphology of the organism, or the growth interval. In all of the enzymes except GST, activity was higher in the yeast than in the mycelia, regardless of the type of nitrogen source, with lower activity from 24 to 72 hours than at 96 hours. In citrulline media, the yeast form showed the maximum GST, GGT, and GPX activity. In ammonia amended media, the mycelial form showed the maximum activity in GGT, whereas in glutamate media, the mycelia showed the maximum activity in GST. The results also showed that the type of nitrogen source had no effect on GPX activity in the mycelial form. Finally, changing the nitrogen source showed no significant effect on GSSGR activity, either in the yeast or mycelial form.

INTRODUCTION

Candida albicans is an opportunistic fungal pathogen which shows pH, temperature and nutrient dependent dimorphism (Vanden Bossche et al., 1992). The ability to change from yeast to mycelial form in response to harsh environmental conditions has been implicated in the infective potential of the organism (Datta, Ganesan, and Natarajan , 1989). Earlier studies have shown how different amino acids can affect the growth and morphogenesis of *C.albicans* (Nishioka, and Silva-Hunter, 1974). Moreover, it has been shown that glutamic acid favored yeast- like growth when serving as the sole nitrogen source, while it favored mycelial growth when used as the sole carbon source (Dabrowa et al., 1974).

A recent study has demonstrated glutathione involvement in alternative morphology in *C.albicans* (Thomas et al., 1991). Glutathione is a biologically active tripeptide involved in several cellular functions ranging from oxidation to protein thiolation (Penninckx, and Elskens, 1993). The intracellular level of glutathione at any given time is a function of the activities of the glutathione metabolic enzymes (Figure 1).

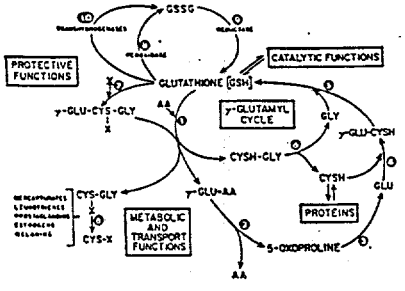


Figure 1. Outline of the metabolism and function of glutathione. Enzymes: 1) γ-glutamyl transpeptidase; 2) γ-glutamyl cyclotransferase; 3) 5-oxoprolinase; 4) γ-glutamylcysteine synthetase; 5) glutathione synthetase; 6) dipeptidase; 7) glutathione S-transferase; 8) glutathione peroxidase; 9) glutathione reductase; 10) transhydrogenases. AA = amino acids; X = compounds that react with glutathione to form conjugates, such as those that lead to formation of mercapturic acids, leukotrienes and other compounds. GSH, glutathione; GSSG, glutathione disulfide.

Glutathione metabolism via γ -glutamyl cycle (Meister, 1984)

Although pH, temperature and nutrient sources are known to influence dimorphic transition in *C.albicans*, a correlative study with regard to nutrient induced dimorphism and consequent changes in glutathione metabolism is lacking. Hence, the effect of using glucose and sucrose as carbon sources and glutamate, ammonia and L-citrulline as nitrogen sources on the activities of glutathione catabolic enzymes during dimorphism in *C.albicans* was studied.

MATERIALS AND METHODS

Culture conditions:

C. albicans, strain 3153A, a thermally inducible dimorphic form, was used in this study. The organism was grown under different cultural conditions to obtain different morphological forms. In the medium, glucose and sucrose, in equimolar concentrations, were individually used as carbon sources while equimolar concentrations of ammonia, glutamate and L-citrulline were separately used as nitrogen sources. Yeast cells were grown under acidic synthetic medium, pH 4.5 and in basal synthetic medium, pH 6.5, at 25° C. Samples were harvested at 24 hour intervals until 96 hours under these conditions. Mycelial cells were grown at 37° C under same conditions as yeast cells and cells were harvested from 24 to 96 hours. The different morphologies were confirmed microscopically.

Enzyme extracts

The crude enzyme source was prepared from the harvested cells by initially flushing with nitrogen and grinding in a mortar with pestle into powder form. This procedure was repeated three times and the cell free homogenates were suspended in extraction buffer (0.1 M phosphate buffer, pH 7.0 with 1 mM PMSF and 2 mM EDTA) in a ratio of 2 ml of buffer per gram of cells. The homogenate was centrifuged at 20,000 X g at 4° C for 15 min and the supernatant was used as the enzyme source for enzyme assays.

Enzyme Assays

Glutathione reductase : Glutathione reductase [GSSGR] was assayed spectrophotometrically (Carlberg, and Mannervik, 1985) at 30°C in a reaction mixture containing 0.5 ml of 0.2 M sodium phosphate buffer (pH 7.0) with 2 mM EDTA, 0.05 ml of 2 mM NADPH (prepared in 10 mM Tris-HCl, pH 7.0), 0.05 ml of 20 mM GSSG and 0.4 ml of crude enzyme in a 1 ml thermo-cuvette and the decrease in absorbance at 340 nm corresponding to NADP formation for 5 min. was monitored. The rate of reductase-independent oxidation of NADPH was measured by monitoring the change in absorbance at 340 nm in the absence of cell lysate.

Glutathione S-transferase : Glutathione S-transferase [GST] was assayed (Mannervik, and Guthenberg, 1985) by following glutathione conjugation with 1-chloro-2,4-dinitrobenzene (CDNB) at 30°C. In a 1 ml thermo-cuvette, 0.9 ml of the diluted cell lysate in 0.1 M sodium phosphate buffer, pH 6.5, containing 1 mM EDTA, 0.05 ml of 20 mM reduced glutathione and 0.05 ml of 20 mM CDNB (ethanol solution) were thoroughly mixed and the increase in absorbance at 340 nm was monitored for 10 min at 30°C.

γ-Glutamyl transpeptidase : γ-Glutamyl transpeptidase [GGT] was assayed spectrophotometrically using L-γ-glutamyl-p-nitroanilide as donor and glycylglycine as acceptor substrates. The p-nitroanilide produced was determined from the increase in absorbance at 410 nm and 37°C (Meister, Tate, and Gfiffith, 1981). In a 1 ml thermo-cuvette, 0.4 ml of 0.2 M glycylglycine and 0.6 ml of a cell lysate diluted with 0.1 M Tris-HCl buffer, pH 8.0, were thoroughly mixed and the increase in absorbance at 410 nm was monitored for 10 min at 37°C.

Glutathione peroxidase : Glutathione peroxidase [GPX] was assayed by continuously monitoring GSSG formation (Flohe, and Gunzler, 1984) at 37°C in a medium containing excess glutathione reductase which maintains a constant level of GSH derived from the GSSG produced by the peroxidase reaction. The concomitant oxidation of NADPH was measured by monitoring the decrease in absorbance at 340 nm. The following reagents were added to a 1 ml thermo-cuvette: 0.5 ml of 0.1 M potassium phosphate buffer (pH 7.0) containing 1 mM EDTA, 0.1 ml of cell lysate, 0.1 ml of glutathione reductase (924 units) and 0.1 ml of 10 mM GSH. This mixture was preincubated for 10 min at 37°C, then 0.1 ml of 1.5 mM NADPH was added. The hydrogen peroxide-independent NADPH consumption was monitored initially for 3 min. at 340 nm and then the reaction was started by addition of 0.1 ml of 12 mM t-butyl hydroperoxide solution (prewarmed at 37°C). The decrease in absorbance at 340 nm was monitored for an additional 5 min. GPX-independent oxidation of NADPH was measured by replacing the enzyme with buffer as an additional blank.

The protein concentration in the cell free extracts was determined by the coomassie dye binding method (Bradford, 1976). All the experiments were repeated three times and the values represent the mean of triplicates.

RESULTS AND DISCUSSION

Candida albicans has been shown to undergo morphological changes, from yeast to mycelia, in response to changing environmental conditions, such as change in pH, temperature, or alteration of nutrients (2). The influence of different carbon and nitrogen sources on the specific activities of four different glutathione metabolic enzymes (GSSGR, GST, GGT, and GPX) in yeast and mycelial forms of *C. albicans* were studied. The data are presented in figures 2 and 3.

In general, the enzyme activities from the cells grown in sucrose media were lower than in glucose media regardless of the enzyme tested, morphology of the organism, or the growth interval (Fig.2A-D). However, the cells in yeast form grown in sucrose media, showed higher GGT activity in all growth periods compared to either yeast or mycelial cells grown in glucose media (Fig. 2C).

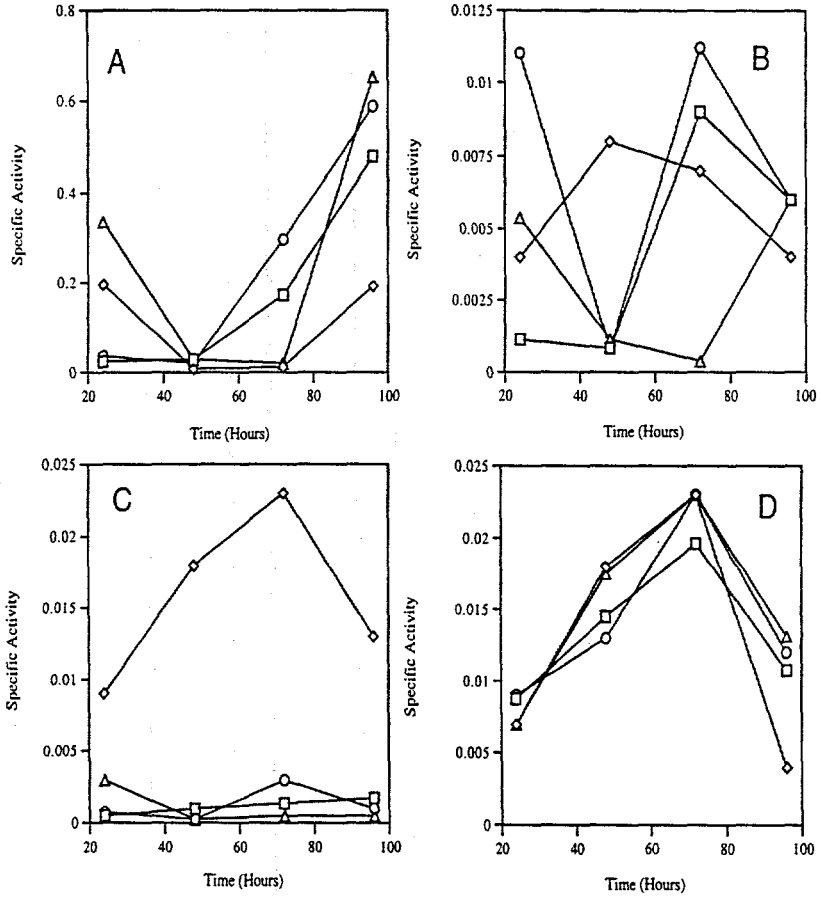


Figure 2. Effect of carbon sources on the activities of glutathione metabolic enzymes in *Candida albicans*. The activities of GSSGR (Fig. A), GST (Fig. B), GGT (Fig. C), and GPX (Fig. D) in yeast cells (Δ) and mycelial cells (○) with glucose as the carbon source and in yeast cells ( ) and mycelial cells(❑) with sucrose as the carbon source are shown.

In all enzymes, activity was higher in the yeast than in the mycelia, regardless of the type of nitrogen source (Fig. 3A-D). Moreover, the activity of all four enzymes was lower from 24 to 72 hours than at 96 hours. However, the transferase activity was higher in the mycelial phase at all growth periods (Fig. 3B).

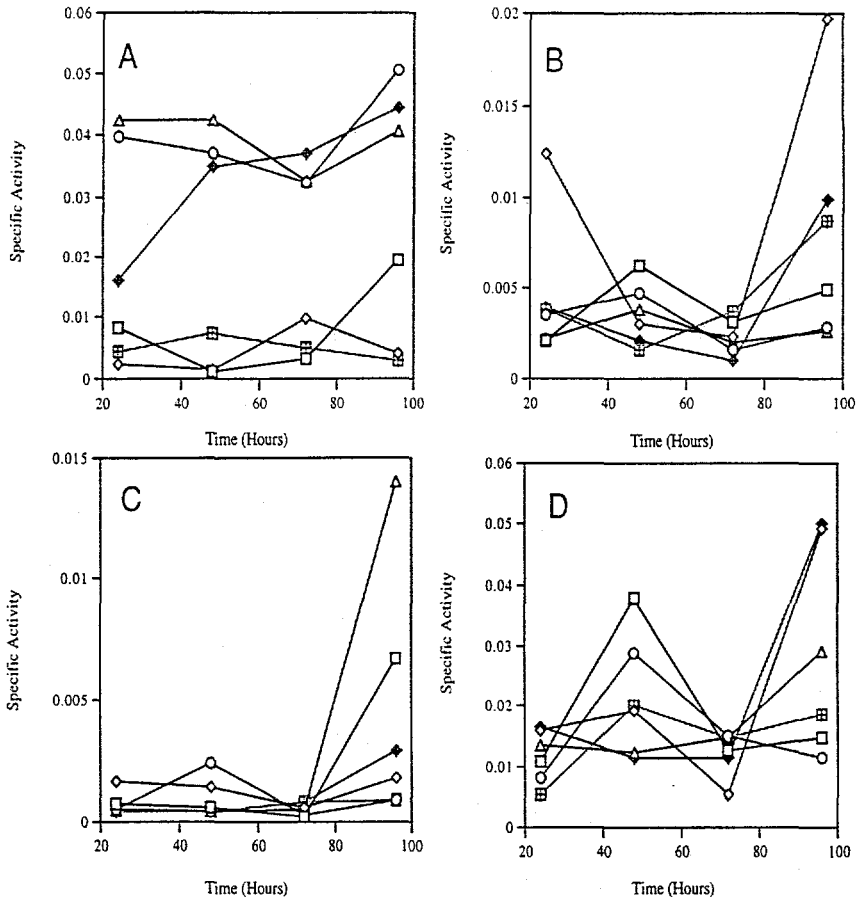


Figure 3. Effect of nitrogen sources on the activities of glutathione metabolic enzymes in *Candida albicans*. The activities of GSSGR (Fig. A), GST (Fig. B), GGT (Fig. C), and GPX (Fig. D) are shown with the three nitrogen sources in the different morphological phases: yeast ( ) and mycelial ( ) cells from ammonia amended media, yeast ( ) and mycelial ( ) cells from citrulline amended media and yeast ( ) and mycelial ( ) cells from glutamate amended media.

In citrulline media, the yeast form showed the maximum GST, GGT, and GPX activity. In ammonia amended media, the mycelial form showed the maximum activity in GGT, whereas in glutamate media, the mycelia showed the maximum activity in GST (Fig. 3C). The results also showed that the type of nitrogen source had no effect on GPX activity in the mycelial form (Fig. 3D). Finally, changing the nitrogen source showed no effect on GSSGR activity, either in the yeast or mycelial form (Fig. 3B). In conclusion, altering the carbon and nitrogen sources affects the glutathione metabolic enzymes; however, in order to directly substantiate the effect, the level of glutathione in yeast and mycelia, in relation to changes in carbon and nitrogen sources must be investigated further.

ACKNOWLEDGEMENTS

This study is supported in part by National Science Foundation grant HRD 92-53037, Kellogg Foundation Grant P0010125, by Howard Hughes Medical Institute grant 71194-527802 and by Department of Education grant P-120A30013.

REFERENCES

Bradford, M.M., A rapid and sensitive method for the quantitation of microgram quantities of protein utilizing the principle of protein-dye binding. Analytical Biochemistry Vol. 72, 1976. pg. 248-254.

Carlberg, I., and Mannervik, B., Glutathione reductase. In S.P. Colowick and N.O. Kaplan (ed) Methods in Enzymology. Vol.113, 1985. pg. 484-485.

Datta, A., Ganesan, K and Natarajan K., Current trends in *Candida albicans* Research. Advances in Microbiol Physiology Vol. 30, 1989. pg. 53-88.

Dabrowa, N., Howard, D.H., Landau, J.W. and Shechter, Y., Synthesis of nucleic acid and protein in the dimorphic form of *Candida albicans*. Sabouraudia Vol. 8 , 1970. pg. 163-169

Flohe, L. and Gunzler, W.A., Assays of glutathione peroxidase. In S.P. Colowick and N.O. Koplan (ed) Methods in Enzymology. Vol.105, 1984. pg. 114-121.

Mannervik, B. and Guthenberg, G., Glutathione transferases from human liver. In S.P. Colowick and N.O. Kaplan (ed) Methods in Enzymology. Vol.113, 1985. pg. 499-501.

Meister, A., New Aspects of glutathione biochemistry and transport - Selective alteration of glutathione metaboilsm. Nutrition Reviews. Vol. 45, 1976. pg. 559-604.

Meister, A., Tate, S.S. and Griffith, O.W., Gamma-glutamyl transpeptidase. In S.P. Colowick and N.O. Kaplan (ed) Methods in Enzymology. Vol.77, 1981. pg. 237-244.

Nishioka, Y. and Silva-Hunter, M., Dimorphism, sensitivity to nystatin and acriflavin uptake in a strain of *Candida albicans* grown with glutamate as sole nitrogen and carbon source. Sabouraudia Vol. 12, 1974. pg. 295-301

Penninckx, M.J., and Elskens, M.T. , Metabolism and functions of glutathione in microorganisms. Advances in Microbial Physiology Vol. 34, 1993. pg. 239-304.

Thomas, D., Klein, K., Manavathu, E., Dimmock, J.R. and Mutus, B., Glutathione levels during thermal induction of the yeast to mycelial transition in *Candida albicans*. Federation of European Microbiology Society Microbiology Letters Vol. 77, 1991. pg. 331-334.

Vanden Bossche, H., Kobayashi, G.S., Edman, J.C., Keath, E.J., Maresca, B and Soll, D.R., Molecular determinants of fungal dimorphism. Journal of Medical and Veterinary Mycology Vol. 30, 1992. pg. 73-76

EXAMINATION OF SOMATIC POLYPLOIDY IN NONSECRETORY CELLS OF *Idothea wosnesenskii*

Katie M. Headley

Department of Biology
Seattle University
Broadway and Madison
Seattle, Wa 98122

Faculty Advisor:
Daniel B. Matlock PhD

INTRODUCTION

Somatic polyploidy is a phenomenon in which a somatic cell possesses more than two complete chromosome sets. This phenomenon has been found in both the plant and animal kingdoms, in vertebrates and invertebrates. It is most commonly found in tissues that show high synthetic activity or multifunctionality. Therefore, a common explanation for this phenomenon has regarded polyploidy as the result of an increased DNA template that allows increased transcription of a specific gene subset. Although this conclusion regarding the immediate function of polyploidy in secretory cells is generally accepted, generalizations as to the evolutionary, adaptive, and developmental significance of somatic polyploidy have yet to be made. Furthermore, the function of somatic polyploidy in cells and tissues that do not secrete a relatively large amount of protein is not fully understood.

The purpose of this experiment was to examine the genome of nonsecretory somatic polyploid cells in the hindgut tissue of the isopod *Idothea wosnesenskii* relative to diploid muscle tissue from the same species to determine if the polyploidy is due to amplification of the total diploid genome, euploidy, or selective amplification of a specific subset of genes. This was accomplished using restriction enzyme digests analyzed by gel electrophoresis.In the case of euploidy one would expect to see identical digestion patterns between the muscle (diploid) and hindgut (ployploid) digests. These patterns would most likely appear as continuous smears down the electrophoresis lanes. In the case of selective amplification one would expect to see the same continuous smear for the muscle (diploid) digests. However, bands would appear in the hindgut (polyploid) digest lanes. These bands would not be apparent in the muscle digests and would represent fragments of the genome that have been selectively amplified to yield the polyploidy in the hindgut tissue.

The polyploid hindgut cells under study are extremely large in comparison with the normal diploid cells in the organism. In addition, the DNA content of the polyploid nucleii in adults was determined to be 32-256C, where 2C is the amount of DNA in the diploid genome.(1)

METHODS AND MATERIALS

Adult *Idothea wosnesenskii* were collected on Whidbey Island and kept alive until dissection in a ten-gallon salt water tank.

Dissection was done on live specimens in seawater so as not to damage the tissues. The hindgut was then removed and sliced longitudinally and carefully washed out with sterile seawater to remove all seaweed and other substances from the gut.

A very gentle DNA extraction procedure was used on the hindguts. Four hindguts, or four side sections containing muscle tissue, were combined with 50uL of 1M NaCL, 50uL of 1M Tris pH 8.5, 50uL of 10% SDS, 50uL of 0.5M EDTA pH 7.4, 5uL of B-mercaptoethanol, 5uL of 10mg/ml proteinase K, and 290uL of distilled water. This was incubated with shaking overnight at 55°C until the tissue disaggregated. The DNA was then extracted three times using a phenol, chloroform, isoamyl alcohol mixture of proportions 49:49:1 respectively. Therefore, 245uL phenol, 245uL chloroform, and 5uL isoamyl alcohol were used. The top aqueous layer containing the DNA was carefully removed with a wide mouth pipet so as not to shear the DNA.

The DNA was precipitated using 1mL of isopropanol for each 0.5 mL of aqueous solution extracted. The solution was centrifuged and the isopropanol poured off. The DNA was washed with 70% ethanol and stored in TE at 4°C. The DNA concentration was determined using a UV spectrophotometer 260-280nm scan. The Beer-Lambert relationship was used

to determine the DNA concentration.

$$\log_{10}(I/Io)=-edc \qquad (1)$$

Where $\log_{10}(I/Io)$ is the absorbance at 280nm, e is the extinction coefficient (25ml/cm mg), d is the cell thickness (1cm), and c is the concentration in mg/ml.

About 10ug of tissue were digested using restriction enzymes Pst I, EcoR I, and BamH I. Double digests were done as well as single digests. Digests were incubated at 37 C for 2 hours, heated at 65 C for 10 min, then plunged in an ice bath to prevent sticky ends from reannealing.

The digested samples were run on a 0.8% agarose gel. The DNA was visualized using ethidium bromide. Polaroid pictures were taken of the resulting gels.

A computer program was used to determine, roughly, what percent of the genome the bands in each column represented. The program consisted of outlining the entire column which represented 100%. Using complete black and white as standards the program determined what percent of the total DNA in the column that the band represented based on its relative intensity.

RESULTS

The following figures are examples of the results obtained from the gels. Unfortunately the bands in the gels are fairly subtle and did not resolve well in these photo-copies of the polaroids.



Figure 1.



Figure 2.



Figure 3.

Figure 1 shows double digests of the tissues. M denotes muscle tissue. G denotes gut tissue. Columns 1 and 2 are Pst I/EcoR I digests. Columns 3 and 4 are Pst I/BamH I digests. Columns 5 and 6 are EcoR I/BamH I digests. Although it is not immediately obvious, each pair of muscle and gut digests matched very well. That is,the one band apparent in the digests matched between the muscle and gut columns. Please note that there appear to be additional bands in some of the columns. These are not present in the original polaroids and are probably a result of copying. All single and double digests turned out very similar to this. Either no bands were apparent in the continuous smears or one band between 2000 and 4000 bp was apparent and matched between the muscle and gut digests.

From previous electron microscope work done by Dr. Daniel Matlock, unpublished, it was known that the anterior portion of the gut was more highly polyploid than the posterior portion. Therefore, to make sure that the posterior gut was not masking amplification in the anterior gut,the anterior third of the gut and the posterior third were digested separately, discarding the middle third. These digests were analyzed and examples of the results are shown in figures 2 and 3. Figure 2 depicts double digests with Pst I/EcoR I in lanes 1-3 and Pst I/BamH I in lanes 4-6. P represents posterior digest and A, anterior digest. It is apparent that the bands present in the anterior and posterior digests match very well to each other. In addition, they also

match to the same digests done on the entire gut tissue which can be seen by comparing figure 2 to figure 1. However, the bands apparent in the muscle digests in figure 1 do not appear in figure 2. Figure 3 depicts digests in which the bands apparent in the muscle digests of figure 1 do appear in relation to the anterior and posterior digests. Lanes 1-3 in figure 3 are EcoR I digests and lanes 3-6 are EcorI/ BamH I digests.

The data obtained from the computer analysis are rough, at best. However, the results obtained are as follows.

TABLE 1
CONTENT OF DIGEST BANDS RELATIVE TO ENTIRE GENOME

Tissue Type	Mean Percent	Standard Deviation	# of Lanes Tested
muscle	6.09	±1.64%	14
gut	5.70	±1.88%	7
posterior	5.55	±2.38%	6
anterior	5.08	±0.472%	5
1st band of MW ladder(control)	14.58	±4.26%	7

DISCUSSION

The digests of the muscle, gut, anterior, and posterior samples revealed continuous smears. The bands that were apparent in these smears were present in and matched between muscle and gut digests, indicating that selective amplification is probably not the source of polyploidy in the hindgut cells. If this were the case, bands present in the gut digests would have been absent in the muscle digests. Thus, the results suggest that replication of the entire diploid genome, euploidy, is most likely responsible for the polyploid condition of the cells in the hindgut tissue.

A proposed mechanism by which euploidy is achieved in cells is endomitosis. In this process the cell prepares for mitosis by doubling cytological contents and chromosomes. However, the nucleolus is not destroyed and spindles are not formed. In other words, mitosis is aborted. This mechanism for euploidy would explain the relative gigantism of the polyploid cells in the hindgut to normal diploid cells. It would also explain why cell volume sometimes seems to correlate to degree of polyploidization because the cell progresses through all the events of the mitotic growth cycle except for division.

The computer analysis is very rough because the polaroids of the gels had to be used instead of the actual gels. The gels were not bright enough to analyze directly.This introduces a problem if the relationship between the brightness of the gel and the brightness of the polaroid is not linear. In addition, only polaroids of gels with discernible bands were used and the boundaries of these bands, since they are faint, were very hard to designate.

Despite this, the results from the computer analysis are surprisingly consistent. The relative percentage of the muscle bands is very similar to the relative percentage of the gut bands. Furthermore, the relative percentages of the anterior, posterior, and gut bands are very similar. These data support the original conclusion that the polyploidy in these cells is due to amplification of the entire diploid genome and not a specific gene subset. In addition, the bands represent a small fraction of the genome, about 5-6%, indicating that they may represent genes that are moderately amplified.

By inspection of figures 1-3 it is obvious that the bands present are very faint in comparison to the background fragments in the rest of the electrophoresis column. This suggests that the bands are a result of moderate selective amplification. In many diploid genomes, genes coding for ribosomal and/or transfer RNA are moderately amplified. Thus the faint bands present in all of the digests may represent moderately amplified genes coding for ribosomal and/ or tranfer RNA proteins. This could be confirmed or disproved by analyzing the gels with probes specific for these genes.

What function then, does polyploidy serve in these cells? No conclusions can be made from these data alone. However, in a study by Matlock in 1981 on the same species it was shown that the degree of polyploidy increased as the isopod matured from an emerger to an adult.(1) Polyploidy, therefore may offer some advantages in the growth of this organ. In other words, the organ may grow by the mechanism of endomitosis, discussed earlier, instead of normal mitosis.

It has also been suggested, based on radiation and mutagen experiments, that the polyploid cell, due to its genetic redundancy, is much more resistant to genetic damage and aberrant mitosis than the diploid cell.(3) If this organ is exposed to genetic damaging agents due to its function or is deficient in protective factors, then polyploidy may serve as an evolutionary adaption to preserve cell life and function.

There are many avenues of exploration left in this area. Further interests and options specific to this experiment may be to analyze the hindgut and muscle tissues using a larger variety of restriction enzymes. In addition, a closely related species, Ligia pallasii lives in the area. These could be collected and analyzed in the same way to see if similar results are obtained. Generalizations between species regarding polyploidy have not always been able to be made. It would be interesting to see how these two species compare.

Somatic ploypoidy continues to be an area in which definite generalizations regarding its evolutionary and developmental significance have yet to be made. Further exploration, especially in nonsecretory tissues, is needed to shed more light on this subject.

ACKNOWLEDGEMENTS

I would like to express my deep gratitude to the Murdock Charitable Trust for their support of this research project. I would also like to thank Dr. Dan Matlock for his help and guidance during this project. In addition, I would like to thank Cheri Peterson who, prior to my research, worked out the procedure used for DNA extraction in this experiment.

REFERENCES

(1)Dornfield&Matlock,Comp Biochem. Physiol. "Somatic Polyploidy in the Marine Isopod Idothea wosnesenskii" Vol.69A 1981, Pergamon Press Ltd. pp771-81

(2)John&Miklos,The Eukaryotic Genome In Development and Evolution,1988, Allen and Unwin Inc.

(3)Nagl&Walter, Endoploidy and Polyteny in Differentiation and Evolution, 1978, North-Holland Publishing Co. pp3-253

(4)Uryvaeva&Brodsky, Genome Multiplication in Growth and Developement, Cell Polyploidy: Its Relation to Tissue Growth and Function, 1985, Cambridge University Press. pp275-326

Genetic Variability Within and Among Local Populations of Dame's Rocket (*Hesperis matronalis*)

Everett Porter

Department of Biology
Gettysburg College
Gettysburg, PA 17325-1484

Faculty Advisor: Dr. Véronique Delesalle

Starch-gel electrophoresis was used to estimate the level of genotypic variability within and among four local populations of Dame's rocket. Of the 16 different enzyme-systems screened, isoenzymatic activity was identified in one system, phosphoglucomutase (PGM), with evidence for possible variability in four others: AAT, IDH, ME, and 6-PGD. Electrophoretic data showed PGM to be a polymorphic enzyme with two alleles: a fast allele (p) and a slow allele (q). The fast allele (p) was more common in population JM1, while a greater frequency of the slow allele (q) was more prevalent in the three other populations: JM2, EM, and RT. X^2-analysis showed significant differences between the observed number of heterozygotes and the number of heterozygotes expected under Hardy-Weinberg conditions in three of the four populations (RT: x^2=7.61, JM2:x^2=11.53, EM: x^2=14.95, where $p \leq 0.05$ and d.f. = 2 for each population, Table 3).

INTRODUCTION

The ability of a species to adapt and evolve in response to environmental change is determined by the level of genetic variability within a species (Hamrick and Godt 1990). A low level of genetic variability within a species limits its potential for adaptive responses to a changing environment, predisposing such species towards extinction (Ridley 1993). In contrast, a high degree of genetic variability within a species can increase its chances of survival in a stressful environment, or increase its response to environmental change (Hamrick and Godt 1990; Mopper and Mitton 1991).

Genetic variability exists at two different levels within a species: variation between individual genotypes *within* a population, and variation in allele frequencies *between* populations (Hamrick and Godt 1990). Genetic variability *between* populations can also indicate the extent to which allele migration is occurring between those populations (Holtsford and Ellstrand 1989). A low degree of genetic differentiation among local populations may indicate that a significant level of inter-population mating is occurring. However, a significant amount of differentiation between such populations suggests that they are reproductively isolated from one another, with little occurrence of migrating alleles.

Hamrick and Godt (1990) have found that the genetic variability of a species is positively correlated with the geographical range of that species. Cosmopolitan species have a greater tendency to exhibit highly variable genotypes than those which are endemic. One explanation for this correlation is that individuals have a higher selective advantage if they have what are called "all-purpose" genotypes (Lynch 1984). Heterozygous, or "all-purpose", genotypes translate into more variable phenotypes, which may increase the survival of an individual under different environmental conditions (Lynch 1984). Such all-purpose genotypes would act as a buffer against environmental stress and change, translating into increased survival under variable climates. This theory is similar to Lerner's (1954) homeostasis hypothesis (Hoffman and Parsons 1992).

Dame's rocket (*Hesperis matronalis*), a short-lived perennial of the Brassicaceae family, is characterized by a cosmopolitan distribution. It is found in many diverse climates and geographical areas. In the United States, populations of Dame's rocket primarily inhabit the eastern coast, between Maine and Georgia. It is also prevalent throughout Europe, and has been identified in locations as remote as Mongolia (Krasnoborov and Rostovtseva 1975). Dame's rocket expresses a polymorphism for flower color, with white- and purple-flowered plants,as well as

a number of intermediate and variegated colors.The widely distributed geographical range of Dame's rocket falls under the same conditions studied by Hamrick and Godt (1990), suggesting that individuals of *Hesperis matronalis* are likely candidates for exhibiting highly variable genotypes.

Starch-gel electrophoresis is a standard method for estimating the level of genotypic variability within and between individuals of a population. For this study, four local populations of Dame's rocket were visited (JM1, JM2, RT, and EM), and transects were laid through the area of highest density within each population. Up to 100 individuals were sampled from each population at 1 meter intervals along each transect.The basic protocols of electrophoretic analysis were taken from Soltis (1983). Following instructions and the blue-print diagrams of Werth (1985), three electrophoresis apparatuses were built. Through electrophoresis, up to 50 individuals from each population of *Hesperis* were screened for isoenzymatic activity in 16 different enzyme systems. The frequency of polymorphic loci within individuals was observed, in an attempt to estimate the level of genetic variability within and among the four local populations of Dame's rocket.

RESULTS

A summary of the preliminary screenings for variable enzyme systems is presented in Table 1. Of the 16 enzymes screened under variable electrode/gel-buffer systems, only five showed evidence for variability: AAT, IDH, ME, PGM, and 6-PGD. Of these, only PGM (phosphoglucomutase) was resolved well enough to yield data on allelic frequencies by population (Table 2).

Table 1
List of Enzymes Screened For Variability

Enzyme tested	Polymorphic	Resolution
ALD (aldosterone)	possible	poor
ADH (alcohol dehydrogenase)	NO	poor
AAT (aspartate aminotransferase)	NO	good
ACON (aconitase)	NO	poor/weak activity
EST (esterase)	possible	good
IDH (isocitrate dehydrogenase)	NO	good
HK (hexokinase)	NO	good
LAP (leucine aminopeptidase)	NO	poor
MDH(malate dehydrogenase)	possible	very good
ME (malic enzyme)	possible	very good
PER (peroxidase)	unknown	very poor
PGI (phosphoglucoisomerase)	NO	very good
PGM (phosphoglucomutase)	YES	very good
6-PGD (6-phosphogluconate dehydrogenase)	NO	good
SkDH (shikimate dehydrogenase)	NO	poor
TPI (triose-phosphate isomerase)	NO	very good

TABLE 2
Allele Frequencies for PGM by Population

Population	Fast allele(p)	Slow allele (q)
JM1	.593	.407
RT	.459	.541
EM	.458	.542
JM2	.490	.510

Electrophoretic evidence showed PGM to be a polymorphic enzyme with two alleles. In the JM1 population, the fast allele (p) was more common than the slow allele (q), with p= .593 and q= .407. However, the other three populations showed a greater frequency of the slow allele (q) than the fast allele (p) (Table 2).

Assuming Hardy-Weinberg conditions and using the observed allele

frequencies within each population, expected values of the genotypic frequencies for the PGM locus were calculated for each population. The observed genotypic frequencies were compared with those expected under Hardy-Weinberg conditions, using x^2-analysis. Observed and expected genotypic frequencies were not statistically different for the JM1 population ($x^2 = 1.76$, $p<0.05$, n.s., Table 3). However, the other populations showed significant differences between the observed number of heterozygotes and the number of heterozygotes expected under Hardy-Weinberg equilibrium (RT: $x^2= 7.61$, JM2: $x^2= 11.53$, EM: $x^2= 14.95$, where $p\leq0.05$ and d.f.= 2 for each population, Table 3).

TABLE 3

Observed allele frequencies and observed-vs.-expected genotypic frequencies of the PGM locus of four populations of *Hesperis matronalis*

Population	#in.	allele freq.	observed genotype	expected
JM1	43	p(.593), q(.407)	AA (.302)=13/43	p^2 (.351)=15.1/43
			Aa (.581) =25/43	2pq (.483)=20.8/43
			aa (.117) =5/43	q^2 (.165)= 7.1/43
		X^2= 1.76, p<0.05, ns df=2		
RT	49	p(.459), q(.542)	AA (.122)= 6/49	p^2(.211)= 10.3/49
			Aa (.673) = 33/49	2pq(.497)= 24.4/49
			aa (.163) = 8/49	q^2(.293)= 14.3/49
		X^2= 7.61, $p\leq0.05$ df=2		
EM	48	p(.458), q(.542)	AA (.063)= 3/49	p^2(.210)= 10.1/48
			Aa (.771)= 37/49	2pq(.496)= 23.8/48
			aa (.166)= 8/48	q^2 (.294)= 14.1/48
		X^2 = 14.95 $p\leq0.05$ df=2		
JM2	50	p(.490), q(.510)	AA (.120) = 6/50	p^2 (.240)= 12/50
			Aa (.740) = 37/50	2pq (.500) = 25/50
			aa (.140) = 7/50	q^2 (.260) = 13/50
		X^2 = 11.53$\leq$ 0.05 df=2		

Errors are possible in scoring the results of the electrophoresis runs when differentiating between heterozygous vs. homozygous genotypes. To ascertain the level of experimental error, a repeat run was performed for 25 of the individuals sampled from the RT population. The observed allelic frequencies for this repetition did not statistically differ from those obtained for the original run (x^2= 0.852, df=1, $p<0.05$, n.s.).

CONCLUSION

Of the 16 enzyme systems screened for variability, only five (AAT, IDH, ME, PGM, and 6-PGD) showed evidence for variability. Of these five enzymes, only one system (PGM) was sufficiently resolved to yield any data on polymorphism for that locus. PGM was determined to be a monomeric enzyme with two alleles, confirming similar findings published for other plants (Gottlieb, 1981).

These results do not provide a conclusive answer to the question of how much genetic diversity exists within and among populations of Dame's rocket. One polymorphic locus, in comparison with the other monomorphic enzymes that were well-resolved (PGI and TPI in Table 1), cannot yield an accurate estimate of the degree of variability within an individual genotype, or of the genetic diversity found at the population level of a species. Multiple polymorphic loci must first be identified and more loci must be resolved before a more conclusive statement about the genetic diversity within and among populations of Dame's rocket can be made.

What is notable is the extent to which Dame's rocket exhibits a predominance of heterozygosity for the PGM locus. X^2-analysis shows that in thee of the four populations sampled, the number of observed heterozygotes significantly exceeded the number expected under Hardy-Weinberg equilibrium

(Table 3). Under Hardy-Weinberg conditions, the maximum frequency of heterozygotes cannot be greater than 50%, when the allele frequencies of p and q are equal for a given population (Lewontin 1974). These three populations: JM2, RT, and EM, show a range of heterozygosity for PGM between 67-77%.

A number of factors may explain this excess of heterozygosity for PGM in these three populations. If Hardy-Weinberg conditions of random mating and no migration are met, then significant evidence for heterosis, or overdominance is present (Lewontin 1974). Overdominance refers to circumstances where individuals with highly heterozygous genotypes have a selective advantage over homozygous genotypes. Heterozygotes at polymorphic loci express a higher mean fitness than individuals which are homozygous for the same loci (Hoffman and Parsons 1992).

The frequency of heterozygous loci of an individual's genotype is often positively associated with the increased fitness of that individual (Hilbisch and Koehn 1985; Mitton and Grant 1984). For example, Mopper and Mitton (1991) show how heterozygosity in two enzymes of the piñon pine is correlated to increased resistance to herbivores. Tress in an area of stress (a region of recent volcanic activity) showed a significantly greater degree of heterozygosity for "enzymes associated with environmental stress" (Mopper and Mitton 1991). Similarly, Lorio and Hodges (1968) found that heterozygosity for the oleoresin locus of the lob-lolly pine translated into increased resistance to herbivore attack under drought conditions. Similar associations of polymorphic, heterozygous genotypes with increased fitness has also been made for invertebrate organisms, as well as for plants (Pogson 1991, Diehl 1986).

However, it is unlikely that heterozygosity for PGM alone is being selected for in these three populations. The phenomenon of overdominance is accepted as being a collective, additive product of all the polymorphic, heterozygous loci of an individual's genotype, which contribute positively to increased viability (Hoffman and Parsons 1992). The observed individuals of *Hesperis* which are heterozygous for PGM are more likely to be heterozygous at other loci. It is the sum total of these heterozygous loci which would collectively confer higher fitness.

Another explanation for the high levels of heterozygosity found at the PGM locus is the migration of alleles between populations (Manwell and Baker 1970). In populations where unequal allele frequencies occur (i.e. less p than q), the migration of the rare allele into a population will result in the production of more heterozygotes than expected under Hardy-Weinberg. Selective, disassortative mating can also increase the frequency of heterozygous genotypes within a population (Manwell and Baker 1970). Because no data on the survival of *Hesperis matronalis* under variable environmental conditions exist, it is impossible to exclude these other factors in favor of overdominance as an explanation for the high levels of observed heterozygosity for the PGM locus. Unfortunately, there are no data available on the degree to which migration is occurring between the four populations of *Hesperis*, nor were data collected by this study on the extent to which selective, disassortative mating does or does not occur within populations of *Hesperis*. Experiments lending insights into the breeding mechanisms occurring within and between populations of *Hesperis matronalis* would indicate the extent to which migration and selective mating may be influencing the level of heterozygosity found among these populations.

This study also shows a certain degree of variability between populations of *Hesperis* for the PGM locus. Allele frequencies differ among the four local populations of Dame's rocket (Table 2). In JM1, the fast allele is more common, where as the slow allele occurs more frequently in the three other populations. This variation between populations is most conspicuous between JM1 and JM2, because the two populations are only 500 meters apart. One explanation for this level of genetic variability is the "founder effect", where a few individuals, which are not representative of their parental population's allelic frequency, form a new, adjacent population (Mayr's Founder Effect; Ridley 1993). Under this condition, if JM1 and JM2 were of recent origin, it is possible that migration of alleles between JM1 and JM2 has not been occurring long enough for migration to equalize the allelic differences between these two populations. Or, if both were well established populations, it could be that no migration of alleles is occurring between JM1 and

JM2, accounting for the difference in PGM allele frequency between the two populations. It is also possible that different selective influences are operating within both populations, causing differentiation in which allele is exhibited with the highest frequency. However, no data is available on the extent to which any of these mechanisms is occurring.

In conclusion, the number of enzymes which have been screened by electrophoresis is insufficient to determine an accurate estimate of the degree of variability both within and among populations of *Hesperis matronalis*. Because of time constraints, only the 16 enzymes have been screened (Table 1), with two positively identified monomorphic enzymes (TPI and PGI) and one variable enzyme (PGM). However, this study did succeed on two important levels. It established protocols for electrophoretic analysis of isoenzymatic activity in *Hesperis*, and it provided preliminary data on increased heterozygosity for the PGM locus in three populations of Dame's rocket.

REFERENCES

Diehl, W.J., et. al., 1986 Physiological and genetic aspects of growth in the mussel *Mytilus edulis*. Physiological Zoology 59: 201-211.

Gottlieb, J.D., 1981 Electrophoretic evidence and plant populations. Progress in Phytochemistry 7: 1-46.

Hamrick, J.L. and M.J. Godt, 1990 Allozyme diversity in plant species, pp. 43-46. In:Plant Population Genetics, Breeding, and Genetic Resources, ed. by Anthony H.D. Brown, et. al. Sinauer Assoc. Inc., Sunderland.

Hilbisch, T.J. and R.K. Koehn, 1985 Dominance in physiological phenotypes and fitness at an enzyme locus. Science 229: 52-54.

Hoffman, Ary A. and Peter A. Parsons, 1992 Evolutionary Genetics and Environmental Stress. Oxford University Press, Oxford.

Holtsford, T.P. and N.C. Ellstrand 1989 Variation in outcrossing rate and population genetic structure of *Clarksia tembloriensis*. Theoretical Applied Genetics 78: 480-488.

Krasnoborov, IM. and T.S. Rostovtseva, 1975 Chromosome number in various plant species of southern Siberia, Botanicheskii Zhurnal 60: 855-61.

Lewontin, R.C., 1974 The Genetic Basis of Evolutionary Change. Columbia University Press, New York.

Lorio, P.L., Jr. and J.D. Hodges, 1969 Microsite effects of oleoresin exudation pressure of large lob-lolly pines. Ecology 49: 1207-1210.

Lynch, Michael, 1984 Destabilizing hybridization, general-purpose genotypes, and geographic parthenogenesis. Quarterly Review of Biology 59: 257-290.

Manwell, Clyde and C.M. Baker, 1970 Molecular Biology and the Origin of Species: heterosis, protein polymorphism, and animal breeding. University of Washington Press, New York.

Mitton, J.B. and M.C. Grant, 1984 Relationships among protein heterozygosity, growth rate, and development stability. Annual Review of Ecology and Systematics 15: 479-499.

Mopper , Susan et. al., 1991 Genetic differentiation and heterozygosity in the piñion pine associated with resistance to herbivory and environmental stress. Evolution 45: 989-999.

Pogson, Grant, 1991 Expression of predominance for specific activity at the Phosphoglucomutase-2 locus in the Pacific oyster, *Crassostrea gigas*. Genetics 128: 133-139.

Ridley, Mark, 1993 Evolution. Blackwell Scientific Publications 127-128, 162, Boston.

Soltis, Douglas E. et. al., 1983 Starch-gel electrophoresis of ferns: a compilation of grinding buffers, gel and electrode buffers, and staining schedules. American Fern Journal 73: 9-26.

Werth, Charles R., 1985 Implementing an isozyme laboratory. Virginia Journal of Science 36: 55-75.

Isolation and Characterization of Yeast Nuclear pre-mRNA Splicing Genes and Factors in *Saccharomyces cerevisiae*

Lin Zhuo Jia

Department of Biology
California Institute of Technology
Pasadena, CA 91125

Faculty Advisor: John N. Abelson

ABSTRACT

Messenger RNA splicing prepares nuclear mRNA precursors for translation into protein by removing non-coding intervening sequences (introns) and joining coding sequences (exons). Although the splicing reaction is generally thought to be catalyzed by the RNA components of the spliceosome, many proteins are required for the process. In order to understand this mechanism, the factors that participate in the splicing process are being identified and their role in the process are being studied.

The goal of this project was to characterize and identify new pre-mRNA processing (*PRP*) genes in *Saccharomyces cerevisiae*. Each of these strains carries a mutation in a previously unknown gene that codes for a protein which participates in the splicing process. To do the initial characterization of these strains, total RNA from each strain was screened on RNA gel blots (Northern Blots) and the splicing phenotype of the actin gene was analyzed by hybridization with an actin intron probe. With this analysis, accumulation of pre-mRNA, intermediates, or excised introns can be detected. To identify the particular mutant genes, transformation of each strain with a wild-type yeast genomic library was carried out.

To date, Northern Blots have been performed for all the mutant strains and are being repeated for confirmation. Transformations are still being carried out for mutant yeast strains and the cloning of new *PRP* genes will be accomplished in the near future.

INTRODUCTION

Messenger RNA splicing occurs within the nucleus. It is the process by which introns are removed from the pre-mRNA, newly transcribed mRNA precursors, and exons are joined to yield a continuous open reading frame that can eventually be translated into protein.

It is now known that pre-mRNA splicing in yeast occurs in two steps (Figure 1). The first step consists of cleavage of the intron from the 5' side of the exon and ligation of the 5' end of the intron to internal intron sequences. This gives way to a lariat intermediate structure. In the second step, the 3' exon bond is subsequently cleaved and the two exons are joined together, giving way to a continuous exon segment and a released lariat intron. The lariat intron then becomes disintegrated within the nucleus. This complex reaction takes place within the spliceosome, a high molecular weight ribonucleoprotein complex. Biochemical work indicates that the spliceosome is composed of five small nuclear ribonucleoproteins (snRNPs) and several other protein factors (1). Although splicing is generally thought to be catalyzed by the RNA components of the spliceosome, many proteins are also required for the process.

The isolation and characterization of genes and their gene products that play a part in the splicing process has been carried out for some years. There have been significant advances in the elucidation of the splicing mechanism. Numerous pre-mRNA processing (*PRP*) genes have been identified. To date,

at least 30 genes and their gene products that directly or indirectly participate in pre-mRNA splicing have been cloned (2). Biochemical and genetic assays are being conducted to determine the role of these gene products in the splicing process. Because of the complexity of the splicing process and the large number of proteins involved, there is a constant search for new genes that might be involved in the splicing process.

As a result of screening a bank of 4,000 temperature sensitive yeast strains, there now exists a new collection of temperature sensitive (*ts*) mutants that are defective in pre-mRNA splicing. These *ts* strains cannot support mRNA splicing at the non permissive temperature of 37°C, but may be able to conduct splicing at the permissive temperature of 23°C. Genetic crosses of each of these new strains to previously known *PRP* mutants showed that the strains carry novel *ts* mutations.

This project therefore had two goals. The first was to identify the specific step of splicing that is affected in each mutant. The second was to identify the *PRP* genes from which these mutations arise. In order to accomplish the first goal of detecting which step of splicing is mutated in the *ts* strains, Northern Blots were performed. In order to accomplish the second goal of isolating the new *PRP* genes that are causing the splicing mutation, yeast transformations were carried out.

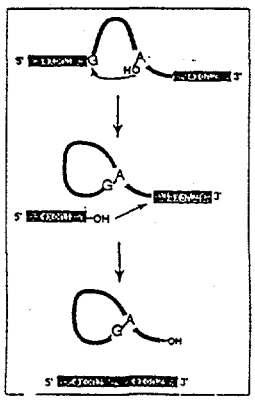


Figure 1: Pre-mRNA Splicing in Yeast (2)

PROCEDURE

Northern Blots

Total cellular RNA was extracted from each of the *ts* mutants. The yeast strains were grown to an optical density of 2 at 600 nanometers. One culture of cells was placed at 23°C to serve as control and another culture was placed at 37°C to inactivate the protein coded by the *ts* gene. Cells were collected and the RNA was purified through phenol extraction and ethanol precipitation. RNA was separated by electrophoresis on a 1.2% agarose gel in pH 7 phosphate buffer. The RNA migrated according to size and shape. The RNA on the gel was then transferred to a sheet of filter (Gene Screen). The transfer occurred by applying pressure to the gel and allowing the RNA to soak through the gel and onto the filter paper (PosiBlot Pressure Blotter, Stratagene). UV crosslink was performed to covalently attach the RNA to the filter. Lastly, a radioactive actin intron probe was made by PCR amplification This intron probe detected existing introns in the RNA. Since the intron probe was radioactive, when the filter was exposed to x-ray film, bands appeared. From the position of the bands, it was deduced which step of the splicing mechanism is mutated. The intron probe detects unspliced active pre-mRNA as well as splicing intermediates and intron lariats because they contain intron sequences.

Yeast Transformations

A YCP 50 genomic plasmid library with a uracil (URA) marker was made. Plasmids were extracted from the library through cesium chloride-ethidium bromide gradient. The plasmid library was added to lithium acetate treated yeast cells followed by a DMSO shock (3). These cells were then plated on growth media lacking URA to select for cells that picked up the plasmids. Those that grew at 23°C were termed "transformants," and were subsequently selected for complementation of the splicing mutation at the 37°C temperature. The process employed was replica plating in which a set of transformants was incubated at 23°C and another identical set was incubated at 37°C. Since they were *ts* mutations, the cells which grew at 37°C represent potential cells that have picked up a plasmid that was able to compensate for the mutation which inhibited correct splicing. The plasmid may then be isolated and the gene responsible for complementation identified.

RESULTS

Analysis of Northern Blots revealed the mutant splicing phenotype of various *ts* strains (Table 1). Strains 270, 1631, and 2820 show accumulation of pre-mRNA, indicating mutation at the first step of splicing. Strains 127 and 2364 show both accumulation of pre-mRNA and lariat intermediate, indicating mutation at the first and second step of splicing. Furthermore, strains 1631, 2364, and 2820 exhibit mutant splicing phenotype at both 23°C and 37°C. However, no *ts* strains display lariat intron accumulator phenotype. To confirm the results for these strains, Northern Blots need to be performed again. In addition, more conclusive results also need to be obtained for other strains.

Various protocols were attempted for transformation of the *ts* strains. The DMSO-enhanced whole cell yeast transformation proved to be most efficient. Thus far, transformation has been carried out for two strains. Several are in the process of being replica plated and the results are yet to be obtained.

Table 1: Preliminary Results of Northern Blots *

	Pre-mRNA		Lariat Intermediate		Lariat Intron	
Strains	23°C	37°C	23°C	37°C	23°C	37°C
110	/	/	/	/	/	/
127	-	+	-	+	-	-
138	-/+	-/+	-/+	-/+	-	-
140	-	-/+	-	-	-	-
270	-	+	-	-	-	-
943	/	/	/	/	/	/
1100	/	/	/	/	/	/
1155	/	/	/	/	/	/
1252	/	/	/	/	/	/
1409	/	/	/	/	/	/
1631	+	++	-	-	-	-
2364	+	++	++	+	-	-
2551	/	/	/	/	/	/
2620	/	/	/	/	/	/
2820	+	+++	-	-	-	-
3013	-	-	-	-	-	-
3188	-	-/+	-	-	-	-

* Intensity of Radioactive Signal

-	none	++	high
-/+	low	+++	very high
+	medium	/	inconclusive

CONCLUSION

The process of mRNA splicing is essential for correct expression of genes in eukaryotic cells and serves as a regulating mechanism for all eukaryotic organisms, including humans. This is what gives us an appreciation of the complexity and elegance of the process, and also a keen desire to know in detail the mechanism of this process.

In addition, a number of hereditary diseases and other ailments are known to be caused by defects in the splicing machinery or defective regulation of it. Knowledge of the mechanism of splicing will aid in understanding the molecular basis of these ailments and thus help to design new therapies.

No doubt, the discovery of new genes and proteins that participate in the splicing process will lead to better understanding of the mRNA splicing mechanism.

ACKNOWLEDGEMENTS

I thank Jaime Arenas and Debra Wiest for technical help and advice. Special thanks to Debra Wiest for valuable comments on the manuscript. This work was supported by John Abelson and the Summer Undergraduate Research Fellowship (SURF) program at Caltech.

REFERENCES

1. Vijayraghavan U, Company M, Abelson J: Isolation and characterization of pre-mRNA splicing mutants of *Saccharomyces cerevisiae. Genes and Development* 1989, 3: 1206-1216.
2. Ruby S, Abelson J: Pre-mRNA splicing in yeast. *Trends in Genetics* 1991, 7: 79-85.
3. Hill J, Ian K. A, Donald G, Griffiths D: DMSO enhanced whole cell yeast transformation. *Nucleic Acid Research* 1991, 19: 5791.

FURTHER REFERENCES

1. Abelson J: RNA Splicing in yeast. *The Harvey Lectures* 1991, 85: 1-42.
2. Cheng S, Abelson J: Spliceosome assembly in yeast. *Genes and Development* 1987, 1: 1014-1027.

Mechanism of the Effect of Citrulline On Valproate(VPA)-Induced Hyperammonemia

Elena Valcarlos

Department of Biology
Seattle University
Broadway and Madison
Seattle, WA 98122

Faculty Advisor:

Jeffrey R. Stephens

Hyperammonemia is a recognized side effect of VPA. We have shown that citrulline, a urea cycle intermediate, reduces blood ammonia and diminishes the associated neurological sequelae in a rat model of VPA-enhanced, NH_4^+-induced encephalopathy (*Epilepsia*, 35(1):161-171, 1994). We hypothesize that this effect is due to enhanced urea cycle activity. In study I, groups of rats received 4.0 or 6.0 mmole//kg NH_4^+ with or without citrulline (5.0 mmole/kg). In study II, groups of rats received VPA (2.5 mmole/kg) and NH_4^+ (4.0 mmole/kg) with or without citrulline (5.0 mmole/kg). Plasma was analyzed for urea and ammonia. In study I, citrulline increased urea concentration at both 4.0 NH_4^+ (5.1 to 7.4 mM, $p<0.05$) and 6.0 NH_4^+ (6.5 to 8.4 mM, $p<0.05$). In study II, citrulline increased urea concentration in animals treated with VPA and NH_4^+ (5.3 to 7.9 mM, $p<0.05$). These findings indicate that citrulline enhances urea synthesis during ammonia intoxication both in the absence and presence of VPA.

INTRODUCTION

Valproic acid (VPA), an anticonvulsant drug used to treat a host of disorders including epilepsy, has a number of side effects. One major and widely-recognized side effect of VPA therapy is hyperammonemia (Zacarra et al., 1984). The inducing role of VPA in hyperammonemia has been examined in studies on both humans and animals. In human studies done by Laub (1986) and Hirsch et al. (1988), VPA was found to cause moderate ammonia level elevations in fasted subjects. VPA-treatment caused greater increases in ammonia levels in subjects given a protein load or fed carbohydrates (Laub, 1986, Hirsch et al., 1988). Likewise, in animal studies conducted by Marini et al. (1988), fasted rats treated with VPA had moderate ammonia level elevations while rats given an ammonia load in the form of amino acids or ammonium-chloride before VPA treatment had greater ammonia level elevations (Marini et al., 1988). Studies of NH_4^+ and VPA induced coma in rats have shown that VPA enhances the neurological complications associated with hyperammonemia. In short, VPA was shown to reduce the threshold concentration of ammonia required to produce encephalopathy (Stephens and Levy, 1994).

The mechanism of VPA-induced hyperammonemia is complex. A portion of the hyperammonemic effect is produced in the kidney. There, VPA stimulates glutaminase to break down glutamine, a nitrogen storage depot, into glutamate and ammonium (Martin et al., 1990). A still larger share of the hyperammonemic effect is produced in the liver where VPA is thought to inhibit urea synthesis.

When VPA is present in the liver, it inhibits the mitochondrial portion of the urea cycle, the mechanism largely responsible for detoxifying the body of ammonia, by inhibiting the activity of carbamoyl phosphate synthetase (CPS I) (Marini et al., 1988). Inactivation of CPS I leads to a decrease in the production of carbamoyl phosphate, a urea cycle intermediate, which in turn leads to a decrease in the synthesis of the other urea cycle intermediates contained in both the mitochondria and cytosol of liver cells.

The purpose of this study was to determine if providing exogenous citrulline would have a protective effect against NH_4+-induced and VPA-enhanced hyperammonemia through increased urea production. Hypothetically, citrulline treatment should counteract VPA's partial inhibition of the urea cycle by stimulating the functioning cytosolic portion of the cycle to increase urea output. To evaluate the efficacy of

citrulline treatment, this study was carried out on a rat model of NH_4^+-induced hyperammonemia.

METHODS

Male Sprague-Dawley rats were divided into two study groups. In study I, groups of rats received NH_4^+ (4.0 or 6.0 mmole/kg) with or without citrulline (5.0 mmole/kg, i.p.). In study II, groups of rats received VPA (2.5 mmole/kg, i.p.) and NH_4^+ (4.0 mmole/kg, i.p.), with or without citrulline (5.0 mmole/kg, i.p.). Both VPA and/or citrulline if administered were given thirty minutes prior to a dose of NH_4Cl. Sampling by aortic puncture occurred half an hour after NH_4Cl administration and one hour after VPA and/or citrulline administration. Blood samples were drawn into heparinized syringes and immediately transferred to tubes containing EDTA as an anticoagulant. The tubes containing the blood samples were then centrifuged at 2,000 rpm for 8-10 minutes. The plasma was removed and kept on ice for immediate analysis or stored at -70°C until such time as an analysis could be performed. All rats were fasted for at least twelve hours before dosing and sampling.

Two colorimetric assays were used to determine plasma urea levels. First, urea+citrulline was assayed in plasma by the method of Rahmatullah and Boyd (1980). Second, a modification of the method of Rahmatullah and Boyd (1980) was used to determine citrulline levels in plasma (Stephens and Levy, 1994). Then, individual urea concentrations were calculated by subtracting citrulline concentrations from the urea+citrulline concentrations determined by the urea assay. Absorbances for all three assays were determined using a Hewett Packard 8451A diode array spectrophotometer. Gas chromatography was used to analyze VPA in plasma by the method of Semmes and Shen (1988). Student's t-tests set at $p<0.05$ significance levels were used to determine statistical differences between treatment groups.

RESULTS

In study I, ammonia levels decreased and urea levels increased overall when animals were treated with citrulline before receiving NH_4^+. Ammonia levels were constant at 0.151 ± 0.095 mM and 0.143 ± 0.021 mM ($p>0.05$) but urea levels increased from 5.1 ± 1.2 mM to 7.4 ± 0.92 mM ($p<0.05$) for animals given citrulline before a 4.0 mmole/kg dose of NH_4^+ (Fig. 1). Animals given citrulline prior to a dose of 6.0 mmole/kg NH_4^+ had ammonia levels that decreased from 0.509 ± 0.138 mM to 0.208 ± 0.140 mM ($p<0.05$) and urea levels that increased from 6.5 ± 1.1 mM to 8.4 ± 1.3 mM ($p<0.05$) (Fig. 1).

In study II, administration of citrulline also decreased ammonia levels and increased urea levels. Citrulline given to rats dosed with VPA and NH_4Cl (4.0 mmole/kg) decreased ammonia levels from 0.544 ± 0.286 mM to 0.289 ± 0.188 mM ($p>0.05$) while increasing urea levels from 5.2 ± 1.0 mM to 7.9 ± 0.78 mM ($p<0.05$) (Fig. 2). Curiously, VPA itself caused a significant rise, from 3.5 ± 0.72 mM to 4.9 ± 0.40 mM, in urea levels over those of basal levels ($p<0.05$) (Fig. 2).

DISCUSSION

This study sought to evaluate the use of citrulline as a treatment for hyperammonemia. The results suggest that citrulline has a protective effect against NH_4^+-induced and VPA-enhanced hyperammonemia through increased urea synthesis.

First of all, citrulline was effective at increasing urea levels when rats were given 4.0 or 6.0 mmole/kg NH_4Cl in the absence of VPA. At the same time, citrulline was able to significantly lower plasma ammonia levels at the higher 6.0 mmole/kg NH_4Cl dose. Since VPA was not present to inhibit the cycle, administration of exogenous citrulline increased the concentrations of and in turn the binding potentials between the urea cycle intermediates to the point where urea production was only limited by the activity of the slowest enzyme in the cycle. In other words, increasing the concentrations of the urea cycle intermediates basically increased the efficiency of the whole cycle.

Second, citrulline was effective at increasing urea levels and correspondingly, decreasing ammonia levels even in the presence of VPA. In this case, although a portion of the cycle was inhibited by VPA, urea synthesis could continue through the cytosol. By increasing the concentrations of the cytosolic based intermediates in the cycle, citrulline treatment increased the efficiency of the cytosolic portion of the cycle and thus caused a significant increase in urea levels.

However, considering that VPA itself can raise urea levels, the increased urea synthesis was probably not solely due to citrulline treatment. The raised urea levels caused by VPA itself suggest that VPA enhanced the kidney's breakdown of glutamine to glutamate and NH_4^+. The glutamate and NH_4^+ would have entered the cytosolic portion of the urea cycle via aspartate, another urea cycle intermediate. The high glutamate levels would have increased aspartate levels thus functioning, like citrulline, to stimulate the cytosolic portion of the cycle to increase urea production. Hence, the increased urea levels could have been due to both citrulline treatment and VPA's enhancement of glutamine breakdown. Without glutamine analysis, which was not performed in the study, it is impossible to determine how great an effect VPA itself had on urea synthesis.

By stimulating the urea cycle, citrulline increased urea levels and decreased ammonia levels in the presence and absence of VPA. These findings suggest that patients who experience VPA-induced hyperammonemia may be helped with citrulline treatment. Also, since it is quite likely that increased urea levels were the product of combined citrulline and aspartate stimulation of the cytosolic portion of the urea cycle, in future, the role of VPA in inducing hyperammonemia in vivo needs to be examined.

REFERENCES

Coudé FX, et al. Letter to the editor: a mechanism for valproate-induced hyperammonemia. *Pediatr Res* 1981;15:974-5.

Hirsch E, et al. Sodium valproate induces a hyperammonemia of renal and hepatic origin depending on diet. In: Soeters PB, Wilson JHP, Meijer AJ, and Holm E, eds. *Advances in ammonia metabolism and hepatic encephalopathy.* Amsterdam: Elsevier Science Publishers BV, 1988:191-6.

Laub MC. Nutritional influence on serum ammonia in young patients receiving sodium valproate. *Epilepsia* 1986;27(1):55-9.

Marini AM, Zaret BS, and Beckner RR. Hepatic and renal contributions to valproate-induced hyperammonemia. *Neurology* 1988;38:365-71.

Martin G, Durozard D, Besson J, and Baverel G. Effect of the antiepiliptic drug sodium valproate on glutamine and glutamate metabolism in isolated human kidney tubules. *Biochim Biophys Acta* 1990;1033:231-66.

Rahmatullah M and Boyde TRC. Improvements in the determination of urea using diacetyl monoxime; methods with and without deproteinisation. *Clin Chim Acta* 1980;107:3-9.

Semmes RLO and Shen DD. Capillary gas chromatographic assay for valproic acid and its 2-desaturated metabolite in brain and plasma. *J Chromatogr* (Biomed Appl) 1988;432:185-97.

Stephens JR and Levy RH. Effects of Valproic Acid and Citrulline on Ammonium-induced Encephalopathy. *Epilepsia* 1994;35(1):161-171.

Zaccara G, Paganini M, Campostrini R, Arnetoli G, Zappoli R, and Moroni F. Hyperammonemia and valproate-induced alterations of the state of consciousness. *Eur Neurol* 1984;23:104-12.

FIGURE 1

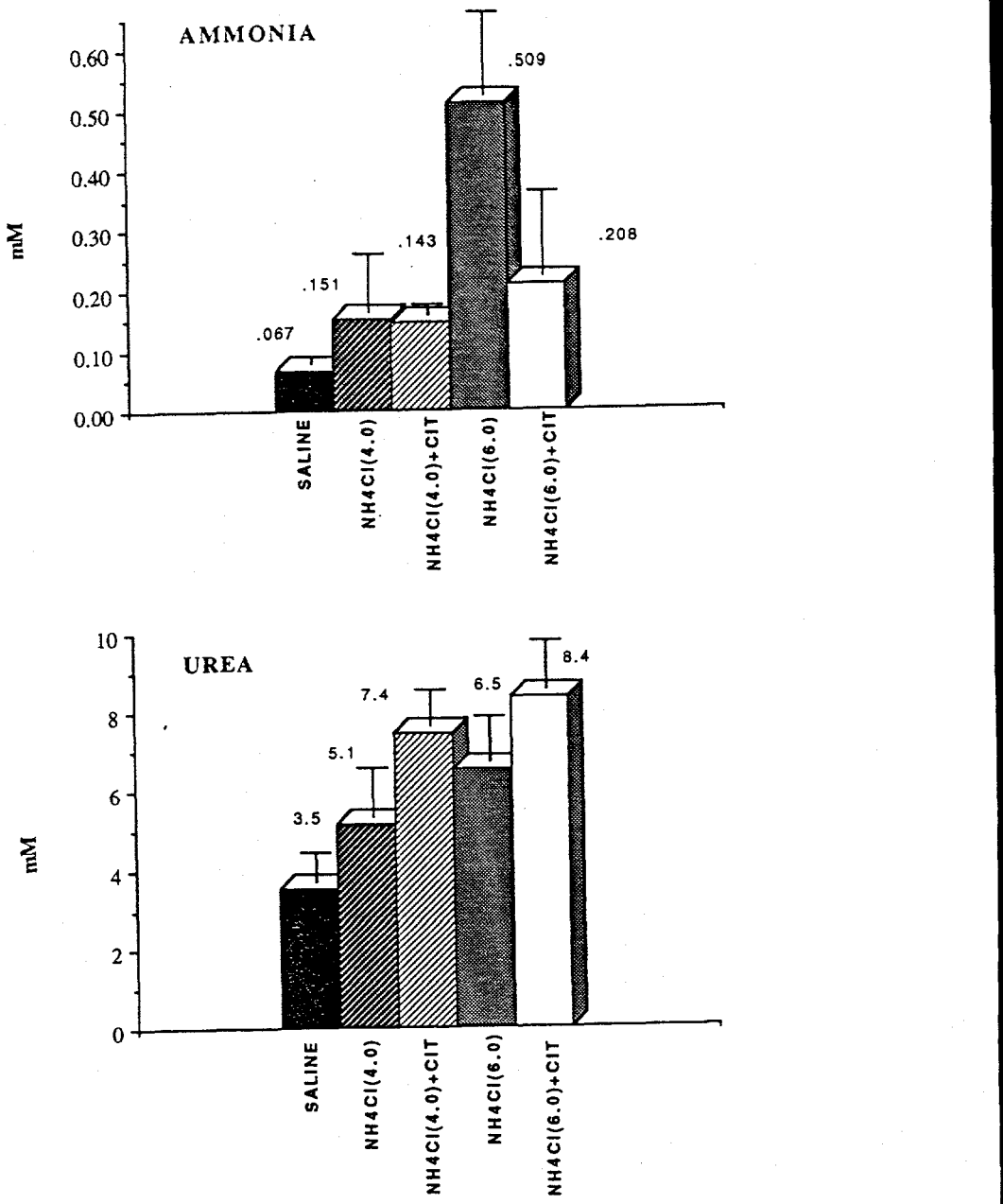


Figure 1: Comparison of mean plasma ammonia and urea concentrations (± standard deviation) in rats administered NH_4Cl (4.0 mmole/kg or 6.0 mmole/kg) and citrulline (5.0 mmole/kg). Samples for plasma ammonia and urea analysis were obtained 30 minutes after NH_4Cl administration. Citrulline was given 30 minutes prior to NH_4Cl. Numbers of rats per group: Saline, (n=5), NH_4Cl, 4.0 (n=8), 6.0 (n=4), NH_4Cl+Citrulline, 4.0 (n=6), 6.0 (n=6).

FIGURE 2

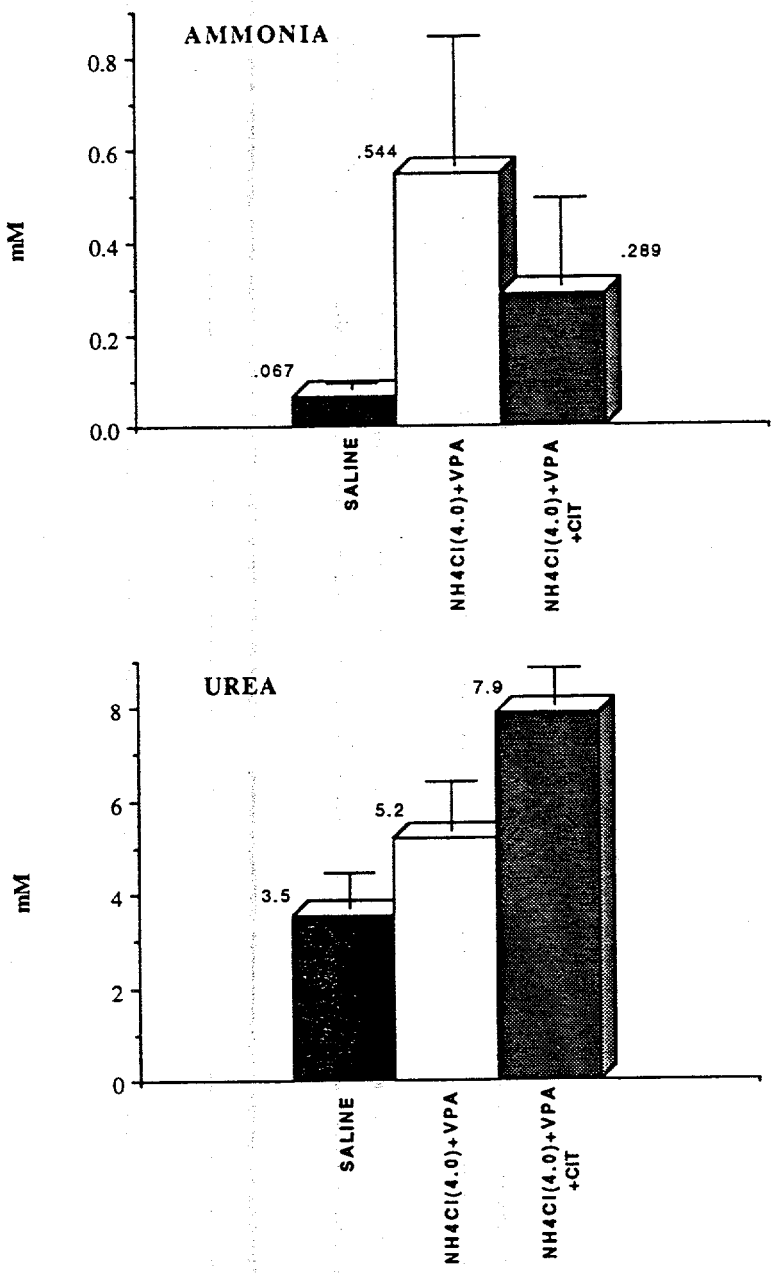


Figure 2: Mean plasma ammonia and urea concentrations (± standard deviation) in rats treated with saline (n=5), VPA (2.5 mmole/kg) (n=4), NH_4Cl (4.0 mmole/kg) and VPA (2.5 mmole/kg) (n=6), or NH_4Cl (4.0 mmole/kg), VPA (2.5 mmole/kg), and citrulline (5.0 mmole/kg) (n=7). Samples for ammonia and urea analysis were obtained 30 minutes after NH_4Cl administration. VPA and citrulline were given 30 minutes prior to NH_4Cl.

Messenger RNA Stability and Membrane Phospholipid Composition in Heat Stressed Barley Aleurone Cells

Paul A. S. Benson

Department of Biology
Knox College
Galesburg, Illinois 61401

Faculty Advisor: Mark R. Brodl, Ph.D.

INTRODUCTION

The barley aleurone layer has served for decades as an excellent model system for studies of hormonal and stress responses in plants. When stimulated by the phytohormone gibberellic acid (GA_3), the aleurone layer synthesizes and secretes a battery of hydrolytic enzymes which serve to degrade the stored food reserves in the endosperm to make the nutrients stored there available to the developing embryo. Under normal conditions, imbibition of water stimulates the embryo to secrete GA_3, which diffuses into the endosperm to bring about these changes in gene expression. In the experimental system, the embryo is removed, and the resulting "half seed" is allowed to imbibe to soften the endosperm. The aleurone layer can then be removed and treated with exogenous GA_3 or other hormones. Data from SDS-PAGE studies have documented that addition of exogenous GA_3 results in a commitment on the part of the aleurone cell to the synthesis of these secreted hydrolases (Pfitzinger *et al.*, 1989).

Of the hydrolases produced upon the addition of GA_3, alpha-amylase is the most prominent, and hence can be used as a marker enzyme. Heat shock (HS) greatly inhibits hydrolase production. Heat shock, in addition, induces the production of a novel set of proteins called heat shock proteins (hsps) (Brown and Brodl, 1988). It has been demonstrated that heat shock results in the degradation of secretory protein mRNAs but not those of non-secretory proteins. The primary distinction between secretory and non-secretory protein mRNAs is a region encoding an amino terminal signal sequence which directs the translation of secretory protein mRNAs to occur at the ER surface (Gilmore, 1993). It has also been shown that ER lamellae are dissociated during heat shock. Because the secretory protein mRNAs are translated at the ER, the stability of the hydrolase mRNA may therefore be affected by ER integrity (Belanger *et al.*, 1986).

This study specifically focuses on dissecting the changes in normal cellular synthesis of heat-shocked aleurone cells by examining the stability of secretory mRNA when subjected to gradual increases in temperature (heat *stress* rather than heat shock). Heat stress appears to permit the cells to make adaptive changes in cellular physiology to adapt to the high temperature. We have observed by SDS-PAGE studies that if aleurone cells are brought from 25°C to 40°C gradually by increments of 2.5°C every 30 (fast ramp) or 60 (slow ramp) min, the synthesis of secretory proteins is sustained at 50% of control levels as compared to less than 5% in heat-shocked samples (Johnston and Brodl, 1994). Using alpha-amylase as our secretory enzyme of study, we report here on the differences between the stability of secretory protein mRNA pools in heat-stressed and heat-shocked samples as seen by northern hybridization analysis. We show the correspondence between these secretory mRNA levels and the resulting rates of synthesis of alpha-amylase as seen by one-dimensional 11% SDS-PAGE of radiolabelled proteins. In addition, the transcription inhibitor cordycepin was used to inhibit hsp synthesis during heat stress to determine whether or not alpha-amylase mRNA levels are thermoprotected even in the absence of hsps.

The final aspect of this study was to examine the fatty acid composition of aleurone cell ER membranes during heat stress. The stability of these membranes may impact secretory protein mRNA stability. Organisms exposed to temperature changes "retailor" their membrane lipid composition to maintain the degree of membrane fluidity essential to membrane function. In previous work from our lab, we have shown using thin layer chromatography (TLC) that heat shock induces the synthesis of phosphatidylcholine (PC), the principal phospholipid of the ER. We have also found that heat stress results in an increased ratio of saturated to unsaturated fatty acids in PC and in ER membrane phospholipids, indicating a possibility that alterations in membrane fluidity may be important in achieving thermal stability (Grindstaff *et al.*, 1995). We document here similar trends in heat-induced alteration of membrane lipid composition.

MATERIALS AND METHODS

Seed preparation

Barley grains (*Horseum vulgare*, cv. Himalaya, obtained from the University of Washington, Pullman Washington) were prepared by removing both the embryo and distal tip of the grain. The resulting "half-seeds" were surface sterilized in a 25% bleach solution for 15 minutes at 45°C. Under aseptic conditions, the half-seeds were placed on filter paper-lined vermiculite plates saturated with incubation buffer (20 mM Na succinate (pH 5.0), 20 mM $CaCl_2$, 1 μg/ml chloramphenicol). The half-seeds were imbibed for four days at 22.5°C. After the incubation period, the aleurone layer was peeled from the softened endosperm under sterile conditions.

In vivo labeling and analysis of proteins

Ten aleurone layers per sample were placed in 2 ml of incubation buffer (20 mM sodium succinate [ph 5.0], 20 mM $CaCl_2$, 10 μg/μl chloramphenicol) in a 25-ml flask. All samples except those involving heat stress by slow ramp (slow heating to heat shock temperature by increments of 2.5°C every 60 min) were incubated for 16 hours at 25°C in the presence or absence of 1 μM GA_3 in a reciprocal shaking water bath at 120 cycles per minute. Heat-shocked aleurone layers were incubated an additional 3 hours at 40°C. Conversely, the non-heat-shocked controls were incubated for the same period at 25°C. Samples heat-stressed under "fast ramp" conditions were incubated for an additional 3 hours with temperature increases of 2.5°C every 30 min, with an optional 2 hour hold at 40°C. Samples heat-stressed under "slow ramp" conditions were incubated for 13 hours at 25°C, then subjected to an additional 6 hours of 2.5°C temperature increases every 60 min, with an optional 2 hour hold at 40°C. For cordycepin-treated samples, cordycepin (Sigma, St. Louis, MO) was added to the buffer at a concentration of 0.1 mM one and one half hours before any subjection to heat shock or heat stress, or one and one half hours before the end of the incubation period if non-heat-treated. One half hour prior to the end of the incubation period the samples were labeled with 50 μCi of [^{35}S]-methionine (NEN, Boston, MA) in 1 ml of incubation buffer.

At the end of the labeling period, the buffer was removed and the layers were washed with 1 mM nonradioactive methionine and homogenized in 300 μl grinding buffer (Laemmli, 1970), 5 μl of 10 μM leupeptin, and 3 μl DNase (1mg/ml). Protein samples synthesized *in vivo* were analyzed by one-dimensional 11% SDS-PAGE as described by Laemmli (1970). Samples were loaded on the basis of equal amounts of trichloroacetic acid-precipitable radioactivity.

RNA isolation and Northern blot analysis

One-hundred aleurone layers per sample were incubated in 20 ml of incubation buffer (as described previously) in a sterile 250-ml flask. RNA was isolated using a guanidine-HCl method outlined by Chirgwin *et al.* (1986). Eighteen μl of total RNA per lane were prepared and electrophoretically separated on formaldehyde-containing 1% agarose gels. RNA was transferred by capillary blotting to "Gene Screen Plus" hybridization membranes (NEN). The blots were probed using the following cDNA clones, nick-translated in the presence of [^{32}P]-dCTP (NEN): pM/C (high pI isozyme of alpha-amylase) (Muthukrishnan *et al.*, 1983), Clone E (the low pI isozyme of alpha-amylase) (Rogers and Milliman, 1983), hsp 70 (Rochester *et al.*, 1986), and protease (Koehler and Ho, 1990).

Phospholipid extraction and TLC analysis

Twenty aleurone layers per sample were incubated in 4 ml of incubation buffer (as described previously) in a sterile 25-ml flask. In one experiment, samples were subjected to a time course of heat shock and heat stress as previously described in the section on *in vivo* labeling and protein analysis. Samples were labeled with 0.4 μCi of [^{14}C]-glycerol three hours prior to grinding. Alternately, samples were subjected to the "slow ramp" time course of heat stress and labeled with 1.2 μCi of [^{14}C]-glycerol during the last one hour prior to their grinding. Slow-ramped aleurone layers were sampled at each temperature increment (27.5°C, 30°C, and so forth).

The incubation buffer was removed, and samples were ground in 300 μl of 100 mM Tris (pH 6.8) and transferred to a 15-ml centrifuge tube. Chloroform-methanol (2:1, v:v) was added to precipitate protein. Phospholipids were extracted according to Geer *et al.* (1986) and were separated on a TLC plate (Whatman Silica Gel A6, Hillsboro, OR) in a solvent of chloroform-methanol-petroleum ether-acetic acid (4:2:3:1, v:v:v:v). Phospholipid spots were visualized by iodine vapors, scraped from the TLC plate, and the amount of radioactivity in each phospholipid was determined by liquid scintillation counting.

RESULTS AND DISCUSSION

For many years it has been thought that heat shock proteins (hsps) played a large role in cells' adaptation to high temperatures. In order to determine whether or not hsps play a role in stabilizing secretory protein and its corresponding mRNA during heat stress, SDS-PAGE was used to visualize proteins synthesized during heat shock and heat stress, either with or without the addition of 0.1 mM cordycepin as a transcription inhibitor (*Fig. 1*). With the addition of cordycepin 1.5 hours before any increase in temperature above 25°C, heat shock proteins were suppressed. However, secretory proteins such as alpha-amylase were unaffected by the addition of cordycepin, since all mRNA for alpha-amylase had been synthesized prior to cordycepin addition (Brodl *et al.*, 1990). Cordycepin, therefore, allows us to see if hsps are responsible for the persistence of alpha-amylase synthesis during heat stress. We have observed little or no dependence upon hsps for the persistence of alpha-amylase synthesis, indicated by the relatively even amounts of protein between heat stressed samples with and without cordycepin (compare lanes 6, 7, 10, and 11 with 8, 9, 12, and 13) (*Fig. 1*). There is no increased stability of alpha-amylase in aleurone cells not treated with cordycepin over those treated with cordycepin, indicating that heat shock alone is responsible for any degradation of alpha-amylase mRNA.

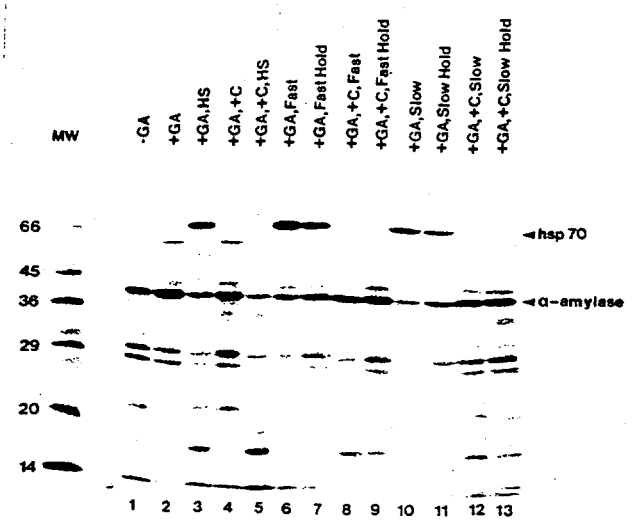


Fig. 1. **Levels of secretory and heat-shock proteins during heat shock vs. heat stress with and without treatment with cordycepin.** Use of cordycepin at a concentration of 0.1 mM 1.5 hours before any heat treatment effectively inhibited the synthesis of any hsps. Even without hsps present, essentially the same amounts of alpha-amylase were seen as in heat stressed lanes, indicating that increased levels of secretory proteins during heat stress are not dependent on hsps.

The idea that increased stability of alpha-amylase during heat stress over heat shock, irrespective of hsps, is further revealed by Northern blot analysis of protease and the high and low pI isozymes of alpha-amylase (*Fig.2*). Secretory protein mRNA levels dramatically drop upon exposure to heat shock, irrelevant of exposure to cordycepin. However, heat stressed aleurone layers are better able to adapt to these higher temperatures, indicated by levels of mRNA at approximately 30% of control in both "fast" and "slow" ramped samples. Comparing secretory protein mRNA levels between heat-stressed samples with and without cordycepin, there is very little difference in the amount of message, indicating that there is little or no dependence on hsps for this increased stability over heat-shocked samples.

Belanger *et al.* (1986) have shown that because secretory protein mRNAs are translated at the ER, the stability of the hydrolase mRNA is therefore affected by ER integrity. One important regulatory factor of ER integrity is the combination of membrane phospholipids present in the ER. Previous work by Grindstaff *et al.* (1995) has shown that certain phospholipids, most notably phosphatidylcholine (PC), are synthesized *de novo* in greater amounts with exposure to heat shock. Here we have examined this trend in heat-*stressed* barley aleurone cells.

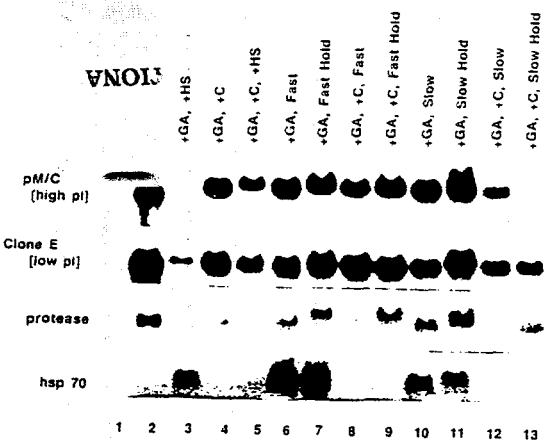


Fig. 2. **Messenger RNA levels of secretory and heat-shock proteins during heat shock vs. heat stress with and without treatment with cordycepin.** mRNA encoding secretory proteins, seen here with protease and both the high (pM/C) and low (Clone E) pI isozymes of alpha-amylase, was selectively suppressed during heat shock, whereas there was an induction of heat shock protein mRNA synthesis with heat shock. Heat stress protein levels were at approximately 50% of control levels as compared to 5% of control levels in heat shocked layers. The levels of message in heat stressed lanes with and without cordycepin were relatively the same.

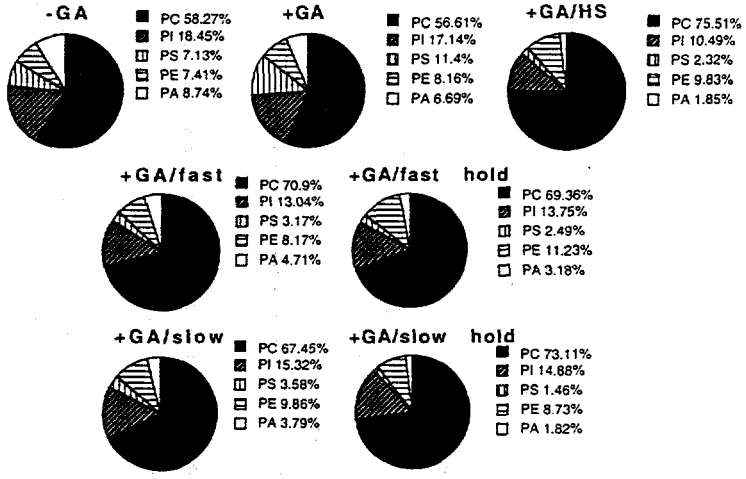


Fig. 3. **Relative amounts of membrane phospholipids produced during heat shock vs. heat stress.** Heat shock resulted in a dramatic increase in the relative amount of phosphatidylcholine (PC), from approximately 57% to 76%. The four ramped samples demonstrated a similar trend, though their relative amounts of PC were not as high as the heat shocked sample, ranging from 67-73%.

To determine the effect of heat stress on phospholipid synthesis, barley aleurone layers exposed to heat stress were labeled with [^{14}C]-glycerol, their lipids extracted, and analyzed by TLC. Figure 3 shows that GA_3 had no effect on the relative amounts of each phospholipid (*Fig. 3*). As has been shown in previous studies by Grindstaff *et al.* (1995), heat shock caused a dramatic increase in the amount of phosphatidylcholine (PC), from approximately 57% to 76%. With regard to heat *stress*, the four ramped samples demonstrated a similar trend, though their relative amounts of PC were not as high (67-73%) as the heat-shocked sample. This suggests that given longer times to adapt, barley aleurone cells are better able to deal with the elevated temperatures and do not require as strong a response as is seen in heat-shocked samples. To examine further at which point barley cells begin to retailor their phospholipid compositions and if there is a temperature where peak amounts of *de novo* PC are synthesized, the process of slow ramp was dissected, and samples were harvested at each temperature in the ramping process (at 27.5°, 30.0°C, etc.). As the temperature was increased during heat stress, the relative amount of PC also increased, but only up to a certain point. The greatest relative amount of PC was made

during the one hour exposure to 37.5°C, after which time the heat-stressed cells had made sufficient PC to maintain alpha-amylase synthesis during the following hour of 40°C. In fact, during the hour at 40°C, the same relative amount of PC is made as in non-heat-shocked samples (*Fig. 4*).

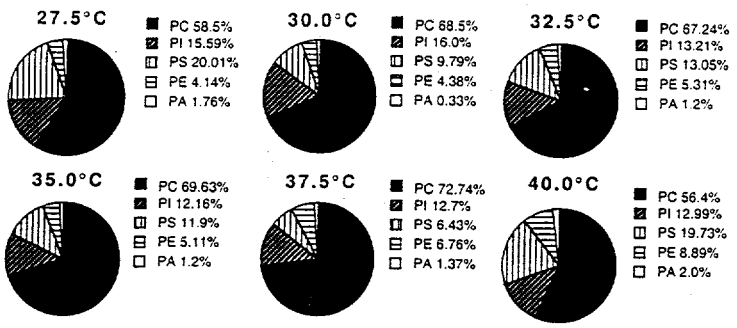


Fig. 4. **Relative amounts of membrane phospholipids produced during each temperature stage of "slow ramp" heat stress.** As temperature was increased during heat stress, the relative amount of PC also increased, but only up to a certain point, that being 73% at 37.5°C. After this time the heat stressed cells had made sufficient PC to cope with the following hour of 40°C. During the hour at 40°C, the same relative amount of PC was made as in non-heat-shocked samples (56%).

REFERENCES

Belanger, F. C., M. R. Brodl, and T-h. D. Ho. 1986. Heat shock causes destabilization of specific mRNAs and destruction of endoplasmic reticulum in barley aleurone cells. *Proc. Natl. Acad. Sci. USA.* 83: 1354-1358.

Brodl, M.R., F.C. Belanger, and T-hD. Ho. 1990. Heat shock protein synthesis is not required for the destruction of endoplasmic reticulum lamellae and alpha-amylase mRNA during heat shock or for the recovery of aleurone cells from heat shock. *Plant Physiol.* **92**: 1133-1141.

Brown, P. H. and M. R. Brodl. 1988. Hormonal and heat stress regulation of protein synthesis in the aleurone layers of barley seeds. *BioEssays* 8: 199-202.

Chirgwin, J. M., A. E. Przybyla, R. J. MacDonald, and W. J. Rutter. 1979. Isolation of biologically active ribonucleic acid from sources enriched in ribonuclease. *Biochemistry* 18: 5294-5299.

Geer, B.W., S.W. McKechnie, and M.L. Langevin. 1986. The effect of dietary ethanol on the composition of lipids of *Drosophila melanogaster* larvae. *Biochem. Genet.* 24: 51-69.

Gilmore, R. 1993. Protein translation across the endoplasmic reticulum: a tunnel with toll booths at entry and exit. *Cell* 75: 589-592.

Grindstaff, K. K., L. A. Fielding, and M. R. Brodl. 1995. Effect of gibberellins and heat shock on protein secretions in barley aleurone cells. *Plant Physiol.* (revisions submitted).

Johnston, M.K., M.R. Brodl. 1994. Shifts in buoyant densities of endoplamic reticulum membranes: Heat shock-induced changes in lipid to protein ratios. *Proc. 8th Natl. Conf. Undrgr. Res.* 8: 928-932.

Koehler S. and T-hD. Ho. 1990. Hormonal regulation, processing, and secretion of cysteine proteinases in barley aleurone layers. *Plant Cell* 2: 769-783.

Laemmli, U. K. 1970. Cleavage of the structural proteins during assembly of the head of bacteriophage T4. *Nature* 227: 680-685.

Muthukrishnan, S., G.R. Chandra, and E.S. Maxwell. 1983. Hormonal control of alpha-amylase gene expression in barley. *J Biol Chem* 258: 2370-2375.

Pfitzinger, H., J. H. Weil, D. T. N. Pillay, and P. Guillemaut. 1989. Preparation of a tRNA-dependent wheat germ protein-synthesizing system. *Plant Molecular Biology* 12: 301-306.

Rochester, D.E., J.A. Winer, and D. M. Shah. 1986. The structure and expression of maize genes encoding the major heat shock protein, hsp 70. *EMBO J.* 5: 451-458.

Rogers, J.C. and C. Milliman. 1983. Isolation and sequence analysis of a barley alpha-amylase cDNA clone. *J Biol Chem* 258: 8169-8174.

ACKNOWLEDGMENTS

This research was funded by National Science Foundation Grants to M. R. Brodl (DCB-9105888 and DCB-9157247) and an HHMI/Knox Summer Fellowship to P. A. S. Benson.

ANTIFUNGAL ACTIVITY OF THIOL-BLOCKERS

Louise McDonald[1] and Tyler Parker[2]

Department of Medicine, Wayne State University[1], Detroit, MI 48201
Department of Biology, Fisk University[2], Nashville, TN 37208

Faculty Advisors:

Dr. Elias Manavathu[1]
Department of Medicine
Wayne State University
Detroit, MI 48201

Dr. Muthukumaran Gunasekaran[2]
Department of Biology
Fisk University
Nashville, TN 37208

ABSTRACT

Aspergillus fumigatus (*AF*) is an opportunistic filamentous fungus which causes severe local and disseminated infections in immunocompromised individuals, especially in cancer patients undergoing protracted chemotherapy. Members of the azole family of antifungals (except itraconazole) are relatively ineffective against *AF* infection. Although amphotericin B is highly effective against *AF* infection, prolonged use of this antifungal agent results in irreversible renal toxicity. Thus, the development of new antifungal agents is essential for effective treatment of fungal infections in the future. Our previous studies revealed that several members of a group of newly synthesized thiol-alkylators inhibited the growth of *Candida albicans*. Therefore, to evaluate the effectiveness of thiol-alkylators as antifungal agents against filamentous fungi, we examined the susceptibility of *AF* to a series of α,β-unsaturated styryl ketones known to be thiol-alkylators, and compared the results to those obtained for *C. albicans*. Among 13 compounds used in our study, one (designated NC1110) inhibited the growth of *AF* completely at low concentrations (minimum inhibitory concentration = 32 μM). Structure-activity analysis of these compounds indicated that the electron attracting property as well as the overall hydrophobicity of the compounds are important parameters for their antifungal activity. These preliminary results suggest that further modification of these molecules to enhance their hydrophobicity and the electron attracting property may result in more active compounds with improved antifungal activity.

INTRODUCTION

Members of the genus *Aspergillus* are typically soil-borne filamentous saprophytic organisms that usually thrive on organic matters utilizing them as nutrients. Because of their existence in relatively nutrient-poor environments, these organisms are equipped with an armamentarium of enzymes capable of breaking down complex organic molecules to simple usable nutrients. Unfortunately, the same degradative enzymes invaluable to the organism for survival act as virulence factors in many pathogenic species. Taxonomically, members of the genus *Aspergillus* are grouped under two fungal classes, namely, Ascomycetes and Deuteromycetes. The latter group is not a natural division, but includes those ascomycetous organisms that do not possess a well-described sexual cycle, most likely not yet discovered.

Among the 100s of species of *Aspergillus* described to date, only a small number of them are pathogenic to man (1). Among the pathogenic species, *A. fumigatus*, capable of producing severe local and disseminated infection, is the most commonly found filamentous fungus in man, followed by *A. flavus*. Sometimes, in extreme cases of immunocompromised patients, species typically found in nature as saprophytes are also capable of causing disease (2-5). Typically found as soil-crganisms, *Aspergillus* species are commonly spread by air-borne conidiospores. The main portal of entry for these organisms in man is the respiratory tract. Consequently, lungs of susceptible individuals are often severely affected and generally develop a condition called aspergillosis. This local infection can subsequently spread hematogenously to cause severe disseminated infection which results in high incidence of mortality.

The incidence of aspergillosis was relatively low a decade ago. The advent of sophisticated life-saving medical procedures such as organ transplants, intense cytotoxic

chemotherapy against cancer, and the prevalence of HIV infection in recent years, dramatically altered the immune status of the patient population during the past 10 years. Consequently, the incidence of *Aspergillus* infection increased significantly. However, it is not clear why certain species of *Aspergillus* are more pathogenic than others. Perhaps the pathogenic species are intrinsically more virulent, either because they are more readily inhaled or because they possess one or more virulence factors such as toxins (6) and extracellular proteases, particularly elastase (7,8). These factors might relate to the ability of the conidia to adhere to the respiratory epithelium, or to prevent clearance by mucociliary mechanisms. In fact, germinating conidia of *A. fumigatus* readily adhere to inert objects such as glass and plastic more than those of relatively non-pathogenic species such as *A. niger* and *A. nidulans* (9). Although fungal infection due to *A. fumigatus* has emerged as a serious clinical problem in many immunocompromised patients (10), the choice of antifungal agents highly effective against *A. fumigatus* is very limited. Since the previous studies (11) revealed that several members of a group of newly synthesized thiol-alkylators inhibited the growth of *C. albicans*, the effect of these compounds on the growth of *A. fumigatus* was investigated.

MATERIALS AND METHODS

Organisms and Culture Conditions: A panel of six clinical isolates of *A. fumigatus* obtained from the Detroit Medical Center were used in this investigation. Working cultures of all the isolates of *A. fumigatus* were maintained on PYG (peptone 1 g; yeast extract 1 g; glucose 3 g; per liter of distilled water) agar slants at room temperature. For long-term storage of the isolates, conidial suspensions were prepared (see below for details), mixed with equal volume of 50 % sterile glycerol and stored as 0.5-ml aliquots at -70 °C. For the preparation of conidial suspension, cultures were grown on PYG agar plates for 6 days at 30 °C, and the conidia were collected by flooding the agar surface with sterile growth medium. The conidial suspension which usually contains fragments of mycelia and other cellular debris was filtered through several layers of sterile cheese cloth, the filtrate was collected and stored at 4 °C. Cell density was determined by hemocytometer counts and adjusted appropriately before use.

Cultures of *C. albicans* B311 were grown in PYG medium at 30 °C with agitation as described previously (11). After determining the cell density by hemocytometer count, the over night cultures were diluted in fresh growth medium to the required cell density before use.

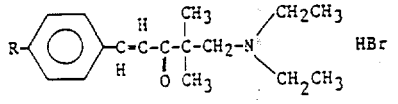
Thiol-alkylators: The thiol-alkylators used in this study were a group of α,β-unsaturated styryl ketones that react reversibly with small molecular weight thiols such as glutathione, but irreversibly with protein-associated thiols (12). These molecules generally react with neither the hydroxyl group of DNA nor with the hydroxyl and the amino groups of proteins; hence they are not generally considered as mutagenic agents (12). The chemical structures of all the compounds used in this investigation are shown in Figure 1. All the compounds were synthesized at the College of Pharmacy, University of Saskatchewan, Saskatoon, Canada as described previously (11) and provided for investigation as a gift by Dr. Jonathan R. Dimmock. The compounds were dissolved in dimethyl sulfoxide (DMSO) as 10 mM stock and diluted appropriately in growth medium just before use to obtain the required concentrations. In all experiments, identical amounts of DMSO were added to the control to evaluate the effect of DMSO on the growth of *A. fumigatus*. DMSO had no significant effect on the growth of *A. fumigatus* at the concentrations used.

Susceptibility studies: The susceptibility of *A. fumigatus* to various thiol-alkylators was examined by determining the minimum inhibitory concentration (MIC) of each compound for *A. fumigatus*. The MIC was determined using a previously developed macrobroth dilution technique suitable for in vitro susceptibility study of filamentous fungi (13). Briefly, the required concentrations (0 μM to 2048 μM) of various thiol-blockers were prepared in 16-ml polystyrene tubes (Falcon 2051) containing 5 ml PYG medium by two-fold serial dilution, and inoculated with freshly prepared conidia to obtain a final cell density of 1×10^3 conidia per ml. The tubes were incubated at 30 °C for 48 hr and then examined visually for growth. The MIC was defined as the lowest concentration of the drug in which no visible growth occurred after incubation at 30 °C for 48 hr.

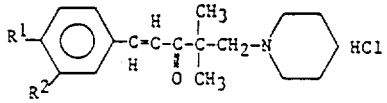
The susceptibility of *C. albicans* B311 to various thiol-alkylators were determined using the microbroth dilution technique essentially as described by the National Committee for Clinical Laboratory Standard (14).

RESULTS AND DISCUSSION

Thirteen thiol-alkylators with the highly reactive α,β-unsaturated ketone or hydrazone, but carrying different substituents on the aryl ring, were examined for their ability to inhibit the growth of six different clinical isolates of *A. fumigatus*. Since all six isolates showed identical susceptibility to these compounds the data obtained for isolate W73355 are presented as representative (Table 1). Since the MIC value of a drug often serves as a measure of its potency against a particular microbial agent, here we express the effect of various thiol alkylators on the growth of *A. fumigatus* as their MIC values. On Table 1, the thiol-alkylators are listed by the designation given at the time of their synthesis (NC numbers) as well as identified by the series number to show their structural relatedness.



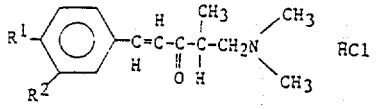
1



2

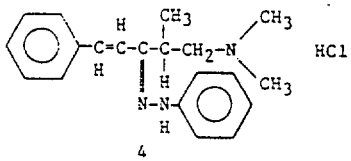
	R
a	Cl
b	OCH_3

	R^1	R^2
a	H	H
b	Cl	H
c	Cl	Cl
d	Br	H
e	CH_3	H
f	OCH_3	H



3

	R^1	R^2
a	H	H
b	F	H
c	H	F
d	H	CH_3



4

Figure 1. Chemical structures of various α,β-unsaturated styryl ketones used in this study. The compounds belonged to four series (Series 1: NC711, NC741; Series 2: NC1128, NC1109, NC1110, NC1184, NC1129, NC1111; Series 3: NC120, NC744, NC816, NC818; Series 4: NC742). Structural analogues were synthesized by substitution at the indicated positions on the aryl ring.

A comparison of the MIC values of NC711 and NC741 reveals that the former analogue with a chloro atom instead of a methoxy group at the para position of the aryl ring is four times more active than the latter. In general, compounds belonged to Series 2 possess greater antifungal activity against *A. fumigatus* (except NC1128 and NC1111) than members of Series 1, 3 and 4. NC1110 with the chloro atom substituents at the para and ortho positions of the aryl ring is the most active compound against *A. fumigatus* with an MIC value of 32 μM. A comparison of the analogues of Series 2 and 3 reveals that perhaps a piperidino function instead of dimethylamino group may contribute significantly to the ability of the former compounds to inhibit the growth of *A. fumigatus*. Similarly, a comparison of the MIC values of compounds of Series 1 and 3 shows that the more hydrophobic diethylamino group

carrying compounds are more active than the ones with dimethylamino group. Therefore, the increased activity of the compounds in Series 1 compared to the activity of those of Series 3 may be due to the increased overall hydrophobicity of the former compounds. NC742 was synthesized to test whether the keto function is absolutely essential for the bioactivity of these compounds. The fact that NC742 has moderate but significant activity against *A. fumigatus* indicates that replacement of the keto function with a hydrazone is somewhat tolerated and the resulting molecule has significant bioactivity. Thus, the hydrazone derivatives of conjugated styryl ketones could be an option to pursue in the future for increased antifungal activity of these compounds. Our previous structure-function studies of α,β-unsaturated styryl ketones revealed that the overall hydrophobicity and the electron attracting property of the molecules are directly correlated with their antifungal activity (11). For instance, NC1110 which is the most active compound against *A. fumigatus* has the highest overall hydrophobicity and electron attracting property.

Table 1. Minimum Inhibitory Concentrations of various thiol-alkylators for *A. fumigatus* and *C. albicans*

Thiol-alkylator	Minimum Inhibitory Concentration (μM)	
	A. fumigatus	*C. albicans*
NC711 (1a)	1024	512
NC741 (1b)	2048	2048
NC1128 (2a)	1024	1024
NC1109 (2b)	256	256
NC1110 (2c)	32	64
NC1184 (2d)	128	128
NC1129 (2e)	128	256
NC1111 (2f)	1024	1024
NC120 (3a)	2048	2048
NC744 (3b)	2048	2048
NC816 (3c)	2048	2048
NC818 (3d)	1024	1024
NC742 (4)	512	256
N-ethylmaleimide	32	318

As shown in Table 1, we also have compared the results obtained for *A. fumigatus* with those obtained for *C. albicans*. Although there are some minor variations in the actual MIC values of these compounds for these two organisms, the pattern of susceptibility of *C. albicans* and *A. fumigatus* to these thiol-blockers is very similar.

N-ethylmaleimide (NEM) is a well-known penetrating thiol-blocker. NEM was used as a control to obtain a comparative estimate of the potency of various α,β-unsaturated styryl ketones we used in the study. As expected, NEM is highly effective against *A. fumigatus*, and more potent than the conjugated styryl ketones. However, in the case of *C. albicans*, both NC1110 and NC1128 were more effective than NEM, and the exact reason for this finding is not understood.

Very little is known about the mode of action of α,β-unsaturated styryl ketones resulting in the inhibition of fungal growth. Low molecular weight thiols as well as protein-associated thiols could be the targets. However, our previous studies with *C. albicans* revealed that the enzymes involved in glutathione utilization are not the primary targets of these thiol-alkylators. For example, inhibition of γ-glutamyltranspeptidase, glutathione S-transferase, glutathione reductase and glutathione peroxidase by these compounds showed no correlation with the MIC values (11). It is known that the synthesis and the assembly of cell wall of fungi are highly dependent on the availability of intracellular thiols (15). Perhaps, a key

component(s) involved in the synthesis of cell wall is inhibited by these compounds. Alternatively, it is reported that the proton translocating ATPase of *Saccharomyces cerevisiae* and *C. albicans* are highly susceptible to non-penetrating thiol-blockers such as p-chloromercuriphenyl sulfonate (16). The susceptibility of the ATPase to thiol-blockers is highly dependent on a critical cysteine (C148) of the enzyme. Mutant enzymes variant at this position are not affected by thiol-blockers. ATPase, a membrane bound enzyme, may be easily accessible to these reagents from outside, and could become a vulnerable target.

ACKNOWLEDGEMENTS

The authors wish to thank the National Science Foundation (Grant HRD 92-53037) and the Howard Hughes Medical Institute (Grant 71194-527-802) for their support.

REFERENCES

1. Rinaldi, M.G. Invasive aspergillosis. Reviews of Infectious Diseases, 5: 1061-1077, 1983.
2. Welsh, R.A. and Buchness, J.M. Aspergillus endocarditis, myocarditis and lung abscesses: report of a case. Am. J. Clin. Pathology, 25: 782-786, 1955.
3. Young, R.C., Bennett, J.E., Vogel, C.L., Carbone, P.P. and DeVita, V.T. Aspergillosis: the spectrum of disease in 98 patients. Medicine, 49: 147-173, 1970.
4. Young, R.C., Jennings, A. and Bennett, J.E. Species identification of invasive aspergillosis in man. Am. J. Clin. Pathology, 58: 554-557, 1972.
5. Gercovich, F.G., Richman, S.P., Rodriguez, V., Luna, M., McCredie, K.B. and Bodey, G.P. Successful control of systemic Aspergillus niger infections in two patients with acute leukemia. Cancer, 36: 2271-2276, 1975.
6. Tilden, E.., Hatton, E.H., Freeman, S., Williamson, W.M. and Koenig, V.L. Preparation and properties of the endotoxins of *Aspergillus fumigatus* and *Aspergillus flavus*. Mycopatholoigia et Mycologia Applicata, 14:325-346, 1961.
7. Kothary, M.H., Chase, T. Jr and Macmillan, J.D. Correlation of elastase production by some strains of *Aspergillus fumigatus* with ability to cause pulmonary invasive aspergillosis in mice. Infection and Immunity, 43: 320-325, 1984.
8. Kolattukudy, P.E., Lee, J.D., Rogers, L.M., Zimmerman, P., Ceselki, S., Fox, B., Stein, B. and Copelan, E.A. Evidence for possible involvement of an elastolytic serine protease in aspergillosis. Infection and Immunity, 61: 2357-2368, 1993.
9. Manavathu, E.K. et al., unpublished data, 1994.
10. Ramundo, M.B. and Koletar, S.L. Invasive Aspergillus infection in AIDS patients.Abs. no. 77, In Abstracts of the 1994 IDSA Annual Meeting, Orlando, Florida.
11. Dimmock, J.R., Kumar, P., Manavathu, E.K., Obedeanu, N. and Grewal, J. Activity of some Mannich bases of conjugated styryl ketones against *Candida albicans*. Pharmazie, 49: (H.12) 909-912, 1994.
12. Mutus, B., Wagner, J.D., Talpas, C.J., Dimmock, J.R., Phillips, O.A. and Reidt, R.S. 1-p-Chlorophenyl-4,4-dimethyl-5-diethylamino-1-penten-3-one hydrobromide, a sulfhydryl-specific compound which reacts irreversibly with protein thiols but reversibly with small molecular weight thiols. Anal. Biochem., 177:237-243, 1989.
13. Manavathu, E.K., Alangaden, G.J. and Lerner, S.A. Manuscript in preparation, 1994.
14. National Committee for Clinical Laboratory Standards. NCCLS Publication M27-P, 1992.
15. Robson, J.E. and Stockly, H.M. Sulfhydryl metabolism of fungi grown in submerged culture. J. Gen. Microbiol., 28:57-68, 1962.
16. Monk, B.C., Feng, W.C., Marshell, C.J., Seto-Young, D., Na, S., Haber, J.E. and Perlin, D.S. Modelling a conformationally sensitive region of the membrane sector of the fungal plasma membrane proton pump. J. Bioenerg. Biomemb., 26:101-115, 1994.

What Is Kamboucha?

Tia M. Barringer

Department of Biology
Russell Sage College
45 Ferry Street
Troy, NY 12180

Faculty Advisors:

Jack Harris and Robert Gehrig

ABSTRACT

In the present study, the phylogenetic status and reproductive physiology of Kamboucha were examined. Kamboucha produces an acidic broth that Kamboucha owners drink. Apparently, Kamboucha produces alleged benefits for the human body, such as, erasing wrinkles, soothing aches and pains, and raising T-cell counts in AIDS patients. Because Kamboucha has gained popularity throughout the United States, it was important to investigate the basic biology of this organism. By performing a series of fermentation and isolation techniques, research concluded Kamboucha to be a fungus composed of a yeast, *Torulaspora delbrueckii* and a bacterium, possibly a Fusiform. By altering growth solutions, results concluded that Kamboucha metabolically grows best in a solution of tea and sucrose or brown sugar. A concern is that people may be improperly growing Kamboucha, thereby, contaminating the broth and possibly producing health risks.

INTRODUCTION

Kamboucha is a fungus that has been known to exist in Asia for over 2000 years (Karlin, 1995). It has recently become popular throughout the United States. Kamboucha is sold in health food stores and by individual Kamboucha farmers. It is grown in a tea and sugar broth and after one week the broth produced by Kamboucha supposedly benefits the human body. Kamboucha is sometimes called the "Magic Mushroom," because there are reports that Kamboucha broth has erased wrinkles and brown spots, eased menopause, soothed aches and pains, fought constipation, multiple sclerosis, bronchitis, asthma, coughing, allergies, aching nerves, kidney problems, cataracts, colitis, nervous stomach, lowered cholesterol levels, burned fat, relieved cellulite, helped insomnia, diarrhea and stopped balding (Pryor, 1993). Also, Kamboucha has been suggested to prevent certain types of cancer, inactivate some viruses, and increase the number of T-cells in AIDS patients (Pryor, 1993). However, as of December 1994, little information about Kamboucha had been published in scientific journals. What is Kamboucha biologically? This was the major focus of my research.

METHODS

It has been stated that Kamboucha is a combination of yeast and bacteria (Karlin, 1995). However, the genera and species of neither component have been identified. The identification of the yeast was accomplished by a series of fermentation and growth experiments. Fermentation experiments included recording the gas production of the yeast within Durham test tubes filled with concentrations of glucose, sucrose, maltose, lactose, trehalose, or cellobiose. Growth experiments included a starvation technique using different carbohydrate-rich media such as cornmeal and malt; inoculations in test tubes of mycosel, urea, nitrate, and citrate; and streak plating nutrient, blood, and cystine heart hemoglobin media. The temperature was also varied between 25 degrees and 42 degrees Celsius. A final experiment was performed with the use of the API 20c clinical yeast system test (bio Merieux, 1992 & Ayerst Labs, 1982), in which the yeast was tested with twenty different sugars (Table I). Data gathered from these techniques were entered into a computerized yeast identification program called "Yeast: Yeast Determination with a New Computerized Program" (DeVroey & Raes-Wuytack).

The bacterium has been quite difficult to identify. The yeast and bacterium share a symbiotic relationship, and the bacterium will not grow without the yeast. By placing a piece of the Kamboucha within the center of a blood agar plate, restricted growth of bacteria did form around the organism. However, after streak plating blood, nitrogen fixing hydrocarbon oxidizers and nutrient mediums with the isolated bacteria, growth discontinued. Additional carbohydrate-rich media, such as egg yolk and burcella, were used and no growth was observed. Also, growth in an anaerobic condition was unsuccessful.

The reproductive physiology of Kamboucha was also investigated. Kamboucha expands horizontally until the ends of its container are met, and simultaneously produces a new layer of membrane each time it receives its nutrients of tea and sugar. To investigate environmental requirements for growth, the growth of Kamboucha was measured in various solutions. By varying types of sugars and sugar substitutes with black tea, using tea without sugar, tap water with sugar, and just tap water broth, the most extensive and rapid growth of Kamboucha was measured.

RESULTS

After conducting the extensive isolation and identification experiments, the yeast was concluded to be *Torulaspora delbrueckii* (Table I.). *T. delbrueckii*, is a white to cream-colored yeast with butyrous colonies, budding, pseudohyphae, and asci (reproductive state). Synonyms of *T. delbrueckii* include organisms of *Debaryomyces*, *Saccharomyces*, and *Zygosaccharomyces* species. Asexually, *T. delbrueckii* is known as *Candida colliculosa*. *T delbrueckii* has existed in ragi (Indonesian starter yeast), grapes, soil, barks of trees, and sheep's milk (Barnett, 1990).

Table I: Fermentation and Growth Analysis of *Torulaspora delbrueckii*

Fermentation:	
Glucose +	Sucrose +
Maltose -	Lactose -
Trehalose -	Cellobiose -
Growth:	
Glucose +	Glycerol -
2 keto-D-	Arabinose -
Gluconate +/-	Xylose -
Adonitol -	Xylitol -
Galactose -	Inositol -
Sorbose +	Methyl-D-
N-Acetyl D-	glucoside +
glucoamine -	Lactose -
Cellobiose -	Sucrose +
Maltose +	Melezitose +
Trehalose +	Raffinose
0.04% Cyclo-	Urea -
heximide -	Nitrate -
25 degrees C +	Blastoconidia +
37 degrees C +	Pseudohyphae +
40 degrees C +	
42 degrees C -	
	+ positive requirement for growth
	- no requirement for growth
	+/- used but not required

Microscopically, the bacteria appear to be gram-negative rods with pointed ends. The bacteria resemble Fusiforms. However, because further testing cannot be conducted until the bacteria are isolated from the yeast, this identification remains only a possibility. To obtain a pure culture, a centrifuge technique has been attempted, in which the Kamboucha broth of organisms has been purified and a pure sample of the bacteria has been placed within the purified Kamboucha broth. Results have not yet been concluded.

Reproductively, results concluded that Kamboucha grew in each solution, however, the most productive growth occurred in the broth consisting of tea with pure or brown sugar (Table II). Further growth analysis was conducted by a time-lapse video recording extended over one week. As long as Kamboucha is placed in an aerobic carbohydrate-rich environment, it will continue to reproduce.

Table II: Reproductive Rates of Kamboucha in Varied Solutions

Solution	Day 1	Day 2	Day 3	Day 4	Day 5	Day 6	Day 7
Sugar + tea							
Sucrose	3.0 x 1.7	same	3.2 x 1.9	3.8 x 2.8	6.5 x 4.0	6.0 x 5.8	6.6 x 5.8
Sucrose, Dextrose	3.0 x 2.0	same	3.1 x 2.4	5.0 x 3.2	5.8 x 4.5	6.0 x 6.1	same
Confectionery sugar	2.8 x 2.0	same	2.8 x 2.2	3.0 x 2.5	6.0 x 3.5	6.3 x 6.1	same
Brown sugar	2.5 x 1.5	same	2.5 x 2.2	2.8 x 2.2	5.2 x 5.1	6.2 x 6.7	same
Maltodextrin, Aspartame (Nutraweet Brand)	2.7 x 2.0	same	same	same	3.1 x 3.1	*	*
Nutritive Dextrose, Calcium, Saccharin (Sweet 'n' Low)	2.8 x 2.0	same	2.8 x 2.0	3.1 x 2.3	4.0 x 6.2	4.2 x 6.2	5.5 x 6.5
Dextrose, Maltodextrin, Aspartame (Equal)	3.0 x 1.9	same	3.0 x 2.0	3.4 x 2.0	6.1 x 5.6	same	same
Tap water:	3.0 x 2.0	same	2.5 x 2.0	2.5 x 2.1	2.5 x 2.0	2.5 x 2.1	same
W/o sugar:	1.2 x 1.2	same	same	3.5 x 3.6	3.1 x 2.8	3.0 x 3.2	same
W/o tea:	1.2 x 1.1	1.2 x 1.2	1.2 x 1.1	3.2 x 3.0	2.8 x 3.5	3.7 x 3.4	same

measured in cm.
* not measurable

CONCLUSIONS

Kamboucha has been loosely termed a "mushroom." But this investigation shows that Kamboucha is not a mushroom. Microscopically, Kamboucha is composed of filaments (actually the mesh of bacteria) that resembles the structure of a mushroom. Also, Kamboucha is cylindrical and gel-like in appearance.

This research has concluded that Kamboucha is a symbiotic association of *Torulaspora delbrueckii* and a Fusiform and that it grows very well in a carbohydrate solution of tea and sugar. The medical effects of Kamboucha were not evaluated, but reason for concern about home use of the Kamboucha broth was uncovered.. Considering, many Kamboucha broth drinkers are naive about the contents of Kamboucha and most likely do not use sterile techniques and because it is aerobically grown at room temperature, an individual's health can be at risk from other organisms that can contaminate the Kamboucha broth. After exposing pieces of Kamboucha membrane in tea and sugar broth to the air, the presence of *Penicillium* and possibly *Humicola* and *Cladosporium* species were observed. Because Kamboucha did not inhibit the growth of these molds, ingestion of Kamboucha contaminants could affect its drinkers.

Kamboucha is a fascinating organism. The research conducted has presented a basis on which additional research of Kamboucha can be planned. For example, currently, examinations of the inhibition of *Staphylococcus aureus* by the acidity of Kamboucha broth and throat cultures administered on Kamboucha broth drinkers and non-drinkers are in progress. Perhaps, in the future, Kamboucha will be investigated from a medical standpoint and the healing powers of Kamboucha will be evaluated.

ACKNOWLEDGMENTS

The author wishes to express great gratitude to Sally Gromadzki and Rama Ramani for enabling her to use the facilities of the Axelrod mycology laboratory and for all their help and patience.

REFERENCES

API, analytical profile index: yeast. Ayerst Laboratories Division of American Home Products Corporation, New York. 1982.

API 20c analytical profile index: clinical yeast system. bioMerieux Vitek, Inc., France, 1992.

Barnett, J.A. et al., Yeasts: Characteristics and identification, second edition. Cambridge University Press, New York. 1990. pg. 647-48.

DeVroey, Ch. and Raes-Wuytack, C., Yeast: Yeast determination with a new computerized program. Lab for Mycology, Institute of Tropical Medicine, Belgium.

Ellis, M.B., Dematiaceous Hyphomycetes. Commonwealth Mycological Institute, Kew. 1971. pg. 59-62, 308-319.

Pryor, B., Network News, AIDS and the enigmatic mushroom, Aug 1993.
Timmons, S., New Age Journal, Fungus among us, Nov/Dec 1994, pg 78-96.

Mechanisms of Phorbol Ester-Induced Cell Death in EL4 Cells

Sandra Fulwood and K. Meyer

Dept of Biology, Claflin College
Orangeburg, SC 29115
and
Medical University of South Carolina
Charleston, SC 29558

Faculty Advisor:

W.W. Gearheart

Cells, as the basic unit of life, are constantly dying and being replaced in multicellular organisms. Two mechanisms of cell death were investigated, programmed and non-programmed. Apoptosis is a form of programmed cell death which occurs through a series of morphologically distinct alterations, including condensation and phagocytosis. Lysis, a form of non-programmed cell death, results from the loss of membrane integrity and can be measured by the release of lactate dehydrogenase (LDH). Wild type (WT) EL4 cells are killed by phorbol esters, while the new variant (NV) EL4 cells are not. The goal of this study was to determine whether phorbol esters caused programmed or non-programmed death in EL4 cells. Two assays were conducted to determine the type of cell death that results from phorbol-12 myristate acetate (PMA) exposure. The apoptosis assay revealed that untreated WT and NV EL4 cells undergo some level of apoptosis naturally. The phorbol ester used did not change the extent of DNA fragmentation, therefore, it was concluded that PMA does not kill WT EL4 cells by apoptosis. Results from the lysis assay showed that incubation of WT cells with PMA for 3 hours resulted in LDH release. It was therefore concluded, that in time, PMA does cause lysis, or non-programmed death, of WT cells.

INTRODUCTION

Sensitive, or wild-type, cells respond to phorbol 12-myristate 13-acetate (PMA) with induction of interleukin-2 (IL-2) synthesis, while insensitive, or variant cells, do not exhibit this response (Harrison et al., 1987). Variant cells, which were originally selected for survival in the presence of chronic incubation with phorbol ester, retain their resistant phenotype when cultured in the absence of phorbol ester (Sando et al., 1982). The nature of the critical differences between wild-type and variant cells has not been established. Activation of the mitogen-activated protein kinase (MAPK) phosphorylation cascade is elicited by various mitogenic agonists, including phorbol esters (Davis, 1993). Meier et al., (1991) has shown that activation of MAPKs is induced by PMA in wild-type but not in variant EL4 cells. The lack of response was also seen for pp90 ribosomal S6 kinase (RSK), a kinase that is activated by MAPK, and for MAPK kinase (MEK), the kinase that activates MAPK (Gause et al., 1993). All of these kinases are expressed in both wild-type and variant EL4 cells, and can be activated in variant cells in response to okadaic acid (OA) (Meier et al., 1991; Gause et al., 1993), a protein phosphatase inhibitor with tumor promoter activity (Cohen et al., 1990).

MATERIALS AND METHODS

Cell proliferation and viability assays

EL4 cells were cultured in multiwell plates (1ml/well) in culture medium to which various compounds were added. PMA, 4-PMA, thymeleatoxin, mezerein, indolactam v, prostratin (12- deoxyphorbol-13-acetate), phorbol 12-tigliate-13-decanoate, and 4-O-methyl PMA were obtained from LC Services. After 20-24 hours, aliquots of cells were resuspended in a solution containing trypan blue and counted using a hemacytometer. Cell viability was assessed by trypan blue exclusion. For experiments in which the effects of PKC activators on cell morphology were examined, EL4 cells were photographed using a Nikon Diaphot microscope with Hoffman interference optics (20X objective).

Apoptosis and LDH Assays

During the apoptosis assay, cell were treated with 100nM phorbol-12 myristate acetate (PMA) overnight. Cells were then collected, washed , resuspended in 500 µl of lysis buffer and added to an equal volume of phenol:chloroform. This solution was centrifuged at 16,000 g for 5 minutes, then mixed with 50 µl of 3M NaACo and 2 volumes of 100% ETOH. The solution was centrifuged again at 16,000 g for 5 minutes. The pellet was collected and washed with 70% ETOH. After a third centrifugation, the pellet was left to air dry. After drying, 25 µl of TE (with .1 mg/ml RNAase) was added and the solution left to incubate overnight at 37 °C. The following morning, 5 µl loading buffer and a DNA standard were added to the mixture. A 1.8% agarose gel was used to electrophorese 20 µl of the mixture at 80 v for 1.5 hours. The gel was then viewed under UV light.

The lactate dehydrogenase (LDH) assay used WT and NV EL4 cells that had been incubated with tumor promoters for 2-24 hours. Microcentrifuge tubes containing cells and/or medium with or without lysis buffer were incubated for 45 minutes at 37 °C. Aliquots of 5, 10 and 25 µl, along with LDH substrate mix, were added to 96 well plates and incubated at room temperature for 30 minutes. A stop solution was added to complete the reaction. The LDH concentration in the medium was used as a measure of cell lysis and LDH concentration in cells indicated cell numbers.

In the viability assay, WT and NV EL4 cells were treated with 100 nM PMA for 1-48 hours. Then 90 µl of cells solution was added to 10 µl of .4% trypan blue. Cells were counted using a hemacytometer and a percentage of viable cells was determined.

RESULTS AND DISCUSSION

Treatment of WT cells with PMA for 24 hrs resulted in much lower cell numbers, while the viability (cell number as % of control) was not decreased in NV EL4 cells (Table 1) . PMA and 4αPMA, compounds used throughout this study, showed 58 and 78 percent viability, respectively with WT cells. Other phorbol esters causing considerable cell death included 4OmethylPMA (20%), thymealotoxin (35%) and mezerein (43%). It appears from these results that phorbol esters that activate protein kinase C was toxic to WT but not NV EL4 cells . The apoptosis assay revealed no difference between WT or NV EL4 cells treated with PMA, since the same amount of laddering was seen in WT and NV EL4 cells (gel not shown). The final assay, for LDH production indicative of non-programmed cell death, indicated that WT EL4 cells were apparantly killed via non-programmed cell death, as were NV EL4 cells (Table 2). As seen in Table 2, WT cells treated with PMA (WTP) had 18% of the maximum release of LDH after three hours, while WT cells treated with 4alphaPMA (WT4P) had released almost 15% of the maximum LDH. Non-programmed cell death also was seen to occur in NV cells also, althought to a lesser degree (Table 2).

In the sensitive (WT) cell line, phorbol ester treatment activates the MAPK phosphorylation cascade. This response is present in most mammalian cells, including primary T-cells and T-cell lines. Resistant (NV) cells represent an exception. NV cells not only fail to show significant activation of MAPK in response to phorbol ester, but are resistant to the toxic effects of this tumor promoter. A causal link between the failure to activate MAPK, failure to synthesize IL-2, and resistance to toxicity remain to be established. A new variant cell line, with a phenotype similar to that of previously-derived variant lines, was readily selected by incubation of WT cells with phorbol ester. This result suggest either that all aspects of the phenotype arise from the same molecular variation, or that these properties arise independently but together contribute to the phorbol ester-resistant phenotype.

These results indicated that PMA-induced cell death in WT EL4 cells appears to arise via a non-programmed mechanism (i.e., does not involve apoptosis). This is consistent with data obtained for other lymphoid cell systems, in which phorbol esters are generally inhibitors of apopotic cell death (Obeid et al., 1993). T-lymphocyte cell lines, unlike fibroblast cell lines, proliferate continuously in culture an dare not easily made quiescent. This may indicate that suppression of proliferation is sufficient to provoke cell death, and that the ability of PKC activators to inhibit cell growth is an

important component of their toxic effect. However, the observation that the activators induce morphological changes in WT but not NV cells suggests that cytoskeletal changes resulting from PKC activation may also be involved in the toxicity. Further studies will be required to address these points.

TABLE 1. Percent viability of WT and NV EL4 cells treated with various phorbol esters.

COMPOUND	CELL TYPE	
	WT EL4	NV EL4
Control	80	80
PMA	58	70
4αPMA	78	82
Thymealotoxin	35	77
Mezerein	43	79
Indolactam V	58	65
Bryostatin	59	70
Prostatin	57	80
4OmethylPMA	20	68
P12tigliate13dec	45	65

TABLE 2. LDH release[a] for WT and NV EL4 cells treated with PMA[b]

COMPOUND	CELL TYPE	
	WT EL4	NV EL4
Control	14	10
PMA	18	8
4αPMA	14	8

[a]LDH release reported as percent of maximum
[b]4αPMA has been shown to be a weak tumor promoter.

LITERATURE CITED

Cohen, P., Holmes, C.F.B., and Tsukitani, Y. (1990) *T.I.B.S.*, 15, 98-102.
Davis. R.J. (1993) *J. Biol. Chem.*, 268, 14553-14556.
Gause, K.C., Homma, M.K., Licciardi, K.A., Seger, R., Ahn, N.G., Petrson, M.J., Krebs, E.G., and Meier, K.E (1993) *J. Biol. Chem.*, 268, 16124-16129, 1993.
Harrison, J.R., Lynch, K.R., an dSando, J.J. (1987) *J. Biol. Chem.*, 262, 234-238.
Meier, K.E., Licciardi, K.A., Haystead, T.A.J., and Krebs, E.G. (1991) *J. Biol. Chem.*, 256, 1914-1920, 1991.
Obeid, L.M., Linardic, C.M., Karolak, L.A., and Hannun, Y.Y. (1993) *Science*, 259: 1769-1771.
Sando, J.J., Hilfiker, M.L., Piacentinin, M.J., and Laufer, T.M. (1982) *Cancer Res.*, 42: 1676-1680.

A Comparison of the Seed Banks of Adjacent Disturbed and Undisturbed North Carolina Wetlands

Carolyn Wells

Department of Biology
University of North Carolina at Asheville
One University Heights
Asheville, NC 28804-3299

Faculty Advisor:

Dr. James Perry

INTRODUCTION

Wetlands represent sources of immense biodiversity and critical habitats for the numerous flora and fauna that inhabit them. However, mountain bogs in the state of North Carolina are being damaged, often irreversibly, by human activity. Only an estimated 500 acres of bogs remain in the southern Appalachians (Weakley and Moorhead, 1991). To prevent the total disappearance of this ecosystem type in the southern Appalachians, restoration of damaged bogs is being encouraged by natural resource managers. One important component of wetlands restoration is the soil seed bank. The soil seed bank consists of the viable seeds located on and in the soil or associated litter (Leck et al. 1989). The seeds represent both current and previous vegetation. Soils can contain viable seed reserves in excess of 400 years old (Gunther et al. 1984). Depth distribution also varies, with the largest percentage of viable seeds generally located within the top 5 cm (Nicholson and Keddy 1983). Numerous studies of soil seed banks have determined characteristics such as the spatial arrangement of seeds in the soil (Lindhart 1976) and species-specific germination requirements (Harper and Benton 1966; Thompson and Grime 1983; Moore and Keddy 1987). Recent studies have assessed the effects of disturbance, either natural or human-induced, upon the seed bank (e.g., Morgan and Neuenschwander 1988; Leck et al. 1989; Wisheu and Keddy 1991; McGee and Feller 1993).

Comparing disturbed and undisturbed habitats using their seed banks can contribute to our understanding of ecosystem disruptions and the possibilities for restoration (McGee and Feller 1993). A greater understanding of seed banks can lead to their integration into ecosystem restoration (e.g., Moore and Wein 1977; Morgan and Neuenschwander 1988; van der Valk et al. 1992), as well as assist with predictions of community responses to disturbances (Keddy et al. 1989).

The objective of this study was to compare the seed banks of adjacent disturbed and undisturbed portions of a mountain bog in western North Carolina. A restoration plan is being developed for the disturbed bog, and the seed bank study was part of a preliminary assessment of the ecosystem.

MATERIALS AND METHODS

Study site

The study area is a wetland (Tulula Bog) located in Graham County, North Carolina. It is 4.8 km west of Topton, at an elevation of 799 m. The site and surrounding floodplain were owned by the U.S. Forest Service until 1989, when they were traded to a developer for the commercial construction of a golf course. Part of the site was classified as representative of a swamp forest-bog complex (Schafale and Weakley 1990).

Tulula Bog is actually a complex of small bogs which are typically less than .40 ha in size (Schafale and Weakley 1990). Portions of the bog were stripped of vegetation and drained for development of the golf greens and fairways. In intact portions of the bog, the dominant vegetation includes red maple (*Acer rubrum*), elderberry (*Sambucus canadensis*), chokeberry

(Sorbus spp.),and tussock sedge (Carex stricta), with scattered peat moss (Sphagnum spp.). Part of the intact bog is covered by an overstory (closed canopy area), and part has thick undergrowth but no overstory (open canopy area).

Field and Lab Methods

In May 1994, a grid of 10x10m plots was established in the wetlands. On June 2, 3, and 4, 1994, soil samples were collected from randomly chosen plots within this grid, including samples from closed canopy undisturbed plots (n=20), open canopy undisturbed plots (n=20), and disturbed plots (n=12). Forty-five soil cores (2.5 x 5.0 cm) were collected from each plot with a soil probe. Loose surface litter was brushed aside before taking each sample, and the probe was wiped clean between plots to avoid transfer of seeds. Samples from each plot were composited and kept on ice in a cooler at the site. On June 6, 1994, samples were transferred to a refrigerator.

Samples were potted on July 16, 1994. Each composite sample was thoroughly mixed before it was potted in triplicate. Approximately 2 cups (8.5 oz) of sterile potting soil were placed in 4-in square pots, and one-third of the composite sample was placed on top of the potting soil. Pots were kept in an unheated greenhouse until October 14, 1994, then transferred to a heated greenhouse.

The pots were watered daily from June 16 until November 20, 1994. After that date, pots were kept moist until February 20, 1995. As seedlings matured to the extent that species characteristics were detectable, they were removed from the pots and pressed. Nomenclature follows Radford et al. (1964).

Data analysis

All species were classified with three variables: as annual or perennial, monocot or dicot, and wetland indicator status (Reed 1988). The four indicator classes were: OBL (obligate wetland species), FACW (facultative wetland species), FAC (facultative species), and FACU (facultative upland species). An obligate species is found >99% of the time in wetland habitats. The remaining categories are distributed as follows: facultative wetland species, 67-99%; facultative species, 33-66%; and facultative upland species 1-32%. For each variable, t-tests (alpha = 0.05) were performed comparing the disturbed vs. undisturbed wetlands and closed vs. open canopy areas of the undisturbed wetland.

RESULTS

Twenty-six species germinated during the course of the study (Table 1). A large number of graminoids (largely grasses, sedges, and rushes) also germinated. However, these never reached reproductive maturity, so they were not identified to species.

Significantly more FAC ($p = 0.02$) and FACW ($p < 0.0001$) seedlings emerged in the disturbed than in the undisturbed wetland (Fig.1a). The disturbed wetland also produced significantly more perennials ($p = 0.0001$) and dicots ($p < 0.0001$) than the undisturbed wetlands (Figs.1b,c). The mean distribution of species by wetland indicator status was similar in the seed banks of both the closed and open canopy undisturbed wetlands (Fig.1d). However, the open canopy area germinated significantly more annuals ($p = 0.01$) and monocots ($p < 0.0001$) than the closed canopy area (Figs.1e,f).

DISCUSSION

Hydrology is an important feature of wetland habitats, and has great influence on seed germination (Mitsch and Gosselink 1993). As hydrology deviates in the disturbed wetlands, the number of facultative species should increase and the number of obligates should decrease. The results of this data supported this transition in the disturbed wetlands.

This study also showed that the open canopy area of the undisturbed wetland contained significantly more annual and

monocot species than the closed canopy area. This may be due to the amount of standing water and sunlight intercepted in this area. A companion study at Tulula Bog is analyzing the above-ground vegetation in these wetlands, and will eventually correlate similarities between the seed bank and standing vegetation. The results of this study will help predict the responses of different parts of the wetland to re-flooding during restoration. Annuals, which have explosive growth patterns and short life cycles, establish rapidly after germination. However, my study has shown that perennials are the most readily germinable seeds in the disturbed wetland.

In conclusion, this study has provided valuable information on the composition of the seed bank at Tulula Bog. Once the analysis of above-ground vegetation is complete, the seed bank will be compared with standing vegetation, and used to plan the restoration of the disturbed wetland.

LITERATURE CITED

Grime, J.P. 1989. Seed banks in ecological perspective. In: "Ecology of soil seed banks" (Leck, M.A., V.T. Parker, R.L. Simpson, eds.). Academic Press, Inc., San Diego, CA.

Keddy, P.A., I.C. Wisheu, B. Shipley, and C. Gaudet. 1989. Seed banks and vegetation management for conservation: Toward predictive community ecology. In: "Ecology of soil seed banks" (M.A. Leck, V.T.Parker, and R.L. Simpson, eds). p.347-363. Academic Press, Inc., San Diego, CA.

Leck, M.A., V.T. Parker, and R.L. Simpson, (Eds.) 1989. Ecology of soil seed banks. Academic Press, San Diego, CA.

McGee, A. and M.C. Feller. 1993. Seed banks of forested and disturbed soils in southwestern British Columbia. Canadian Journal of Botany 71: 1574-1583.

Mitsch, W.J. and J.G. Gosselink. Wetlands. 1993. 2nd ed. Van Norstrand Reinhold, NY.

Moore, J.M. and R.W. Wein. 1977. Viable seed populations by soil depth and potential site recolonization after disturbance. Canadian Journal of Botany 55:2408-2412.

Morgan, P. and L.F. Neuenschwander. 1988. Seed-bank contributions to regeneration of shrub species after clear-cutting and burning. Canadian Journal of Botany 66:169-172.

Nicholson, A. and P.A. Keddy 1983. The depth profile of a shoreline seedbank in Matchedash lake, Ontario. Canadian Journal of Botany 61: 3293-3296.

Radford, A. E., H.E. Ahles, and C. R. Bell. 1964. Manual of the flora of the Carolinas. The University of North Carolina Press, Chapel Hill, NC.

Reed, P.B., Jr. 1988. National list of plant species that occur in wetlands: Southeast (Region 2). Biolog. Rep. 88 (26.2). U.S. Fish and Wildl. Serv., Washington, D.C.

Roe, C. 1984. Report to the North Carolina Natural Heritage Program. North Carolina Dept. Environ. Health and Natural Resourc. Raleigh, NC.

Schafale, M.P. and A.S. Weakley. 1990. Classification of the natural communities of North Carolina. Third Approximation. North Carolina Natural Heritage Program. North Carolina Dept. Environ. Health and Natural Resourc. Raleigh, NC.

van der Valk, A.G., R.L. Pederson and C.B. Davis. 1992. Restoration and creation of freshwater wetlands using seed banks. Wetlands Ecology and Management 1:191-197.

Weakley, A.S. and K.K. Moorhead. 1991. Conservation of southern Appalachian bogs and fens. Paper presented at: Annual meetings of The Association of Southeastern Biologists. Boone, NC.

Wisheu, I.C. and P.A. Keddy. 1991. Seed banks of a rare wetland plant community: distribution patterns and effects of human-induced disturbance. Journal of Vegetation Science 2:181-188.

Table 1. Species list with categories* of emerged seedlings.

Family	Species	IND	HAB	FORM
Aceraceae	Acer rubrum L.	FAC	P	D
Asteraceae	Erechtites hieracifolia (L.) Raf.	FAC	A	D
Asteraceae	Eupatorium perfoliatum L.	FACW	P	D
Cyperaceae	Cyperus retrorsus Chapman	FACU	P	M
Cyperaceae	Cyperus strigosus L.	FACW	P	M
Cyperaceae	Eleocharis obtusa (Willd.) Schultes	OBL	A	M
Cyperaceae	Eleocharis sp.	U	U	M
Euphorbiaceae	Acalypha rhomboidea Raf.	FAC	A	D
Hypericaceae	Hypericum mutilum L.	FACW	P	D
Juncaceae	Juncus spp.	U	U	M
Lamiaceae	Lycopus virginicus L.	OBL	P	D
Melastomataceae	Rhexia mariana L.	FACW	P	D
Onagraceae	Ludwigia palustris (L.) Ell.	OBL	P	D
Oxalidaceae	Oxalis stricta L.	U	U	D
Plantaginaceae	Plantago sp.	U	U	D
Polygonaceae	Polygonum pensylvanicum L.	FACW	A	D
Polygonaceae	Polygonum sagittatum L.	FACW	U	D
Poaceae	Panicum dichotomum L.	OBL	U	D
Rosaceae	Potentilla sp.	U	P	D
Rosaceae	Rosa palustris Marshall	OBL	P	D
Rosaceae	Rubus hispidus L.	FACW	P	D
Rubiaceae	Galium tinctorium L.	FACW	A	D
Scrophulariaceae	Lindernia dubia (L.) Pennell	OBL	U	D
Scrophulariaceae	Verbascum thapsus L.	U	P	D
Violaceae	Viola blanda Willd.	FACW	U	D
Violaceae	Viola primulifolia L.	FACW	U	D
Vitaceae	Vitis aestivalis Michaux	FAC	P	D

*IND= Wetland Indicator Status; HABIT= Annual (A) or Perennial (P); FORM= Monocot (M) or Dicot (D).

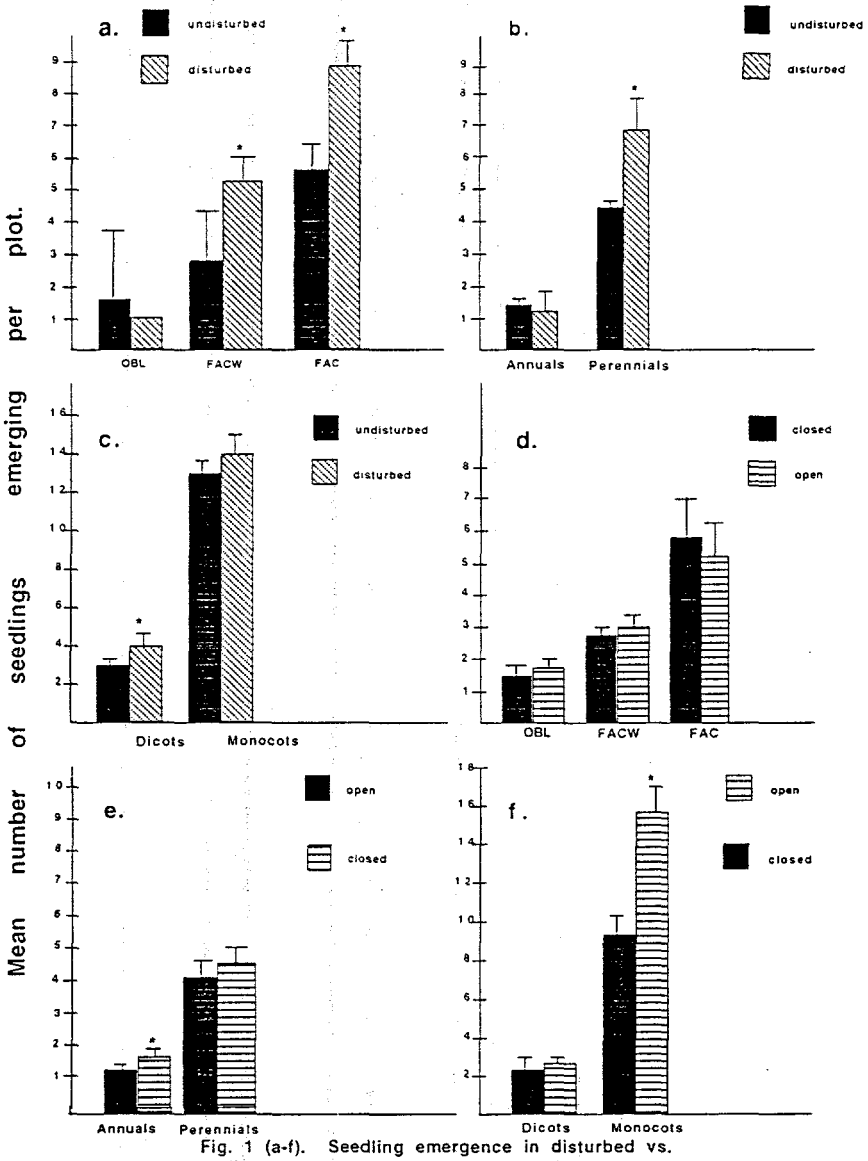


Fig. 1 (a-f). Seedling emergence in disturbed vs. undisturbed wetlands (a-c) and closed vs. open canopy areas of the disturbed wetland (d-f). Means are ± 1 SE. Asterisks indicate a significant difference ($P \leq 0.05$) in the means.

MULTIPLE BIOASSAY OF HOUSATONIC RIVER WATER ABOVE AND BELOW TWO INDUSTRIAL USE SITES

Erik Carlson, Heather Martin and Ana C. Ribeiro

Department of Biology
Western Connecticut State University
181 White St.
Danbury, CT 06810

Faculty Advisor:
Frank J. Dye

Two commonly used bioassays to monitor the quality of natural waters are the Modified Allium Test, and Mouse Cell Line Analysis. The Modified Allium Test is a versatile, short term test that is inexpensive, simple to set up, and sensitive. Allium cepa, common onions, were exposed to water upstream and downstream of two factories on the Housatonic River, in Connecticut. The onions were observed macroscopically (for root length and C-Tumor formation abnormalities), and microscopically (Mitotic Index and Abnormal Cell Division). In addition, 15 day CD-1 Mouse Fetal Cells and Cell Line Analysis were used. Cell cultures were exposed to the same test waters and Mitotic Indices were recorded. Time-lapse video microscopy, colcemid chromosome spreads, and microscopic computer imaging were also used. From all these studies one can conclude that in general the quality of the river water was not as bad as expected, or as depicted by in previous studies. Furthermore, it was found that the biggest shift in water quality occurred between the factories.

INTRODUCTION

Water pollution is an ever growing ecological problem in the industrial regions of the world. Any analysis of natural waters should include a study of the biological effects of the contaminants. Our study involved the use of two bioassays to monitor the toxicity of river water taken from both above and below two industrial plants which utilize Housatonic River water. The Housatonic has a long history of contamination (U.S. Geological survey, 1988). From the early 1930's to 1977, polychlorinated biphenyls (PCBs) were used in the manufacturing of transformers at the General Electric Company plant in Pittsfield, Massachusetts. In 1978, leakage from this plant was found to be the major source of PCBs in the Housatonic River. In 1977, trout fillets from the river were found to contain greater PCB concentrations than the DEP's 5mg PCB per kilogram of fillet tolerance level. In 1984 the Department of Environmental Protection (DEP) lowered the tolerance level for human consumption to 2 mg/kg. Since the termination of their use, PCB levels in the river have dramatically decreased to 0.32 mg/kg in Great Barrington, MA, and less than 0.1 mg/kg (the detectable level) in Kent, CT. Because Kent is some 20 river miles above New Milford it seems that PCB pollution from the electric plant will probably not affect the two test sites' results due to its extremely low levels. The two tests used were the modified Allium Test and Mouse Fetal Cell Line Analysis.

The Allium Test is a recognized test in the study of the effects of mutagenic or carcinogenic pollutants in various waters such as natural waters, drinking water and industrial wastes. This technique is inexpensive, simple to set up, and sensitive. This experiment involves the use of the modified version of the Allium Test as first proposed by Fiskesjo (1985a). Results obtained can be observed both macroscopically and microscopically. Macroscopic observations included both root length and c-tumor formation, while microscopic results were seen in the chromosomal analysis of the root tip cells. Results of the test have been found to compare quite well with other environmental monitoring test systems such as: mammalian cell lines (including human cells), bacteria, and other plants (Fiskesjo, 1985).

Cell cultures grown in test water allow one to view possible in vivo toxicity by the use of in vitro techniques. In vitro toxicity testing is being more frequently used by biomedical researchers due to public demands for more ethical and humane approaches. This relatively new science including in vitro test systems is called in vitro cytotoxicology (Barile, 1994).

To our knowledge neither the Allium Test nor Mammalian Cell Culture Analyses have been conducted on the Housatonic River in Western Connecticut and Massachusetts, but it seems to be a prime candidate for observation. In New Milford, Connecticut, there are several factories which utilize Housatonic River water such as Fidco and Kimberly-Clark. Also, water is pumped from the Housatonic River uphill to Candlewood Lake then allowed to flow down-hill back into

the river by the Rocky River Power Plant on Route 7 in New Milford. These various locations could possibly contaminate the river along with isolated illegal dumping and sewage discharge.

MATERIALS AND METHODS

TEST WATERS

Water samples were collected only once, at the beginning of the semester, and then stored in Finast Brand spring water, one gallon containers. This water was used throughout the semester for our various bioassays. Water samples were categorized as:

AF= Above Fidco
BF= Below Fidco
AK= Above Kimberly-Clark
BK= Below Kimberly-Clark
+ = Positive Control Higgins-Annex water (causes mutation)
- = Negative Control-Well water (doesn't cause mutation)

BIOLOGICAL TEST MATERIAL

The test materials used were onion bulbs from two populations of onions. One population was from Deep's Market in Danbury, CT, and another was from a North Carolina farm. Onions from Deep's Market were tested first followed by the onions from the North Carolina farm. The species of onions used was Allium cepa. This species has 16 large chromosomes with clear and characteristic morphological features suitable for rapid mitotic studies (Fiskesjo, 1985b).

We used CD-1 mouse fetal cells for our cell culture analysis. One reason for using CD-1 mouse fetal cells was because they are easily obtained from mice and are easy to study through cell culture analysis.

MACROSCOPIC METHODS

The Allium Test was done as follows: bulbs of equal size were carefully cleaned and placed on the beakers filled with the water samples to be tested. The onions were supported on the beakers with toothpicks. Each water sample was tested by a series of three individual bulbs. On day three the root lengths were recorded.

MICROSCOPIC METHODS

Allium root tip squash Fixations were made after three days of cultivation. The staining procedure was the acetoorcein squash method to prepare slides. The mitotic index was recorded for each slide (100 observations per slide). Also the metaphase and anaphase cells (50 observations per slide) were classified as: normal anaphase, normal metaphase, delayed anaphase, and sticky anaphase and metaphase. Normal metaphases are ordinarily more frequent than the normal anaphases, but this order may be reversed due to influence of toxic substances (Fiskesjo, 1985b). An accumulation of early anaphases indicates an abnormal situation and is a reliable sign of lowered speed of the entire mitotic process (Fiskesjo, 1981). Abnormal mitosis includes c-mitosis, sticky stages of mitosis and bridges or fragments. Also computer imaging pictures were obtained showing different stages of mitosis (Figures 1-5).

Cell culture McCoy's media was prepared with the six different test waters. Two separate cell cultures per type of growth medium were prepared.

Each cell culture was observed under the phase contrast microscope and computer imaging pictures were obtained (Figure 6). Mitotic indices were determined and abnormalities in mitosis were observed.

Mitotic chromosome spreads were prepared and the slides were stained and studied under a light microscope. Abnormalities in the chromosomes were recorded.

RESULTS

MACROSCOPIC OBSERVATIONS

The growth of Allium roots was shown to be highly variable, and no obvious explanation was found for this variability. This is apparent in onions tested from different populations which grew at highly different rates (Table 1). Also variations were seen between onions of the same population and in the same test water. For example three onions growing in the same water would have very different root lengths, which is reflected in the standard deviations of both populations (Table 1). Due to the discrepancies in root length a definite conclusion could not be made, but some trends were seen. For both populations the positive control roots grew less than the negative control roots. Also below Kimberly-Clark water allowed for the least amount of growth out of the test samples from the river.

MICROSCOPIC OBSERVATIONS

Microscopic observations showed more reliable results. The results obtained microscopically from the two different populations of onions correlated better than the macroscopic results. Both the mitotic index and the classification of dividing cells were interpretable (Table 2).

All slides prepared from root tips grown in the positive control showed no cell division (Figure 2). The cell chromatin was clumped together, yet the nuclear membrane was present. Because of the lack of cell division, mitotic indices could not be determined; however in the discussion we speculate about the relationship between cell division and chromosome clumping.

The mitotic index decreased as the samples were further down stream (Table 2). The highest mitotic index was observed above Fidco, and the lowest was below Kimberly-Clark. The negative control had a higher mitotic index than any test water.

The negative control had 59% of its metaphase and anaphase cells exhibiting normal metaphase (Figure 2), and 40% in normal anaphase. Only 1% of the cells showed delayed anaphase (Figure 3). This water showed the highest percentage of cells in metaphase. Test waters showed a decreasing percentage of metaphase cells and an increasing percentage of anaphase and delayed anaphases stages. Also downstream samples (above and below KC) started showing sticky chromosomes (AK= 0.5%, BK= 0.2%)(Figure 4). Vagrant chromosomes (Figure 5) are also strong evidence of toxicity, which was observed below KC.

Mammalian cell culture analysis gave less clear results. The cells that were cultured seemed to grow equally well in all water samples (Figure 6). Observation under a phase contrast microscope showed no apparent differences in cell morphology or number. All the cultures seemed to become confluent at the same time. No abnormal mitoses were observed in the cultures. We were unable to obtain any chromosome spreads by the colcemid treatment. The LeukoStat stained slides showed some nuclei but no chromosomes were found.

DISCUSSION

From our observations of this experiment we conclude that the Allium test gave better results than the mammalian cell line. The Allium test was the better of the two for the following reasons: 1) results from the Allium test were more quickly observable, 2) the Allium test used less materials and therefore was less expensive to run, compared to cell culture, 3) the Allium test did not involve aseptic procedure and there was no fear of bacterial contamination, unlike the cell line analysis 4) the results in this experiment proved to be more conclusive in the Allium test, and 5) results in the Allium test were both microscopic and macroscopic.

Due to the variability of onions from the same population in the same test water no significant conclusions can be made about any test waters when observed macroscopically. In both populations, the average root length of onions taken from water above and below Fidco were longer than those taken from above and below KC. This could be due to more toxic water found between the point below Fidco and the point above Kimberly-Clark. No EPA reports were available on these areas of the river. The first population of onions tested (from Deep's Market) did not show a striking drop off in root length between the two points although it did decrease slightly. The second population of onions tested (from South Carolina) showed a more accentuated drop off. This can be explained as a possible increase in toxicity found in the water below Fidco and above Kimberly-Clark. In both populations the water below Kimberly-Clark showed the least root growth of the river water samples. Also in both populations the positive control (Higgins Annex tap water, WCSU) proved to be highly toxic and this inhibited root growth.

Microscopic results proved to be more conclusive than the macroscopic results in determining the toxicity of the samples. The mitotic index decreased in the samples as the samples were taken further downstream, with the highest index found above Fidco and the lowest index from below Kimberly-Clark. When compared to the negative control the river water gave lower mitotic indices. The percent of mitotic cells seemed to show a reversal in percent metaphase and anaphase stages. This reversal has been shown to be an indication of toxic water by Fiskesjo (Fiskesjo, 1985b). Apparently if there are more anaphases than metaphases, this is a sign of toxicity. Also the appearance of more delayed anaphases in water samples taken downstream indicate toxicity due to a slower rate of mitosis. Finally sticky chromosomes seen in above KC and below KC samples indicate extreme toxicity of the water samples. In all cases the positive control was found to be the most toxic sample and no dividing cells were found. Statistical analysis of the data for the Allium test indicated that there was no significant difference between the two populations of onions, one from Deep's Market and the other from South Carolina. Furthermore, statistical tests also showed that the differences in mitotic indices and root length from the different test waters were not significant.

From the cell culture analysis no conclusions could be made. Mouse cells seem to grow equally well in all water samples, with the exception of the positive control (Higgins Annex Water). No differences were observed under the phase contrast microscope. Chromosome spreads obtained from the colcemid treatment also gave no results that would lead to any

determination of toxicity. Therefore, cell culture analysis proved to be more difficult in observing the toxic effects of the water samples on cells.

From the results obtained by the Allium test, the toxicity of Housatonic River Water increased slightly as water samples were taken further downstream. Therefore the toxic source could not be traced to either factory since the shift in toxicity occurred between the two. This shift in toxicity could be due to the greater distance between the sampling site below Fidco and above KC when compared to the distances between sites above and below each factory. This would allow a greater distance for toxic build up between Fidco and KC. There are several brooks and streams that enter the river between Fidco and KC, as well as a hydroelectric plant that uses both Housatonic River Water and Candlewood Lake Water. Also between the two factories lies the town of New Milford, including small factories and storage facilities. Although the Allium test provided some helpful information about the toxicity of the Housatonic River water more tests should be run to accurately determine the source of contamination of the river.

As for the relationship between cell division and chromosome clumping, a possibility is that the contaminants in the water affect the stability of the microtubules that compose the spindle fibers. This would culminate in totally condensed chromosomes, with no division and no lining up of the chromosomes in the metaphase plate, which is exactly what was seen in the positive control (Higgins Annex Water). Further investigation would be needed to accurately determine the exact relationship between chromosome clumping and lack of cell division.

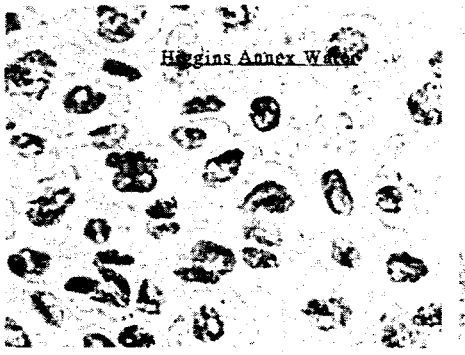


FIGURE 1 Acetoorcein squash of root tips grown in Higgins Annex Water (Positive Control) 400X.

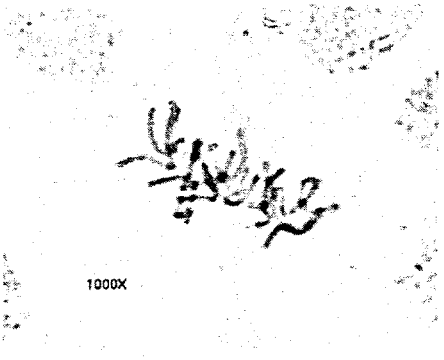


FIGURE 2 Normal Metaphase (Negative Control) 1000X.

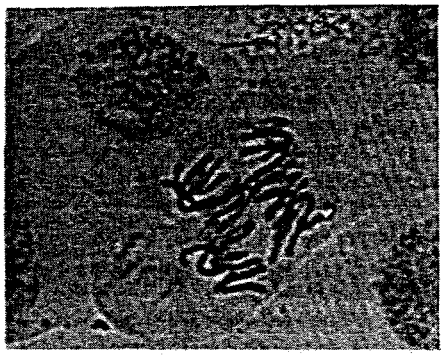


FIGURE 3 Delayed Anaphase, possible Stickiness (Below KC) 1000X.

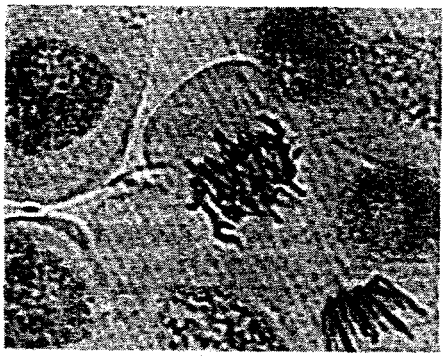


FIGURE 4 Sticky Chromosomes (Below KC) 1000X

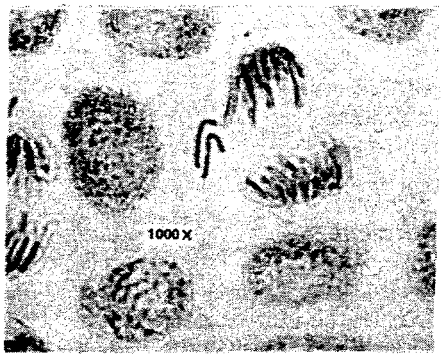


FIGURE 6 Vagrant Chromosome (Below KC) 1000X.

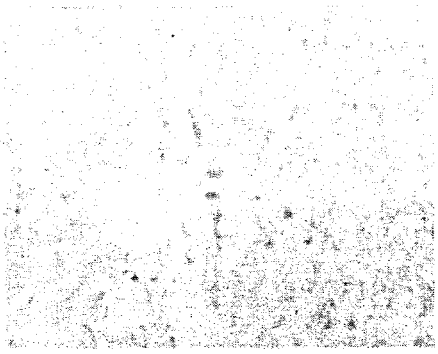


FIGURE 7 Normal Anaphase Cell in Mammalian Cell Culture (Above Fidco)400X.

TABLE 1 Macroscopic Observations of Root Length, in cm..

Sample Site	Trial 1 (n=3) x	Trial 1 (n=3) Std. Deviation	Trial 2 (n=4) x	Trial 2 (n=4) Std. Deviation
AF	1.6	1.06	1.1	0.32
BF	2.8	0.43	1.2	0.27
AK	1.6	0.37	0.8	0.16
BK	1.4	0.69	0.6	0.22
Pos. Control	0.9	0.37	0.7	0.1
Neg. Control	2.6	0.99	1.2	0.08

TABLE 2 Microscopic Observations of the roots of *Allium cepa*.

Sample Site	Avg. Mitotic Index *	% of Dividing Cells in Metaphase and Anaphase			
		Normal Metaphase	Normal Anaphase	Delayed Anaphase	"Stickiness"
AF	45.3	58	40	2	-
BF	44.3	56	40	4	-
AK	41.3	46	46	7	0.5
BK	39.3	38	52	9	0.2
Pos. Control	-	-	-	-	-
Neg. Control	62.5	59	40	1	-

* = Number of Dividing Cells per 1000 cells.

REFERENCES

Barile, Frank A. Introduction to In Vitro Cytotoxicity Mechanisms and Methods. CRC Press. London. 1984. Preface

Dye, Frank J. 1985. Cell Culture Made Easy. Journal of College Science Teaching. reprint

Fiskesjo, Geirid. 1981. Allium Test on Copper in Drinking Water. Vatten 37/3: 232-240.

Fiskesjo, Geirid. 1985a. The Allium Test as a standard in environmental monitoring. Hereditas 102: 99-112.

1988. Concentration and Transport of Polychlorinated Biphenyls in the Housatonic River between Great Barrington, Massachusetts, and Kent, Connecticut, 1984-88. U.S. Geological Survey. Water Resources Investigations Report 91-4014.

Productivity of Grassland Bird Species at Iroquois National Wildlife Refuge, NY

Kathleen M. Hartman

Department of Biology
SUNY at Brockport
Brockport, NY 14420

Faculty Advisor:
Dr. Chris Norment

INTRODUCTION

Populations of many grassland birds in the northeast have declined during the last two decades (Bollinger and Gavin 1992). Between 1966 and 1988, Breeding Bird Survey (BBS) counts for Savannah Sparrows (*Passerculus sandwichensis*) decreased by 46%, while Bobolink (*Dolichonyx oryzivorus*) counts decreased by 38% (Bollinger and Gavin 1992). These trends have created a need for more data on the life history of declining grassland bird species. Data on clutch size, brood number, and nesting success are necessary to understand the vulnerability of declining populations, and may provide insight into effective management techniques (Martin and Geupel 1993).

In response to this need, a multiyear grassland bird study was started in 1994 at Iroquois National Wildlife Refuge in New York. Data were collected for several grassland nesting bird species including: Savannah Sparrow, Bobolink, Song Sparrow (*Melospiza melodia*), and Red-winged Blackbird (*Agelaius phoeniceus*). The purpose of this study was to correlate nesting success with habitat types and management techniques used on the refuge and to identify optimal nesting habitat for grassland species. In turn, this will allow for more informed management decisions about northeastern grasslands.

METHODS

The study was conducted at Iroquois National Wildlife Refuge and on adjacent New York State operated Tonawanda and Oak Orchard Conservation Areas. Field work was conducted from May to July 1994 in cool and warm season grasslands, pastures, old fields, and fallow fields.

Nests were located using the rope-dragging method (Martin and Geupel 1993). Success with this method was restricted to a large continuous 0.92 km^2 pasture. Additional nests were found by following incubating females or attendant males to their nests. Although locating nests during construction is ideal for effective estimation of nest success, no nests were located during the nest building stage (Martin and Geupel 1993).

Nest were flagged 5m north of the nest and followed throughout the breeding season. Upon location of a nest the date, species, nest number, location, number of eggs or nestlings, and estimated age of nestlings were recorded. Each nest was checked every 2 to 4 days until completion. Number of eggs or nestlings, age of nestlings, and condition of the nest were recorded. A nest was considered complete if it had been depredated, abandoned, or the young had fledged. If the eggs were cold with no sign of the female in the area, it was considered abandoned. Nests were considered depredated if the

eggs or nestlings disappeared prior to the anticipated fledging date, or the nest had been disturbed.

RESULTS

In this study 26 Savannah Sparrow, 23 Bobolink, six Song Sparrow and 11 Red-winged Blackbird nests were followed to completion (Table 1). Generally, a nest size of 20 is required to calculate nest success adequately (Martin and Geupel 1993). The small sample sizes for Red-winged Blackbirds and Song Sparrows mean that estimates of productivity for these species should be considered very rough.

Table 1. Productivity of Savannah Sparrows, Bobolinks, Song Sparrows, and Red-Winged Blackbirds nesting on the Refuge.

	Savannah Sparrow (25)[1]	Bobolink (23)	Song Sparrow (6)	Red-winged Blackbird (11)
Mean clutch size	4.09±.49	5.17±.58	4.17±.75	3.55±.82
Hatchability	.94	.93	.83	1.0[2]
Hatching Success (%)	69	87	40	36
Fledging success (%)	87	75	100	21
Egg success (%)	60	65	40	8
Nest success (%)	84	70	50	9
#Fledged/nest	3.08± 1.58	3.35± 2.40	1.67± 2.25	.27± .9

1 Sample sizes are in ().
2 Only for 1 successful nest of 11.

Nesting cycles of Savannah Sparrows, Bobolinks, and Red-winged Blackbirds were similar with a mean hatch date of 11 June (Table 2). Mean fledge dates of the Savannah Sparrow and Bobolink were close at 19 June and 21 June respectively. The Song Sparrow had a much earlier mean hatch date of 2 June and therefore, had an earlier mean fledge date of 12 June. Only one Red-winged Blackbird nest survived, which fledged on 13 June.

Table 2. Hatch and Fledge Dates for each species.

Species	Mean Hatch Date	Hatch Date Range	Mean Fledge Date	Fledge Date Range
Savannah Sparrow	11 June (15)[1]	30 May-23 June	19 June (13)[1]	8 June-1 July
Bobolink	11 June (18)	4 June-19 June	21 June (15)	15 June-27 June
Song Sparrow	2 June (3)	31 May-5 June	12 June (3)	9 June-15 June
Red-winged Blackbird	11 June (3)	2 June-21 June	13 June[2] (1)	13 June

1 Sample sizes for mean hatch and fledge dates are shown in parentheses.
2 Only 1 of the 11 nests fledged young, so this is based on one nest.

Nest success and egg success were calculated using the Mayfield (1975) method, which adjusts for differences in the length of time each known nest is monitored. Both the Red-winged Blackbird and Song Sparrow sample sizes were not large enough to warrant use of

this method. Nest Success was 79.4% for the Savannah Sparrow and 64.6% for the Bobolink.

DISCUSSION

The most relevant information for determining effective management and the present status of these populations on the refuge are: (1) clutch size, (2) nest success, and (3) nest chronology.

Clutch Size

This study found the clutch size of the Savannah Sparrow to be 4.09. Savannah Sparrow clutch size at Iroquois National Wildlife Refuge (4.09) was very close to clutch sizes of other populations at similar latitudes (4.1; Wiens 1969, Dixon 4.02;1975, Welsh 4.2;1975). The mean clutch size, 5.17 for the Bobolinks was similar to the mean of 5.47 found in a study conducted in Oregon (Martin 1974).

Nest Success

Savannah Sparrow nest success (% of nests fledging > 1 young) at Iroquois National Wildlife Refuge (84%) was higher than for populations in Nova Scotia (58%; Dixon 1975) and Michigan (50%; Potter 1974). Bobolink nest success at Iroquois (70%) was comparable to nest success for an Oregon population (73.4%; Martin 1974). Both the Song Sparrow and Red-winged Blackbird are not true grassland species. The Song Sparrow prefers shrubby, early successional habitats, while the Red-winged Blackbird prefers cattail marshes. One might expect a lower nest success for the Song Sparrow; it nest near edges, and nests placed near edges suffer higher predation rates (Johnson and Temple 1990). Red-winged Blackbirds nest success of 9% was low compared to 37% found in a similar study done in Ithaca, New York (Westneat 1992). The suboptimal breeding habitat most likely accounts for the low nesting success and it is probably not indicative of the success of the population as a whole on the refuge. The true grassland species on the refuge, the Savannah Sparrow and the Bobolink both appear to have had successful breeding seasons. The second year of this study will be important in determining the status of these populations.

Nest Chronology

Nest chronology is particularly important for determining the timing of management activities. Dixon's study (1978) found the mean hatch date to be 30 June for Savannah Sparrows, which is much later than our findings (Table 2). This inconsistency could be due to the differences in location; Dixon's study was done on Kent Island in Canada.

Likewise, the mean fledge date for Savannah Sparrows (19 June) was much earlier than the 9 July date for the population in Canada (Dixon 1975). Bobolinks fledged from 15 June to 27 June, with the mean being 21 June. In a study conducted from 1984 to 1988 by Bollinger and Gavin (1992) in Madison County, New York, 75% of the Bobolink fledged by 25 June, which is directly comparable to our findings. Since Savannah Sparrows and Bobolinks had the same mean hatch date, differences in mean fledge dates represent differences in nestling periods.

Management implications for these species are that no mowing, haying, or grazing should be done prior to July 1 (Table 2). Any activities such as these prior to this date would cause a large decrease in nest productivity.

ACKNOWLEDGMENTS

The author thanks Dr. Chris Norment for his extensive help with this paper as well as the opportunity of working on this study.

LITERATURE CITED

Bollinger, E.K. and T. Gavin. 1992. Eastern Bobolink populations: ecology and conservation in an agricultural landscape. Pages 497-506 *in* Ecology and conservation of Neotropical migrant landbirds. J.M. Hagan III and D.W. Johnston, editors. Smithsonian Institution Press, Washington, D.C..

Dixon, C.L. 1978. Breeding biology of the Savannah Sparrow on Kent Island. Auk 95: 235-246.

Forbush, E.H. and J.B. May. 1939. Natural history of the birds of eastern and central North America. Houghton-Mufflin, Boston, Massachusetts.

Holm, C.H. 1973. Breeding sex ratios, territoriality, and reproductive success in the Red-winged Blackbird (*Agelaius phoeniceus*). Ecology 54: 356-365.

Johnson, R.G. and S.A. Temple. 1990. Nest predation and brood parasitism of tallgrass prairie birds. Journal of Wildlife Management 54: 106-111.

Martin, S.G. 1974. Adaptations for polygynous breeding in the Bobolink, *Dolichonyx oryzivorus*. Amer. Zool. 14: 109-119.

Martin, S.G. and G.R. Geupel. 1993. Nest-monitoring plots: methods for locating nests and monitoring success. Journal of Field Ornithology 64: 507-519.

Mayfield, H.F. 1975. Suggestions for calculating nest success. Wilson Bulletin 87: 456-466.

Potter, P. 1974. Breeding biology of Savannah Sparrows in southeastern Michigan. The Jack Pine Warbler 52: 51-63.

Welsh, D.A. 1975. Savannah Sparrow breeding and territoriality on a Nova Scotia dune beach. Auk 92: 235-251.

Westneat, D.F. 1992. Nesting synchrony by female red-winged blackbirds: effects on predation and breeding success. Ecology 73: 2284-2294.

Wiens, J.A. 1969. An approach to the study of ecological relationships among grassland birds. American Ornithologists' Union, Ornithological Monographs. No 8:35.

The Effect of Environmental pH on the Morphology of Gill Tissue in *Carassius Auratus* (Goldfish)

Randy L. Durren

Department of Biology
University of North Carolina at Asheville
One University Heights
Asheville, NC 28804-3299

Faculty Advisor:
Dr. Gregg Kormanik

Acid rain has a profound effect on the physiology of aquatic organisms. Especially affected are the gills of teleosts. On this tissue are chloride cells, which are instrumental in ion regulation, acid/base balance and respiration. Scanning electron microscopy was used to observe changes in morphology of the gills of goldfish exposed to sublethal levels of acidified fresh water (pH 3.5 to 4.5), and alkaline freshwater (pH 8.3) Primary and secondary lamellar cells under control conditions displayed smooth apical regions with apical crypts, which are associated with chloride cells. Exposure to lower pH resulted in damage to gill tissue and/or an increase in the number of apical crypts representing chloride cells. Increased pH resulted in a decrease in the number of apical crypts and an increase in the size of the cells in the secondary lamellae. Even short term exposure to minor acidic challenge results in structural changes to the cells involved in ion regulation, acid/base balance and respiration in this species.

INTRODUCTION

The gills are one of the most important structures of fishes that are affected by exposure to an acidic environment. Important functions of the gills include osmotic, ionic, and acid/base regulation. Mitochondrial-rich cells in the gill, called chloride cells, are responsible for ion regulation as well as acid/base balance, at least on the basis of circumstantial evidence (Heisler 1993).

In most species, chloride cells are located mainly at the base of the secondary lamellae on the primary filament, in the interlamellar regions where they are irregularly spaced or form clusters of cells in the primary epithelium (Laurent and Dunel 1980). The ultrastructural characteristics of chloride cells are well known. Chloride cells display numerous mitochondria associated with a densely branched tubular system that opens on the basolateral plasma membrane. The apex of each cell has microvilli and is firmly bound to the neighboring pavement cells by a long and tight junctional apparatus. A terminal web is anchored by parietal desmosomes. Vesicles of various sizes are concentrated in the apical region (Laurent and Dunel 1980).

In freshwater teleosts, gills are the site of Na^+ and Cl^- absorption which contribute to the maintenance of ionic balance. This transport capacity has been attributed to the chloride cells even though *in vivo* studies have not permitted such precise localization (Avella *et al* 1987). It has long been hypothesized the $Na^+/H^+(NH_4^+)$ electroneutral exchange is the principle mechanism of acid/base regulation in the gill epithelium of fish. Several authors have concluded that the fish gill has an electrogenic proton pump in the mucosal membrane similar to that reported for frog skin and toad bladder, rather than a Na^+/H^+ exchange mechanism (Avella and Bornancin, 1989; Lin and Randall 1991). The electrogenic proton pump, or H+-translocation ATPase, on the apical membrane removes protons from the cell. A $Na^+/K^+(NH_4^+)$-ATPase in the basolateral membrane pumps sodium out of the cell into the blood, thus, proton excretion and sodium uptake are intimately, but indirectly, linked (Lin and Randall 1991). Avella *et al* (1987) showed that branchial sodium uptake was proportional to the number of chloride cells in the gills. Furthermore, since proton pumps consume energy and chloride cells are rich in mitochondria and can supply the energy demand, it is likely that the electrogenic proton pump is located in the chloride cells (Avella *et al* 1987; Lin and Randall 1991). Chloride cells are thus implicated in the response of the fish to acidic challenge.

This study examined, using scanning electron microscopy (SEM), gill morphology and the effect of acidic and alkaline environments on the numbers of chloride cells as indicated by changes in the number of apical crypts.

MATERIALS AND METHODS

One fifty gallon aquarium was stocked with goldfish. Ten gallon aquaria containing tap water (pH 6.8 to 7.2) were used as control. Alkaline tanks were titrated with 0.1M KOH, to a pH of 8.3, and acidic tanks were titrated with 0.1M H_2SO_4, to a pH of between 3.5 and 4.5. Experimental tanks were titrated daily to maintain pH for 14 days. Acidic tanks were maintained with 0.05M H_2SO_4 and the alkaline tanks with 0.1M KOH.Fish were maintained at room temperature, about 20°C, and all fish were fed identical amounts of food. One-third of the water was changed every second day in all tanks.

In preparation for scanning electron microscopy, at the end of 14 days the fish were killed by decapitation, gill tissue was quickly dissected out and fixed in 2.5% glutaraldehyde for two hours. Gills were then dehydrated in ascending strengths of ethanol, critical point dried (Structure Probe,Inc.), attached to studs, sputter coated (Anatech, LTD) and placed in the SEM (Cambridge Instruments Steroscan 90) for viewing.

Another set of fish were subjected to the same set of experimental conditions, for determination of gill surface area. At the end of two weeks, these fish were then sacrificed and the second gill arch on the left sided gill was removed, placed on a wet mount, and then placed in a projection microscope. The fifth, seventh, and ninth primary lamellae were traced on to paper. Tracings were cut-out and weighed to determine any change in lamellar area.

RESULTS

Gill tissue from a representative control fish is shown in Figure 1. Fish exposed to a pH of 6.8 to 7.2 showed smooth tissue on the primary and secondary lamellae, with little or no damage. Primary lamellae were observed to have 2-4 apical crypts per lamella.



Figure 1. A SEM micrograph of a representative fish gill from the control group. The tissue was removed, fixed in 2.5% glutaraldehyde, critical point dried, sputter coated and placed in the SEM for viewing. The primary lamella shows smooth tissue with 2-4 apical crypts (Arrows).

The fish exposed to alkaline freshwater (pH 8.3) are shown in figure 2. Alkaline exposure resulted in a decrease in the number of apical crypts and an increase in the size of the cells of the secondary lamellae.

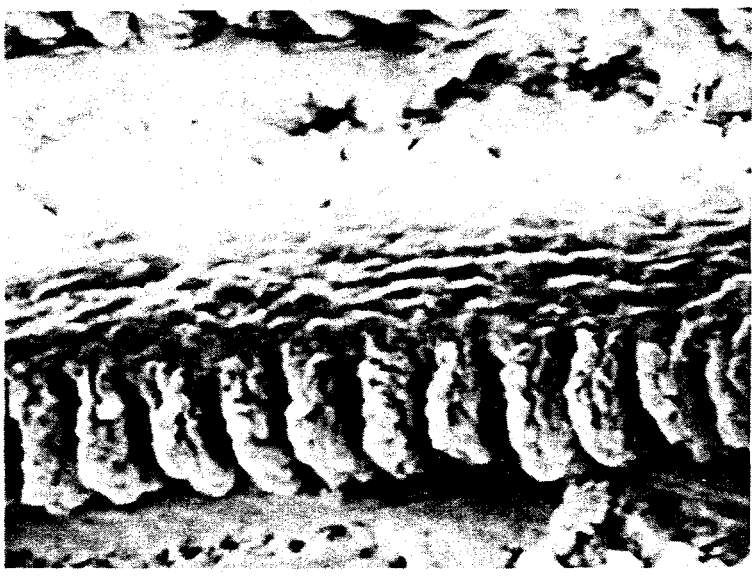


Figure 2. SEM micrograph of representative fish from the alkaline group. Note the decrease in apical crypts.

The fish exposed to acidic freshwater (pH 3.5 to 4.5) are shown in Figure 3. Exposure to acidic freshwater resulted in an increase in the number of apical crypts, a decrease in the area of the primary lamellae themselves, and visible tissue damage, in the form of a constriction of the primary lamellae. Tissue damage was consistently observed in all the fish from the acidic environment, as was the increase of the number of apical crypts.



Figure 3. This SEM micrograph is from a representative sample from the acidic environment. There is an increase in the number of apical crypts and visible tissue damage to the primary lamella in the form of a constriction. This damage was consistent in all gills from this group (Arrows).

DISCUSSION

This study showed that exposure to an acidic or alkaline environment modified the morphology of the gill primary and secondary lamellae in goldfish, as well as the number of chloride cells.

Exposure to an acidic environment (Fig. 3) increased the number of apical crypts, indicating that the number of chloride cells also increased. An increase in the number of chloride cells would help to maintain ionic and acid/base balance in this stressful environment. However, exposure to an acidic environment had a damaging effect on the tissue of the gills, causing a reduction in surface area, and even destruction of the tissues themselves. This would likely cause a decrease in the surface area necessary for gas exchange in respiration and also a decrease in the surface area for ionic and acid/base balance.

WORKS CITED

Avella, M., A. Masoni, M. Bornancin, and N. Mayer-Gostan (1987). Gill morphology and sodium influx in the rainbow trout (*Salmo gairdneri*) acclimated to artificial freshwater environments. J. exp. Zool., 241:159-169.

Avella, M., and M. Bornancin (1989). A new analysis of ammonia and sodium transport through the gills of the freshwater rainbow trout (*Salmo gairdneri*). J. exp. Zool.,142:155-175.

Heisler, N. (1993). Acid-Base Regulation. In The Physiology of Fishes (ed. D.H. Evans), pp343-379. Boca Raton:CRC Press.

Laurent, P., and S. Dunel (1980). Morphology of gill epithelia in fish. Am. J. Physiol., 238:R147-R159.

Lin, H., and Randall (1991). Evidence for the presence of an electrogenic proton pump on the trout gill epithelium. J. exp. Biol. 161:119-134.

Oikawa, S., and Y. Itayawa (1985). Gill and body surface area of the carp in relation to body mass, with special reference to the metabolism-size relationships. J. exp. Biol. 117:1-14.

Long-Term Nutrient Assimilation by a Diked Lake Erie Coastal Marsh

Michael Liptak
Department of Biology
University of Toledo
2801 West Bancroft St.
Toledo OH 43606

Faculty Advisor: Dr. Johan F. Gottgens

ABSTRACT

Marshes can be used by environmental engineers to filter unwanted substances and keep them from entering other waterways. This pilot study examined the long-term assimilation of nutrient runoff by coastal marshes, using two marshes which have been diked from Sandusky Bay since the early 1900s. In the past, both marshes received nutrient runoff from farms in the watershed. The North Marsh still received agricultural runoff as of 1994, while the West Marsh had not since 1978. Sediment cores from the two marshes were analyzed for total organic matter, total carbon (TC), total nitrogen (TN), and total phosphorus (TP), and were dated using lead-210 (^{210}Pb), cesium-137 (^{137}Cs), and americium-241 (^{241}Am). Measuring the activities of these radioisotopes, which have known half-lives, allowed the determination of the transfer rates of material between water and sediment for the past 100-150 years. The increase in accumulation of sediment, TP, and organic matter was 2-3 times higher in the North Marsh than in the West Marsh since the diversion of farm runoff from the latter. TC and TN accumulation rates increased also, but the difference between the North and West marshes was less pronounced (1.7 and 1.8 times, respectively). The difference between the North and West Marsh accumulation rates persisted over a more recent time period (since 1985) suggesting no assimilative saturation. The data from this pilot study supported the hypothesis that Lake Erie coastal marshes may function in long-term water-quality improvement and agricultural waste water treatment. More extensive study is needed to fully support this hypothesis.

INTRODUCTION

Wetlands have traditionally been seen as wastelands which serve no useful purpose. Only recently has their role in the ecosystem and the watershed been identified. Wetlands play a critical role in the nutrient cycle. They transform nitrogen, phosphorus, sulfur, carbon, and other elements and deposit them in the sediments, release them into the air, or leave them in the water column. Phosphorus is one of the most important elements in the wetland ecosystem, and has been found to be a major limiting nutrient in freshwater marshes (Klopatek 1978, from Mitsch and Gosselink 1993). Phosphorus occurs as soluble and insoluble complexes in wetland soil, and is filtered in wetlands through adsorption and precipitation reactions with iron, aluminum, calcium, and clay particles (Mitsch and Gosselink 1993).

Wetlands have been shown to be sinks for certain nutrients and sources for others. Constructed wetlands have been shown to be effective in removing suspended solids, nitrogen, and phosphorus (Hey *et al.* 1994). Hence, wetlands may remove nutrients, carbon, and suspended solids from agricultural runoff. Farm runoff may contribute to eutrophication in Lake Erie when this runoff, which contain fertilizers, nutrients, and organic matter, drains directly into the lake. This increase in nutrient inflow may change the trophic status of the lake. If wetlands were used as nutrient filters, the water quality of Lake Erie might be improved. However, there is currently no information on the longterm filtering capabilities of Lake Erie marshes. Some wetlands have been shown to become saturated with nutrients over the years and gradually lose their ability to remove these nutrients from water inflow (Spangler *et al.* 1977, from Mitsch and Gosselink 1993). This pilot study proposed the use of sediment cores for the analysis of a wetland's history. These cores may be used to establish a chronological description of the wetland in question, and may be used to quantify changes in the net accumulation rates of a variety of biologically important materials over time.

One way of dating the sediments contained in a core is by radiodating. For extremely old cores, ^{14}C dating can be used, but for the period of time covering the last 100-150 years, analyzing the sediments for ^{210}Pb (Goldberg 1963) has become the preferred method of radiodating. ^{210}Pb is an intermediate in the ^{238}U decay series with a half-life of 22.2 years. It is deposited from the atmosphere into lakes and wetlands, and accumulates in their

sediments, where it decays. Some ^{210}Pb is present within the sediment due to the decay of ^{222}Rn gas which is trapped in the sediment. The ^{210}Pb exists in an equilibrium with the ^{222}Rn and is called supported ^{210}Pb, while the ^{210}Pb which enters the sediment through precipitation from the atmosphere decays according to its half-life and is called unsupported ^{210}Pb. The age of a layer of sediment can be determined by the amount of unsupported ^{210}Pb in the sediment, and this method can be used to date sediments deposited in the last 100-150 years. ^{137}Cs and ^{241}Am can be used as supporting age markers, because they are products of atmospheric testing of nuclear weapons in the late 1950s and early 1960s. These isotopes are not a natural component of the soil matrix. Analysis by direct gamma ray measurement (Gäggeler *et al.* 1976) has advantages in establishing geochronologies in cores because, unlike alpha counting, it requires relatively little preparation time and does not involve destruction of the sample. This method is now commonly used in paleolimnology on a wide range of sediments from tropical to arctic systems.

Despite their possible role in reducing the amount of pollutants which enter a lake, diked marshes have not been studied as long-term nutrient filters for agricultural runoff. This pilot study was designed to address the question of whether these marshes do in fact filter C, N, and P from agricultural nutrient runoff and whether this activity is sustainable over long periods of time, or whether these wetlands would eventually become saturated and lose their ability as nutrient sinks. In order to answer these questions, sediment cores from two adjacent marshes at the Winous Point Shooting Club on Sandusky Bay were taken and sedimentation rates were determined by radiodating, using ^{210}Pb, ^{137}Cs, and ^{241}Am as age markers. The sediments were also analyzed for bulk density, percent solids, organic matter, carbon, nitrogen, and phosphorus. From these data the history of the marshes and the ability of the marshes to absorb nutrients was determined.

SITE DESCRIPTION

The Winous Point Shooting Club (WPSC) is a privately owned hunting club founded in 1856. WPSC owns the largest private wetland in Ohio, consisting of 1800 hectares of wetlands near the western shore of Sandusky Bay. These wetlands were diked from Sandusky Bay in the early 1900s, and have been managed for emergent vegetation to attract waterfowl. This management involves periodic lowering of water levels in the marshes between mid-June and mid-August when the potential for the establishment of plants is the highest. The marshes are under water the rest of the year. The North Marsh is a 260 hectare wetland which currently (1995) receives runoff from approximately 900 hectares of corn/soybean farmland and which has from the beginning of agriculture in the Sandusky area, while the 220 hectare West Marsh has not received agricultural runoff since 1978.

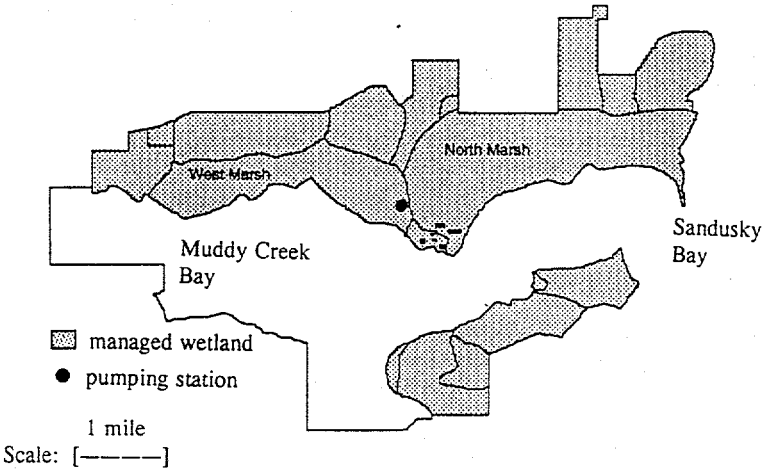


Fig. 1. Map of the Winous Point Shooting Club, Port Clinton, Ohio, showing Sandusky Bay, the club's managed wetlands (shaded), Muddy Creek Bay, and the North and West Marshes.

METHODS AND MATERIALS

A sediment core was taken from each marsh using a piston corer (7.6 cm i.d.). Samples were extruded from the top of the core and sectioned at 1 cm intervals. Subsamples of 1 or 2 cm^3 of sediment from each section were weighed, dried at 100° C for 24 hours, and reweighed to determine bulk density (g/cm^3) and percent solids (g/g). The remaining portions of the sections were refrigerated. The subsamples were then ignited at 550° C for 1 hour to burn off all organic material in each sample, and were reweighed to determine the organic matter content (g/g). Percent nitrogen (g/g) and percent carbon (g/g) of dried samples were determined using a CHN analyzer. Subsamples (2mg) of oven-dried, finely ground sediment were placed in tin vials and ignited in a pure oxygen environment at 925° C. The C, H, and N in the samples were converted into gases, separated, and measured under steady-state conditions as a function of their thermal conductivity.

Subsamples were analyzed for P using an acid digestion method (Andersen, 1976). Oven-dried sample (100mg) was ignited at 550° C for 1 hour. The ash was digested by heating with 25 ml 1N HCl for 15 minutes. Subsamples were filtered and diluted to 100 ml. A portion (5 or 10 ml) of the diluted filtrate from each sample was neutralized, diluted to 50 ml, and analyzed using the ascorbic acid test (APHA 1992). In this test, a combined reagent containing ascorbic acid, potassium antimonyl tartrate, and ammonium molybdate in an acid medium was mixed with the filtrate. The molybdate reacted with the phosphate in the sample to produce a blue reaction product. The amount of color produced was proportional to the amount of phosphate in the sample according to Beer's Law. Absorbance values for the samples were measured with a spectrophotometer at 880 nm.

For radiodating, an intrinsic germanium well detector was used. Subsamples were prepared for gamma ray analysis by drying at 40° C, pulverizing using a mortar and pestle, and redrying at 40° C. Subsamples were weighed, placed into small plastic tubes (length: 5 cm, diameter: 1.3cm) and sealed to prevent ^{222}Rn gas from escaping. Since ^{222}Rn is a precursor of ^{210}Pb, its presence served to stabilize the supported levels of ^{210}Pb at an equilibrium in the tube. The contents were allowed to equilibrate for a minimum of 21 days and were then analyzed for ^{210}Pb (supported and total), ^{137}Cs, and ^{241}Am using the germanium well detector. Age-depth relatioships were calculated using the Constant Rate of Supply point transformation (Goldberg 1963). Accumulation rates were then calculated by multiplying the concentration of each analyte with the radiochemically determined bulk sedimentation rates.

RESULTS AND DISCUSSION

The ^{210}Pb activities showed a typical decline in the sediments due to decay, while the earliest presence of ^{137}Cs and ^{241}Am occurred in sediments which were dated to the late 1950s and early 1960s in both marshes. This served as a supporting line of evidence for the reliability of the ^{210}Pb dating technique (Fig 2).

The sediment composition of each marsh differed both before and after 1978 (Table 1). Before 1978, the two marshes had similar C:N ratios, but their N:P ratios were different. After 1978, the sediments in the North Marsh became enriched with phosphorus relative to the other elements, which was shown by the decreasing C:P and N:P ratios. However, the C:N ratio in the North Marsh were fairly stable, showing that the amounts of C and N remained in about the same proportions with continued influx of agricultural runoff. The C:N:P ratios in the West Marsh showed that the marsh's sediment composition remained similar to its pre-1978 composition after it no longer received farm runoff.

Table 1. Total carbon, nitrogen, phosphorus ratios (w/w) for North and West Marsh sediments, WPSC, Ohio.

LOCATION	TIME PERIOD	C: N: P
North Marsh	Post 1985	121: 11: 1
North Marsh	Post 1978	125: 11: 1
North Marsh	Pre 1978	190: 17: 1
West Marsh	Post 1985	95: 9: 1
West Marsh	Post 1978	98: 9: 1
West Marsh	Pre 1978	88: 9: 1

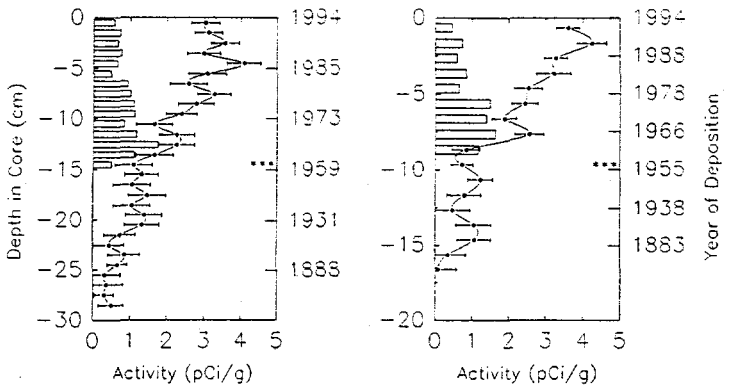


Figure 2. Radio-isotope activities (pCi g^{-1})for the North (left) and West Marsh (right) cores showing depth in core (left axis) and ^{210}Pb-age of sediment sections (right axis). Unsupported ^{210}Pb activity is represented by a solid line with counting errors (± one standard deviation) indicated. ^{137}Cs activity (open bars) is corrected for decay since deposition and the deepest core section with detectable ^{241}Am levels is marked with ***.

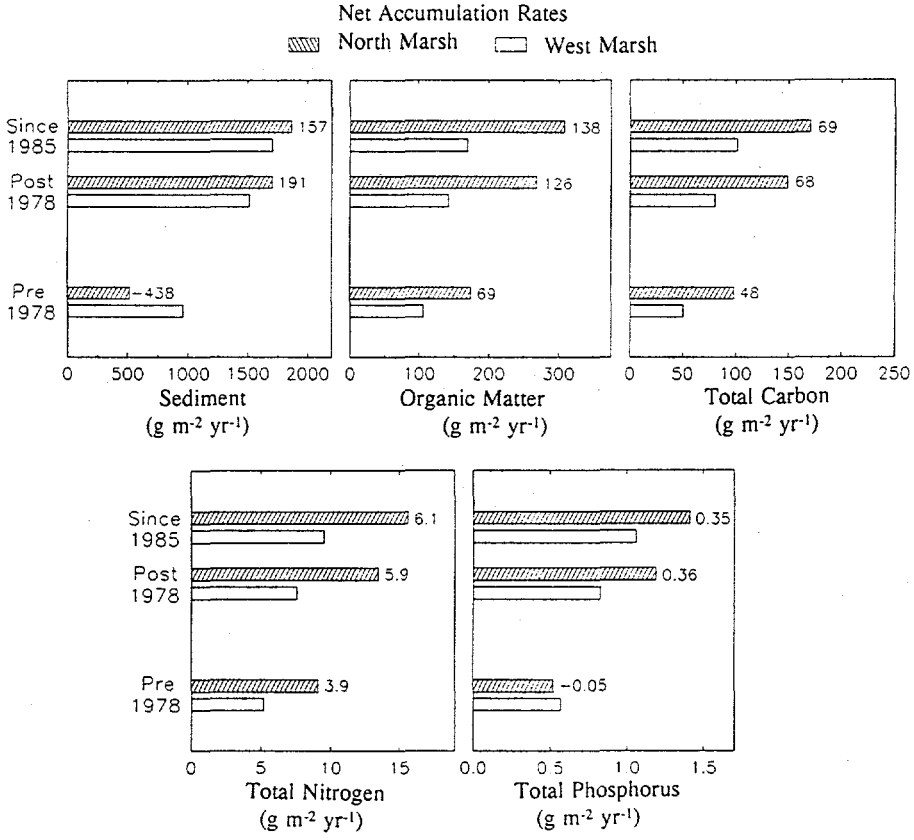


Figure 3. Net accumulation rates for total sediment, organic matter, total carbon, total nitrogen, and total phosphorus (g m^2yr^{-1}) of the North and the West Marsh cores (hatched bars and open bars, respectively). Net accumulation rates are based on CRS-calculated ^{210}Pb chronology (see text) and reported for the time period since 1985, post 1978 (i.e. post diversion of farm runoff from the West Marsh), and pre 1978 (average rate from the turn of the century to 1978, i.e. during the time when both marshes were still receiving agricultural drainage). Numbers next to the North Marsh bars indicate the difference (in g m^{-2} yr^{-1}) in accumulation rate between both core sites.

Accumulation rates showed a pronounced difference between the two marshes after 1978, when the agricultural runoff was diked away from the West Marsh but not from the North Marsh (Figure 3). The pre-1978 data showed that the accumulation rates for carbon, organic matter, and nitrogen were somewhat higher in the North Marsh than in the West Marsh. Pre-1978 accumulation of total sediment and phosphorus was lower in the North Marsh than the West Marsh.

The post-1978 data showed that both marshes increased their accumulation rates over pre-1978 levels, and all of the North Marsh accumulation rates exceeded those in the West Marsh. Increased trapping of sediments, organic matter, and TP was particularly pronounced in the North Marsh. The difference between the North and West Marsh average sedimentation rates rose from -438 $g/m^2.yr$ before 1978 to 191 $g/m^2.yr$ after 1978. The difference between their phosphorus accumulation rates rose from -0.05 $g/m^2.yr$ to 0.36 $g/m^2.yr.$, and the difference in organic matter accumulation rates rose from 69 $g/m^2.yr$ to 126 $g/m^2.yr$. These data suggest that the North Marsh was an effective trap for sediments, for organic matter, and for phosphorus. The difference in TC and TN accumulation rates between the two marshes (pre- and post-1978) was smaller, perhaps because these chemicals have an atmospheric sink in addition to sediment storage. The differences in the post-1978 accumulation rates of the two marshes seemed to persist in the most recent sediments (post-1985), which suggested that the North Marsh had not become saturated with nutrients, but continued to serve as a filter for farm wastewater inflow.

CONCLUSION

There was a measurable difference in the sedimentation and accumulation rates between the North and West marshes both before and after the diversion of agricultural runoff from the West Marsh This difference became much more pronounced after 1978 and can be correlated with the fact that the North Marsh still received agricultural runoff as of 1995, while the West Marsh has not since 1978. The results of this study showed that these freshwater marshes can trap considerable amounts of inorganic particles (e.g. silts and clays) and phosphorus, thus preventing these nutrients and sediments from entering downstream bodies of water. For example, the North Marsh absorbed an average of 12 kg TP/ha/yr since 1978, and in excess of 17,000 kg sediment/ha/yr. The effect of these nutrients on the productivity of the wetland deserves further study, and these marshes will be the site of more extensive studies using more cores from each marsh. This long-term filtering capacity may be used to prevent downstream large bodies of water from undergoing cultural eutrophication and may play an important role in the management of lakes which border agricultural areas.

REFERENCES

Andersen, J.N. 1976. An ignition method for determination of total phoshorus in lake sediments. Water Research. 10: 329-331.

American Public Health Association. 1992. Standard methods for the examination of water and wastewater. Washington, D.C.

Gäggeler, H., H.R.Von Gunten, and U. Nyffler.1976. Determination of ^{210}Pb in lake sediments and air samples by direct gamma ray measurement. Earth Planet Sci. Lett. 33: 119-121.

Goldberg, E.D. 1963. Geochronology with ^{210}Pb. Radioactive Dating. IAEA, Vienna. 121-131.

Hey, D.L., A.L. Kenimer and K.R. Barrett. 1994. Water quality improvement by four experimental wetlands. Ecological Engineering, 3: 381-397.

Klopatek, J.M. 1978. Nutrient dynamics of freshwater riverine marshes and the role of emergent macrophytes. In Freshwater Wetlands: Ecological Processes and Management Potential. R.E. Good, D.F Whigham, and R.L. Simpson, eds. Academic Press, New York. 195-216.

Mitsch, William J., and James G. Gosselink. 1993. Wetlands, second edition. Van Nostrand Reinhold, New York.

Spangler,F.L., C.W. Fetter, Jr., and W.E. Sloey. 1977. Phosphorus accumulation-discharge cycles in marshes. Water Resource Bulletin, 13:1191-1201.

Ingestion rates of an estuarine copepod, Acartia tonsa, in labratory mesocosms.

B. Wysor

Natural Science Division
Southampton College of Long Island University
Southampton, NY 11968

Faculty Advisor:

M. Roman

Center for Estuarine Studies
Horn Point Environmental Labratory
Cambridge, MD 21613

Abstract

Ingestion rates of the estuarine, calanoid copepod *Acartia tonsa* were estimated from samples collected at the MEERC (Multiscale Experimental Ecosystem Research Center), a 2300 sq. ft. laboratory housing 27 multicosms under naturally simulated conditions. Zooplankton were sampled twice weekly from three mesocosms of the constant depth series in collaboration with the larger, interdisciplinary project of the MEERC designed to assess scale-dependent variability as it relates to ecosystem health. Copepods were individually selected from collection filters and levels of gut fullness determined using the gut fluorescence method. Ingestion rates were determined according to the equation I = KG, where I is the ingestion rate of *A. tonsa* in ng chlorophyll *a* copepod^{-1}, K is the instantaneous gut evacuation rate constant in units of time according to the empirical formula of Dam and Peterson (1988) and G is the level of gut fullness in ng chlorophyll *a*. Ingestion rate data were plotted against time and compared to phytoplankton pigment concentrations and copepod densities to assess trophic relationships in each mesocosm. Results suggest that scale does not affect rate of ingestion in *A. tonsa*; however, the effect of scale may be apparent at lower trophic levels.

Introduction

Marine copepods have been shown to contribute significantly to the transfer of energy between primary producers and larger predatory zooplankton and the nekton (Frost, 1972). The understanding of such interactive relationships between primary producers and primary consumers is necessary to assess marine food webs on large spatial and temporal scales (Berggreen et al., 1988). Elucidation of these scales is important because herbivorous zooplankton are primary components of marine food webs and thus provide energy for a broad diversity of organisms (Pomeroy, 1974).

The use of whole animal fluorescence has been used to assess ingestion rates of marine copepods because it is reflective of the amount of phytoplankton ingested immediately prior to collection (Dagg and Wyman, 1983). This methodology is particularly useful because the measurements are reflective of the zooplankton's response to mechanisms of its environment (Kleppel, 1988), such as temperature (Dam and Peterson, 1988), food concentration (Paffenhöfer, 1971; Frost, 1972; Berggreen et al., 1988;), and food particle size (Frost, 1972; Berggreen et al., 1988). These factors affect gut evacuation and gut passage rates which must be considered in determining ingestion rates. Furthermore, comparisons between ambient chlorophyll concentrations and ingestion rates can be easily assessed as fluorometry is used in both instances.

A limited number of investigations have researched the effect of scale in experimental design (Crossland and La Point, 1992) and more specifically, the effect of scale on ingestion rates of copepods. Such investigations, however, are imperative to understanding the limitations of laboratory experiments. Paffenhöfer (1971) conjectured that one *Calanus helgolandicus* is more likely to come into contact with the walls of a 500mL beaker than are 16 in an eight liter container. He also noted that the grazing potential of a copepod may still be masked in the larger cosm. Paffenhöfer (1988) later investigated variations between different experiments carried out in variable container sizes and concluded that grazing performance was limited by container size such that container size and ingestion rate are positively correlated.

In this study the gut fluorescence method was used for assessing the ingestion rate of the calanoid, estuarine copepod, *Acartia tonsa*, in laboratory mesocosms. The effect of tank size on the ingestion rate of the copepod was investigated.

Materials and Methods

The study was part of a collaborative effort on the larger, interdisciplinary project of the MEERC (Multiscale Experimental Ecosystem Research Center) designed to assess scale-dependent variability as it relates to ecosystem health. The MEERC is a 2300 sq. ft. laboratory containing 27 circular multicosms. Fluorescent and incandescent illumination simulated the spectral composition of photosynthetically active radiation (PAR). The light:dark cycle is 12h:12h. Ten cm of sediment lined the bottom of each cosm. The tanks were filled with water from the Choptank River, Cambridge, Maryland, USA initially, and each day of experimentation a 10% raw water exchange was completed (10% of tank volume was removed and subsequently replaced with fresh, raw Choptank River water). Each tank had an automated mixing system on a 4h:2h on:off mixing cycle. Each tank was also equipped with thermistors for continuous water temperature recording (Reyes, 1994). Table 1 summarizes the dimensions of the three mesocosms investigated in this study.

Table 1. Mesocosm dimensions.

Tank	Radius (m)	Depth (m)	Capacity (m^3)
A1	.178	1.0	0.1
C1	.565	1.0	1.0
E1	1.78	1.0	10

Copepods were collected on 202 μm mesh sieves drawn through the water of mesocosms A1, C1, and E1 in the MEERC laboratory. To avoid potential problems associated with diurnal feeding patterns collections were consistently made between 1400 and 1600 hrs on specified sampling days (Marshall and Orr, 1955; Kiørboe et al., 1985). Once collected, animals were covered to minimize exposure to light and taken to a dimmed light laboratory where they were washed and prepared for freezing. Animals were washed for 10-15 seconds in each of three filtered sea water baths by gently agitating the collection sieve in the baths. The copepods were then washed off of the collection sieve with filtered sea water into a Millipore hand pump filtration unit and collected on Whatman GF/C filters. After filtration, filters were immediately wrapped in aluminum foil and placed in a -80°C freezer until extractions were made (with in approximately 24 hrs.) (Dam and Peterson, 1988).

Gut Fluorescence. Fifty copepods (adults and copepodites) were used (fewer were used in instances of inadequate collection) for gut fluorescence measurements. To minimize photodegradation of gut contents during the selection process, all selections were completed in either dim or dark ambient light conditions. In addition, red acetate was placed over the microscope platform to prevent potential chlorophyll degrading wavelengths of light from reaching the copepods directly. Copepods were selected randomly and in duplicate from frozen filters using jewelers forceps and placed directly in 8 ml of 90% acetone for extraction of chlorophyll. Samples were then immediately placed in a -20°C freezer and allowed to extract overnight (18-24 hours). Samples were then diluted with 90% acetone to a final volume of 10 ml prior to centrifugation for 10 minutes at 2050 rpm. Following centrifugation, fluorescence measurements of the supernatant were taken using a Turner D (model 10-005) fluorometer before and after acidification with 10% HCl (Dam and Peterson, 1988).

Ingestion rates. Assuming that egestion and ingestion are in equilibrium and that egestion occurs at a constant rate, ingestion rate (I) is calculated using the following equation

$$I = KG \qquad (1)$$

where K is the gut evacuation rate constant (min) and G is the amount of food animal^{-1} (Dam and Peterson, 1988).

The instantaneous gut evacuation rate constant can be estimated using the equations of Dam and Peterson (1988) if the size of the copepod and the temperature of the ambient water are known. The equation follows:

$$K = 0.0119 + 0.001904T \qquad (2)$$

where K is the instantaneous gut evacuation rate constant (time) and T is the temperature (°C). Dam and Peterson (1988) investigated the effect of temperature on ingestion rates in *Temora longicornis* to determine an equation for K. As *Temora longicornis* and *A. tonsa* are approximately equal in size, no account was made for relative copepod size; consequently, temperature alone, according to the equations, was used to determine K.

Mesocosm Copepod Densities. Copepod densities were determined to assess the trophic behavior of *A. tonsa* in the mesocosms. Twice each week, a 10 L sample of water was taken from mesocosm A, and a 20 L sample was taken from the C and E mesocosms (samples for ingestion rate and copepod density were collected on the same day) and poured through a 44μm mesh sieve. The sample was then washed off of the sieve and preserved in 1% buffered formalin. Using an image analysis system and a double-channeled Plexiglas wheel two 5 ml aliquots of the preserved sample were counted and an average density calculated.

Pigment Concentration. Pigment concentrations in each mesocosm were determined using the fluorescence method. All measurements were made on the same Turner Designs fluorometer as was used for gut fluorescence measurements. Pigment concentration data were obtained from J. Cornwell (University of Maryland, pers. comm.).

Results and Discussion

There are no apparent trends in ingestion rate on a per mesocosm basis. Generally the ingestion rate of *A. tonsa* increased throughout the experiment in all tanks (Fig. 1a). This suggests that mesocosm size may only play a significant role in the ingestion rate to the extent which it controls trophic relationships through regulating organismal density and

diversity. It is worthwhile, then, to consider the relationships of pigment concentration vs. ingestion rates (Fig. 1a), density of *A. tonsa* vs. ingestion rate (Fig. 1b), and finally, pigment concentration vs. density of *A. tonsa* (Fig. 1c) in detail.

In tank A1 pigment concentration appears to be the controlling factor of the trophic behavior of *A. tonsa*. Density of *A. tonsa* responds directly to shifts in pigment concentration; as pigment concentration decreases the number of copepods decreases (Fig. 1c). Figure 2 depicts this response in a different way. The ingestion rate was multiplied by the density of *A. tonsa* to obtain a value for the amount of pigment consumed (ng chlorophyll *a* m^{-3} d^{-1}). When this value is compared to the pigment concentration a functional relationship is revealed, i.e. when less food is available for consumption, less food is consumed. This implies that tank A1 copepods are food limited and, as a result, mortality increases. The distinct decrease in copepodite density illustrates this mortality.

Food availability was determined by dividing the mesocosm pigment concentration by the density of *A. tonsa*. The general trend in food availability (Fig. 3) and ingestion rate (Fig. 1a) in mesocosm A1 is very similar. Changes in ingestion appear to be a response to the pigment concentration. By the nature of the equation used, a change in mesocosm pigment concentration translates directly to a similar change in the ingestion rate ,assuming temperature remains relatively consistent through the course of the experiment (temperature range=1.7°C).

Despite having the lowest mesocosm pigment concentration as well as the lowest food availability, tank A1 generally had the highest values of ingestion rate. This may simply suggest, however, that there exists a saturation point in relation to food availability and ingestion rate. That is, even though the food availability is low it is at least sufficient, but probably more than enough, to feed the number of copepods in the tank. Tanks C1 and E1, having higher pigment concentrations and greater food availability, would be expected to have similarly higher ingestion rates based on research that has shown ingestion rates to increase with increasing algal cell concentration (Deason, 1980; Kiørboe et al., 1982). This may suggest that community structure is different in the C1 and E1 tanks such that *A. tonsa* is feeding on alternative sources of food.

Pigment concentration does not appear to influence components of the C1 mesocosm as in the A1 mesocosm. On day 203 food availability appears to be greater than day 200 (Fig 3). Because there is more food present, more food is, in fact, ingested (Fig. 2). This increase in ingestion is apparent in the decrease of the mesocosm pigment concentration (Fig. 1a) and, ultimately, the increase in density of *A. tonsa* on day 207 (Fig. 1c). Alternately, it may be argued that the pigment concentration decreases as a result of a change in the trophic structure of the tank. For example a flagellate bloom may have occurred, thus providing *A. tonsa* with an alternate food source. Such an event would still provide food enough to support an increase in the total density. With the elevated density grazing pressure increases and less food is available (Fig. 3) which results in a decrease in the density on day 210. However, there was also a decrease in the ingestion rate between day 207 and day 210.

The decrease in ingestion rate was not mediated by a change in the mesocosm pigment concentration as appeared to be the case in tank A1 which reveals a potential shortcoming of the fluorescence method. That is, if *A. tonsa* is feeding on a food source that does not contain chlorophyll the ingestion rate will be underestimated, showing up as a decrease where it is not expected. Between days 207 and 210 the decrease in density and increase in food availability would be expected to yield higher ingestion rates. However, as this is not the case, utilization of alternate food sources such as detritus and flagellates/protozoans can be suspected. The decrease in density on day 210 gives way to greater ingestion as the amount by which the density decreases does not exceed the decrease in pigment concentration (Fig. 1c). As a result, the ingestion rate of *A. tonsa* over the final sampling days increases.

It seems that pigment concentration mediates the trophic dynamics of tank E1 as the pigment consumed and the pigment concentration express a similar trend during the first three sampling days (Fig. 2). However, the extreme difference (i.e. the distance between lines) between these variables suggests otherwise. It is apparent, by considering the pigment concentrations of both mesocosm A1 and C1, that the pigment concentration of mesocosm E1 is sufficient enough to support greater ingestion and thus higher ingestion rates. The amount of pigment consumed by E1 organisms is slightly lower, however, than that of either tank A1 or C1 organisms, which is evident in the comparatively lower ingestion rates (Fig. 1a).

Between days 200 and 203 both density and pigment concentration decrease, however, food availability increases. Despite this, pigment consumption experiences a decline (Fig. 2) which is reflected in the ingestion rate (Fig 1a). Likewise, between days 210 and 214 there is a decrease in density. Over this time the pigment concentration decreases, while food availability increases. Here again, the pigment consumption decreases, bringing with it the ingestion rate. In both of these instances it appears as if ideal conditions exist for an increase in ingestion rate from the previous measurement. As this is not the case, utilization of alternate food sources is suspected.

Conclusions

In tanks C1 and E1 trophic relationships do not appear to be regulated strictly by mesocosm pigment concentration. Inconsistencies in apparent trends suggest that *A. tonsa* is feeding on organisms and/or substances that do not contain chlorophyll, and are consequently not measurable by the fluorescence method.

Tanks C1 and E1 are more likely to have a broader diversity of organisms simply based on the greater volume of each of these mesocosms as compared to the A1 tank. This, in itself, may serve to provide alternate food sources to *A. tonsa*.

The design of the mesocosms may lend itself to altering the community structure as well. Walls are constructed of translucent Fiberglas. With increasing tank volume there is an accompanying threefold increase in the radius of each mesocosm (Fig. 1, Table 1). In the larger tanks, this translates to a darker water column in the center of the tank. In tank A1 the combination of direct lighting and penetration of light through the walls is such that light penetrates the entire water column. In tank C1 this occurs to a lesser extent (the sediment in the tank was not visible as in the A1 tank when viewed from directly above the cosm) and in the E1 tank, to an even lesser extent. The dark zone in the E1 tank has a larger diameter than that in the C1 tank.

Less light in the tanks may be responsible for changing community structure. With a proportionately larger light zone, tank A1 may better suit non-flagellated microalgae, as opposed to protozoans/flagellates, such that non-flagellated food organisms exist throughout the mesocosm. Another consideration is that due to the small volume of the tank, diversity is limited to non-flagellated microalgae. In tanks C1 and E1 where there is a dark zone, flagellates may occur in larger numbers. Production of the flagellates is not necessarily limited by light penetration as they are able to move to areas where light levels are sufficient. As a result there is competition between non-flagellated microalgae and flagellates. This relationship is enhanced by the volumes of the C1 and E1 tanks which allow for a broader diversity of organisms. In considering just the mesocosm pigment concentration data for each tank it appears that tank A1 is comprised of less chlorophyll containing microalgae than either of the other tanks (Fig. 1a). This in itself may be a factor of scale.

Another consideration in the differences in community structure within the mesocosms is the design of the mixing system. While dye dispersion studies were completed (Reyes, 1994) to test the mixing capacity of the mixing bars in each mesocosm, insufficient mixing may alter community structure in favor of flagellates. Non-flagellated microalgae depend on the mixing system to remain suspended. If there are dead spaces (spaces of insufficient mixing) in a particular mesocosm the non-flagellated microalgae will sink making flagellates more desirable to feeding copepods in that area. Dead spaces have been observed in tank E1.

Instances of optimum feeding potential (when food availability is greatest) with corresponding low ingestion rates may reveal differences between mesocosms due to scale. Elucidation of the hypothesized effects of mesocosm design discussed above will be necessary in order to more accurately assess variation due to scale.

ACKNOWLEDGMENTS

The author kindly thanks the following: University of Maryland Sea Grant Research Experience for Undergraduates program for sponsoring this fellowship; Ann Gauzens and Louise Wootton for supportive and stimulating suggestions; Jeff Cornwell, Sherry Pike, and Tom Wozniak for pigment concentration data; and Tim Goertemiller, Eric Nicholson, Alison Sipler and Tom Wozniak for sampling assistance in the MEERC.

REFERENCES

Berggreen, U., B. Hansen and T. Kiørboe. 1988. Food size spectra, ingestion and growth of the copepod *Acartia tonsa* during development: implications for determination of copepod production. Mar. Biol. 99:341-352.

Crossland, N. and T. La Point. 1992. The design of mesocosm experiments. Envir. Toxi. Chem. 11:1-4.

Dagg, M. and K. Wyman. 1983. Natural ingestion rates of the copepods *Neocalanus plumchrus* and *N. cristatus* calculated from gut contents. Mar. Ecol. Prog. Ser. 13:37-46.

Dam, H. and W. Peterson. 1988. The effect of temperature on the gut clearance rate constant of planktonic copepods. J. Exp. Mar. Biol. Ecol. 123:1-14.

Deason, E. 1980. Grazing of *Acartia hudsonica* (*A. clausi*) on *Skeletonema costatum* in Narragansett Bay (USA): Influence of food concentration and temperature. Mar. Biol. 60:101-113.

Frost, B. 1972. Effects of size and concentration of food particles on the feeding behavior of the marine planktonic copepod *Calanus pacificus*. Limnol. Oceanogr. 27:805-815.

Kiørboe, T., F. Møhlenberg, and H. Nicolajsen. 1982. Ingestion rate and gut clearance in the planktonic copepod *Centropages hamatus* (Lilljeborg) in relation to food concentration and temperature. Ophelia 21(2):181-194.

Kiørboe, T., F. Møhlenberg and H. Riisgård. (1985). *In situ* feeding rates of planktonic copepods: a comparison of four methods. J. Exp. Mar. Biol. Ecol. 88:67-81.

Kleppel, G. 1988. On the diets of calanoid copepods. Mar. Ecol. Prog. Ser. 99:183-195.

Marshall, S. and A. Orr. 1955. The biology of a marine copepod. Oliver and Boyd, Edinburgh. 188 p.

Paffenhöfer, G. 1971. Grazing and ingestion rates of nauplii, copepodids, and adults of the marine planktonic copepod *Calanus helgolandicus*. Mar. Biol. 11:286-298.

Paffenhöfer, G. 1988. Feeding rates and behavior of zooplankton. Bull. Mar. Sci. 43(3):430-445.

Pomeroy, L. 1974. The Ocean's Food Web, A Changing Paradigm. BioSci. 24:499-504.

Reyes, E. 1994. Science Advisory Council Mid Year Project Review. April 1994. 20 pp., unpublished.

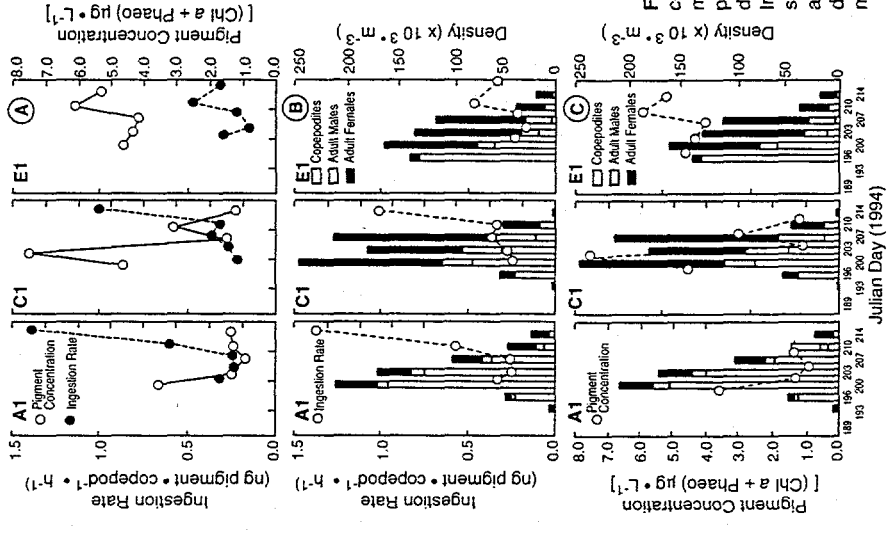


Fig. 1. a) Comparision of ambient pigment concentrations and ingestion rates for each mesocosm. There is a one day lag between pigment concentration data and ingestion rate due to MEERC sampling restrictions. Ingestion rate points are the mean of two samples. b) Comparision of *A. tonsa* density and ingestion rate. c) Comparison of *A. tonsa* density and pigment concentration for each mesocosm.

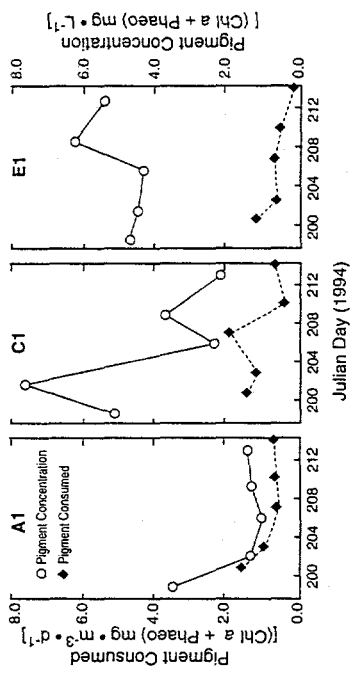


Fig. 2. Comparisons of mesocosm pigment concentration to pigment consumption by *A. tonsa*. Pigment consumption is determined by multiplying the ingestion rate by the *A. tonsa* density.

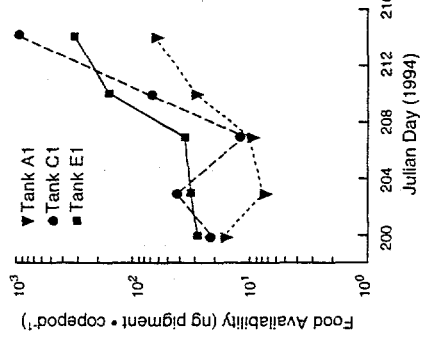


Fig. 3. Changes in food availability. Food availability is determined by dividing the mesocosm pigment concentration by the *A. tonsa* density.

PHOTOPERIOD AND SEASONAL DIFFERENCES OF ENDOPHYTIC AND FREELIVING FORMS OF THE TWO MARINE GREEN ALGAE, *ACROSIPHONIA* AND *MONOSTROMA*

Ami C. Ongstad

Department of Biology
Seattle University
Broadway and Madison
Seattle, Washington 98122-4460

Faculty Advisor: Margaret L. Hudson

INTRODUCTION

Acrosiphonia and *Monostroma* are two green algae found in cool marine waters, including the coast of Whidbey Island, Washington. They exist in two alternating life stages, gametophyte and sporophyte. The life cycle of *Acrosiphonia* is an alternation of generation between sporophyte and gametophyte. Multicellular gametophytes mature and produce gametangia which release biflagellate gametes. Opposite mating types fuse and form a planozygote that germinates into the sporophyte generation which has been found in nature within certain red host algae. These endophytic sporophytes are very small, between 20 and 220 micrometers in diameter (Ongstad, 1994). For this study the red host algae include *Iridaea*, *Schyzimenia* and *Constantinea*. *Acrosiphonia's* life cycle is diagrammed below in figure 1. *Monostroma's* life history is reported to be variable. Blades are reported to produce quadriflagellate zoospores in some species and bifalgellate gametes in other species. Zoospores and zygotes are reported to sometimes produce a discoid stage (Abbott and Hollenberg,1976). A stage in the life history of *Monostroma* has been found to be endophytic within *Iridaea* and *Schizymenia* (Ongstad, 1994). In this study will investigate *Acrosiphonia's* gamete release with relation to photoperiod, sporophytic competition between *Acrosiphonia* and *Monostroma*, and distribution studies of intertidal algae on Whidbey Island. These issues were investigated to gain insight into the complicated challenges these two marine green algae face in nature.

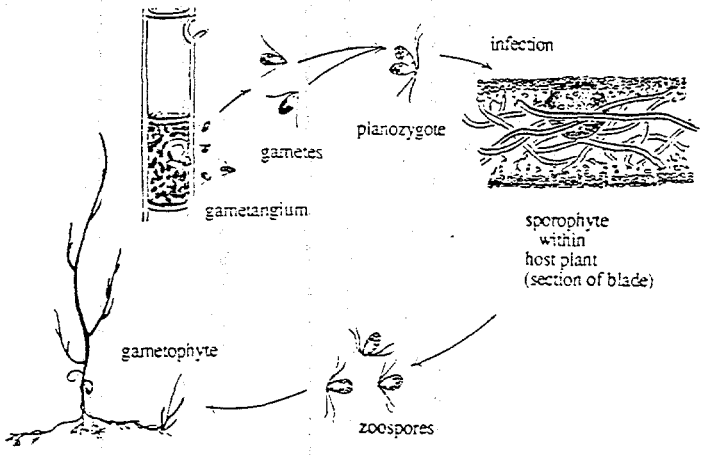


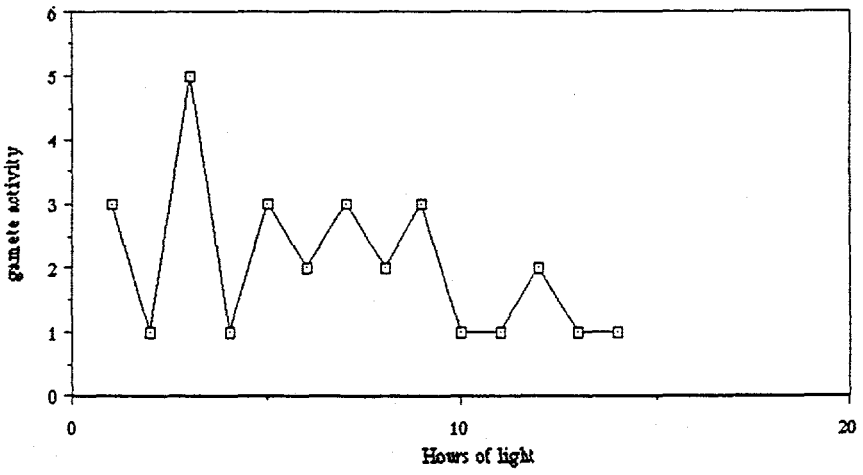
Figure 1: *Acrosiphonia's* Life cycle: Alternation of generation

ACROSIPHONIA'S GAMETE RELEASE WITH RELATION TO PHOTOPERIOD

Acrosiphonia gametophytes growing in culture with Provasoli's enriched sea water, under 14L:10D, in a culture chamber at temperatures near 10C, equipped with cool white light were used for this study. Mature gametophytes were cut into pieces approximately one centimeter in length and ranging from 35 to 90 cells long. They were placed in a depression slide with sterilized sea water. The slide was kept in the culture chamber

and taken out every two hours to be checked on a compound microscope for gamete release, and gamete release activity was ranked. The scale is as follows, 1- no gamete activity, 2-gametes moving inside one gametangium, 3- gametes releasing from one gametangia to the outside of the cell, 4- two gametangia containing active gametes, 5-three gametangia containing active gametes 6-more than three gametangia containing active gametes. Gamete release was also studied in the dark hours. Depression slides were prepared with mature *Acrosiphonia* gametophytes cut as described above in light hours and placed in the culture chamber. During dark hours the slide was removed from the cold room covered up so that exposure to light would be minimal. The slide was then scanned quickly for active gametes in the gametangium. Activity was rated the same as above and the slide was not used again, since the dark period had been interrupted.

During the light hours, gamete release was found most likely to occur between the first and the eighth hours of light. The greatest activity in gamete release was observed at three hours into the light period, with an average rating of 5 (more than two gametangium containing active gametes). In the dark hours gamete release was minimal. A total of fourteen *Acrosiphonia* filaments was checked. Gametes are very small and live within a large volume of sea water in nature. In order to form a planozygote and continue their life cycle, these gametes must find other gametes of opposite mating types and fuse with them. *Acrosiphonia* must release its gametes at a time when the probability of finding opposite mating types is highest. Therefore a timed gamete release is advantageous to the reproductive success of *Acrosiphonia*. It appears that this timed gamete release is a photoperiod response since all other factors were kept constant. Gametes of *Acrosiphonia* contain an eyespot and display positve phototaxis which would also help them to find each other during the light period (Hudson, 1974). Graph 1. summarizes these results.



Graph 1. *Acrosiphonia* Gamete Release over Time

SEASONAL DIFFERENCE IN PRESENCE OF SPOROPHYTES OF GREEN ALGAE

Red host algae *Iridaea, Schizymenia* and *Constantinea* were collected on Whidbey Island from June 1993 to January 1995. Sporophytes were isolated from their red host algal blades, rinsed in three changes of sterile sea water in a spot plate and placed in small, sterile petri dishes with sterilized sea water. The cultures were placed in a cold room equipped with cool white light at 14L:10D and temperatures remaining near 10 C. Since sporophytes of these two genera cannot be distinguished from each other using a microscope, these isolations were done to better

observe the change from sporophyte to gametophyte. Since the gametophytes of these two genera are quite different in structure (blades in *Monostroma* and branched filaments in *Acrosiphonia*), it is possible to determine the genus after spores released by the sporophytes have grown up into gametophytes. The cultures were checked approximately once every two weeks. Any changes in morphology or mortality were noted along with the date. Results are summarized on the following page in table 1.

Table 1. Seasonal Differences in Presence

Month of Isolation	Number and Genus of sporophytes that survived to produce gametophytes	
	Acrosiphonia	*Monostroma*
June	0	3
July	1	7
August	3	1
September	0	0
October	0	1
November	0	2
December	2	0
January	0	1
February	0	0
March	0	0
April	0	0
May	0	0

Fifteen *Monostroma* sporophytes survived to produce gametophytes and six *Acrosiphonia* sporophytes survived to produce gametophytes over 19 months and 21 out of 220 isolated sporophytes. This can be explained three ways: *Monostroma* is either hardier in a culture environment, more prevalent in red host algae, or both. Sporophytic *Monostroma* is present in red host algae between June and January. Sporophytes identifiable as *Monostroma* were most prevalent during June and July, making up 11 out of 15 total sporophytes that survived to produce *Monostroma* gametophytes. Sporophytes identifiable as *Acrosiphonia*, were present in red host algae between July and December. Sporophytes identifiable as *Acrosiphonia* were most prevalent in red host algae in August. Three out of the 6 sporophytes that survived to produce *Acrosiphonia* gametophytes were present in red host algae in August. There does not appear to be a seasonal difference in presence between *Acrosiphonia* and *Monostroma*. *Monostroma* does appear to be hardier and more prevalent in the red host algae than *Acrosiphonia* from the results of this study. However, until there is a way to identify the genus of the sporophytes directly, or increase the number of sporophytes which release spores in culture, these results will remain preliminary.

DISTRIBUTION OF INTERTIDAL ALGAE ON WHIDBEY ISLAND

Six quadrat studies total were done on November 4, 1994, December 30, 1994 and January 29, 1995 on Whidbey Island. Tidal heights at times these quadrat studies were done ranged from -2.6 to -1.4 feet, between these three months. The quadrats were five feet square and subdivided into four parts consisting of a northwest, northeast, southwest and southeast each approximately two and one-half feet square. Genera were recorded along with approximate percentages of covered area by that genus within the subdivided quadrats. Genera were not recorded for the phylum Chlorophyta because identification of the greens can be difficult without the help of a microscope; therefore all green algae were recorded together. The majority of the greens appear to be *Ulva fenestrata* and *Enteromorpha linza*, but to be avoid misidentifying any genera within Cholophyta they will remain grouped together. Although *Acrosiphonia* gametophytes were looked for, Acrosiphonia was not observed during these winter months in this study.

Genera and species from the phylum Rhodophyta observed in the quadrat were *Mastocarpus papillatus, Iridaea splendens, Laurencia spectabilis, Odonthalia floccosa* and *Neorhodomela larix.* Genera and species observed from the Phylum Phaeophyta include *Alaria marginata, Laminaria saccharina* and *Fucus gardneri.* All numbers recorded for each genus and species in the subdivided quadrats for each date were averaged and the range was found. Results are summarized onthe following page in Table 2.

Table 2.

Average Percent Coverage of Algae

	Nov.		Dec.		Jan.	
Genus species	avg.	range	avg.	range	avg.	range
Mastocarpus papillatus	23	17-27	9	0-15	8	0-15
Laurencia spectabilis	0.6	0-5	5	0-15	0.5	0-2
Odonthalia floccosa	0	0	1.4	0-5	0.3	0-1
Neorhodomela larix	0	0	0.6	0-5	0.6	0-2
Alaria marginata	7	0-7	1	0-7	0.1	0-1
Laminaria saccharina	3	0-5	6	0-20	0.5	0-2
Fucus gardneri	15	5-20	7	0-15	7	2-12
Greens	21	15-30	5	0-8	3	1-7
Total coverage	76.6		39		23	

The average total area of coverage decreased over time. November had an average percent coverage of 77.6%, December had 38.4%, and December had 22.4%. The coverage during these winter months is expected to decrease due to shorter daylength and the increase in winter storms and freezing. It is expected that harsh conditions during winter would result in loss of algal mass and these results are consistent with this assumption.

Iridaea splendens is of significant importance in this study since it is the only red host alga for *Acrosiphonia* and *Monostroma* present in these quadrats. In November it was found to have an average area of coverage of 7%, 4% for December and 3% for January. Most of the *Iridaea splendens* was present as very small blades arising in groups. Its presence during the winter months suggests a possible way for sporophytic *Acrosiphonia* and *Monostroma* to survive during the winter. Gametophytic *Acrosiphonia* and *Monostroma* were not observed during these months in the quadrats. *Acrosiphonia* is known to go to a rhizoidal form over the winter and then appear between February and April in its gametophytic form (Hudson, 1974). In addition, sporophytes of *Acrosiphonia* are commonly found in the crustose *Petrocelis* phase of *Mastocarpus papillatus*, in which *Acrosiphonia* is called *Spongomorpha coalita* (Fan, 1959). It may also be advantageous to find a durable, always present host in which to over winter in the sporophytic form; in spring, when the threat of winter storms have past they can release gametes and continue their life cycle as the gametophyte. Distribution of potential hosts is an important aspect of the life cyle of endophytic algae. It is necessary that hosts be available during the times in which zygotes are formed, and that they are numerous enough to allow the zygotes to incorporate themselves into the blade and form endophytes. *Gigartina papillata* (now known as *Mastocarpus papillatus*) at Partidge Point on Whidbey Island, has been reported to contain *Acrosiphonia* sporophytes (Hudson, 1974). *Mastocarpus papillatus* was the most abundant alga on average for November (23%), December (9%), and January (8%). In this study endophytes in *Mastocarpus*

papillatus have not been found, but the high distibution of this red alga could make a favorable host for endophytes.

The average percent coverage from the phylum Chlorophyta and Phaeophyta was highest also during November and decreased in December , and January. Phylum Phaeophyta was represented by *Alaria marginata*, *Laminaria saccharina* and *Fucus gardneri* . Although green endophytes have not been reported in these algae they could have an effect on both gametophytic and sporophytic *Acrosiphonia* and *Monostroma*, through competition for intertidal space for both red host algae, and also the gametophytes.

CONCLUSIONS:

In summary, these studies have discovered some of the challenges and means by which these two marine green algae deal with these challenges. One of these challenges is reproductive success. To increase it's reproductive success, *Acrosiphonia* has evolved eye spots and a photoperiod response for gamete release. This allows for an increased probability that other gametes will find each other and fuse in order ot carry out their life cycle. Another challenges faced by *Acrosiphonia* and *Monostroma* is competition. Sporophytic *Acrosiphonia* and *Monostroma* compete with each other for red algal hosts, but results on the intensity of this competition are preliminary due to the difficulty in identifing the sporophytes of these genera and in the low number of sporophytes releasing spores in culture. Distribution of red host algae is important in understanding the competition red host algae face which would effect sporophytic *Acrosiphonia* and *Monostroma*. Distribution was found to vary in the months of November, December and January. The red host algae *Iridaea splendens* was present through out these months along with *Mastocarpus papillatus* which suggests that these host algae are available during these months for possible infection by sporophytic *Acrosiphonia* and *Monostroma*. More work needs to be done on *Acrosiphonia* and *Monostroma* to understand the intricate balance these two marine green algae have with each other and their hosts in nature.

BIBLIOGRAPHY

Abbott, Isabella A. and Hollenberg, George J. 1976. Marine Algae of Califonia. Stanford University Press. Stanford, Cailfonia.

Fan, K. C. 1959. Studies on the Life-histories of marine algae. I. *Codiolum petrocelidis* and *Spongomorpha coalita*. Bull. Torrey Bot. Club 86: 1-12.

Gabrielson, P.W., Scagel, R.F., and Widdowson, T.B. 1990. Keys to the Benthic Marine Algae and Seagrass of British Columbia, Southeast Alaska, Washington and Oregon. Phycological Contribution Number 4. University of British Columbia Department of Botany 187pp.

Hudson, Margaret L. 1974. Field, Culture and Ultrastructural Studies on the Marine Green Algae *Acrosiphonia* in the Puget Sound Region. PhD. Dissertation. University of Washington.

Ongstad, Ami C. Life Cycle Relationships of the Green Alga *Acrosiphonia* on Whidbey Island, Washington. 1994. Proceedings eighth National Conference on Undergraduate Research. VIII. University of North Carolina July, 1994 pp 810-814.

Provasoli, L. 1968. Media and Prospects for the cultivation of marine algae. In: Watanabe, A. and Hattori, A. (eds.), Cultures and Collections of Algae. Proc. U.S. Japan Conf. Hakone, Sept. 1966. Japan Society of Plant Physiology pp 63-75.

Special Thanks to Dr. Margaret Hudson for allowing me the wonderful opportunity to work with her over the past two years and her unending support and guidance.

The Distribution and Ecology of Freshwater Sponges in Connecticut with an Emphasis on the Thames River Basin.

Elizabeth M. De Santo
Department of Zoology
Connecticut College
New London, CT 06320

Faculty Advisor:
Paul E. Fell

ABSTRACT

A study of the distribution and ecology of freshwater sponges was conducted during the summer and fall of 1994 (June to December). Sites surveyed included both lentic and lotic environments. Sponges were found in 21 out of 53 survey locations: *Spongilla lacustris* at 11, *Ephydatia muelleri* at 8, *Eunapius fragilis* at 5, *Anheteromeyenia ryderi* at 4 and *Corvomeyenia everetti* at 2. This is a previously unrecorded species in Connecticut. In addition, siliceous sponge spicules were found in surface sediments of 33 out of 45 lakes. Sites where live sponges and/or spicules were found were slightly acidic with low conductivities, low chlorophyll-*a* concentrations, and low alkalinities as compared with sites where no evidence of sponges was found. Sexual reproduction and gemmule formation by the sponges also was studied. An extended drought substantially lowered water levels at some sites by mid-summer, and many sponges at these sites were killed. Thick-walled gemmules of *Spongilla lacustris* were found to be desiccation tolerant, but thin-walled gemmules of this sponge were not.

INTRODUCTION

The Spongillidae is the only family of the class Demospongiae found in freshwater. The Demospongiae comprise 95% of the world's sponge species (Hickman *et al.* 1988). Of the thousands of sponge species, only 170 species are known to occur in freshwater environments (Penny and Racek, 1968; Schwandes and Collins, 1994).

Sponge reproduction may be sexual and/or asexual. Sexual reproduction typically results in the release of free-swimming larvae. Asexual reproduction may occur by fragmentation (Wulff 1991), the production of external buds that separate from the parent sponge (Saller 1990) and/or the formation of gemmules (Harrison, 1982; Simpson, 1984; Fell, 1993). Gemmules are reproductive bodies that are sometimes formed by the parent sponge as a response to environmental stress (Harrison 1982; Bazer and Fell 1986). These spherical structures consist of an internal mass of undifferentiated cells enclosed by a secreted outer layer, often containing spicules (Pennack, 1953; Harrison, 1982; Simpson, 1984). Gemmule production is a characteristic process of freshwater sponges. Factors apart from environmental stress that regulate gemmule formation are largely unknown (Bazer and Fell 1986). In some cases gemmules are produced well in advance of the onset of unfavourable conditions. Thorough field studies examining gemmule formation and hatching have been carried out on few freshwater sponges, and information concerning sexual reproduction is also sparse (Simpson and Gilbert 1973).

Freshwater sponges are common in ponds, lakes, streams and rivers; they may occur in clear or turbid waters. Due to their sessile nature and inconspicuous coloration, sponges are frequently overlooked. Freshwater sponges attach and grow on almost any substratum, but there are species-specific preferences for different water flow conditions (Harrison 1974). Excessive water turbulence tends to eliminate sponges from habitats, however these animals can thrive in areas of good circulation that bring food and oxygen and remove wastes and sediments. Other factors affecting sponge distribution may include light intensity, water temperature and color, and water chemistry. Little is known about the ecology of freshwater sponges in Connecituct, and no comprehensive study of their distribution in this state has been reported.

METHODS AND RESULTS

Throughout the summer and fall of 1994, 53 sites were surveyed, and at 21 (40%) of these, sponges were observed. *Spongilla lacustris* was found at 11 sites, *Ephydatia muelleri* at 8, *Eunapius fragilis* at 5, *Anheteromeyenia ryderi* at 4 and *Corvomeyenia everetti*.at 2.

The study of the geographical distribution of the freshwater sponges concentrated around the following river systems: the Thames River basin, which includes the Quinnebaug, Shetucket, Yantic and Willimantic rivers; the Pawcatuck River basin, including Shunock Brook; the Connecticut River basin, including Eight Mile River; the

Hammonasset River basin and the Housatonic River basin. These systems are located for the most part in the eastern upland half of the state, with the exception of the Housatonic system, located west of the central valley region. *Spongilla lacustris* , *Ephydatia muelleri* and *Corvomeyenia everetti* were each found in one site in this western region, whereas *Spongilla lacustris* and *Ephydatia muelleri* were present at many locations throughout the eastern region. *Anheteromeyenia ryderi* and *Eunapius fragilis* were found only in the eastern half of the state and in fewer locations than the other species.

Table 1 shows the distribution of sponges found, as well as their relative abundances and reproductive activity. Sites surveyed included both lentic and lotic environments, corresponding to 15 lakes or ponds and 6 river sites. Sponges found in lakes or ponds were frequently located in areas of moving water, near dams. Seven of the 15 lake sites where sponges were found were in fast-moving water below dams, while 8 of the lakes sites were in still areas within the body of the lake.

Table 1. Species distribution, lentic vs. lotic environments.
Key: P = present; C = common; A = abundant; g = gemmules; e = embryos

	S.l.	*E.m.*	*A.r.*	*E.f.*	*C.e.*
I. Fast-moving water					
THAMES RIVER BASIN					
Quinnebaug River					
below Glasgo Pond dam	C-g	-	-	-	-
below Pachaug Pond dam	C-g,e	C	-	P-g	-
below Hopeville Pond dam	A-g,e	A-g	-	C-g	-
Snake Meadow River	C-e	-	C-g	-	-
Shetucket River					
at Willimantic	C-g	C-g	-	-	-
Willimantic River					
at Mansfield Depot	-	-	-	P-g	-
below State Line Pond dam	-	-	P-g	-	-
below Crystal Pond dam	C-g	-	C	C-g	-
Yantic River					
Pease Brook	-	P	-	-	-
PAWCATUCK RIVER					
Shunock Brook	-	C-g,e	-	-	-
CONNECTICUT RIVER BASIN					
Eight Mile River	-	C-e	-	-	-
HAMMONASSET RIVER BASIN					
below Hammonasset dam	C-g,e	-	-	-	-
HOUSATONIC RIVER BASIN					
Winchester Lake	P	-	-	-	-
II. Still-water					
THAMES RIVER BASIN					
Quinnebaug River					
on Beach Pond dam	C	-	-	-	-
Shetucket River					
Black Pond	C	-	C-g	-	-
Arboretum Pond	-	-	-	-	-
PAWCATUCK RIVER					
on Gallup Pond dam	-	-	-	C	-
CONNECTICUT RIVER BASIN					
Pocotopaug Lake	-	C	-	-	-
Hayward Lake	P-e	-	-	-	-
Uncas Lake	-	-	-	-	P
HOUSATONIC RIVER BASIN					
Mohawk Pond	-	P	-	-	P

Table 2. Comparison of chemical data (means ± SD, **range**), lakes with sponges, lakes with sponges and/or spicules and lakes where neither sponges nor spicules were seen. Key: Chl-*a* = Chlorophyll-*a*; Cond = Conductivity.

Parameter	Units	Lakes with sponges	Lakes with sponges and/or sponge spicules	Lakes surveyed with neither sponges nor spicules
Secchi Disk	m	3.3 ± 1.2, **1.2-4.6**	3.7 ± 1.8, **0.9-9.2**	3.08 ± 1.2, **1.4-5.8**
Total P	µg/L	27.1 ± 11.8, **11-52**	27.8 ± 17.4, **9-96**	44.3 ± 77.7, **10-334**
Total N	µg/L	303.9 ± 105.9, **211-543**	388.1 ± 238.3, **119-1263**	588.9 ± 871, **208-3831**
Chl-*a*	µg/L	3.8 ± 4.2, **0.69-14.9**	6.2 ± 12.2, **0.2-69.1**	8.5 ± 17.2, **1.2-71.8**
Cond	µS/cm	53.6 ± 22, **25-101**	73.2 ± 49.4, **23-274**	146.2 ± 91.2, **36-317**
pH		6.6 ± 0.39, **5.9-7.1**	6.8 ± 0.93, **4.5-8.6**	7.4 ± 0.91, **4.8-8.9**
Alkalinity	meq/L	0.11 ± 0.05, **0.02-0.20**	0.30 ± 0.46, **-0.03-2.41**	0.66 ± 0.72, **0.0-2.37**
Cl	meq/L	0.19 ± 0.15, **0.02-0.55**	0.22 ± 0.13, **0.05-0.69**	0.37 ± 0.26, **0.05-1.04**
SO_4	meq/L	0.11 ± 0.02, **0.08-0.15**	0.13 ± 0.05, **0.07-0.33**	0.23 ± 0.14, **0.07-0.55**
K	meq/L	0.02 ± 0.01, **0.01-0.03**	0.03 ± 0.01, **0.01-0.06**	0.04 ± 0.01, **0.02-0.06**
Na	meq/L	0.21 ± 0.15, **0.06-0.59**	0.22 ± 0.11, **0.11-0.59**	0.41 ± 0.31, **0.11-1.02**
Ca	meq/L	0.15 ± 0.04, **0.07-0.21**	0.26 ± 0.24, **0.06-1.26**	0.53 ± 0.41, **0.12-1.44**
Mg	meq/L	0.08 ± 0.02, **0.03-0.09**	0.17 ± 0.24, **0.02-1.27**	0.29 ± 0.27, **0.05-0.95**

This survey also included the examination of sediment samples from many lakes for sponge spicules. These samples were preparations of siliceous remains from the surface layer of cores taken in deeper areas of the lakes. Spicules were seen in 33 out of 45 lakes (73%) surveyed for siliceous remains. The spicules found indicate the recent presence of sponges in many more lakes than those in which live sponges were found during the summer survey.

Smooth megascleres were present at 31 sites. There were 21 sites where *Spongilla lacustris* microscleres were found. *Ephydatia muelleri* -like megascleres were seen at 11 sites, and *Anheteromeyenia ryderi* -like megascleres also were found at 11 sites. *Corvomeyenia everetti*. microscleres were not seen in the spicule survey. There were 18 sites where live *E. muelleri* and/or *E. muelleri*-like spicules were seen, and 15 sites where live *A. ryderi* and/or *A. ryderi* spicules were seen.

In general, the water bodies where sponges occurred were slightly acidic, with low ion concentrations and conductivities, low chlorophyll-*a* levels and low alkalinities. Table 2 shows the chemical conditions of the lakes where live sponges were found, in comparison with sites where sponges and/or spicules were found, and sites where no evidence of sponges was found.

The sponges collected from the various sites were examined for embryos and gemmules, evidence of sexual and asexual reproduction respectively. *Spongilla lacustris* showed stages of both sexual and asexual reproduction, as did *Ephydatia muelleri* . *Eunapius fragilis* and *Anheteromeyenia ryderi* were only found with gemmules, and *Corvomeyenia everetti* was not found with reproductive bodies.

The life cycle events of one species, *Spongilla lacustris*, were examined in detail in the Pachaug system of the Thames River basin (Table 3). Two types of gemmules were observed, thick-walled and thin-walled. Thick-walled gemmules (brown) were produced early in the summer, while thin-walled gemmules (yellow) formed in the fall. Experiments involving rehydration of thick-walled gemmules have demonstrated that such gemmules are tolerant of dessication. In contrast, the thin-walled gemmules are not.

Table 3. Lifecycle events of *Spongilla lacustris* within the Pachaug River system of the Thames River basin during 1994.
Key: d = developing; M = mature

Date	Site	H_2O Temp. (°C)	Embryos	Gemmules	
				Brown	Yellow
22-Jun	Pachaug		*	-	-
7-Jul	Hopeville	26	*	-	-
7-Jul	Glasgo	27	-	-	-
24-Jul	Pachaug	(dry)	-	*	-
25-Jul	Hopeville	26	-	*d, M	-
16-Sep	Hopeville	(dry)	-	*M	-
12-Oct	Hopeville	10	-	-	*d, M
21-Oct	Glasgo	15	-	-	-
18-Nov	Glasgo	10	-	-	*d, M

CONCLUSION

The four major species found in this survey were *Spongilla lacustris, Ephydatia muelleri, Eunapius fragilis and Anheteromenia ryderi*, in order of relative abundance. In addition, a fifth species, *Corvomeyenia everetti*, was collected. This is a species previously unrecorded in Connecticut.

The abundance of freshwater sponges in the eastern region of the state indicates that the chemical and physical conditions of the lakes and rivers are favourable for these animals. However, spicule surveys of siliceous sediments that date back to five years show sponges in areas where they were not seen in the live-sponge survey. Live sponges were found more frequently in areas of fast-moving water. Spicules were present in still areas of lakes, however, indicating that the survey for live sponges probably missed sponges in some sites, or else the sponges that were present in lakes a few years ago have since died off.

The chemical analyses of lakes containing live freshwater sponges suggest preferences for specific conditions (Table 2). The survey concentrated in the eastern half of the state, and consequently fewer sponges were found in the central or western reions. Water bodies situated in the eastern and coastal regions of the state, where most of the specimens were found, are in general more dilute than lakes in the central and western geographic regions (Canavan and Siver 1994).

Experiments involving the desiccation-resistance of *Spongilla lacustris* have indicated that the thick-walled gemmules may serve as a protective mechanism against drying of the habitat. The ability of this species to reproduce asexually in this way may increase its chances of survival under adverse conditions.

ACKNOWLEDGEMENTS

Chemical data was provided by Dr. Peter Siver, Connecticut College, funded in part by National Science Foundation grant #DEB-9306587 to Dr. Siver.

LITERATURE CITED

Bazer, L.J. and Fell, P.E. 1986. Gemmules of *Anheteromeyenia ryderi* and *Heteromeyenia tubisperma* (Porifera: Spongillidae) from southern New England undergo diapause. *Freshwater Biology*, **16**: 479-484.

Canavan, R.W. and Siver, P.A. 1994. Chemical and physical properties of Connecticut lakes with emphasis on regional geology. *Lake and Reserv. Manage.*, **10**(2): 175-188.

Fell, P.E. 1993. Porifera: in *Reproductive Biology of Invertebrates* IV. Asexual propogation and reproductive strategies. K.G. and R.G. Adiyodi (eds): 1-43. New Delhi: Oxford & IBH Publishing Co.

Harrison, F.W. 1982. Developmental Biology of Freshwater Sponges. In: *Developmental Biology of Freshwater Invertebrates*. F.W. Harrison and R.R. Cowden (eds): 1-67. New York: Alan R. Riss, Inc.

Hickman, C.P., Roberts, L.S. & Hickman F.M. (eds). 1988. *Integrated Principles of Zoology*: Porifera pp. 166-177. St. Louis: Times Mirror/Mosby College Publishing.

Pennack, R.W. 1953. *Freshwater Invertebrates of the United States.* Spongillidae: 77-97. New York: The Ronald Press Co.

Penney, J.T. and Racek, A.A. 1968. Comprehensive revision of a worldwide collection of freshwater sponges. *U.S. Nat. Mus. Bull.*, No. 272, pp. 1-148.

Saller, U. 1990. Formation and construction of asexual buds of the freshwater sponge *Radiospongilla cerebellata* (Porifera, Spongillidae). *Zoomorphology*, **109**: 295-301.

Schwandes, L.P. and Collins, M.E. 1994. Distribution and significance of freshwater sponge spicules in selected Florida soils. *Trans. Am. Microsc. Soc.*, **113**(3): 242-257.

Simpson, T.L. and Gilbert, J.J. 1973. Gemmulation, gemmule hatching, and sexual reproduction in fresh-water sponges, (1) The life cycle of *Spongilla lacustris* and *Tubella pennsylvanica*. *Trans. Amer. Micros. Soc.*, **92** (3): 422-433.

Wulff, J.L. 1991. Asexual fragmentation, genotype success, and population dynamics of erect, branching sponges. *J. Exp. Mar. Biol. Ecol.*, **149**: 227-247.

Immunolocalization of a Conserved Tektin Peptide Sequence

Aimee M. deCathelineau

Department of Cell Biology and Neuroanatomy
University of Minnesota
Minneapolis, MN 55414

Faculty Advisor
Richard W. Linck

A polyclonal antibody to a conserved tektin peptide sequence was used to localize the conserved sequence in sea urchin (*Lytechinus pictus, Strongylocentrotus purpuratus*) sperm flagellar axonemes and basal bodies. The anti-peptide antibody recognizes three tektin polypeptides (55-, 51-, and 47- kD) by immunoblot analysis. Immunofluorescence microscopy has shown that the anti-peptide antibody stains the entire length of the flagellar axoneme and all nine doublet microtubules, as well as a region corresponding to the basal body and the acrosome in both methanol fixed and native, unfixed microtubules of both species of sea urchin.

Introduction

The cytoskeleton is composed of three major types of filaments. Microfilaments, intermediate filaments, and microtubules are responsible for essential cell functions such as cell division, cytoplasmic motility, and intracellular structure and organization. Flagellar microtubules have been shown to be similar to cytoplasmic microtubules and are highly conserved among species ranging from single cell algae to human cells. Thus, flagellar microtubules provide a useful means for studying general microtubule protein assembly, structure, and function.

Most eukaryotic flagella have an axoneme consisting of nine outer doublet microtubules and two central singlet microtubules. Tubulin, the major protein component of microtubules, forms protofilaments from *alpha*- and *beta*-tubulin heterodimers. In flagellar microtubules, the A-tubule in each doublet is constructed of thirteen protofilaments, and the adjacent B-tubule contains ten protofilaments and an eleventh, junctional component. Another class of proteins, tektins, are known to be associated with flagellar microtubules (Linck and Langevin, 1982). Tektins are an integral part of the A-tubule (Nojima *et al.*, 1995; Pirner and Linck, 1994) and are possibly involved in the attachment of several structures to the A-tubule, including the B-tubule and flagellar appendages such as dynein arms and radial spokes. Immunological evidence indicates that tektins, or tektin-like proteins, are present in centrioles, centrosomes, and mitotic spindles of many cell types, including human and other mammalian cells (Steffen and Linck, 1988).

Originally, tektins were found to be insoluble components of sea urchin sperm flagellar axonemes (Linck and Langevin, 1982). Detergent extraction of flagellar axonemes leaves a protofilament ribbon of three tektin isoforms as well as *alpha*- and *beta*-tubulin. Further extraction yields purified tektin filaments. Analysis by Sodium Dodecyl Sulfate - Polyacrylamide Gel Electrophoresis (SDS/PAGE) showed that tektins A, B, and C have apparent relative molecular weights of 55,000, 51,000 and 47,000 daltons, respectively. Genetic sequence analysis predicts the presence of alpha-helical rod domains separated by non-helical linker domains; this sequence analysis also revealed a conserved nine residue amino acid sequence in tektins A, B, and C (Chen *et al.*, 1993). This consensus sequence (RPNVELCRD) is located in a non-helical linker domain which disrupts the second alpha-helical rod domain and possibly forms a protruding loop from the tektin filament. Because it is conserved among all three tektins, this region may have significant function in the assembly or structure of stable microtubules and their associations with other proteins.

In previous studies, antibodies raised to tektins A, B, and C were used to study the location of tektins in axonemal microtubules using immunofluorescence and immunoelectron microscopy techniques (Linck *et al.*, 1987: Linck, *et al.*, 1985). Each of the three antibodies stained flagellar axonemes along the entire length of the axoneme. A thin fibril extending past the end of the axoneme was also stained by the antibodies, as well as the basal body and acrosomal region of the sperm head.

In this study, an antibody raised to the consensus peptide sequence of tektins A, B, and C, (an "anti-peptide") was characterized by immunoblot analysis and used to localize the conserved peptide sequence in methanol fixed and native *L. pictus* and *S. purpuratus* sperm flagellar axonemes.

Materials and Methods

Abbreviations

Bovine serum albumin (BSA), 3-[Cclohexylamino]-1-propanesulfonic acid (CAPS), 5-bromo-4-choro-

3-indoyl phosphate (BCIP), nitro blue tetrazolium (NBT), phosphate-buffered saline (PBS: 10 mM phosphate, 0.15 M NaCl, 2.7 mM KCl, pH 7.4), PBS containing 0.05% Tween 20 and 0.02% NaN_3 (PTN), polyacrylamide gel electrophoresis (PAGE), room temperature (RT), sodium dodecyl sulfate (SDS), Tris buffered saline (TBS: 20 mM tris, 0.5 M HCl, pH 7.5)

Affinity Purification

SDS denatured tektin filaments were conjugated to cyanogen bromide linked sepharose beads (Pharmacia). Crude anti-peptide sera was diluted in PBS, applied to the column and incubated. Unbound sera was washed from the column with PBS. Bound antibody was eluted from the column using 0.2 M Gylcine, pH 3.0 and neutralized with 0.4 M Tris/HCl, pH 9.0.

Preparation of peptide sequence

Sequence analysis of tektins A, B, and C and the preparation of the anti-peptide antibody were conducted as detailed in previously published studies. (Chen *et. al*, 1993, Norrander *et. al*, 1992). The peptide RPNVELCRD was synthesized by the Microchemical Facility, University of Minnesota. The peptide was conjugated to Keyhole Limpet Hemocyanin by maleimide (Pierce, Rockford, IL) and used to raise antisera in rabbits, using standard immunization protocols by A.Rostovtsev and R.W. Linck (unpublished).

Immunoblot analysis

L. pictus flagellar axonemes and *S. purpuratus* protofilament ribbons, prepared according to Linck and Langevin (1982), were resolved on 7.5% SDS/PAGE gels (Laemmli, 1970) and transferred to nitrocellulose in 10 mM CAPS, 10% methanol, pH 11.0. (Towbin, Staehin, and Gordon, 1979). Blots were blocked for 1 h, RT in TBS/3% BSA and washed 3 times (10 min) in TBS/0.05% Tween-20. Primary antibody was applied in TBS/0.05% Tween/1% BSA for 4 h, RT. Alkaline phosphatase conjugated secondary antibody was applied for 2 h, RT. BCIP in NBT (in 100 mM tris/HCl, 5 mM MgCl, pH 9.5) at 1:100 was used to develop the blots.

Immunofluorescence microscopy

L. pictus and *S. purpuratus* sperm were collected and attached to poly-L-lysine treated coverslips, fixed in 100% methanol (-20° C) for a minimum of 30 minutes, washed in PTN 3 times (10 min). The coverslips were blocked in PTN/1% BSA for 20 min, incubated with primary antibody (monoclonal anti-acetylated alpha tubulin, polyclonal anti-RPNVELCRD, affinity purified polyclonal anti-RPNVELCRD) in PTN/1% BSA for 2 hours at 37° C, and washed 3 times (10 min) in PTN. The cells were then incubated in Hoechst stain at 10 mg/ml for 15 min, and washed 3 times (10 min) in PTN. Cells were incubated in secondary antibody (Texas Red conjugated goat anti-rabbit, fluorescein conjugated goat anti-mouse) in PTN/1% BSA for 1 h at 37° C, washed 3 times (10 min) in PTN, and mounted in parphenline diamine (1 mg/ml in 90% glycerol, 0.1 M tris HCl, pH 9.0).

Results

Both the anti-peptide antibody sera and the affinity purified anti-peptide antibody were used to determine their reactivity with tektins A, B, and C. One dimensional SDS/PAGE immunoblot analysis of Sarkosyl-resistant protofilament ribbons showed the expected cross reactivity of antibodies to tektins A, B, and C with bands at their respective relative molecular weights. The anti-peptide antibody as well as the affinity purified anti-peptide antibody cross reacted with bands corresponding to those of tektins A, B, and C. The affinity purified anti-peptide antibody did not behave significantly different from the anti-peptide crude sera, which illustrates the specificity of both antibodies for the tektin consensus sequence by recognizing epitopes, as expected, in all three tektins.

The anti-peptide sera and the affinity-purified anti-peptide antibody were used to localize the consensus sequence in methanol fixed and native, unfixed flagellar axonemes from two species of sea urchin, *L. pictus* and *S. purpuratus*. In both native and methanol fixed flagellar axonemes, the antibodies stained the entire length of the flagellar axoneme, similar to results seen with antibodies raised to tektins A, B, and C. Also labeled by both antibodies was a region corresponding to the basal body and acrosome.

To show the individual doublet microtubules, the axonemes were splayed by pressing coverslips with attached sperm cells onto parafilm. This process causes the separation of the flagellar axoneme into its nine doublet microtubule components. Each of the anti-peptide antibodies (crude sera and affinity purified) labeled the entire length of all nine doublet microtubules in native microtubules as well as in those which were methanol fixed.

Discussion

An antibody was raised to a conserved peptide sequence among three tektins found in sea urchin sperm flagellar microtubules. Immunoblot analysis shows that this anti-peptide antibody recognizes all

three known tektins in sea urchin sperm flagellar axonemes. This antibody was also used to study the localization of the conserved peptide sequence in methanol fixed and native *L. pictus* and *S. purpuratus* sperm using immunofluorescence microscopy techniques.

Anti-peptide antibody staining of unfixed, whole flagellar axonemes and individual doublet microtubules indicates that the conserved tektin peptide sequence is oriented in such a way that its epitope is exposed on the surface of native flagellar microtubules. The presence of the consensus sequence in each doublet microtubule supports the possibility that this peptide domain plays a role in the binding of flagellar appendages such as radial spokes or dynein arms, which are attached to all nine doublet microtubules and found along the entire length of the axoneme.

Staining of the regions corresponding to the basal body and acrosome indicates that the peptide is located there as well. Antibodies raised to tektins have recognized tektins or tektin-like proteins in centrioles and centrosomes of other cell types, including mammalian and human cells. The staining of the basal body by the anti-peptide antibody will lead to the testing for the presence of the conserved amino acid sequence in the centrioles and centrosomes of other species.

Tektins are a highly insoluble component of flagellar microtubules that may have a variety of functions, including roles in microtubule assembly and stability or the attachment of flagellar appendages such as dynein arms and radial spokes. While the function of tektins in flagellar axonemes, basal bodies, and centrioles remains unknown, there are many possibilities based on their characteristics. Because they are highly stable, insoluble filaments they may play a role in the assembly of microtubules and mitotic spindles. Abnormalities in these processes may be factors in diseases such as cancer, Alzheimer's disease, and other neurological diseases.

References

Chen, R., Perrone, C.A., Amos, L., and Linck, R.W., (1993). Tektin B1 from ciliar microtubules: primary structure as deduced from the cDNA sequence and comparison with tektin A1. *J. Cell Sci.* 106: 909-918.

Laemmli, UK, (1970). Cleavage of structural proteins during the assembly of the head of bacteriophage T4. *Natue, Lond.* 227: 680-685.

Linck RW, Amos LA, and Amos WB, (1985). Localization of tektin filaments in microtubules of sea urchin sperm flagella by immunoelectron microscopy. *J. Cell Bio.* 100: 126-135.

Linck, RW, Goggin, MJ, Norrander, JM and Steffen, W, (1987). Characterization of antibodies as probes for structural and biochemical studies of tektins from ciliary and flagllar microtubules. *J. Cell Sci.* 88: 453-466.

Linck, RW, and Langevin, GL, (1982). Structure and chemical composition of insoluble filamentous components of sperm flagellar microtubules. *J. Cell Sci.* 58: 1-22.

Nojima, D, Linck, RW, and Egelman, EH, (1995). At least one of the protofilaments in flagellar microtubules is not composed of tubulin. *Curr. Biol.* Vol. 5, No. 2: 158-167.

Norrander, JM, Amos, LA, and Linck, RW, (1992). Primary structure of tektin A1: Comparision with intermediate filament proteins and a model for its association with tubulin. *Proc. Natl. Acad. Sci.* 89: 8567-8571.

Pirner, MA, and Linck RW, (1994). Tektins are Heterodimeric Polymers in Flagellar Microtubules with Axial Periodicities Matching the Tubulin Lattice. *J. Biol. Chem.* Vol 269, No. 50: 31800-31806.

Steffen, W, and Linck, RW, (1988). Evidence for tektins in centrioles and axonemal microtubules. *Proc. Natl. Acad. Sci.* 85: 2643-2647.

Towbin, H, Staehin, T, and Gordon, J (1979). Electrophoretic transfer of proteins from polyacrylamide gels to nitrocellulose shetts: procedure and some applications. *Proc. Natl. Acad. Sci* 76: 4350-4354.

ARTISANAL TRAPPING OF LAND CRABS IN PUERTO RICO

Darwin Caraballo-Burgos. Faculty advisor: Dr. Frank Barnwell

Department of Ecology, Evolution & Behavior
University of Minnesota
St. Paul, MN 55108

The neotropical land crab Cardisoma guanhumi ("juey terrestre") is a large (carapace width ≤ 8.5 cm, weight ≤ 250 g) burrowing inhabitant of mangrove forests and adjoining coastal lowlands. This crab is a prized food in Puerto Rico and other countries in Latin America. Studies by the Department of Natural Resources showed a dramatic 93% decrease in the harvest of C. guanhumi from 1971 to 1977 in Puerto Rico. Even though crab populations still appear to be reduced, fishermen known as "cangrejeros" continue to harvest them commercially at low levels. In this study, we videotaped interviews with two cangrejeros from Guanica in southern Puerto Rico and documented their methods for constructing and setting wooden live traps. The design of these traps allows for selective harvesting of the crabs and minimizing the environmental impact of collection, both important concerns of the cangrejeros.

BACKGROUND

The neotropical land crab Cardisoma guanhumi commonly known as "juey terrestre" is a burrowing inhabitant of flat and swampy coastal areas in the western hemisphere. Its distribution on tropical islands of the Western Atlantic extends from Bermuda to the lesser Antilles. Continental limits extend from southern Florida and Texas to South America. This species is one of the largest land crabs. It is comestible and usually trapped for human consumption. In Puerto Rico C. guanhumi can be found in mangrove forests and adjoining coastal lowlands. The distribution of this blue colored land crab from the sea to the land is determined by its size, with the juveniles located closer to the shoreline (Morales de Rojas, 1981).

During the last decades harvesting of this crab or "juey" has been of considerable economic and nutritional importance to the Puerto Rican population. Nowadays its meat is traded alive, fresh or processed. The price for a dozen crabs has risen from $1.25 in 1957 to $15.00 in 1993. At present the processing and packaging of the meat is not done in Puerto Rico, reportedly because of the high cost and lack of this product on the island. As a consequence, almost half a million pounds of Cardisoma meat is imported from foreign countries annually. The price for frozen meat fluctuates from $3.00 to $6.00 per pound. Therefore, considering the actual cost of this nutritious product and that its importation fees have increased by a factor of five from 1971 to 1977, fishing of land crabs has produced an impact on the economy of Puerto Rico.

During recent decades, an apparent dramatic reduction has been observed in the harvesting of C. guanhumi. Compiled data from the harvesting of crabs in Puerto Rico show a reduction of about 93% from 1971 to 1977. The fishery of crabs that added up to 7% of the total fishery in Puerto Rico by 1971 is now less than half a percent (1/2 %) (Fig. 1).

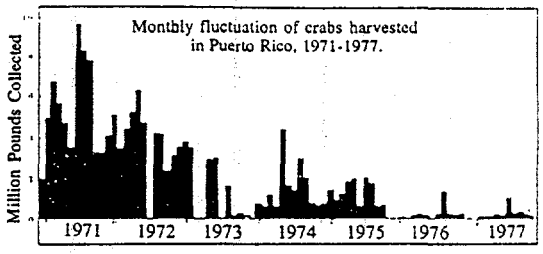


Figure 1.
The decrease in harvests of land crabs between 1971-1977.(Sea Grant Bolletín Marino, 1991).

The reduction in harvesting presumably reflects a reduction in the population of crabs on the island. Reasons for that reduction have not been defined so far. However, possible causes can be suggested. First, increased human population during the last 20 years may have increased demand of the product and resulted in over-harvesting. Secondly, the expansion of urban areas around flat low coastal lands may have reduced the natural habitat of the land crab. Finally, Cardisoma has been considered an agricultural pest because of the damages it has done to the sugar cane and rice fields on the island. Agriculturists and settlers decided to eliminate the crabs using pesticides, and this eradication campaign may have reduced the numbers.

Nevertheless, not everything points towards the elimination and extinction of this blue colored juey terrestre in Puerto Rico. On two visits to the island on September and December, 1994, I had the opportunity to interview two fishermen (cangrejeros) from southern Puerto Rico and to learn of their ecological concern about the slow extinction of the crab on the island. Through the interviews, I was able to compile data about the methodology used by these fishermen to collect crabs while at the same time preserving the habitat of this valuable source of food and income.

First interviewed was Mr. Santos "Frenchi" Martinez-Friend. He has been dedicated to the fishing of crabs since childhood. During the afternoons between the months of April to June, Frenchi collects crabs at sector La Cueva in the town of Guánica, PR. To start his job, Frenchi checks the outside of different burrows in search of fresh excrement as a sign that the crab is inside the burrow. He reports that the shape of the fecal pellet gives him an idea of the sex of the animal. He affirms that long-shaped pellets are characteristic of males while round-shaped pellets indicate a female.

Having identified the presence of the crab, Frenchi places a trap over the hole on the ground, taking care not to destroy the entrance of the burrow. He uses a very rustic wooden box trap known as a "trampa cuadrada" or square trap. The trap is placed against burrows that open horizontally from a vertical surface such as the face of a bank. (Fig. 2)

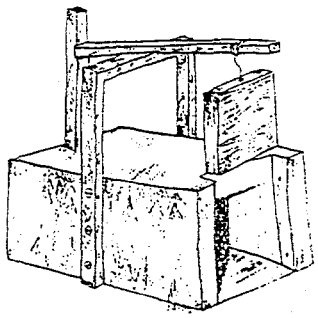


Figure 2.
Common crab trap known as "trampa cuadrada".

The trap has a small sliding door at the front, that can be easily raised vertically and kept in that position by the use of a wooden stick. The stick is set in a horizontal position that enables it to lay down over the hanger of the trap and be inserted into a notch in another piece of wood at the end of the trap. This second stick of wood is placed in a vertical position that enables it to be inserted inside the trap through a small hole at the back of the trap. The bait that attracts the crab is attached to the end of the vertical stick within the trap. The vertical stick is notched on its anterior face and hooked under the top of the trap.

Frenchi uses pieces of sugar cane covered with cane juice syrup as bait. In addition, if the ground seems to be very dry and the temperature very high, he adds fresh water to the burrow before placing the trap. This will cause the crab to leave the burrow. Once placed, the traps are kept untouched for several hours. Frenchi believes that the smell of the sugar cane attracts the crab inside the trap. When the crab goes inside the trap, it touches the lower end of the back wood stick where the bait was attached. This action dislodges the vertical stick, freeing the horizontal stick from its notch and allowing the door to fall shut.

After removing the crabs from the trap, Frenchi cleans and feeds them with water and corn for few days before selling them. He believes that this diet helps to take out any source of contamination from the meat of the crab and improves its flavor.

A second fisherman interviewed was Mr. Agapito " Papo" Ruiz-Pacheco who lives in the town of Yauco, PR. He prefers to collect crabs in sector San Jacinto, Guánica, PR. Like Frenchi, Papo uses traps, but in addition to the square trap used by Frenchi, he employs an "osicua or sharp trap. This trap has a sloping extension from the front that allows it to be placed over a burrow opening on flat ground (Fig. 3).

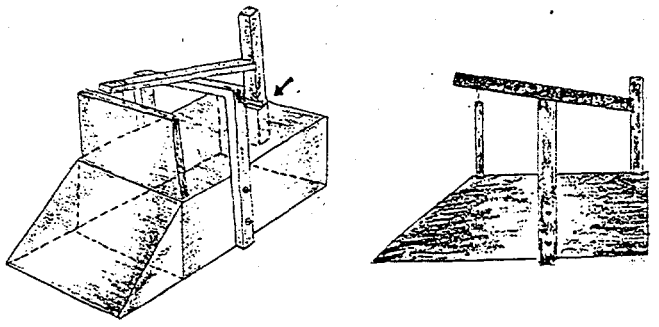


Figure 3.
Sharp "osicua" trap. The front has an opening at the bottom, which is covered with a lid of wood.

Using a small portable saw and hand tools, Papo takes around 45 minutes to construct a trap from the wood of old empty dry cod fish boxes. At the time of the interview, he had a total of 45 wooden box traps. When collecting crabs, he uses around 10 to 15 of those traps, depending on how long he plans to stay harvesting crabs. Depending on the location and orientation (facing upwards or to a side) of the entrance of the burrow, Papo chooses the type of trap for collecting. Papo stays with his traps and never leaves them unattended because of his concern about theft. After several hours, he checks the traps. Harvested crabs are then taken home to be fed with water, rice and corn for several days, before selling them.

Both cangrejeros confirmed their concern about sustaining harvestable populations of crabs. They argued that the use of a trap facilitates the selective harvesting of C. guanhumi. In other words, since no threat to the life of the crab is posed by the use of a trap, juveniles and egg-laying females crabs are set free without any injury. Both fishermen affirmed that the trap does not require the destruction of the crabs burrows or habitats, an important concern of both men.

CONCLUSION

Even though there has been an apparent decrease in the population of land crabs in Puerto Rico, some fishermen continue to harvest them. The two interviewed were concerned about maintaining sustainable levels by the use of live traps. In addition, an article published in 1991 by the Sea Grant Program Boletín Marino from the University of Puerto Rico-Mayagüez Campus listed a series of recommendations to help increase the actual population of land crabs in the island. The first suggestion is the protection of certain areas of crabs habitat from the industrial development. Secondly, the fishery of crabs should be prohibited during the months of June and September when crabs copulate and reproduce. Finally, harvesting should be limited to crabs with carapaces greater than 3 inches in length.

If implemented these suggestions should help in the recovery of Cardisoma guanhumi on the island. Meanwhile, artisanal fishing of crabs in Puerto Rico seems to be the starting point for a new era of human concern about ecological and environmental issues.

ACKNOWLEDGEMENTS

Thanks to Mr. Santos "Frenchi" Martinez Friend and Mr. Agapito "Papo" Ruiz Pacheco for their collaboration during the course of the study. In a very special way, we would like to thank Mr. Ruiz Pacheco for the Artisanal Crab Trap that he designed for my formal presentation of the study. In addition, we thank Mr. Richard Ramos Irizarry and Mrs. Luz E. Irizarry in the production of the video of the interviews. Also, we thank Miss Lourdes Cancel for the drawings. Finally, we would like to thank the staff of the library of the Department of Natural Resources in Puerto Rico for providing references.

REFERENCES

Benedetti, Mariana.. Dos cangrejos de Puerto Rico. Sea Grant Boletin Marino Marzo-Abril 1991.

Morales de Rojas, Hilda,. Estudios sobre el cangrejo de tierra en Guanajibo, Mayagüez y Guayanilla: su tamaño, relación de peso a tamaño y resultados preliminares de su cultivo. Octavo Simposio de Recursos Naturales 7 de Diciembre de 1981. pg. 100-105

Morales de Rojas, Hilda,. El cangrejo terrestre (*Cardisoma guanhumi* Latreille) y su aparente disminucion poblacional en Puerto Rico. Quinto Simposio de los Recursos Naturales. 20 de Septiembre de 1978. pg. 120-127

TOTAL HEMOCYANIN CONTENT IN RESPONSE TO VARYING OXYGEN AND SALINITY IN THE BLUE CRAB *CALLINECTES SAPIDUS*

Toren Andrew Prawdzik

Department of Marine Science
Jacksonville University
Jacksonville, FL. 32211

Faculty Advisor: Dr. Lee Ann Clements

ABSTRACT

Oxygen and salinity variations occur naturally in Estuarine systems. How an organism adapts to these stresses is of great importance to commercial fisherman and to the ecosystem itself. Blue crabs were collected in the St. Johns River and maintained in aquarium to examine how they adapted hemocyanin and protein concentrations to survive high salinity-high oxygen, high salinity-low oxygen, low salinity-high oxygen, and low salinity-low oxygen conditions. Crabs were fed an artificial food made by mixing Agar, Albumin, and ground fish. This gave all crabs the same nutritional base. Blood samples were taken bi-weekly and analyzed for total protein and total hemocyanin. Reduced oxygen treatments resulted in a relative increase in total hemocyanin and total protein. Elevated oxygen and salinity treatments resulted in a relative decrease in total hemocyanin and total protein. No conclusive correlation between oxygen concentration and hemocyanin content were found. Further study into seasonality may yield more accurate data.

BACKGROUND

Callinectes sapidus, the common blue crab, is a commercially important species (Williams 1984). C. sapidus is a very adaptable species. It ranges from freshwater to hyper saline lagoons, such as Laguna Madre De Tamaulipas, Mexico. Blue crabs can be found in salinities ranging from 4 ppt to 117 ppt. They can also be found in temperature ranges of three degrees to thirty-five degrees Celsius, and in sewage treatment ponds with oxygen levels that have dropped to 0.08 mg/l (Williams 1984).

Blue crabs are coastal creatures found at water depths varying from shallow waters to waters ninety meters deep. Mass mortality of marine and estuarine benthic communities due to hypoxic bottom waters has been widely reported (Harper et al., 1981, Officer et al. 1984, Rabalais et al., 1984). Hypoxic bottom water masses may persist for weeks. Reports suggest that fish and crustaceans try to avoid or escape hypoxic bottom waters (Pavela et al., 1983). In well harvested areas it is necessary to know how salinities and oxygen levels affect protein synthesis, growth, and respiration in C. sapidus.

Total blood hemocyanin volume in C. sapidus may be affected by changing oxygen concentrations and varying salinities in their environment. Crabs respond to short-term hypoxia by increasing the ventilation of water over their gills and this has been shown to induce an adaptive alkalosis in the hemolymph (Truchot 1975, Burnett and Johansen 1981, Lallier and Truchot 1989). Overall long-term effects were the emphasis in these experiments. It is hypothesized that crabs in low oxygen environments will tend to increase total blood hemocyanin volume and that crabs in high oxygen environments will tend to decrease total blood hemocyanin volumes. It is also hypothesized that salinity gradients may cause the crab to divert energy usage to water regulation and thus slow or reduce hemocyanin production in either low or high salinities.

Hemocyanin is a protein in the globulin group (Lockwood 1967) that serves to increase the oxygen carrying capacity in the blood of crustaceans. Hemocyanin binds to oxygen and aids its transfer to the bodily tissues. Without hemocyanin, the fluids of a blue crab can carry oxygen, but not as efficiently. Furthermore, without hemocyanin, crustacean blood cannot deliver enough oxygen to the tissues in stressful situations. Hemocyanin is a copper containing protein which is colorless when deoxygenated and blue when oxygenated (Warner 1977, Lockwood 1967). In the oxygenated form, hemocyanin has a spectral absorption band at 275nm and at 340nm (Lockwood 1967). Spectral absorbance varies from species to species. For crustaceans, including genera closely related to Callinectes (e.g., Carcinus and Cancer), the spectral absorbance of hemocyanin is 335-336nm (Nickerson and Van Holde 1971). An absorbance at either of these numbers will yield accurate results for C. sapidus. Hemocyanin in C. sapidus exists in the blood as a mixture of hexamer (1x6) and dodecamers (2x6) (Mangum et al 1991). The respiratory significance, if any, of oligomerization is relatively unknown.

MATERIALS AND METHODS

Male crabs of carapace sizes ranging from 13cm to 19cm, measured point to point, were collected from the St. Johns river in Jacksonville Fl. for the first run of the experiment in the Fall of 94. Male and female crabs purchased from a local distributor were used in the second run of the experiment in the winter and spring of '94-'95. Crabs were acclimated from 6-10 days at 20ppt and saturated oxygen concentration. Four treatments were set up: 1) high salinity, high oxygen (HSHO). 2) high salinity, low oxygen (HSLO). 3) low salinity, high oxygen (LSHO).

4) low salinity, low oxygen (LSLO). Two sets of experiments were done, one in the Summer-Fall of '94 (denoted by a large C in figures) and another done in the winter of '94-'95 (denoted by a small c in figures). The crabs were fed a mixture of fish, egg albumin, and non-nutrient agar. This mixture was allowed to solidify into 12-14g blocks. Approximately one block of the food mixture was fed to each crab every 48hrs. The artificial food source was used to maintain a constant feeding ration and quality throughout the experiment. The food source gave all the crabs a consistent protein intake of approximately 400mg/L. Approximately 1cc of blood was extracted from the base of the fifth leg, or swimming leg, with a standard sterile syringe fitted with a 27 gauge hypodermic needle. The blood was then homogenized in a tissue homogenizer and centrifuged to remove any remaining solids. One fraction was analyzed for protein concentration using a Sigma protein assay Kit (SIGMA CHEMICAL Co. Procedure No. P 5656). The other fraction was analyzed for hemocyanin concentration using the documented methods of Nickerson and Van Holde (1971). Random samples of the food source were assayed for protein to determine an average protein intake of the crabs. Protein content of the food mixture was increased as necessary through the addition of egg albumin. The carbohydrate source in the food mixture was the agar. The treatment tanks were monitored to verify the salinity and oxygen concentrations during the experiment.

RESULTS

Salinity and Oxygen Concentration

Through both experiments the salinities were kept consistently different among the experimental tanks (Fig. 1). In the first experiment measurements were taken only at the beginning and end of the experiment and some salinity change did occur over time. In the second experiment, the salinities of the high and low salinity treatments were gradually changed over the first test week to the final salinity (high = 28ppt, low = 12ppt) and maintained at these levels throughout the experiment.

Fig. 2 shows the relationship of oxygen concentration vs. time for both experiments. In the first experiment oxygen concentrations were held constant for each experimental treatment. The high oxygen treatments were on average 1-2mg/L above the control and the control treatment was 2-3mg/L above the low oxygen treatment. In the second experiment the oxygen concentration was different among the experimental treatments, but with a smaller average difference. Overall, the oxygen concentrations in the second experiment were higher than the first experiment. The change was probably due to the different methods of aeration used in the two experiments. In the first experiment air stones with external aquarium pumps (Whisper 800)were used to aerate the tanks. In the second experiment under gravel filters attached to a compressed air system set up in the lab were used. The compressed air system proved to be harder to control as the pressure was much higher overall. Furthermore, oxygen concentration values were affected by the lowered temperatures and consistent higher gas solubility during the winter months (avg temp = 7-12 C less than summer months).

Protein concentration

Protein concentrations varied extensively throughout the duration of the experiment. In the first experiment (Fig. 3) the protein levels changed quite a bit from their initial level. In the second experiment (Fig. 4) protein concentration of the blood of the crabs varied with time for the duration of the experiment. Although there was variation in the protein levels, none was significant enough to affect the experiment.

Hemocyanin concentration

Hemocyanin concentration vs. time (Fig.5) shows the overall levels of hemocyanin in the blood samples of the crabs at the extraction time. There was little variation among the treatments and in some cases, extreme differences in similar treatments. In the first experiment there was a general downward sloping trend in hemocyanin levels. In the second experiment there was almost no change in hemocyanin concentration over time.

As seen in the individual graphs of the treatments over time there is a variability that was due to different responses by individual crabs (Fig. 6,7,8,9,10). In the high salinity and high oxygen treatment (Fig. 6) there is a spike of hemocyanin concentration by crab #17 followed by a reduction to the level shown by the other crabs. In the high salinity and low oxygen treatment (Fig. 7) we see contrasting responses between t1 and t2 for all the crabs. As one crab increases hemocyanin concentrations the other decreases. Crab #8 shows similarities to crab #6 in hemocyanin concentration even though crab #8 went through a molt between t0 and t1 while #6 did not. In the control treatment (Fig. 8) there is a wide variation in hemocyanin levels and only at the end of the experiment did the hemocyanin concentrations converge. In the low salinity and high oxygen treatment (Fig. 9) #8 and #2 (of the second experiment) converged with similar slopes. Crab #7 did the exact opposite and increased hemocyanin concentration, initially this was thought to be a precursor to a molt but after 4 weeks of high hemocyanin no molt occurred. In the low salinity and low oxygen (Fig. 10) Once again there is a great variation and no correlation, in this case some crabs increased hemocyanin while others in the same treatment decreased. Although some of the crabs in the experiment responded as expected, there were still individuals that did not.

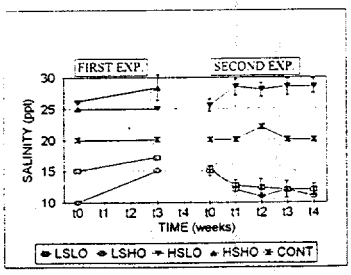


Fig. 1-Salinity Vs. Time

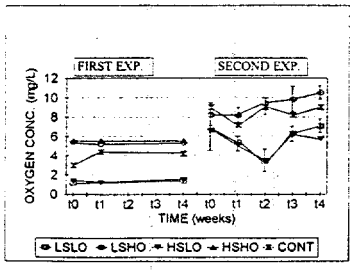


Fig. 2-Oxygen concentration Vs. Time

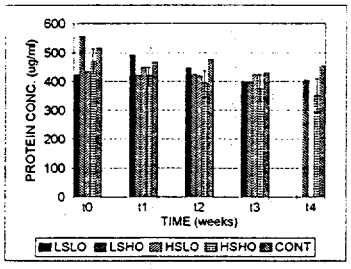


Fig. 3- Total Blood Protein Vs. Time for first experiment.

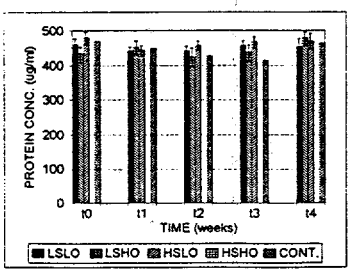


Fig. 4- Total Blood Protein Vs. Time for second experiment.

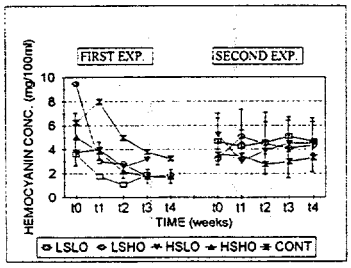


Fig. 5- Hemocyanin Concentration Vs. Time. Individual crabs in each treatment are averaged together.

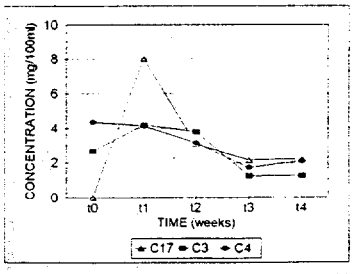


Fig. 6- Hemocyanin Concentration Vs. Time for high salinity and high oxygen

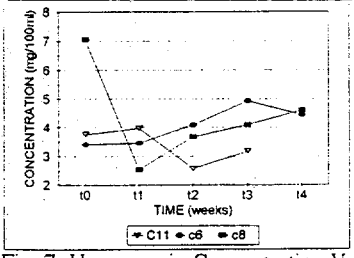


Fig. 7- Hemocyanin Concentration Vs. Time for high salinity and low oxygen

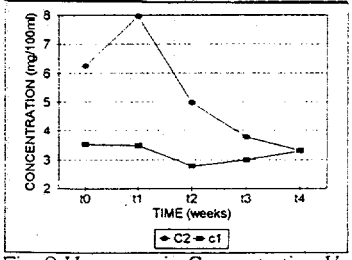


Fig. 8-Hemocyanin Concentration Vs. Time for control.

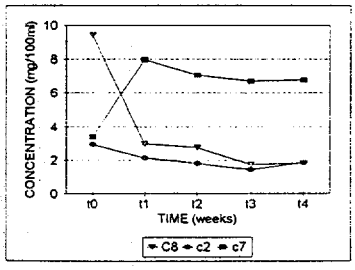


Fig. 9- Hemocyanin Concentration Vs. Time for low salinity and high oxygen

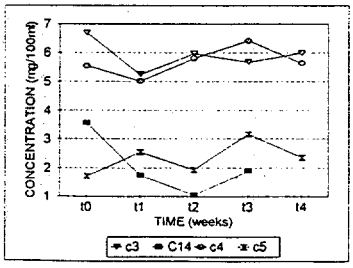


Fig. 10- Hemocyanin Concentration Vs. Time for low salinity and low oxygen

DISCUSSION

Hemocyanin vs. time

Hemocyanin levels varied significantly over time (Fig. 6,7,8,9,10). This contradicts what was expected to happen to the hemocyanin concentrations in the blood. The hypothesis stated that hemocyanin should increase as oxygen levels decreased and hemocyanin should decrease as oxygen levels are increased above control levels. The data suggest that there is no correlation between oxygen concentration and hemocyanin concentration.

The overall hemocyanin concentrations for the first and second experiments differ (Fig. 5). The final concentration in the first experiment was lower than the average concentration in the second experiment. This can be attributed to seasonal differences in hemocyanin (Mangum, 1982). Winter hemocyanin is found in winter conditioned crabs; this hemocyanin binds poorly with oxygen because high oxygen affinity is not necessary in hibernating crabs (Mangum 1982). Summer hemocyanin is found in summer crabs; this form readily binds with oxygen (Mangum 1982). The hemocyanin differences can be accounted for by the seasonal behavior of the crabs. In winter, crabs burrow into the sand and suspend many of their activities (i.e.. feeding, reproduction, locomotion) for several months, a response known as "hibernation" (Warner 1976). As the water temperature rises in the summer (above 10 C) the crabs become more active and move or swim upwards of 2km per day (Mangum 1975). The added aerobic need for oxygen necessitates a form of hemocyanin that can readily bind and carry oxygen to the body tissues, while the winter crab in its state of hibernation does not need an over abundance of oxygen in its tissues and adjusts to a hemocyanin that does not readily bind and does not carry oxygen well. The result is that most of the oxygen consumed in the winter crab is free oxygen in the blood stream and most of the oxygen consumed by the summer crab is from oxygen bound to hemocyanin.

The activity level of crabs in our first experiment may have been the overriding factor in determining hemocyanin concentration. We took crabs that were normally active and traveling up to 2km per day and put them into a 20 gallon tank, thus limiting their range of movement. The aerobic need for oxygen can deminish. There was a slight decline in hemocyanin concentration over time for the first experiment. In the second experiment the hemocyanin concentration did not change appreciably. It is hypothesized that a crab with poor binding hemocyanin in an active environment should show an overall increase in hemocyanin concentration levels over crabs with hemocyanin that can bind well. In our second experiment the overall hemocyanin was higher than in the first experiment. Winter crabs can delay changing their hemocyanin for extended periods of time (Mangum, 1982). This is a built in safety measure to prevent premature acclimation to summer hemocyanin on days or weeks of abnormal highs in the winter months and to effectively prevent being caught in the cold upon return of normal winter temperatures (Mangum 1982). If the second experiment had been carried out over a longer time period, a change in the form of hemocyanin may be seen. A biological clock may also play a part in delaying the change of hemocyanin structure.

The hemocyanin oligomers are built of five to six different polypeptide chains, four of which exhibit considerable quantitative variability in natural populations (Mangum et al., 1991). Crabs imersed into prolonged hypoxic conditions have been seen to change the structure of their hemocyanin by changing concentrations of three of the six oligomers (3, 5, and 6) (Mangum et al 1991, Burnett 1992). Oxygen affinity can specifically be attributed to the levels of the chains of oligomers 3 and 6 (Mangum and Rainer 1988, Rainer 1989, deFur et al 1990). The contribution of the other oligomers is still not known. What may be happening is not a change in volume of hemocyanin over time but a change in the subunits of the hemocyanin proteins.

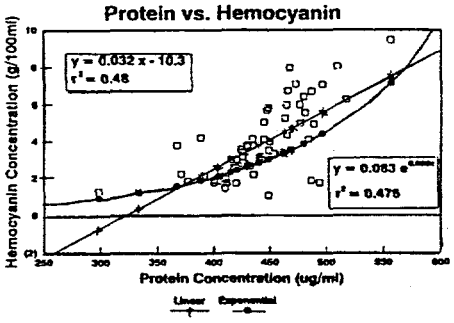


Fig. 11-Linear and logarithmic regressions of Hemocyanin Vs. Protein.

Hemocyanin vs. Protein

Hemocyanin may have an effect on total blood protein levels. Blood protein levels were positively correlated with blood hemocyanin concentrations (Fig. 11). The correlation is not a spectacular one with a r-squared value of only 0.48. A exponential regression also supplies a positive r-squared value but it too is not outstanding at 0.476.

CONCLUSION

In conclusion there is very little change in hemocyanin concentrations over time for increased or decreased oxygen levels and salinities in our experimental set up. Although some individuals showed the predictable response, it is impossible to determine the cause of hemocyanin change in these individual cases. Hemocyanin does seem to be correlated with blood protein levels. Finally, the activity level of the crabs seems to be the most important variable affecting hemocyanin concentration. The examination of the differences between winter and summer hemocyanin, the effects of temperature differences, the effects of urea and other wastes, and a better control of oxygen levels would help to provide more accurate experimental results. Hemocyanin is an important aspect of the crabs ability to adapt, not only does hemocyanin deliver oxygen to the bodily tissues in times of stress, but it also acts as a storage unit for bodily tissues when oxygen is not needed as much. How the blue crab changes its hemocyanin and adapts to its environment is an interesting problem that needs further experimentation.

REFERENCES

Bliss, D.E., and Mantel, L.H. .1985 . The Biology of Crustacea: Integuments, Pigments, and Hormonal Processes. New York: Academic Press.

Burnett, L.E., and K. Johansen. 1981. The role of branchial ventilation in hemolymph acid-base changes in the shore crab *Carcinus maenas* during hypoxia. *J. Comp. Physiol.* 141:489-494

Burnett, L. 1992 . Integrated Function of the Respiratory Pigment Hemocyanin in Crabs. *Amer. Zool.*, 32:438-446

deFur, P., Mangum, C., and Reese, J. 1990 . Respiratory Responses of the Blue Crab *Callinectes sapidus* to Long-Term Hypoxia. *Biol. Bull.* 178:46-54.

Harper, D. E., et al. 1981. The occurrence of hypoxic bottom water off the upper texas coast and its effect on the benthic biota. *Contrib. Mar. Sci.* 24:53-79

Lallier, Fl., F. Boitel, and J-P. Trunchot. 1987. The effect of ambient oxygen and temperature on haemolymph L-lactate and urate concentrations in the shore crab *Carcinus maenas*.. *Comp Biochem. Physiol.* 86A:255-260

Lockwood, A.P. 1967 . Physiology of Crustacea. San Francisco: W.H. Freedman.

Mangum, C.P., Weiland, A.L. 1975. The function of hemocyanin in respiration of the Blue Crab *Callinectes sapidus. J. Exp. Zool.*, 193:257-264.

Mangum, C., and Rainer, S. 1988 . The Relationship Between Subunit Composition and O2 Binding of Blue Crab Hemocyanin. *Biol. Bull.* 174:77-82

Mangum, C. et al. 1991 . Oligomer Composition and Oxygen Binding of the Hemocyanin of the Blue Crab *Callinectes sapidus. Biol. Bull.* 181:453-458

Mangum, C. 1992 . Phusiological Aspects of Molting in the Blue Crab *Callinectes sapidus. American Zoology* 32:459-469

Mantel, L.H. .1983 . The Biology of Crustacea: Internal Anatomy and Phisiolgy Regulation. New York: Academic Press

Mauro, N.D. .1978 . The Effects of Temperature on Oxygen Transport in Decopod Crustaceans. *American Zoology*. 18.693

Nickerson K. W., Van Holde K. E. .1970. A Comparison of Molluscan and Arthropod Hemocyanin-I. Circular Dichroism and Absorption Spectra. *Comp. Biochm. Physiol.* Vol. 39b pg 855-872.

Officer, C. B. et al. 1984. Chesapeake Bay anoxia: origin, development and significance. *Science* 223:22- 27.

Pavels, J.S., et al. 1983. Sharp reductions in abundance of fishes and benthic macroinvertibrates in the Gulf of Mexico off Texas associated with hypoxia. *Northeast Gulf Sci.* 6:167-172.

Rabalais, N. N. et al. 1985. Nationwide review of oxygen depletion and etrophication in estrarine and coastal waters: Gulf of Mexico (Alabama, Mississippi, Louisiana, and Texas). Final Rep. NOAA, National Ocean Service, Ocean Assessment Division, Rockville, MA. 60pp.

Rainer, J.S. 1989. Distribution of the heterogencous hemocyanin subunits along a salinity gradient. M.A. Thesis, College of William and Mary, Williamsburg, Virgina. 62pp.

Rittschof, D. 1992 . Chemosensation in the Daily Life of Crabs. *Amer. Zool.*, 32:363-369

Schram, F.R. 1986 . Crustacea. Oxford University Press, New York, NY.

Stickle, W et al. 1989 . Metabolic Adaptions of several Species of Crustaceans and Molluscs to Hypoxia: Tolerance and Microcalorimetric Studies. *Biol. Bull.* 177:303-312

Talbot, H., and Watelman. 1960 . Physiology of crustacea. New York: Academic Press.

Trunchot, J-P. 1973. Fixaation et transport de l'oxygene par le sang de *Carcinus meanas:* vaariations en rapport avec diverse conditions de temperature et de salinitie. *Neth. J. Sea Res.*, 7:482-495

Warner, W.W. 1976. Beautiful Swimmers. Little, Brown and Co. New York, 304pp.

Warner, G.F. 1977 . The Biology of Crabs. Van Nostrand Reinhold Company, New York

Williams, A.B. 1984 . Shrimps, Lobsters and Crabs of the Atlantic Coast. Washington, D.C. : Smithsonian Press.

Verenberg, F.G., ed. 1975. Physiological Adaptations to the Environment. New York: Intext Educational Publishers.

BETA-HYDROXYBUTYRATE-INDUCED TERATOGENESIS IN THE SEA URCHIN EMBRYO

Jeffrey B. King

Biology Department
Susquehanna University
Selinsgrove, PA 17870

Faculty Advisor: Margaret T. Peeler

INTRODUCTION

Diabetes mellitus, the condition in which blood glucose levels are abnormally elevated due to a deficiency in insulin, assumes a variety of onset times and severity. The disease may begin during childhood, pregnancy, or late adulthood and may be treated through diet, oral agents, or insulin therapy.

Pregnant women who are insulin-dependent diabetics have been known to have a higher than normal incidence of spontaneous abortions and births of abnormal infants. The availability of insulin has resulted in a decline in the percentage of abortions but not in the incidence of birth defects (Lufkin et al, 1984). Birth defects that are commonly observed in the infants of such women are rarely observed otherwise; these include caudal regression (Mills, 1982), respiratory distress (Lufkin et al, 1984), macrosomia, birth trauma, hypertrophic cardiomyopathy, vascular thrombosis, neonatal hypoglycemia, erythrocytosis, and hyperbilirubinemia (Jovanovich-Peterson et al, 1991). While common to infants of insulin-dependent diabetic mothers, these defects are rare in infants born to gestational diabetic women (Mills, 1982).

The high incidence of abnormal births to diabetic mothers prompted studies to determine the causes of these defects. A number of factors were examined, including vascular disease, hypoxia, hormone imbalances, glycosylated proteins, and ketone body and amino acid abnormalities (Mills, 1982). Some attention was focussed upon beta-hydroxybutyrate (BHOB), a ketone body, as a possible teratogen responsible for observed defects. BHOB is normally produced during periods when blood glucose levels are low; during these times, BHOB serves as an alternate energy source for muscle (Rawn, 1989). BHOB is known to inhibit the pentose phosphate pathway, thus resulting in decreased pyrimidine and protein synthesis (Shum and Sadler, 1990). BHOB concentration has also been found to increase in cases of abnormal glucose metabolism, such as is common in diabetics. Normal BHOB serum concentration is about 0.2mM; during periods of low glucose it can rise fifty-fold and even higher levels have been observed in diabetics (Hall et al, 1984).

The teratogenic effects of BHOB have been studied in experiments using rat and mouse embryos. Results have confirmed that higher BHOB concentrations, along with earlier times of exposure during embryogenesis, are more detrimental to development (Moore et al, 1989). The teratogenic period in rats was found to be between days 6 and 10 of gestation (at concentrations of 8mM, 16mM, and 32mM), a period which corresponds to weeks 2 through 4 in humans (Eriksson et al, 1989). Among those abnormalities observed were failure of neural tube closure and retardation of development (Horton and Sadler, 1983).

However, few studies have addressed the effects of BHOB upon invertebrate embryogenesis. Therefore, the present study of the effects of BHOB upon the development of the sea urchin embryo was undertaken. The sea urchin embryo is a particularly suitable animal model for studying development because of the ease with which it is cultured and its relatively short developmental time; cleavage, blastula, gastrulation, and pluteus stages are all achieved between 36 and 72 hours after fertilization, depending on species and temperature. In addition, the extracellular matrix (ECM) of the sea urchin embryo is remarkably similar to that of humans with regard to both structure and function (Evans, personal communication), as are the primary germ layers

(ectoderm, mesoderm, and endoderm). The present experiments were performed to elucidate whether or not the sea urchin embryo is a useful model for studying BHOB-induced teratogenesis in humans.

METHODS

Embryo culture:

Experiments were performed with *Lytechinus pictus* and *Lytechinus variegatus*. Gametes were obtained by injecting adults with 0.5M KCl. Eggs were washed 3 times through cheesecloth using normal sea water (NSW), fertilized with dilute sperm suspension, and cultured in glass bowls; *Lytechinus pictus* embryos were cultured at 17°C and *Lytechinus variegatus* at room temperature.

Determination of critical dosage of BHOB:

Lytechinus pictus embryos were exposed to BHOB levels ranging from 20mM to 160mM (at 20mM increments); a control culture (no BHOB added) was also maintained. BHOB solutions were made by diluting a 320mM BHOB stock solution with NSW; the stock solution itself was made by dissolving the Na^+ salt of BHOB (Sigma Chemical Company) in NSW. Embryos were exposed immediately following fertilization.

Embryos were observed at cleavage, mesenchyme blastula, and gastrulation stages using light microscopy. Counts were performed with embryos of each [BHOB] at each stage (n=300) to determine the percentage of abnormal embryos.

This experiment was also performed with *Lytechinus variegatus* to ensure that both species had comparable susceptibility to BHOB.

Determination of critical exposure time:

Lytechinus pictus embryos were exposed to 80mM BHOB immediately following fertilization; 80 mM BHOB was also added at 2, 4, 6, 8, 10, 12, and 25 hours after fertilization. A culture of control embryos (no BHOB added) was also grown.

Counts of embryos (n=300) for each time point were performed at mesenchyme blastula and gastrulation stages to determine the percentages of abnormal embryos.

The experiment was also performed with *Lytechinus variegatus* to ensure similar susceptibility.

Recovery from BHOB:

Embryos of *Lytechinus variegatus* were exposed to 80mM BHOB immediately following fertilization; a control culture of embryos (no BHOB added) was also maintained. At time points of 2 and 4 hours, embryos were gently centrifuged (centrifugation is known not to affect the presence or absence of abnormalities in sea urchin embryos) and BHOB solution was removed and replaced with NSW. A culture was also grown in which BHOB was not removed at all.

Counts were performed (n=300) at the mesenchyme blastula stage for control embryos, embryos that had BHOB removed, and embryos kept constantly in BHOB to determine the percentage of abnormal embryos.

Primary mesenchyme cell (PMC) expression:

Control embryos and embryos exposed to 80mM BHOB were fixed with cold methanol (MeOH) at mesenchyme blastula, gastrulation, and pluteus stages. Embryos were kept in MeOH for 30 minutes and then washed 3 times with NSW. Following washing, they were incubated with the monoclonal antibody (mAb) 6e10 (Ettensohn and McClay, 1988) in a 1:10 dilution with NSW for 1 hour. This 1° Ab recognizes a family of PMC-specific glycoproteins. Following this incubation, embryos were washed 3 times with NSW and then incubated for 30 minutes with a 2° goat anti-mouse Ab (1:100 dilution in NSW) which recognizes the 6e10 mAb; the 2° Ab was conjugated with either FITC (a fluorescent tag) or horseradish peroxidase. This incubation was also followed by 3 washes with NSW. The FITC-conjugated 2° Ab was utilized with *Lytechinus pictus* and control pluteus embryos of *Lytechinus variegatus*. These embryos were observed using fluorescent microscopy. The

remaining *Lytechinus variegatus* embryos, which were incubated with the horseradish peroxidase-conjugated 2° Ab, were incubated in a solution of chloronaphthol (Harlow and Lane, 1988), which forms a blue-black product via the action of horseradish peroxidase. These embryos were observed using light microscopy.

RESULTS

Embryos of both *Lytechinus pictus* and *Lytechinus variegatus* were found to be sensitive to BHOB, demonstrating a range of abnormal phenotypes, which increased in severity and frequency with increased concentration. A sigmoidal relationship was observed between the percentage of abnormal embryos and [BHOB] (Figure 1). A sharp rise in the percentage of abnormal embryos was observed at 80mM. Abnormalities were present at the cleavage, mesenchyme blastula, and gastrulation stages.

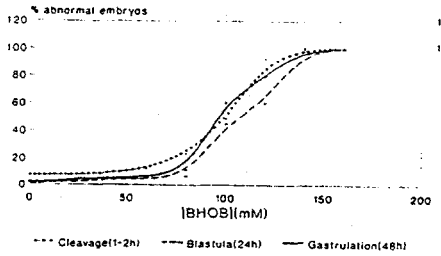


Figure 1: Effect of BHOB on *Lytechinus pictus*

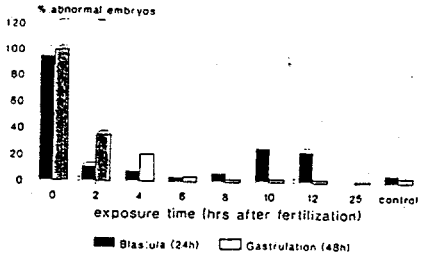


Figure 2: Effect of exposure time on BHOB-induced abnormality in *Lytechinus pictus*

Both species exhibited greater sensitivity to BHOB at earlier stages of development. The highest percentages of abnormality were observed following treatment during the first 2 hours of development. This observation was valid for embryos observed at both the mesenchyme blastula and gastrulation stages (Figure 2).

A wide variety of abnormalities was observed for embryos of *Lytechinus pictus*. Among them were pigment cell clumping, exogastrulation, absence of gut formation, abnormal vegetal plate morphology, abnormal overall shape, and retardation of development. *Lytechinus variegatus* embryos did not display nearly as wide a range of abnormalities as *Lytechinus pictus*, but did demonstrate retarded development.

Embryos appear to be capable of recovery from exposure to BHOB. *Lytechinus variegatus* embryos that had BHOB removed earlier (2 hours after fertilization) displayed a lower percentage of abnormality than those that had it removed 4 hours

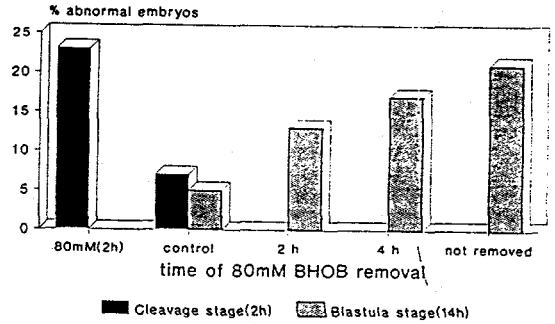


Figure 3: Recovery from BHOB in *L. variegatus*

after fertilization (Figure 3). Both cultures in which BHOB was removed had higher percentages of abnormalities than control embryos but lower percentages than those embryos that were kept in constant exposure to 80mM BHOB.

PMC ingression was observed to be delayed in some, but not all, of the embryos treated with 80mM BHOB for both species. PMC ingression was delayed in embryos that were also retarded developmentally. However, no embryos were observed in which the only abnormality was delayed PMC ingression or absent PMC expression.

DISCUSSION

The objective of our experiments was to determine whether or not the sea urchin embryo would prove a useful model for studying the role of BHOB in the malformations of infants of diabetic women. Experiments using rats and mice as models have indicated that BHOB can act as a teratogen. We wished to determine if BHOB-induced teratogenesis also occurs in the sea urchin embryo, which might therefore make a model system more amenable to study than mammalian systems.

Embryos were observed to show increasing sensitivity to higher [BHOB] and earlier exposures to BHOB (Figures 1 and 2). Both of these observations corroborate findings that were made in BHOB-induced teratogenesis of rat and mouse embryos (Moore et al, 1989). At cleavage, mesenchyme blastula, and gastrulation stages, 80mM BHOB was found to be a critical dosage, as the percentage of abnormality increases sharply above this concentration (Figure 1). This concentration is within the [BHOB] observed in the serum of diabetic women (Hall et al, 1984). These results demonstrate that BHOB definitely has the potential to act as a teratogen, though they do not prove that BHOB is exclusively responsible for malformations observed in the infants of diabetic mothers. Nonetheless, they do strongly support the possibility that BHOB plays a role in such malformations. It is also believed that acetoacetate, another ketone body and immediate precursor to BHOB, may also play a teratogenic role; further experimentation on rats and mice, as well as sea urchins, are necessary to determine this.

The fact that earlier exposure to BHOB was more detrimental to the development of sea urchin embryos demonstrates that early cell development and cell interactions are vital to the overall development of the sea urchin embryo. Cell differentiation occurs as early as 4 hours after fertilization with the 16-cell stage, when the embryo is composed of mesomeres, macromeres, and micromeres (Gilbert, 1991). Abnormalities in these cell types can lead to, among other things, abnormal skeletogenesis, vegetal plate formation, basal lamina and ECM formation, and gastrulation.

The removal of 80mM BHOB after 2 and 4 hours of development resulted in lower percentages of abnormal embryos than in cultures that were maintained constantly in 80mM BHOB (Figure 3). Though these cultures were exposed to BHOB for shorter periods of time, they were exposed during the most critical period of development (Figure 2). Thus, it seems more likely that the lower percentages of abnormality were due to embryonic recovery rather than just shorter exposure time to BHOB. In addition, percentages of abnormality at the late blastula stage were lower for these embryos than at the cleavage stage when the BHOB was first removed (Figure 3). Even those embryos that were constantly exposed to 80mM BHOB showed a degree of recovery at later stages; percentages of abnormality decreased for the lower [BHOB] from the cleavage stage to the blastula stage (Figure 1), and those embryos that were exposed to 80mM BHOB at various time points following fertilization showed decreased abnormality from the blastula stage to the gastrulation stage (Figure 2). These findings are in agreement with similar experiments performed with rat and mouse embryos (Shum and Sadler, 1988).

BHOB is most likely teratogenic in nature due to the fact that it inhibits the pentose phosphate pathway, thereby decreasing the synthesis of proteins and pyrimidines (Shum and Sadler, 1990). Pyrimidines, which comprise nucleic acids, are

important in cell division and peptide translation. Proteins, in turn, are vital to nearly every aspect of cell function, including cell division, migration, differentiation, signalling, and interactions. Thus, BHOB can inhibit virtually all developmental functions. Examples of this include abnormal gastrulation, pigment cell clumping, and retardation of development, all of which were observed in our experiments. The delayed PMC ingression that we observed was most likely due to inhibited cell signalling or cell-cell interactions (particularly with the ECM), as PMC ingression was observed to be delayed only in embryos that had other abnormalities and overall retardation.

Based on our results, it appears that the sea urchin embryo is an appropriate model for studying the factors that lead to developmental abnormalities in the infants of insulin-dependent diabetic women. Further studies will involve the characterization of specific molecular changes in ectoderm, mesoderm, endoderm, and ECM (which mediates numerous cell interactions) expression resulting from exposure to BHOB.

Besides their relevance to developmental biology as a whole, our findings also have a particular relevance to human embryogenesis as well as medicine. The existence of teratogenic properties of BHOB may play a role in abnormal embryonic development in humans. Further studies are needed to elucidate the exact cause (or causes) of abnormalities in the infants of insulin-dependent diabetic women.

REFERENCES

Eriksson, R.S.M., Thunberg, L., and Eriksson, U.J. (1989). Effects of interrupted insulin treatment on fetal outcome of pregnant diabetic rats. *Diabetes*. 38, 764-72.

Ettensohn, C.A., and McClay, D.R. (1988). Cell lineage conversion in the sea urchin embryo. *Developmental Biology*. 125, 396-409.

Gilbert, S. (1991). *Developmental Biology*. Sunderland, Massachusetts: Sinauer Associates.

Hall, S.E.H., Wastney, M.E., Bolton, T.M., Braaten, J.T., and Berman, M. (1984). Ketone body kinetics in humans: The effects of insulin-dependent diabetes, obesity, and starvation. *Journal of Lipid Research*. 25, 1184-94.

Harlow, E., and Lane, D. (1988). *Antibodies: A Laboratory Manual*. Cold Spring Harbor, New York: Cold Spring Harbor Laboratory.

Horton, W.E. Jr., and Sadler, T.W. (1983). Effects of maternal diabetes on early embryogenesis: Alterations in morphogenesis produced by the ketone body, beta-hydroxybutyrate. *Diabetes*. 32, 610-6.

Jovanovich-Peterson, L., Peterson, C.M., Reed, G.F., Metzger, B.E., Mills, J.L., Knopp, R.H., Aarons, J.H., and the National Institute of Child Health and Human Development. (1991). Maternal postprandial glucose levels and infant birth weight: The diabetes in early pregnancy study. *American Journal of Obstetrics and Gynecology*. 164, 103-11.

Lufkin, E.G., Nelson, R.L., Hill, L.M., Melton, L.J., O'Fallon, W.M., and Evans, A.T. (1984). An analysis of diabetic pregnancies at Mayo Clinic, 1950-79. *Diabetes Care*. 7, 539-47.

Mills, J.L. (1982). Malformations in infants of diabetic mothers. *Teratology*. 25, 385-94.

Moore, D.C.P., Stanisstreet, M., and Clarke, C.A. (1989). Morphological and physiological effects of beta-hydroxybutyrate on rat embryos grown in vitro at different stages. *Teratology*. 40, 237-51.

Rawn, J. David. (1989). *Biochemistry*. Burlington, North Carolina: Neil Patterson Publishers.

Shum, L., and Sadler, T.W. (1988). Embryonic catch-up growth after exposure to the ketone body D,L,-beta-hydroxybutyrate in vitro. *Teratology*. 38, 369-79.

Shum, L., and Sadler, T.W. (1990). Biochemical basis for D,L,-beta-hyroxybutyrate-induced teratogenesis. *Teratology*. 42, 553-63.

ZEBRA MUSSEL (*Dreissena polymorpha*) BIOFILTER REDUCTION OF WATERBORNE MICROBES

Mary L. Seaman
NSF Research Experience For Undergraduates
Center for Great Lakes Studies
600 E. Greenfield Avenue
University of Wisconsin - Milwaukee
Milwaukee, Wisconsin 53204
Faculty Advisor:
Dr. Jerry L. Kaster

The zebra mussel (*Dreissena polymorpha*) is notorious for its negative impact on water users. This study examined the use of zebra mussels as biofilters for pretreating water by removing microbial flora. The apparatus consisted of a vertical filtering chamber with three compartments linked together, each housing 1000 g. of zebra mussels. Samples were collected from four ports to measure changes in water quality through the system. Test metrics included: temperature, dissolved oxygen, specific conductance, pH, ammonia, membrane filtration rates and bacterial counts. Biofiltration removed enough particles to increase the flow rate of water through membrane filters by 30 to 400% depending upon harbor conditions. Total coliform colony counts were reduced about 69% from inlet to outlet. Heterotrophic bacteria plate counts decreased 75% between inlet and outlet. The trend indicated the first compartment was most efficient in reducing microbial flora. Water flow can be adjusted to obtain maximum filtration. The potential uses of the biofilter for water management purposes were very positive.

INTRODUCTION

The zebra mussel (*Dreissena polymorpha*) was introduced into Lake St. Clair around 1985. It is native to Europe, and was probably transported to Lake St. Clair in the veliger larval form in the ballast water of a transoceanic ship. Zebra mussels are serious biofouling pests. Europeans can attest to their nuisance effects: clogging intake and distribution pipelines; corroding metals; contaminating potable water supplies and encrusting hulls of boats (Claudi and Mackie, 1994). Millions of dollars have been spent for controlling zebra mussels, but with little success. They continue to spread throughout the central, southern and eastern watersheds in the United States.

Why is *D. polymorpha* so successful? Several features make it unique among the bivalves: First, they are very efficient suspension feeders. Each adult mussel (approximately 25 mm) is able to filter approximately one liter of water per day. Their prime food source is algae, primarily the 15-40 micrometer size range, which are utlimately processed as feces or as pseudofeces. Pseudofeces are undigested material that is bound with mucous into pellets and expelled from the shell into the water column (Synder, 1991). Second, the zebra mussel's reproductive cycle allows for rapid dispersal and high abundance. A mature female mussel may produce as many as one million eggs in two years (Claudi and Mackie, 1994). Peak reproduction is usually late in May and then again in late July or early August. Eggs are fertilized outside the shell and develop into free swimming veliger larvae. Veligers are carried by the current as part of the planktonic load, thus allowing for their rapid dispersal. After 3 to 4 weeks, the veligers attach themselves to hard substrates. At this stage they are called juveniles and within a year the zebra mussels become adults. The adult growth rate is very high, as much as 0.5 mm per day. The adult life span is about 1.5 to 2 years (Claudi and Mackie, 1994). Third, they have the ability to generate byssal threads. These threads enable the mussels to anchor to hard surfaces. Juveniles can detach from hard surfaces and generate new buoyant threads which allow them to drift in the currents and find new surfaces (Snyder, 1991). *Dreissena* is epifaunal, unlike the majority of other freshwater bivalves which are infaunal (Claudi and Mackie, 1994). Byssal threads allow them to colonize hard surfaces such as rocks, metal, wood, glass, rubber, plants, paper and other aquatic organisms (Snyder, 1991).

Zebra mussels are most numerous in the 3 to 7 m depths. Once they are established, large clumps of mussels (called translocators) can break free and form the substrate for new colonies (Claudi and Mackie, 1994). Knowledge of the zebra mussel's environmental requirements can be helpful in predicting where they will colonize even perhaps aiding in lessening their negative impact. The most critical parameters for colonization are: salinity (0-4 ppt), temperature (17-23°C), pH (7.4-9.0), dissolved oxygen (8-10 ppm), calcium concentrations of 20-125 ppm and water velocity of 0.2-1.2 m/s (Ludyanskiy, McDonald, and MacNeill, 1993).

Most research has focused on the biofouling properties of *D. polymorpha*. Recently some research activities have started to concentrate on the beneficial aspects of the zebra mussel, especially for water management, because of their ability to clarify water through their efficient natural biofiltering system (Claudi and Mackie, 1994).Currently, studies are being conducted on use of zebra mussels as biological filters in the freshwater inlet of Lake Volkerak-Zoommeer in The Netherlands. The process involves hanging cultures of zebra mussels in the lake and letting them filter out the suspended material and deposit the pseudofeces in the sediment (Reeders, bij de Vaate, Norodhuis, 1993). The objective of the study reported here is to examine the use of zebra mussels as biofiltering agents for waterborne microbial flora within an artificial environment.

METHODS AND MATERIALS

Apparatus

A biofiltering chamber comprised of three vertical compartments (Figure 1) was constructed from 3 inch (7.6 cm) diameter PVC pipe. A screen was placed in each compartment to prevent migration between compartments. Changes in the microbial flora and water quality were measured at four sampling ports: Port 1 (inlet) received water directly from Milwaukee Harbor; port 2; port 3; and port 4 (outlet).

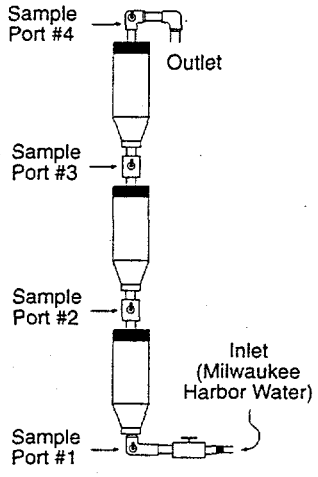


Figure 1. Biofiltering apparatus.

Procedure

Zebra mussels (*D. polymorpha*) were collected from Lake Michigan at the Wisconsin Electric Power Company in Oak Creek, Wisconsin. They were placed in a sieve and drained for 10 minutes and then weighed. Fresh weight included zebra mussels, sediment, shells and small stones. Each compartment in the biofilter was filled with 1000 g. of live zebra mussels. Prior to testing, mussels were acclimated within the chamber for 72 hours. Loading rates through the filter bed were determined by timing how many seconds it took to fill a 500 ml graduated cylinder.

Before testing, each of the four ports were opened and flushed for 15 seconds. A fresh 100 ml sample was used for each test parameter. Test metrics included: temperature; dissolved oxygen (YSI Model 51B Oxygen Meter); specific conductance (TDS Digital Tester); pH (Type 40 Chemtrix); ammonia nitrogen (Perkin-Elmer Lambda 3B UV/VIS

Spectrophotometer) measured at 425 nanometers and syringe-filtered prior to analysis with 0.45 micrometer Metricel 25 mm membrane filters.

A Gomco vacuum and Millipore filtration unit were used to measure filtration rates. Three aliquots of 200 ml each (600 ml total) were collected from each of the four ports, then filtered using Nucleopore 47 mm, 0.8 micrometer membrane filters weighed to constant weight. Time required for 600 ml to pass through the filter was determined. To obtain particle weights, filters were dried for 15 min. at 43°C and then weighed to constant weight (Am. Public Health Assoc. 1992).

Bacterial samples were collected from each port using sterile 250 ml bottles. Analyses were conducted by personnel at the City of Milwaukee Linnwood Water Filtration Plant and included the following: *Clostridium perfringens* (100 ml dilution) using Modified mCP media, incubated anaerobically at 35°C plus or minus 0.5°C for 24 hours; Heterotrophic plate counts (l ml dilution) using 12-15 ml Standard Plate Count media, incubated for 48 hours at 35°C; Total and Fecal Coliform using Colilert by IDEXX®, incubated at 35°C for 24 hours.

RESULTS

Water temperature in the Milwaukee Harbor ranged from 19.5°C to 21.7°C during the study (June through August). Loading rates were variable in the biofiltering system for all test metrics (1.1, 1.8, 2.9, 4.2 and 5.0 l/min) respectively. Specific conductance showed little variability across all ports and loading rates. The range at port 1 (inlet) was 415 to 470 microsiemens/cm and at port 4 (outlet) 430 to 470 microsiemens/cm. A small but consistent increase in pH occurred from inlet (6.6 to 6.9) to outlet (7.1 to 7.6) at all loading rates. Dissolved oxygen concentration decreased from inlet (6.0 to 8.4 mg/l) to outlet (4.6 to 7.9 mg/l) at all loading rates. Ammonia nitrogen stayed the same at ports 1 and 2, but then decreased considerably between ports 2 and 3 (.305 to .235 mg/l) only at the 1.8 l/min loading rate. Table 1 gives an example of the typical trends that were observed for all test metrics. At the loading rate of 1.8 l/min., temperature averaged 19.5°C; pH increased across all ports (6.9 to 7.3); dissolved oxygen, nitrogen ammonia and specific conductance decreased across all ports (6.8 to 5.3 mg/l, .305 to .240 mg/l and 415 to 430 microsiemens/cm respectively).

Table 1. Results (except for bacteria and solids) at loading rate of 1.8 liters/minute.

	pH	Dissolved Oxygen (mg/l)	Nitrogen Ammonia (mg/l)	Specific Conductance (µsiemens/cm)	Temperature (Celsius)
Port 1	6.9	6.8	0.305	415	19
Port 2	7.2	5.8	0.305	415	19
Port 3	7.3	5.5	0.235	430	19
Port 4	7.3	5.3	0.240	430	19

Influent (Port 1) membrane filtration rates ranged from 152.2 ml/min to 6.8 ml/min. depending upon harbor conditions. Effluent (Port 2) membrane filtration rates ranged from 654 ml/min to 286 ml/min. The relationship between influent water quality (measured indirectly by membrane filtration) and improvement in water quality by the zebra mussels is shown in Figure 2. Water quality improved by almost 400% (ratio of IMFR to EMFR = 39.0) when influent was high in particulates (influent membrane filtration rate 7.3 ml/min) and when influent was low in particulates (influent membrane filtration rate 152 ml/min) water quality only improved by 30% (ratio of IMFR to EMFR = 3.0). Particle weight and membrane filtration rate showed an inverse relationship. The expected relationship between high influent membrane filtration rates (IMFR) and low influent particle weights is seen in columns one and two of Table 2. In 3 out of 4 trials yielding complete data, effluent particle weight was higher than influent particle weight. In one trial not yielding complete data, the effluent particle weight probably was high since the membrane filter plugged. Fine particles were observed at port 1 and coarse particles at ports 2 through 4, indicating the biofiltering system coagulated the fine particles leading to increased flow of water through the system and reduced membrane filter clogging.

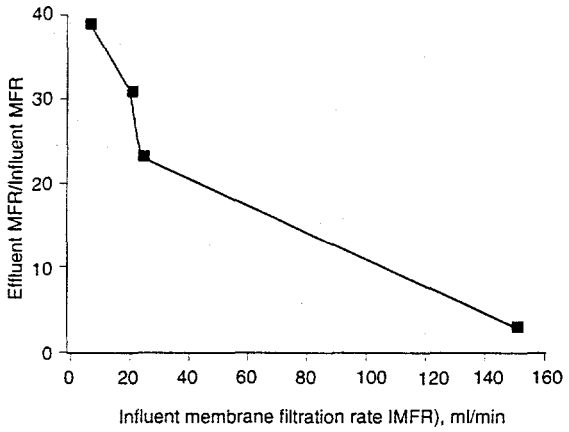


Figure 2. Relationship between influent particulate water quality and improvement in water quality by zebra mussels. Loading rates variable.

Table 2. Relationship between particle weight and membrane filtration rates.

Membrane filtration rate (ml/min.) *infuent*	Particle weight (mg/l) *influent*	Particle weight (mg/l) *effluent*
152.0	2.0	2.5
25.0	2.8	5.4
21.0	2.7	4.8
7.3	2.2	0.8
6.8	4.2	not available

Reduction of microbial organisms are shown in Figure 3. Counts of *Clostridium perfringens* were reduced about 33% overall between inlet and outlet. Heterotrophic plate counts decreased about 75% and total coliform colonies were reduced about 69% overall. Fecal counts from all ports were zero.

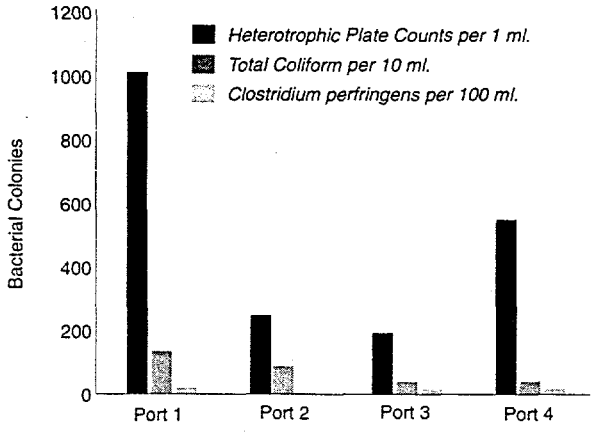


Figure 3. Reduction of number of microbial organisms.

CONCLUSIONS

This study demonstrated that zebra mussels could be used effectively as biofilters in the pretreatment of water. The biofilter biologically coagulated fine particulates which reduced membrane filter clogging resulting in increased flow through membrane filters by at least 30% and as much as 400% depending on the condition of the inlet water. The first compartment proved to be the most efficient; microbial flora were decreased substantially. The design of the biofilter could be studied further to see if a two compartment vertical filter, or possibly a two or three parallel compartment design would obtain optimal results better than the current design.

ACKNOWLEDGEMENTS

Special thanks to Dr. Jerry Kaster from the Center For Great Lakes Studies for his time, assistance and patience in helping me with this project, and Dr. Frederic Spangler from the University of Wisconsin Oshkosh for his assistance in analysing the data and writing of this paper. Also, thanks to Pat Klappa from the City of Milwaukee Linnwood Water Filtration Plant for analysing the bacterial samples. Funding for this project was provided by the National Science Foundation's Research Experience for Undergraduates program.

REFERENCES

American Public Health Association (1992). Standard methods for the examination of water and wastewater, 18th ed. APHA.

Claudi, Renata, & Mackie, Gerald L. (1994). Practical manual for zebra mussel monitoring and control. Boca Raton: Lewis Publishers.

Ludyanskiy, Michael L., McDonald, Derek, & MacNeill, David (1993). Impact of the zebra mussel, a bivalve invader. BioScience. 43(8), 533-544.

Reeders, Harro H., Bij de Vaate, Abraham, & Norodhuis, Ruurd (1993). Potential of the zebra mussel (*Dreissena polymorpha*) for water quality management. In Nalepa, Thomas F., & Schloesser, Donald W. (Eds.), Zebra mussels biology, impacts, and control. (pp. 439-451). Boca Raton: Lewis Publishers.

Snyder, Fred L. (1991). Zebra mussels in the Great Lakes: The invasion and its implications. (Report No. OHSU-FS-045). Ohio Sea Grant College Program.

Altering Serum IGF-1 Concentration and its Relationship to Reproductive Performance to Lactating Holstein Cows

Lance Baumgard

Department of Animal Science
University of Minnesota
130 Haecker Hall
1364 Eckles Ave.
St. Paul, Mn 55108

Faculty Advisor:
Dr. Brian Crooker

BACKGROUND

Multiparous Holstein cows were used to evaluate the effects of bovine somatotropin and supplemental dietary fat on plasma progesterone and IGF-1 concentrations and reproductive measures during early lactation.

INTRODUCTION

A good reproductive program is imperative to a dairy producer if the dairy operation is to be successful. A goal of a dairy producer is to achieve a 365 day calving interval. Gestation period of a cow is 280 days and the cow requires about a 60 day dry period to prepare for the subsequent lactation. The first and second estrus cycles are sometimes difficult to detect because negative energy balance alters secretion of the hormones responsible for maintenance of cyclicity. Most producers do not initiate breeding until day 50-60 of lactation, when cycling becomes more prominent and regular. Thus, to achieve a 365 day calving interval, cows must become pregnant prior to day 90 of lactation. In this situation producers have, at most, two estrus cycles to get their cows pregnant. In order to make it possible to shorten the amount of time between parturition and conception, the dynamics that exist between hormone secretion and reproductive success must be understood.

Progesterone is the primary ovarian hormone responsible for maintenance of pregnancy. It is produced by the ovary, in particular the granulosa and theca interna cells of the corpus luteum, and by the placenta during gestation. Progesterone prepares the uterus for fertilization and maintains it during pregnancy. It also aids in the initiation of lactation. Insulin-like growth factor-1 (IGF-1) is one of the primary hormones involved with tissue growth. The primary site of production is the liver. Its production is stimulated by the presence of somatotropin. IGF-1 stimulates cell proliferation, differentiation and steroidogenesis.

Energy balance (EBAL) and general health have been implicated as major contributors to impaired reproductive performance in lactating dairy cows. EBAL is the net result of associations between yield, energy intake, and use of nutrients by the cow. About 90% of dairy cows experience a negative EBAL (NEBAL) during the early stages of lactation, but the magnitude and duration of NEBAL varies among cows. Dairy producers have attempted to alleviate this problem by feeding supplemental dietary fat which increases the energy density of the diet. This helps, but usually does not eliminate, the NEBAL.

Severe NEBAL, during the early postpartum period, is generally associated with poor reproductive performance (difficulty to breed back) because of reduced luteal function, according to Villa-Goday *et al.* (1988), during the second and third postpartum luteal phases. Luteal function is associated with reproductive events that determine fertility in cattle. Attempts to correct the NEBAL before the second luteal phase should help the reproductive performance of the cow. According to Spicer *et al.* (1990), there is a positive relationship between EBAL and serum IGF-1 concentrations.

Administration of bovine somatotropin (bST) to lactating dairy cows results in metabolic changes that lead to increased milk production. Although bST is

helpful in milk production, it can either increase the magnitude, or prolong the duration of NEBAL, or possibly do both, depending on the amount of increased milk yield and the corresponding increase in feed intake. Thus, there is concern about the potential negative influence of bST on reproductive performance of bST-treated cows. According to Stanisiewski *et al.* (1992.), one action of bST is to stimulate synthesis and secretion of IGF-1, and there is evidence that IGF-1 stimulates the production of progesterone. There are also data that suggest a direct involvement of bST or IGF-1 in ovarian follicular growth in cattle (Lucy *et al.*, 1993).

MATERIALS AND METHODS

Cows and treatments. Thirty six-multiparous Holstein cows were housed in a tie stall barn and milked twice a day. They were blocked in groups of six by date of calving (56 d interval), and were randomly assigned within blocks to one of six treatments (2 diets x 3 bST doses). One cow was removed from the study because of health (lameness). Depending on treatment assignment, cows received daily intramuscular injections of 0, 0.6, or 1.6 ml of solubilized bST. This provided doses of 0, 5, or 14 mg of bST/d. The daily treatment was initiated 14 days postpartum and continued through the entire lactation.

Data collected. Blood samples used to determine progesterone concentration, were obtained by vacutainer on Monday, Wednesday, and Friday mornings from the tail vein. Wednesday samples were also used to determine IGF-1 concentrations. Vacutainers contained potassium oxalate and sodium fluoride to prevent coagulation and to minimize degradation of hormones. Blood sampling was initiated at calving and continued through the second confirmation of pregnancy or until 150 days postpartum, whichever came first. Samples were kept on ice until plasma was harvested (2,000 x g, 10 min in a refrigerated centrifuge). Plasma was stored at -10° C until assayed.

Progesterone content of the samples was determined quantitatively by the Diagnostic Products Corporation, Coat-A-Count progesterone assay. A validated RIA of bovine plasma was used to quantitate IGF-1 content. These assays have been optimized for linearity of logit-log plots. Extensive experiments have shown that the assays are accurate over a broad spectrum of progesterone and IGF-1 concentrations, assay sensitivities are approximately 0.03 and 0.5 ng/ml, respectively.

Calculations. Progesterone concentrations were plotted against day of lactation for individual cows. Progesterone concentrations greater than or equal to 0.5 ng/ml indicated a rise above baseline. Two consecutive samples with a progesterone concentrations greater than or equal to 0.5 ng/ml indicated initiation of an estrus cycle. End of an estrus cycle occurred when progesterone concentration decreased to less than 0.5 ng/ml. Area under the curve (AUC) was calculated by trapezoid summation of areas defined by successive pairs of concentration and day data within a cycle.

EBAL was computed as energy intake minus energy expenditure corrected for body weight change. Energy intake was calculated as dietary dry matter intake times net energy content (Mcal/kg) of the diet. Energy expenditure for maintenance and production was calculated according to NRC (1989).

Statistical analysis. Data were evaluated for treatment effects through GLM procedures of SAS. Production data were analyzed by the model $Y = \mu$ + block + fat + bST + fat*bST + covariate + error where fat was dietary fat and bST was bST dose. Covariate data were collected through days 7-13 postpartum. Effects of treatment on days open (number of days from calving to conception) and endocrine data were not covariately analyzed: $Y = \mu$ + block + fat + bST + fat*bST + error. Other reproductive data were not analyzed because of the limited number of animal observations. Linear regression was used to evaluate the relationship between variables (mean EBAL and progesterone AUC, mean IGF-1 concentration and EBAL, and progesterone AUC and mean IGF-1) during each cycle. Repeated measures was used to detect the effect of treatments on mean plasma IGF-1 concentrations. Differences were considered significant when $P < 0.10$.

RESULTS

Administration of bST increased ($P < 0.05$) serum IGF-1 concentrations (Figure 1). There was no effect of treatment on mean EBAL (Table 1) during day 1-10 postpartum (-4.4 Mcal/d), day 1-20 postpartum (-4.73 Mcal/d), or day 1-150 postpartum (6.53 Mcal/d). EBAL curves (not shown) were consistent among treatments.

Length and AUC of the first and second estrus cycles were not altered by treatment (Table 1). Length and AUC of the third estrus cycle of cows receiving no bST and no supplemental fat were considerably greater than those of other cows in this study (Table 1). This difference appears to be real as the results were consistent among the cows receiving this treatment. Length and AUC of the third estrus cycle were reduced when cows received 5 mg bST/d and this resulted in an overall curvilinear response of cycle length and AUC to bST dose (Table 1; $P < 0.05$). There was an interaction ($P < 0.10$) of bST and dietary fat on length and AUC of the third estrus cycle. Inclusion of dietary fat appeared to reduce length and AUC of the third cycle of cows not receiving bST but length and AUC of the third cycle of cows consuming additional fat and receiving bST were slightly greater than that of cows treated with bST and not consuming additional fat. No relationship between mean IGF-1 and progesterone AUC (Figure 2), EBAL and AUC, or IGF-1 and EBAL were observed.

DISCUSSION

Dairy cattle are typically in NEBAL for several weeks postpartum and the cows in this study were no exception. Although cows receiving 5 and 14 mg bST/d were expected to have a more severe NEBAL than control cows, the data did not support this (Table 1). Positive effects were also expected for 4% supplemental dietary fat on EBAL of cows. Supplemental dietary fat tended to lower the severity of NEBAL in the 0 and 5 mg treatments. However, overall NEBAL was not altered by inclusion of dietary fat. This is most likely due to the small number of cows used in this study and the large standard error in the EBAL analysis. A larger data set would improve the ability to determine if supplemental dietary fat reduces the intensity of NEBAL.

Treatments used in this study had little effect on estrus cycle length and AUC of Holstein cows in early lactation. Although length and AUC of the third estrous cycle were altered by bST and the interaction of bST and dietary fat, the limited number of observations restricts our ability to develop a conclusive interpretation. There was no relationship between mean EBAL during each estrous cycle and progesterone AUC. Thus, we detected no effects of EBAL on reproductive performance. In contrast to Hammond *et al.* (1988), this study found no correlation between plasma IGF-1 and plasma progesterone concentrations (Figure 2). Lack of a relationship may be due to a limited number of observations. A larger data set would improve the ability to determine an accurate association.

REFERENCES

Hammond, J.M., C.J. Hsu, J.S. Mondschein, and S.F. Canning. 1988. Paracrine and autocrine functions of growth factors in the ovarian cycle. J. Anim. Sci. 66 (Suppl. 2):21.

Lucy M.C., T.L. Curran, R.J. Collier, and W.J. Cole. 1994. Extended function of the corpus luteum and earlier development of the second follicular wave in heifers treated with bovine somatotropin. Theriogenology 41: 561-572.

National Research Council. 1989. Nutrient requirements of dairy cattle. 6th rev. ed. Natl. Acad. Sci., Washington, DC.

Spicer, L.J., W.B. Tucker, and G.D. Adams. 1990. Insulin-like growth factor-1 in dairy cows: relationships among energy balance, body condition, ovarian activity, and estrous behavior. J. Dairy Sci. 73:929.

Stanisiewski E. P., L. F. Krabill, and J. W. Lauderdale. 1992. Milk yield, health, and reproduction of dairy cows given somatotropin (Somavubove) beginning early postpartum. Dairy Sci 75: 2149-2164.

Villa-Goday, A.T.L. Hughes, R.S. Emery, L.T. Chapin, and R.L. Fogwell. 1988. Association between energy balance and luteal function in lactating dairy cows. J. Dairy Sci 71: 1063-1070.

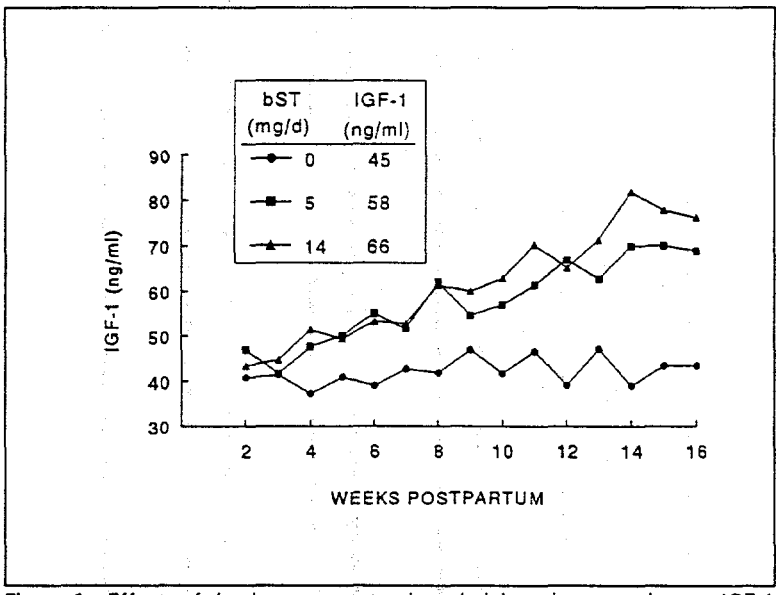


Figure 1. Effect of bovine somatotropin administration on plasma IGF-1 concentrations.

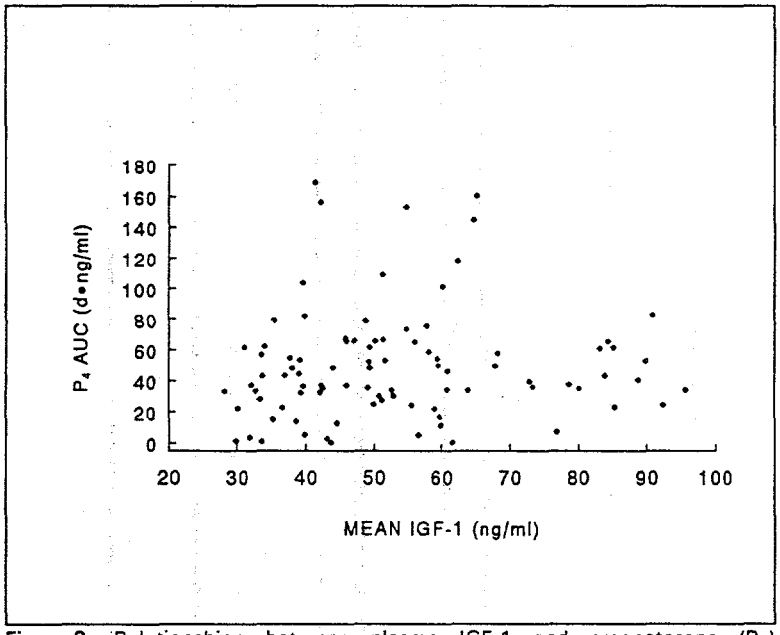


Figure 2. Relationshiop between plasma IGF-1 and progesterone (P_4) concentrations.

TABLE 1. Effect of supplemental dietary fat and bovine somatotropin (bST) on lactational performance, plasma progesterone and estrus cycle lengths of Holstein cows during the first 150 days of lactation.[1]

	Treatment[2]							P^3		
Variable	0F-0B	4F-0B	0F-5B	4F-5B	0F-14B	4F-14B	SE	F	B	I
Cows, n	6	6	5	6	6	6	--	--	--	--
3.5% FCM, kg/d	33.8	33.0	35.0	36.3	36.6	35.6	1.2	NS	*[a]	NS
DMI,kg/d	24.0	21.7	24.8	23.0	24.6	23.8	.7	**[b]	NS	NS
Energy balance[4], Mcal/d										
d 1-10	-6.26	-2.62	-5.61	-2.74	-4.34	-5.23	1.95	NS	NS	NS
d 1-20	-5.82	-3.76	-6.02	-2.83	-4.68	-5.27	1.90	NS	NS	NS
d 1-150	6.85	5.72	7.56	6.18	5.89	7.02	.89	NS	NS	NS
Cycle AUC[5]										
First	52.6	37.0	15.9	38.2	33.8	50.0	14.2	NS	NS	NS
Second	50.1	49.8	62.6	40.4	29.8	38.4	12.6	NS	NS	NS
Third	140.0^{x}	68.1^{y}	22.5^{y}	39.5^{y}	38.0^{y}	56.5^{y}	23.6	NS	**[c]	*
Overall mean[6]	69.3	50.9	34.4	40.9	31.6	47.4	8.7	NS	***[d]	NS
Cycle length, days										
First	20.0	21.5	11.4	20.0	18.6	22.8	3.6	NS	NS	NS
Second	22.1	22.1	23.4	18.3	19.6	22.1	3.1	NS	NS	NS
Third	41.4^{x}	24.8^{y}	16.3^{y}	18.6^{y}	22.6^{y}	24.4^{y}	4.5	NS	***[e]	*
Overall mean[6]	25.2	22.3	16.8	19.5	19.1	23.0	2.0	NS	**[f]	NS

[a]0B, 33.4^{x}; 5B, 35.6^{y}; 14B, 36.1^{y}.
[b]0F, 24.4; 4F, 22.8.
[c]0B, 104.3^{x}; 5B, 31.1^{y}; 14B, 47.4^{y}.
[d]0B, 60.1^{x}; 5B, 37.7^{y}; 14B, 39.5^{y}.
[e]0B, 35.1^{x}; 5B, 17.5^{y}; 14B, 23.0^{y}.
[f]0B, 23.7^{x}; 5B, 18.2^{y}; 14B, 21.0^{y}.
[1]Least squares means.
[2]Treatments were 0 and 4% supplemental fat (0F, 4F) and 0, 5 and 14 mg bST/d (0B, 5B, 14B).
[3]F, fat; B, bST; I, interaction; NS, non-significant; *, $P<.10$; **, $P<.05$; ***, $P<.01$.
[4]NEL intake - (NE_L maintenance + NE_L production).
[5]Area under the progesterone curve (d · ng/ml).
[6]All cycles through 150 days of lactation.

THE FUNCTION AND EVOLUTION OF RABBIT C REPEATS

Gabrielle A. DeVere, Jeanne L. Uy and Carri R. Eagler

Department of Biological Sciences
Wright State University
Dayton, OH 45435.

Faculty advisor:

Dan E. Krane

Within the rabbit genome, the predominant family of short interspersed repetitive elements (SINEs) are known as C repeats. These elements have been estimated to comprise approximately 12% of all rabbit nuclear DNA. Previous work characterizing 45 rabbit C revealed that this family of repeats had propagated in at least three discrete waves over the evolutionary history of rabbits. A significant number of these identified repeats were also found to provide polyadenylation signals that act to increase the stability of translated messenger RNAs. This study has focused on the characterization of additional, previously unidentified C repeats with an emphasis on further elucidating the role that they and other short repetitive elements play in eukaryotic genomes. 57 new C repeats have been found; eight of these repeats may provide polyadenylation signals; one a critical element of an essential gene's promoter.

INTRODUCTION:

Multiple copies of highly repetitive sequences interspersed throughout eukaryotic genomes contribute significantly to the size and possibly the function of these genomes. These interspersed repetitive elements in mammals are classified by length as either short interspersed repetitive elements (SINEs), typically < 500bp in length, or long interspersed repetitive elements (LINEs) whose full-length copies range in size from 6 to 8 kb (Singer, 1982). Both SINE and LINE classes appear to be propagated by retrotransposition, a process by which a progenitor repeat is transcribed into an RNA that is reverse transcribed into DNA and reinserted into the genome. Insertion events occur at staggered breaks in chromosomes and the repair of these break points create short direct repeats that flank the repetitive elements. Families within the shorter class of repeats can be identified on the basis of sequence similarity and each mammalian order examined to date appears to possess its own characteristic family.

The predominant SINE in primates, *Alu* repeats, appears to have arisen from a 7SL RNA gene shortly after the mammalian radiation 80 million years ago. Similarly, the SINEs in many other mammalian orders, including rabbit C repeats, appear to be derived in part from tRNA genes (Krane, *et al.*, 1991). Despite the extensive sequence differences between families of these repeats, most mammalian SINEs share several structural features including internal promoters for RNA polymerase III, A-rich tracts at their 3' ends, full lengths of approximately 300 nucleotides, and a general absence of conserved open reading frames.

Approximately 500,000 *Alu* repeats comprise roughly 10% of the human genome and can be divided into at least three subfamilies of differing ages. Members of each subfamily can be readily distinguished by examination of diagnostic nucleotides within each sequence. The ability to separate these repeats into well-defined subfamilies supports a model that invokes a small number of sequences, progenitor repeats, as being capable of generating new repeats that can successfully be retrotransposed and fixed within a population (Deininger, 1993).

The predominant repetitive element in lagomorphs, rabbit C repeats, are typical SINEs. With approximately one million copies interspersed throughout the rabbit genome and an average length of 324 bp, they account for 12% of rabbit nuclear DNA. Alignment of the nucleotide sequences of C repeats shows that they too fall into at least three distinct subfamilies whose progenitors contain diagnostic sites that have changed in a progressive and apparently punctuated manner (Krane, *et al.*, 1991). Several individual C repeats have been found to contribute useful sequences to rabbits by providing functional polyadenylation signals to the genes into which they have inserted (Krane and Hardison, 1990).

Further characterization of these repetitive elements and determination of which provide potentially functional sequence elements to rabbit genes was made possible by the discovery and analysis of 57 previously unrecognized members of this family available in the GenBank database. These newly recognized C repeat sequences have also been used to improve a consensus sequence for this family of SINE (now based on a total of 102 members). This improved consensus sequence was used to design a C repeat-specific probe that has been used to screen a rabbit lung cDNA library. cDNA clones found in this way have been isolated and are being characterized by restriction enzyme mapping, Southern blotting and dideoxynucleotide sequencing to gain further insights into the rate and evolutionary history of C repeats and SINEs in general.

Table 1. Sources of C Repeat Sequences.

Repeat	Acc. Number	Start[a]	End[a]	Orientation[b]	Location[c]	Reference(s)[d]
C46	M98536	5213	5570	+	3' UT of serum amyloid	Ray and Ray 1991
C47	M98536	2110	2465	-	Intron 2 of serum amyloid	Ray and Ray 1991
C48	D90378	1290	1614	+	Intron 1 of lambda R-1	Sasaki 1992
C49	D90378	3526	3783	+	3' UT of λ R-1 ANA	Sasaki 1992
C50	D90378	4372	4676	+	3' UT of λ R-1 ANA	Sasaki 1992
C51	D90378	2012	2251	-	Intron 1 of λ R-1 ANA	Sasaki 1992
C52	M33582	1932	2276	+	5' UT of Beta-casein	Thepot *et al.* 1991
C53	M33582	2408	2796	+	5' UT of Beta-casein	Thepot *et al.* 1991
C54	M33582	1432	1780	-	5' UT of Beta-casein	Thepot *et al.* 1991
C55	M33582	7617	7983	-	Intron 7 of Beta-casein	Thepot *et al.* 1991
C56	M33582	8745	9123	-	3' UT of Beta-casein	Thepot *et al.* 1991
C57	M33582	10436	10760	-	3' UT of Beta-casein	Thepot *et al.* 1991
C58	X07791	566	900	+	5' UT of MT-2	Thirion p.c.
C59	X07791	1299	1646	+	3' UT of MT-2	Thirion p.c.
C60	X07791	1403	1470	+	3' UT of MT-2	Thirion p.c.
C61	X07791	1642	1811	+	3' UT of MT-2	Thirion p.c.
C62	X07791	140	520	-	5'UT of MT-2	Thirion p.c.
C63	L05833	3560	3800	+	Unknown	Hardison *et al.* 1993
C64	L05833	6333	6596	+	Unknown	Hardison *et al.* 1993
C65	M12180	1213	1527	-	In rabbit Ig	Bernstein *et al.* 1985
C66	M12180	1635	1981	-	In rabbit Ig	Bernstein *et al.* 1985
C67	M12180	2596	3034	+	In rabbit Ig	Bernstein *et al.* 1985
C68	M24901	1347	1705	+	Unknown	Xu *et al.* 1989
C69	M83085	1099	1382	+	Unknown	Sasaki *et al.* 1991
C70	Y00761	1762	2046	+	Unknown	Fujii *et al.* 1988
C71	M94359	176	386	+	Unknown	Ayres *et al.* 1992
C72	X60985	122	499	-	Contains C46 and C47	Hardison 1991
C73	X53765	334	646	-	Intron of NAT1	Blum 1990; Blum *et al.* 1990
C74	X53765	602	980	-	Intron of NAT1	Blum 1990; Blum *et al.* 1990
C76	Z19092	1082	1425	-	Intron 1 of Trichohyalin	Fietz and Rogers 1992; Fietz p.c.
C77	Z19092	1685	1945	-	Intron 1 of Trichohyalin	Fietz and Rogers 1992; Fietz p.c.
C78	Z12842	1676	2095	-	3' UT of unknown protein	Boll 1992; Boll *et al.* 1993
C79	D90377	2695	3040	+	3' UT of λ S-1 ANA	Sasaki *et al.* 1991; Sasaki 1992
C80	D90377	3316	3676	+	3' UT of λ S-1 ANA	Sasaki *et al.* 1991; Sasaki 1992
C81	D90377	336	636	-	5' UT of λ S-1 ANA	Sasaki *et al.* 1991; Sasaki 1992
C82	D90377	626	964	-	5' UT of λ S-1 ANA	Sasaki *et al.* 1991; Sasaki 1992
C83	X60986	900	1309	-	3' UT of MHC fragment	Marche p.c.; Marche *et al.* 1991
C84	X60986	2481	2726	-	3'UT of MHC fragment	Marche p.c.; Marche *et al.* 1991
C86	X52564	4	100	+	5' UT of WAP	Devinoy 1990; Devinoy *et al.* 1990
C87	X52564	91	441	-	5'UT of WAP	Devinoy 1990; Devinoy *et al.* 1990
C88	M93344	206	500	-	Unknown	Ray and Ray 1992
C89	M93344	2030	2405	-	Unknown	Ray and Ray 1992
C91	M77195	7670	8085	+	Intron 9 of αs1-casein	Jolivet *et al.* 1992
C92	M77195	140	550	-	5' UT of αs1-casein	Jolivet *et al.* 1992
C93	M77195	2675	3055`	-	Intron 1 of αs1-casein	Jolivet *et al.* 1992
C94	M77195	3924	4252	-	Intron 2 of αs1-casein	Jolivet *et al.* 1992
C95	M77195	6526	6892	-	Intron 8 of αs1-casein	Jolivet *et al.* 1992
C96	M77195	8316	8684	-	Intron 9 of αs1-casein	Jolivet *et al.* 1992
C97	M77195	11184	11500	-	Intron 13 of αs1-casein	Jolivet *et al.* 1992
C98	M77195	13732	14065	-	Intron 15 of αs1-casein	Jolivet *et al.* 1992
C99	M77195	16408	16784	-	Intron 18 of αs1-casein	Jolivet *et al.* 1992
C100	M33291	6417	6839	-	Unknown	O'Prey *et al.* 1989
C101	L10931	1803	2163	+	3' UT of monoxygenase	Burnett and Philpot p.c.
C102	L10931	2269	2584	+	3' UT of monoxygenase	Burnett and Philpot p.c.
C103	M93174	4	282	+	part of coding region	Knight and Becker 1990
C104	X53766	2140	2325	+	Intron of NAT2	Blum 1990; Blum *et al.* 1990
C105	M31245	1	522	-	5'UT contains TATA	Chan 1990

[a]Positions of repeats within GenBank files. Several repeats appear to be longer than the repeats' average length of 324 nucleotides, because of the insertion of additional repeats. All sequences are available in GenBank using the accession numbers provided in the column labeled Acc. Number.

[b]A plus sign (+) indicates that the repeat is read 5' to 3', left to right on the top strand of the sequence, while a minus sign (-) indicates the opposite orientation.

[c]3'UT = 3' untranslated region; 5'UT = 5' untranslated region; MHC = major histocompatibility complex; WAP = whey acid protein; ANA = arylamine N-acetyltransferase.

d p.c. = personal communication.

MATERIALS AND METHODS:

Previously unrecognized C repeat sequences (Table 1) were found in the GenBank R81.0 database using the C repeat consensus sequence reported by Krane and Hardison (1990), and the MacDNAsis software package (Hitachi, 1993). The 57 new rabbit C-repeats found were added to a multiple alignment of 45 previously reported C repeats (Krane and Hardison, 1990), using pairwise alignments generated by MacDNAsis and optimized by hand. The PAUP (phylogenetic analysis using parsimony) program (Swofford, 1991) was used to generate a phylogenetic tree based upon this alignment.

The alignment containing 102 C repeat sequences was also used to generate an improved consensus sequence for this family of SINEs. A highly conserved sequence from position 138 to 163 of this consensus sequence, 5'- CGATGGCCCAAGTGCTTGGGCCCC TGCCA -3', was used as a probe in a series of screens of a rabbit lung cDNA library cloned in λgt10. Filters for Southern hybridization (Church and Gilbert, 1984) were prepared by lifting

nitrocellulose membranes from LB agarose (+10 mM $MgSO_4$) plates containing isolated plaques on a lawn of *E Coli* C600Hfl. Phage DNA was fixed to these membranes by UV crosslinking.

The 25 nucleotide-long probe was labeled with gamma-P^{32} using polynucleotide kinase. Once radiolabeled, the oligonucleotide probe was used to identify plaques containing C repeats. The filters were warmed with prehybridization solution in a Techne hybridiser HB-1D for four hours at 46°C prior to addition of the probe. Filters were probed for twenty hours at 64°C. Upon completion of the hybridization, they were rinsed twice at 46°C with 2X SSC and 0.05 SDS for one hour and fifteen minutes, respectively. Filters were then exposed to X-ray film for 3-12 days at -70°C with two intensifying screens.

Approximately 4% of the 5,500 cDNA clones screened were determined to hybridize to the C repeat-specific probe and were isolated and purified. PCR using primers flanking the poly-linker of λgt10 and *Eco*RI restriction enzyme digests were performed to determine the length of each clone's insert. DNA sequencing of unique clones is currently in progress using the Sanger dideoxynucleotide method and the fmol DNA sequencing system with S^{35}.

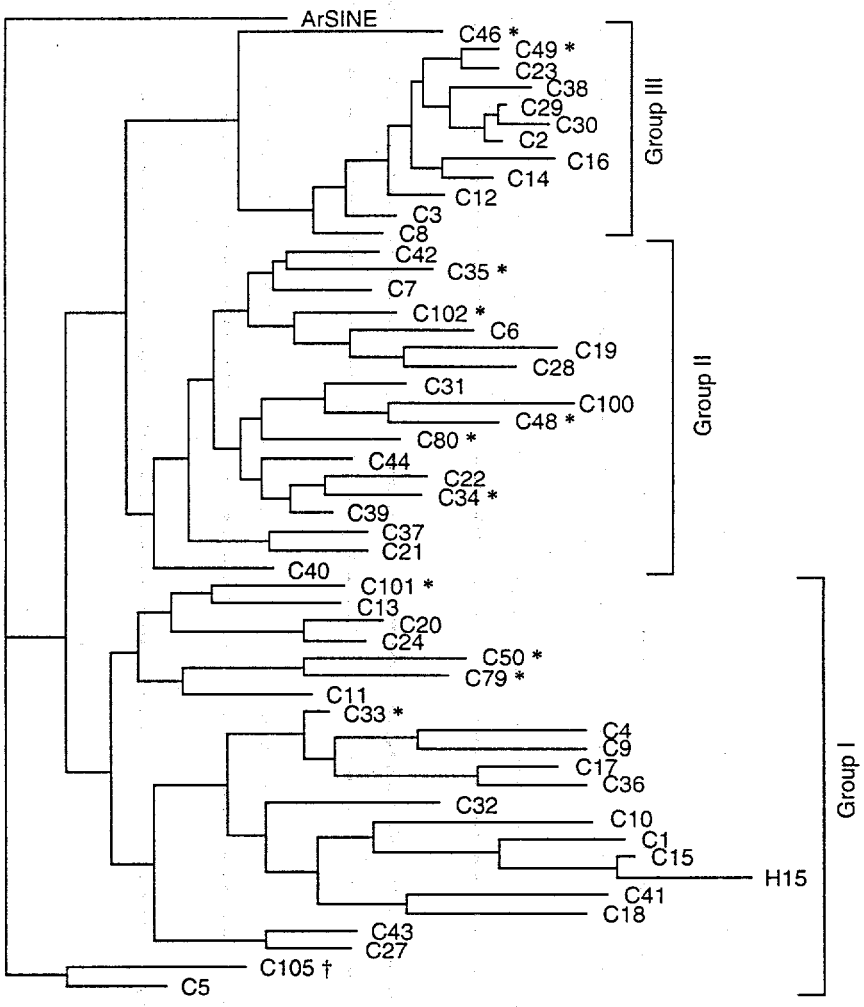


Figure 1. Phylogram of 54 rabbit C repeats. The relatedness of the first 45 C repeats to be characterized plus nine found to contribute potentially useful elements to rabbit genes in this study is shown. Horizontal distance is proportional to the evolutionary distance separating repeats. Subfamilies to which repeats have been assigned are bracketed and are consistent with those determined by Krane and Hardison (1990). C repeats that provide functional polyadenylation signals are marked with asterisks (*) and the repeat that provides a TATA box (C105) is marked with a dagger (†).

RESULTS:

This work reports the characterization of 57 previously undescribed rabbit C repeats (Table 1) and brings the total number of these repeats whose sequences are known to 102. Analyses of these newly described C repeats confirms that this family of repetitive elements can be divided into at least three distinct subfamilies that have been propagated at different times during lagomorph evolution (Krane and Hardison, 1990). Sites shown to be diagnostic in previous work have indeed proven to be useful in the characterization of newly recognized members of this family and additional diagnostic sites have been elucidated (data not shown).

Interestingly, almost 8% of all rabbit genes presently in the GenBank database were found to contain C repeats that provide sequences important to their proper function or expression. this finding is consistent with our observation that approximately 4% of rabbit long cDNA clones hybridize to a C repeat specific probe. The most common (a total of 11% of all characterized C repeats) putative role for these C repeats remains one involved in polyadenylation as seen in the rabbit genes for rabbit cytochrome p-450 isozymes 4 and 6 (Okino *et al.*, 1985), rabbit lambda S-1 gene for arylamine N-acetyltransferase (Sasaki *et al.*, 1991; Sasaki, personal communication), rabbit lambda R-1 gene for arylamine N-acetyltransferase (Sasaki, personal communication), rabbit serum amyloid A gene (Ray and Ray, 1991) and rabbit flavin-containing monooxygenase (Burnett and Philpot, personal communication). Additionally, one repeat (C105) was found to contain an important promoter element (the TATA box) of the rabbit cytochrome P45011C3 (Chan, 1990).

The repeats C46 and C49 in particular that are described here are very similar to the consensus sequence for Group III repeats that have been propagated only in the past 15 million years. Thus , it is likely that little evolutionary time if any is required for their polyadenylation signals to supplant those presumed to be associated with their genes originally.

Rabbit C repeats that provide elements that may play essential functional roles in gene expression and function are equally represented among all three of the subfamilies of this repeat (Figure 1). The dispersion times of these repeats appears to span the entire evolutionary history of lagomorphs. C repeats and their analogs in other mammalian orders may confer a sufficient selective advantage through effects upon transcribed regions alone as described in this work to justify their extensive propagation and maintenance in high copy numbers.

CONCLUSION:

The short, interspersed repetitive elements known as C repeats comprise approximately 12% of the rabbit genome and are analogous to the *Alu* repeats found in abundance in the human genome. The role that repetitive DNA elements play in the evolution and function of mammalian genomes has been a matter of debate since their discovery (reviewed in Rogers 1985; Weiner *et al.*, 1986). Initial studies of C repeats (Krane and Hardison, 1990) were the first to provide evidence that they , and SINEs in general, may confer a selective advantage to the organisms in which they are found by providing functional polyadenylation signals to the genes into which they have inserted. The more comprehensive survey of rabbit C repeats reported here confirms that preliminary work and reveals that a statistically significant fraction (11%) of sequenced C repeats provide potentially functional elements to lagomorph genes. Almost 8% of all currently sequenced rabbit genes and approximately 4% of rabbit lung cDNA clones contain C repeats that could play roles important to the regulation of gene expression. The C repeats providing potentially functional elements to genes for which sequence information is available have been placed in each of the rabbit C repeat subfamilies (propagated 65 to 40 million years ago, 40 to 15 million years ago and 15 million years ago to the present) and are likely to have played these roles throughout their own and lagomorph evolution in general.

ACKNOWLEDGMENTS:

The authors appreciate the valuable insights and assistance that Scott Jenkins, Keri Steinbrugge and Adam Skepner provided during the course of this work. This work was supported in part by an Ohio Research Challenge grant to DEK and a U.S. Department of Education grant for summer research projects by woman and minority students to JLU and CRE.

REFERENCES:

Ayres, J.A., D.K. Price, D.M. Pasqualone, C.H. Cabell, W. Miller and R.C. Hardison. 1992. Genomics. The 5' end of LINE1 repeats in rabbit DNA define subfamilies and reveal a short sequence conserved between rabbits and humans. Vol. 14, pp. 320-331.

Bernstein, K.E., C.B. Alexander and R.G. Mage. 1985. J. Immunol. Germline VH genes in an a3 rabbit not typical of any one VHa allotype. Vol. 134, pp. 3480-3488.

Blum, M., M. Heim and V.A. Meyer. 1990. Nucleic Acids Res. Nucleotide sequence of rabbit NAT1 encoding monomorphic arylamine N-acetyltransferase. Vol. 18, pp. 5287-5287.

Blum, M., M. Heim and V.A. Meyer. 1990. Nucleic Acids Res. Nucleotide sequences of rabbit NAT2 encoding the polymorphic liver enzyme arylamine N-acetyltransferase. Vol. 18, pp. 5295-5295.

Boll, W., T. Schmid-Chanda, G. Semenza, and N. Mantei. 1993. J. Biol. Chem. Messenger RNAs expressed in intestine of adult but not baby rabbits. Isolation of cognate cDNAs and characterization of a novel brush border protein with esterase and phospholipase activity. Vol. 268, pp. 12901-12911.

Chan, G., 1990. Biochemistry. Structure of the rabbit cytochrome P45011C3, a constitutive member of the P45011C subfamily. Vol. 29, pp. 3743-3750.

Church G.M. and W. Gilbert 1984. Proc. Natl. Acad. Sci. USA. Genomic Sequencing. Vol. 81, pp. 1991-1995.

Deininger, P.L. and M. A. Batzer. 1993. Evol. Biol. Evolution of Retroposons. Vol. 27, pp. 157-195.

Devinoy, E., D. Thepot, M.L. Fontaine, C. Hubert and L.M. Houdebine. 1990. Nucleic Acids Res. Complete sequences of rabbit WAP gene. Vol. 18, pp. 3641-3641.

Fujii, J., J. Lytton, M. Tada, and H. MacLennan. 1988. FEBS Lett. Rabbit cardiac and slow twitch muscle express the same phospholamban gene. Vol. 227, pp. 51-55.

Hardison, R.C., D.E. Krane, C. Vandenbergh, J.F. Cheng, J. Mansberger, J. Taddie, S. Schwartz, X. Huan and W. Miller. personal communication.

Hardison, R.C., J. Xu, J. Jackson, J. Mansberger, O. Selifonova, B. Grotch, H. Petrykowska, J. Biesecker and W. Miller. 1993. Nucleic Acids Res. Comparative analysis of the locus control region of the rabbit beta-like globin gene cluster: HS3 increases transient expression of an embryonic epsilon-globin gene. Vol. 21, pp. 1265-1272.

Hitachi Software Engineering Co., Ltd. HIBIO MacDNAsis Pro (DNA and Protein Sequence Analysis System). San Bruno, CA. October, 1993.

Jolivet, G., E. Devinoy, M.L. Fontaine and L.M. Houdebine. 1992. Gene. Structure of the gene encoding rabbit alpha-s-1-casein. Vol. 113, pp. 257-262.

Knight, K.L. and R.S. Becker. 1990. Cell. Molecular basis of the allelic inheritance of rabbit immunoglobulin VH allotypes: Implications for the generation of antibody diversity. Vol.60, pp. 963-970.

Krane, D.E., A.G. Clark, J.-F. Cheng and R. C. Hardison. 1991. Mol. Bio. Evol. Subfamily relationships and clustering of rabbit C repeats. Vol. 8(1), pp. 1-30.

Krane, D.E. and R.C. Hardison. 1990. Mol. Bio. Evol. Short Interspersed Repeats in Rabbit DNA Can Provide Functional Polyadenylation Signals. Vol. 7(1), pp. 1-8.

Okino, S.T., L.C. Quattroch, H. J. Barnes, S. Osanto, K.J. Griffin, E.F. Johnson, and R.H. Tukey. 1985. Proc. Natl. Acad. Sci. USA. Cloning and Characterization of cDNAs Encoding 2,3,7,8, tetra-chlorodibenzo-p-dioxin-inducible Rabbit mRNAs for Cytochrome P450 isozymes 4 and 6. Vol. 82, pp. 5310-5314.

O'Prey, J., J. Chester, B.J. Thiele, S. Janetzik, S. Prehn, J. Fleming and P.R. Harrison. 1989. Gene. The promoter structure and complete sequence of the gene encoding the rabbit erythroid cell-specific 15- lipoxygenase. Vol. 84, pp. 493-499.

Ray, B.K. and A. Ray. 1991. Biochem. Biophys. Res. Commun. Complementary DNA cloning and nucleotide sequence of rabbit serum amyloid A protein. Vol. 178, pp. 68-72.

Ray, B.K. and A. Ray. 1991. Biochem. Biophys. Res. Commun. Rabbit serum amyloid A gene: Cloning, characterization, and sequence analysis. Vol. 180, pp. 1258-1264.

Ray, B.K. and A. Ray. 1992. Biochem. Biophys. Res. Commun. Cloning and structural characterization of a rabbit genomiv DNA for acid alpha 1 acid glycoprotein. Vol. 185, pp. 69-77.

Rogers, J.H. 1985. Int. Rev. Cytol. The Origin and Evolution of Retroposons. Vol. 93, pp. 2066-2074.

Sasaki, Y., S. Ohsako and T. Deguchi. 1991. J. Biol. Chem. Molecular and genetic analysis of Arylamine N-acetyltransferase polymorphism of Rabbit liver. Vol. 266, pp. 13243-13250.

Singer, M.F. 1982. Cell. SINES and LINES: Highly repeated short and long interspersed sequences in Mammalian Genomes. Vol. 28, pp. 433-434.

Swofford, D.L. 1991. PAUP: Phylogenetic Analysis Using Parsimony, Version 3.0s. Computer program distributed by the Illinois Natural History Survey, Champagne, Illinois.

Thepot, D., E. Devinoy, M.L. Fontaine and L.M. Houdebine. 1991. Gene. Structure of the gene encoding rabbit beta-casein. Vol. 97, pp. 301-306.

Weiner, A.M., P. L. Deininger and A. Efstratiadis. 1986. Annu. Rev. Biochem. Nonviral Retrotransposons: Genes, Pseudogenes, and Transposable Elements Generated by the Reverse Flow of Genetic Information. Vol. 55, pp. 631-661.

Xu, J., C. Richardson, C. Ford, T. Spencer, Y. Li-juan, G. Mackie, G. Hammond and F. Possmayer. 1989. Biochem. Biophys. Res. Commun. Isolation and characterization of the cDNA for pulmonary surfactant-associated protein-B (SP-B) in the rabbit. Vol. 160, pp. 325-332.

SUPPLEMENTATION RATE OF BREAST FED BABIES AT A LOCAL HOSPITAL AND POSSIBLE EFFECTS ON THE DURATION OF BREAST FEEDING IN INFANT NUTRITION

Anne M. Delles

Department of Biology
Nazareth College of Rochester
4245 East Ave.
Rochester, NY 14618

Faculty Advisors:
Christine Gruhn, Ph.D. Matthew Temple, Ph.D., and Cynthia R. Howard ,M.D.

Breast feeding can be extremely beneficial to infant health. On the average, breast fed babies have fewer medical problems than formula fed babies (Winick, 1985). However, national statistics show that only a small percentage of mothers continues to breast feed their children past the first four months of life. The Healthy Children 2000, established by the Surgeon General of the United States, includes a policy for promoting breast feeding in America. Hospitals should adopt Baby Friendly policies that will encourage mothers to breast feed so that the total number of mothers choosing to breast feed their infants increases over the next few years. The first few days in the hospital are crucial for establishing breast feeding as the main source of nutrition for the baby (Newman, 1990).

Cup feeding is the one method that does not discourage breast feeding when supplementation must be implemented. The baby does not begin to position its tongue and lips in a way that conflicts with feeding from the breast. Infants that learn to feed on a bottle may have difficulties switching back to the breast. Cup feeding is a way of avoiding certain problems, and can hopefully encourage a longer course of breast feeding (Newman, 1990).

A chart review was conducted to determine how often supplementational feedings occurred during newborn stays at Rochester General Hospital. Patient charts (mothers and infants) were reviewed to determine why supplementation was implemented, what types of infants were supplemented, and if the infants were cup or bottle fed during the additional feedings. Approximately 70% of breast fed infants were supplemented at some time during their stay at the hospital. Of the infants sampled, the major means of supplementation was through bottle feeding rather than cup feeding. This study may help change nursing practices in the nursery at Rochester General Hospital so that the total number of supplementational feedings decreases, and that cup feeding becomes the primary procedure for additional feedings. Hopefully an awareness of this data may lead to a prolonged and improved duration of breast feeding.

INTRODUCTION

Breast feeding is the most natural form of nutrition for infants and there are many associated health benefits. For example, immunologically active factors are transmitted through breast milk. Breast fed babies have three times the amount of serum IgG than do formula fed babies (Rodwell-Williams and Worthington-Roberts, 1993). Breast fed babies receive 0.5-1g of sIgA daily. This can be compared to the production of 2.5g of sIgA per day for a 60kg adult (Hansen et al., 1994). The baby receives this passive immunity from the transmission of the mothers milk. The Ig transmission, in particular IgA and IgG, can help the newborn fight infection, and there may also be an enhanced vaccination response from this passive immunity (Rodwell-Williams & Worthington-Roberts, 1993). Also, babies that are breast fed tend to develop gut flora more quickly than formula fed babies and this aids in digestion. Formula fed babies tend to suffer from indigestion and gas more often than breast fed infants. Possibly due to the differences in their gut flora (Wharton et al., 1994). Further, breast fed infants have a much lower frequency of illness, in particular otitis media. It is not clearly understood if this is due to antibodies transmitted in the

breast milk, the mechanics of breast feeding or a combination of the two. The position that infants assume during suckling from the breast allows for proper drainage of the eustachian tubes which can help prevent ear infection. Sasses et al. (1994) showed that babies who were breast fed for the first four months showed 40% fewer cases of otitis media than formula fed babies.

Some of the benefits of breast feeding are more difficult to determine scientifically. Breast feeding helps promote mother and infant bonding. Breast fed infants on the average have fewer allergies. Some controversial studies have also demonstrated that breast feeding can possibly contribute to neurological development in children (Lanting et al., 1994). Also, breast fed infants have fewer cases of Sudden Infant Death Syndrome (SIDS), than do formula fed babies.

Even though breast feeding is clearly beneficial to infant health, there is a low rate of breast feeding in the United States. A little over 50% of expectant mothers decide to breast feed, and the number of breast feeding mothers decreases drastically each month after the birth of the baby. At six months, approximately 20% of those that initiated breast feeding continue to do so (US Dept. of Health and Human Services, 1990). There are many contributing factors to the low rate of breast feeding in America. Some of the factors that influence breast feeding rates include age, income, education, employment and area of residence.

Healthy Children 2000 is a program created by the Surgeon General of the United States. Hopefully, by the year 2000 at least 75% of expectant mothers in the U.S. initiate breast feeding as the main source of food for the infant in the early postpartum months and have the number of mothers that continue to breast feed their children to the age of five to six months will increase to at least 50% (U.S. Dept. of Health and Human Services, 1990).

A hospital that implements a Baby Friendly Policy to encourage breast feeding must follow a written policy that is understood by all medical staff. Staff must be thoroughly trained so that they can properly instruct mothers how to breast feed, how to manage their breast feeding and how to maintain their milk supply in case of mother/child separation. Breast feeding should be initiated immediately after the delivery of the infant. Supplemental feedings should only be given when medically necessary, in a hospital that has adopted a Baby Friendly policy (Moxley et al., 1994).

The time spent in the hospital when the baby is born is crucial for the establishment of a solid course of breast feeding. When a mother has made the decision to breast feed, care must be taken in the hospital to properly teach her how to breast feed and to encourage it. Support is crucial for some mothers, especially if they are young, or uncomfortable with breast feeding at first. It is also extremely important that infants are not given any artificial teats or nipples. Cup feeding should be utilized in cases when additional feedings are required because it does not require the use of artificial nipples (Aurbach & Riordan, 1993).

There are occasions in which supplementational feedings are required for a variety of medical reasons at which time the infant is unable to breast feed. When feeding intervention must take place, care must be taken to do it in the least invasive manner. Cup feeding is the one means of supplementing an infant in such a way that it does not conflict with feeding from the breast. Although cupfeeding is significantly more work for the nursing staff, it should be standard practice in a hospital with a Baby Friendly Policy. Newborn infants are learning to feed for the first time. Cupfeeding avoids training breast fed infants to bottle feed from an artificial nipple. There is good evidence that early supplementation with a bottle is associated with reduced breast feeding duration (Newman, 1990).

Feeding is a complicated process that involves coordination between sucking, swallowing, and breathing. When a baby is feeding on the breast, the mouth is opened very wide and the tongue is positioned at the gum line. The infant does not have to suck very hard because the mother has a milk ejection reflex that helps with the delivery of milk. Bottle fed infants do not need to open the mouth very wide and the tongue controls the amount of milk coming in. Breast feeding does not require as much energy

expenditure for the infant and they also tend to stay more relaxed (Rodwell-Williams & Worthington-Roberts, 1993).

Nipple confusion can occur when a baby that has learned to bottle feed switches to breast feeding. The infant will not open the mouth wide enough and attaches to the point of the nipple only. This is an inefficient means of milk delivery because only a small amount of liquid is obtained. The mother's breasts can become very sore because the baby tends to suck very hard(Rodwell-Williams & Worthington-Roberts, 1993).

Cupfeeding involves touching the baby's lower lip with a small cup(usually a medicine cup) and then introducing a few drops of fluid. The baby learns to swallow when the feeder tilts the head back after the fluid has been poured into the moth. The baby is then allowed sufficient time to swallow and then the procedure is repeated. The infant should also be burped frequently (Unpublished Data, Rochester General Hospital Dept. of Nursing).

METHODS AND RESULTS

This study was initially created to study cupfeeding. Rochester General's policy is to cupfeed breast fed babies at times when supplementation is required. This project was initiated to see how infants benefited from supplementation through cupfeeding. It deemed important to study physiological responses to cupfeeding, such as heart rate and respiration rate, during infant feeding. However, researchers were unable to procede with this original task because so few babies were being cupfeed.

Approximately 42 sets of charts were reviewed (mothers and infants). Data sheets were completed from infant charts for gestational age, weight, APGAR scores, which record the babies health immediately after delivery, feeding log information and general information on the babies health throughout the hospital stay. Mothers charts were reviewed for gestation length, number of total births, type of delivery, breast feeding problems and general health during the hospital stay. After data sheets were completed information was analyzed using Epi Info.

There was an alarming 70% supplementation rate for breast fed infants in the nursery. This goes against current policy of being a Baby Friendly Hospital. Although cupfeeding is the policy for additional feedings in the nursery, data on cupfeeding was contradictory to this. Of the babies that were supplemented once, only 28% were cupfed. Also, only 50% of the one day old babies were cupfed on their first supplementation. This can be counterproductive to the course of breast feeding. This may be the first feeding that the baby has received and already 50% of them have learned to use an artificial nipple.

It was determined that the weight of the supplemented babies was on the average 253g less than non-supplemented infants. It is true that low birth weight infants sometimes require additional feedings, but the infants should be of significantly lower birth weight to receive those additional feedings. A possible reason for this could be that the nurses observed that the babies were smaller and may have felt that they needed to gain weight. As a result, these babies were supplemented more often than babies of average weight.

Supplementation rates did correlate with nursing shifts. The number of supplementations greatly increased with later shifts. A total of 62% of the supplementations occurred during the 11PM-7AM shift. A possible reason for this is that it is easier for the nursing staff to supplement the infants, rather than to wake a sleeping mother to initiate breast feeding.

Were the supplementations justified? A total of 31% of the babies were supplemented and no reason at all was given for this action. All motives for additional feedings are required to be logged in on infant charts. Also, all additional feedings should only be given when absolutely necessary. The majority of the reasons, a total of 73%, indicated on the charts for supplementation were not valid for medical problems. Hospital policy specifically states that supplementation should be avoided unless it is medically necessary.

Incases when supplementation was implemented, these are some of the acceptable reasons that were given: an infant with health problems being observed in the Special Care Nursery who was unable to breast feed; infant with respiratory distress; maternal illness and cesarean section. Some examples of medically unsubstantiated reasons for

supplementation include: mother requested to sleep through night; and baby too tired to breast feed. It is understandable that the mother is extremely tired from the delivery, but if she was clearly informed about the problems associated with supplementation, she would most likely not request it. This is why Rochester General encourages rooming in. The baby can sleep in the same room as the mother to make breast feeding at night more convenient. Also, if the baby is too tired to breast feed supplementation should not be given as well. After the baby has rested breast feeding can be initiated once again.

CONCLUSION

As the rate of supplementation decreases, breast feeding duration will hopefully increase. This will help meet the Healthy Children 2000 Goals by enforcing a breast feeding policy that is encouraging, rather than discouraging.

By enforcing the current Baby Friendly policy at Rochester General Hospital, quality assurance in nursing practices will be improved. It is the job of every member of the nursery staff to help mothers learn how to breast feed their infants to ensure a strong and lengthy duration of breast feeding for improved infant nutrition.

REFERENCES

Auerbach K.; Riordan, Breast Feeding and Human Lactation. Boston: Jones and Bartlett Publishers, Inc., 1993.

Hanson, L.A.; Hahn-Zoric, M.; Berndes, M.; Ashraf, R.; Herias, V.; Jalil, F.; Bhutta, T.I.; Laeeg, A.; Mattsby-Baltzer, I., "Breast feeding: overview and breast milk immunology"., Acta-Paediatr-Jp., vol 36(5), Oct. 1994.

Lanting, C.I.; Fidler, V.; Huisman, M.; Touwen, B.C.; Boersma, E.R., "Neurological differences between 9-year-old children fed breast-milk or formula-milk as babies", Lancet, vol 344(8933), Nov. 12, 1994.

Moxley, S.; Kennedy, M., "Strategies to support breastfeeding. Discarding myths and outdated advice." Canadian Family Physician, vol 40, Oct. 1994.

Newman, J. "Breast feeding Problems Associated with the Early Introduction of Bottles and Pacifiers." Journal of Human Lactation, vol 6(2), 1990.

Rodwell-Williams S.; Worthington-Roberts, B., Nutrition in Pregnancy and Lactation: Fifth Edition. St. Louis: Mosby Publishers, Inc., 1993.

Sassen, M.L.; Brand, R.; Grote, J.J., "Breast feeding and acute otitis media.", American Journal of Otolaryngology, vol 15(5), Spt-Oct. 1994.

U.S. Department of Health and Human Services, Public Health Service, Healthy people 2000: National Health promotion and disease prevention objectives. PHS Pub No 79-55071, Washington DC: Government Printing Office, 1990.

Wharton, B.A.; Balmer, S.E.; Scott, P.H., "Sorrento studies of diet and fecal flora in the newborn.", Acta-Paediatr-Jpn., vol 36(5), Oct. 1994.

Winick, Myron, Feeding the Mother and Infant. New York: John Wiley & Sons, Inc., 1985.

TRUNCATED PREPROSOMATOSTATIN TARGETS α-GLOBIN TO STORAGE GRANULES IN A MOUSE ANTERIOR PITUITARY CELL LINE.

Nanditha J. Vivekananthan

Department of Animal Science
North Carolina State University
Raleigh, NC 27695-7621

Faculty Advisors: Jeanne B. Koger and Evan E. Jones

Cells export digestive enzymes, peptide hormones and regulatory factors via a regulatory secretory pathway. The structural elements which direct proteins to this pathway have yet to be identified. In 1991, Kizer and Tropsha hypothesized a "sorting motif": a serine (or threonine), N-terminal to two or more leucines, all on the same side of a highly amphipathic α-helix. In order to test this hypothesis, we have synthesized four shuttle vectors containing the DNA encoding a marker protein, α-globin, preceded by various segments of rat preprosomatostatin (ppSRIF), under control of the inducible metallothionein promoter. The four segments encode the following portions of ppSRIF: 1)amino acids 1-24, the signal sequence only; 2)amino acids 1-42, containing a single putative sorting motif; 3) amino acids 1-59, containing two such sorting motifs; and 4) amino acids 1-116, the full length ppSRIF which is known to target α-globin to storage granules. AtT-20 cells have been stably transfected with these constructs and clones have been isolated. The translation products have been identified in cellular homogenates of clones induced with $CdCl_2$ (Figure 3). Subcellular fractionation studies suggest that only the pS59- and pS116-α-globin translation products colocalize with ACTH, a marker for the secretory granule fraction.

INTRODUCTION

Proteins of the regulated secretory pathway begin as precursors composed partly of a signal or leader peptide, which is cleaved in the rough endoplasmic reticulum (RER), and a pro-region or extrapeptide sequence which guides the precursor from the RER to the secretory granules (Kelly 1985). It is in the RER where core glycosylation and folding of the nascent proteins occur, forming a three-dimensional structure. Transport proceeds through the Golgi apparatus to the trans-Golgi network (TGN), the site of sorting into the regulated or constitutive secretory pathway (Farquhar 1985; Griffiths and Simons 1986). Both pathways involve transport and fusion of vesicles to the plasma membrane and discharge of vesicular contents (Figure 1).

Proteins of the regulated pathway can be stored for long periods of time and released upon stimulation of the cell by secretagogues (Burgess and Kelly 1987). As a result of stimulation, calcium acts as a second messenger, assisting in transport of peptides to the plasma membrane. It is thought that proproteins aggregate in the TGN and are targeted by a sorting signal sequence within extrapeptide regions (Burgess and Kelly 1987; Miller and Moore 1990; Sevarino and Stork 1991). The structural elements which target proteins to the regulated pathway have yet to be identified. By contrast, proteins of the constitutive pathway undergo calcium-independent, continuous secretion and fusion with the plasma membrane. This pathway involves bulk flow and requires no known sorting signal (Figure 1).

Previous research has been done on the rat hormone, preprosomatostatin, composed of a leader peptide of 24 residues and a pro-region of 64 residues (Montminy et al. 1984). It has been determined that the amino-terminal 78 residues are sufficient to correctly target the protein to regulated secretory vesicles (Sevarino and Stork 1991). In 1991, Kizer and Tropsha hypothesized a sorting motif: a serine (or threonine), N-terminal to two or more leucines, all on the same side of a highly amphipathic α-helix (Kizer and Tropsha 1992). In order to evaluate this hypothesis, we have constructed vectors encoding various lengths of preprosomatostatin which lack or possess this motif (Figure 2). We find that the amino-terminal 59 residues are sufficient for correct sorting. Our data do not rule out the Kizer motif; however, we cannot definitively characterize the sorting signal at this time.

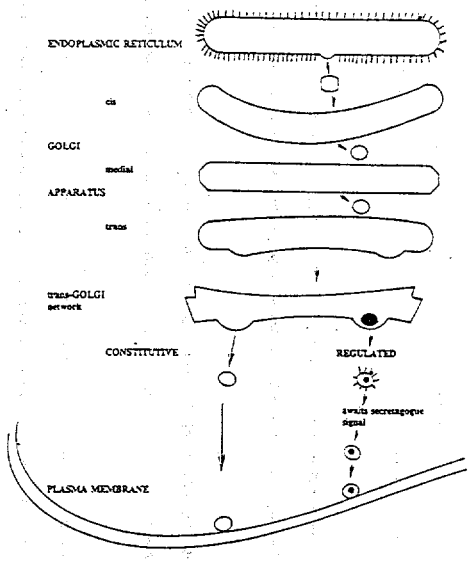


FIGURE 1: TRANSPORT OF SECRETORY PROTEINS
Nascent secretory proteins undergo core glycosylation and folding in the rough endoplasmic reticulum and proceed through the Golgi apparatus to the trans-Golgi network, the site of sorting into the constitutive or regulated secretory pathway. Proteins of the constitutive pathway are continuously secreted and vesicle membranes fuse with the plasma membrane. Proteins may reside in the plasma membrane (as integral membrane proteins) or be externalized and leave the site of export altogether. Proteins of the regulated pathway, by contrast, aggregate in the trans-Golgi network prior to sorting. They are sorted first to immature secretory vesicles which undergo maturation. Both the immature and mature proteins are stored within the cell until secretagogue elicits their secretion. Furthermore, nascent vesicles of this pathway are covered with a clathrin coat which is removed once a mature protein is formed.

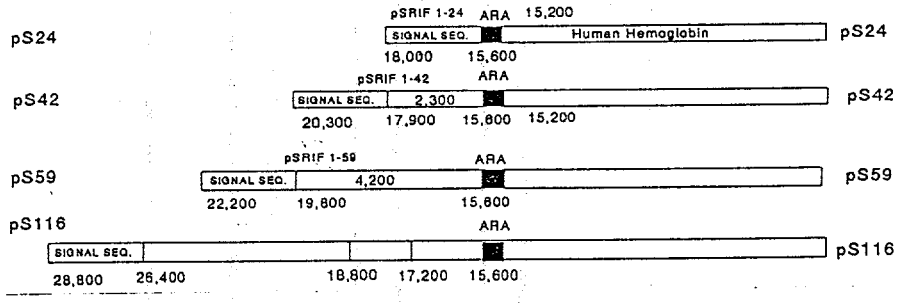


FIGURE 2: DIAGRAM OF VECTOR CONSTRUCTS
All constructs contain a marker protein, α-globin, preceded by various segments of rat preprosomatostatin, under control of the metallothionein promoter. Constructs were inserted into the pMT.neo vector and AtT-20 cells were stably transfected and clones were isolated. The resultant cell lines were named based upon the number of amino acids present in preprosomatostatin.

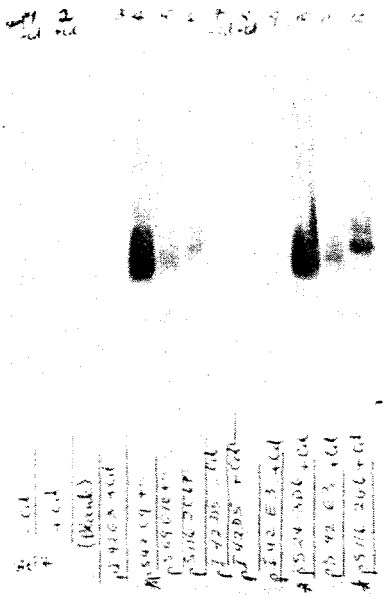


FIGURE 3: NORTHERN BLOT ANALYSIS OF AtT-20 CELLS TRANSFECTED WITH THE α-GLOBIN CONSTRUCTS

Transcription products have been identified in cellular homogenates of clones induced with 10 μM $CdCl_2$. The prominent bands in each lane reflect the relative size of the product expected from each construct.

METHODS: mRNA was isolated and electrophoresed on a 1.5% agarose/formaldehyde gel and membrane. Detection was by hybridization to a biotinylated α-globin cDNA probe and visualization was by addition of a streptavidin alkaline phophatase conjugate and colorimetric substrates.

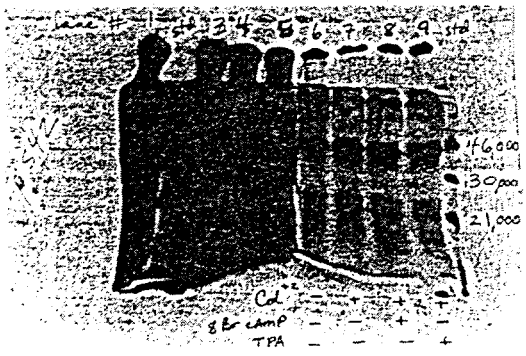
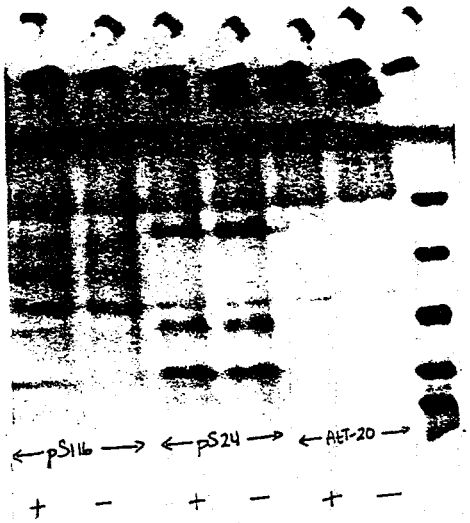


FIGURE 4: STIMULATED SECRETION IN pS42 CELLS

Cells containing the preprosomatostatin-42 construct were cultured for 16 hours in the absence (lane 5) or presence (lanes 6-9) of 10 μM $CdCl_2$. Secretion was evaluated after 1 hour of no stimulation (lanes 6, 7), stimulation with 5 mM 8-bromoadenosine 3':5'-cyclic monophosphate (8-Br cAMP; lane 8), or stimulation with 10^{-7} M phorbol 12-myristate 13-acetate (TPA). Media of non-stimulated cells and of cells stimulated with 8-Br cAMP appear to contain the same protein products.

METHODS: Cellular proteins were radiolabeled with ^{35}S-methionine (250 μCi) for three hours. Media were harvested, immunoprecipitated with rabbit anti-human hemoglobin antiserum and protein A Sepharose, and the eluted material was electrophoresed on 15% SDS-polyacrylamide gels. Detection was by autoradiography.

5.



6.

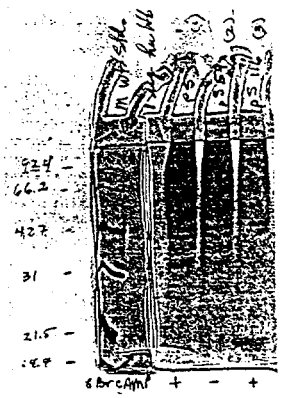


FIGURE 5: STIMULATED SECRETION IN pS24 AND pS116 CELLS
Media analysis of the pS116 cell line stimulated with 8-bromoadenosine 3':5'-cyclic monophosphate (8-Br cAMP) reveals products migrating at 20,000 and 14,500 which do not appear in the media of non-stimulated cells or AtT-20 cells. Media of pS24 cells reveal export of the same products in stimulated and non-stimulated cells.
METHODS: Similar to those of Figure 4, except that only 8-Br cAMP was used to stimulate secretion.

FIGURE 6: STIMULATED SECRETION IN pS59 CELLS
Cells containing the preprosomatostatin-59 construct were cultured for 16 hours in the presence of 10 μM $CdCl_2$. Secretion was evaluated after one hour of either stimulation with 8-bromoadenosine 3':5'-cyclic monophosphate (sample 1) or no stimulation (sample 2). Only the medium from stimulated cells reveals a protein comigrating with the monomeric form of authentic human α-globin.
METHODS: Cells were cultured as indicated. Media were harvested, treated with protease inhibitors (phenylmethylsulfonyl fluoride, leupeptin, and pepstatin) and concentrated in a Microcon 3 concentration unit (Amicon). The concentrate was analyzed by SDS-polyacrylamide gel electrophoresis (15% gels) and the gels were stained with Coomassie Blue.

7.

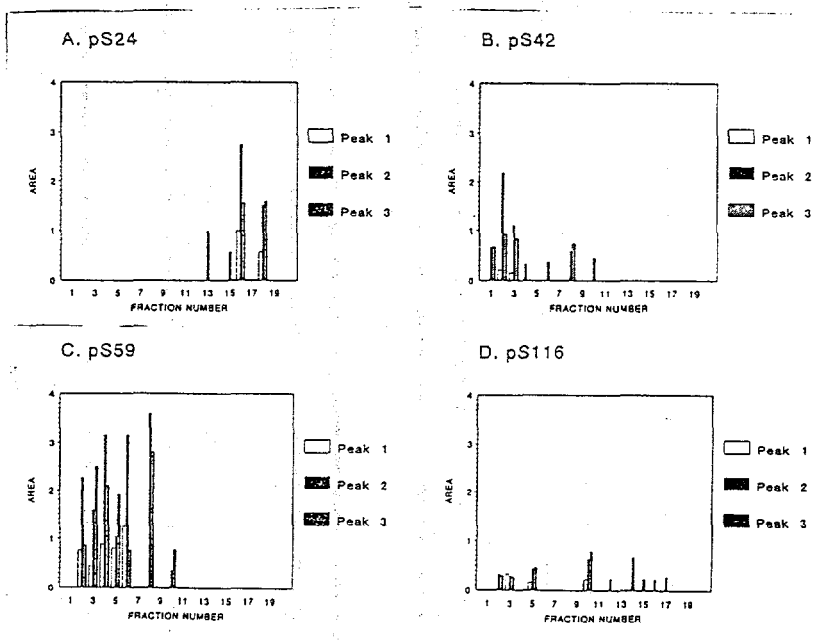


FIGURE 7: SUBCELLULAR DISTRIBUTION OF α-GLOBIN RELATED PROTEINS
Bar graphs showing the density gradient distribution of the three major, unique α-globin immunoreactive proteins obtained for each clonal cell line. Results were normalized to the intensity of a constant precipitating antibody band in each sample. (There were no unique peaks for the AtT-20 cell lines; data not shown.)
METHODS: Cells were cultured for 16 hours in the presence of 20 μM $CdCl_2$ and harvested in a 10 mM triethanolamine/acetic acid buffer. Cells were ruptured by passage through a 26 gauge needle and the light mitochondrial fraction was obtained by differential centrifugation. The pellet was resuspended in a 17.5% OptiPrep iodixanol density gradient solution and centrifuged at 270,000 *x g*, 3 hr, 4°C. Gradient fractions (0.5 mL each) were collected, dense end first, and immunoprecipitated as previously described. The eluent was electrophoresed on 15% SDS-polyacrylamide gels and proteins were visualized by western blotting and chemiluminescent detection.

DISCUSSION

As shown in Figure 3, the relative sizes of the mRNA transcription products in each cell line have been identified when induced with $CdCl_2$. Media analysis of both the pS24 and pS42 cells as shown in Figures 4 & 5 reveal that α-globin immunoreactivity is detected without stimulation by 8-Br-cAMP. This suggests that the α-globin related products of these cell lines are released constitutively. However, the pS59 and pS116 cells each export a product in stimulated cells which do not appear in non-stimulated cells (Figures 5 & 6). We can conclude from these results that a sorting signal exists within the first 59 amino acids of preprosomatostatin. If the sorting signal per se resides in the first 42 amino acids, then additional sequence is required for the proper conformation to be achieved and for proper sorting into the regulated secretory pathway.

Subcellular fractionation indicates that distribution of α-globin related products varies with each cell line (Figure 7). Results obtained from the pS116 cell line are not understood. We expected to find that the major α-globin related products would appear in a limited portion of the gradient; however, products appear scattered throughout (Figure 7D). Perhaps the large size and/or the conformation of this product result in its partial degradation and generalized distribution. Examination of the less dense fractions (14-17) reveals that only fully processed α-globin is present. ACTH, a marker for the secretory granule fraction has been identified in fractions 1 to 3 and 17 to 19 (data not shown). These data are difficult to reconcile since stimulated secretion studies indicate that only pS59 and pS116 products are secreted in a secretagogue-dependent manner. It is tempt ing to conclude that fractions 4 to 10 contain the secretory vesicles, but the ACTH immunoreactivity suggests otherwise. Further characterization of these fractions by marker enzyme analysis is required. Presently, we have established that a sorting signal exists within the first 59 amino acids of preprosomatostatin. However, the exact nature of the signal has not been determined. Site-directed mutagenesis is necessary for further testing of the hypothesis.

REFERENCES

Burgess, T.L. and Kelly, R.B. (1987) *Ann. Rev. Cell Biol.* 3:243-293.
Farquhar, M.B. (1985) *Ann. Rev. Cell Biol.* 1:447-488.
Griffiths, G. and Simons, K. (1986) *Science*. 234:438-443.
Kelly, R. (1985) *Science*. 230:25-32.
Kizer, J.S. and Tropsha, A. (1992) *Biochem. Biophys. Res. Comm*. 174: 586-592.
Miller, S.G. and Moore, H.P. (1990) *Curr. Opin. Cell Biol.* 2:642-647.
Montminy, M.R. et al. (1984) *Proc. Natl. Acad. Sci.* 81:3337-3340.
Sevarino, Kevin and Stork, Philip. (1991) *Biol. Chem.* 266:18507-18513.

Superior Olivary Complex Inputs to the Dorsomedial Inferior Colliculus of the CBA Mouse Model of Presbycusis Remain Stable With Age

Jonathan D. Byrd

Division of Otolaryngology
Depts. of Surgery & Physiology
University of Rochester Medical Center
601 Elmwood Ave.
Rochester, NY 14642-8629

Faculty Advisors: Robert D. Frisina, Ph.D., and Joseph P. Walton, Ph.D.

INTRODUCTION

Many people throughout the world develop hearing loss as they grow older. This is known clinically as presbycusis. The causes of presbycusis and therapies to alleviate it have been difficult to find. To study presbycusis, some researchers use a mouse-model of the disorder. The particular strain used in this experiment is the CBA mouse. The CBA loses its hearing with a timecourse remarkably similar to that of humans, after correcting for the shorter overall lifespan of the mouse is made. That is, hearing is relatively normal for approximately the first half of life, and then it gradually declines in the last half. Researchers have also used chinchillas and guinea pigs (Saint Marie & Baker, '90; Kelley et al., '92), cats (Adams, '79; Adams & Mugnaini, '84; Glendenning et al., '81; Brunso-Bechtold et al., '81), and bats (Zook & Casseday, '82; Covey & Casseday, '86, '91; Frisina et al., '89; Zettel et al., '91) in their study of normal hearing.

Earlier experiments confirmed presbycusis physiologically in the old CBA mice. Previously, it has been observed in this laboratory that single nerve cells in the central nucleus of the inferior colliculus (ICC) of old CBAs have decreased temporal processing capabilities relative to young CBAs (Walton et al., ARO abstract, 17:83, 1994). . With these findings in mind, this experiment poses the question of what happens on an anatomical and cellular level in the auditory brainstem as mice grow older.

One area or nucleus of the brain that provides significant input to the inferior colliculus is the superior olivary complex (SOC). The SOC is located just superior to the cochlear nucleus and dorsal to the trapezoid body in what is known as the auditory brainstem. The major subnuclei that comprise the SOC are the lateral superior olive (LSO), the medial superior olive (MSO) and the medial nucleus of the trapezoid body (MNTB). Less understood subdivisons include the superior paraolivary nuclei (SPN), dorsolateral and anterolateral periolivary nuclei (DLPO & ALPO), and the ventral and lateral nucleus of the trapezoid body (VNTB & LNTB).

Neural impulses enter the SOC bilaterally from the ventral cochlear nucleus (VCN) by way of terminating fibers from the ipsilateral trapezoid body (TB) or collaterals from the TB. The SOC also receives inputs from the dorsal cochlear nucleus (DCN) by way of a small projection from the dorsal tract of *Held*. The neural information that reaches the SOC continues to the IC by way of the fibers of the lateral lemnicus (LL). The neural information about sound goes through increased divergence at the SOC and LL levels and convergence at the level of the IC (Gulick et al, '89).

Functions of the SOC have started to be characterized. The ability to locate sounds in space is believed to be due to the arrangement of the incoming terminals that code for binaural time (MSO) and intensity (LSO) differences. Since each SOC receives systematic input from both ears, this is where the first levels of binaural neural impulse processing can occur along the ascending pathways. Therefore the importance of the SOC rests in its ability to accurately locate sounds. Thus, an inability to locate sound accurately could implicate the SOC in presbycusis. In this study, the SOC was observed on a neuroanatomical and neurocellular level to determine if its inputs to the dorsomedial ICC changed significantly with age.

METHODS

Fourteen experimental animals from the CBA mouse strain were used. Single nerve cell responses to pure tones and temporal features of sounds were mapped in the central nucleus of the ICC of each mouse while it was mildly tranquilized and placed in a stereotaxic/recording apparatus. At the conclusion of the physiological mapping experiment, focal injections of 10% horseradish peroxidase(HRP-Sigma Type XII) were made through the recording electrode into the tonotopic location corresponding to 18-24 KHz.

Following a 24hr survival time, the mice were anesthetized with 0.8mL of Sodium Pentobarbital and intracardially perfused with heparinized saline(0.9%) for 10 minutes and fixed with 1.25% gluteraldehyde/1% paraformaldehyde in 0.2M phosphate buffer for 40 minutes. This was followed by 3% glycerol in buffer for 10 minutes. The brains were dissected and placed in 10%, 15%, and 20% buffered glycerol solutions for 24 hrs. each at 4° C.

Three serial sets of coronal sections were cut at 60 μm on a freezing microtome. Two sets were reacted with 3,3,5,5-tetramethylbenzidine (TMB), then one counterstained with Safranin-O; the other was not counterstained. The third set was processed with diaminobenzidine(DAB) and counterstained with Cresyl Violet.

The CBA mice were tested at three ages: Young adult, 2-4 mon(n=5); Middle age, 14-16

mon(n=4); Old, 22-27 mon(n=5). During the counting of cells, a stained entity was counted as a cell if the soma was distinguishable and a process, either dendrite or axon, was attached to the soma, or a nucleus was present. All cell counts were made by hand, ie. without the aid of an electronic cell counting machine; and were done blindly, i.e. the investigator did not have knowledge of the age of the mouse being counted. Numbers of cells as well as quality of staining were evaluated.

Statistical analysis was performed on the data using Mann-Whitney Tests and Kruskal-Wallis tests. Size of injection sites were measured for total diameter and plotted against cell counts. Linear regression was performed on the data, and it was determined that cell counts were proportional to the size of the injections sites. Thus, the raw data were corrected with a correction coefficient directly relating size of injection site to cell counts.

RESULTS

One characteristic that changed with age was the labelling density of the neurons in the SOCs. As the animals grew older, the total amount of HRP that had stained the cell noticeably decreased. Figs. 1, 2, and 3 are from ipsilateral ALPO divisions of young, middle age, and old mice respectively. The labeling density completely fills the cells in the young mice, then gradually loses staining density as the mice age.

Another noticeable trend among the mice was that the SOC, relative to other auditory brainstem nuclei, had lower total cells counts. From one particular animal, the SOC, CN, and LL were compared. Fig. 4 shows five cells in the ipsilateral MSO. This is representative of the SOC for practically all the the animals. Fig. 5 shows the ipsilateral AVCN having about twenty-one cells scattered throughout the nucleus. Lastly, Fig. 6 shows the drawings for the well stained nuclei of the LL. This section contains fifty-seven cells.

In addition, the number of inputs to the constituent nuclei of the SOC were remarkably constant as the animals grew older except in the ipsilateral ALPO and DLPO. Figures 10, 11, and 12 illustrate this phenomenon with mean cell counts in the three age groups respectively. The mean cell counts remain very stable througout the life of the animals except for a noticeable drop in the ALPO region and a less noticeable decline in the DLPO region. In addition, the ALPO region far exceeds cell counts in other regions of the SOC as noted by figures 10 and 11-young and mid age mice respectively, while figure 12 shows that the total cell counts of the SOC regions in the old mice are very similar. Figures 7, 8, and 9 pictorially illustrate this finding with photomicrograph drawings of ALPO sections of young, mid age, and old mice respectively.

In the ALPO region the greatest changes take place from the young to the mid age animals and young to old. However in the DLPO region the largest change occurs from the young to the old. The ramifications of these changes are not well understood at this time, however, the stability of the SOC as an entire nucleus is most significant since age-related declines in labeled cells take place in all 3 divisions of the cochlear nucleus (Lynch-Armour et al., 95).

While the SOC is apparently stable, the ALPO and DLPO are the only sub-nuclei that changed during the life of the animal. The Kruskal-Wallis p-value for the ALPO region over the entire lifespan was $0.01<p<0.05$. The p-value for the Mann-Whitney test of young and mid age mice was $p<0.001$. For the DLPO region, the only significant difference was in the Mann-Whitney test of young and old mice with the $p<0.01$ (Table 1).

DISCUSSION

Although there are dynamic changes in the superior olivary complex of the CBA as it ages, what is most noteworthy are the many nuclei that change only slightly, especially the MSO and LSO. Equally remarkable is the fact that while the SOC is the first systematic processing nucleus for binaural sounds, very few cells are found stained with HRP, though nuclei before and after the SOC in the ascending pathways have much higher staining densities. The reason for high numbers of stained cells around,but not within, the SOC is not entirely clear since the SOC lies between the cochlear nucleus and the LL in the ascending pathway. One obvious difference could be attributed to the SOC itself since it is physically smaller than either the CN or LL in mice. Another reason could be the long physical distance from the injection site. However, if the SOC was not being stained densely because of the distance from injection site, it follows that the cochlear nucleus should be less darkly stained as the SOC, if not equally, since the labeling is retrograde. This was not found to be the case, as demonstrated in Fig. 5. While the cell counts are relatively stable, the connections of the SOC with the ICC seem to be changing with age (Figs 1-3). In addition, changes in ALPO and DLPO, while not well understood, could contribute to the problems associated with presbycusis. These insights may help in determining how the aging brain copes with presbycusis.

ACKNOWLEDGEMENTS

Many thanks to Drs. William O'Neill and D. Robert Frisina for their help and support. Appreciation also goes to Martha Lynch-Armour and Patty Bardeen for essential assistance. Reseach sponsored by NIH Grant P01 AG09524-03 and the International Center for Hearing & Speech Research (RICHS), Rochester, NY.

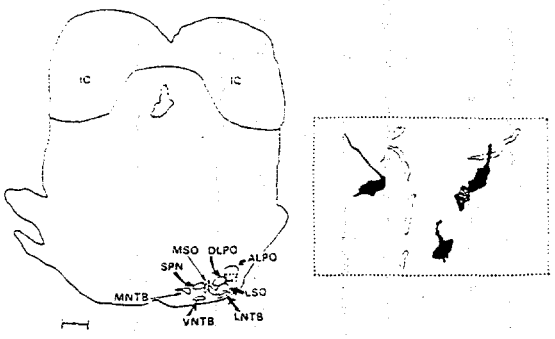
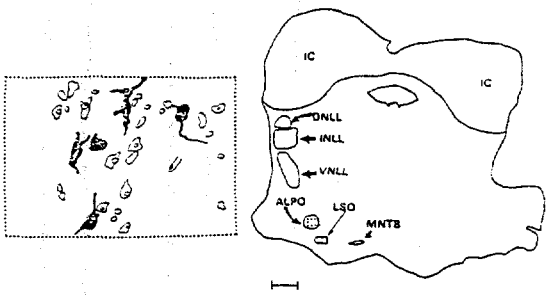


Figure 1-Animal # 19, young, ipsi ALPO, 40x mag.- Shows how labelling density is higher at young ages. Drawings are of coronal sections at 60 µm. Dotted boxes are drawings of photomicrographs.

Figure 2- #9, mid age, ipsi ALPO, 40x mag.- Shows that as the mouse grows older, labelling density is slightly decreasing.



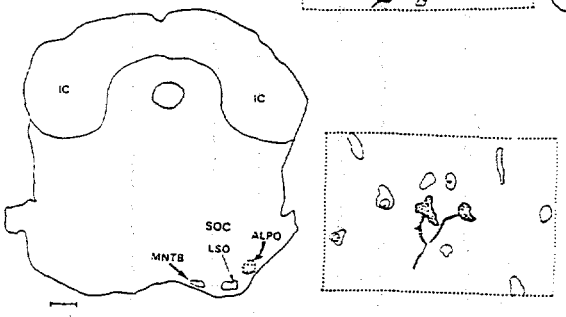


Figure 3- #13, old, ipsi ALPO, 40x mag.- Illustrates how labelling density has further decreased in the old mouse. Calibration bar in each figure is equal to or 0.5mm.

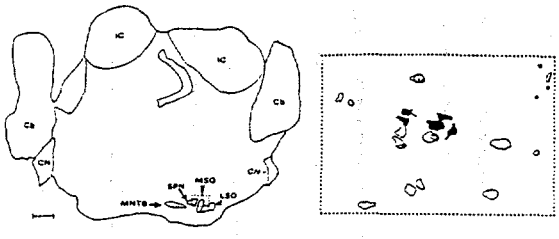
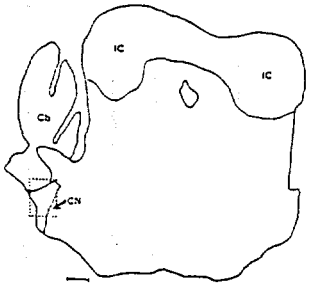


Figure 4- #20, young, ipsi MSO, 20x, - Typical section in the SOC with an average number of cells stained, 5.

Figure 5- #20, young, ipsi AVCN, 10x mag.-Typical cochlear nucleus cell count of 21.



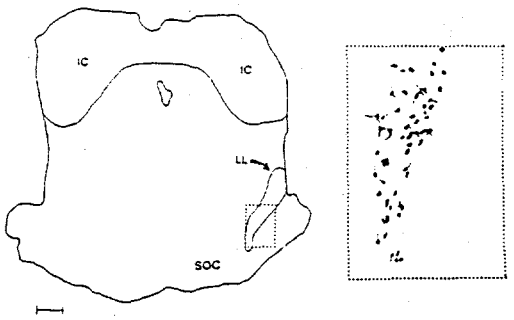


Figure 6- #20, young, ipsi LL, 10x mag.- Illustrates further how the SOC has few cells in comparison to surrounding nuclei. There are 57 labeled cells.

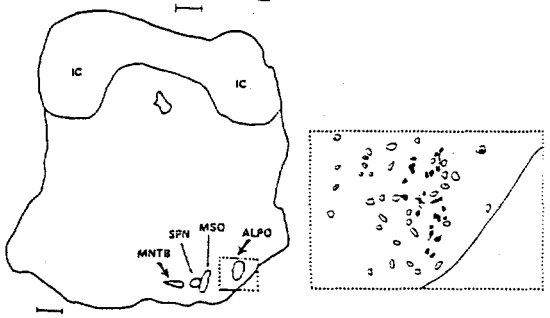
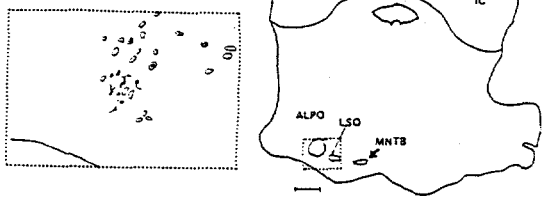


Figure 7- #20, young, ipsi 10x mag.- Illustrates how the ipsilateral ALPO has many stained cells in the young age group. This particular section has 24 stained cells.

Figure 8- #9, mid age, ipsi ALPO, 10x mag.- Depicts a mid age ALPO with a declining cell count as it ages. This section has 8 stained cells.



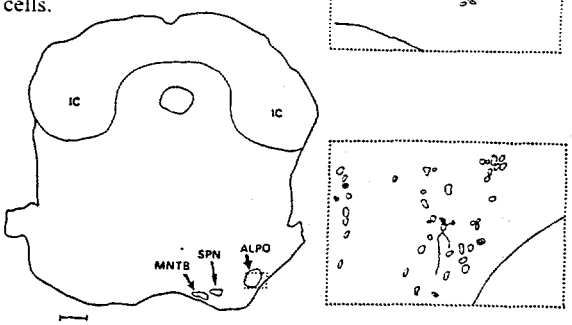


Figure 9- #13, old, ipsi ALPO, 20x mag.- shows the decline in cell count with age in the ALPO nuclei. This section contains 2 cells.

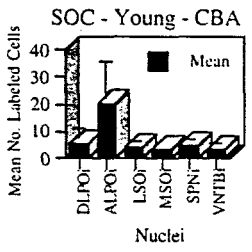


Fig. 10

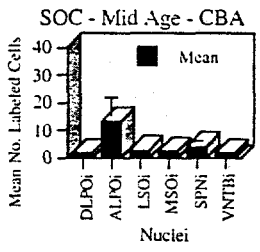


Fig. 11

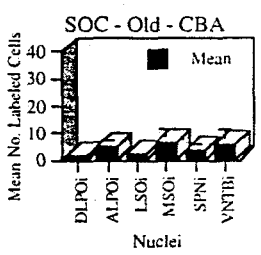


Fig. 12

Fig. 10-Graph of young mean cell counts for each divsion in the SOC. The high number of cell counts in the ALPOi stands out while the cell counts of the other regions remain fairly constant.All counts are in ipsilateral divisions in the SOC. Fig. 11-Graph of mid age cell counts. The significant decline in ALPOi and less striking decline in DLPOi can be seen while cell counts in other divisions remain stable. Figure 12-Graph of old cell counts showing how ALPOi and DLPOi regions have significantly declined while other regions continue to show stable and constant cell counts.

Kruskal-Wallis Analysis for Superior Olivary Complex - Overall Age Effect N.S.

Nuclei	Young vs. Mid Age	Mid Age vs. Old	Young vs. Old	Total
DLPOi	N.S.	N.S.	P < 0.01	N.S.
ALPOi	P < 0.001	N.S.	P < 0.001	P < 0.05
degrees of freedom	1	1	1	2

Table 1. The overall age effect on the SOC was not significant. However, the table shows that from young-to-old in DLPO and from young-to-middle and young-to-old in ALPO the changes were significant.

REFERENCES

Adams, J.C. (1979) Ascending Projections to the Inferior Colliculus. Journal of Comparative Neurology. 183: 519-538.

Adams, J.C., Mugnaini, E. (1984) Dorsal Nucleus of the Lateral Lemniscus: A Nucleus of GABAergic Projection Neurons. Brain Research Bulletin 13: 585-590.

Brunso-Bechtold, J.K., Thompson, G.C., Masterton, R.B. (1981) HRP Study of the Organization of Auditory Afferents Ascending to Central Nucleus of Inferior Colliculus in Cat. Journal of Comparative Neurology 197: 705-722.

Covey, E., Casseday, J.H. (1986) Connectional Basis for Frequency Representation in the Nuclei of the Lateral Lemniscus of the Bat *Eptesicus Fuscus*. Journal of Neuroscience 6(10): 2926-2940.

Covey, E., Casseday, J.H. (1991) The Monaural Nuclei of the Lateral Lemniscus in the Echolocating Bat: Parallel Pathways for Analyzing Temporal Features of Sound. Journal of Neuroscience 11(11): 3456-3470.

Frisina, R.D., O'Neill, W.E., Zettel, M.L. (1989) Functional Organization of Mustached Bat Inferior Colliculus: II. Connections of the FM_2 Region. Journal of Comparative Neurology 284: 85-107.

Glendenning, K.K., Brunso-Bechtold, J.K., Thompson, G.C., Masterton, R.B. (1981) Ascending Auditory Afferents to the Nuclei of the Lateral Lemniscus. Journal of Comparative Neurology 197: 673-703.

Gulick, W.L., Gescheider, G.A., Frisina, R.D. (1989) Hearing: Physiological Acoustics, Neural Coding, and Psychoacoustics. New York, Oxford University Press.

Kelley, P.E., Frisina, R.D., Zettel, M.L., Walton, J.P. (1992) Differential Calbindin-Like Immunoreactivity in the Brain Stem Auditory System of the Chinchilla. Journal of Comparative Neurology 319: 196-212.

Lynch-Armour, M.A., Frisina, R.D., McReynolds, E.E., Byrd, J.D., Walton, J.P.(1995) Cochlear Nucleus Imputs to a Functionally-Characterized Region of the Inferior Colliculus Decline with Age for the CBA mouse model of Presbycusis. Association for Research in Otolaryngology Abstract 18:71.

Saint Marie, R.L., Baker, R.A. (1990) Neurotransmitter-specific Uptake and Retrograde Transport of [^{3}H] Glycine from the Inferior Colliculus by Ipsilateral Projections of the Superior Olivary Complex and Nuclei of the Lateral Lemniscus. Brain Research 524: 244-253.

Walton, J.P., Frisina, R.D., O'Neill, W.E.(1994) Effects of Age On Single-Unit Temporal Processing in the Inferior Colliculus of the CBA Mouse Model of Presbycusis. Association for Research in Otolaryngology Abstract, 17:83.

Zettel, M.L., Carr, C.E., O'Neill, W.E. (1991) Calbindin-Like Immunoreactivity in the Central Auditory System of the Mustached Bat, *Pteronotus parnelli*. Journal of Comparative Neurology 313: 1-16.

Zook, J.M., Casseday, J.H. (1982) Cytoarchitecture of Auditory System in Lower Brainstem of the Mustache Bat, *Pteronotus Parnelli*. Journal of Comparative Neurology 207: 1-13.

The Amygdala Kindling Rat Model as a Tool for Screening Novel Anticonvulsant Compounds

Teresa Seo

Department of Pharmacology
University of Toledo
2801 W. Bancroft Street
Toledo, OH 43606

Faculty Advisor:
Christine N. Hinko, Ph.D.

The amygdala kindling model of epileptogenesis in rats has been suggested as a viable model for complex partial seizures, the most prevalent seizure type in adults as well as the most refractory to drug therapy. The kindling phenomenon refers to the observation that repeated stimulation of the amygdala structure of the brain with initially subconvulsive electrical stimulation leads to the development of focal and secondarily generalized seizures which progress in a stepwise manner through the seizure stages 1-5. Once fully kindled, the animals represent a stable and reliable model of epilepsy in that seizures can be elicited upon stimulation for at least one year. Since the level of stimulation delivered remains a constant, changes in brain function are inferred. We have established this model in our laboratory for the preclinical screening of novel antiepileptic agents and have evaluated the anticonvulsant effects of the standard compound valproic acid by measuring behavioral (motor seizure latency, motor seizure duration, forelimb clonus latency, forelimb clonus duration) and electrical (amygdala afterdischarge duration) changes as recorded on an electroencephalograph. Valproic acid was found to reduce seizure severity significantly without overt motor impairment as well as effectively reduce motor seizure duration and forelimb clonus duration.

INTRODUCTION

Epilepsy is a chronic neurological disorder afflicting approximately 2% of the American population and 20-40 million people worldwide (Rall and Schleifer, 1990; Garnett, 1989). This disorder is characterized by recurrent seizures which may manifest themselves as abnormal motor, sensory, psychic, or autonomic activity. The seizures arise from excessive electrical discharge of neurons from cortical or subcortical areas of the brain which usually can be noted on an electroencephalograph as "spikes" or sharp waves. The clinical presentation of these seizures depends upon the site of the focus, the functions of the cortical areas involved, and on the propagation to other areas of the brain (Scheur and Pedley, 1990).

Accurate diagnosis of seizure type is essential in determining which treatments to employ since the seizure types exhibit varying degrees of resistance and respond differently to the same drug treatments (Loscher and Schmidt, 1988). There is not a single drug capable of treating all types of epilepsy. Approximately 20-30% of epileptic patients cannot be treated with currently available antiepileptic drugs (AEDs), and many patients must discontinue drug therapies because of undesirable side effects (Loscher and Schmidt, 1994). Of the seizure types, complex partial seizures are the most prevalent and refractory to drug therapy in adults. The amygdala kindling model has been suggested as a viable model for complex partial seizures. This model has been found to correlate well with complex partial seizures in man in that AEDs effective against that seizure type in man have also been found to be effective against amygdala kindled seizures.

Kindling refers to the observation that repeated stimulation of an area of the brain, such as the amygdala, with initially subconvulsive electrical stimulation leads to the development of focal and secondarily generalized seizures. Behavioral motor seizures elicited develop in a stepwise manner generally evolving through the stages 1) facial movement, 2) head nodding, 3) forelimb clonus, 4) rearing, and 5) rearing and falling (Racine, 1972). Once the enhanced sensitivity has developed, i.e. reached criteria of 10

consecutive stage 5 seizures, the animal is considered "kindled." This effect is long lasting, and there have been no reports of reversal. The behavior observed in the various seizure stages mimic those seen in human seizures. Compounds that reduce seizure severity below a stage 3 and/or decrease duration or increase latency to seizure may hold promise as complex partial seizure therapy.

METHODS

Animals. Male Sprague-Dawley rats (Harlan Sprague-Dawley, Indianapolis, IN) were used in the experimentation. Prior to surgery, the animals were housed in colony cages under standard laboratory conditions (controlled temperature, 12 hr light/dark cycle) with food and water available ad libitum.

Chemicals. Sodium pentobarbital (Mallinkrodt Inc., St. Louis, MO) was used as the anesthetic, and atropine sulfate (Sigma Chemical Co., St. Louis, MO) was administered to reduce bronchial secretions. Valproic acid was purchased from the Sigma Chemical Co. (St. Louis, MO) for use as the reference anticonvulsant agent. The sodium pentobarbital was prepared in distilled water with the addition of a small amount of anhydrous sodium carbonate (Mallinkrodt Inc., St. Louis, MO) to aid in the dissolution. Valproic acid was prepared as a suspension in corn oil, and atropine sulfate was prepared in 0.9% saline solution. All solutions and suspensions were administered by intraperitoneal injection.

Surgery. Rats, weighing 267-301 gm at the time of surgery, were deeply anesthetized with sodium pentobarbital (65 mg/kg) and surgically implanted with two bipolar, twisted nichrome wire electrodes (Plastics One, MS303/2, 0.25 mm outer diameter) using stereotaxic techniques. The electrodes were insulated to the tip and aimed at the right basolateral amygdala nucleus (-2.2 mm AP, -4.8 mm ML, -8.6 mm DV) and the left frontal cortex (+1 mm AP, +2.0 mm ML, -2.0 mm DV) according to the atlas of Paxinos and Watson (1982). The electrode tips were spread 0.5 mm and oriented in the rostral-caudal plane. Electrodes were secured to the skull using two stainless steel screws and fast-curing dental acrylic. Silk 4-O suture (Look Inc., Norwell, MA) and Nexaband^{R} (Veterinary Products Laboratories, Phoenix, AZ) were used to close the incision site and facilitate healing of the skin.

Animals were allowed at least one week recovery after surgery before beginning afterdischarge (AD) threshold determinations (Tietz et al., 1989). The AD was defined as an EEG recording in which spikes had at least twice the amplitude of prestimulus baseline and had a frequency greater than 1 spike/second. The current which elicited an AD was recorded as the AD threshold. Subsequently, beginning the day following AD threshold determinations, the rats were stimulated once daily at a suprathreshold, 200 microampere current for 1 second until at least 10 consecutive stage 5 seizures were produced. Behavioral (motor seizure latency, motor seizure duration, forelimb clonus latency, forelimb clonus duration) and electrical (amygdala afterdischarge duration) changes as recorded on an electroencephalograph were scored according to the methods of Tietz et al. (1989).

Drug testing. The day after reaching the criterion of 10 consecutive stage 5 seizures, the fully kindled animals were stimulated on two consecutive days to record baseline data. The results of the baseline recordings were averaged for comparison to the drug testing data. On the next Thursday (1-2 days following baseline recordings), the first dose of drug was given. A four day wash-out period followed, after which the vehicle treatment was given. A three day wash-out period followed before the next drug treatment. On days of drug treatment, electrical stimulation was given 30 minutes after injection. The animals were subjected to three motor function tests 5 minutes prior to electrical stimulation to assess degree of motor impairment, muscle relaxation, sedation, and muscle tone (Tietz et al., 1989). Four doses of valproic acid were tested in this manner (100 mg/kg, 150 mg/kg, 175 mg/kg, 200 mg/kg).

Analysis. Statistical analysis was conducted on behavioral seizure, forelimb clonus seizure, and amygdala AD duration and latency measurements using multifactor analysis of variance tests. Friedman's two-way analysis of variance by ranks was used for analysis of behavioral seizure stage. Multifactor range analysis was used to determine in which groups statistically significant differences lay. All analysis was performed on version 5 of the Statgraphics computer program (Statistical Graphics Corporation, 1991).

RESULTS

Afterdischarge thresholds were obtained for 5 animals with values ranging from 40-80 microamps with a mean of 64 ± 8.12 microamps (± SEM). These values were well below the 200 microamp current used for the kindling procedure. All 5 animals were kindled as expected and exhibited reliable generalized seizures. Drug effects were compared against an average of 2 baseline measurements obtained after kindling criterion was reached.

There was a statistically significant reduction in seizure severity obtained at a dose of 200 mg/kg valproic acid. Reductions in forelimb clonus duration at this dose were also statistically significant ($p \leq 0.01$). Behavioral seizure duration was shortened at 200 mg/kg valproic acid but was not statistically significant. Valproic acid at 175 mg/kg appeared to increase latency to behavioral seizure and forelimb clonus, but the increase was not statistically significant. No other doses of valproic acid were shown to produce a significant change.

None of the animals showed any signs of motor impairment at doses of 100 mg/kg, 150 mg/kg, or 175 mg/kg of valproic acid at the time of motor function testing. Two of the 5 animals exhibited very mild ataxia and muscle relaxation at a dose of 200 mg/kg valproic acid.

Table 1 - Percent Reduction in Behavioral Seizure Stage Produced by Valproic Acid (VA)

Animal	VA 100 mg/kg	VA 150 mg/kg	VA 175 mg/kg	VA 200 mg/kg
Rat 1	5	5	5	1
Rat 2	5	5	5	3.5
Rat 3	4	1	1	1
Rat 4	5	5	5	0
Rat 5	4.5	5	1	3.5
Average	4.7	4.2	3.4	1.8
SD ±	0.45	1.79	2.19	1.6
% decrease in seizure stage	6%	16%	32%	64%

CONCLUSION

The amygdala kindling model provides a useful method for the pharmacological testing of compounds for antiepileptic activity, particularly those effective in treatment of complex partial seizures. Both electrographic and behavioral response can be measured using this model, and because seizures can be evoked on demand, compounds can be tested at the time of expected maximum activity (Albright and Burnham, 1980; McNamara, 1984). Amygdala kindled seizures are controlled most effectively by agents used for the treatment of complex partial seizures, suggesting that kindling may model epileptogenesis of focal human epilepsy or complex partial seizures with secondary generalization (Albright and Burnham, 1980). The kindling effect has been elicited in a number of species, including primates, and there have been reports of a kindling-like effect produced in humans. Another feature of this model is that animals who have received numerous stimulations have been observed to develop spontaneous seizures, thereby more closely paralleling the disease state (Pinel and Rovner, 1978).

Although criticisms have been made that kindling is a labor intensive and time consuming process, this model has proven to be a reliable one in that once kindled, animals retain their enhanced sensitivity to the stimulus for up to a year or longer (Racine, 1978). Although the mechanisms underlying the kindling effect have not yet been elucidated, several hypotheses have been proposed, including long term potentiation and

neurotransmitter involvement. Tissue damage and deposits from metal electrodes have generally been ruled out as causative agents.

Valproic acid produced a decrease in seizure severity that was comparable to results reported from other investigators (Loscher et al., 1986; Albertson et al., 1980). Motor impairment was minimal with valproic acid with none evident at any of the doses except for mild ataxia and muscle relaxation observed in two of the animals at the 200 mg/kg dose. Forelimb clonus duration seemed to be the most easily discernable and sensitive predictor of drug effect in this model as has been noted by others (Tietz et al., 1989).

In conclusion, the amygdala kindling paradigm serves as a viable model of epilepsy. The parallels between the kindled seizures and those observed in human complex partial seizures in behavioral seizure and electrographic patterns support the validity of the amygdala kindling model as a screening test for novel drugs (Albright and Burnham, 1980). Valproic acid was found to be active in this model as expected. The dose of 200 mg/kg valproic acid was significant in reducing seizure severity and forelimb clonus duration with minimal motor toxicity.

REFERENCES

Albertson TE, Peterson SL, and Stark LG. Anticonvulsant Drugs and Their Antagonism of Kindled Amygdaloid Seizures in Rats. *Neuropharmacology* 1980; 19: 643-652.

Albright PS and Burnham WM. Development of a New Pharmacological Seizure Model: Effects of Anticonvulsants on Cortical- and Amygdala-kindled Seizures in the Rat. *Epilepsia* 1980; 21: 681-689.

Garnett WR. Epilepsy. In: Dipiro JT, Talbert RL, Hayes PE, Yee GC, Posey LM, eds. *Pharmacotherapy: A pathophysiologic approach.* New York: Elsevier Science Publishing Co., 1989: 611-631.

Loscher W, Jackel R, Czuczwar SJ. Is Amygdala Kindling in Rats a Model for Drug-Resistant Partial Epilepsy? *Experimental Neurology* 1986; 93: 211-226.

Loscher W and Schmidt D. Which Animal Models Should be Used in the Search for New Antiepileptic Drugs? A Proposal Based on Experimental and Clinical Considerations. *Epilepsy Res* 1988; 2: 145-181.

Loscher W and Schmidt D. Strategies in Antiepileptic Drug Development: Is Rational Drug Design Superior to Random Screening and Structural Variation? *Epilepsy Res* 1994; 17: 95-134.

McNamara J. Kindling: An Animal Model of Complex Partial Epilepsy. *Ann Neurol* 1984; 16 (Suppl): S72-S76.

Paxinos G and Watson C. *The Rat Brain in Stereotaxic Coordinates.* New York: Academic Press, 1982.

Pinel JPJ and Rovner LI. Experimental Epileptogenesis: Kindling-induced Epilepsy in Rats. *Experimental Neurology* 1978; 58: 190-202.

Racine RJ. Modification of Seizure Activity by Electrical Stimulation: II. Motor Seizure. *Electroenceph clin Neurophysiol* 1972; 32: 281-294.

Racine R. Kindling: The First Decade. *Neurosurgery* 1978; 3 (2): 234-252.

Rall TW and Schleifer LS. Drugs Effective in the Therapy of the Epilepsies. In Rall TW, Nies AS, and Taylor P, eds. *Goodman and Gilman's The Pharmacologic Basis of Therapeutics*, eight edition. New York: Pergamon Press, 1990: 436-462.

Scheur ML and Pedley TA. The Evaluation and Treatment of Seizures. *N Engl J Med* 1990; 323 (21): 14687-1472.

Statistical Graphics Corporation. *Statgraphics: version 5.* Maryland: STSC, Inc., 1991.

Tietz EI, Rosenberg HC, and Chiu TH. A Comparison of the Anticonvulsant Effects of 1,4 and 1,5 Benzodiazepines in the Amygdala-kindled Rat and Their effects on Motor Function. *Epilepsy Res* 1989; 3: 31-40.

JUVENILE GROWTH RATES IN SIX TURTLE SPECIES

Jeannine Mogavero and Christopher Benetatos

Department of Biology
Saint Joseph's University
Philadelphia, PA 19131

Faculty Advisor: Scott P. McRobert

INTRODUCTION

There have been numerous studies documenting the growth rates of turtles, typically under natural conditions (Carr & Goodman, 1970; Dunham & Gibbons, 1990; Germano, 1988). The limitations to these studies are that juvenile specimens, which are difficult to mark, release, and recapture (Janzen, 1993), and which are subject to high rates of predation, are often not included. Cox, *et al.* (1991) stated that hatchlings have long been overlooked for study because of their small size, secretive nature, possible occupancy of different microhabitats, and different daily activity cycles. Therefore, detailed analyses of the growth of turtles during their first one-to-two years of life are not adequately represented in the literature.

The first year in the life of a turtle is a time that includes dangers that will not be encountered at any other point in the animal's life. Due to their small size and relatively thin shell, juvenile turtles are preyed upon by birds, fish, snakes, frogs, mammals and even other turtles. Indeed, predation on young turtles can be so intense that, in some species, less than two percent of the turtles that hatch survive to adulthood (Bertoni, 1994). As a turtle matures, however, its increased size and harder shell reduce much of this predation pressure.

Since predation is a major selective force in the evolution of life history characteristics (Endler, 1995), and since turtles are unusual in that only as juveniles do they experience serious predation pressure, this suggests that growth rate during the first two years of a turtle's life should be a highly-selected trait. Furthermore, juveniles of different species might be expected to exhibit different rates of growth if they have evolved under significantly different predatory pressures.

In this study, which was begun in August, 1993, turtle growth is monitored under laboratory conditions to determine whether different 'innate' rates of growth exist between juveniles of different species. In the initial year of the study, the growth rates of three species (*Pseudemys nelsoni, Trachemys scripta elegans, and Graptemys geographica kohni*) were examined (Benetatos & McRobert, 1994). In this report, the growth of turtles from the first year, as well as hatchlings from three new species (*Pseudemys peninsularis floridana, Trachemys scripta scripta* and *Pseudemys concinna hieroglyphica*), are reported.

MATERIALS AND METHODS

Turtles

The turtles used in the first year of the study included: five red-eared sliders (*Trachemys scripta elegans*), which were hatched from eggs laid in the laboratory; three Mississippi map turtles (*Graptemys geographica kohni*) and two Florida red-bellied turtles (*Pseudemys nelsoni*), which were acquired from professional breeders.

Turtles added in the second year of the study included: two red-eared sliders (*Trachemys scripta elegans*), which were hatched from eggs collected near the Cooper River in New Jersey; three captive-bred red-eared sliders (*Trachemys scripta elegans*); one Florida red-bellied turtle (*Pseudemys nelsoni*), six Mississippi map turtles (*Graptemys geographica kohni*), three yellow-bellied turtles (*Trachemys scripta scripta*), three hieroglyphic turtles (*Pseudemys concinna hieroglyphica*), and three Florida cooters (*Pseudemys peninsularis floridana*), which were acquired from professional breeders.

All turtles were housed in 40 gallon aquaria, in groups of 9-15, containing approximately eight inches of water and slate basking platforms. The water was maintained at 22-26^{o}C under a 12:12 LD cycle.

The turtles were fed a daily diet of commercial turtle food (Reptile-10, Wardley Corporation) which was provide *ad libitum*.

All turtles were less than 3 months of age at their introduction to the study.

Growth Assays

Growth measurements were taken on the first day of each month using a one-arm balance and calipers. Measurements included total body weight (in grams) and carapace length (in millimeters).

Statistics

A one-way analysis of variance was performed on each of the measures, followed by a Tukey HSD test.

RESULTS

During the periods described in this study, all turtles fed readily on the commercial turtle food provided. At the beginning of the first year of the study, the mean weights of the different species were 8.7 grams (*T. s. elegans*), 7.4 grams (*G. g. kohni*), and 9.4 grams (*P. nelsoni*). At the end of 18 months, the mean weight gain in *P. nelsoni* (437.8 +/- 30.5 g) was significantly greater than seen in *T. s. elegans* (171.4 +/- 27.4 g) and *G. g. kohni* (221.6 +/- 96.1 g). $P < .01$; see Table 1. Average carapace length at the onset of the study was 34.2 mm (*T. s. elegans*), 33.2 mm (*G. g. kohni*), and 35.5 mm (*P. nelsoni*). At the end of 18 months, the mean increase in carapace length for *P. nelsoni* (142.5 +/- 3.5 mm) was significantly greater than seen in *T. s. elegans* (102.2 +/- 6.1 mm) and *G. g. kohni* (115.0 +/- 16.9 mm). $P < .01$; see Table 1.

For turtles added in the second year of the study, no significant differences in growth rates were observed during the first five months. The mean weight change for these species was 10.0 g (*P. nelsoni*), 9.9 g (*T. s. elegans*), 10.9 g (*G. g. kohni*), 9.1 g (*P. p .floridana*), 8.7 g (*T. s. scripta*), and 13.8 g (*P. c. hieroglyphica*). The mean carapace lengths were 37.0 mm (*P. nelsoni*), 33.8 mm (*T. s. elegans*), 38.6 mm (*G. g. kohni*), 34.5 mm (*P. p. floridana*), 33.7 mm (*T. s. scripta*), and 39.3 mm (*P. c. hieroglyphica*); See Table 2.

Table 1 Mean Changes in Total Body Weight and Carapace Length after 18 months

Species	Mean Weight Change (± SD)	Mean Carapace Length Change (± SD)
P. nelsoni N=2	437.8 ± 30.5 g**	142.5 ± 3.5 mm**
G. g. kohni N=2	221.6 ± 96.1 g	115.0 ± 16.9 mm
T. s. elegans N=5	171.4 ± 27.4 g	102.2 ± 6.1 mm

** Significantly different from other means
Weight: $F(2, 6) = 23.33$. $P < .01$
Carapace length: $F(2, 6) = 15.51$. $P < .01$
(One-way analysis of variance followed by a Tukey HSD test).

Table 2 Mean Changes in Total Body Weight and Carapace Length after 5 months

Species	Mean Weight Change (± SD)	Mean Carapace Length Change (± SD)
P. nelsoni N=1	65.0 ± 0 g	70.0 ± 0 mm
T. s. elegans N=5	47.9 ± 27.8 g	59.0 ± 15.3 mm
G. g. kohni N=6	36.1 ± 12.9 g	58.2 ± 9.1 mm
P. p. floridana N=3	41.2 ± 13.8 g	60.3 ± 6.5 mm
T. s. scripta N=3	25.4 ± 9.5 g	47.7 ± 6.8 mm
P. c. hieroglyphica N = 3	43.2 ± 18.7 g	61.7 ± 10.9 mm

No significant differences across groups
Weight: $F(5, 15) = 1.00$. $P > .05$
Carapace Length: $F(5, 15) = 0.89$. $P > .05$
(One-way analysis of variance followed by a Tukey HSD Test)

DISCUSSION

Growth rates in turtles have been the subject of numerous research studies (for reviews see Auffenberg & Iverson, 1979; Bury, 1979). Indeed, certain features of turtles make them ideal subjects for such work. Turtle shells can be marked in a variety of ways to allow individuals to be recognized in either the laboratory or the field (Cagle, 1939). The age of many turtle species can be roughly determined by counting the annual rings of epithelial tissue of the carapace scutes and since turtles are very long lived animals many growth measurements can be made per individual (Gibbons, 1987; Gibbons & Semlitsch, 1982).

However, despite characteristics that make turtles good candidates for the study of growth, very little research has been done concerning the growth rates of juveniles. Since the first year or two of a turtle's life is a time involving intense predation pressure, analysis of juvenile growth rate may answer important questions regarding the evolution of life-history traits. Accordingly, this study was initiated to monitor growth rates of juvenile species under laboratory conditions.

These results show that during the first 18 months of life, significant differences exist in the growth rates of the red-bellied turtle (*P. nelsoni*), the red-eared slider (*T. s. elegans*), and the map turtle (*G. g. kohni*). Red-bellied turtles gained significantly more weight and added significantly more carapace length than did either red-eared sliders or map turtles. For the turtles added in the second year of the study, no significant differences were seen in growth rates. However, it is possible that these results are a function of the short period of time in which these animals have been studied and that differences in the growth rates of these turtles will be evident in the coming months.

These results show that under identical conditions, different turtle species grow at different rates. This is not to imply that these growth rates represent the rates of growth of these species in nature. Certainly, differences in food quality and other environmental conditions should have a strong impact on growth rate. However, this method shows that different species exhibit distinct growth rates when housed under identical conditions. If it is found that these growth rates are reproducible, it may indicate the presence of underlying genetic components that have been molded during the evolution of each species.

In future studies, the growth rates of more species and more individuals of existing species will be monitored. In addition, the growth rates of conspecific turtles from different ecological populations will be compared. If the theory that juvenile growth rate is responsive to selective pressure from the environment, this would assume that conspecifics from populations experiencing different levels of predation would demonstrate distinctly different growth rates.

ACKNOWLEDGMENT

Supported by Howard Hughes Medical Institute grant 71194-535101, and the Wardley Corporation, Secaucus, NJ.

LITERATURE CITED

Auffenberg, W. and Iverson, J. B. 1979. Demography of terrestrial turtles. *In* Turtles: Perspectives and Research. Edited by M. Harless and H. Morlock. John Wiley & Sons, New York. pp. 541-569.

Benetatos, C. and McRobert, S. P. 1994. Juvenile growth rates in three species of turtle. Proceedings of the Eighth National Conference on Undergraduate Research: 956-959.

Bertoni, R. M. 1994. Painted turtles. Reptile and Amphibian Magazine 2-1994: 8-16.

Bury, R. B. 1979. Population ecology of freshwater turtles. *In* Turtles: Perspectives and Research. Edited by M. Harless and H. Morlock. John Wiley & Sons, New York. pp. 571-602.

Cagle, F. R. 1939. A system of marking turtles for future identification. Copeia, 1939: 170-172.

Carr, A. and Goodman, D. 1970. Ecological implications of size and growth in *Chelonia*. Copeia, 1970: 783-786.

Cox, W. A., Haxelrig, J. B. , Turner, M. E., Angus, R. A., and Marion, K. R. 1991. A model for growth in the musk turtle, *Sternotherus minor*, in a North Florida spring. Copeia, 1991: 954-968.

Dunham, A. E. and Gibbons, J. W. 1990. Growth of the slider turtle. *In* Life History and Ecology of the Slider Turtle. Edited by J. W. Gibbons. Smithsonian Institution Press, Washington, D. C.

Endler, J. A. 1995. Multiple-trait coevolution and environmental gradients in guppies. Trends in Ecology and Evolution 1995: 22-29.

Germano, D. J. 1988. Age and growth histories of desert tortoises using scute annuli. Copeia 1988: 914-920.

Gibbons, J. W. 1987. Why do turtles live so long? Bioscience 37: 262-269.

Gibbons, J. W. and Semlitsch, R. D. 1982. Survivorship and longevity of a long-live vertebrate species: how long do turtles live? Journal of Animal Ecology 51: 523-527.

Janzen, F. J. 1993. An experimental analysis of natural selection on body size of hatchling turtles. Ecology 74(2): 332-341.

A COMPARISON OF INSECTICIDE SUSCEPTIBILITY AND ESTERASE ACTIVITY USING A RESISTANT STRAIN OF THE GERMAN COCKROACH, *BLATTELLA GERMANICA*, (DICTYOPTERA:BLATTELLIDAE)

Brian R. Wamhoff and Michael S. Sabom

Department of Biology
Rhodes College
Memphis, TN 38112

Faculty Advisor:
Dr. Bobby R. Jones

ABSTRACT

A resistant strain of the German cockroach, named Texas A&M, was evaluated to determine the relative susceptibility to Dursban, a chemically unstable organophosphate insecticide. A refined method was employed to test the susceptibility of the A&M German cockroach to a controlled dosage of Dursban, also known as chloropyrifos. The survivors of this A&M population (renamed S&W) were housed and allowed to reproduce. The S&W population was then tested for susceptibility to Dursban. A comparison of the LD_{50} values of the A&M and S&W populations reveals an increase in insecticide resistance in the S&W survivors. An analysis of esterase activity on animals resistant to organophosphate insecticides was completed on the S&W population selecting male nymphs for the experiment. These data were compared to the esterase activity of the original A&M population (McCanless and Domon, 1989). The enzyme assay revealed that the esterase activity of the S&W population was significantly different than the esterase activity of the original A&M population.

INTRODUCTION

The German cockroach, *Blattellagermanica*, is a common pest to many parts of the world. Because these cockroaches, like many insects, are known to carry dangerous pathogens, it has been necessary to employ the use of insecticides in order to control their growth. However, this has become increasingly difficult due to the resistance the cockroach populations have acquired to many of the common insecticides (Koehler and Patterson, 1986). This all too often leads to results in increasing application and the use of multiple pesticides, leading to economic and environmental problems.

Some insecticides are known as organophosphates, cholinesterase (ChE) inhibitors which exert their toxic action on the nervous system of vertebrates as well as insects. This action is the result of the inhibition of acetylcholinesterase involved in the hydrolysis of acetylcholine (Bevan and Thompson, 1983). When a ChE inhibitor is applied, synaptic transmission is altered, causing increased skeletal muscle contraction, increased activity of organs, increased activity of tissues receiving postganglionic parasympathetic innervation, increased ganglion transmission, and cholinergic effects of the central nervous system. We specifically chose an organophosphate insecticide called Dursban, also known as chloropyrifos, for this investigation.

In 1956, a common method, the jar test, was developed for detecting insecticide resistance in the German cockroach (Keller et al., 1956). This method was adopted by the U.S. Armed Forces Pest Control Board (1959) and the World Health Organization (1970). Essentially, 2.5 ml of a 0.05% insecticide solution is added to a 500 ml jar and the insects are then exposed directly to the insecticide. In 1983, a survey of German cockroaches from various apartment complexes in Gainesville, FL, revealed no chlorpyrifos (Dursban) resistance based on the jar test (Milio et al., 1987). These findings, though, did not correlate with the control problems experienced by some chloropyrifos control operators. Further testing suggested that the jar test can produce inaccurate results when assessing chlorpyrifos susceptibility in field populations of German cockroaches (Milio et al., 1987).

Using an unpublished method proposed by Bancroft and Jones, we produced a strain of German cockroaches resistant to chlorpyrifos. This resistance revealed a decrease in mortality in comparison with the original population. Previous analysis of esterases indicated a higher enzyme activity in resistant strains when compared with the susceptible strains (Prabhakaran, 1993). Thus, to achieve a quantitative assessment of this resistance, enzyme assays were employed to compare the levels of esterase activity in our resistant and susceptible populations. An increase in esterase activity of the S&W population was observed.

METHODS

animal care

The strain used in this investigation, *Blatellagermanica*, Texas A&M, was provided by Bobby Jones, Rhodes College. These animals were reared in a 32 gallon container in an incubator set at a constant temperature of 27° C and constant relative humidity of 52%. They were fed a continuous supply of commercial dog food and water. The containers were cleaned on a regular basis. A thin film of 1:1 mineral oil and petroleum jelly around the top of the containers prevented the roaches from escaping.

insecticide

Dursban® (*O,O*-diethyl *O*-3,5,6-trichloro-2-pyridyl phosphorothioate), or chlorpyrifos, is

an organophosphate produced by Dow Chemical Company that is commonly used as an insecticide. This cholinesterase inhibitor is moderately residual on plants but quite residual on wood, glass, linoleum, concrete, and other hard surfaces where insects might be sprayed for by control operators. In this investigation, a 1% solution of Dursban was used to test for chloropyrifos resistance in the A&M population.

method for detecting chloropyrifos resistance

This method is an unpublished method. A 19.6 x 19.6 cm^2 area was marked off on a glass plate. The desired concentration of a 1% Dursban solution was spread on the plate, allowed to dry and covered with four acetate strips. Forty animals were anesthetized with carbon dioxide and placed on the strips. These animals were covered in groups of 10 with petri dishes coated on the inside with 1:1 mineral oil and petroleum jelly (this allows the animals to remain exposed to the insecticide). When the animals resumed consciousness, the acetate strips were removed exposing them to the insecticide for one hour. After one hour, the animals were placed in recovery chambers and mortality counts were taken at 24 and 48 hours. The survivors were placed in their respective housing units and allowed to regenerate for future testing.

selection for resistance

Over a period of 3 months, the above LD_{50} procedures were carried out on male and female nymphs of the Texas A&M population. At high concentration dosages of Dursban, 31.6 mg/m^2 and up, a mortality rate of approximately 90% was observed. This correlates to about 3-4 surviving animals for every 40 tested; the majority of the survivors were females. Because of time constraints, an insecticide concentration level of 15.6 mg/m^2 was chosen to produce a greater population of survivors. Once this desired concentration level was determined, 480 animals (50% of each gender) were tested (Table 1). After 3 months of chloropyrifos application to the A&M population, LD_{50} values were recorded and the population was allowed to regenerate over a period of another 3 months (Fig 1). This population of survivors at Dursban dosage 15.6 mg/m^2 was renamed S&W or Sabom and Wamhoff.

Keeping within the same time frame, 480 animals of the S&W population were exposed to the same levels of Dursban as the A&M population. A decrease in the percent mortality (Table 2, Fig 3) was observed marked by an increase in the LD_{50} values of the S&W population (Fig 2).

esterase determination

Male nymphs, similar in weight, were homogenized in 0.04 M sodium phosphate buffer (1 ml of buffer per 10 mg of roach). Male nymphs were selected for this part of the experiment because of the extremely high levels of esterase activity that females possess. Each homogenized sample was added to a reaction mixture containing 5 ml of ß-napthyl acetate, acetone, and 0.04 M sodium phosphate buffer. The concentration of ß-napthyl acetate was determined for A_{560} described by Jones (1994). A_{560} was monitored and esterase activity was analyzed using R.A. Fisher's least significant difference (LSD), $P > 0.05$, (Prabhakaran, 1993). The data used for esterase levels in the A&M population were provided by McCanless and Domon (1989). When the A&M data were compared to absorbance values of the S&W population, there was a significant difference calculated between the two means of each population (Table 3).

RESULTS AND DISCUSSION

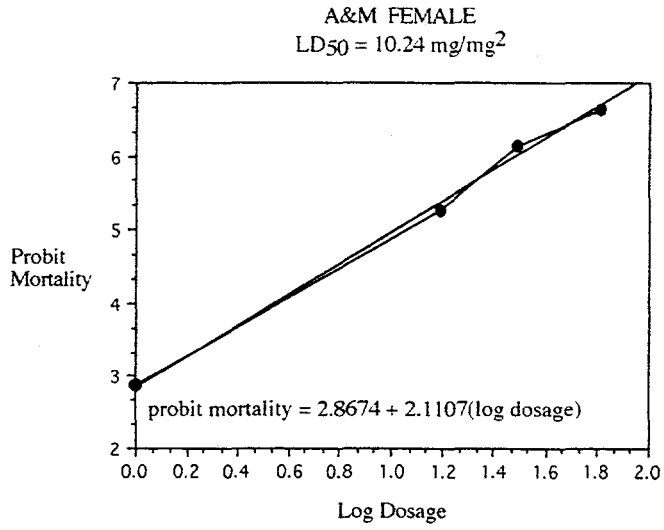
An analysis of our results reveals remarkable differences between the % mortalities, LD_{50}s, and esterase activities of the A&M and S&W populations. There is an obvious decrease in the mortality rates between the A&M and S&W populations at the dosage of 15.6 mg/cm^2. The LD_{50} value likewise increases in the S&W population in comparison to the A&M population. The LD_{50} values and mortality rates between the susceptible and resistant populations indicate an induction of resistance within the progeny.

A corresponding increase in the level of esterase activity was evident in the S&W population when compared to the A&M (Prabhakaran, 1993). These results suggest that there is a significant difference in the levels of esterase activity between both populations (Table 3). Although it has not been clearly established, a modification in the efficiency of the enzyme, ChE, or increased production of ChE might be the mechanism by which this resistance is being established. Nonetheless, it has been shown that building a population of German cockroaches resistant to chlorpyrifos is possible through the proliferation of animals surviving a moderate exposure to Dursban (15.6 mg/cm^2). Furthermore, there is a relevant correlation between insecticide resistance and increased esterase activity in the resistant S&W population.

The unpublished method employed to detect chloropyrifos resistance in the German Cockroach proved to be valid. In contrast to the universally accepted jar test, this method shows the capacity of a cockroach to develop a noticeable immunity to a common insecticide. There are several problems with the jar test. Specifically, the insect is placed in an unrealistic situation where it is constantly exposed to an insecticide in a fumigated chamber. Our method illustrates that there is a serious problem in controlling these pests. These findings provide information for further research on the involvement of esterases in the resistance mechanism of German cockroaches.

Table 1. Percent mortality rates calculated 48 hours post exposure to a 1% Dursban solution of a desired concentration for 1 hour.

SELECTION FOR RESISTANCE IN THE A&M POPULATION		
concentration (mg/m2)	% mortality male	% mortality female
0.00	2.5	1.7
15.6	66.4	60.7
31.2	92.5	87.5
62.4	99.5	95.0



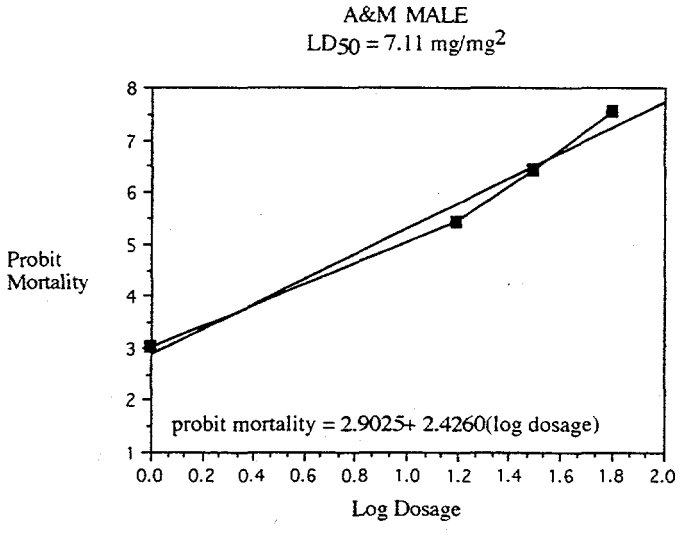


Figure 1. This figure represents the LD_{50} determination by plotting mortality rates as a function of probit values against the log of Dursban concentrations used in this experiment. The LD_{50} of the female A&M roach was determined to be 10.24 mg/m2 of a 1% Dursban solution. The male LD_{50} value was determined to be 7.11 mg/m2. These are the concentrations which will kill approximately half of the female/male populations.

Table 2. Percent mortality rates calculated 48 hours post exposure to a 1% Dursban solution of a desired concentration for 1 hour.

SELECTION FOR RESISTANCE IN THE S&W POPULATION		
concentration (mg/m2)	% mortality male	% mortality female
0.00	1.6	2.1
15.6	40.4	15.2
31.2	89.7	76.5
62.4	91.7	82.0

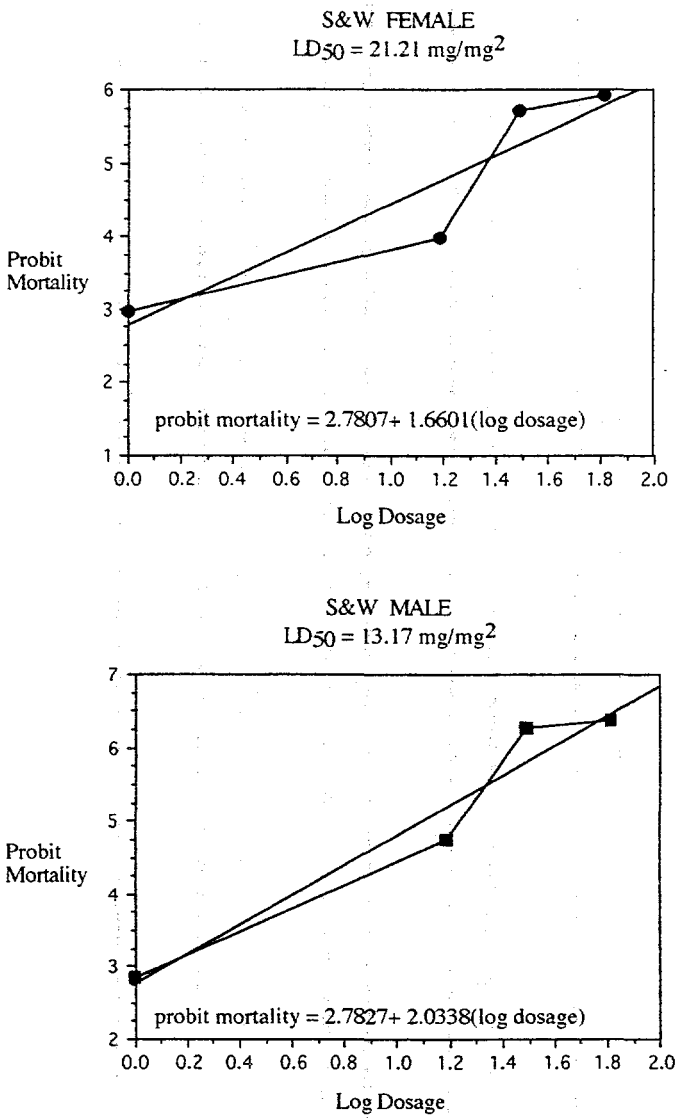


Figure 2. This figure represents the LD_{50} determination by plotting mortality rates as a function of probit values against the log of Dursban concentrations used in this experiment. The LD_{50} of the female S&W roach was determined to be 21.21 mg/m² of a 1% Dursban solution. The male LD_{50} value was determined to be 13.17 mg/m². These are the concentrations which will kill approximately half of the female/male populations.

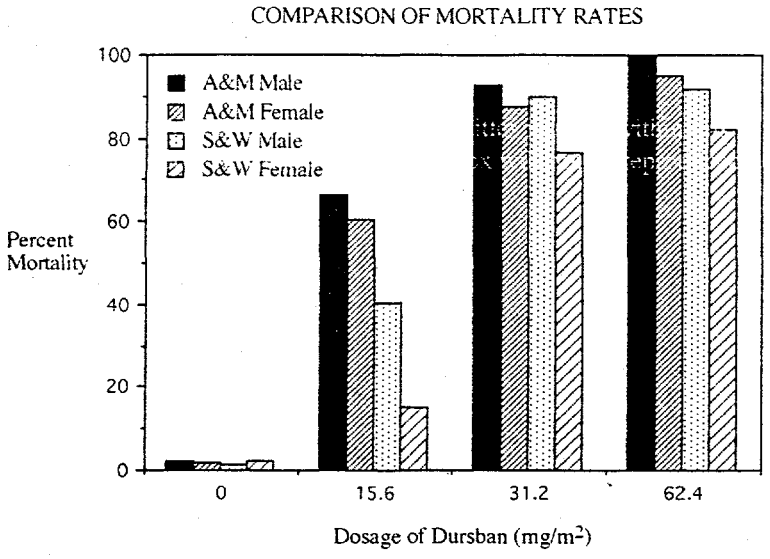


Figure 3. This bar graph depicts the decrease in percent mortality when the S&W population is compared to the A&M population.

Table 3. The means for both populations were derived from the absorbance values (560 nm) collected during the esterase assay. These data were analyzed to determine the relationship between the mean and esterase activity according to Prabhakaran, 1993. Means with the same grouping letter are not significantly different (LDS, P> 0.05).

ANALYSIS OF VARIANCE IN THE A&M AND S&W POPULATIONS

strain	mean	grouping
A&M	7.5692	A
S&W	3.3648	B

ACKNOWLEDGMENTS

Special thanks goes out to Bobby Jones for allowing the use of his lab and for providing this research with the LD_{50} techniques and critical knowledge that went into this manuscript. Also, a special thanks goes out to David Killilea who helped provide us with some essential aspects of pharmacology.

REFERENCES

Bevan, J.A. & J.H. Thompson. 1983. Essentials of Pharmacology. Pennsylvania, Harper and Row, Publishers, Inc.

Jones, Bobby. 1989. (Unpublished data). Memphis, TN., Department of Biology, Rhodes College.

Keller, J.C., P.H. Clark & C.F. Lofgren. 1956. Results of USDA sponsored research in cockroach control. Pest Control 24: 12; 14; 17-20.

Koehler, P.G. & R. S Patterson. 1986. A comparison of insecticide susceptibility in seven nonresistant strains of the German cockroach. J. Med. Entomol. Vol. 23, no 3.: 298-299.

McCanless & Domon. 1989. (Unpublished data). Memphis, TN., Department of Biology, Rhodes College.

Milio, J.F., P.G. Koehler & R.S. Patterson. 1987. Evaluation of three methods for detecting chlorpyrifos resistance in German cockroach populations. J. Econ. Entomol. 80: 44-46.

Prabhakaran, S.K. 1993. Activity and electrophoretic characterization in insecticide-resistant and susceptible strains of German cockroach. J. Econ. Entomol. 86: 1009-1013.

THE EFFECTS OF MATING ON SEXUAL RECEPTIVITY IN *DROSOPHILA BIARMIPES*

Carissa R. Adams

Department of Biology
St. Joseph's University
Philadelphia, PA 19131-1395.

Faculty Advisor, Scott P. McRobert

INTRODUCTION

In 1915, Sturtevant first described the courtship of *Drosophila melanogaster*, giving rise to numerous studies directed towards understanding the complex sexual behavior of Drosophilids. In many Drosophilids, males engage in a series of courtship behaviors elicited by visual, olfactory, and tactile cues provided by the female (reviewed by Tompkins, 1984). These behaviors include, orientation, in which the male orients his body with respect to the sexually attractive fly, following, if the female runs away, tapping where the male extends his fore-tarsi attempting to touch the females abdomen, singing, where the male extends and vibrates one wing to produce sounds known as the courtship-song, male licking, where he extends his proboscis and licks the female's genitalia, and attempted copulation. Copulation, which is under the control of the female, apparently occurs if she has received the proper stimulation from the male's courtship. The duration of copulation varies between species. Drosophila female's are "sperm-storers", and will lay eggs fertilized by a single copulation for a number of days.

Following mating, *D. melanogaster* females undergo a series of dramatic changes. Sexual attractiveness and sexual receptivity decrease significantly, while oviposition rates increase. The decrease in sex appeal is related to a dramatic reduction of the female's major sex pheromone, (Z, Z)-7, 11-heptacosadiene (HCD) (Antony and Jallon, 1982; Antony et al., 1985). The decrease in receptivity, and increase in oviposition may involve temporary changes in the female's central nervous system. Over a period of days, as the female depletes her sperm reserves, attractiveness, receptivity, and oviposition rates return to their original (virgin) levels. The female will now stimulate courtship, remate, and the entire process will be repeated. This pattern apparently continues throughout the female's life.

Changes seen in *D. melanogaster* females immediately after mating are mediated by a compound known as a sex peptide, which is transferred to the female during copulation. In *D. melanogaster*, female attractiveness, receptivity, and oviposition are all linked by their response to sex peptide in the female's system.

Drosophila biarmipes is a small Asian pomace fly, also known as *D. rajasekari*. Based on morphological features, this species has been assigned to the *suzukii* subgroup of the *melanogaster* species group in the subgenus *Sophophora* (Sreerama Reddy and Krishna Murty, 1968). *D. biarmipes* and *D. melanogaster* are, thus, distantly related.

During initial studies in which the courtship behavior of *D. biarmipes* males was described (McRobert and Jackson, 1988), it was revealed that the sexual attractiveness and receptivity of *D. biarmipes* females decreased following mating (as in *D. melanogaster*). However, while the sexual attractiveness of mated females returned, *D. biarmipes* females rarely, if ever, remated.

Accordingly, the present study which compared the remating behavior of *D. biarmipes* and *D. melanogaster* females under conditions in which females are given multiple chances to remate was initiated. In addition, the study examined the offspring production of both species following one successful mating.

MATERIALS AND METHODS

Stocks

D. biarmipes and *D. melanogaster* were maintained in mass culture on Carolina instant Drosophila media (Formula 4-24). The bottles were cleared and virgin males and females were collected. Flies were collected under CO_2 anesthesia within 12 hours of eclosion. Females were stored in groups of 10-15 in vials containing media. Males were kept individually in vials containing media.

Behavioral Assays

The remating frequency of *D. biarmipes* females was determined by performing an "exhaustive mating regime". Mated females were produced by placing virgin females into vials with two mature males (3-7 days old). The vials were observed at five minute intervals for two hours and those containing copulating pairs were set aside. Following the termination of copulation, the males were removed by aspiration. The mated females were

stored for 24 hours, then tapped into new vials, containing two males. The vials were observed at five minute intervals for two hours. After the two hour time limit, the two males were aspirated out while the females were stored in the vials for twenty-four hours, when the process was repeated. Virgin males were attempted to be used throughout this process. However, occasionally males were used more than once. Vials from the experiment were kept so that offspring production could be monitored.

Offspring Production

Offspring production for females from the exhaustive mating regime, and from the females mated only once, was determined by using a media submersion technique. After 6 days, the contents of each vial were removed, mixed with a 20% sucrose solution, and stirred with a glass rod. This technique resulted in media sinking to the bottom and larvae floating to the surface where they were counted.

Statistical Analysis

The significance of differences between means was determined using a contingency Chi-square test or by calculating t (student's t test, two-tailed).

RESULTS

D. biarmipes females remated at a significantly lower rate than *D. melanogaster* females during the two week period following their initial mating (Table 1). *D. biarmipes* females also produced a significantly lower number of offspring than *D. melanogaster* females during the two week period following initial mating (Table 2).

D. melanogaster females that were given chances to remate produced significantly more offspring than *D. melanogaster* females that mated only once (Table 2). *D. biarmipes* females which were given a chance to remate did not produce any more offspring than *D. biarmipes* females that mated only once (Table 2). Therefore, *D. melanogaster* females, appeared to benefit from remating while *D. biarmipes* females did not.

Table 1. A comparison of mating and remating behavior between *D. biarmipes* and *D. melanogaster* females

Copulation Frequency-Virgin Females

Species	Copulation	Frequency
D. biarmipes	46/50	92%
D. melanogaster	20/20	100%

($\chi^2 = 1.70$. $p > .05$)

Remating Within 14 Days of Initial Mating

Species	Remating	Frequency
D. biarmipes	5/16	31%
D. melanogaster	12/13	92%

($\chi^2 = 60.71$. $p < .001$)

Mean Time Until First Remating

Species	Mean Remating Latency
D. biarmipes	10.8 (± 2.5) Days
D. melanogaster	6.4 (± 1.9) Days

($t(15) = 4.0$. $p < .001$)

Mean Number of Rematings/Remating Females

Species	Mean Number of Rematings
D. biarmipes	0.2 (± 0.4)
D. melanogaster	1.2 (± 0.7)

($t(37) = 5.95$. $p<.001$)

Table 2. A comparison of offspring production between *D. biarmipes* and *D. melanogaster* females

Mean Offspring Production

Species	N	Mean Offspring Production
D. melanogaster *	21	158.3 (± 10.8)
D. melanogaster Δ	16	358.3 (± 102.8)
		(t(36) = 7.31. p < .001)
D. biarmipes *	8	93.6 (± 34.9)
D. biarmipes Δ	22	95.9 (± 31.5)
		(t(29) = 0.36. p > .05)
D. melanogaster *	21	158.3 (± 70.8)
D. biarmipes *	8	93.6 (± 34.9)
		(t(27) = 2.45. p < .05)
D. melanogaster Δ	16	358.3 (± 102.8)
D. biarmipes Δ	22	95.9 (± 31.5)
		(t(38) = 11.69. p < .001)

* Once-Mated Females
Δ Females Given Multiple Chances to Remate

DISCUSSION

Virgin *D. Biarmipes* females elicited high levels of courtship from mature males and were highly receptive to copulation. Following mating, both attractiveness and receptivity significantly declined. Within two weeks of their initial mating, the sexual attractiveness of *D. biarmipes* females returned to levels seen in virgins.

This is similar to the pattern seen in *D. melanogaster* females. However, unlike the *D. melanogaster* system, sexual receptivity of *D. biarmipes* females did not return to virgin levels within two weeks of initial mating. During this period, only 31% of *D. biarmipes* females remated. This is significantly lower than the 92% remating frequency of *D. melanogaster* females. In addition, *D. melanogaster* females remated significantly faster than *D. biarmipes* females, and *D. melanogaster* females often remated more than once. *D. biarmipes* females never remated more than once.

This study raises questions as to why the sexual behavior of these two species differs so greatly. The system seen in *D. melanogaster* seems logical: females become unattractive and unreceptive during the egg-laying period that follows mating. Then, as the female depletes her levels of stored sperm, attractiveness returns, the females remates, and the process is repeated. The system seen in *D. biarmipes* seems to be more unusual. While the attractiveness of *D. biarmipes* females returns a few days after mating, sexual receptivity does not.

With respect to fecundity, our results show that "once-mated" *D. melanogaster* females produced significantly higher numbers of offspring than "once-mated" *D. biarmipes* females. Furthermore, when females of both species are given multiple chances to remate, *D. melanogaster* females produce even more offspring, while no change is seen in the fecundity of *D. biarmipes* females. Thus, *D. melanogaster* females benefit from remating while *D. biarmipes* females do not.

One possible explanation for the behavior of *D. biarmipes* females is that they may have the ability to store and utilize sperm over longer periods of time than *D. melanogaster* females. If so, and if sexual receptivity returns when sperm supplies are depleted, then the offspring production and remating frequency of *D. biarmipes* females might eventually reach the levels seen in *D. melanogaster* females. In future studies we will examine this possibility by monitoring egg-laying and receptivity in *D. biarmipes* for longer periods of time following their initial mating.

ACKNOWLEDGMENT

Supported by Howard Hughes Medical Institue grant 1194-535101.

REFERENCES

Antony, C., and Jallon, J.-M. 1982. The chemical basis for sex recognition in *Drosophila melanogaster*. J. Insect Physiology. 28:873-880.

Antony, C., Davis, T.L., Carlson, D.A., Pechine, J.-M., and Jallon, J.-M. 1985. Compared behavioral responses of male *Drosophila melanogaster* (Canton-S) to natural and synthetic aphrodisiacs. J. Chem. Ecol. 11:1617-1629.

Hall, Jeffrey C. 1994. The Mating of a Fly. Science. 264:1702-1714.

McRobert, Scott P., and Jackson, Larry L. 1988. Description of Sexual Behaviors of *Drosophila rajasekari*. Journal of Chemical Ecology. 15:1423-1432.

Sreerama Reddy, G., and Krishna Murty, N.B. 1968. *Drosophila rajasekari a* new species from Mysore (India). Proc; Indian Acad. Sci. 68B:202-205.

Sturtevant, A.H. 1915. Experiments on sex recognition and the problem of sexual selection in *Drosophila*. J. Animal Behavior. 5:351-366.

Tompkins, L. 1984. Genetic analysis of sex appeal in *Drosophila*. Behavioral Genetics. 14:411-440.

PROTEASE ACTIVITY IN DEVELOPING SILKMOTH EMBRYOS

Yashoda Sharma

Department of Biology
Skidmore College,
Saratoga Springs, NY 12866

Faculty Advisor: Elaine Rubenstein

Yolk proteins stored in developing oocytes during oogenesis in the silkmoth Hyalophora cecropia are subsequently degraded during embryonic development (Rubenstein and Han, 1991). Using zymography, we analyzed protein samples from different stages of embryonic development for protease activity. Embryo protein samples were separated on SDS-polyacrylamide gels containing the protein substrate casein or gelatin, and then activated by incubation with buffers of different pHs, ranging from 5.0 to 11.0. The greatest protease activity was detected on days 11 and 12 of a 13 day developmental period. Proteases able to digest the substrate casein were identified with the relative molecular masses of 197, 153, 141, 130, 101.5, 101, 64, 52, 50, and 40.5 kDa. The pH optima for these proteases appear to be in the range of pH 9.0. Proteases able to digest the substrate gelatin were identified with the relative molecular masses of >200, 153, 71, 62, 42, 33, 31, 22, and 16.5 kDa. The pH optima for the gelatin protease appear to be in the range of 7.0. Because the proteases we detected exhibit substrate specificity, we believe it is likely that these enzymes also exhibit specificity for their natural substrates, one of the four yolk proteins.

INTRODUCTION

Macromolecules stored in developing oocytes during oogenesis support subsequent embryonic development. Four major yolk proteins have been identified in oocytes of the silkmoth Hyalophora cecropia; these are degraded during embryonic development to supply the embryo with amino acid building blocks and energy (Rubenstein and Han, 1991). The predominant yolk protein is the glycolipoprotein Vitellin, which is composed of two polypeptides that are easily identified on SDS-polyacrylamide gels.

In this study, zymography was used to identify proteases that are present in developing embryos, to determine at what times during embryonic development the enzymes are present, and to measure what their pH optima are. Zymography is an electrophoretic technique in which a protein substrate is co-polymerized with acrylamide during the preparation of the separating gel, allowing detection of both active and latent proteolytic enzymes present and estimation of their molecular weights.

RESULTS AND METHODS

Yolk Proteins are degraded during embryogenesis

A developmental series of embryos was analyzed by SDS-PAGE followed by protein staining with Coomassie Brilliant Blue-R250 (Figure 1). The two polypeptide subunits of the major yolk protein, Vitellin, are labeled. Over developmental time, there is a very gradual decrease in concentration of all the yolk proteins. By day 11, however, a dramatic change is evident. For example the Vitellin polypeptides are no longer visible; many new polypeptides, presumably the breakdown products of the yolk proteins, can now be detected.

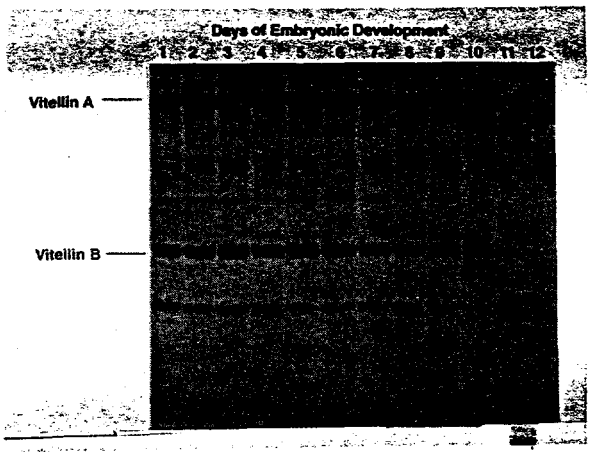


Figure 1. This is a 13 day developmental series of embryos of Hyalophora cecropia, lasting 12 days with hatching on the 13th day. Five embryos at each day of development were homogenized in 300 µl of pH 7.0 phosphate buffered saline, and then diluted 1:3 with SDS sample buffer [25 mM Tris-HCl (pH 6.8), 2% SDS, 10% Glycerol, 5% 2-mercaptoethanol, 0.006% Bromophenol Blue]. Five µl of the diluted samples were placed in each well of a 10% SDS-polyacrylamide gel, and then separated at 90 V for 2 hours, or until the dye reached the bottom of the gel.

Casein zymograms reveal protease activity late in embryonic development.

Protease activity is detected by the digestion of the casein substrate, evident as clear bands on the darkly stained background (Figure 2). No protease activity was observed until day 11, when three bands were detected (Mr = 141,500, 101,000, 52,000). On day 12, seven bands of protease activity are evident (Mr = 197,000, 153,000, 130,000, 101,500, 64,000, 50,000, 40,500). The location of Vitellin A is indicated on this gel.

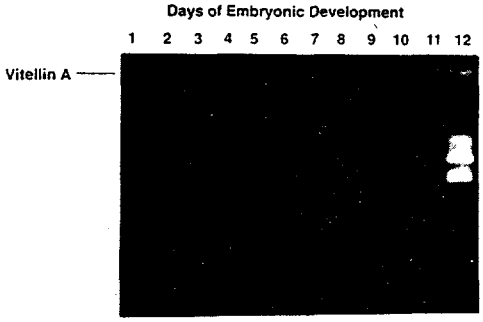


Figure 2. For zymography, the same embryo samples as used in the regular SDS-PAGE were separated on a 10% SDS-polyacrylamide gel that was co-polymerized with 0.2% casein (Kleiner and Stetler-Stevenson. 1994). Following electrophoresis at 90 V, the gel was rinsed with 2.5% Triton X-100, and then incubated for 1 hour, at 37°C, in a 0.05 M Tris-HCl buffer (pH 9.0). The gel was then stained with Coomassie Brilliant Blue R-250, and destained with 10% acetic acid, 10% methanol.

Casein proteases have optimal activity around pH 9.0

In order to determine the pH optima of those protease bands detected in the casein gel, the enzymatic activity in digesting casein was compared

in gels incubated at different pHs (Figure 3). Embryo samples from days 10, 11, and 12 were separated on casein- containing gels (no activity was detected in earlier samples). The bands indicating protease activity appear to be most intense at pH 9.0. One new band, however, is evident at day 11 only, at pH 11.0 (Mr = 52,000). The heavy subunit, Vitellin A, is labeled on the gel.

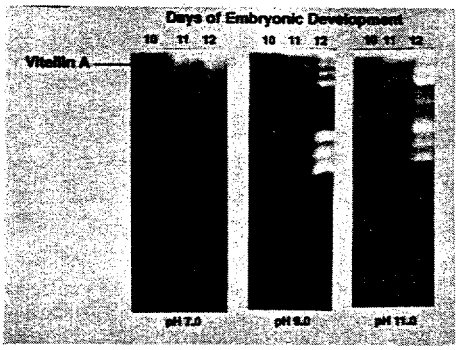


Figure 3. Embryo samples were separated on casein-containing gels as described earlier. After rinsing in 2.5% Triton X-100, the gel was cut into three sections and each was incubated in a different buffer: 0.1 M Potassium phosphate buffer, pH 7.0 or 0.05 M Tris-HCl buffer, pH 9.0, or 0.1 M Sodium phosphate buffer, pH 11.0.

Densitometric Analysis of the 64, 50, 40.5, kDa Protease Bands

The optical density of an area around the 64,00, 50,000, and 40,500 bands, at each pH, was quantified as described in the legend to Table 1. An equal area of the gel without bands was quantified, as the background value. From this comparison it is clear that the pH optimum for the proteases with molecular masses of 64,000, 50,000, and 40,500 on the protein substrate casein is 9.0.

Table 1. Images of the gels incubated in the pH 7.0, 9.0, and 11.0 buffers were digitized using a UVP video image analysis system. The images were then quantitatively analyzed using "NIH Image" software.

pH	Optical Density (minus background) in arbitrary units
7.0	4.51
9.0	36.07
11.0	17.16

Gelatin zymograms reveal different proteases

In order to find out if there were any proteolytic enzymes which were active on different substrates, gelatin was used. Again protease activity is evident by the presence of clear bands (Figure 4). No protease activity was observed until day 10, when two bands were detected (Mr = 153,000 and 16,500). On day 11, four bands of protease activity were observed (Mr = >200,000, 71,000, 31,000, and 16,500). On day 12, six bands of protease activity are evident on the gelatin substrate (Mr = >200,000, 62,000, 42,000, 33,000, 22,000, and 16, 500). The location of the heavy and light polypeptides of Vitellin are indicated on the gel.

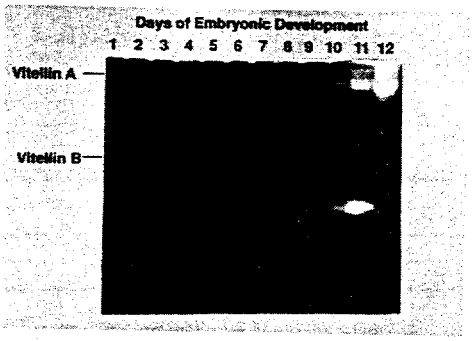


Figure 4. The same embryo samples described earlier were used, but they were diluted with a different SDS sample buffer (0.4 M Tris-HCl pH 6.8, 5% SDS, 20% Glycerol, 0.03% Bromophenol Blue). The embryo samples were separated on a 10% SDS-polyacrylamide gel that was copolymerized with 0.09% gelatin. Following electrophoresis, the gel was rinsed in 2.5% Triton X-100 for 1 hour, with shaking, and then incubated in buffer [50 mM Tris - HCl (pH 7.5) 200 mM NaCl, 5 mM $CaCl_2$, 0.02% Brij-35] for 18 hours, at 37°C (Roche, et. al. 1983). The gel was then stained with Coomassie Brilliant Blue R-250, and destained with 10% acetic acid, 10% methanol.

Gelatin proteases have optimal activity around pH 7.0

In order to determine the pH optima of those protease bands detected in the gelatin gel, enzymatic activity in digesting gelatin in gels incubated at different pHs was compared (Figure 5). Embryo samples from days 10, 11, and 12 were studied. The same proteases were seen at all pHs tested, however, they differed in intensity, with pH 7.0 appearing to be the optimum.

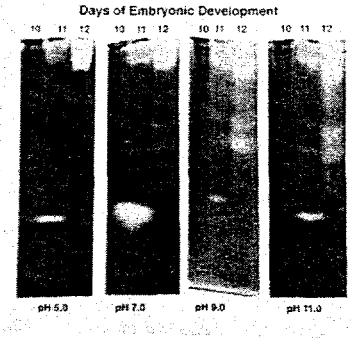


Figure 5. Embryo samples were separated on the gelatin-containing gels as described earlier. After electrophoresis, the gel was rinsed in 2.5% Triton X-100 for 1 hour, with shaking, and then cut into four sections. Each section was incubated in a different buffer: 0.1 M Potassium acetate enzyme buffer, pH 5.0 or 0.1 M Potassium phosphate enzyme buffer, pH 7.0, or 0.05 M Tris enzyme buffer, pH 9.0, or 0.1 M Sodium phosphate enzyme buffer, pH 11.0.

Densitometric Analysis of the 16.5 kDa Protease Band

The optical density of an area around the 16,500 band was quantified at each pH as described in the legend to Table 2. An equal area of the gel without bands was quantified as the background value. From this comparison it was concluded that the pH optimum for the protease with molecular mass of 16,500 on the protein substrate gelatin is 7.0.

Table 2. Images of the gels incubated in the pH 5.0, 7.0, 9.0, and 11.0 buffers were digitized using a UVP video image analysis system. The images were then quantitatively analyzed using "NIH Image" software.

pH	Optical Density (minus background) in arbitrary units
5.0	2.58
7.0	12.43
9.0	not detectable
11.0	2.69

CONCLUSION

Because the proteolytic enzymes detected exhibit substrate specificity, that is, most enzymes degraded one but not the other of the two substrates tested, these enzymes may also exhibit specificity for their natural substrates, one of the four major yolk proteins.

REFERENCES

Kleiner, D. and Stetler-Stevenson, W. G., Analytical Biochemistry, Quantitative Zymography: Detection of Picogram Quantities of Gelatinases, Vol. 218, (1994), pg. 325-329.

Roche, P., Campaeu, J. D. and Shaw, T., Biochemica et Biophysica Acta., Comparative Electrophoretic Analysis of Human and Porcine Plasminogen Activators in SDS-Polyacrylamide Gels Containing Plasminogen and Casein, Vol. 745 (1983), pg. 82-89.

Rubenstein, E. and Han, J-Y., American Zoologist, Yolk Protein Degradation During Embryonic Development in *Hyalophora cecropia*, Vol. 31 (1991), pg. 79A.

Morphological Examination of Spermathecae from Three Grasshopper Species

Rita Michelle Roberts

Department of Zoology, Box 7617
North Carolina State University
Raleigh, N.C. 27695-7617

Faculty Advisor:

Marianne Niedzlek-Feaver

The spermathecae or sperm storage organs of three grasshopper species were examined under light microscopy and scanning electron microscopy. Sensillae were found internally and externally. Basiconic internal sensillae were numerous and accompanied by pores and tracks. High interspecific variation related to differences in reproductive biology argue for a function for this organ in addition to sperm storage.

INTRODUCTION

Recently investigators have focussed on the realization that the race to fertilize eggs may not end with copulation (Eberhard,1991). In some species for example, a second mating may swamp out the sperm contributed by the first male. Males in some species even have appendages that they can use to scoop out sperm from previous males. Lately, investigators are asking what role the female plays in postmating strategies (Cronin, 1991; Rosenquist and Berglund, 1993). Do females simply decide to solicit a second mating or do they play a more active role in determining paternity by influencing sperm survivorship and storage?

Using the grasshopper as a model mating system has benefits. Some examples include, grasshoppers are not disturbed by human observation while copulating, and they are easily raised in large numbers in the laboratory. Males are not aggressive, therefore any role played by the female in choosing among males should be apparent. The first step in documenting any active female choice is the examination of the spermatheca or the sperm storage organ. Does the morphology of the organ indicate that females may have some potential to influence sperm behavior or sperm survival?

METHODS

This experiment first involved collecting three different species, *Dichromorpha viridis*, *Chortaphaga viridifasciata*, and *Schistocerca americana* from their natural environment. Grasshoppers were individually marked with airplane paint and maintained on a diet consisting of grass and water. Grasshoppers were allowed to mate in fiberglass cages that allowed the behavior of the individuals to be observed from the initiation of courtship to the end of copulation. Then the female's spermatheca was dissected out and examined under the light microscope. Dissection occurred in Hoyle's solution in order to emphasize features of interest and preserve sperm viability. Later, various spermathecae were examined using a Phillips 505 Scanning Electron Microscope. Before the spermathecae could be viewed under S.E.M., the organs were put through an alcohol series (30-50-70-95-100). Specimens were also critically point dried and gold coated (20-30nm/side).

RESULTS

The spermathecae of all three species, *Dicromorpha viridis*, *Chortaphaga viridifasciata*, and *Schistocerca americana* were found to contain three chambers (Fig. 1). In the first species examined, *D. viridis*, the chamber communicating with the environment, and the first to receive sperm was the largest and labeled one. The next chamber was knob-like, small, and blind at one end. The third chamber was also blind, and approximated the first chamber in length, although it was much narrower than the first chamber. In *C. viridifasciata*, the same three chambers were present, although it was the third and blind chamber that was the widest of the three. In *S. americana*, all three chambers were approximately the same size with the two blind chambers forming a Y at the end of the

chamber into which sperm first entered. Protein coated the outside of all chambers, while in mated females the protein coat was thicker.

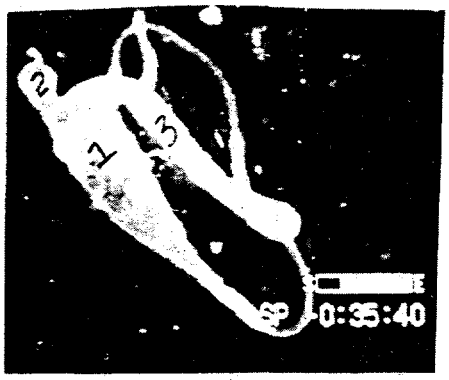


Fig. 1: Spermatheca of *Dichromorpha viridis*, light microscopy, 50x

In *D. viridis* and *C. viridifasciata*, after the first mating sperm bundles were found at the beginning of the spermathecae. After their second mating, most of the sperm was found in the last chamber, and a few times the sperm was viewed in the little knob-like structure. In *S. americana*, sperm was found evenly distributed throughout the spermathecae. Sperm appeared to be transferred with proteins in the form of bundles. The leftover debris made the appearance of the wall of the spermatheca hard to see. This was one of the main reasons why the spermathecae had to be cleaned with the alcohol series.

After cleaning, under S.E.M. the external surface was found to contain sensillae and the internal surface of the spermatheca was found to contain sensillae, pores, and tracks (Fig. 2). Some of the micrographs displayed a few sperm with their heads and protein still embedded in the hairlike sensillae. In *D. viridis*, internally similar sensillae were evenly spread throughout the chambers (Fig. 3). The only exception was the knob- like chamber two, that contained fewer sensillae. The same is true for *S. americana*, although the internal surface of the spermatheca contained only about 1/10 the sensillae found per unit area in *D. viridis*. The internal surface of the spermatheca in *C. viridifasciata* was more complex. Different sections of chambers appear to have a diverse number of sensillae. Also, the sensillae appear to vary in size. All sensillae examined at higher magnification to date are similar in that they are essentially blunt tipped hairs (Fig. 2). These hairlike sensillae when found in other organs are characterized by other scientists as basiconic, or sensillae olfactory as well as tactile in function (Bland, 1987).



Fig. 2. Pores, tracks and sensillae in *Chortophaga viridifasciata*, S.E.M. 2700x, Note various sizes of sensillae

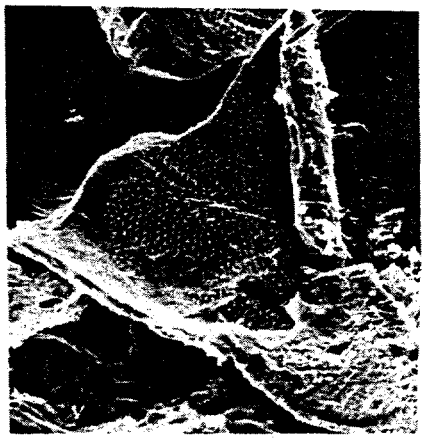


Fig. 3. Spermatheca of *Dichromorpha viridis*, S.E.M. 250x, Note even distribution of sensillae

DISCUSSION

That the internal structure of the spermathecae in all three species was complex, containing numerous sensillae, pores and tracks, indicates that the spermatheca may play a more important role than simply serving as a sac for temporary sperm storage. Sensillae have been implicated in other studies to be olfactory and their function may play some role in assisting the quality or quantity of the protein contribution by males that accompanies sperm transfer (Bland, 1987). Tracks may direct sperm migration throughout the spermatheca. A number of blind chambers may allow females to shunt some sperm into chambers farther removed from eggs.

Interspecific variation in spermathecae morphology could be related to difference among species in mating biology. *S. americana* females are very selective sometime mating only with one or two males throughout the season (Kosal, 1995). The amount of protein that can be transferred by the male also appeared small compared to the other two species. Strong premating choice is exerted in this species and the amount of nutrients transferred by the male may not be important. This may explain why so few sensillae (relative to the two other species) were found on the internal surface of the spematheca in *S. americana*. In *D. viridis*, however, all choice appears to be exerted postmating with females allowing males in lengthy copulations (2-72 hours) to transfer sperm bundles only as long as such bundles are preceded by protein (pers comm. M. Niedzlek-Feaver). Perhaps the abundant sensillae found internally aid the female in assessing if sufficient protein is being transferred. In *C. viridifasciata*, females do exhibit premating choice, mating with "heavier" males in relatively short copulations (Niedzlek-Feaver, 1995). However, "mistakes" are corrected by second matings. Perhaps, the complex internal morphology of the spermatheca aids the females in not only assessing the quality of the nutrients transferred during mating, but also influences which sperm will be allowed to fertilize eggs. More work has to be done, especially in correlating sperm absence and presence in various chambers with the number of matings and characteristics of males such as size.

CONCLUSION

A spematheca appears to be a most complex organ internally containing numerous sensillae, tracks and pores. Even in the three species examined, tremendous interspecific variation in morphology was observed.

BIBLIOGRAPHY

Bland. 1987. Antennal Sensilla of Acrididae (Orthoptera) in Relation to Subfamily and Food Preference. Ann. Entomol. Soc. Am. Vol. 82. pg. 368-384.

Cronin, H. 1991. The Ant and the Peacock. Oxford University Press. Oxford.

Eberhard, W.G. 1991. Copulatory courtship and cryptic female choicein insects. Bio. Rev. Vol. 66. pg. 1-31.

Kosal, E. 1995. The natural history and mate choice of *Schistocerca americana* (Orthoptera: Acrididae). University of North Carolina. MS thesis.

Niedzlek-Feaver, M. 1995. Crepitation, Pair Formation and Female Choice in *Chortophaga viridifasciata* (DeBeer) (Orthoptera: Acrididae). J. of Orthoptera Res. Vol. 4. pg. 1-12.

Rearing and Pathogenic Biological Control of the Citrus Leafminer, Phyllocnistis citrella Stainton

Dorothy Hoppe

Division of Natural Sciences
New College of the University of South Florida
5700 North Tamiami Trail
Sarasota, FL 34243

Faculty Advisor:

Sandra L. Gilchrist

This study was conducted in an effort to provide a supplementary control of the citrus leafminer, Phyllocnistis citrella, an insect new to Florida (first noted May 1993). A citrus leafminer colony was established. Bioassays were then developed to test activity of entomopathogens against the leafminer larvae. Bioassays were based on mortality of larvae in isolated citrus leaves. Two techniques were used: direct injection into the leaf mine and topical application. Bioassays were tested for two attributes: insecticidal activity (virulence of the pathogen) and penetration of virulent mixtures into leaf mines to affect larvae. Nematodes, Heterohabditis bacteriophora and Steinernema riobravis, the bacterium Bacillus thuringiensis (Bt), and a nuclear polyhedrosis virus, the celery looper virus, were tested for virulence with and without an organosilicone surfactant, Silwet L-77. L-77 killed larvae at low concentrations when topically applied as well as when injected into the mine. Topical applications of commercial Bt preparations were active against the leafminer at high concentrations. L-77 synergized the activities of Bt preparations, producing up to 90% mortality at 0.01% L-77 and 20% Bt. The nematodes H. bacteriophora and S. riobravis and the celery looper virus were active against leafminers when injected into mines. Rearing and bioassay techniques and results will be discussed as will be possible application of the bioassays.

INTRODUCTION

The citrus leafminer, Phyllocnistis citrella Stainton, is a small moth (Lepidoptera: Phyllocnistidae) pest of citrus. Leafminer is native to eastern and southern Asia, and is now widely distributed in citrus-growing areas in Asia, Papua New Guinea, Australia, northern and central Africa, and Florida. It was first found in Florida in May 1993. Within six months, infestation had spread throughout the state.

Damage is caused by the leafminer larvae, as they feed on parenchymal tissue below the epithelial layer of the leaf; the effect is a "mine" under the epithelium. Symptoms of infestation include twisted and curled leaves. Severe damage can retard the growth and yield of nursery and newly planted trees; infestation on mature trees is usually less serious. Hence, the leafminer is a special concern to commercial nursery owners. Infestation usually occurs in the summer and autumn, but can be seen in Florida as early as late spring.

On the basis of experience in China, Thailand, and Australia, it is believed that biological control with parasitoids provides the best chance of effective management (Beattie & Smith, 1993). The successful importation, introduction, and establishment of parasitoids may, however, require years. This study proposed the use of insect pathogens such as host-specific viruses and bacteria as supplementary, short-term control.

The initial priority was to establish self-sustaining colonies of the insect. These were intended to serve as a source of larvae for bioassays. Difficulties encountered

included molding or drying of leaves containing pupae, presence of parasites, and fragility of emerged adults. An effective and simple method was found and several colonies begun. However, the colonies did not become sufficiently robust to provide a consistent source of test larvae.

Bioassays targeted the larva. A significant problem was posed by the protection offered to the larva by the leaf epithelium. In order to enter the mine and affect a leafminer larva, the pathogen must first penetrate the epithelial layer, either through leaf stomata or between or through the epithelial cells. The leaf and larva must also be kept alive for a period sufficient for the pathogen to act. Slow-acting agents such as viruses and nematodes are particularly demanding; it must be certain that mortality results from pathogenic activity, not factors such as leaf death.

Bioassays were begun with the aim of testing two attributes of potential biocontrols: insecticidal activity and ability of virulent pathogens to penetrate leaf mines and affect the larvae. Insecticidal activity was tested using Bacillus thuringiensis (Bt), nematodes, and a nuclear polyhedrosis virus, the celery looper virus. These were injected directly into the mine. The question of penetration was addressed with the use of an organosilicone surfactant, Silwet L-77; it is proposed that the very low surface tension of such surfactants (Knoche et al., 1991) may strongly increase penetration of pathogens into leaf mines. L-77 was both injected directly and applied topically, alone and in solution with proven pathogens. Thus, the activity and applicability of pathogens was tested.

MATERIALS

Rearing and bioassays were accomplished using larvae and pupae collected from a nursery in Apopka, Florida and from seedlings of various cultivars at the U.S. Horticultural Research Laboratory, Orlando, Florida.

Silwet L-77 (Loveland Industries, Greeley, CO), commercial preparations of Bt (Condor, Ecogen, Langhorne, PA, Florbac HPWP, Biobit HPWP, Entotech, Davis, CA), an HD-73 Bt strain (Entotech, Davis, CA), a celery looper virus (Biosys, Davis, CA), and nematodes (Steinernema riobravis and Heterohabditis bacteriophora, Biosys, Davis, CA) were provided by manufacturers.

METHODS

Rearing

Leaves containing pupae were cut from trees and placed in polyethylene bags (Fisher) at quantities ranging from 60-80 pupae per bag. The bags were lightly inflated, tied, and placed under a lamp. Bags were checked daily for emerged adults. Adults were caught in the bag using 1cm petri dishes. All adults were released into the colonies. Colonies were housed in plastic cages in incubators set at a constant temperature of 26°C and 83% humidity. The colonies were supplied with citrus plants with new leaf flush. All plants were obtained from an isolated chamber in a laboratory greenhouse; the plants were completely stripped of leaves and flush was allowed to grow. Plants in the colonies were changed weekly to provide new flush for the laying of eggs. Adults were fed small drops of honey beaded on a strip of Para-film and placed on the walls of the cage.

Bioassays

Actively feeding second or third instar larvae were used for bioassays. A direct mine injection assay was used to test insecticidal activity of pathogens or the surfactant. Under a stereomicroscope, the mine epithelium above the head of the larva was punctured with a #0.10 minutin pin. 4 microliters of solution were then placed directly over the puncture site and allowed to flow into the mine. To test the penetrability of a compound or pathogen, 4 microliters of solution were placed onto the intact mine surface directly above the head of a feeding larva. Blue food coloring (FD&C Blue dye No.1, McCormick Company) was added to all samples to 10% of total

volume to allow the viewing of ingestion and movement of the sample through the gut. Following treatment, the tip of the leaf petiole was cut and the leaf was placed into a 2-mL sample vial filled with water; the petiole was secured in the vial with a cotton wick. Vials were kept in the laboratory at room temperature (23°C) inside a closed plastic box (19x13.5x10.5 cm). The time course of L-77 was observed completely; all other mortalities were monitored daily at particular observation periods (discussed in Results).

To observe the effects of L-77, mines were injected or topically treated and larvae observed for cessation of mandibular feeding movement and midgut peristalsis. Initial observations were continuous for 15 min, then every 15 min up to 1 hr after treatment, every 30 min for the next 3 hr, and every 24 hr thereafter. Mortality was recorded when larvae showed no external or peristaltic movement when probed.

RESULTS AND DISCUSSION

Citrus leafminer larvae feed on the parenchymal tissue of a leaf using coordinated sweeping semicircular movements of the mandibles. Consumed tissue quickly enters the pharynx and foregut and continues through the digestive system. At times, mandibular movement stops briefly during feeding, while ingestion continues through "sucking" in of materials; ingestion is independent of mandibular movement. Movements of the head and mandibles ceased within 10 sec of injection of a water/dye solution, but ingestion continued through peristaltic movement of the pharynx and gut. Mandibular and head movement and ingestion of leaf tissue resumed once all injected liquid was cleared from the mine. Ingestion and excretion were rapid (15-20 min from ingestion to excretion) and easily observed with the dye marker. Larvae were not affected by control solutions of water/10% dye; 90-100% survived to pupate within 3 days. In all types of treatment, larvae did not recover once gut peristalsis ceased.

Injection of increasing concentrations of L-77 in water showed direct toxicity. Larvae were killed within minutes by concentrations greater than 0.02%. 100% of control larvae treated with water/dye survived. When L-77 was topically applied to mines, mortality also resulted. At a concentration of 0.01% L-77, normal feeding and peristalsis continued; some L-77/dye solution did penetrate into the mine, was ingested, and excreted.

Table 1. Mortality and mean times until cessation of feeding and midgut peristalsis (the latter observed and recorded in dead larvae only). Leaf mines were injected with increasing concentrations of L-77 with 10% dye in water. See Materials and Methods for timing of observations.

Concentration (%)	Mortality (%)	Time to Cessation (hr)	
		Feeding	Peristalsis
0.006	40	0.8	1.0
0.010	70	0.2	0.3
0.016	80	0.3	0.4
0.025	100	0.3	0.4

Table 2. Mortality and mean times until cessation of feeding and midgut peristalsis (death) when leaf mines were topically treated with increasing concentrations of L-77 with 10% dye in water. See Materials and Methods for timing of observations.

Concentration (%)	Mortality (%)	Time to Cessation (hr)	
		Feeding	Peristalsis
0.010	50	*	65
0.016	40	*	53
0.020	70	0	31
0.025	50	*	11
0.050	100	3	9
0.10	100	3	3
0.50	100	0.05	0.3
1.0	100	0.02	0.08
5.0	100	0.02	0.07

*Ceased feeding between 4 and 24 hr after treatment

Condor was initially tested by mine injection to determine toxicity. A solution of 20% Condor Bt/10% blue dye was injected into the mines of 5 larvae. Feeding stopped in four of the five larvae within 1-2 hours; peristalsis in these four larvae stopped within 22 hours. Next, suspensions of three commercial Bt preparations were applied topically in 20% Bt solutions with and without L-77. An additional control of water/10% dye was also performed and gave 100% survival. L-77 was included at a concentration of 0.01%; this concentration had been shown to cause minimal mortality with topical application, yet enhanced penetration. With all preparations, larvae topically treated with Bt/water showed higher mortality than those treated with just 0.01% L-77, and those treated with solutions containing both Bt and 0.01% L-77 sustained the highest mortalities. Thus, L-77 appeared to synergize the activity of the Bt.

Table 3. Percent mortality of larvae in mines topically treated with Silwet L-77 only ("L-77 Control"; 0.01% in water), one of four different *Bt* formulations ("*Bt*"; 20% of full concentration in water), or L-77 and *Bt* together ("L-77+*Bt*"). Percentages are (v/v) for flowable *Bt* formulations and L-77, or (w/v) for wettable *Bt* (HPWP) powders. (N=10).

	Percent Mortality		
	L-77 Control	*Bt*	L-77+ *Bt*
Biobit HPWP	10	40	100
Condor	10	50	80
Entotech HD-73	20	70	90
Florbac HPWP	10	20	60

Mortality of leafminers topically treated with Bt/0.01% L-77 correlated directly with Bt concentration. However, it was always less than the observed mortality at 20% Bt concentration. Larvae treated with Biobit and Condor showed slightly higher mortalities than HD-73 or Florbac. Bt preparations at 0.01% resulted in mortality only slightly above the usual mortalities of 0.01% L-77 controls. Dead larvae treated with Bt appeared to have no differentiated internal organs; all internal matter was uniform.

Table 4. Mortality of larvae in mines topically treated with varying concentrations of *Bt* (percent w/v for wettable powders and percent v/v for flowable preparations) in 0.01% L-77 (N=10, except for HD-73 at 0.10% N=9).

Bt Preparation	*Bt* Concentration			
	0.01%	0.10%	1%	5%
Biobit HPWP	20	20	60	60
Condor	10	30	50	60
Entotech HD-73	10	33	40	30
Florbac HPWP	0	20	30	40

When entomopathogenic nematodes and the celery looper virus were injected into mines in water, leafminer larvae sustained mortality, though it was always less than 100%. High concentrations (10/microliter) of H. bacteriophora produced 70% mortality within 5 days; concentrations of 20/microliter of S. riobravis gave 50% mortality within 6 days. .205x10 PIB virus produced 80% mortality in 6 days. Larvae treated with H. bacteriophora had a characteristic brownish-pink color when dead, those treated with S. riobravis retained their yellow color but appeared to have no internal organs; all had been destroyed. Virus-treated larvae turned a bright red-pink color when dead.

This study refined and put in use a rearing methodology for the citrus leafminer. It also developed and demonstrated

the utility of two bioassays, one for assessing direct activity of several biocontrol agents against larval citrus leafminer, and another to test penetration of the agents into leaf mines. Using these assays, it was demonstrated that Bt, an NPV virus, and nematodes are directly active against the leafminer larva; activity increases with concentration. Furthermore, Bt evidently penetrated leaf mines to affects the larvae, and penetration was enhanced by the surfactant L-77.

Surfactants have long been used to increase uptake, retention, and persistence of conventional pesticides and other agricultural chemicals; they may also increase the efficacy of biological control agents. Organosilicones are particularly effective due to their exceptionally low surface tension; they are excellent wetting agents. L-77 penetrated leaf mines at concentrations lower than those required to kill miners, as evidenced by tracing the penetration of blue dye. The high concentrations of L-77 required to produce mortality imply drowning as a mode of action. In order to test whether L-77 increased penetrability of Bt, a low (0.01%) concentration of L-77 that is nontoxic to larvae yet penetrates leaf mines was used. Higher concentrations of organosilicone surfactants may further enhance penetrability of Bt into leaf mines. In addition, these surfactants may enhance the retention and persistence of Bt beneath the leaf epithelium. These results demonstrate that Bt activity is enhanced when applied with low concentrations of L-77, probably due to increased penetration into leaf mines.

The effects of L-77 as an adjuvant have not yet been tested with nematodes of NPV virus. Although this was not tested in the leafminer system, Bt and NPVs can synergize each other (Navon 1993). This combination could be an effective form of pest management.

Field application may differ from these tests in several aspects. Field treatments may use L-77 concentrations as high as 0.05% on citrus without damage. Since higher concentrations increase penetration, synergism with Bt should be enhanced by them. High concentrations of Bt were used to offset the low L-77 concentration; higher filed applications of L-77 may require less Bt. Results showed that Bt gave workable activity at low concentrations. A typical field rate may be 1 lb/acre at 100 gals/acre; this translates to 0.12% Bt. Activity of Bt/0.01% L-77 over controls was seen at Bt concentrations as low as 0.1% Bt.

The results of this project demonstrate several practical biocontrol agents for the citrus leafminer and a method of their delivery. The study shows promise for effective supplementary, short-term management of an important agricultural pest.

ACKNOWLEDGEMENTS

This work was funded by Florida Department of Agriculture & Consumer Services grant #1957. The project was carried out at the U.S. Horticultural Research Laboratory in Orlando, FL. I wish to thank Drs. Jeffrey P. Shapiro and William J. Schroeder for sponsoring and supervising this project, and Nancy Maynard and Hunter Smith for their invaluable assistance.

REFERENCES

Beattie, G.A.C., Smith, D., 1993, Citrus Leafminer, Agfacts H2.AE.4: 1-6.

Knoche, M., Tamura, H., Bukovac, M.J., 1991, Performance and stability of the organosilicone surfactant L-77: Effect of pH, concentration, and temperature, J. Agric. Food Chem., 39: 202-206.

Navon, A., 1993, Control of lepidopteran pests with Bacillus thuringiensis, pp. 125-143, In Entwistle, P.F., Cory, J.S.,Bailey, M.J., Higgs, S. (eds.), Bacillus Thuringiensis, an Environmental Pesticide: Theory and Practice, John Wiley & Sons Ltd.

The Effect of Thorax Temperature on Flight Speed in Honey Bee Drones (*Apis mellifera*)

Allan J. Ross

Department of Biological Sciences
Western Illinois University
900 W. Adams St.
Macomb, IL 61455-1396

Faculty Advisor: Joseph R. Coelho

Though flight speed is believed to be an important aspect of survival and evolution in insects, little useful information exists on factors which affect it. Thorax temperature (T_{th}) had a significant, positive, linear effect on ground speed (approximating airspeed) in drone honeybees (*Apis mellifera* L) as measured with a radar gun. This effect was similar to that observed in the two other insect species for which data are available, but did not match the established effect of T_{th} on force production in drones. Differences in thermoregulatory ability among drones could influence reproductive success in that hotter drones, through faster flight, may reach pursued queens more quickly than cooler drones. Curiously, there was no significant effect of any morphological variable on flight speed in drones. An effect of size on flight speed appears to be demonstrable interspecifically, but not intraspecifically.

INTRODUCTION

Flight speed is believed to be an important aspect of many survival and reproductive activities in insects, including foraging (Schmid-Hempel *et al.*, 1985) and mating (Chappell, 1984). The evolutionary diversification of insects is thought to be profoundly influenced by selection pressure for increased flight speed (Dudley, 1991). In spite of its significance, little useful information exists about insect flight speed or factors that influence it (see DeVries and Dudley, 1990).

Perhaps the lack of data results from the technical difficulties involved in measuring free-flight speed. In addition, it may be difficult to capture the insect afterward so that morphological or physiological measurements can be made and related to variation in flight speed. During a previous study (Coelho, 1991a), it was discovered that honey bee drones (*Apis mellifera* L.) taken from the entrance board of the hive and released some distance away will often return directly to the hive. In preliminary experiments, when the drone was held aloft and slowly rotated, presumably providing it with orientation cues, the frequency with which drones returned increased dramatically (Coelho, 1989). In this study doppler radar and the homing behavior of drones was used to examine effects of thorax temperature (T_{th}) and several morphological variables on ground speed (V). Drones are abundant in healthy colonies, and many aspects of their biology are well understood. Honey bees alter the altitude of flight to compensate for changes in wind speed, so that ground speed is nearly independent of wind speed (Wenner, 1963). This effect obviated the task of calculating the vector sum of wind speed and ground speed to estimate airspeed. Nonetheless, results are reported as ground speed.

Increasing T_{th}, within limits, results in improved muscle function (Josephson, 1981; Goller and Esch, 1990a; 1990b); hence, V should increase in direct proportion to T_{th}. Drones have a consistently higher T_{th} than workers (Coelho, 1991a; 1991b), which may represent a product of sexual selection based on flight speed. However, force production during flight describes a convex upward curve as a function of T_{th} in drones, so that force decreases with increasing T_{th} from 40.3°C to 50.5°C, the lethal upper limit (Coelho, 1991b). Within this range, V should decrease as well.

As size increases, V is expected to increase, assuming geometrical similarity (Lighthill, 1977). Hence, we predict that V should increase with measures of size,

such as body mass (M_b), thorax mass (M_{th}), forewing length (R), and wing area (S). Similarly, V should increase with increasing wing-loading (p_w).

The ratio of flight muscle mass to body mass (Flight Muscle Ratio, or FMR) is an excellent predictor of maximal force production and maneuverability in insects, birds, and bats (Marden, 1987). Honeybees alter the allocation of total power output between lift and thrust by changing body angle (Esch *et al.*, 1975). By maintaining a horizontal body angle, more force is exerted as thrust. Hence, one would predict that greater force production would support higher V; therefore, V should vary with FMR.

MATERIALS AND METHODS

A drone was captured from the hive porch by seizing a leg with self-closing forceps, carried ~30 m from the hive, marked on the thoracic tergum with a spot of paint, held aloft, rotated 360 degrees, and released. Ground speed was measured with a police-type K-band doppler radar gun as described previously (Coelho, 1991a) while the bee returned to the hive. The highest speed observed was recorded. Wind speed was measured immediately afterward at a point 2 m above the ground using an Alnor® ThermoAnemometer (CompuFlow 8575). The drone was captured when it arrived at the hive, and its T_{th} was measured within 5 s with a 26 AWG type T thermocouple probe (Physitemp MT 26/2) connected to a digital thermometer (Omega® HH-72 T) calibrated against a precision mercury thermometer. Ambient shade temperature (T_a) was measured with the same equipment after the thermocouple probe was wiped clean and allowed to equilibrate. The drone was sealed in a 1.5-ml centrifuge tube and frozen.

For all drones, M_b and M_{th} were measured to the nearest 0.1 mg on an analytical balance (Ohaus® AP110S). For approximately half of the drones, R and S were measured as described previously (Coelho 1991b). Wingloading was calculated as gM_b/S (where $g = 9.8$ m/s^2, the acceleration of gravity), and aspect ratio (AR) as $4R^2/S$.

Data were taken only for drones that returned to the hive within 15 s of their release in order to minimize the time lag between V and T_{th} measurements. Data collected when wind speed exceeded 3 m/s were excluded from the analysis to minimize effects of wind on V. This provides a maximum difference of ~1 m/s between the ground speed of bees flying against the wind and those flying with the wind, and much smaller potential errors in neutral winds (Wenner, 1963). Since winds were usually much slower than 3 m/s and predominantly from neutral directions, differences between V and airspeed are expected to be small. The experiment was performed during the summer months of 1990 and 1994 in Boulder County, CO and McDonough County, IL, respectively, using managed honey bee colonies of mixed European origin.

RESULTS

Thorax temperature had a significant linear effect on V (Figure 1A). Flight speed (m/s) was related to T_{th} (°C) according to the following equation: $0.35(T_{th}) - 8.46$ ($N = 66$, $r^2 = 0.212$, $P < .001$). This equation provides a Q_{10} of flight speed for drones of 2.01 Ambient temperature ranged from 22.1 to 35°C, and there was no effect of T_a on V.

Simple linear regression also revealed significant positive effects of M_b and M_{th} on V; however, stepwise multiple linear regression including T_{th}, M_b, and M_{th} demonstrated that only T_{th} had a significant effect on V ($n = 58$, $r^2 = 0.298$, $P < .001$). This effect may have occurred because T_{th} was correlated with M_{th} ($r = 0.348$, $P = 0.044$) and weakly correlated with M_b ($r = 0.331$, $P = 0.067$). Flight muscle ratio also had no effect on V ($N = 58$, $r^2 = 0.04$, NS). Among drones for which data were available, log-log regressions revealed no significant effect of M_b, M_{th}, R, S, p_w, or AR on V ($N = 34$, $P > .05$).

DISCUSSION

Thorax temperature had a significant, positive, linear effect on V in drones. The Q_{10} of V for drones was 2.01, which matches that for maximal oxygen consumption during hovering, 2.1 (Coelho, 1991a). The intensity of muscle potentials also describes a direct linear function of T_{th} (Goller and Esch, 1990a). In tethered worker honeybees in a servomechanically controlled wind tunnel, V also increases linearly with T_{th} (Esch, 1976). These concordances support expectations that effects of temperature on measures of muscle performance produce similar effects on free-flight performance.

The linear effect of T_{th} on flight speed in drones is also strikingly similar to that observed in the sheep blowfly (*Phaenicia sericata*; Yurkiewicz and Smyth, 1966) and in a tropical moth (*Urania fulgens*; DeVries and Dudley, 1990). Q_{10} ranges from 1.23 to 1.33 in the sheep blowfly, while *U. fulgens* exhibits a Q_{10} of flight speed of 2.1. The large taxonomic differences between these insects suggest a common mechanism and universality of the temperature effect.

In contrast, V does not seem to be affected by T_{th} in the same manner as force production. Greater FMR should result in larger amounts of excess force production (beyond the lift required to support body mass) which could presumably be invested in thrust. However, in spite of adequate variation, FMR was not correlated with V.

The relationship between V and T_{th} appears quite different from that between force production and T_{th} (see Figure 1B). Above a T_{th} of 40.3°C, V continued to rise, while force production decreases (Coelho, 1991b), suggesting that V is not limited by force production. Force production may not be translated into flight speed in a straightforward fashion. Perhaps our analysis was not sufficiently sensitive to detect a subtle decrease in V in this range of T_{th}. It would be interesting to see, however, how V is affected by higher T_{th}, perhaps by collecting data in hotter environments.

A biophysical model demonstrates that greater size results in higher T_{th} in drones, and T_{th} is, in fact, correlated with M_b and M_{th} (Coelho, 1991a). Thus, greater size augments V because it results in higher T_{th}. However, the lack of a direct, T_{th}-independent size effect runs contrary to predictions based upon isometric design (Lighthill, 1977). The size effect appears to be demonstrable interspecifically, but not intraspecifically. Lewis and Taylor (1967), who examined a diversity of insects, found a strong, positive size effect on V. Similarly, airspeed is strongly correlated with size and among neotropical butterflies (Dudley, 1990; Dudley and Srygley, 1994). But airspeed is not correlated with body mass in *U. fulgens* (DeVries and Dudley, 1990). It is curious that the size effect does not appear to hold intraspecifically, since one would expect greater geometric similarity within a species than among different ones.

To examine the level of geometrical similarity in drones we drew upon morphometric data from this study and our previous work (Coelho, 1991a; 1991b). Wing area is expected to scale with $M_b^{2/3}$ (Lighthill, 1977), but we found $S\ (cm^2) = 201.1M_b^{.40}$ ($R^2 = .33$, $P < .01$, $N = 106$). The expected exponent is not included in the 95% confidence interval of the empirically derived one (.29 to .51). Wing loading is expected to scale with $M_b^{1/3}$, but we found $p_w\ (N/m^2) = 201M_b^{.597}$ ($R^2 = .53$, $P < .01$, $N = 106$). Again, the expected exponent did not fall within the 95% confidence interval (.49 to .71). It appears that in drones wing-loading increases with body size more steeply, and wing size less steeply, than predicted from geometrical similarity. The lack of a size effect on V is even more surprising in light of these relationships.

The wing loading effect might be neutralized if drones were all of similar size and differences in p_w resulted from drones carrying different loads. This is, in fact, the effect observed in *worker* honey bees, which are of rather uniform size, but quite variable in M_b because of variation in filling of the honey crop (Coelho, unpublished data). Consequently, workers loaded with nectar fly slower than unloaded workers (Wenner, 1963; Coelho, 1989). This effect is unlikely in drones, however, because

they are quite variable in size, and carry only 10μl on average in the honey crop (Coelho, 1995).

It has been suggested, but never proven, that elevated T_{th} in males of certain insect species is adaptive in providing additional flight speed for mate-seeking, territorial defense, and other types of intermale mate competition (Chappell, 1984). For drones the effect of temperature on flight speed may have significant impacts on reproductive success. Mating occurs following a high-speed aerial chase wherein a large number of drones pursues a single queen (Ruttner, 1956). It is not clear precisely which characteristics of drones affect mating success (see review by Coelho, 1995), though size may be a factor (Coelho and Taylor, in press). It is conceivable that drones that are hotter, and hence faster in flight, have a higher probability of reaching the queen first and mating successfully.

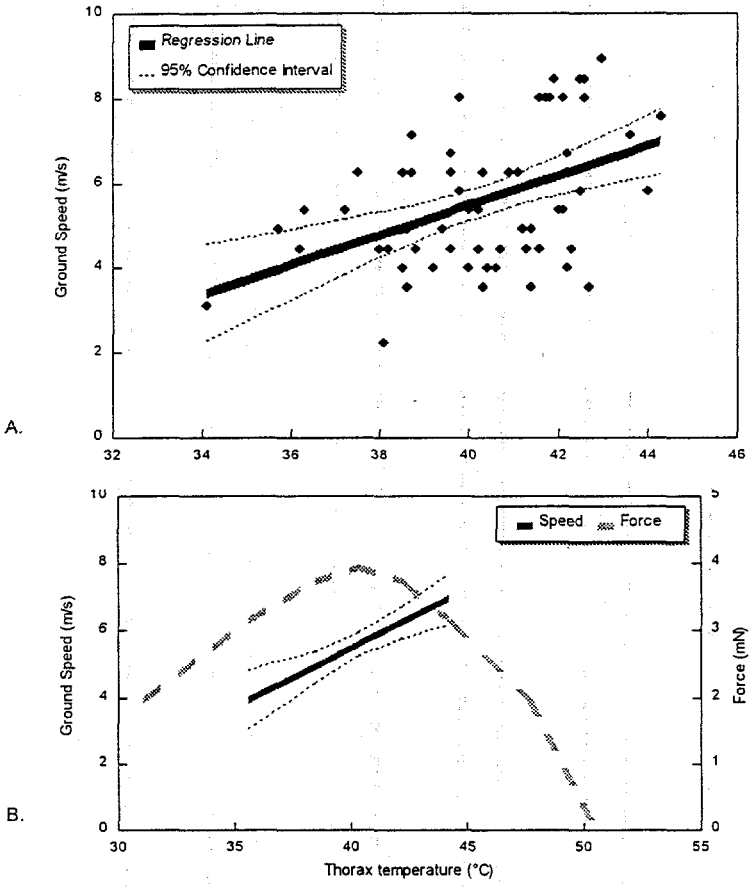


Figure 1. A. The effect of thorax temperature on ground speed. B. A comparison of the effect of thorax temperature on ground speed (solid line, regression only) and force production (dashed line, from Coelho, 1991b) in honey bee drones.

ACKNOWLEDGEMENTS

This study was supported by a WIU Research Council Grant to JRC, a WIU Honors Council minigrant to AJR, and a Summer Undergraduate Research Fellowship to AJR from the Council on Undergraduate Research.

REFERENCES

Chappell, M.A. (1984). Temperature regulation and energetics of the solitary bee *Centris pallida* during foraging and intermale mate competition. *Physiological Zoology* 57, 215-225.

Coelho, J.R. (1989). The effect of thorax temperature and body size on flight speed in honey bee drones. *American Bee Journal* 129, 811-812 [abstract].

Coelho, J.R. (1991a). Heat transfer and body temperature in honey bee (Hymenoptera: Apidae) drones and workers. *Environmental Entomology* 20, 1627-1635.

Coelho, J.R. (1991b). The effect of thorax temperature on force production during tethered flight in honey bee (*Apis mellifera*) drones, workers, and queens. *Physiological Zoology* 64, 823-835.

Coelho, J. R. (1995). The flight characteristics of drones in relation to mating. *BeeScience* 4,2-6.

Coelho, J.R. and Taylor, O.R., Jr. (in press). Size-related mating preferences of honeybee drones. *Journal of the Kansas Entomological Society.*

DeVries, P.J. and Dudley, R. (1990). Morphometrics, airspeed, thermoregulation, and lipid reserves of migrating *Urania fulgens* (Uraniidae) moths in natural free flight. *Physiological Zoology* 63, 235-251.

Dudley, R. (1990). Biomechanics of flight in neotropical butterflies: morphometrics and kinematics. *Journal of Experimental Biology* 150, 37-53.

Dudley, R. (1991). Comparative biomechanics and the evolutionary diversification of flying insect morphology. In *The Unity of Evolutionary Biology* (ed. E. Dudley), pp. 503-514. Portland:Dioscorides Press.

Dudley, R. and Srygley, R.B. (1994). Flight physiology of neotropical butterflies:allomery of airspeeds during natural free flight. *Journal of Experimental Biology* 191, 125-139.

Esch, H. (1976). Body temperature and flight performance of honey bees in a servo-mechanically controlled wind tunnel. *Journal of Comparative Physiology* 109, 265-277.

Esch, H., Nachtigall, W. and Kogge, S. (1975). Correlations between aerodynamic output, electrical activity in the indirect flight muscles and wing positions of bees flying in a servomechanically controlled wind tunnel. *Journal of Comparative Physiology* 100, 147-159.

Goller, F. and Esch, H. (1990a). Muscle potentials and temperature acclimation and acclimatization in flight muscles of workers and drones of *Apis mellifera*. *Journal of Thermal Biology* 15, 307-312.

Goller, F. and Esch, H. (1990b). Comparative study of chill-coma temperatures and muscle potentials in insect flight muscles. *Journal of Experimental Biology* 150, 221-231.

Josephson, R.K. (1981). Temperature and the mechanical performance of muscle. In *Insect Thermoregulation* (ed. B. Heinrich), pp. 19-44. New York: John Wiley and Sons.

Lewis, T. and Taylor, L.R. (1967). *Introduction to Experimental Ecology*. London: Academic Press.

Lighthill, J. (1977). Introduction to the scaling of aerial locomotion. In *Scale Effects in Animal Locomotion* (ed. T.J. Pedley), pp. 365-404. London: Academic Press.

Marden, J.H. (1987). Maximum lift production during takeoff in flying animals. *Journal of Experimental Biology* 130, 235-258.

Ruttner, F. (1956). The mating of the honeybee. *Bee World* **37**, 1-15.

Schmid-Hempel, P., Kacelnik, A. and Houston, A.I. (1985). Honeybees maximize efficiency by not filling their crop. *Behavioral Ecology and Sociobiology* 17, 61-66.

Wenner, A.M. (1963). The flight speed of honeybees: a quantitative approach. *Journal of Apicultural Research* 2, 25-32.

Yurkiewicz, W.J. and Smyth, T., Jr. (1966). Effect of temperature on flight speed in the sheep blowfly *Journal of Insect Physiology* 12, 189-194.

The Influence of Menstrual Cycle Phases on the Chaotic Behavior of R-R Intervals in College-Age Women

Allyson Rich and Stephanie Duncan

Department of Biology
Saint Joseph's University
Philadelphia, PA 19131

Faculty Advisor:

James J. Watrous, Ph.D

ABSTRACT

Heart rate variability is a phenomenon of physiology which has been studied for many years in relation to such things as aging and disease. The R-R intervals of a normal electrocardiogram (ECG) have been shown by others to exhibit chaotic behavior. This study focuses on the relationship between phases of the menstrual cycle and R-R intervals. The R-R intervals of six female subjects showed differences in chaotic behavior, as determined by the parameters of Fast Fourier Transform (FFT), Lyapunov exponent, capacity, and correlation dimensions, at certain phases of the menstrual cycle, specifically ovulation and menses. The male subject in this study showed considerably less variability for the duration of the study. We conclude that the phases of the menstrual cycle appear to have some influence on the variability of R-R intervals; thus, chaotic behavior in heart rate can help determine or possibly predict the phases of the menstrual cycle.

INTRODUCTION

This study focuses on the relationship between heart rate variability and phases of the menstrual cycle in college-aged women. Previous research has shown the connection between variability of heart rate and other changes in the body. Common examples are the loss of chaos with age (Lipsitz & Goldberger, 1992) and the prediction of risk for sudden cardiac death. The goal of this study is to examine the changes that take place in the female body as part of the menstrual cycle and their relationship to the heart rate, specifically the chaotic characteristics of the interval between successive R waves.

Chaos can be defined by understanding the definition of randomness and periodicity. Random behavior never repeats itself, is unpredictable, and is disorganized. Very few biological processes are considered fundamentally random, such as genetic translocation and fertilization. Periodic behavior, however, is predictable because it always repeats itself over some time interval and is governed by an underlying deterministic process. It is considered normal for biological systems to be periodic, such as sinus rhythm and menstruation. Chaos is distinct from these two concepts, yet has characteristics of both. Chaotic behavior seems disorganized, yet it is deterministic. A few biological systems are considered chaotic, such as evolution models, the electroencephalogram, and models of cardiac behavior (Denton et al, 1990).

Chaos theory dates from the work of Henri Poincare in the late 19th century. The chaotic system essentially produces random looking results that are not truly random (Peters, 1991). Traditional theory would lead us to believe that the ECG time series is periodic; however, analysis of the time series reveals a number of irregularities. Goldberger et al (1985), among others has concluded that the normal human heart follows deterministic dynamics of a chaotic nature (West, 1990).

Several techniques are available to distinguish chaos, both quantitatively (Lyapunov exponent) and qualitatively (Phase-space plot). Many analytic techniques are used to detect nonlinear dynamic behavior (chaos). The Fast Fourier Transform (FFT) is one such technique which results in a graph of the frequency vs. the signal amplitude and permits determination of the most predominant frequencies for the data. The graph of the data as phase-space plots usually represents the two dimensions of state space and plots of chaotic signals together exhibit a definite pattern, but do not have periodic trajectories. Therefore, they should not appear as a closed loop. The Dominant frequencies view the data in terms of a finite number of complex poles of discrete frequency, similar to an FFT. Random and chaotic data give rise to broad spectra versus the few dominant peaks for periodic data, and chaotic data show a basic linear relationship with a negative slope. Several quantitative techniques distinguish chaos from data which is simply periodic, random, or noisy. Three common parameters are the Lyapunov exponents, capacity, and correlation dimensions. Chaotic orbits will have at least one positive Lyapunov exponent, a measure of the rate at which nearby trajectories in phase space diverge. Capacity dimension, which is calculated by successively dividing the phase space with embedding dimension D, should saturate at some value less than five for chaotic data (Sprott, 1992).

The theory of chaos in heart rate variability is important for many reasons and has several implications as far as its clinical usefulness. Chaos in cardiac physiology is commonly being studied to determine whether it is indicative of a healthy heart or certain arrhythmias. Nonlinear dynamics of the female subject and the female subject's heart rate variability extends the study to include specifically women's physiological events and could be used to diagnose pathologies specific to females or to explain or predict changes specific to physiolgical events which occur at different phases of a woman's life, e.g., menstrual cycle.

MATERIALS AND METHODS

Electrocardiograms (ECGs) recorded of six female college-age subjects were taken in the quiet, awake state in the upright seated position, following a five-minute period of acclimation, three times a week over a sixty-day period.

A medical history was taken of each subject, all of which revealed no significant variables and normal menstrual cycles. Duration of each menstrual phase and the onset of ovulation was determined based upon the length of each individual's cycle. One healthy male subject was added to the study as a control; ECGs were taken once a week and beginning in the sixth week, taken three times a week. All of the volunteers signed a written consent form after the test protocol was described.

ECGs were recorded by applying Vermed EL503 vinyl disposable electrodes, one on the inside of each wrist and one on the inside of the left ankle (a ground electrode). Using a Biopac system including an EKG100A module set to receive only R waves at a gain of 5000 and a MP100 amplifier module, data were recorded for 900 seconds at 50 samples per second, resulting in approximately 1000 R-R intervals. These records were stored in a Microscan 3G/AD1 (486, 33 mHz). The AcqKnowledge (Version 2.0, 1992-93 BIOPAC Systems Inc.) program was used to calculate the change in time between R waves, and the results were stored in a text file. The data files were analyzed using a Chaos Data Analyzer program (1992, J.C. Sprott, University of Wisconsin, 53706) for phase-space plots, dominant frequencies, and return maps.

RESULTS

The results obtained for all subjects qualitatively exhibited a basic linear relationship with broad spectra in dominant frequencies, discernible fractal structure for phase-space plots, and little dispersion in return maps (Figure 1). The phase space plots remained constant throughout the menstrual cycle, yet minor differences in the distribution of points were evident in all the female subjects' plots. These changes were not phase-specific and were not evident in the phase space plots of the male subject.

Fast Fourier Transforms of the male subject displayed shifts of the predominant frequency (1.3 Hz) of no more than (+ or -) 0.2 Hz. Generally, three peaks were evident in the FFTs of the six female subjects; the predominant peak was between 1 and 2 Hz. Consistent shifts in the predominant peak were noted in most of the female subjects from menses to ovulation (Figure 2). Three subjects did not show a third frequency distribution peak immediately prior to ovulation.

The graphs of the values for Lyapunov exponent, capacity dimension, and correlation dimension showed variation from individual to individual and from phase to phase of the menstrual cycle. Capacity dimension was the strongest piece of evidence. Subject A (the male subject) did not show nearly the amount of variation for his values as compared to those of the female subjects. The Lyapunov graph showed a low value toward the beginning and a gradual decrease in values with time. For all of the female subjects, values for each parameter varied from subject to subject, the most obvious being consistent increases during menses for the capacity dimension.

DISCUSSION

Chaotic behavior was evident for all subjects according to the parameters that were measured. For all subjects, R-R intervals revealed broad spectra with a linear relationship in frequency distribution. The dominant frequencies along with the discernible structure in the phase-space plots indicated chaos rather than a simply periodic system or noise (Figure 1). The phase-space plots also showed chaotic structure, differing from subject to subject, with no phase-related pattern. The male subject showed less variability than the females in his phase-space plots, which may suggest some underlying phase-related influence on the chaotic behavior of R-R intervals.

The shifts in the FFTs varied individually from subject to subject from menses to ovulation. The presence of a third peak was questionable for Subject X immediately prior to and post menses, and Subject Z during ovulation. This may suggest that the presence of this peak is a potential indicator of a particular phase of the menstrual cycle. The shifts in the predominant peak for the male subject were considerably smaller in comparison to the female subjects, again emphasizing less variability for the control.

The graphs for the values of Lyapunov exponents, capacity dimension, and correlation dimension varied from individual to individual, with differences for each parameter according to phase. Phase-dependent differences, consistent for all female subjects, were not obvious;

yet trends became apparent during consecutive cycles. For example, Subject U and Subject V's Lyapunov exponents decreased right after ovulation. Subject X's Lyapunov increased right after ovulation. Therefore, some distinctive change in value may suggest the onset or completion of the phase of ovulation.

Capacity dimension at the three phases of the menstrual cycle for all of the female subjects was the strongest piece of evidence of chaotic behavior. Some oscillations were obvious for the subjects' values since all of the subjects' data was recorded for two cycles. For each subject, the changes which occurred according to the three phases were consistent; however, at which phase the change occurred, differed from individual to individual. Significant jumps in the numbers were obvious around the time of menses and ovulation for many of the subjects: Subjects U, X, and Y showed either a significant increase or decrease in value during menses or ovulation. It seems difficult to make general predictions according to the menstrual cycle for all of the female subjects. Significant changes are obvious yet seem to be dependent on the individual rather than the phase (individual-specific over phase-specific). Factors such as medication, movement, talking, noise distractions, stress, and other external stimuli may have served as variables when recording the ECG. Uncertainty in predicting the phase of ovulation and the small sample size may affect conclusions as well.

This study suggests many practical applications as far as the possibility of predicting phases of the cycle. The fact that this experiment provides a method for describing, with chaotic behavior, the phases of the menstrual cycle suggests a new approach to pinpointing these phases. This would be particularly exciting in terms of fertility problems or menstrual irregularity. Also, the lack of or decline in chaotic behavior points to disease or death, as suggested by previous studies in cardiac physiology. With more subjects and an increased frequency and duration of the study, more could be said, universally, about menstrual phase-related changes in R-R intervals. Data suggest, however, underlying patterns in the chaotic behavior of R-R intervals, specific to the individual.

ACKNOWLEDGEMENTS

This study was supported by a grant from the Howard Hughes Medical Institute.

REFERENCES

Glass L, Hunter P, McCulloch A. Theory of Heart: Biomechanics, Biophysics, and Nonlinear Dynamics of Cardiac Function. New York: Springer-Verlag, 1991.

Denton KA, Diamond GA, Helfant RH et al. A fascinating rhythm: a primer on chaos theory and its application to cardiology. Amercian Heart Journal 1990.(6):1419-1435.

Lipsitz LA, Goldberger MD. Loss of 'Complexity' and Aging. Potential Applications of Fractals and Chaos Theory to Senescence. Journal of the American Medical Association 1992; Vol 267, No. 13. pg. 1806-1809.

Peters EE. Chaos and Order in the Capital Markets. A New View of Cycles, Prices and Market Volatility. New York: John Wiley & Sons, 1991.

Pool R. Is it Healthy to be Chaotic? Science 1989. (243): 604-607.

West BJ. Fractal Physiology and Chaos in Medicine. Singapore: World Scientific, 1990.

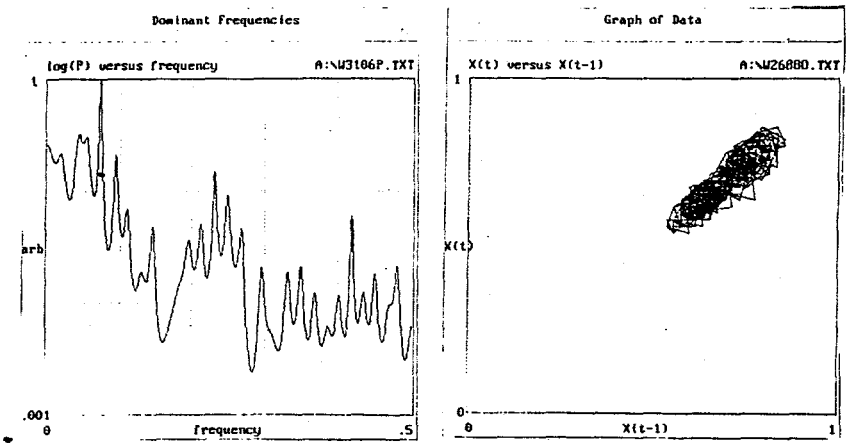


Figure 1- Dominant frequencies (power spectrum in log-linear form) and phase-space plot of typical chaotic behavior of female subject

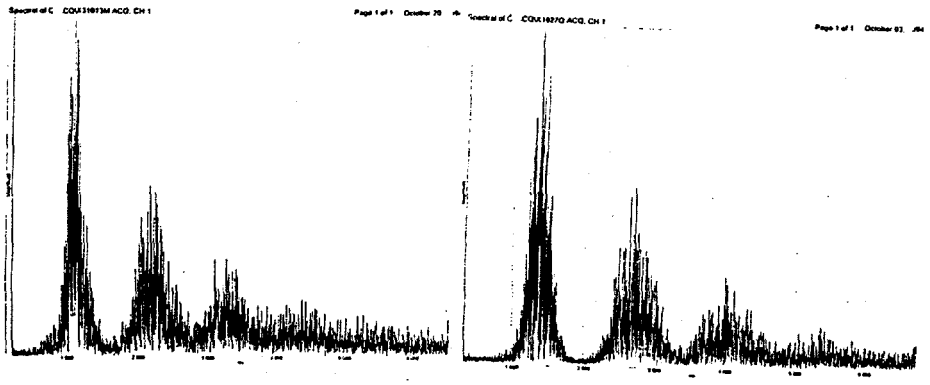


Figure 2- Fast Fourier Transform of female subject during menses and ovulation, exhibiting shift in predominant peak of frequency distribution.

ALCOHOL CONSUMPTION AND ITS EFFECTS ON GRADE POINT AVERAGE AND ACUTE ILLNESS IN COLLEGE STUDENTS

Marlene A. Faust
Nazareth College of Rochester, 4245 East Avenue
Rochester, NY 14618

Advisor: Robert Byrd, M.D.
Rochester General Hospital

To investigate correlations between frequency of alcohol consumption, grade point average and illness in a college population. Convenience sampling of 360 students at a small, private northeastern college using a questionnaire format to collect data. Eight graduate students were eliminated from the analysis, resulting in a sample study where N= 352. Students who consume more than 8 alcoholic drinks a week are 3.3 (1.9, 6.0) times as likely to have a low GPA as compared to students who do not drink at all, or drink less than 8 drinks a week. This ratio remains constant when controlling for gender, age and year in school. There was no correlation found between students who exhibit a high frequency of consumption and increased frequency of illness. Increased alcohol consumption can have a detrimental effect on a student's academic performance, but does not seem to effect frequency of illness.

Introduction:Excessive alcohol abuse is a serious problem on college campuses. One study reports that 7 out of 8 college students drink (Wechsler, et al., 1994). Alcohol consumption has social, educational and physiological impacts. Research has shown that increased alcohol consumption may have a detrimental effect on GPA (Lall and Schandler, 1991), and may follow trends based on gender (Gleason, 1994 and Svenson, et al., 1994), family history of abuse (Lichtenfeld and Kayson, 1994), year in school and level of self-esteem (Maney, 1990).

There are several physiological effects of alcohol consumption which may contribute to lower academic performance and a decrease in the general health of the drinker. Alcohol depresses the central nervous system which can result in impaired judgment and also impairs cognitive and perceptual motor abilities (Mungas, et al., 1994). Alcohol inhibits vitamin and calcium uptake; repeated drinking episodes may cause damage to hair and skin (Harding, 1993). In addition, persons who engage in repeated use of alcohol may develop alcohol dependency (Harding, 1993). All these negative side effects of frequent alcohol consumption may influence the frequency of illness for the consumer.

An individual's drinking behavior may also be affected by their environment. Subjects who typically have lower self-esteem may use alcohol to fit into the crowd or raise their self image (Maney, 1990). Previous studies have shown that increased alcohol consumption is also correlated with a lower grade point average (Lall and Schandler, 1991; Maney, 1990 and Harding, 1993). The purpose of this study is to replicate these results in a target population and investigate if a further correlation exists between alcohol consumption and increased frequency of illness.

Methods: The sample population is a small, private, predominately Caucasian liberal arts college in Rochester, New York with an enrollment of 1,745 undergraduates and 885 graduates in which the male/female ratio is 30/70. A pilot study consisting of 40 students was conducted prior to the distribution of the survey to the sample population. The questionnaire was then modified slightly before it was distributed to the sample population. From this population 400 students were sampled. Participation consisted of completing an eleven item questionnaire of closed ended questions designed to obtain information on typical drinking behaviors, academic performance and history of illness. Students were asked to provide self-reported GPA as well as the frequency of illness and number of days and amount of alcohol consumed in the past week. Students were sampled in classes, laboratories and the dining facilities on campus. Three hundred and sixty usable questionnaires were returned

resulting in a 90% return rate. Eight graduate students were eliminated from the sample before analysis, since the focus of the study was the undergraduate populatio resulting in N = 352.

Data collected on frequency of illness was dichotomized based on information presented in Garibaldi (1991). This article reported that adults experience an average of three upper respiratory infections per year. Therefore, the data was divided into two groups: those who were sick 0-2 times (considered healthy) and those who were sick 3 or more times. The data collected on grade point average was dichotomized based on the guidelines and policies outlined in the Nazareth College Student Handbook (1992-93). A GPA of 3.0 or better was considered high, while a GPA below 3.0 was considered low. Finally, the information collected on the number of alcoholic drinks consumed in a week was divided based on information obtained from Maney (1990). Zero to light drinking was defined as eight or less drinks per week, while moderate to heavy drinking was defined as more than eight drinks per week.

Results:The study sample was compared to the college population in terms of gender, and it was determined that there was not a significant difference between the two populations (p= >0.1). Therefore, the study sample was representative of the college population in terms of gender.

Data was also collected in regards to age and place of residence. 56% of the sample were aged 18-20 years, 28% were 21-23 years old and 16% were 24 years or older. 69% of the students lived on campus while the remaining 31% had residence off campus. Table 1 presents distributions of the dependent and independent variables of this study, specifically the frequency of alcoholic consumption per week (independent variable), self-reported GPA (dependent variable) and frequency of illness in the past semester (dependent variable).

Table 1: Distribution of Dependent and Independent Variables in Study Sample

Variable	Percent	Variable	Percent
Number of Drinks		GPA (self-reported):	
Consumed in a Week:		4.0-3.5	25
0	39	3.49-3.0	30
1-2	17	2.99-2.5	32
3-4	13	2.49-2.0	10
5-8	10	Below 2.0	2
9-16	9	Frequency of illness:	
17-20	4	0	41
21-24	2	1-2	49
25 or more	7	3 or more	9

Table 2: Odds Ratios and Confidence Intervals for Stratified Analysis of Frequency of Alcohol Consumption and GPA

Variables	Odds ratio	Confidence Intervals
Frequency of alcohol consumption and gpa:		
	3.32	(1.9, 6.0)
Frequency of alcohol consumption, gpa and gender:		
male	2.82	(1.2, 6.6)
female	3.65	(1.3, 10.4)
combined	3.14	(1.7, 5.7)
Frequency of alcohol consumption, gpa and year:		
freshman	2.40	(.7, 8.7)
sophomore	7.27	(2.2, 26.0)
junior	2.77	(.8, 10.4)
senior	1.57	(.4, 5.9)
combined	3.12	(1.8, 5.4)
Frequency of alcohol consumption, gpa and age:		
18-20 yrs.	3.94	(1.8, 8.9)
21-23 yrs.	2.04	(.7, 5.7)
24 yrs. or more	0	(0, 67.9)
combined	2.92	(1.7, 5.1)

The frequency of alcohol consumption and gpa were analyzed through a cross sectional cumulative index to indicate if an association existed between variables. An odds ratio of 3.32 (1.9, 6.0) showed that students who consume alcohol frequently (defined as 8 or more drinks a week) are approximately three times as likely to have a lower GPA (defined as below a 3.0 on a 4.0 scale). The odds ratio remained fairly constant when the data was controlled for gender, age and year of study. This data is presented in Table 2. No correlation was found between frequency of alcohol consumption and frequency of illness. It was also shown that of students missing more than five classes, they are 2.2 (1.2, 3.8) times as likely to be male.

Conclusions: This study demonstrates a negative correlation between the frequency of alcohol consumption and GPA, that is an inverse relationship exists between the two fields. This finding is consistent with similar studies conducted in high school seniors (Schulenburg, et al., 1994) and college students (Prendergast, 1994). There are several reasons why increased alcohol consumption might lead to decreased academic performance. For example, when students party regularly they are re-directing energy which might otherwise have been spent on academic work (Lall and Schandler, 1991). Party behavior may be interfering with a student's sleeping habits which may make an improperly rested student perform poorly in class and take additional time away from academic studies. In cases where excessive or binge drinking occurs, students may experience physical sickness and hangovers which may result in lowered performance and missed classes.

An alternative hypothesis suggested by previos studies is that it is low academic performance which drives students to work out their frustrations through alcohol use (Prendergast, 1994). This type of cross-sectional study does not show cause and effect, it is clear that alcohol consumption and grade point average are associated. The specifics of this relationship have yet to be elucidated.

Despite the numerous, well documented physiological effects of alcohol, no correlation was found between the number of alcoholic drinks consumed and the number of times a student was sick. P-values were insignificant ($p = .576$) when the frequencies of alcohol consumption and the frequencies of illness were compared. Males and females reported similar frequencies of illness indicating that there was no reporting bias for that particular field. The data collected on GPA was self-reported, therefore there may be some error in the data, as people may tend to round up or over exaggerate their gpa.

Previous studies have defined heavy drinking as an average of 1 ounces or more of alcohol per day and problem, or heaviest, drinking as more than two ounces of alcohol per day (Maney, 1990). Using that definition, and data collected concerning number of drinks consumed per week and the number of days in which alcohol was consumed, it was determined that 7% of the sample exhibited heavy/problem drinking. Studies at large universities indicate that between 7%-16% of the student population exhibit heavy/problem drinking behaviors (Lall and Schandler, 1991). Therefore, the sample in this study falls within the previously reported range at the lower end of the scale.

Data analysis also indicated other interesting trends. Students who live on campus reported higher frequencies of alcohol consumption than students who lived off campus ($p = .003$). This might be due to the fact that students who live off campus are typically older students. They are also more likely to be holding down part-time jobs, or married, possibly with children, and may have less time and energy to devote to partying and drinking. It was also shown that students who were sick more than three times did not miss more classes than those students who reported being sick 0-2 times ($p = .00008$). This data suggests that students do not typically miss classes because they are sick. Rather, they may miss classes due to oversleeping, lack of interest, or various other reasons besides physical health.

This work will help to identify trends and relationships associated with alcohol consumption in college populations. Colleges can use data concerning frequency of drinking and impacts of alcohol consumption to assess alcohol problems on campus and develop strategies for identifying and helping problem drinkers. This data, focused on a small, private, liberal arts college, is useful for comparison with studies focused on large universities and clusters of smaller colleges.

Works Cited:
Garibaldi RA. Epidemiology of Community Aquired Respiratory Tract Infections in Adults. *The Americal Journal of Medicine.* 1991; 78: 32-37.
Gleason NA. College Women and Alcohol: a relational perspective. *Journal of American College Health.* 1994; 42: 279-289.
Harding FM. *Teamwork for Healthy Campuses, NYS College Alcohol and Other Drug Programs.* New York State Office of Alcoholism and Substance Abuse; Albany, NY: 1993.
Lall R, Schandler SL. Michigan Alcohol Screening Test (MAST) Scores and Academic Performance in College Students. *College Student Journal.* 1991; 21: 245-251.
Lichtenfeld M, Kayson WA. Factors in college students' drinking. *Psychological Reports.* 1994; 74: 927-30.
Maney DW. Predicting University Students' Use of Alcoholic Beverages. *Journal of College Student Development.* 1990; 31: 23-32.
Mungas D, Ehlers CL and Wall TL. Effects of Acute Alcohol Administration on Verbal and Spatial Learning. *Alcohol and Alcoholism.* 1994; 29: 163-169.
Nazareth College of Rochester Undergraduate Catalog 1992-1993.
Prendergast, ML. Substance Use and Abuse Among College Students: a Review of Recent Literature. *Journal of American College Health.* 1994; 43: 99-113.
Schulenburg J, Bachman JG, O'Malley PM, Johnston LD. High School Educational Success and Subsequent Substance Abuse: a Panel Analysis Following Adolescents into Young Adulthood. *Journal of Health and Social Behavior.* 1994; 35: 45-62.
Svenson LW, Jarvis GK, Campbell RL. Gender and age differences in the drinking behaviors of university students. *Psychological Reports.* 1994; 75: 395-402.
Wechsler H, Isaac NE, Grodstein F, Sellers DE. Continuation and Initiation of Alcohol Use from the First to the Second Year of College. *Journal of Studies on Alcohol.* 1994; 55: 41-45.

Alcohol Inhibits Tumor Necrosis Factor-alpha Production by Alveolar Macrophages during Pneumonia caused by *Streptococcus pneumoniae*

Paul Nelson and Elaina Bleifield

Department of Clinical and Population Sciences
University of Minnesota, Twin Cities
225 Veterinary Teaching Hospitals
1365 Gortner Ave
St. Paul, MN 55108

Faculty Advisor:

Martha A. Mellencamp

Chronic alcohol abuse increases susceptibility to community-acquired pneumonia caused by *S. pneumoniae* (Pn). This observation along with laboratory studies suggest that alcohol impairs host defense mechanisms against bacterial infection. The purpose of this study was to investigate how ethyl alcohol (ethanol) affects early lung defense mechanisms against Pn including production of the proinflammatory cytokine, tumor necrosis factor-α (TNF-α). TNF-α is produced by lung macrophages after bacterial challenge. The function of TNF-α is to recruit and activate other phagocytic cells to fight the infection. Male Sprague-Dawley rats were fed ethanol or control diet for 7 d prior to challenge with Pn. At 3 h post challenge, alveolar secretions were collected from the lungs by bronchoalveolar lavage, concentrated, and assayed for TNF-α activity using the L929 bioassay. TNF-α was present in lung fluids from control-fed rats (mean ± SD= 61.4 ± 72.14 pg/ml, n=11). However, ethanol consumption significantly reduced the amount of TNF-α recovered in lung fluids to 52% ± 28% of control levels (25.3 ± 29.0 pg/ml, n=9, $P<0.05$). In vitro studies using ethanol-treated macrophages confirmed these results. Reduction of early inflammatory mediators such as TNF-α may, in part, be responsible for increased lethality of Pn in the alcoholic host.

INTRODUCTION

Pneumonia caused by *Streptococcus pneumoniae* (Pn), is the most common cause of community-acquired pneumonia in adults and may be a lethal disease in immunocompromised patients (Coonrod, 1989). Alcoholics are immunocompromised and are especially susceptible to pneumococcal pneumonia (Research Triangle Institute, 1985). The immunomodulatory effect of ethanol on these patients has been the object of a great deal of study.

Pn is a gram positive, encapsulated diplococcus that often colonizes the human nasopharynx and can proceed from there to the lungs and cause disease (Coonrod, 1989). Pn are aspirated into the lungs where alveolar macrophages (AM) are the first line of cellular defense (Coonrod, 1989). The capsule of Pn inhibits phagocytosis by AM and other phagocytes even in the presence of opsonins. An acute inflammatory response is, however, induced by the Pn cell wall components teichoic acid and peptidoglycan (Tuomanen,

Rich, Zak, 1987). This inflammatory response consists largely of neutrophils (PMNL) and is a characteristic sign of pneumococcal pneumonia.

In addition to phagocytosis, an important function of AM is to produce biochemical signals called cytokines. Cytokines initiate and modulate immunologic responses to bacterial or viral challenge. TNF-α is an AM-derived cytokine that recruits and activates PMNLs as part of the inflammatory response. We have shown that AM can be induced by Pn to produce TNF-α in vitro. Recently, Nelson and colleagues found that acute ethanol administration in rats significantly suppressed LPS-induced TNF-α production and PMNL aggregation in the lungs (Nelson, Bagby, Bainton, and Summer, 1989). Our purpose here was to investigate TNF-α production in the lungs during experimental Pn pneumonia and to determine how its production is modulated by ethanol.

MATERIALS AND METHODS

Bacteria. *S. pneumoniae* type 3 (Pn 3) or R36a (an noncapsulated type 2 mutant) were grown by inoculating 100 µl of stock culture into 10 ml of Todd-Hewitt broth (Difco Labs). Bacteria were incubated at 37°C in 5% CO_2 for 10 h to obtain a large number of Pn in the log phase of growth. Pn were washed 3 times with Hanks' Balanced Salt Solution (HBSS) and resuspended in HBSS to the desired concentration. To confirm the number of bacteria in each experiment, bacterial suspensions were serially diluted in sterile saline and plated onto sheep blood agar plates in duplicate. After overnight incubation, colonies were counted, averaged, and expressed as colony-forming units/ml.

Animals and diets. Male Sprague-Dawley rats (120-140 g, Sasco, Inc.) were fed nutritionally adequate liquid diets (Dyets, Inc.) formulated by DeCarli and Lieber (DeCarli and Lieber, 1967). Ethanol diet contained 36% of calories from ethanol. The control diet was calorically matched to the ethanol diet by the addition of dextrin maltose. At approximately 150 g, rats were weight-paired and fed control diet for 3 d. Following this acclimation period, one rat of each pair was fed ethanol diet and the other the control diet for 7 d. To maintain equal calorie intake, the control rat was fed the volume its ethanol pair consumed the previous day.

In vivo experiment. The purpose of this study was to determine if Pn infection of the lungs induced detectable TNF-α production in alveolar secretions. In addition, the effects of alcohol diet on TNF-α production were assessed. Two experiments (control n=11, ethanol n=9) were performed (Fig. 1). Rats were fed liquid diets as described above. On day 7, rats were transtracheally challenged with Pn R36a (Bakker-Woudenberg, 1979). After 3 h, alveolar secretions were collected by bronchoalveolar lavage (BAL), and TNF-α levels in these secretions determined by bioassay. Detailed methods are given below.

Pn challenge and bronchoalveolar lavage. Rats were anesthetized and the trachea exposed by blunt dissection. A 22 guage catheter was inserted into the trachea and approximately 2 x 10^7 cfu of Pn (R36a) were delivered into the lungs followed by 0.2 ml of air. The wound was closed with a sterile metal clip. At 3 h post-infection rats were anesthetized and the trachea and lungs removed. BAL was performed with cold HBSS+heparin (10 U/ml) until 30 ml were recovered. Cells were removed by centrifugation and the BAL fluid (BALF) was concentrated by ultrafiltration using a membrane

(Amicon, Inc.) with a 10,000 Da molecular weight cut-off (TNF-α M.W.=17,000 Da). Concentrated BALF was frozen at -80°C for later analysis in the TNF-α bioassay.

In vitro experiment. The purpose of this experiment was to confirm TNF-α production by AM and alcohol modulation of this system *in vitro*.

Culture of AM. AM obtained by BAL were washed 3 times and suspended in Dulbecco's Modified Eagle Medium (DMEM) with 5% fetal bovine serum (FBS), L-glutamine, gentamicin, and 0.5% ethanol. Cells were counted and plated in 96-well plates at 2.5 x 10^5 cells/well. After overnight incubation at 37°C with 5% CO_2, ethanol or medium was added. After an additional 4 h, heat-killed Pn 3 (40:1 Pn 3:AM) were added in the presence of 0.5% ethanol or medium. Culture supernatants were collected and frozen at -80° C.

TNF-α bioassay. Bioactive TNF-α was determined using the L929 fibroblast assay (Mosmann, 1983). Recombinant mouse TNF-α (R&D Systems) was used as a standard. Cytotoxicity was measured colorimetrically using (3-[4,5-Dimethylthiazol-2-yl]-2,5-diphenyltetrazolium bromide) (MTT) uptake by viable cells and measuring the absorbance at 570 nm. Samples were assayed in duplicate, using two-fold dilutions to reach the approximate 50% cytotoxicity point. The amount of TNF-α in the sample was calculated from the standard curve and is expressed as pg/sample or pg/ml.

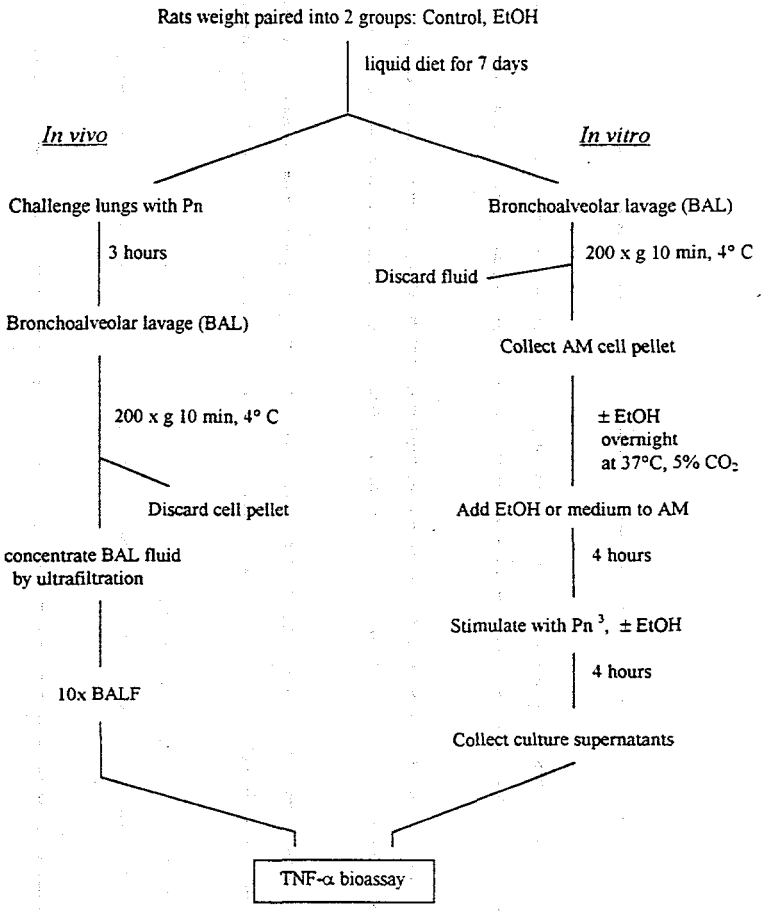


Fig. 1. Experimental Design

RESULTS AND DISCUSSION

Figure 2 shows that TNF-α was present in alveolar secretions 3 h after pulmonary challenge with Pn (panel A). These results confirmed our initial hypothesis that Pn induces production of TNF-α by AM . Ethanol diet decreased the amount of TNF-α in the lungs by one-half when compared with control rats (panel B, 53% of controls). These results are consistent with the *in vitro* experiments demonstrating that ethanol diet or exogenous ethanol in tissue culture medium (0.5%) significantly suppressed TNF-α production by isolated AM (Fig. 3).

Reduced levels of TNF-α during the early stages of Pn infection could have a number of implications. Lower levels of TNF-α mean that there will be less up-regulation of adhesins in vascular endothelial cells which means that fewer PMNLs will reach the alveolar space. However, we know that in this model PMNL recruitment is not affected. This would imply that another mechanism of chemotaxis or recruitment is involved. It is also possible that the PMNLs are able to migrate into the infected lung tissue but are not activated due to the low TNF-α concentration. This might result in the accumulation of large numbers of neutrophils that exert little or no antimicrobial effect. These possibilities are being investigated in our laboratory.

REFERENCES

Bakker-Woudenberg, deJong-Hoenderop, Michel,. Infection and Immunity, Efficacy of antimicrobial therapy in experimental rat pneumonia: effects of impaired phagocytosis, Vol. 25, 1979. pg. 366-75

Coonrod JD,. Seminars in Respiratory Infection, Pneumococcal pneumonia, Vol. 4, 1989. pg. 4-11

DeCarli, Lieber,. Journal of Nutrition, Fatty liver in the rat after prolonged intake of ethanol with a nutritionally adequate new liquid diet, Vol. 91, 1967. pg. 331-36

Mosmann T,. Journal of Immunological Methods, Rapid colorimetric assay for cellular growth and survival: application to proliferation and cytotoxicity assays, Vol. 65, 1983. pg. 55-63

Nelson, Bagby, Bainton, Summer,. Journal of Infectious Disease, The effects of acute and chronic alcoholism on tumor necrosis factor and the inflammatory response, Vol. 160, 1989. pg. 422-29

Research Triangle Institute (1985) Report to the National Institute on Alcohol Abuse and Alcoholism (administrative document). Research Triangle Park, NC: RTI.

Tuomanen, Rich, Zak,. American Review of Respiratory Disease, Induction of pulmonary inflammation by components of the pneumococcal cell surface, Vol. 135, 1987. pg. 869-74

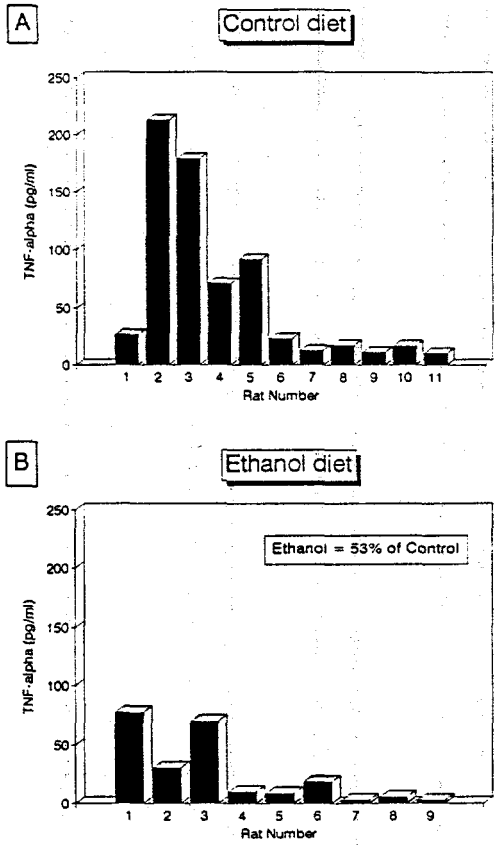


Figure 2. Effects of control (panel A) or ethanol (panel B) diet on TNF-α production in the lungs following Pn challenge. Rats were fed ethanol or control diet for 7 d before transtracheal challenge with *S. pneumoniae* R36a. Alveolar secretions were collected by BAL three hours later and assayed for TNF-α.

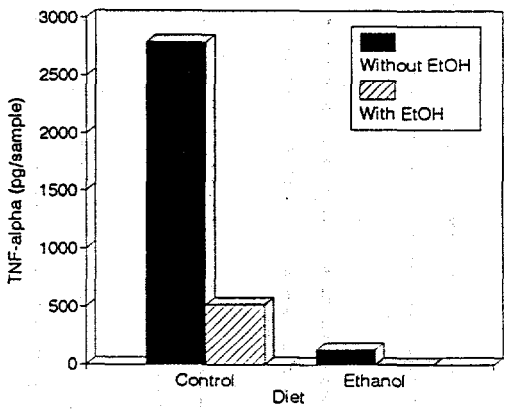


Figure 3. Effect of diet on TNF-α production by rat AM stimulated with Pn 3 *in vitro*.

A Study of the Acceptance Rates of Prenatal Genetic Testing Among Women with High Risk Pregnancies

Tara Butler

School of Natural Science
Hampshire College
Amherst, Massachusetts 01002-5001

Faculty Advisors:
Ann McNeal and Chris Jarvis

Prenatal genetic testing is an area that is quickly growing in technology and usage. This study looked at whether or not the distribution of four prenatal services (genetic counseling, alpha-fetoprotein screening, stage II ultrasound, and amniocentesis) was equal among different demographic groups and socioeconomic levels. The study sample consisted of 252 women, all of advanced maternal age (>35). It was found that procedures were offered more frequently to women who were >37 and to those who had other known risks present with their pregnancies. There were no significant differences visible across other demographics or across socioeconomic levels.

INTRODUCTION

The past few decades have seen a great deal of advancement in many areas of science. Despite some controversy, the field of reproductive medicine and the accompanying technology have been growing rapidly in many directions since the 1970's. The 1960's saw a dramatic increase in public concern about genetic disorders, leading modern medicine to investigate many new issues in genetics (Bergsma et al., 1974). Issues that were merely ideas 20 years ago have rapidly moved into reality. With the concepts come new sets of medical, ethical and societal issues which affect the perception and usage of technologies.

Within the field of reproductive medicine, prenatal genetic testing and screening is one specific area which has grown at an outstanding pace. With this growth we have seen ethical, legal and financial controversies arise from many sources. For the first time in history women are being offered prenatal tests that may be harmful to the fetus they are carrying (Evans et al., 1989). This creates a whole new area of thought in the field of medical and personal ethics. There are endless directions from which this issue of medical and legal importance could be looked at and explored. As genetic screening tests become more available to the public, it is interesting to see when and under which circumstances health care providers and patients choose to utilize the technology.

This study focuses on a population of all the women over 35 who delivered babies or terminated a pregnancy (due to abnormal screening) at a western Massachusetts hospital in one year. Medical records for these women were used to obtain information regarding the delivery of prenatal genetic testing procedures. Specifically, differences in the availability and utilization of genetic counseling services, maternal serum screening, stage II ultrasound, and amniocentesis will be compared between pregnant women who all are at risk for having a genetically abnormal baby due to advanced maternal age (35 or greater). It was hypothesized that there would be differences in the rates that procedures were accepted by different people of different religions, races, insurance brackets, marital status, and age. Evidence has shown that some of these factors contribute to whether or not a person decides to receive prenatal genetic services.

Many studies have been done which focus on the distribution of prenatal genetic testing. Smith and Miller (1989) and Murray et al. (1980) both discuss the special considerations and the areas that are lacking in equal distribution of care. Issues of genetic testing and insurance coverage are discussed at length in Harper (1993), who focuses on potential discrimination resulting from genetic testing, and Sui (1993) looks at how insurance companies are reacting to the new availability of genetic information. Beeson et al. (1983) and Rapp (1993) both review the issues and implications of amniocentesis and genetic diagnosis in general. Beeson et al. (1983) found that three important themes were consistently present in the information that was gathered through their field work. They are. problems of access, the meaning of informed consent, and the grounds on which women accept or reject prenatal testing. Rapp et al. (1993) conclude that in many ways the impact and consequences of prenatal diagnosis are less examined than the techniques themselves.

MATERIALS AND METHODS

The data for this study was collected from pregnancy delivery records and termination records kept at Baystate Medical Center Hospital in Springfield, Massachusetts. The sample of 274 records obtained for the purpose of this study consisted of all women over the age of 35 who gave birth or terminated a pregnancy due to a positive screen for a genetic disorder in 1993. The records were requested from the medical records department under physician supervision and were all reviewed in a private records office.

Information from the records was recorded during January and February of 1995. Basic demographic information was taken from each patient's record: age at time of pregnancy, ethnicity, religion, zip code, marital status, and insurance status (private insurance, Medicaid, or private pay for services rendered). If the patient or doctor knew of any other risk factors present in the pregnancy this was recorded. Information regarding prenatal services offered and those received was obtained from each record. This information included whether or not a patient was informed of and/or accepted genetic counseling options, Alpha-fetoprotein screening, stage II ultrasound, and amniocentesis. If a patient underwent a diagnostic procedure the results were recorded, though these are not of importance in this study, with the exception of terminations, which were recorded in the final category of pregnancy outcome.

The data was recorded by hand and entered onto a spreadsheet Minitab statistical package version 8 was used to perform statistical analysis on the data obtained. Chi square tests and T- tests used $P=<.05$ as the level of significance.

RESULTS

The sample used in this study was predominantly married, white, and privately insured as shown in Table 1. For purposes of further analysis, race categories were translated into white (N=209) and non-white (N=43).

A summary of procedures offered and accepted is shown in Table 2. As expected, both the percents offered and the percents received for procedures decreases with the complexity of the test procedure.

The acceptance of procedures did not vary across most demographic categories (race, estimated socioeconomic status, insurance coverage, or marital status). All P values for these demographics were insignificant.

The rates of receiving prenatal testing procedures were higher for women aged 37+ than for those aged 35-36 (Table 3). In particular the rate of receiving stage II ultrasound was significantly higher for the older age category ($P<.025$). There was also significant ($P<.05$) difference in the rates that amniocentesis was received by women 35-36 and those 37 and over. While the overall percentage of women over the age of 35 receiving amniocentesis is 40.08%, percentages vary greatly between the two age breakdowns: among 35 and 36 year old women 35.75% receive amniocentesis,

Table 1: Demographic breakdown of the 252 women in the sample population

Demographic	Count	Percentage
Insurance Status		
Medicaid	22	10.7
Private Carrier	225	89.3
Marital Status		
Single	22	8.7
Married	214	84.9
Divorced	16	6.4
Race		
White	209	82.9
Black	12	4.8
Hispanic	18	7.1
Other	4	1.6
Unknown	9	3.6
Religion		
Catholic	122	48.4
Protestant	41	16.3
Jewish	8	3.2
Other	23	9.1
None/Unknown	58	23.0

Table 2: Tallies of total percents of population that were offered and total percents of population who received particular procedures

		Count	Percent
Offered Genetic Counseling	Yes	236	93.6
	No	16	6.4
Received Genetic Counseling	Yes	218	86.5
	No	34	13.5
Offered AFP Screening	Yes	222	88.1
	No	30	11.1
Received AFP Screening	Yes	139	55.2
	No	113	44.8
Offered Stage II Ultrasound	Yes	73	29.0
	No	179	71.0
Received Stage II Ultrasound	Yes	37	14.7
	No	215	85.3
Offered Amniocentesis	Yes	199	79.0
	No	53	21.0
Received Amniocentesis	Yes	101	40.1
	No	151	58.9

Table 3: Percent of women who received genetic procedures by age

Procedure	Age 35-36 N=179	Age 37+ N=73	Overall % N=252
Genetic Counseling:			
Received	86.0%	87.7%	86.5%
Not-received	14.0%	12.3%	13.5%
AFP Screening:			
Received	57.5%	49.3%	55.2%
Not-received	42.5%	50.7%	44.8%
Stage II Ultrasound:			
Received	11.2%	23.3%	14.7%
Not-received	88.8%	76.7%	85.3%
Amniocentesis:			
Received	35.8%	50.7%	40.1
Not-received	64.2%	49.3%	59.9%

Table 4: Percent of women who received prenatal procedures by other known risk factors

Procedure	Other Known Risks N=59	No Other Known Risks N=193	Overall % N=252
Genetic Counseling:			
Received	94.9%	83.9%	86.5%
Not-received	5.1%	16.1%	13.5%
AFP Screening:			
Received	55.9%	54.9%	55.2%
Not-received	44.1%	45.1%	44.8%
Stage II Ultrasound:			
Received	22.0%	12.4%	14.7%
Not-received	78.0%	87.6%	85.3%
Amniocentesis:			
Received	37.3%	40.9%	40.1%
Not-received	62.7%	59.1%	59.9%

that percentage jumps to 50.68% for women 37 and older. Amniocentesis and stage II ultrasound procedures were offered to women 37+ more often than they was offered to women aged 35-36, this accounts for the differences in the amounts receiving the procedures. Out of those offered the procedures the acceptance rates were not significantly different for the two groups.

The other category which showed significance was that of the other known risks to the fetus, shown in Table 4. Women with other known risks to their fetus showed an increased rate of receiving of all the procedures noted in this study. While the increase between known risk and no known risk is minimal in for some procedures, there is a significant difference ($P<.025$) in the acceptance of genetic counseling between the two groups. Again, women who had a known risk to their fetus were more likely to have been offered the option of the procedure than were women with no other known risks. The rates of acceptance did not differ significantly between the two groups.

CONCLUSION

The sample size used in this study was not extensive enough to draw any real conclusions from. While some interesting information regarding physician distribution to women of advanced maternal age and those with other known risk factors in their pregnancies was obtained, in general the sample size did not allow conclusions to be made. This study examines some very interesting data regarding the distribution of prenatal genetic services. it attempts to answer some questions while pointing us in the direction of others at the same time. In general the data obtained is very helpful in completing a mental understanding of the delivery of prenatal care and prenatal genetic services.

ACKNOWLEDGMENTS

The author would like to express her extreme gratitude to Dr. Gabriel Cohn and Michelle Murray, at Baystate Medical Center for their help with this study.

REFERENCES

Beeson, Diana, PhD, Rita Douglas, MA, Terry F. Lundsford, JD, PhD "Prenatal Diagnosis of Fetal Disorders Part II: Issues and Implications", Birth, Vol. 10: 233-241, 1983

Bergsma, Daniel, MD, Marc Lappe, PhD, Richard O. Roblin, PhD, James M. Gustafson, PhD, Natalie W. Paul. Ethical, Social and Legal Dimensions of Screening for Human Genetic Disease, Symposia Specialists, New York, 1974

Evans, Mark I., MD, Alan O. Dixler, JD, LLM, John C. Fletcher, PhD, Joseph D. Schulman, MD. Editors. Fetal Diagnosis and Therapy: Science Fiction and the Law, J.B. Lippencott Company, Philadelphia, 1989

Harper, Peter S., editorial. "The Human Genome Project and Medical Genetics", Genetics, Vol. 29: 1-2, 1992

Murray, Robert F., Jr., MD, Naomi Chamberlin, MS, John Fletcher, PhD, Ernest Hopkins, MD, Rudolph Jackson, MD, Patricia A. King, JD, Tabitha Powledge, MS. "Special Considerations for Minority Participation in Prenatal Diagnosis", Journal of the American Medical Association, Vol. 243, No. 12: 1254-1256

Rapp, Rayna. "Sociocultural Differences in the Impact of Amniocentesis", Fetal Diagnosis and Therapy, Vol. 8, (suppl. 1): 90-96, 1993

Siu, Albert J., MD, MSPH. "Conflicting Aims: Voluntary Health Insurance and Contemporary Medical Practice", Archives of Internal Medicine, Vol. 153: 457-463

Smith, Stephanie C., MS, Jenny Miller, BS, RN, MPH. "Prenatal Diagnosis Technology: Equal Access For All Women", Human Genetics Program, Tulane University School of Medicine, 1989

Microcurrent Versus a Placebo for the Control of Pain and Swelling in Acute Ankle Sprains

Ann Samuelson

Department of Kinesiology
Dow Center Training Room
Hope College
Holland, MI 49423

Faculty Advisors:

Richard Ray, EdD, ATC

John Shaughnessy, PhD
Department of Psychology
Hope College

The use of microcurrent electrical stimulation therapy (MES) has increased in recent years despite the uncertainty of its clinical effectiveness. Manufacturers claim that devices such as MENS,™ Biopulse,™ Electro-Acuscope,™ and My-O-Matic,™ alleviate a range of signs and symptoms. Studies have been conducted to determine its effect on swelling,[1] pain,[2,5] range of motion,[10] delayed onset muscle soreness,[9] and wound healing.[4] This treatment is thought to facilitate the healing process by re-establishing the body's natural direct current which has been disturbed at the injury site. Unfortunately, the basis for the clinical effects of MES is so poorly understood that its definition varies widely and its effects cannot be clearly defined.[2,6,8]

The purpose of this double-blind study is to determine the effectiveness of MES therapy compared to a placebo for the control of pain and swelling on acute lateral ankle sprains. There are two distinct characteristics of this study which contribute to its significance. First, this is a double-blind study that reduces researchers' bias. Also, by employing both a placebo and a control group, the claims of MES effectiveness can be better substantiated or refuted. Second, this study controls for injury type by including only first and second degree lateral ankle sprains. Previous attempts to document claims of MES effectiveness have involved comparisons of a variety of injuries within the same study. Because all joints respond differently to treatment, it is difficult to compare the response of various structures to the same treatment. The focus of the present study is to determine the effects of MES relative to a placebo control and a control group on one specific injury.

MES therapy is a subsensory stimulation that is normally not perceived, even when the unit is functioning properly. For this reason, it is critical to know whether the effects of MES can be attributed to the actual treatment or to a placebo effect. To test for this requires the use of a placebo and a control. To double-blind the study, the wires of one set of leads were cut so that the MES unit would not function, and the second set of leads remained intact. Both sets of leads were made to look identical by covering the wires with tape. One set was covered with red tape, and the other with black.

Walcott et al[3] (cited in Babcock, 1993) studied the effect of microcurrent on 83 ischemic ulcers and found that subjects in the study group (n=75) healed at a rate of 13.4% a week, while those in the control group (n=8) at a rate of only 5% a week. It is uncertain if this increased rate of healing is attributed to the use of the modality or to a placebo effect. Small control group sample size may have influenced the results.

Babcock[3] compared the pain perception of injured athletes with a variety of injuries before and after MES treatment. Three study groups were used: subjects who received the actual treatment, subjects who received a placebo, and subjects who served as a control. The placebo group experienced 15% greater pain reduction than the actual

treatment group, indicating the presence of a placebo effect. In spite of this relatively large difference, the results were not statistically significant. Both the pattern of mean differences and the lack of statistical significance indicate that the treatment is not more effective than the placebo.

A controlled study conducted by Rolle et al[10] on patients suffering from elbow epicondylitis offers similar results. This double-blind study tested subliminal electric stimulation on a treatment group (n=15) and a placebo group (n=16). Measurements in pain perception, grip strength, pain-free range of motion and pain phase were taken. ANOVA results revealed no greater effects among the treatment group than the placebo group for the control of symptoms. Again, this study shows no treatment effect attributable to the use of MES therapy.

METHODS

Subjects

Fifteen subjects from Hope College volunteered to participate in this study. Table 1 lists the subjects' demographic information. All subjects sustained a first or second degree lateral ankle sprain. Mean degrees of ankle sprain for the treatment, placebo, and control groups were 1.9, 1.6, and 1.6, respectively. The first treatment was administered within 24 hours of the injury. Potential subjects who had ankles with suspected fractures were sent for x-rays, and were disqualified if the results were positive. Subjects signed an informed consent document verifying that they were not pregnant, were free of disease or heart condition, were not allergic to acetaminophen, and that they were not familiar with and had never received MES therapy. Subjects refrained from the use of all medication except acetaminophen as needed for pain. Subjects agreed to be randomly placed into one of three groups. Group one received the actual MES treatment, group two received a placebo treatment, and group three served as the control, receiving no MES treatment. Neither the subject nor the researchers knew which group received the actual MES treatment.

Table 1: Demographic Information

Group	Sex (n)	Age (Median)	Degree of Injury (Mean)
Treatment	M= 2 F= 3	19	1.9
Placebo	M= 2 F= 3	20	1.6
Control	M= 3 F= 2	21	1.6

Materials

The device used in this study was a Microcurrent Electrical Stimulation Ultima XS unit. The MES unit was attached to each subject's ankle using ComfortEase 2" x 2.5" pin conductor polymer gel electrodes.

Procedures

Prior to collecting data, a reliability study was conducted to determine uniformity of the measurements of foot and ankle volume and range of motion taken by the three researchers. Interclass correlation coefficients were analyzed at range of motion (ROM)=.90 and volume (VOL)=.99, indicating high levels of interclass reliability for the measurements.

Subjects reported to the training room and received their first treatment within 24 hours of the injury, at which time they were randomly assigned to one of the three groups. Four variables were measured on each subject before and after treatment - pain at rest (PAR), weight bearing pain (WBP), pain-free range of motion (ROM), and foot/ankle volume (VOL). PAR was assessed by having the subject plantar- and dorsi-flex their ankle three times and having them place a vertical mark on a 100 mm visual

analog scale (VAS) that represented their perceived pain (Figure 1). Weight bearing pain was assessed by having the patient take three steps and place a vertical mark on the VAS that represented their level of pain. Pain-free ROM was determined by first having the subject relax their ankle over the end of a treatment table. The angle between the relaxed position and the point at which pain was felt, or at which pain increased from the relaxed position was measured as pain-free ROM. Foot and ankle volume was assessed through water displacement using a foot and ankle volumeter.

No pain at all	Worst pain imaginable

Figure 1: Visual Analog Scale

Treatment consisted of applying the MES unit to the lateral aspect of the injured ankle of subjects in the treatment and placebo groups. Four electrode pads were arranged in an interferential crossing pattern. Subjects were read a standard statement explaining that most patients do not feel MES and that the presence or absence of tingling was not evidence for or against the presence of the real or the placebo MES treatment. The MES unit was turned up to maximal levels. If the subject experienced a slight tingling, the unit was turned down until the sensation disappeared. The machine was set at 0.5 Hz for ten minutes, and at 80 Hz for ten minutes. During this treatment, subjects were instructed to sit with their leg straight on a treatment table, and were to read or study quietly. Subjects in the control group read or studied quietly, with no MES between the pre and post measurements. Following the 20 minutes of treatment, all subjects' ankles were iced, wrapped with a compression wrap, and elevated for 20 minutes. Subjects then performed 10 minutes of active range of motion exercises by hanging their ankle off the end of a treatment table and moving the ankle through a pain-free range of motion. Subjects' ankles were wrapped with a compression wrap with a felt "U" shaped pad. This procedure was repeated twice daily for three consecutive days.

RESULTS

A one-way analysis of variance (ANOVA) was performed comparing the responses of each of the three groups to the MES treatment. Table 2 lists the total change in the variables from the beginning of the first treatment to the end of the last treatment. Mean decreases of PAR in mm for the treatment, placebo, and control groups were 20.2, 22.0, and 28.2, respectively. The analysis showed a non-statistically significant effect; $F(2,12)=.30$, $p=.75$. Mean decreases in WBP in mm for the three groups were 43.6, 33.2, and 33.6. No statistically significant effect was seen; $F(2,12)=.27$, $p=.77$. Mean increases in ROM measured in degrees were 16.6, 8.8, and 5.2. These findings were not statistically significant; $F(2,12)=.79$, $p=.44$. Mean decreases in foot and ankle volume measurements in ml were 29.6, 4.0, and 0.0. Again, no statistically significant differences were seen; $F(2,12)=.79$, $p=.48$.

Table 2: Mean Change Over Three Day Treatment Period

	Dependent Variable			
Group	Pain at Rest (mm)	Weight Bearing Pain (mm)	Pain-free ROM (degrees)	Foot/Ankle Volume (mL)
Treatment	20.2	43.6	16.6	29.6
Placebo	22.0	33.2	8.8	4.0
Control	28.2	33.6	5.2	0.0

Table 3 displays the mean values for each of the four variables after a one-way analysis of variance was performed of the sum of the six pre-treatment results minus the sum of the six post-treatment results. Mean decreases in PAR for the treatment, placebo, and control groups were 4.6, 17.8, and 6.8 respectively. No statistically significant differences were seen; $F(2,12)=1.17$, $p=.34$. Mean changes in WBP were 2.4, 15.6, and -8.4. These differences were not statistically significant; $F(2,12)=1.47$, $p=.27$. Mean changes in ROM were 36.2, 25.8, and 19.2. These values were not statistically different; $F(2,12)=.44$, $p=.65$. Mean decreases in VOL for the three groups were 36.0, 12.0, and 2.0. Again, no statistically significant effects resulted; $F(2,12)=.43$, $p=.66$.

Table 3: Sum of Pre-Treatment Measurements Minus Sum of Post-Treatment Measurements

	Dependent Variable			
Group	Pain at Rest (mm)	Weight Bearing Pain (mm)	Pain-Free ROM (degrees)	Foot/Ankle Volume (mL)
Treatment	4.6	2.4	36.2	36.0
Placebo	17.8	15.6	25.8	12.0
Control	6.8	-8.4	19.2	2.0

Following the six treatments, subjects in the treatment and placebo groups were asked whether they thought they had received the actual MES therapy. Possible replies were yes, no, or not sure. Table 4 lists the subjects' responses. The results indicate that the double-blinding of this study was effective, as there is a non-systematic distribution of responses.

Table 4: "Do you think you received the actual MES therapy?"

	Response		
Group	Yes	No	Not Sure
Treatment	2	1	2
Placebo	3	1	1

DISCUSSION

From the data in Table 2, it appears that the treatment group was positively affected by the MES treatment over the three day period, as the mean measurements for three of the four variables were more favorable than the placebo or control groups. In contrast, the analysis revealed no statistical significance ($p<.05$) among the changes in measurements across the three groups.

Table 3 displays the values for the mean changes when the sum of all six post-treatment measurements were subtracted from the sum of the six pre-treatment

measurements for each variable. This analysis accounts for variability within the three day treatment period. The data indicate that WBP within the control group increased by an average of 8.4 mm during the treatment period, which may lead one to believe that both treatment and placebo effects can be attributed to MES therapy. These values, however, are not statistically significant at $p < .05$. Based on the results of our study alone, it cannot be conclusively stated that MES therapy is or is not effective for the control of pain, swelling and range of motion in patients who have sustained acute lateral ankle sprains.

Additionally, previous studies that are similar to the present study which use a placebo and a control group and focus on one specific injury[1,2,5] have found no clinical effects among patients receiving MES treatment. Our findings confirm the conclusions reached in these studies. Data collection in the present study is ongoing, and more definitive results will be published upon completion.

Research indicates a variety of clinical effects attributed to MES therapy, including decreased pain,[4,5] increased rate of wound healing,[4] and increased ROM[6]. Other research has claimed that the effects of microcurrent cannot be immediately observed; rather, improvement of symptoms is observed up to 24 hours after treatment[9]. The best controlled studies have indicated that MES therapy is not an effective treatment for these symptoms. We support these studies which refute the clinical effects of MES.

CONCLUSIONS

Based on this double-blind controlled study and previous research using similar conditions, it is concluded that MES therapy is not effective for decreasing pain at rest, decreasing weight bearing pain, increasing pain-free range of motion, and decreasing swelling for subjects with acute first and second degree lateral ankle sprains.

Some suggestions to increase the sensitivity in future experiments would be to use probes in place of electrodes for the conduction of the MES treatment, and regulate the time of day at which the treatment is administered to control for the amount of ankle swelling throughout the day. Because chronic and acute injuries may respond differently to the same MES therapy, a similar study using subjects with chronic pain is suggested. Finally, by increasing the number of subjects in each of the three groups, the sensitivity of the experiment would be increased.

REFERENCES

1. Akers,L., Collidge, F., Daly, A., Goldberger, E., Gur, O., Iannuzzi, R., Miller, M. Effect of subliminal electrical stimulation on acute ankle sprain: two case studies. University of Maryland School of Medicine, Department of Physical Therapy.
2. Alon, G., (1993). "Micro current:" subliminal electric stimulation. Sports Medicine Update, 9, 8-11.
3. Babcock, TA., (1993). The use of microcurrent therapy for management of pain in the acute phase of soft tissue injury. (Master of Science Thesis). University of Idaho.
4. Carley, PJ., Wainapel, SF. (1985).Electrotherapy for acceleration of wound healing: Low intensity direct current. Archives of Physical Medicine and Rehabilitation, 66, 443-446.
5. Lerner, FN., Kirsch, DL. (1981). A double-blind comparative study of micro stimulation and placebo effect in short term treatment of the chronic back patients. The Journal of the American Chiropractic Association, 15, S101-S106.
6. Picker, RI. (1993). Current trends: low-volt pulsed microamp stimulation, Part I. Clinical Management, 9(2), 10-14.
7. Picker, RI. (1993). Current trends: low-volt pulsed microamp stimulation, Part II. Clinical Management, 9(3), 28-32.
8. Prentice, WE. (1990). Therapeutic Modalities in Sports Medicine. St. Louis: Times Mirror/Mosby College Publishing.

9. Rapaski, D., Isles, S., Kulig, K., Boyce, D. (1991). Microcurrent electrical stimulation. Journal of the American Physical Therapy Association, 71, S116. (Abstract No. R286)

10. Rolle, WC., Alon, G., Nirschl, RP. (1991). Comparison of subliminal and placebo stimulation in the management of elbow epicondylitis. Journal of the American Physical Therapy Association, 71, S114. (Abstract No. R280)

The Reliability of the Biodex Stability System

Stephanie Smith

Department of Biology
University of North Carolina at Asheville
One University Heights
Asheville, NC 28804

Faculty Advisor:

John Bernhardt

INTRODUCTION

The Greek philosopher Aristotle was the first to define sensation when he described the five senses. Sir Charles Bell much later described a "sixth sense". This "sixth sense" was the sensation related to limb position and motion. Articular sensation has been the subject of research only in the last two centuries. Duchenne and Charcot (Daniel,1990) began studies on articular sensations and their clinical importance in 1865. In 1932, Sherrington and Adrian (Daniel,1990, Prentice,1990) won a Nobel Prize for their studies on the mechanism of sensation.

Neurological control mechanisms allow the movement of the human body. Receptors that detect movement and provide feedback to the central nervous system are found in the skin, muscles, tendons, articular structures, and visual and vestibular systems (Harrison,1994).

Proprioception and kinesthesia are terms used to describe articular sensations. Prentice (1990) defines proprioception as a specialized variation of the sensory modality of touch that encompasses the sensations of joint movement and joint position. According to Mountcastle (1974), proprioception is the conscious awareness of a limb's position in space, whether moving or still. Kinesthesia is the awareness of joint position while in motion. Many of our daily activities rely on proper joint function through conscious proprioception. Muscle function and reflex stabilization are controlled by unconscious proprioception.

The ligaments of the knee are innervated. In 1944, LeRoy Abbott (1944) reported that these ligaments are the first step in the kinetic chain that provides knee stabilization. Recently, much research has been performed on knee joint innervation. The cruciate ligaments have a rich nerve supply that originates mainly from the posterior articular nerve (PAN) as well as from the terminal branch of the obturator nerve (Kennedy,1982). Hilton stated, over 100 years ago, that "joints are innervated by articular branches of the nerves supplying the muscles that cross the joint."(Barrack,1989) This is known as Hilton's Law. Neuronal tissue comprises 1.0% to 2.5% of the total volume of the anterior cruciate ligament (Johansson,1991). The nerves serving the cruciate ligaments run beside the blood vessels that supply the ligament. This caused investigators to erroneously believe that these nerves serve in vasomotor control only. Current research has shown that the nerves have much broader functions.

Palmer (Daniel,1990) studied the role of proprioceptive input from knee ligaments. He proposed that proprioception may play a protective role in acute knee injury through reflex muscular splinting. One such reflex causes contraction of the hamstring and vastus medialis upon valgus force hyperextension. He also observed that this reflex is weakened when the anterior cruciate ligament is injured. Mechanoreceptors are located in the cruciate ligaments (Boyd,1954, Burgess,1969, Freeman,1967, Kennedy,1982, Schultz,1984). They are transducers that convert mechanical energy to electrical energy of nerve action potential. These mechanoreceptors detect stretch and pressure, and send impulses to the brain to prevent injury. Proprioceptive ability would be impaired in cases where there is an injury to a ligament.

Stauffer and Prodromos (Barrack,1989), in two separate experiments, studied patients with diseased knees. They utilized gait analysis and concluded that the loss of proprioceptive feedback might cause patients to alter their gait patterns. They would do this to decrease pain and to increase proprioceptive feedback. The authors concluded that an increase in proprioceptive feedback would increase stability and

muscle control.

Studies have been done to determine the effect injury has on knee proprioception. Kennedy (1982) has shown that injury to the ligaments of the knee decreases neural feedback and may cause disability and progressive degeneration of the knee itself. Barrack (1989) found that patients with complete ACL tears and moderate to severe rotary instability may also experience a decline in proprioceptive function in the affected joint. Barrett (1991) found that when the ACL is torn, kinesthesia of the knee joint is decreased. Glencross (1981) found that there was a loss of precision in judging position sense following an injury.

Barrack (1983) studied the effect of intraarticular anaesthesia of the knee on gait patterns and joint proprioception. The anesthesia had no effect on the proprioceptive ability of the subject. Clark and Burgess (1975) concluded from their study that local anaesthetics infiltrate the joint and interfere with the sensory input to the central nervous system. This would cause a slowing and distortion of joint position sense.

An age-related decline in proprioceptive ability has been observed. Skinner (1982) tested the ability of subjects to reproduce passive positioning and the sensitivity they showed in detecting passive motion. It was found that there is a significant correlation between the two tests of position sense and age. Kaplan (1985) also found an age-related decline in proprioception. Other studies have correlated an increase in falls in the elderly with the loss of proprioception. It seems apparent, based on multiple studies, that there is a decline in proprioception as an individual ages.

Standing balance is often used to evaluate lower-limb neuromuscular function. If a patient has difficulty with standing balance, it is important to prescribe a program to correct this deficiency. Zatterstrom *et al.* (1994) studied the effect of ACL deficiency on standing balance. They found that impaired standing balance may not be due merely to physical inactivity. It could be caused by impaired sensory feedback from the injured joint. The relearning of postural control in this study proved to be slow when compared with the amount of time it took to regain muscle strength. Proper neuromuscular function can be regained by modification of existing motor programs for rehabilitation to correct altered sensory situations.

These findings suggest that there is a need to condition the proprioceptive apparatus of the knee. Stabilometry has been used as a quantitative measure of balance. Freeman (1967) introduced this technique in 1967 when he used an unstable board to study ankle injuries. Today, proprioceptive training is usually accomplished by performing single leg balancing exercises on a multi-axial tilting board or force plate. This technique analyzes postural sway by determining the displacement of the center of pressure. These tests are classified as closed chain tests. The feet usually remain in the same position with little movement of the center of gravity. This apparatus is used to measure steadiness (lack of motion), symmetry (even distribution of weight), and motion control (transfer of the vertical center around the base of support) (France,1992). These tests attempt to teach patients to improve postural balance by increasing their awareness of their center of gravity.

Restoration of proprioceptive ability from the ACL is an important aspect of the rehabilitation process. The object of proprioceptive rehabilitation is the prevention of reinjury. Proprioception can be more important than muscle strength in preventing reinjury. It is important that rehabilitation include the types of activities that the patients will perform when they are discharged. In performing these exercises, conscious and unconscious pathways are utilized and kinesthetic awareness is maximally stimulated (Prentice,1990). It can often take more than one year before full proprioceptive abilities are regained in the affected joint (Daniel,1990).

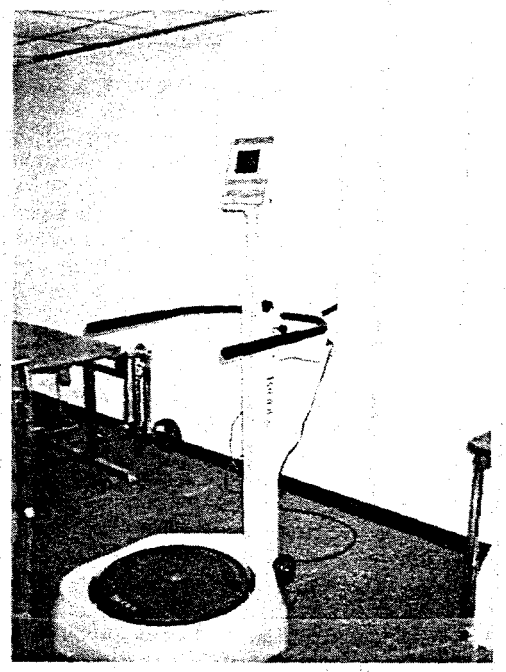
Despite the apparently significant role of proprioceptive training, only 28% of the physical therapy clinics that participated in a study by Beard (1992) include proprioceptive training in their treatment of injuries. The clinician must have reliable means of training and testing proprioceptive abilities. It is also vital to have an accurate assessment of a patient's abilities before they are allowed to return to their normal level of functioning after an injury.

The Biodex Stability System (Biodex Medical Systems, Shirley, NY) was used in this experiment (Figure 1). This equipment was designed for neuromuscular assessment and functional rehabilitation in a clinical setting. It consists of an unstable platform that can achieve varying degrees of instability. Level 1 is most unstable and level 10 is most stable; level 6 is prescribed for initial testing of patients by Biodex. A small screen can be adjusted to the line of vision of the subject for a visual image of

how well they are holding the platform level. The disk is marked with a grid for foot placement.

Each test begins when the stable platform becomes unstable. The ability of the subject to maintain postural stability on the unstable surface is recorded. Then the equipment generates a stability index (quantifies overall stability), anterior/posterior index, and medial/lateral index. "The patient's ability to control the platform's angle of tilt is quantified as a variance from the center, as well as degrees of deflection over time."(Biodex,1994) The equipment reports the amount of time spent in each quadrant of the disk and in each concentric region of the disk. The purpose of this research was to test the reliability of the Biodex Stability System.

Figure 1: The Biodex Stability System



EXPERIMENTAL DESIGN

Subjects:

Thirty-four subjects were recruited from the Physical Therapy Division of the School of Allied Health at the University of Kentucky. Ten males and twenty-four females participated in the study. The subjects were selected if there was no history of lower limb surgery, trauma to the head or neck or current illness that would alter balance abilities. The average age of the subjects was 23.4 years old (standard deviation 3.5). The ages ranged from 20 to 34.

Survey:

Information obtained from the subjects included age, weight, height, and gender. Each subject was asked to rate his or her activity level on the following scale: sedentary (activities of daily living only), slight (exercise 1 or 2 times a week), moderate (exercise 3 times a week), or very (exercise 4 to 7 times a week).

Protocol:

The test protocol consisted of a series of seven twenty second tests using the Biodex Stability System with a thirty second rest between each test. The degree of platform instability was set at level 6. Subjects were given identical directions and allowed a one minute practice period before testing began. The foot placement the subject chose was recorded for the first test of each set using the grid on the disk. The foot position was recorded for each test using the grid on the disk. The foot position was the same on the second day. A single bilateral test was performed. Three tests were performed on each single leg. The legs tested were chosen in a randomly assigned order. Two identical sets of test were run on each subject on two consecutive

days.

ANALYSIS

Data collected consisted of computer generated stability indexes, anterior/posterior indexes and medial/lateral indexes for each test. The mean for each subject was determined for the three unilateral tests done on each day. Nine tests were run on the data (Table 1). Data were examined for homogeneity of variances using the Levine's Test. Data were determined to be homogeneous (ie. assumption of equal variances was valid). Analysis of variances was used to determine the differences between day one data and day two data of the examined groups. Data were determined to be heterogeneous (ie. assumption of equal variances was not valid. Significant differences between groups was determined by Satterwiatte's Approximation (Millken and Johnson, 1984). The "Messy Assistant" (Barger, Yearout, Yates and Massey, 1995) was used for this analysis. Since only two groups were used in the analysis, it was not necessary to apply Bonforoni's Adjustment to the given 95% confidence level (Milliken and Johnson, 1984).

Table 1: Analysis of Day One Data vs. Day Two Data

TEST #	
1A	Stability Index for both legs
1B	Medial/Lateral Index for both legs
1C	Anterior/Posterior Index for both legs
2A	Stability Index for right leg
2B	Medial/Lateral Index for right leg
2C	Anterior/Posterior Index for right leg
3A	Stability Index for left leg
3B	Medial/Lateral Index for left leg
3C	Anterior/Posterior Index for left leg

RESULTS

No statistical significant differences were found at the 95% confidence level for all nine tests. The result of the survey showed that the average activity level of the subjects was between slight and moderate.

DISCUSSION

Determining the reliability of the Biodex Stability System is important. If it is not reliable, it will not be effective for use in a clinical setting. Because the purpose of rehabilitation is the prevention of reinjury, a physical therapist must be positive patients are not allowed to return to activities they are not able to perform after an injury. More studies need to be performed to test the effectiveness of the Biodex Stability System as a training apparatus. A learning curve may be detected in use over long periods of time.

During the course of my pilot study, fatigue became a factor when the testing time was longer than thirty seconds. Further research could be performed to examine the effect of muscle fatigue on proprioceptive abilities. This research establishes a baseline pertaining to normal subjects. The normative data allow physical therapists to evaluate the effectiveness of the equipment in testing patients. With the reliability of the equipment established, it is now possible to test patients who are rehabilitating a lower limb injury.

CONCLUSION

This research project verified the reliability of the Biodex Stability System.

ACKNOWLEDGEMENTS

The author greatly appreciates the generous funding for this research provided

by the University of North Carolina at Asheville's Undergraduate Research Program. Thanks also to Terry Malone, PT, EdD, Arthur Nitz, PT, PhD, and Gail Friedhoff, PT, MS of the Physical Therapy Division at the University of Kentucky for their patience and support in designing and conducting this project. The author also wishes to thank
Dr. Robert Yearout for his assistance in the completion of this research.

REFERENCES

Abbott, JC, JB Saunders, M Dec. Injuries to the ligaments of the knee joint. Journal of Bone and Joint Surgery. 26: 503-521, 1944.

Barrack, RL, et al. Functional performance of the knee after intraarticular anesthesia. American Journal of Sports Medicine. 11(4): 258-261, 1983.

Barrack, RL, HB Skinner, ME Brunet. Proprioception in the anterior cruciate deficient knee. American Journal of Sports Medicine. 17(1): 1-6, 1989.

Barrett, DS, AG Cobb, G Bentley. Joint proprioception in normal, osteoarthritic, and replaced knees. Journal of Bone and Joint Surgery [Br]. 73: 53-56, 1991.

Beard, DJ and CM Fergeson. The conservative management of anterior cruciate ligament deficiency: a nationwide survey of current practice. Physiotherapy. 78(3): 181-186, 1992.

Biodex Medical Systems, Inc. Reflexions. Summer, 1994.

Boyd, IA. The histological structure of the receptors in the knee-joint of the cat correlated with their physiological response. Journal of Physiology. 124: 476-489, 1954.

Burgess, PR and FJ Clark. Characteristics of knee joint receptors in the cat. Journal of Physiology (Lond). 203: 317-335, 1969.

Clark, FJ, PR Burgess. Slowly adapting receptors in cat knee joint: Can they signal joint angle? Journal of Neurophysiology. 38: 1448-1463, 1975.

Daniel, DM. Knee Ligaments: Structure, Function, Injury, and Repair. Raven Press, 1990.

France, EP, G Derscheid, J Irragang, T Malone, R Petersen, S Tippett, K Wilk. Preliminary Clinical Evaluation of the Breg K.A.T.: Effects of Training in Normals. Isokinetics and Exercise Science. 2(3): 133-139, 1992.

Freeman, MAF and B Wyke. The innervation of the knee joint, an anatomical and histological study in the cat.Journal of Anatomy. 101: 505, 1967. Glencross, D and E Thornton. Position sense following joint injury. Journal of Sports Medicine. 21: 23-27, 1981.

Harrison, EL, N Duenkel, R Dunlop, G Russell. Evaluation of Single-Leg Standing Following Anterior Cruciate Ligament Surgery and Rehabilitation. Physical Therapy. 74(3): 245-252, 1994.

Johansson H, P Sjolander, P Sojka. A Sensory Role for the Cruciate Ligaments. Clinical Orthopaedics and Related Research. 268: 161-178, 1991.

Kaplan, FS, JE Nixon, M Reitz, L Rindfleish, J Tucker. Age-related changes in proprioception and sensation of joint position. Acta Orthopaedic Scandinavia. 56: 72-74, 1985.

Kennedy, JC, IJ Alexander, KC Hayes. Nerve supply of the human knee and its functional importance. American Journal of Sports Medicine. 10: 329-335, 1982.

Mountcastle, VB. Medical Physiology. 13th ed. St Louis: Mosby, 1974.

Prentice,WE. Rehabilitation Techniques in Sports Medicine. Times Mirror/Mosby, 1990.

Schultz, RA, AG Cobb, G Bentley. Mechanorecptors in human cruciate ligaments: a histological study. Journal of Bone and Joint Surgery. 66[A]: 1072-1076, 1984.

Skinner, HB, RL Barrack, SD Cook. Age-related Decline in Proprioception. Clinical Orthopaedics and Related Research. 184: 208-211, 1982.

Zatterstrom, R, T Friden, A Lindstrand, U Moritz. The Effect of Physiotherapy in Chronic Anterior Cruciate Ligament Insufficiency. American Journal of Sports Medicine. 22(4): 531-536, 1994.

Current Science Textbooks: How Do They Rate with the Ohio Science Model?

Anne Fay

Department of Curriculum and Educational Technology
University of Toledo
2801 West Bancroft Street
Toledo, Ohio 43606

Faculty Advisor:

Andrew T. Lumpe

There are a number of current movements in Ohio and nationally to reform science curricula. These efforts include: Moving Toward the Twenty-First Century: Strengthening Mathematics and Science Learning for All Ohioans (Mathematics and Science Advisory Commission), Project 2061: Science For All Americans (American Association for the Advancement of Science, Inc., 1989), and Science: Ohio's Model Competency-Based Program (State Board of Education, 1994). These movements are important both to educators and to students. For educators reform means that they will be given guidelines for educating their students that will influence or even change the way they teach. For students the changing curriculum means their teachers will be guiding them in a more directed manner, leading to higher level thinking. The effort to improve science education would have a considerable impact if focused on the correspondence between textbooks and the goals of science curricula. The focus on textbooks is relevant when estimates show that 75 percent of classroom time and 90 percent of homework time involve the use of textbooks (Blystone cited in Jablon, 1992).

Authors and publishers of science textbooks should work to balance curriculum goals in an effort to develop a scientifically and technologically literate society. Many of the commercially prepared textbooks stress facts and present science as a complete body of information (Chiappetta, Sethna, & Fillman, 1991b), while a more broad view of science information may better aid in developing a scientifically literate society.

The move for science education reform in Ohio, as with many other states throughout the country, must focus on the ability to relay concepts, skills, and processes in order to build a scientifically literate society. Curriculum reform efforts in Ohio have been developed to accomplish this goal. There are four strands to the new Ohio Model Competency-Based Science Curriculum: 1) Scientific Knowledge, relay of scientific information, such as definitions, 2) Scientific Inquiry, encouraging students to think and learn by searching for answers, as through discovery activities, 3) Conditions for Learning, classroom setup and how students are expected to respond to information, such as group activities with results presented to the class, and 4) Applications for Science Learning, relating what has been learned to real world experience and technology, such as building upon knowledge about wind resistance and having students build their own airplanes (Ohio Department of Education, 1994). These four strands set a standard to guide school districts in developing instructional and performance objectives for students. They represent the optimal performance of the essential knowledge and skills Ohio expects of students at all grade levels. These objectives focus on both the processes and content of science, where traditionally only the content was addressed in the curriculum.

PURPOSE

The purpose of this investigation is to analyze current secondary science curriculum materials to determine which best address the goals proposed in the Model Competency-Based program in Ohio, and to describe general content and characteristics of the materials.

METHODS

In similar research, Chiappetta, Fillman, and Sethna suggest four categories for analyzing science textbooks. The categories for analyzing science textbooks listed in the article are:

The Knowledge of Science: Check this category if the intent of the text is to present, discuss, or ask the student to recall information, facts, concepts, principles, laws, theories, etc. It reflects the transmission of scientific knowledge where the student receives information.
The Investigative Nature of Science: Check this category if the intent of the text is to stimulate thinking and doing by asking the student to "find out." It reflects the active aspect of inquiry and learning, which involves the student in the methods and processes of science such as observing, measuring, classifying, inferring, recording data, making calculations, experimenting, etc.
Science as a way of Thinking: Check this category if the intent of the text is to illustrate how science in genera, or a certain scientist in particular, went about "finding out." This aspect of the nature of science represents thinking, reasoning, and reflection, where the student is told about how the scientific enterprise operates.
Interaction of Science, Technology, and Society: Check this category if the intent of the text is to illustrate the effects or impacts of science on society. This aspect of scientific literacy pertains of the application of science and how technology helps or hinders humankind. In addition, it involves social issues and careers. Nevertheless, the student receives this information and generally does not have to find out. (Chiappetta, et al., Sethna, 1991a)

The Ohio science model does not include science as a way of thinking in the four strands; thus this category will not be considered for analysis. The conditions for learning science strand will be substituted as a category. Conditions for learning science will be checked if the intent of the text is to convey classroom set up and how the student is expected to respond to the information. The interaction of science, technology, and society category parallels the applications science learning strand of the Ohio science model; thus for purposes of analysis, the stipulations of this category will be applied to the applications science learning strand. The same arrangement was made for the other two strands in the Ohio science model, and the categories previously listed as knowledge of science and the investigative nature of science.

The units for analysis (data points) include: complete paragraphs, questions, figures, tables with captions, and marginal comments. Units that are not included for analysis are: pages with fewer than two analyzable units, a page that contains only review questions and vocabulary words, and goal and objective statements (Chiappetta, et al., 1991a). Random number tables were used to generate page numbers corresponding to five percent of each text which results in a representative sample of each text (Garcia 1985 cited in Chiappetta, et al., 1991a). This coding method provides an objective look at the content of each of the textbooks. Thus it is included in the analysis of the textbooks. General observations of each text will also be included in addition to the analysis according to the Ohio science model. The textbooks under investigation are: Biology Visualizing Life, Modern Chemistry, Modern Biology, Science Plus Level Blue, ChemCom: Chemistry in the Community, BSCS Green Version, BSCS Investigating Diversity and Limits Level B, Science Interactions Course Two. These textbooks were chosen for analysis because of the large market share of each book.

RESULTS

Each text has some characteristics in common with all of the other texts being analyzed. These characteristics include vocabulary words, laboratory activities, chapters, and pages. Table 2 illustrates the common characteristics among the texts. The total number of vocabulary words found in the analyzed texts ranged from 95 in BSCS Level B to 1412 in Modern Biology. The number of laboratory activities ranged from 18 in Modern Chemistry to 81 in Science Plus. The number of chapters ranged from 8 units in Science Plus to 53 chapters in Modern Chemistry. Modern Chemistry had the most pages, and BSCS Level B had the least. Table 1 illustrates this data.

Table 1: Common Characteristics Among Science Textbooks

	# Vocab	# Labs	# Chapters	# Pages Total	# Pages Text
Biology Vis. Life	492	34	34	850	811
Modern Chemistry	594	18	29	909	875
Modern Biology	1412	53	53	880	831
Science Plus	197	81	8 units	658	500
ChemCom	351	37	42	518	500
BSCS Green	704	72	24	800	869
BSCS Level B	95	44	15	340	299
Science Interactions	163	42	21	708	658

Results of the analysis may be seen in Table 2. The total number of data points ranged from 166 in Modern Chemistry, to 63 in BSCS Level B. The percent of each text devoted to the scientific knowledge strand ranged from 66.67 percent in BSCS Level B to 89.76 percent in Modern Chemistry. The percent of each text devoted to scientific inquiry ranged from 1.87 percent in Science Plus to 16.78 percent in Science Interactions. The conditions strand was only represented in two of the texts, Biology Visualizing Life, 0.87 percent, and BSCS Level B, 14.29 percent. The percent of each text devoted to applications science learning ranged from 2.01 percent in Science Interactions to 12.70 percent in BSCS Level B.

Table 2: Analysis of Data Points

	Total Data Pts	Raw Count as a Percentage of Total Data Points			
		Knowledge	Inquiry	Conditions	Applications
Biology Vis. Life	115	80.87%	12.17%	0.87%	6.09%
Modern Chemistry	166	89.76%	5.42%	0.00%	4.82%
Modern Biology	165	88.48%	4.85%	0.00%	6.67%
Science Plus	107	85.98%	1.87%	0.00%	12.15%
ChemCom	127	82.68%	10.24%	0.00%	7.09%
BSCS Green	136	86.03%	8.82%	0.00%	5.15%
BSCS Level B	63	66.67%	6.35%	14.29%	12.70%
Science Interactions	149	81.21%	16.78%	0.00%	2.01%

DISCUSSION

Several observations may be drawn from the data gathered: 1) current science textbooks focus mainly on conveying scientific knowledge; 2) the number of laboratory activities a text contains does not necessarily relate to the inquiry level of that text; 3) conditions of science learning and applications science learning are minimally addressed in current science texts; 4) the textbooks analyzed do not match the goals of the Ohio science model. These observations are important because they may become the basis for suggestions to science textbook writers and publishers. By adding aspects of scientific inquiry, conditions for learning, and applications for science learning to current science textbooks publishers may find that their products will more closely match the demands of curriculum committees that are influencing changes in the current market.

CONCLUSION

This information, in addition to supplemental information on the materials that have been studied, will aid curriculum committees in choosing the best materials for their school districts. This information should also be useful to writers and publishers of secondary science textbooks, by indicating areas in textbooks in need of improvement.

REFERENCES

American Association for the Advancement of Science. (1989). *Project 2061: Science for all Americans.* Washington D.C.

American Chemical Society. (1993). *ChemCom: Chemistry in the Community.* Dubuque, Iowa: Kendall/Hunt.

BSCS. (1994). *Investigating Diversity and Limits, Level B.* Dubuque, Iowa: Kendall/Hunt.

BSCS. (1992). *Biological Science: An Ecological Approach.* Dubuque, Iowa: Kendall/Hunt.

Chiappetta, Eugene L., Fillman, David A., & Sethna, Godrej H. (1991a). A Method to Quantify Major Themes of Scientific Literacy in Science Textbooks. *Journal of Research in Science Teaching.* 28(8), 713-725.

Chiappetta, Eugene L., Sethna, Godrej H. (1991b). A Quantitative Analysis of High School Chemistry Textbooks for Scientific Literacy themes and Expository Learning Aids. *Journal of Research in Science Teaching.* 28(10), 939-951.

Glenco. (1993). *Science Interactions, Course Two.* Columbus, Ohio: Macmillan/McGraw-Hill.

Holt, Rinehart, Winston. (1993). *Science Plus Level Blue.* Chicago.

Jablon, Paul C. (1992). A Generic Biology Textbook Review: It Is Time to Stop Placing Band-Aids on Our Biology Curricula. *The American Biology Teacher.* 54(2), 72-74.

Johnson, George B. (1994). *Biology: Visualizing Life.* Chicago: Holt, Rinehart, Winston.

Mathematics and Science Advisory Commission. (199?). *Moving Toward the Twenty-First Century: Strengthening Mathematics and Science Learning for All Ohioans.* Columbus, Ohio: The Ohio State University.

Ohio Department of Education: Division of Curriculum, Instruction, and Professional Development. (Working Draft January 20, 1994). *Science: Ohio's Model Competency-Based Program.* Columbus, Ohio.

Towle, Albert. (1993). *Modern Biology.* Chicago: Holt, Rinehart, Winston.

Tzimopoulos, Metcalfe, Williams, Castka. (1993). *Modern Chemistry.* Chicago: Holt, Rinehart, Winston.

THE IDENTIFICATION OF THE KINETIC PATHWAYS IN THE THERMAL DECOMPOSITION OF ZINC (II) ACETYLACETONATE

Jennifer Ann Condon

Chemistry Department
James Madison University
Harrisonburg, Va. 22807

Faculty Advisor:

Dr. Thomas C. DeVore

ABSTRACT

Evolved Gas Analysis-FTIR (EGA-FTIR) was used to investigate the thermal decomposition of zinc (II) acetylacetonate dihydrate. Both the open and closed cell experiments consistently showed two separate peaks indicating that the decomposition of zinc acac occurred in three steps. EGA-FTIR spectroscopy of the gaseous products indicated the loss of 2,4-pentanedione and the waters of hydration in each step. The first peak, occurring at approximately 359 K, is believed to be $Zn_4O(AcAc)_6 \cdot X H_2O$ (where X can be any integer from one to six). The further decomposition of this material at 401 K formed $Zn_x O_{x-1}(AcAc)(OH)$ (where $X \geq 6$). This second intermediate then decomposes into ZnO. Identification of the products was conducted using solid-state pellet IR spectroscopy and combustion analysis.

INTRODUCTION

Chemical vapor deposition (CVD), often used in the high temperature synthesis of coatings and powders, creates an environment in which gaseous species react to form more condensed phase compounds.[1-4] Recently the CVD process using beta-diketonates, such as acetylacetonate compounds, has become a more common method for forming metal oxides.

The thermal decomposition of $Zn(AcAc)_2 \cdot 2 H_2O$ was investigated previously by Ismail (1991) and Hussien (1990).[5,6] Each reported the appearance of water and hydrocarbons in the IR spectra. Based upon this analysis, they determined that the anhydrous $Zn(AcAc)_2$ and the zinc carbonate were formed as intermediates during this reaction. However, the IR spectra of the evolved gases does not support this analysis. This investigation demonstrates that 2,4-pentanedione is a principle decomposition product. Therefore, the products of the individual phases have been reassigned to account for this discrepancy.

EXPERIMENTAL

Instrumental Analysis

The experimental procedure used has been described in detail previously.[7] The IR cell was constructed from a stainless steel four-way cross vacuum flange (MDC Corp.). One arm was used to connect the IR cell to the vacuum system, while the remaining opposing arms were attached to KBr windows with O-ring vacuum connectors to furnish an optical path. The remaining port was connected to the sample container and the heating elements. The data obtained from pumping the cell (open cell experiments) resembled DTA-like results, while the data from a non-pumped cell (closed cell experiment) was characteristic of TGA-like results.

Open cell experiments in the presence of water vapor were done by placing a sample of zinc acac into a glass tube that was connected to a teflon needle valve. The valve was used to control the flow of water vapor into the IR cell. The sample was then placed inside a larger Vycor tube, which was wrapped with Nichrome heating wire. The Vycor tube was used as a separate furnace for heating the sample. Temperature changes were monitored using a chromel-alumel thermocouple connected to a Keithley Digital Thermometer. The temperature of the sample could be determined within ±3 degrees. Zinc acac hydrate (99.9%) was obtained from Aldrich Chemical Co.

Closed cell experiments were also done on the sample and compared to the results of the open cell experiments. A sample of zinc acac was placed into a glass tube which was sealed at one end. To obtain a closed cell system the vacuum was first allowed to remove any atmospheric gases that had become trapped in the system. It was then closed so that the evolved gases from the reaction could not escape. The closed cell sample was heated and monitored using the same method as described for the open cell.

Evolved Gas Analysis: Open Cell

Evolved gases were monitored using rapid-scan Fourier transform infrared spectroscopy. The Nicolet 740 FTIR collected and stored one spectrum approximately every two seconds for the length of the reaction time up to 40 minutes. Each spectrum was displayed over a range of 400 to 4000 cm^{-1} with four wavenumber resolution. A reconstruction curve was then obtained for the reaction, and the IR spectra of each consecutive peak was plotted against a reference point in order to show the relative absorbance over time. [Figures 1,2] Water was subtracted out by taking the reference point at a point in the plateau of water absorbance before the actual reaction occurred.

Each glass tube containing solid zinc acac hydrate was weighed before and after heating. The mass losses were then recorded and used to determine possible chemical formulas. The remaining solid and sublimed material were identified using solid-state pellet IR spectroscopy. A combustion analysis was also executed on the remaining solid to determine the amount of zinc in the product.

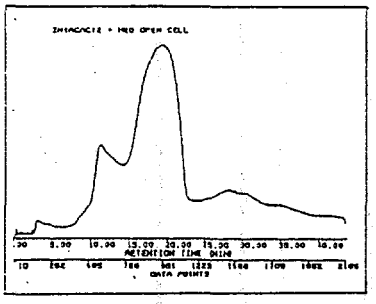


Figure 1. DTA-like reconstruction curve for the open cell experiment.

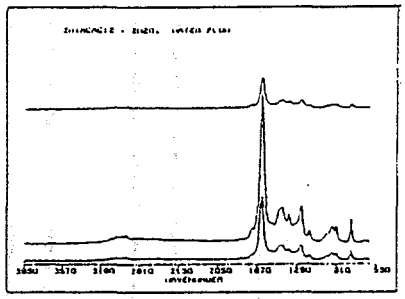


Figure 2. IR scans of the evolved gases for each peak in the open cell experiment.

Evolved Gas Analysis: Closed Cell

Evolved gases were monitored using the Nicolet 740 FTIR as described above. The peaks of the reconstruction curves were then compared to the reconstruction curves of the open cell experiments. Solid-state pellet IR spectroscopy was done on the white solid and the sublimed material in the glass tube, and the IR spectra of the evolved gases were compared to the spectra for the open cell experiments. [Figures 3,4]

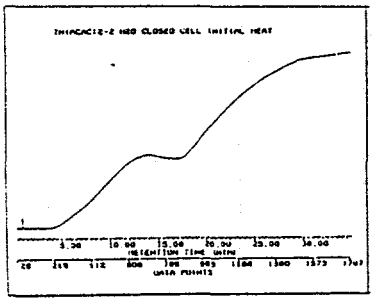


Figure 3. TGA-like reconstruction curve for the closed cell experiment.

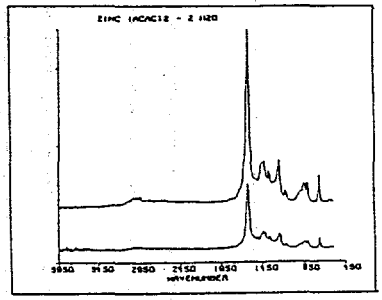


Figure 4. IR scans of the evolved gases for each peak in the closed cell experiment

Kinetic Analysis

Absorbances were obtained every 30 seconds of the individual sample runs and plotted on SOLVE, a graphics program. The activation energy (ΔE) was then calculated based on the fractional reaction, α, defined as[8]

$$\alpha = m_0 - m / m_0 - m_f \quad (1)$$

where m is the mass at any time during the decomposition, m_0 is the initial mass of the sample, and m_f is the mass at the completion of decomposition. Using the absorbance of the evolved gases in the closed cell experiments α can be determined by

$$\alpha = A / A_{max} \quad (2)$$

where A is the individual absorbance observed and A_{max} is the observed absorbance when the sample is depleted to completion. For open cell experiments α is found by integrating the area under the EGA curve.

The kinetic parameters can be obtained for open cell experiments from the fractional reaction as a function of temperature using non-linear least squares to determine $d\alpha / dT$:

$$d\alpha / dT = (A/\theta)\, g(\alpha) \exp(-E_a / RT) \quad (3)$$

where A is the steric factor, θ is the heating rate, $g(\alpha)$ is a function that depends on the order of reaction, and E_a is the activation energy. In these open cell experiments, $g(\alpha)$ was found to be $(1-\alpha)$, indicating that the reaction is first order.

RESULTS

Analysis of the open and closed cell experiments of hydrated zinc acac revealed two specific curves. The first appeared around 86°C (359 K). EGA-FTIR spectroscopy indicated that the gaseous products of the decomposition were 2,4-pentanedione and water vapor. The rate of this reaction was determined to be first order, based on the non-linear least squares fit of the EGA curve. Open cell experiments yielded an average of 15.56% mass loss for the first peak. Combustion analysis showed an average of 27.80 % zinc in the product of the first peak.

The first peak was assigned the chemical formula $Zn_4O(AcAc)_6 \cdot X H_2O$. The absolute value of X was not determined because several values of X may be possible. Theoretically, it was found that four waters of hydration corresponded to 27.71% zinc. Based on the combustion analysis, this percentage was most representative of the average found for this intermediate phase. Consequently, $Zn_4O(AcAc)_6 \cdot 4 H_2O$ was used when referring to this phase.

The second peak appeared at 128°C (401 K) and contained 70.54% zinc. It was assigned the chemical formula, $Zn_xO_{x-1}(AcAc)(OH)$, because it also undergoes a number of rearrangements before decomposing to ZnO. The idea of rearrangement corresponds consistently with the observed data from the combustion analysis and with the IR spectra. $Zn_9O_8(AcAc)(OH)$ will be used when referring to the product of the second peak, since it was most representative of that phase. A value of X = 9 is equivalent to 70.69% zinc in the compound.

The activation energy (E_a) was then calculated using the average slopes of $d\alpha / dT$ for each peak. The first peak, having an average slope of $-2.29 \times 10^4 \pm 0.03$, had an activation energy of 190.43 ± 2.49 kJ/K· mol. The second peak with an average slope of $-1.34 \times 10^4 \pm 0.04$ had an activation energy of 111.28 ± 0.33 kJ/K· mol.

CONCLUSION

Both the open and closed cell experiments consistantly yeilded IR spectra of 2,4-pentanedione (1624 cm^{-1}) and water (1558 cm^{-1}) as the evolved gases for the decomposition of $Zn(AcAc)_2 \cdot 2 H_2O$. The two intermediates of this decomposition were determined to be $Zn_4O(AcAc)_6 \cdot 4 H_2O$ with an activation energy of 190.43 ± 2.49 kJ/K· mole occuring around 86°C and $Zn_9O_8(AcAc)(OH)$ with an activation energy of 111.28 ± 0.33 kJ/K· mole occuring around 128°C. The final product of this decomposition was determined to be ZnO based on the combined weight loss. This agrees with the results obtained by Ismail (1991) and Hussien (1990) using X-ray diffractometry (XRD) of the final product.[5,6]

REFERENCES

1. K. E. Spear, R. R. Dirkx; "Role of High Temperature Chemistry in CVD Processing," Materials Chemistry at Hight Temperatures, Volume 2: Processing and Proformance, J. W. Hastie, ed., Humana Press, Clifton, NJ, 1990, p. 107 - 130.

2. C. Bernard; "Thermochemical Modeling of Vapor Deposition," ibid. p. 131 - 142.

3. E. Defoort, J. L. Ponthenier, T. J. Anderson; "A Thermodynamic Analysis of Germanium Nitride CVD," ibid. p. 143 - 158.

4. H. Griener, E. Schnedler; "Modeling of High Temperature Transport Reactions," ibid. p. 199 - 208.

5. H. M. Ismail; "A Thermodynamic Study of Metal Acetylacetonates," Journal of Analytical and Applied Pyrolysis, 21 (1991) p. 315 - 326.

6. G. A. M. Hussein; "Characterization of the Thermal Genesis Course of Zinc Oxide from Zinc Acetoacetonate Dihydrate," Thermochim. Acta., vol. 186, no. 2, (1990), p. 187 - 197.

7. T.C. DeVore and T. N. Gallaher, Journal of Chemical Education, vol. 63, (1986), p. 729.

8. M. E. Brown; "Introduction to Thermal Analysis," Chapman and Hall, New York, 1988, p. 127 - 151.

THE EFFECTS OF ION BINDING ON THE ADENINE - THYMINE BASE PAIR

Angela Felicia Chatman

Department of Chemistry
Spelman College
350 Spelman Lane
Atlanta, Georgia 30314

Faculty Advisor: Dr. Beatriz H. Cardelino

For this theoretical study, MOPAC, a quantum mechanical program, was used to investigate the effect of ion binding on the relative stability of various tautomeric forms of adenine, thymine and the pairing of their tautomeric forms. For the latter case, the two lowest energy tautomers of adenine were paired with all possible tautomers of the complementary thymine partner. The relative energies of these paired bases were calculated with and without perturbing ions.

This study predicts that ion binding induces a reordering of the relative energies of the free tautomers and of the paired tautomeric forms of adenine and thymine.

Introduction

Interactions of ions with nucleic acids are believed to induce tautomerization and, thus, cause base mispairing. This effect is important because it may lead to spontaneous and induced mutagenesis, and carcinogenesis. DNA double helices can achieve many different stable conformations. These conformations depend on the base sequence as well as on their environment (1, 2). The binding of metal ions, which may be present in the environment, to nucleic acid bases may induce tautomerization of the bases (3). The changes in conformation of the bases may affect the primary and secondary structures of the nucleic acids, and mispairing may occur. Mispairing of the DNA bases during replication may be responsible for mutations observed in biological systems, and may be the cause for spontaneous (4) or induced mutagenesis (5) and carcinogenesis (6).

This study involved the prediction of the relative stability of adenine paired with thymine before and after they were perturbed by the presence of either a positive or negative charge in the environment. The primary step was to determine the relative stabilities of the unperturbed free tautomers and the unperturbed paired tautomeric forms. Secondly, the relative stabilities of the free tautomers and the paired tautomers were determined in the presence of ions. The goal was to determine which reordering of relative energies occurred among the paired tautomers due to different ion binding.

The perturbing ions used were either monovalent or divalent (a) cations placed close to the centers of high electron density or (b) anions placed close to the centers of low electron density. The usual centers of high and low electron density consisted of the oxygens of the exocylic keto/enol groups for thymine and the carbons to which those keto/enol groups were attached respectively (2).

Methods

The quantum mechanical program MOPAC (7), was used to study the stability of the free tautomers and the paired tautomers. All methods for theoretical calculations on large molecules involve considerable approximations. When different tautomers are being paired, an important factor is the initial geometry selected for the calculation, since it may lead to different energy minima. Theoretical predictions have been found to be very dependent on the geometry selected. Since the total energy of a paired tautomer is strongly dependent on the position of the hydrogen atoms involved in hydrogen bonding, it has been suggested that complete geometry optimization be performed (5).

The minimum energy of the paired tautomeric structures was determined by performing complete geometry optimization on several initial structures. Every optimization was performed with respect to all bond distances, bond angles, and dihedral angles. A "sparkle" was then incorporated into the six structures of the paired tautomers with lower relative energies. Sparkles consist of electric charges with no associated atomic orbitals or masses (7). Positive charges (cations) were incorporated close to the centers of high electron density. Negative charges (anions) were placed close to the centers of low electron density. The distances between the charges and the centers were fixed and chosen close to the van der Waals bond distances for K^{+}, Ca^{2+}, Cl^{-}, and O^{2-} (8).

Results

All tautomeric forms of the nucleic acid bases were identified. Tautomers were defined as structures that:

a) contain the same number of double bonds,

b) have sp^2 hybridization for all carbon atoms of the rings,

c) have sp2 hybridization for nitrogen with either the nonbonding electrons on an orbital prependicular to the ring or the nonbonding electrons on one of the sp2 orbitals,

d) have hydrogen atoms attached to the ring at the same carbon positions,

e) differ by one the following conditions:

1) contain a hydrogen atom attached to a different nitrogen atom of the rings,

2) the carbonyl functional group may be in the keto (-C(=O)-) or enol (=C(OH)-) form,

3) the amino functional group may be in the amine (=C(-NH^2)-) or the unsubstituted imine (-C(=NH)-) form.

Of the purine family, there are eight structures for adenine. Of the pyrimidine family, there are six structures for thymine. Figures 1 and 2 show the tautomer structures of adenine and thymine.

Table 1 summarizes the results obtained for all tautomers of unperturbed adenine and thymine. With respect to adenine, the lower energy structures contained the amino group in the amine form, and an H atom attached either to N 7 or N 9 of the five-membered ring (see fig. 1), with the latter position being preferred. With respect to thymine, the lower energy structures consisted of carbonyl groups in the keto/keto or in the enol/enol forms (see fig. 2), with the latter form being preferred.

The two adenine structures with lower energy were selected to be paired with all possible tautomers of the thymine partner. Tables 2 and 3 specify the location and the distance where the charges were placed and figure 3 depicts the exact position. The 1^+ and 2^+ charges were placed 2.73A and 2.39A, respectively, from the oxygen of the exocylic keto/enol group at C 2 of thymine (referred to as O 24). The 1^- and 2^- charges were placed 4.41A and 4.90A away from C 2 in thymine, respectively. These distances were selected by adding the van der Waals radius of the atom in the molecule where the charge would bind and the van der Waals radii for K^+, Ca^{2+}, Cl^-, and O^{2-} respectively.

Table 4 summarizes the relative energies obtained for the unperturbed and perturbed base pairs of adenine and thymine. For the unperturbed pair, the two adenine forms paired with the keto/keto thymine tautomers showed the lowest energy. However, when positive charges were incorporated, the two adenine forms paired with the enol/keto thymine and keto/enol thymine tautomers were preferred; the former for the 1^+ charge and the latter for the 2^+ charge. In the case of the negative charges, the two adenine forms paired with the enol/keto thymine form were preferred. It is also interesting to note that the H atom at position 9 in adenine was preferred when there were no charges incorporated and with the negative charges. When positive charges were present, the H atom at position 7 in adenine gave lower energies.

Conclusion

The normal Watson-Crick base pairing in thymine involves hydrogen bonding to adenine through the keto oxygen attached to C 4 and to the hydrated N 3 (see fig. 3). These conditions are present in two of the stable unperturbed tautomers selected. For the unperturbed pairs, the two lowest energy structures contained the two adenine forms paired with the keto/keto thymine. But the presence of any of the charges favored the enol/keto, keto/enol thymine paired structures.

Whenever a charge was present, the energy of the two adenine forms paired with the keto/keto thymine tautomer increased. As for the two adenine forms paired with the enol/keto and keto/enol thymine tautomers, there were changes in their energies from being unstable to being stable. Overall, there is an indication that ion binding might have a greater effect on the lowest energy structure of the adenine-thymine pair (in reference to the unperturbed pairs of ade 9n-thy kk and ade 7n-thy kk). This was exhibited by the increase of energy on the two adenine forms paired with the keto/keto thymine tautomer.

The fact that the lowest energy structure for the unperturbed adenine-thymine pair was not the lowest energy structure when any of the charges were incorporated, indicates that the ions may be affecting the structures of these two pairs. Specifically, the thymine keto/keto tautomer would be affected since this was the site for ion binding in the base pair of adenine-thymine. In particular, ion binding could be affecting the thymine tautomer in such a way that induced mispairing may result.

Acknowledgements

This research was supported by the NIH/BRIP Minority Biomedical Research Support (MBRS) grant #S06 GM-08241 at Spelman College. The acknowledgement also extends to Leslie Gooch and Sonya McCall for their valuable discussions and insight.

References

1. Wang, A.H.J.; Nature (London), Vol. 282, pp. 680, 1979.

2. Saenger, W.; Principles of Nucleic Acid Structure. New York: Springer-Verlag, 1984, pp. 201-219.

3. Barr, R.G. and Pinnavaia, T.M.; J Phys Chem, Vol. 90, pp. 328, 1986.

4. Watson, J.D. and Crick, F.H.; Nature (London), Vol. 171, pp. 964, 1953.

5. Flavell, R.A., Sabo, D.L., Bandle, E.F., and Weissmann, C.; J Mol Biol, Vol. 89, pp. 255, 1974.

6. Barton, J.K. and Lippard, S.J.; Nucleic Acid-Metal Ion Interactions. Spiro, Ed. New York: Wiley & Sons, 1980, ch. 2.

7. Quantum Mechanical Program Exchange #455, (Version 4.0).

8. Dean, J.; Lange's Handbook of Chemistry. New York: McGraw-Hill, 1973, pp. 118-123.

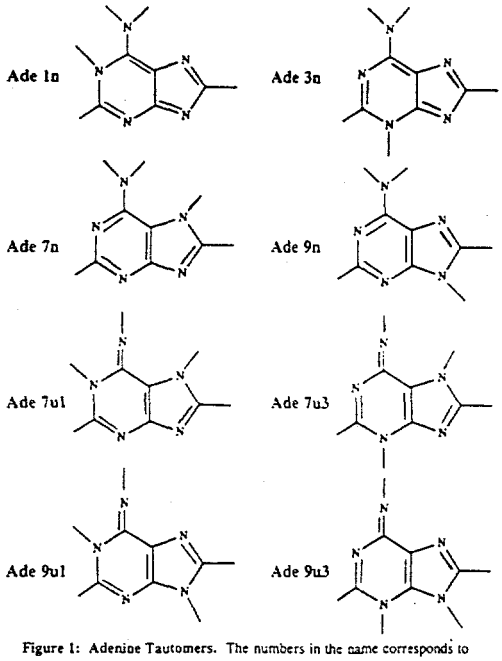


Figure 1: Adenine Tautomers. The numbers in the name corresponds to the locations where H atoms are bonded to N atoms in the ring(s); the O atom can either be in the keto (k) form or enol (e) form; the amino group can either be in an amine (n) or an unsubstituted imine (u). All ring C atoms have sp^2 hybridization.

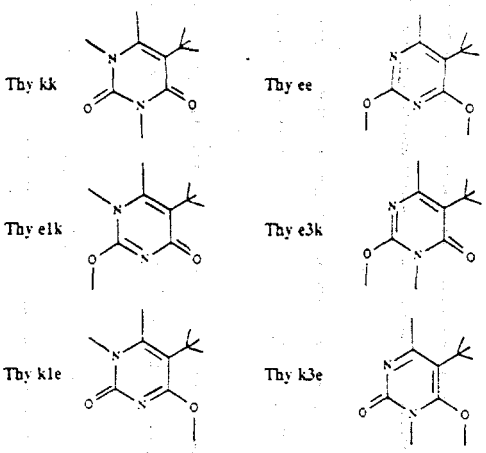


Figure 2: Thymine Tautomers. The numbers in the name corresponds to the locations where H atoms are bonded to N atoms in the ring(s), the O atom can either be in the keto (k) form or enol (e) form; the amino group can either be in an amine (n) or an unsubstituted imine (u). All ring C atoms have sp^2 hybridization.

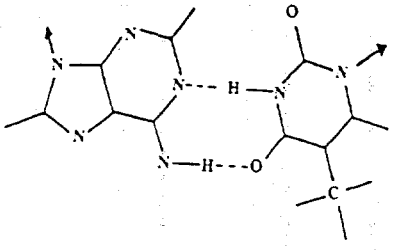


Figure 3: Basic Adenine-Thymine Structure. Reference to the structure of the base pair adenine 9n - thymine kk.

TABLE 1

Molecule	Total number of H atoms	Total number of Double Bonds	Total number of Resonance Structures	Relative Energy (KCal/Mol)
Ade 1n	5	4	1	20.78
Ade 3n	5	4	1	11.27
Ade 7n	5	4	1	8.15
Ade 9n	5	4	1	0.00
Ade 7u1	5	4	1	40.79
Ade 9u1	5	4	1	37.28
Ade 7u3	5	4	1	45.37
Ade 9u3	5	4	1	50.79
Thy kk	6	3	1	13.58
Thy ee	6	3	1	0.00
Thy e1k	6	3	1	21.09
Thy e3k	6	3	1	19.20
Thy k1e	6	3	1	23.13
Thy k3e	6	3	1	21.95

Notes:

ade = adenine, thy = thymine, n = amine, u = unsubstituted imine, k = keto, e = enol, the numbers correspond to the locations where H atoms are bonded to N atoms in the rings.

TABLE 2

ION BONDING

BASE PAIR	CHARGE	LOCATION	DISTANCE
Ade 9n-Thy kk	1+	O 24	2.73A
	2+	O 24	2.39A
Ade 7n-Thy kk	1+	O 24	2.73A
	2+	O 24	2.39A
Ade 9n-Thy e3k	1+	O 24	2.73A
	2+	O 24	2.39A
Ade 7n-Thy e3k	1+	O 24	2.73A
	2+	O 24	2.39A
Ade 9n-Thy k3e	1+	O 24	2.73A
	2+	O 24	2.39A
Ade 7n-Thy k3e	1+	O 24	2.73A
	2+	O 24	2.39A

Note:

1+ charge = K, Potassium and 2+ charge = Ca, Calcium. See additional note in table 4.

TABLE 3

ION BONDING

BASE PAIR	CHARGE	LOCATION	DISTANCE
Ade 9n-Thy kk	1-	C 2	4.41A
	2-	C 2	4.90A
Ade 7n-Thy kk	1-	C 2	4.41A
	2-	C 2	4.90A
Ade 9n-Thy e3k	1-	C 2	4.41A
	2-	C 2	4.90A
Ade 7n-Thy e3k	1-	C 2	4.41A
	2-	C 2	4.90A
Ade 9n-Thy k3e	1-	C 2	4.41A
	2-	C 2	4.90A
Ade 7n-Thy k3e	1-	C 2	4.41A
	2-	C 2	4.90A

Note:

1- charge = Cl, Chlorine and 2- charge = O, Oxygen. See additional note in Table 4

TABLE 4

RELATIVE ENERGIES (KCAL/MOL)

BASE PAIR	NO ION	1+	2+	1-	2-
Ade 9n-Thy kk	0.00	1.77	4.94	76.15	77.11
Ade 7n-Thy kk	0.83	1.14	8.37	78.21	85.59
Ade 9n-Thy e3k	44.89	0.43	72.20	0.00	0.00
Ade 7n-Thy e3k	44.94	0.00	69.27	1.07	5.32
Ade 9n-Thy k3e	164.10	25.02	2.66	84.36	104.45
Ade 7n-Thy k3e	202.99	24.66	0.00	70.44	117.13

Notes:

ade = adenine, thy = thymine, k = keto, e = enol, n = amine, the numbers correspond to the locations where the H atoms are bonded to the N atoms in the rings.

The tert-Butylbenzyl Moiety, a New Protecting Group for Alcohols

Jason Stamm, Ronald Aungst, Ann Bullion, Stephen Cairone, Bryan Firth, and Lisa Jarrell

Department of Chemistry
Lycoming College
Williamsport, PA 17701

Faculty Advisor:

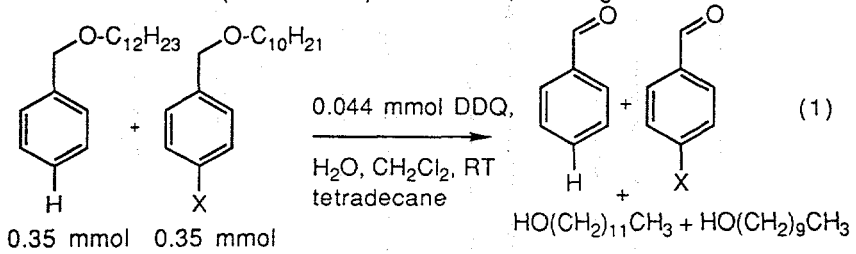
Chriss McDonald

INTRODUCTION

The efficacy of the para-methoxybenzyl (PMB) moiety as an alcohol- protecting group has been clearly demonstrated (Oikawa, Yoshioka, and Yonemitsu, 1982). PMB ethers may be synthesized using the standard conditions for ether synthesis and subsequently deprotected by treatment with 2,3-dichloro-5,6-dicyanobenzoquinone (DDQ) and water (Greene and Wuts, 1991). A mechanism involving initial rate-limiting oxidation to a stabilized para-methoxybenzylic carbocation, followed by addition of water and decomposition of the resultant hemiacetal has been postulated (Horita, et. al., 1985). Previous work in this laboratory has shown that benzyl ethers substituted with a more modest electron-donating group are also subject to oxidative deprotection with DDQ (McDonald, Nice, and Kennedy, 1994). Herein we more fully describe the effect of various substituents on the oxidative deprotection of para-substituted benzyl ethers, and a general method for utilizing the para-tert-butylbenzyl (PTBB) moiety as a protecting group for the alcohol functional group.

SUBSTITUENT EFFECTS ON THE DEPROTECTION REACTION

Kinetic studies on the effect of various para - substituents (OCH_3, CH_3, $C[CH_3]_3$, C_6H_5, Br, and Cl) on the rate of DDQ-induced deprotection of benzyl alkyl ethers relative to an unsubstituted benzyl ether were carried out. The requisite benzyl ethers were constructed from the readily available para-substituted benzyl alcohols via treatment of the corresponding alkoxide with the appropriate alkyl bromide (1-bromododecane for para-H, 1-bromodecane for all of the rest). The heterogeneity of the reaction mixture necessitated that the kinetic studies be carried out as competition reactions (Hanzlik and Leinwetter, 1978), Equation 1. Reproducible relative initial rates were obtained by the use of an internal standard (tetradecane) and small, limiting amounts



(1)

of DDQ. Data points in Figure 1 represent average values for two or three trials per substituent. The relative amount of each alcohol was

then determined by gas chromatographic analysis. The molar ratio of decanol to dodecanol was used as a measure of k_X/K_H. The sum of the yields of the two alcoholic products was always within 5% of 0.044 mol. Aldehyde products were not quantified. The large negative ρ+ value of -2.9 (R = 0.95) is reasonable based on the aforementioned mechanism which invoked a benzylic carbocation intermediate. Clearly the identity of the para-substituent plays an important, well-defined role in the rate of DDQ-induced removal of the benzylic moiety.

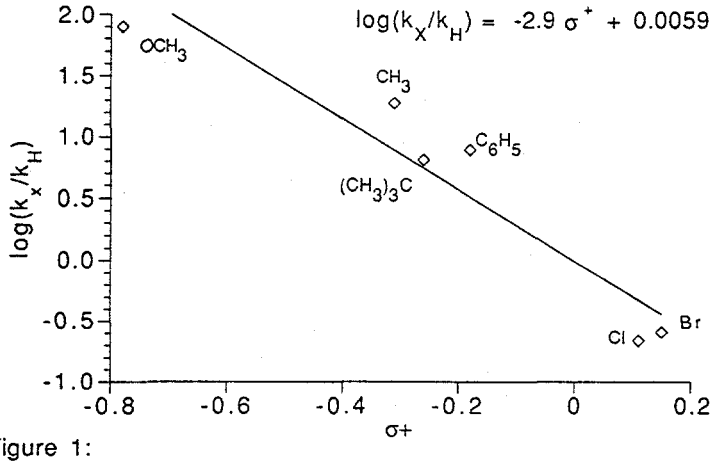
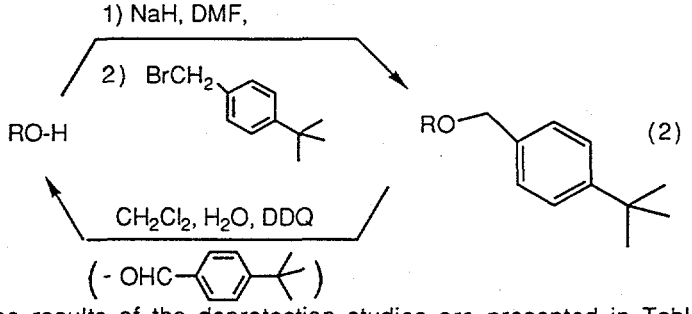


Figure 1:

DEPROTECTION OF PARA-TERT-BUTYLBENZYL ETHERS

The para-tert-butylbenzyl group was further examined regarding its synthetic utility as a protecting group. Protection of alcohols as PTBB ethers is straightforward, involving deprotonation with sodium hydride and subsequent reaction with the commercially available para-tert-butylbenzyl bromide (Equation 2). This well established protocol afforded the corresponding ethers in 60-80% yields.



The results of the deprotection studies are presented in Table 1. In most cases, excellent yields of the alcohol products are obtained. The deprotections were typically complete after three hours. A notable exception is the ribofuranoside derivative shown in entry 4. This reaction was significantly more sluggish, full deprotection requiring 30 hours. The deprotection of the PTBB ether of 3-octanol shown in entry 2 is also worthy of note. When the reaction was performed with 2.0 eq of DDQ, approximately 7% of the product was

converted into the corresponding ketone, 3-octanone. The oxidation of secondary alcohols to ketones with DDQ has been previously reported (Iwamura and Hirao, 1973). Lessening the amount of DDQ to 1.5 eq obviated these difficulties (< 3% of 3-octanone being formed). The primary alcohol products are apparently much less susceptible to oxidation by DDQ as evidenced by the lack of production of the corresponding aldehydes. The para-tert-butylbenzaldehyde that is also liberated in the deprotection reaction was quantified for entries 1-3. Yields were consistently in the 80 - 90% range. Entries 5 and 6 illustrate the selectivity of the deprotection. We were gratified to see that the more reactive PMB group could be removed selectively in the presence of the PTBB group as shown in entry 5. The liberated aldehydes were also quantified in this procedure (83% para-methoxybenzaldehyde and 6% para-tert-butylbenzaldehyde as determined by gas chromatography). Attempted removal of the PTBB group in the presence of the benzyl group was less satisfactory. Only 45% of the pure 5-benzyloxy-1-pentanol could be isolated. The gas chromatographically determined yields for para-tert-butylbenzaldehyde and benzaldehyde were 78% and 22% respectively.

CONCLUSION

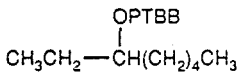
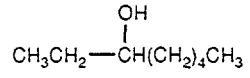
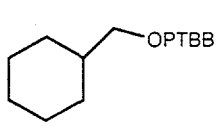
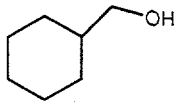
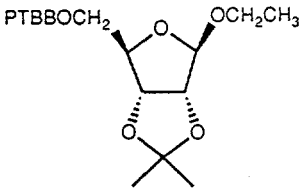
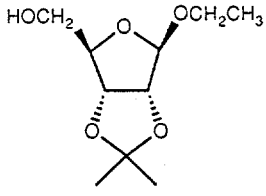
The PTBB group has been shown to be a useful protecting group for alcohols. It is sufficiently less reactive than the PMB group to allow selective cleavage of the PMB ether. There is not sufficient reactivity difference between the PTBB group and the benzyl group to allow selective removal of PTBB. Future plans include an examination of the protection/deprotection sequence with other functionality and an evaluation of dialkylbenzyl groups (perhaps 3,4-dimethylbenzyl) as oxidatively removable protecting groups.

TYPICAL EXPERIMENTAL PROCEDURES

Competition between p-tert-butylbenzyl decyl ether and benzyl dodecyl ether. A 20 mL screw-capped vial equipped with a stir bar was charged with 113 mg (0.372 mmol) of p-tert-butylbenzyldodecyl ether and 102 mg (0.370 mmol) of benzyl dodecyl ether. To this mixture was added 7 mL of dichloromethane, 0.7 mL of water, 23 mg (0.12 mmol) of tetradecane (internal standard) and 10 mg (0.044 mmol) of DDQ. The reaction mixture was stirred for 24 h. Gas chromatographic analysis of the dichloromethane layer showed the yields for decanol and dodecanol were determined by to be 0.037 mmol and 0.0054 mmol respectively (log k_X/k_H = 0.84).

Deprotection of ß-ethyl-2,3-O-isopropylidene-5-O-p-tert-butylbenzyl-ribofuranoside. A 20 mL screw-capped vial equipped with a stir bar was charged with 210 mg (0.576 mmol) of the protected ribofuranoside. Dichloromethane (2.9 mL), water (0.29 mL) and DDQ (261 mg, 1.15 mmol) were added. The heterogenous reaction mixture was stirred for 30 h, at which time thin-layer chromatographic analysis indicated complete consumption of starting material. Water was added (5 mL) and the mixture was extracted with ether (4 X 5 mL). After solvent removal, the residue was chromatographed on a 35 X 1 cm column of silica gel using mixtures of ethyl acetate in hexane (5% --> 20%) to provide 100 mg (0.458 mmol, 80%) of the corresponding known alcohol (Levene and Stiller, 1933) as a colorless syrup.

Table 1. Oxidative Removal Of the para-tert-Butylbenzyl (PTBB) Protecting Group[a,b]

entry	protected alcohol	product	eq DDQ	yield[c]
1	$n\text{-}C_{10}H_{21}OPTBB$	$n\text{-}C_{10}H_{21}OH$	2.0	91%[d]
2			1.3	95%[d]
3			2.0	65%[d]
4			2.0	80%
5	$PMBO\text{—}(CH_2)_5\text{—}OPTBB$	$HO\text{—}(CH_2)_5\text{—}OPTBB$	1.0	89%
6	$BnO\text{—}(CH_2)_5\text{—}OPTBB$	$BnO\text{—}(CH_2)_5\text{—}OH$	1.4	45%

a. Reaction conditions: CH_2Cl_2 (0.2M), H_2O, RT.
b. *PTBB = para-tert-butylbenzyl, PMB = para-methoxybenzyl, Bn = benzyl.*
c. Isolated yield except where noted.
d. Yield determined by GC using tetradecane as an internal standard.

REFERENCES.

Greene, T.; and Wuts, P., 1991, Protective Groups in Organic Synthesis, 2nd Edition, Wiley, New York.

Hanzlik, R.; and Leinwetter, M., J. Org. Chem., Vol. 43, 1978, pg. 438-440.

Horita, K.; Yoshioka, T.; Tatsuyoshi, T.; Oikawa, Y.; Yonemitsu, O., Tetrahedron, Vol. 42, 1986, pg. 3021-3028.

Iwamura, J.; and Hirao, N., Tetrahedron Lett., Vol. 27, 1973, pg. 2447-2450.

Levene, P.; and Stiller, E., J. Biol. Chem., Vol. 102, 1933, pg. 187-192.

McDonald, C.; Nice, L.; and Kennedy, K. Tetrahedron Lett., Vol. 35, 1994, pg. 57-60.

Oikawa, Y.; Yoshioka, T.; Yonemitsu, O., Tetrahedron Lett., Vol. 23, 1982, pg. 885-888.

Enantioselective Addition of Metal-Based Nucleophiles to Unsaturated Aldehydes

Cynthia A. Papesch

Department of Science
Pennsylvania State University at Erie
The Behrend College
Station Road
Erie, PA 16563

Faculty Advisor:

Dr. Timothy L. Friebe

Enantiomeric selectivity is a vital goal in synthetic chemistry. Our research focuses on novel methods of achieving enantioselective addition of Zn-, Mg- and Cu-based nucleophiles to unsaturated aldehydes. Unsaturated aldehydes were first converted to chiral 1,3-dioxolan-4-ones and then reacted with metal-based nucleophiles including phenyl, allyl, butyl, and vinyl organometallics to give addition products. These reactions were performed both in the presence and absence of a transition metal catalyst.

INTRODUCTION

Enantiomeric control of reaction products is crucial in synthetic organic chemistry. Animal life and its environment is filled with both optically active and biologically active natural products. Many of these compounds are active only in one enantiomeric form, while the other enantiomer exhibits no activity at all or possibly even detrimental behavior. For this reason, it is vitally important for the synthetic chemist to be able to control the enantioselectivity of the reactions carried out to create a natural or biological product. Our research focuses on the optimization of novel methods for achieving enantioselectivity in addition reactions to α,β-unsaturated aldehydes.

The α,β-unsaturated aldehyde, acrolein, was converted to a dioxolanone in order to facilitate the addition of a metal-based nucleophile. Dioxolanones contain easily accessible alkenyl and acetal carbons. These carbons are the targets of our direct (1,2)- and conjugate (1,4)- addition reactions. The dioxolanone was reacted with various Grignard and organozinc reagents in order to generate a new chiral center at the 2-alkenyl and/or the acetal carbon. The organozinc reagents were formed by mixing the corresponding Grignard reagent with zinc dust in THF for approximately one hour prior to the addition of the reagent to the reaction flask containing a THF solution of the dioxolanone. The nucleophilic groups used in the organometallic reagents were benzyl, phenyl, allyl, butyl, and vinyl.

EXPERIMENTAL

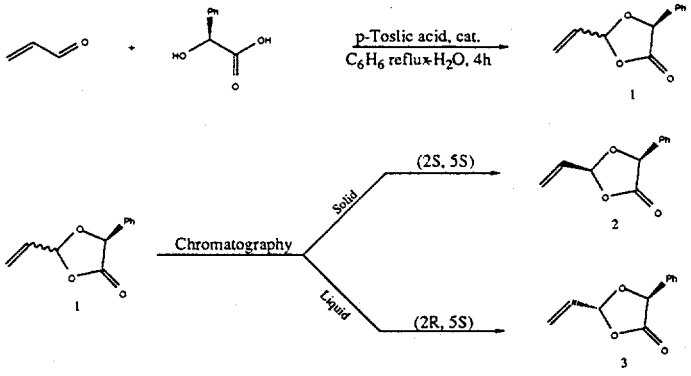
Synthesis of Starting Material

Our starting material was (2R, S, 5S)-2-ethenyl-5-phenyl-1,3-dioxolan-4-one. A mixture of 21.5 g of (S)-(+)-mandelic acid, 11.2 mL of acrolein, and 0.27 g of *p*-toluenesulfonic acid in benzene was refluxed for four hours with the azeotropic removal of water.[1] Three milliliters of water were collected. After some cooling, the warm solution was quickly washed with two 50 mL portions of saturated $NaHCO_3$ and one 50 mL portion of saturated NaCl. The yellow

benzene layer was isolated and dried over $MgSO_4$, filtered and concentrated under vacuum. The resulting liquid was vacuum distilled at 84°- 87° C to give 15 g of a very light yellow, clear liquid. (Equation 1, Product 1)

The yellow liquid consisted of two diastereomers, which were separated by column chromatography into the (2S, 5S) and (2R, 5S) diastereomers. (Equation 1, Products 2 and 3) The cis isomer formed long, white crystals with a melting point of 22° C, while the trans isomer remained a clear, colorless liquid at room temperature.

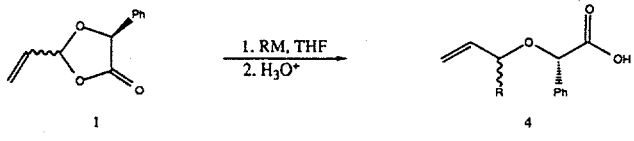
Equation 1



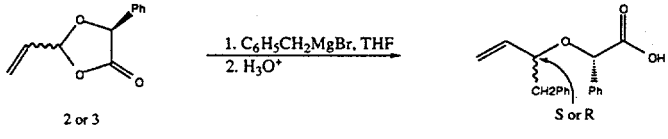
Organometallic Reactions

Our starting material was used both as a racemic mixture (product 1) and as a pure diastereomer (product 2 or 3). The starting material and an organometallic nucleophile (1:1 ratio) were mixed together in dry THF under a nitrogen atmosphere. The solution was stirred for three days forming a cloudy, white mixture. The reaction mixture was then quenched with aqueous HCl (10%) solution, extracted with ether, and the ether layer washed with saturated NaCl, dried over $MgSO_4$ and concentrated under vacuum. The products were stored in desicators, since they exhibited hygroscopic properties. Equations 2 and 3 show general reactions for the schemes described.

Equation 2



Equation 3



M = ZnCl or MgBr R = allyl, vinyl, butyl, phenyl, benzyl

RESULTS

The major product of the described organometallic reaction with the racemic starting material was identified as a carboxylic acid by both FT-Infrared (FT-IR) and Nuclear Magnetic Resonance (NMR) spectroscopic methods.

Interestingly, these results were in direct contrast with results reported using six-membered ring dioxolanones in which the nucleophilic attack occurred at the lactone carbon and yielded a keto-alcohol.[2] The percent yields of isolated crude carboxylic acid (product 4) formed by various nucleophiles were as follows: phenyl, allyl, and vinyl -- greater than 75%; butyl and benzyl -- greater than 90%, respectively. Yields and reaction conditions were not optimized.

When one of the pure diastereomers of the starting material was used in an organometallic reaction, only one major carboxylic acid isomer was observed on the ^1H NMR spectrum. Yields and diastereomeric excess of products have yet to be determined.

Furthermore, preliminary results using organocuprate nucleophiles indicate 1,4-addition occurring rather than the 1,2-additon observed with the other metal-based nucleophiles.

ACKNOWLEDGMENTS

Pennsylvania State University at Erie, The Behrend College
PSU Undergraduate Research Fund

REFERENCES

(1) Dr. Timothy L. Friebe, Doctoral Thesis, Northwestern University, June **1990**.

(2) Schreiber, S. L.; Reagan, J. *Tetrahedron Letters*, **1986**, *vol. 27*, pp. 2945-2948.

Production and HPLC Purification of Siderophores: Enterobactin and Ferric Eneterobactin

William C. Putnam

Department of Chemistry
Pittsburg State University
Heckert-Wells Hall
Pittsburg, KS 66762

Faculty Advisors:

Dick van der Helm

Department of Chemistry and Biochemistry
University of Oklahoma
602 Parrington Oval
Norman, OK 73019

Iron has long been established as a bioessential element for cellular growth. Iron appears in earth's environment as iron(III) due to the oxidative atmosphere. This poses a large problem due to insolubility. To elevate this problem gram-positive microbateria and fungi secrete to the extracellular environment, low molecular weight compounds called siderophores. This is followed by induction to the cell through a specific membrane protein system. Production, and purification techniques of enterobactin a siderophore produced in Escherichia coli have been established as well as the ferriation procedure.

INTRODUCTION

During the anaerobic stage of life iron was established as a bioessential element.[1] Due to the oxidative nature of the Earth's environment iron exists in its trivalent state. This poses an extreme problem of insolubility due to the high solubility product of iron(III) hydroxide (10^{-38}). To combat this problem most aerobic microorganisms secrete low molecular weight iron chelating complexes called siderophores. Siderophores chelate the iron in the extracellular environment in a hexadentate, octahedral structure. This chelation is followed by an introduction to the cell through a system of siderophore-specific membrane receptor proteins.[2] This involves active transport across the outermembrane, periplasm, and inner membrane of gram-negitive bacteria to the cytoplasm. These proteins have high affinity to the specific siderophore produced by the organism, or closely related ones. Production of more than one type of siderophore allows the organism to compete better for the iron, this is seen in fungi. This can also be done by acquiring genes for uptake systems and siderophores which are not produced by the organism, a method apparently used by bacteria. The ongoing research is directed toward purification of the siderophores from the extracellular environment, and eventual structural determination using single crystal x-ray diffraction. The specific siderophore examined in this paper is enterobactin and the ferriated complex of enterobactin. Enterobactin(See Figure 1) is a siderophore secreted by Escherichia coli bacteria when orientated in low concentrations of iron.

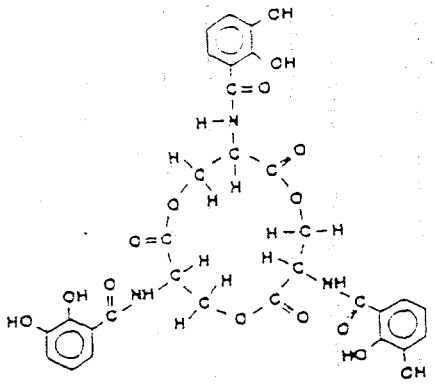


Figure 1: Structure of Enterobactin

EXPERIMENTAL METHOD

Enterobactin, from Escherichia Coli strain AN102, was grown in deferriated growing media for 24 hours at 37°C on a rotary shaker. The growing media was deferriated using Chelex 100. The cells were separated from the supernatant using centrifugation for 30 minutes at 3500 rpm. The supernatant was adjusted to pH = 4.0 with concentrated HCl. The supernatant was then run through a XAD-2 column (8cm diameter*10cm). The column was then washed with MilliQ water. The enterobactin was eluted off of the column using HPLC grade methanol. The elute was then concentrated using a rotovap(room temperature). A LH-20 column was prepared and packed in methanol(HPLC grade). The compound was allowed to run through the column and a number of bands were detected. The elute was collected in fractions with about a 5mL volume in each tube. The fractions were tested for the presence of siderophores using thin layer chromatography(TLC). The solvent system used was 35:12:1 -(chloroform, methanol, water). The TLC paper was allowed to dry and then sprayed with 5.0% $FeCl_3$ in HCl. A black spot was noted at Rf = 0.75. This Rf value was consistent with previous lab results for enterobactin. The target fractions in which the siderophore was detected were combined and concentrated using a rotovap(room temperature). The purification was then performed on a Gilson HPLC using a {(250*8)mm Nucleosil 300 RP-C18 7 micron} column. A gradient was found running from 0 to 68% acetonitrile in water, and the gradient lasted 50 min. The detector was set to 280nm, and a flow rate of 1 ml/min was used. Both solvents were filtered, degassed and contained 0.1% trifluroacetic acid(TFA) as to maintain a pH of about 2.5. Establishment of protocol for the purification of the ferriated complex of enterobactin was the next step.

The complexation was completed under Argon using Schlenk apparatus. The equation under which the reaction proceeds is as follows[3]:

$Fe(acac)_3 + H_6(Ent) + 3\ KOH \Longrightarrow Fe(Ent)^{-3} + 3\ H^+ + 3\ H_2O + 3\ H(acac)$

Stoichiometric solutions of $Fe(acac)_3$, KOH, and Enterobactin are produced in methanol (HPLC grade). The concentration of enterobactin is deduced using ultraviolet spectroscopy and an extinction coefficient $\varepsilon_{316}(MeOH) = 9500$[4]. The solution of enterobactin is added to the schlenk flask, and the

solvent is degassed in the schlenk flask. The tris(acetylacetonate)iron(III) is added to another schlenk flask and separately degassed. The metal complex is added to the enterobactin flask using a gas tight syringe. The KOH solution is degassed in a separate flask. The KOH is then slowly cannulated over to the reaction flask using small diameter teflon tubing, this proceeds over a two minute period. The pH is checked and found to be slightly basic(7.5). The solvent is removed from the complex. The complex can then be placed under a second solvent if recrystalization is deemed necessary. The solution was then taken to paper electrophoresis for further purification due to the triply negitative state of $Fe(ent)^{3-}$. The major band was collected and, dissolved in methanol. The ferric enterobactin was identified on a {(7.8*300)mm c18-RP Waters Nova-pak 6micron} column using a 0 to 85% acetonitrile in water gradient. The detector was set to 280nm and the flow rate was set at 1ml/min. The solvents contained 0.1% TFA to maintain the pH at 2.5.

DISCUSSION OF RESULTS

When enterobactin was injected on the HPLC column small peaks were found at retention times (10.2, 14.4 and 21.5) minutes. These are probable decomposition peaks corresponding to the monomer, dimer and trimer receptively. These peaks were omnipresent in the chromatograms. These peaks are believed to be decomposition peaks due to their increase in intensity when the sample was subjected to denaturing conditions (i.e. large temperature fluctuations). The retention time for enterobactin was found to be 23.4 min(See Figure 2).

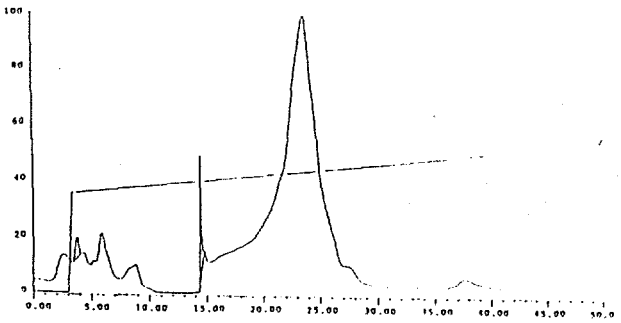


Figure 2: HPLC of enterobacin after LH-20, and concentration

All peaks were collected and tested for the presence of siderophores through TLC. Only the peak at 23.4 min. was found to contain enterobactin. To test the purity after HPLC the Rt(23.4) peak was reinjected and the chromatogram was deemed pure due to the lack of intensity of secondary peaks (See Figure 3). The ferric enterobactin was then tested on the HPLC for purity after the complexation reaction. Further purification was needed and the answer was found in paper electrophoresis. The FeEnt was then reinjected after paper electrophoresis and the results were extremely positive(Figure 4). The ferric enterobactin was found to be pure. A retention time was established for the gradient at 61.0 min.

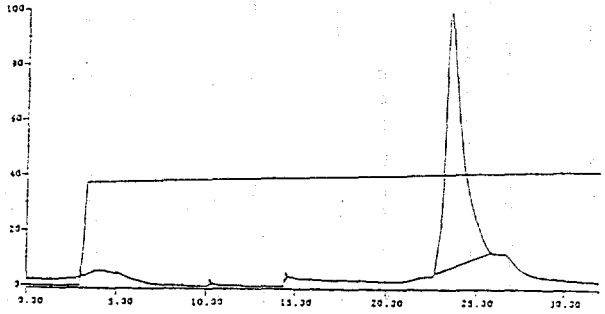


Figure 3: Injection of Enterobactin Peak

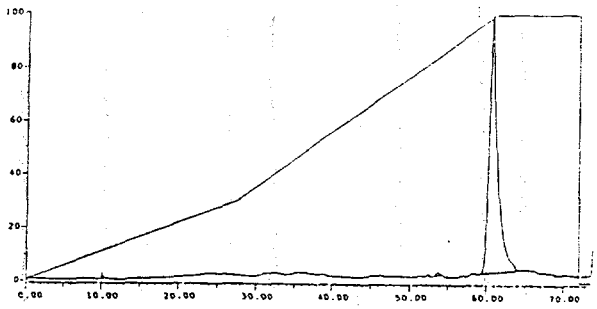


Figure 4: HPLC of Ferric Enterobactin

CONCLUSION

Establishment of the protocol of production and purification of Enterobactin and Ferric Enterobactin have been obtained using HPLC techniques. Many more wide range studies can be planned using this powerful separation technique and iron transport agents. The protocol is also very useful in the development of similar protocol for the purification of other siderophores, such as Pseudobactin from Pseudomonas Florescens.

ACKNOWLEDGMENTS

The author would like to thank Dr. van der Helm, his staff, the University of Oklahoma, the National Science Foundation, and Dr. Gerald Caple for making this possible.

REFERENCES

1. J.B. Neilands (1984), Structure and Bonding, p.p. 6-7
2. J.B. Neilands (1982), Microbial envelope proteins related to iron. Annual Reviews inMicrobiology. 36 285-309.
3. T.B. Karpishin, and K.N. Raymond (1992), The first characterization of a Metal-Enterobactin complex: $[V(enterobactin)]^{2-}$. Angewandte Chemie, 31(4): 466-468.
4. L.D. Loumis and K.N. Raymond (1991), Inorganic Chemistry, 30: 906-911.

CONTACT ANGLE STUDY OF PORPHYRIN MONOLAYERS ON SOLAR CELLS

Thea J. Wilmarth

Department of Chemistry
Willamette University
900 State St.
Salem, OR 97301

Faculty Advisor:
Carl C. Wamser
Department of Chemistry
Portland State University
Portland, OR 97207

The technique of contact angle pH titration (observing the contact angle made on a solid surface by various aqueous buffers as a function of the buffer pH) is used to characterize the porphyrin layer of solar cell electrode surfaces. Porphyrins used are tetrakis (4-carboxyphenyl)-porphine (TCPP), tetrakis(4-aminophenyl)-porphine (TAPP), and poly-TAPP (prepared by electropolymerization.) Ultraviolet spectroscopy is used to determine the length of time required for maximum adsorption of each porphyrin onto glass used in the solar cell system. Theoretical calculations of the absorbance of a porphyrin monolayer using Beer's Law are related to the porphyrin film thickness obtained in experimental results. TCPP adsorption was more than six times that of TAPP to glass. Contact angle pH titrations show that TCPP reacts distinctly opposite to poly-TAPP. This is consistent with the surface acid-base reactions which show the charged form of the carboxylic acid or amine functional group to be more hydrophilic (lower contact angle) than the neutral form. The pKa of TCPP was found to be between 5-7, while the pKa of poly-TAPP was found to be between 7-10.

BACKGROUND

"Harvesting light energy." Solar power. Photovoltaic (PV) cells. The future of energy resources. Artificial photosynthesis has been the subject of countless hours of research and debate. In recent years, scientists have been looking for ways to maximize efficiency while minimizing costs of solar cells to make solar energy feasible on a macroscopic scale.

Liquid-electrolyte solar cells, designed by Michael Gratzel of the Swiss Federal Institute of Technology in Lausanne, are one of the newest possibilities for generation of solar energy. The system is "an electrochemical cell -- two electrodes in contact with a liquid that contains charge-carrying ions. One of the electrodes is covered with a layer of titanium dioxide particles, which is in turn coated with a special dye. . . The photosensitive dye molecules absorb photons of incoming light, . . . and release electrons to the titanium dioxide underneath." (Beardsley, 1992) The ruthenium-based dye used in Gratzel's model has similar characteristics to chlorophyll, the light-absorbing pigment found in plants and photosynthetic bacteria that facilitates photosynthesis.

TiO_2 colloid has been shown to be useful in the solar cell system because it creates a large surface area for the binding of photosensitizer. The more porphyrin or the surface of the cell, the more light can be absorbed.

The dye is one of the key elements of the solar cell. It enables the system to utilize more wavelengths in the solar spectrum, and to separate the charge once energy is absorbed. This is similar to the work of the pigments in chlorophyll which "collect light in various regions of the solar spectrum and transfer the resulting excitation energy to a reaction center where the photochemistry occurs." (Gust & Moore, 1989) Increased light absorption is one way to maximize efficiency.

Dyes made of porphyrin molecules have shown an asymmetric structure that effectively directs charge transport. (Wamser et al . , 1989) "The idea is to get the charges to separate and flow across a load to produce electricity before they recombine. . . You want to get the charges as far apart as you can as quickly as you can." (Amato, 1990) The charge separation is directional, "involving transfer of electrons toward the acid-rich surface of the film." (Wamser et al . , 1989)

At Portland State University working with porphyrin dyes in the context of a solar cell system, a contact angle study of monolayer films of either tetrakis(4-carboxyphenyl)-porphine (TCPP) or tetrakis(4-aminophenyl)-porphine (TAPP) adsorbed onto plain glass, conductive indium-tin oxide (ITO) glass, and TiO_2 colloid was undertaken.

The use of contact angle titrations to characterize surfaces is a relatively new technique. By observing the angle between a liquid drop on a solid surface, one can determine the chemical interactions that are taking place The contact angle indicates the strength of interaction between the liquid and solid. If the contact angle of several buffered drops of various pH upon a surface is observed, the acidity or basicity of the surface can be determined. This is a surface-sensitive technique, the interaction between liquid and solid occurring between the first few molecular layers. As the surface functional groups interact with the buffered drop, the solid-liquid component of the surface free energy will change as a function of pH. This explanation of free energy comes from a modification of Young's equation (Wamser, 1992.) Contact angle titrations would be a useful way to identify and characterize the surfaces of porphyrin-coated, solar cell electrodes quickly and easily.

METHODS

Materials. Buffer solutions were prepared to a 0.05M concentration
The pH was finely adjusted using small amounts of either NaOH or HCl. The buffers used were HCl (pH 1), maleic acid (pH 2), tartaric acid (pH 3), succinic acid (pH 4), acetic acid (pH 5), maleic acid (pH 6), HEPES, 4-(2-hydroxyethyl)-1-piperazineethanesulfonic acid (pH7 and 8), Borax/ HCl (pH 9), CAPS, 3-(cyclohexylamino)-1-propanesulfonic acid (pH 10 and 11), phosphate (pH 12), and NaOH (pH 13). Buffers chosen reflect previous research done by Mark Gilbert (Wamser, 1992.) Porphyrins used were the purest commercially available (see Figure 2.)

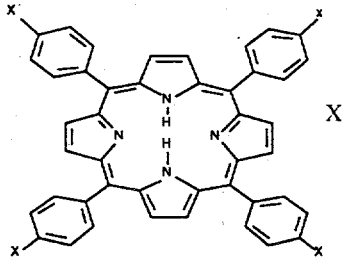


Figure 1: Porphyrin Structures

Preparation of Glass. The glass used was fluorine-doped indium tin oxide (ITO). After cutting into small pieces, 1x1.5 cm, they were washed in a sonic cleaner with Micro cleaner and distilled water for thirty minutes. After the initial cleaning, glass was rinsed with distilled water and soaked for one hour in either acid, base, or neither. Then, the glass was rinsed again with distilled water in the sonic cleaner for thirty minutes. Finally, the glass pieces were dried in an oven above 100 °C for at least two hours.
TiO_2 Colloid Preparation. TiO2 colloids were prepared using commercial TiO_2 (P-25). The TiO_2 (3 g) was combined with a small volume of water (1 mL) containing acetic acid (0.1 mL) to prevent reaggregation of the crystals and mixed with mortar and pestle to form a thick paste. Water (4 mL) was added dropwise to dilute the paste. To facilitate the spreading of the colloid, a detergent (0.05 mL Triton X-100) was added.

A clean piece of ITO glass, 3x8cm, was lined lengthwise with Scotch tape to 1.5cm on either side. A small spatula was used to spread a thin line of TiO2 across one end of the glass. Using a cylindrical glass rod, TiO2 colloid was spread evenly back and forth over the entire length once. After drying in air for at least one hour, the TiO2 colloid was cintered in a muffle furnace at 420C for twenty minutes and allowed to cool slowly. (Nazeeruddin et al, 1993.)

Soaking Procedures. Each photosensitizer was applied in a similar manner. Generally, the porphyrin of choice was prepared to a 0.1 mM concentration in absolute ethanol. Then, 3mL of porphyrin solution was poured into a small vial with a tight fitting cap. A piece of glass was placed in the solution and allowed to sit, undisturbed, for a specific length of time. The cap was on tightly at all times to prevent evaporation of the ethanol solvent. The sample was removed, rinsed with ethanol, and allowed to air dry.

Preparation of poly-TAPP Sample Films. Graduate student Judith Lebzelter deposited poly-TAPP films on ITO glass using electropolymerization. This technique produced even films, which are needed for contact angle studies.

Absorption Spectroscopy. Absorbance measurements were taken using a Shimadzu 260 UV-spectroscopy instrument. The reference samples were plain, ITO glass rinsed with ethanol and allowed to air dry. Both reference and sample were attached to the instrument for analysis using double-sided tape.

Contact Angle Measurements. Using a Kayeness Model D1060 contact angle analyzer, glass pieces were placed on a flat surface and inserted into the machine for measurement. A 1-μL drop of buffer solution was dispensed onto the glass coated with photosensitizer of choice by a fixed syringe. The contact angle was measured by estimating the tangent to the liquid curve at the point of contact. Although measurements were taken quickly after placing the drop, significant evaporation occurred after thirty seconds. Drops were placed in either of two ways: on a fresh location of the film for each drop, or on the same spot each time. For the latter, the glass was washed with distilled water and then pure (200 proof) ethanol between drops. Measurements were taken at least twice for each film. The order for placement of buffer solution drops was variable, but most often occurred in either an ascending or descending series.

RESULTS

ADSORPTION PROPERTIES

I found the adsorption of porphyrin to ITO glass varied with time at a different rate for both TAPP and TCPP. The peak adsorbance for TCPP was at one hour with a Soret band absorbance of 0.115, while the peak adsorbance of TAPP was after five hours. TCPP was found to be more than twice as adsorbent as TAPP. The low adsorbency of TAPP onto glass suggests that the molecules had a stronger affinity for ethanol than for glass. After reaching a maximum peak, the adsorbency of TCPP then decreased. This behavior suggests that the porphyrin molecules were approaching an equilibrium between the amount adsorbed onto glass and the amount dissolved in ethanol solution.

Using Beer's law, the thickness of a monolayer of porphyrin molecules can be calculated. The typical Soret band of a porphyrin film has a molar absorptivity of $1X10^5$ $L \cdot M^{-1} \cdot cm^{-1}$, and a density of $0.9g/cm^3$ (Wamser Notebook, 1992.) A UV-visible spectrum was taken of each sample as a film on a piece of ITO glass, approximately 0.3 cm thick. The path length of a monolayer of porphyrin will be the sum of the glass thickness and the thickness of one molecule (approx. 20 Å.) From this information, it can be shown that the absorbency resulting from a uniform monolayer of typical porphyrin molecules is the following:

$$Abs. = E \cdot c \cdot l$$

$$Abs. = (1X10^5 L \cdot M^{-1} \cdot cm^{-1})\ (0.9g/cm^3)\ (6X10^{-8}cm)\ (1000cm^3/L)(1mol/\ x\ g)$$
$$Abs. = 5.4g/x\ g \qquad (x = \text{mol. wt. of porphyrin})$$

Therefore, a monolayer of TCPP (mol. wt.- 794.83g/mol) has an absorbency of 6.79 x 10^{-3} and that for a monolayer of TAPP (mol. wt.- 674.70 g/mol) is 8.00 x 10^{-3}. From these calculations, it can be seen that the film of TCPP was more than sixteen layers thick at maximum adsorbency. Interestingly, the TAPP film was only about 2.5 layers thick at maximum adsorbency. (The poly-TAPP films were too thick to analyze using UV-spectroscopy.)

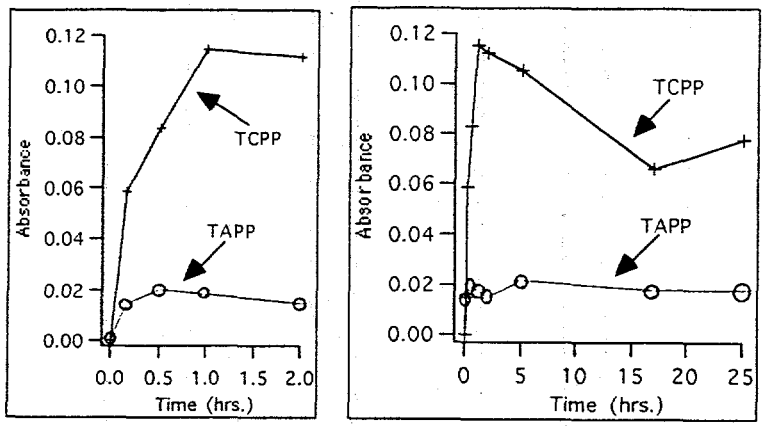


Figure 2: Absorbance vs. time data for adsorption experiments of TCPP and TAPP on ITO glass.

SURFACE EFFECTS

The acidity or basicity of the ITO glass surface caused very different adsorption properties. Acidic washing of glass prior to soaking with any porphyrin causes a significant decrease in adsorption. Base washing, however, causes TCPP to adsorb to a greater extent than if no base had been applied. It is believed that the base causes ionization of the hydroxyl groups on the glass surface, which allows a maximum amount of covalent bonding between porphyrin and glass to occur.

Application of these properties involves storage of porphyrins. Prewashing of containers with strong acid prior to storage of porphyrin solutions will minimize loss of porphyrin to the sides of a beaker.

CONTACT ANGLE pH TITRATIONS

It was found that porphyrins react quite differently to the pH buffers (See Figure 3.) TCPP showed a high affinity for basic solutions while avoiding acidic ones. This is reasonable because the reactive functional group on TCPP is a carboxylic acid. The pKa of TCPP was shown experimentally to be between 5-7.

Poly-TAPP showed distinctly opposite behavior to TCPP. The surface showed strong hydrophobicity to higher pH, basic solutions and hydrophilicity to lower pH, acidic buffer solutions. The pKa for poly-TAPP was shown to be between 7-10 depending on the film used for measurements.

TAPP on TiO_2 colloid also showed some sign of hydrophilicity towards acidic buffer solutions. However, the points scattered greatly so that a conclusion is difficult. The liquid buffer solutions may be soaking down into the absorbent TiO_2 , therefore skewing the measurements. This would explain the overall occurrence of very low angles (22 degrees or less).

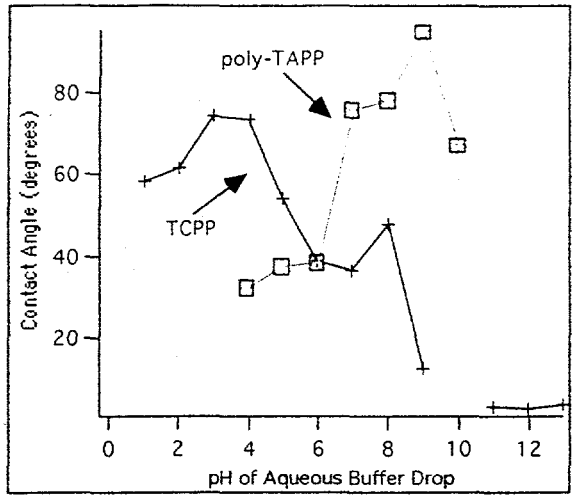


Figure 3: Example of pH contact angle titration for poly-TAPP and TCPP on ITO glass.

DISCUSSION

Results were not highly reproducible. Porphyrin coverage may have been slightly uneven due to the adsorption technique utilized. This was not noticeable by UV spectroscopy, but perhaps is important when utilizing a surface-sensitive technique such as contact angle studies. The porphyrin molecules may also have stacked up in a non-uniform manner, causing microscopic nooks for the buffered drop to soak into.

It is possible that the drop size was not appropriate, as contact angles are affected by drop size (Drelich, 1993.) Previous studies utilized drops of 1 μL volume, but this may not be small enough (Wamser, 1992.) In the future, drop size should be varied.

REFERENCES

Amato, I. "Lab-made molecule taps light's energy," Science News 1990, 247.

Beardsley, T. "Current Event: Bright future for a new photovoltaic cell," Scientific American 1992, 138.

Drelich, Jaroslaw; Miller, Jan D.; and Hupka, Jan "The Effect of Drop Size on Contact Angle over a Wide Range of Drop Volumes," Journal of Colloid and Interface Science 1993, 155, 379-385.

Gust, D. & Moore, T.A. "Mimicking Photosynthesis," Science 1989, 244, 35-41.

Nazeeruddin, M. K.; Kay, A.; Rodicio, I.; Humphry-Baker, R.; Muller, E.; Liska, P.; Vlachopoulos, N.; & Gratzel, M. "Conversion of Light to Electricity by cis-X2Bis(2,2'-bipyridyl-4,4' dicarboxylate) ruthenium(II) Charge-Transfer Sensitizers (X= Cl , Br ,I , CN , and SCN) on Nanocrystalline TiO2 Electrodes," J. Am. Chem. Soc. 1993, 115, 6382-6390.

Wamser, Carl C. Portland State University Research Notebook 1992, 36, 8.

Wamser, C.C.; Bard, R.R.; Senthilathipan, V.; Anderson, V.C.; Yates, J.A.; Lonsdale, H.K.; Rayfield, G.W.; Friesen, D.T.; Lorenz, D.A.;Stangle, G.C.; Eikeren, P.; Baer, D.R.; Ransdell, R.A.; Golbeck, J.H.; Babcock, W.C.; Sandberg, J.J.; & Clarke, S.E. "Synthesis and Photoactivity of Chemically Asymmetric Polymeric Porphyrin Films Made by Interfacial Polymerization," Journal of the American Chemical Society 1989, 111, 8485-8491.

Wamser, Carl C. & Gilbert, Mark I. "Detection of Surface Functional Group Asymmetry in Interfacially-Polymerized Films by Contact Angle Titrations," Langmuir 1992, 8, 1608-1614.

Whitesides, George M. & Ferguson, Gregory S. "Organic Chemistry In Two Dimensions: Surface-Functionalized Polymers and Self-Assembled Monolayer Films," Chemtracts- Organic Chemistry 1988, 1, 171-187.

REDUCTION AND PURIFICATION OF WATER SOLUBLE PORPHYRINS

Tom Newman

Department of Chemistry
Western Connecticut State University
181 White Street
Danbury, CT 06810

Faculty Advisor: Russ Selzer

The reduction of a water soluble porphyrin is performed to yield a stable water soluble tetrahydroporphyrin product. Tetrasodium Meso-Tetra-p-Sulfonatophenyl porphyrin is reduced with diimide to the chlorin intermediate and ultimately to the bacteriochlorin. The purification includes the removal of the air sensitive bacteriochlorin from water and hydrazine solution to yield a solid bacteriochlorin product. This bacteriochlorin product is characterized using its visible spectra as well as its oxidation with quinones.

Introduction

The chemistry of porphyrins is important due to the existence of porphyrin molecules in biological systems. Porphyrins in blood serve to bind respiratory gases while in plants the reduced porphyrins (bacterioclorin and chlorin) aid in the aid in the transfer of electrons within a cell. These reduced porphyrins convert light energy into chemical energy. This role of photosynthetic porphyrins is being explored in vitro to understand its role as a renewable source of chemical energy.

The increasing need to explore alternative sources of energy has made many researchers explore the chemical system that exists in photosynthetic organisms such as plants and bacteria. In these systems light energy is used to synthesize energy yielding organic compounds, specifically carbohydrates. This chemical system is also ideal because the by-product of the reactions is molecular oxygen making this a system that can harness light energy and yield a desirable waste product. Models must be explored in vitro to copy the light harvesting chemical potential that is performed in vivo.

In these photosynthetic organisms the porphyrins exist in the cell in the reduced (hydrogenated) form as opposed to the basic porphyrin that is found in Heme. The reduced porphyrins are found in these organisms as the free base as well as porphyrins with metal centers, as in the chlorophyll molecule where a magnesium atom is bound in the center of the porphyrin.

The goal of this research was to synthesize stable reduced water soluble porphyrin in relatively high yield so that this reduced porphyrin may be characterized and reacted in further synthesis. The porphyrin selected would be a free base so that upon reduction various metal centers could be introduced and chelated to the porphyrin. The porphyrin investigated must also have some electrostatic charge so that the reduced porphyrin may be electrostatically bound to an unreduced porphyrin to synthesize an electrostatic diporphyrin compound.

Experimental Procedure

The reduction of Tetrasodium meso-Tetra-Para-Sulfonatophenyl porphyrin($TSOPPNa_4$) was carried out by first dissolving this compound in a minimum of water. To this solution hydrazine/50% hydrogen peroxide was added at a 4/3 ratio always keeping the hydrazine in excess so the porphyrin was not oxidized. The peroxide served to oxidize the hydrazine to diimide[1] (H-N=N-H) which reduced the porphyrin.

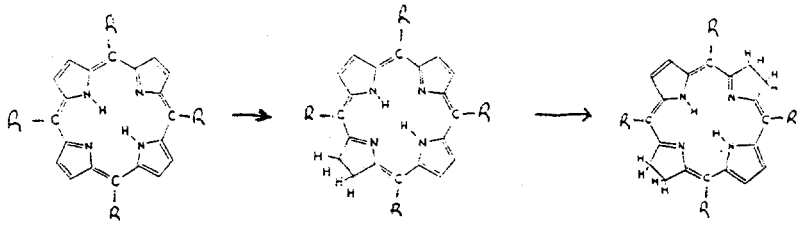


Figure 1: stepwise reduction of the porphyrin to the chlorin and bacteriochlorin. $R=C_6H_4SO_3^-,Na^+$

The hydrazine is then removed with the addition of benzaldehyde to form benzalazine which is an insoluble precipitate.

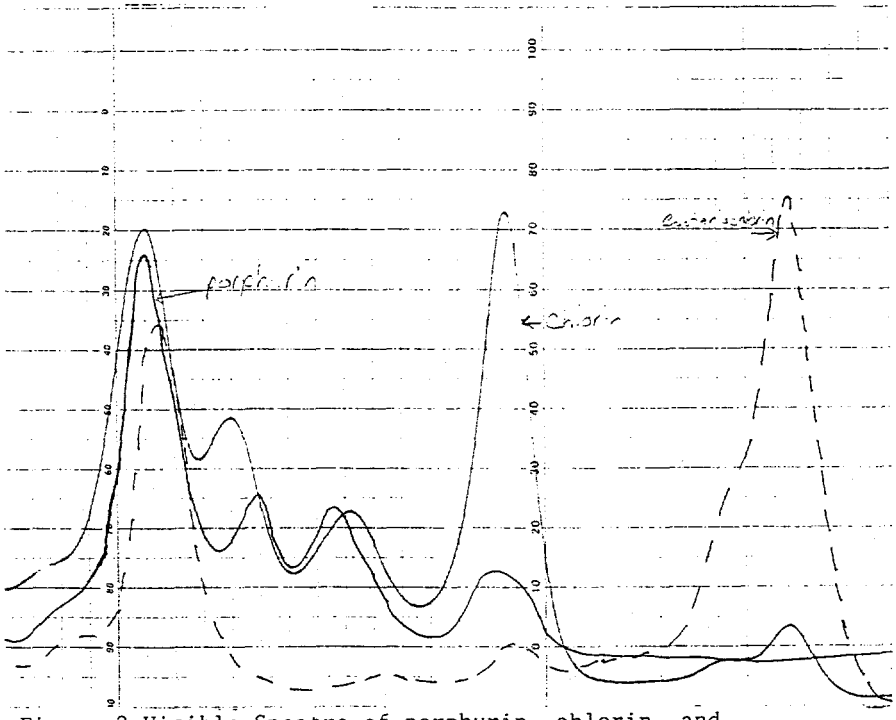


Figure 2:Visible Spectra of porphyrin, chlorin, and bacteriochlorin -------(450-775 nanometers)

The bacteriochlorin and benzalazine mixture was cooled to 20°C for 36 hours to ensure that all of the hydrazine was removed from solution. The mixture was then dried, and a solid remained that was a mixture of benzalazine and bacteriochlorin. The benzalazine was removed by placing the solid in an extraction thimble and extracting the benzalazine with methylene chloride. The solid bacteriochlorin remained and was washed with acetone repeatedly and allowed to dry.

Results

This proved to be a successful method for the isolation of bacteriochlorin which was obtained at a yield of 97%. The extraction method removed the hydrazine in a safe manner which did not require distillation of hydrazine or of the water in the solution. The Tetrasodium Meso-Tetra-Para-Sulfonatophenyl Bacteriochlorin that is produced is characterized by its visible spectrum[2](see figure 2) and is oxidized to the original porphyrin with phenylsulfonic benzoquinone to confirm its existence.

References

1. H.W. Whitlock, Diimide Reduction of Porphyrins, Journal of the American Chemical Society, 7485,1969.

2. G.D. Dorough, An Attempted Preparation of a Simple Tetrahydroporphine, Journal of the American Chemical Society,7,6106,1952.

SECOND-ORDER POLARIZABILITIES OF SUBSTITUTED SCHIFF'S BASES

Sonya D. McCall

Department of Chemistry
Spelman College
350 Spelman Lane S.W.
Atlanta, Georgia 30314

Faculty Advisor: Dr. Beatriz H. Cardelino

The second-order polarizabilities of substituted Schiff's bases have been predicted and compared to experimental data. The goal of this project was to develop a procedure useful for material's scientists in the selection of good candidate molecules for synthesis. The calculations were based on the finite-field method and involved empirical corrections for dynamic fields and intermolecular effects. The experimental data was obtained from dc-induced second-harmonic generation (EFISH) by Sanghadasa from UAH and the compounds were synthesized by M. Aggarwal's group at Alabama A&M University. The comparison demonstrates the qualitative ability of the method to predict the relative magnitudes of second-order polarizabilities for this class of compounds.

Introduction

Calculations of second-order polarizabilites (β) were performed on Schiff's bases derived from four aldehydes: benzaldehyde, salicylaldehyde, anisaldehyde and isovanillin; and six anilines: unsubstituted, p-nitro, p-cyano, p-formyl, p-carbamyl and o-methyl-p-nitro (Figure 1). Values of $\mu\beta$ (μ=permanent dipole moment) relative to 2-methyl-4-nitroaniline were obtained for single molecules in a static field. These values were compared with experimental data to derive adjustment parameters applicable to Schiff's bases for dynamic and bulk effects.

Method

For relatively large molecules, two types of calculations may be used: the sum-over-states (based on a perturbative expansion in terms of molecular eigenstates in the absence of an external field) and the finite-field approach (which diagonalizes a molecular Hamiltonian with a static-field dipolar perturbation). In the first case, the magnitude of the properties is obtained for a specific dynamic field, and the static field value can be extrapolated to zero frequency. In the second case, the nonlinear terms are obtained for static conditions and, if they are to be compared with experiments involving electromagnetic radiation, the latter should be corrected for dispersion effects. Our work employs the finite-field method because it is better suited for larger molecules.

The procedure we have used is a modification to the method implemented by Dewar and Stewart[1] for calculating molecular linear polarizabilities. Dewar and Stewart include isolated point charges in the description of the molecule, with no associated electrons or atomic orbitals. An appropriate selection of these point charges simulates the effect of a uniform electric field on a molecule, allowing for the corresponding changes in polarization to be calculated directly.

The all valence-electron AM1[2] Hamiltonian is employed to obtain molecular polarizations in the presence of 252 static fields utilizing a modified version of the MOPAC program[3]. The data of molecular polarizations versus static fields are then incorporated into the HYPER program[4]. Based on equation 1, the HYPER program performs polynomial

regressions with these data and calculates all tensor elements of the static polarizabilities. The values of the tensor elements are extracted from polynomial expansions of orders four to eighteen, to allow for an evaluation of numerial instabilities.

$$P_q=\mu_q + \Sigma_j\alpha_{qj}F_j + \Sigma_j\Sigma_k\beta_{qjk}F_jF_k + \Sigma_j\Sigma_k\Sigma_l\gamma_{qjkl}F_jF_kF_l + \ldots \quad (1)$$

where P_q represents qth component of the polarization, F_i the ith component of the applied electric field, α the linear polarizability, β the second-order polarizability, γ the third-order polarizability, etc. The magnitude of the vector part of β corresponds to the effective measure of polariability for second-harmonic generation (SHG):

$$\beta_{vec} = (\beta_x^2 + \beta_y^2 + \beta_z^2)^{1/2} \quad (2)$$

where x, y, and z are the molecular coordinate axes. The symmetry of β with respect to interchange of the last two indices determines that the vector components be:

$$\beta_q=\beta_{qqq} + (\Sigma_j\beta_{qjj} + 2\ \Sigma_j\beta_{jqj})/3 \quad (3)$$

Results and Discussion

Synthesis and laboratory measurments of $\mu\beta$ relative to MNA (2-methyl-4-nitroaniline) were performed by Sanghadasa on Schiff's bases derived from the above four aldehydes and six anilines. These compounds were synthesized by M. Aggarwal's group at Alabama A&M. No experimental data on Schiff's bases is available to obtain the adjustment factors for dispersion and solvent effect. The correlation between the unadjusted calculated values and the measured values is 0.91. A slope of 0.36 seems to indicate that 2.8 should be the adjustment factor for Schiff's bases and the corresponding experimental conditions the data is summarized in Table 1.

Figure 2 shows the correlation between the experimental and the predicted values. The two points that most deviate from the straight line correspond to the 2-methyl-4-nitroaniline substituent; the highest point in the graph correponds to the anisaldehyde group, the second to the right to the salicylaldehyde group. Steric effects may cause these substituents to rotate. These rotations may have small effects on the energies of the compounds but may affect their β values.

Conclusion

Comparison between 24 experimental and calculated β values for Schiff's bases show that the latter may be used to predict trends in the second-order polarizabilities for these compounds. Moreover, the correlation between the experimental and the calculated values indicate that the bulk and dispersion effects increase β on these compounds by a factor of 2.8.

References

1. M. J. S. Dewar and J. J. P. Stewart; Chem Phys. Lett. 111, p. 416 (1984).

2. M. J. S. Dewar, E. G. Zoebisch, E. F. Healy, and J. J. P. Stewart, J. Am. Chem. Soc., 107, 3902 (1985).

3. QCPE; MOPAC, Quantum Chemistry Program Exchange, Version 6 (1990).

4. B. H. Cardelino, C. E. Moore, and R. E. Stickel; J. Phys. Chem., 95, 8645 (1991).

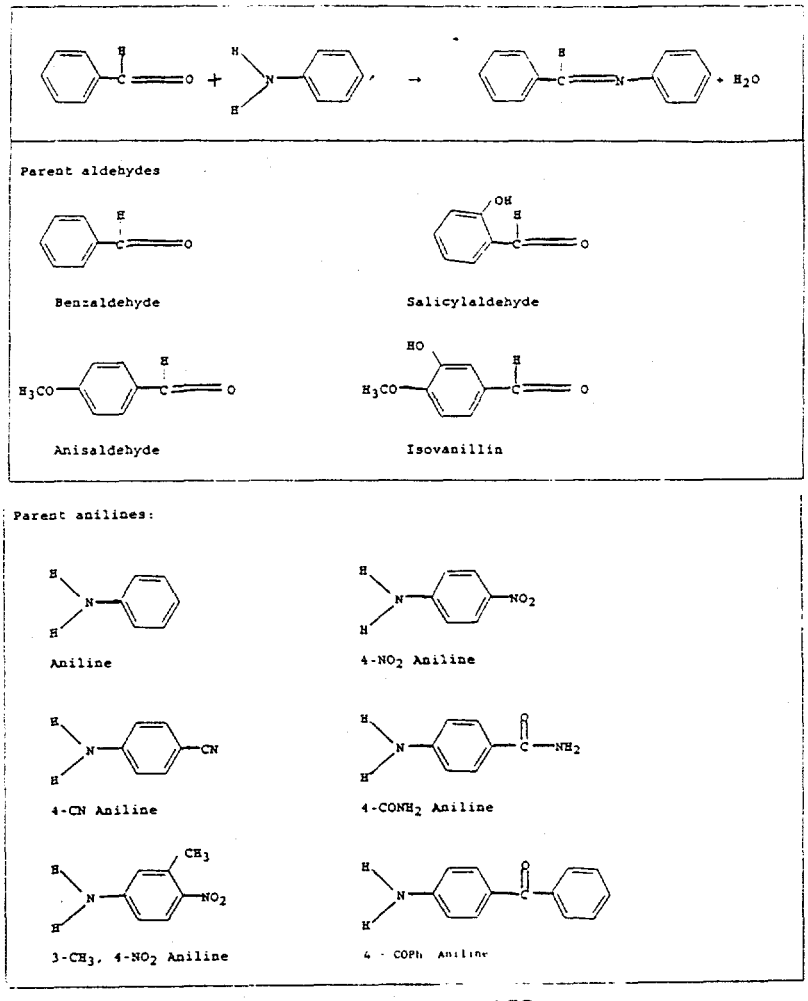


FIGURE 1 - SCHIFF'S BASES

TABLE 1 - SCHIFF'S BASES

Structure		μ_x	μ_y	μ_z	β_x	β_y	β_z	$\langle\beta\rangle$	β_e
1-NH2 2-CH3 4-NO2		+7.25	+0.29	+1.26	+17.57	+1.27	+0.02	+17.62	+0.81
Aldehyde	**Aniline**								
p-OCH3	unsub	+2.90	+0.85	+0.57	+10.55	+4.93	-0.50	+11.73	+2.16
p-OCH3	p-CN	+5.76	-1.67	+0.51	+20.63	+0.83	+0.24	+20.69	+1.78
p-OCH3	p-C(O)NH2	+6.08	+0.78	+2.96	+15.45	+3.18	+0.31	+15.92	+2.89
p-OCH3	p-C(O)Ph	+3.56	-1.12	+2.84	+20.62	-0.64	-0.43	+20.81	+3.02
p-OCH3	p-NO2 o-CH3	+7.56	-3.58	+1.09	+34.74	-6.35	+2.37	+35.53	+3.08
p-OCH3	p-NO2	+7.58	-3.07	+0.50	+24.47	+2.99	+0.95	+24.90	+2.48
p-OCH3 m-OH	unsub	+2.16	-0.08	+0.38	+15.41	+6.31	+0.90	+16.77	+1.90
p-OCH3 m-OH	p-CN	+4.81	-2.41	+0.88	+22.67	+2.71	-0.10	+22.88	+1.53
p-OCH3 m-OH	p-C(O)NH2	+5.39	-0.15	+2.67	+18.56	+5.37	+0.51	+19.54	+0.99
p-OCH3 m-OH	p-C(O)Ph	+2.59	-1.83	+3.23	+23.18	-1.59	+3.64	+23.65	+4.44
p-OCH3 m-OH	p-NO2 o-CH3	+6.63	-4.33	+1.35	+37.31	-4.75	+3.17	+37.92	+2.94
p-OCH3 m-OH	p-NO2	+6.67	-3.84	+0.79	+29.21	+3.62	+2.05	+29.67	+2.46
unsub	unsub	+1.81	+1.47	+0.01	+2.28	-1.94	-0.11	+3.02	+1.21
unsub	p-CN	+4.57	-1.09	-0.04	+10.04	-5.81	-0.61	+11.63	+1.11
unsub	p-C(O)NH2	+4.89	+1.34	+2.43	+7.43	-3.72	+0.37	+8.43	+0.84
unsub	p-C(O)Ph	+2.38	-0.51	+2.32	+7.92	-7.43	+2.09	+11.74	+4.66
unsub	p-NO2 o-CH3	+6.25	-3.02	+0.56	+20.86	-13.78	+1.34	+25.12	+1.92
unsub	p-NO2	+6.30	-2.53	-0.06	+13.25	-5.23	+1.20	+14.54	+1.32
o-OH	unsub	+0.49	+1.46	-0.44	+4.72	-4.52	+1.97	+6.84	+0.74
o-OH	p-CN	+3.19	-1.13	-0.52	+10.85	-8.15	+2.39	+13.87	+1.57
o-OH	p-C(O)NH2	+3.64	+1.31	+1.87	+10.06	-7.69	+3.56	+13.25	+1.96
o-OH	p-C(O)Ph	-0.12	-0.96	+1.10	+6.83	-8.32	+3.48	+11.37	+0.59
o-OH	p-NO2 o-CH3	+4.78	-3.11	-0.02	+20.52	-15.05	+3.21	+25.70	+4.05
o-OH	p-NO2	+4.90	-2.60	-0.55	+14.08	-7.16	+3.16	+16.32	+0.39

μ=(Debyes)
β=10^{-51} $Cm^{-3}v^{-2}$

TABLE 2 - SCHIFF'S BASES

Structure			μβ	μβ/μβ(MNA)	error*	experimental
1-NH2 2-CH3 4-NO2			+127.78	+1.000	+0.046	1.00
Aldehyde	**Aniline**					
p-OCH3	unsub		+34.50	+0.270	+0.050	1.75
p-OCH3	p-CN		+117.57	+0.920	+0.079	1.68
p-OCH3	p-C(O)NH2		+97.33	+0.762	+0.138	2.50
p-OCH3	p-C(O)Ph		+72.90	+0.571	+0.083	1.92
p-OCH3	p-NO2	o-CH3	+287.95	+2.254	+0.195	3.10
p-OCH3	p-NO2		+176.78	+1.384	+0.138	2.90
p-OCH3	m-OH unsub		+33.12	+0.259	+0.029	2.13
p-OCH3	m-OH p-CN		+102.42	+0.802	+0.054	1.78
p-OCH3	m-OH p-C(O)NH2		+100.59	+0.787	+0.040	2.50
p-OCH3	m-OH p-C(O)Ph		+74.70	+0.585	+0.110	1.84
p-OCH3	m-OH p-NO2	o-CH3	+272.21	+2.130	+0.165	4.60
p-OCH3	m-OH p-NO2		+182.55	+1.429	+0.118	2.90
unsub	unsub		+1.27	+0.010	+0.004	1.40
unsub	p-CN		+52.24	+0.409	+0.039	1.42
unsub	p-C(O)NH2		+32.25	+0.252	+0.025	1.92
unsub	p-C(O)Ph		+27.49	+0.215	+0.085	1.61
unsub	p-NO2	o-CH3	+172.74	+1.352	+0.103	3.72
unsub	p-NO2		+96.63	+0.756	+0.069	1.84
o-OH	unsub		-5.15	-0.040	-0.004	0.67
o-OH	p-CN		+42.58	+0.333	+0.038	1.50
o-OH	p-C(O)NH2		+33.20	+0.260	+0.038	2.00
o-OH	p-C(O)Ph		+11.00	+0.086	+0.004	1.35
o-OH	p-NO2	o-CH3	+144.83	+1.133	+0.179	4.24
o-OH	p-NO2		+85.87	+0.672	+0.016	2.73

*error in ratio is based on error in β values.

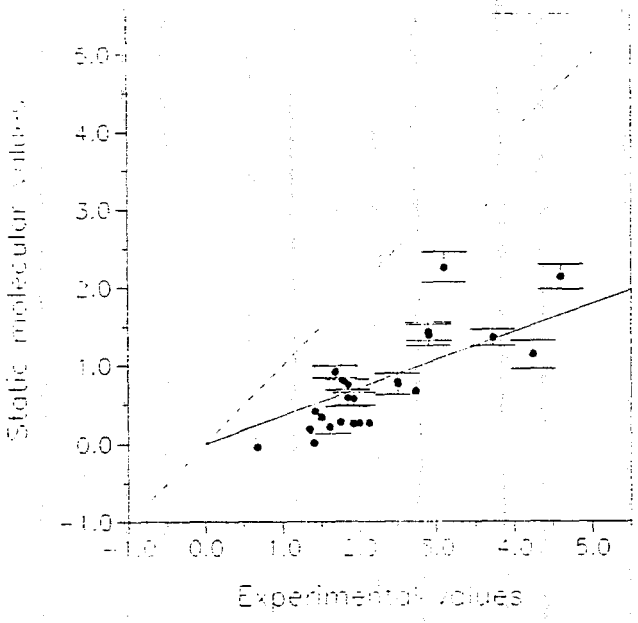


FIGURE 2- CORRELATION BETWEEN EXPERIMENTAL AND PREDICTED VALUES

Substance Isolated from the Marine Bryozoa Bugula Stolonifera

Angelo Volpe
Department of Biological Sciences
SUNY College at Old Westbury
Old Westbury, NY 11568
Faculty Advisor: Dr. Rita Colon-Urban

It has been previously reported that crude extracts from several different marine bryozoans inhibit the growth of gram positive organisms but not the growth of gram negative ones. The purpose of this study was to further purify and characterize the antibiotic component(s). Methanol homogenates were prepared from the bryozoan Bugula stolonifera which was collected in a local marina. These extracts were partitioned with chloroform and concentrated under reduced pressure. This fraction was then subjected to silica gel and thin layer chromatography. The compound(s) obtained were analyzed by IR and NMR spectroscopy. IR scans showed bands indicating the presence of aromatic C-C and C-N bonds suggesting the presence of an indole structure. This data was further supported by NMR spectral analysis. The details of the IR and NMR data are presented.

BACKGROUND

This report attempts to analyze chemically and structurally a crude bryozoan extract, which has been shown in the laboratory to inhibit the growth of several gram positive organisms (Colon-Urban 1991). The crude bryozoan extracts were prepared from a local marine bryozoan, Bugula stolonifera. Christopherson has reported that compounds isolated from Bugula dentata have also shown antimicrobial activity (Christopherson 1990).

For the past few years many interesting compounds have been purified and structurally characterized from marine bryozoans by Pettit and colleagues (Pettit 1986, 1991). Some of these are presently undergoing clinical trials for the treatment of leukemia.

EXPERIMENTAL

Methanol homogenates were prepared from frozen specimens of Bugula stolonifera, and partitioned with chloroform and concentrated under reduced pressure. It was redissolved in ether and placed onto a silica gel column. The standard set of solvents ranging in polarity from hexane to methanol were used, concentrated, and analyzed by Thin Layer Chromatography (TLC). TLC solvents used for migration were a mixture of chloroform : 2-butanol (10:1). TLC plates were developed using a detection reagent for the presence of alkaloids. Spots were recovered from TLC plates and prepared for IR (Perkin Elmer 1600 Series FTIR) and NMR (Bruker Wp100SY) scans. The antimicrobial activity was done using disk diffusion technique and those fractions that inhibited the growth of gram positive bacteria were used for the analyses.

RESULTS & DISCUSSION

TLC plates sprayed with KI/I detection reagent (Stahl 1969) gave a positive reaction with an R_f value of .65. TLC and its solvent recovery suggested the presence of a polar compound.

Further structural studies were done using IR & NMR. Infrared bands (Figure 1) were found at 3000 - 3300cm^{-1}, and 1690cm^{-1} which suggest N-H strecthes. Other aromatic C-N stretches (moderate and narrow) at 1100cm^{-1} and 1140cm^{-1} were apparent, as well as aromatic C-C stretches found at 1380, 1450, and 1480cm^{-1}. This gave an indication that the compound may have contained an indole structure due to the fact that when compared to compounds isolated from different species of bryozoan (Wright 1984) aromatic C-N and C-C bonds present may have been those contributed from an indole structure. This assumption was based because the only nitrogen in the compound is contained in the indole structure.

NMR data (Figure 2) gave peaks downfield from TMS at 6.5 - 8.0 ppm. These peaks clearly indicate an aromatic structure, further more the doublet at 6.94 and 6.83 ppm and the doublet at 7.31 and 7.41 ppm were indicative of an "ab" splitting pattern (two pairs of adjacent hydrogens each giving a doublet) of a benzene ring which may be part of a ring system consisting of an indole structure. Peaks which are present at 6.54 and 7.59ppm were not necessarily corresponding to hydrogens inside the ring structure. These peaks were not assigned. However a multiplet of peaks which were in the range of 3.66 and 4.02 ppm also gave a strong indication that an aromatic N-H system was present. Peaks upfield from TMS at 2.44 - 1.77 ppm were believed to either be an impurity of the sample or perhaps were due to the incomplete drying of the sample.

These preliminary studies suggest that the active antibiotic fraction is aromatic and contains an indole structure but further attempts to purify these samples by HPLC will be forthcoming.

ACKNOWLEDGEMENTS

The author would like to thank Dr. Evelyn Garrity, Dr. Robert M. Hoyte, and Dr. Steve Samuel of the Chemistry department at S.U.N.Y Old Westbury for their time and assistance in the research. This work was supported by NIH-MBRS RR 08180 and SUNY Old Westbury Presidential Faculty Development Award to RCU.

REFERENCES

Christopherson, C., Anthoni, U., Nielson, P.H., Pereira, M., *Comp. Biochem. Physiol.*, 1990, 96B: 431-437.

Colon-Urban, Rita D., Urban, Carl M., Oppenheim, Joel D., *Bull. Soc. Sci. Nat. Quest Fr., Mem.*, HS 1, 1991, 89-95.

Matsunaga, S., Fusetani, N., Hashimoto, K., *Experientia*, 1984, 42: 741-744.

Pettit, G.R., Kamano, Y., Herald, C.L. Schimdt, J.M. and Zubrod, C.G., *Pure Appl. Chem*, 1986, 58: 415-421.

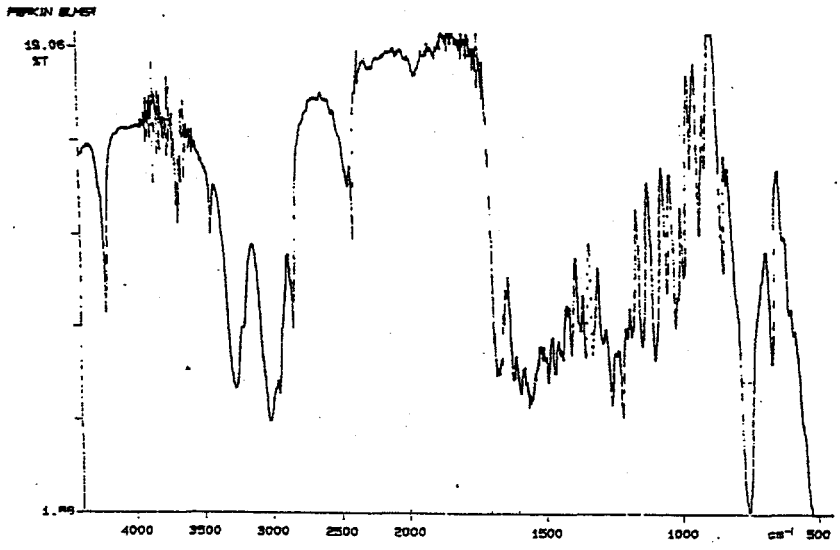
Pettit, G.R., Gao, F., Sengupta, D., Coll, J.C., Herald, C.L., Schmidt, J.M., Van Vamp, J.R., Rudloe, J.J., and Nieman, R.A., *Tetrahedron*, 1991, 47: 3601-3610.

Prisep, M.R., Blunt, J.W., Munro, Murray H.G., *J. Nat. Prod.*, Jul.-Aug. 1991, 54, 1068-1076.

Stahl, Egon, Thin Layer Chromatography, 2nd edition,; Springer-Verlag Berlin Heidelberg New York, 1969; pp 421-462.

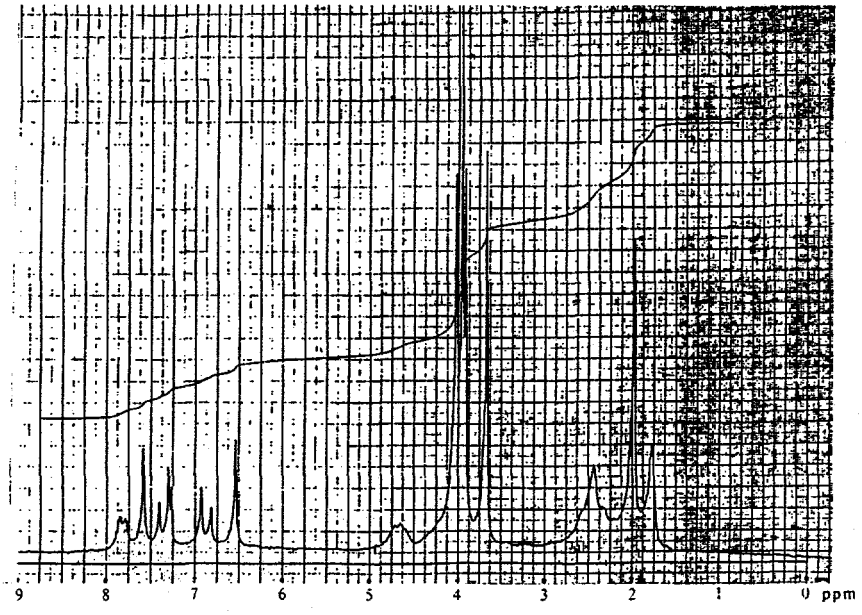
Wright, J.L.C., *J. Nat. Prod.*, Sept.-Oct. 1984, 893-895.

Figure 1



IR Spectra of Bryozoan Extract (64 scans, 4.0 cm^{-1})

Figure 2



NMR Spectra of Bryozoan Extract (100 scans)

Determination of Structural Changes of Conductive Vapor Deposited Polyaniline Films

Traci Simpson

Department of Chemistry
Northern Arizona University
P.O. Box 5698
Flagstaff, Arizona 86011

Faculty Advisor:

Gerald Caple

Polyaniline·1 M HCl was vapor deposited on glass and NaCl slides at currents of 14A, 17A, 18A, and 20A. The resulting polyaniline·1 M HCl films were then reprotonated with gaseous HCl in a closed system or a solution concentrated with HCl. UV-Vis spectra of the films demonstrated changes with reprotonation. The most noticeable change was an increased absorbance between 375 and 475 nm with reprotonation. The color of the films was also altered with reprotonation, from light purple to blue-green when reprotonated. The UV-Vis spectrum of the polyaniline films also changed with oxidation. The absorbance of the UV-Vis spectra increased between 375 and 825 nm with oxidation. Oxidation also caused the films to turn from light purple to black-gray.

INTRODUCTION

Vapor deposited organic films have been the recent topic of many research projects because of their possible future use as conductive surfaces in electrical devices. These films are important as conductive surfaces because of the ease in controlling their thickness and placement on a surface. Research for this paper was completed in order to investigate how the structure of vapor deposited films of polyaniline change under conditions such as protonation and oxidation. Light scattering was also used to help determine the size of the polyaniline chains on the films. Polyaniline was the chosen polymer for this research because this compound is easily vapor deposited.

EXPERIMENTAL

Two samples of polyaniline were prepared, which differed only in the solvent used for each. The solvents were 1 M hydrochloric acid and 1 M sulfuric acid. The polyaniline·1 M HCl was prepared by dissolving 9.3 mL of aniline in 150 mL of 1 M HCl, and dissolving 11.200 g of ammonium persulfate in 100 mL of 1 M HCl. To dissolve the aniline in the first solution, 14 mL of 12 M HCl were added. Both solutions were cooled to 0°C and then the ammonium persulfate solution was mixed into the aniline solution. The aniline-ammonium persulfate mixture was allowed to react for twenty-four hours. The remaining solvent was then vacuum filtrated from the solid polyaniline·1 M HCl product. The polyaniline·1 M HCl solid was washed three times with 40 mL of 1 M HCl, and then dried for twenty-four hours. The polyaniline·1 M H_2SO_4 was prepared using the same method as described for polyaniline·1 M HCl; however, 11.000 g of ammonium persulfate were used and 100 mL of distilled water were needed to dissolve the aniline into the H_2SO_4 solution.

For this study, polyaniline·1 M HCl was used more often than polyaniline·1 M H_2SO_4. The vapor deposition apparatus that was used to produce the polyaniline films was a Kinney KSE-2A-M Vacuum Evaporator. For each vapor deposition, a set of two slides was made; one of glass and one of NaCl. The NaCl slides were necessary to make IR spectra of the films using a Perkin-Elmer 1420 Ratio Recording Infrared Spectrophotometer. UV-Vis spectra were produced from the films on both the glass and NaCl

slides using a Hewlett Packard 8452A Diode Array Spectrophotometer. One set of glass and NaCl slides with polyaniline·1 M HCl film was produced at each of the following currents: 14 A, 18 A, and 20 A. Four sets of slides were made at 17 A.

UV-Vis and IR spectra were taken after each set of films was vapor deposited. Three sets of the films produced at 17 A were reprotonated with gaseous HCl. IR and UV-Vis spectra were then taken of the reprotonated films. Gaseous HCl was used five different times to reprotonate the films produced at 20 A. UV-Vis and IR spectra were taken after each reprotonation in the series. For reprotonation by gaseous HCl, concentrated sulfuric acid was placed in the separatory funnel, and allowed to drip into a flask below, which contained NaCl crystals. The H_2SO_4 and NaCl generated the HCl gas that reprotonated the polyaniline films in an airfree chamber connected to the flask.

The polyaniline·1 M HCl films could also be reprotonated by adding concentrated HCl directly to a solution in which the films had been dissolved. The polyaniline·1 M HCl film vapor deposited at 14 A on a glass slide was reprotonated by this method. The film on the glass slide was dissolved in ethanol. Hydrochloric acid was added to the ethanol solution, and a UV-Vis spectrum was made of this solution. The films on glass slides from two of the sets made at 17 A were also dissolved in ethanol and then reprotonated by adding concentrated hydrochloric acid to the solutions. The UV-Vis spectra were also taken from these reprotonated solutions.

The set of films of vapor deposited polyaniline·1 M HCl produced at 18 A was oxidized before it was reprotonated by placing them in a sealed canister of oxygen, which was left in an 383 K oven for two days. UV-Vis spectra were then taken of the oxidized slides. These films were then reprotonated with gaseous HCl using the apparatus previously described, and UV-Vis spectra were taken of the reprotonated films. Light scattering experiments were then conducted with a Nicomp Laser Particle Sizer Model 200 using the glass slide, to determine the mean diameter of the chains of polyaniline·1 M HCl present on the film. The film from the glass slide was dissolved in methanol. The particle sizing apparatus used a laser of wavelength 632.8 nm and maintained a temperature of 293.00 K.

One set of vapor deposited films was produced using the polyaniline·1 M H_2SO_4 sample. This set of films was vapor deposited at 17 A. The film on the glass slide of this set was reprotonated by dissolving the film in distilled H_2O and then adding a few drops of fuming sulfuric acid. After the reprotonation, a UV-Vis spectrum was made of the solution.

RESULTS and DISCUSSION

The most obvious results that occurred when the polyaniline·1 M HCl films were reprotonated or oxidized were changes in color. Most of the films of polyaniline·1 M HCl were light purple upon vapor deposition. Those films reprotonated by gaseous HCl, turned dark blue-green after the films were exposed to HCl. Two sets of films, however, were produced from the vapor deposition of the polyaniline·1 M HCl that were light brown in color. These two sets of films were both produced at 17 A. The films on the glass slides from these two sets were reprotonated in solution. The initial color of the solutions in which the films were dissolved was transparent light brown. The resulting solutions, after the reprotonation, were transparent and light blue. The reprotonation in solution of the film on the glass slide made at 14 A, caused the solution of ethanol to turn from light purple, the original color of the film, to light transparent blue upon reprotonation.

The only spectral data collected that demonstrated consistent variations which occurred when the color of the polyaniline·1 HCl films was changed with reprotonation or oxidation was that of the UV-Vis spectra. The IR spectra demonstrated changes upon reprotonation of the polyaniline·1 M

HCl films; however, the changes in the spectra were not consistently occurring at one set of peaks and may have been due to the apparatus not working properly. The Physics Department conducted XPS and conductive studies on the vapor deposited polyaniline·1 M HCl films before and after reprotonation. The XPS and conductive studies demonstrated no conclusive changes in the structure of the films even though the color of films the Physics Department produced would change from emerald green, unprotonated, to dark blue when protonated.

The reprotonation of the polyaniline·1 M HCl vapor deposited films caused reproducible changes in the UV-Vis spectra. Upon reprotonation, the absorbance between 375 and 475 nm on the UV-Vis spectra would increase. The amount of increase in absorbance varied; but, the increase occurred consistently in the range of 375 to 475 nm on the UV-Vis spectra, with both methods of reprotonation (by gaseous HCl or in solution). This type of change is demonstrated in Figure 1a and 1b for the films on the NaCl slides and in Figure 2a and 2b for the films on the glass slides.

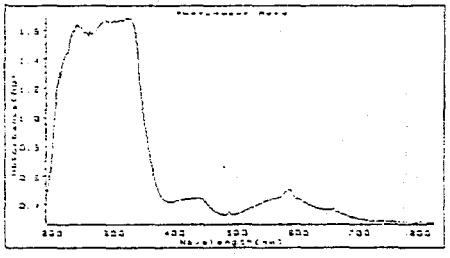


Figure 1a: Vapor deposition of polyaniline·1 M HCl on an NaCl slide before reprotonation.

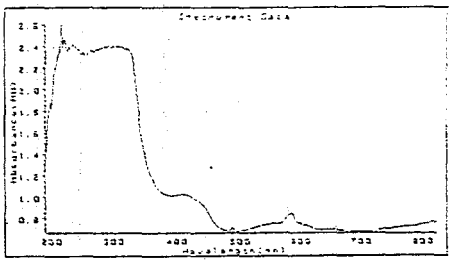


Figure 1b: Vapor deposition of polyaniline·1 M HCl on an NaCl slide after reprotonation.

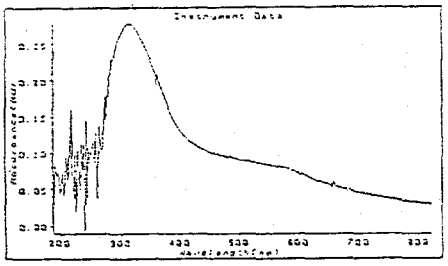


Figure 2a: Vapor deposition of polyaniline·1 M HCl on a glass slide before reprotonation.

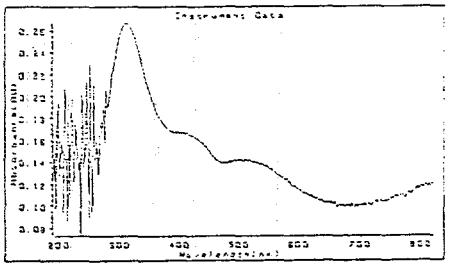


Figure 2b: Vapor deposition of polyaniline·1 M HCl on a glass slide after reprotonation.

The set of the vapor deposited polyaniline·1 M HCl that was produced at 20 A and reprotonated five times, started as light purple films. These films turned dark blue-green upon reprotonation and then turned to light purple two to three days afterward. After the first two reprotonations, the absorbance on the UV-Vis spectra would increase between 375 and 475 nm right after reprotonation and then decrease again after a couple of days. After the third reprotonation, the absorbance between 375 and 475 nm on the UV-Vis spectra increased and then did not decrease with time or fluctuate after the fourth and fifth reprotonation. This lack of change in the UV-Vis spectra was apparent with the films both on the glass and the NaCl slides. After the third reprotonation, the films on both of the slides also remained dark blue-green.

The oxidation of the polyaniline films made at 18 A caused the films to turn from light purple to black-gray when oxidized. These films then turned dark blue when reprotonated by gaseous HCl. The absorbance of the UV-Vis spectra increased

between 375 and 825 nm when the films were oxidized. This increase is demonstrated in Figure 3a and 3b for the film on the NaCl slide and in Figure 4a and 4b for the film on the glass slide.

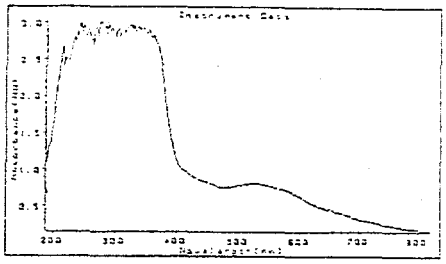


Figure 3a: Vapor deposition of polyaniline·1 M HCl on an NaCl slide before oxidation.

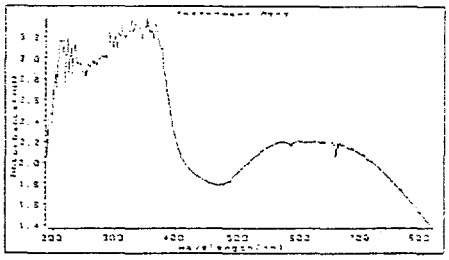


Figure 3b: Vapor deposition of polyaniline·1 M HCl on an NaCl slide after oxidation.

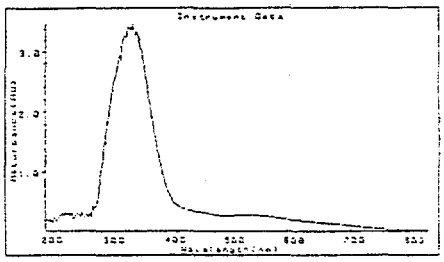


Figure 4a: Vapor deposition of polyaniline·1 M HCl on a glass slide before oxidation.

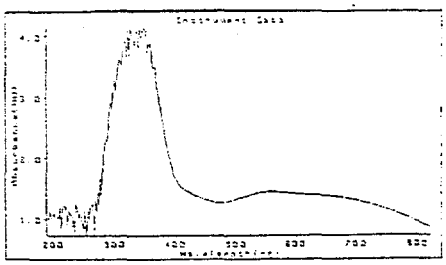


Figure 4b: Vapor deposition of polyaniline·1 M HCl on a glass slide after oxidation.

Once the films were reprotonated, the absorbance on the UV-Vis spectra increased between 375 and 475 nm, as occurred for the other films that were reprotonated. The results from the light scattering experiments performed on the film from the glass slide after reprotonation were not reproducible. The mean diameter was calculated twice using light scattering. The first time the mean diameter of the polyaniline·1 M HCl chain on the glass slide was found to be 2922.7 nm and the second time it was calculated as 97.6 nm.

The vapor deposition of the polyaniline·1 M H_2SO_4 created light brown films on both the glass and NaCl slides. When dissolved in distilled water, the film from the glass slide turned the solution light transparent brown. When the fuming sulfuric acid was added, the solution turned light blue and transparent. The UV-Vis spectrum of the solution from the film of the glass slide demonstrated a small increase in absorbance between 375 and 475 nm after reprotonation. The changes in the UV-Vis spectrum due to reprotonation of the polyaniline·1 M H_2SO_4 solution are shown in Figure 5a and 5b.

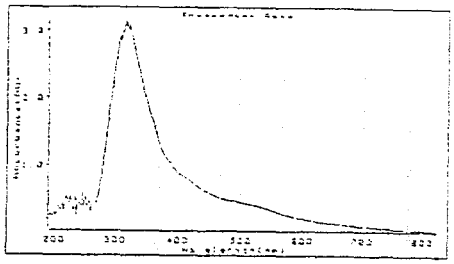


Figure 5a: Vapor deposition of polyaniline·1 M H_2SO_4 on a glass slide before reprotonation.

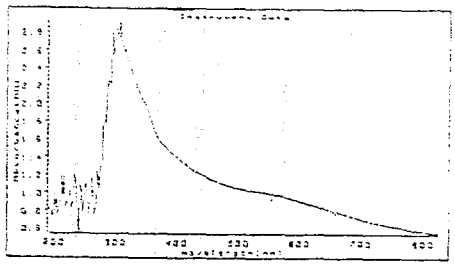


Figure 5b: Vapor deposition of polyaniline·1 M H_2SO_4 on a glass slide after reprotonation.

CONCLUSIONS

Due to the inconclusive results from the XPS and UV-Vis experiments, more work needs to be done concerning the changes vapor deposited polyaniline·1 M HCl films undergo with protonation as well as oxidation. A more complete study also needs to be conducted to determine the mean diameter of the polyaniline chains. Once these studies are completed and better understood, polyaniline films will have the potential for use in electrical devices.

ACKNOWLEDGEMENTS

The author would like to thank Dr. Randy Dillingham and Dr. David Cornelison for contributing the information from their XPS studies of polyaniline to this paper.

REFERENCES

Kang, E. T., Neoh, K. G., and Tan, K. L., "The Intrinsic Redox States in Polypyrrole and Polyaniline: A Comparative Study by XPS", Surface and Interface Analysis, Vol. 19(1992), pp. 33-37.

Kang, E. T., Neoh, K. G., and Tan, K. L., "Polyaniline with High Intrinsic Oxidation State", Surface and Interface Analysis, Vol. 20(1993), pp. 833-840.

Angelopoulos, M., Asturias, G. E., Ermer, S. P., Ray, A., Scherr, E. M., MacDiarmid, A. G., Akhtar, M., Kiss, Z., and Epstein, A. J., "Polyaniline: Solutions, Films and Oxidation State", Mol. Cryst. Liq. Cryst., Vol. 160(1988), pp. 151-163.

Dannetun, P. and Uvdal, K., "Physical Vapor Deposition of Polyaniline", Chemtronics, Vol. 5(1991), pp. 173-177.

Uvdal, K., Logdlund, M., Dannetun, P., Bertilsson, L., Stafstrom, S., Salaneck, W. R., MacDiarmid, A. G., Ray, A., Scherr, E. M., Hjertberg, T., and Epstein, A. J., "Vapor Deposited Polyaniline", Synthetic Metals, Vol. 29(1989), pp. E451-E456.

NMR AND FT/IR STUDIES OF TRYPTOPHANASE

Karen N. Toppin

Department of Chemistry
Claflin College
Orangeburg, S.C. 29115

Faculty Advisor:

Dr. Herbert Ashline

Studies are being conducted in this lab to determine the mechanism for tryptophanase reaction. This enzyme uses a cofactor vitamin B-6, or pyridoxal 5'-phosphate (PLP). Metzler (Biochem. Biophys. Res. Comm. 1991) has observed that proton NMR can be used to study PLP-bound enzymes. The bands observed are in the 15-20 ppm range. Martinez-Carrion (Arc. Biochem. Biophys.1991) has observed that FT/IR can be used to study the same hydrogen bound to phosphate. These two methods were employed to study the structure of the B-6 in the protein. Sample of the enzyme cofactor complex were titrated from pH 6.0 to pH 8.5 in increments of .5 pH units and both NMR and FT/IR spectra were taken of each sample.
Inhibitor was added to each sample and spectra taken. It was observed that there was a significant change in the NMR spectra with change in pH, in both cases. The FT/IR spectra of the enzyme and PLP showed significant changes with pH, however, the inhibited samples showed no change with changes in pH.

BACKGROUND

Escherichia coli bacteria containing the trn A gene on plasmid pm06 was cultured to produce tryptophanase. The first step in this process was to make the the medium used to grow the bacteria, containing: 2 grams of yeast extract, 10 grams casein enzymatic hyrolsytate, 2 grams of KH2PO4, .02 grams pyridoxine hydrochloride, and .1 gram of ampicillin. The pH was adjusted to 7.45 by adding 1m of NaOH to the solution and then the ampicillin was added after the autoclave. The broth was then sterilized at 110 degrees Celsius. Broth was cooled and culture was added; it was left for sixteen hours at a temperature of 37 degrees Celsius. The next morning the L-trytophan was introduce to the medium and the mixture was shaken for an additional three hours. The addition of this amino acid started the production of the enzyme, tryptophanase.

The mixture was centrifuged for 30 minutes at 10,000xG. Then the supernatant was discarded and the pellets suspended a 1 molar phosphate buffer. The solution was sonicated in three periods of one minute each and then centrifuged at 25,000xG. The supernatant was collected and the sample weighed 8.30 grams. The centrifuge bottles were sterilized with alcohol to kill any bacteria left in the residue.

A gel column was selected and equilibrated with a buffer of (NH4)2SO4 at 40% saturation, 121.5 grams in 500ml. The sample obtained was 25 ml. This sample was chromatographed overnight at 8ml/hr to separate the tryptophanase from the other byproducts. The sample was eluted in 20%(NH4)2SO4 at 28ml/hr. The samples were stored in 1ml vials at -70 degrees centigrade.

As needed, samples of enzyme were thawed and chromatographed to remove excess PLP that was not bound to the tryptophanase. The B-6 vitamin (PLP) is needed to ensure the stability of the enzyme. A buffer of KCl, 0.05 molar pH 7.0 was used to chromatograph the samples. The concentration and activity of the enzyme was confirmed by UV/Visible spectra by adding 30ul of 2mm Pyridoxal Phosphate, 300 ul 1.2mm 2-(O Nitrophenyl)-L-Cysteine, 21 ul of distilled water and 10 ul of enzyme solution. Distilled water was used as a blank and the results are shown in figure 1.1.

The tryptophanase was titrated with HCl and NaOH to set the pH at a range of 6 to 8 in increments of 0.5. The deuterium oxide was added and NMR spectrum taken. After this was completed the pH was checked and they were prepared for analysis for the FT/IR. A background spectrum was taken before running each sample.

There was a significant change in NMR with pH for samples of enzyme and enzyme with inhibitor (Oxindolyl-Alanine). The most significant changes were observed in the FT/IR spectra of enzyme vs pH. The enzyme that had their pH change from 6.5 to 7.5 had a peak in 1453-1452 range rise slowly which is illustrated in figure 1.2, while those that had a pH change of 8 to 8.5 showed that the same peak (1453-1452) proceeded to drop below its original size as seen in figure 1.2. . When Oxindyl-L-Alinine (the inhibitor) was added the change that had occurred in the range of 1453-1452 with pH was not observed, which can be noted in figure 1.3. Prior to taking the spectrum of the FT/IR the samples were checked for their pH value. It was noted that the enzyme had titrated to its original pH value of 6.8; though the spectrum noted that a change had occurred.

This data obtained is not conclusive and studies are still being conducted. New possibilities have been presented with this additional information obtained from the IR spectra; which in turn could support the NMR results. It is believed that a configurational change occurred when the pH of the enzyme was altered. Also, results showed that the inhibitor affected the altered enzyme of tryptophanase by binding to one of it's sites. The question is where and how is the Oxindolyl-Aliaine affecting the enzyme. Finally, why has

the enzyme titrated itself to its original pH, yet has given different results for each spectrum taken.

ACKNOWLEDGEMENTS
The author desires to express her thanks for the influential individuals who helped in every way possible through out this research: Dr. Richard Dluhy, Dr. Robert Phillips, Quincy Teng, and Dr. Herbert Ashline.

REFERENCES
Gollinck, P.D. and Phillips, R.S (1989).Evidence That Cysteine Is in the Active Site of Tryptophan Indole-lyase, (Journal of Biological Chemistry)
Metzler, C.M., Metzler, D.M., Kintanat, A., Scott, R.D., and Marceu, M.,(1991) Biochemistry Biophysic Res. Comm., 178, 385-392
Morino, Y. and Snell, E.E. (1970) Methods of Ezymol, (Journal of Boiolgical Chemistry)
Ruiz-Sanchez, J.M., Iriate, A. and Martinez-Carrion (1991), Arc. Biochem. Biophys., 286, 38-45.

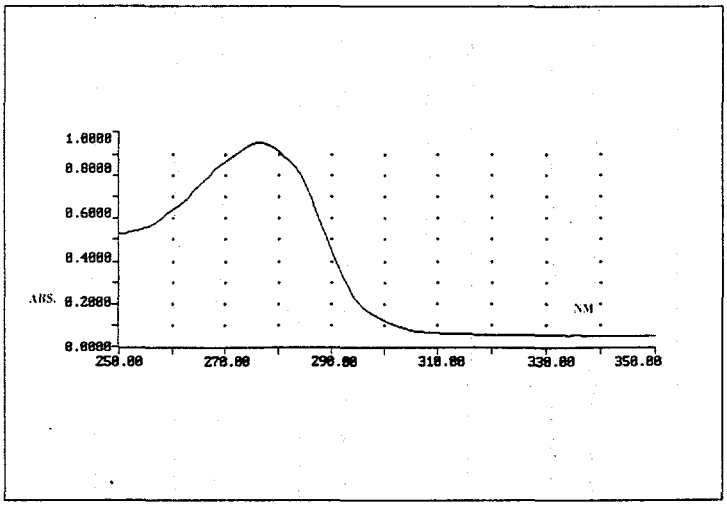


FIGURE 1.1 ACTIVITY OF TRYPTOPHANASE WITH UV SPECTRA

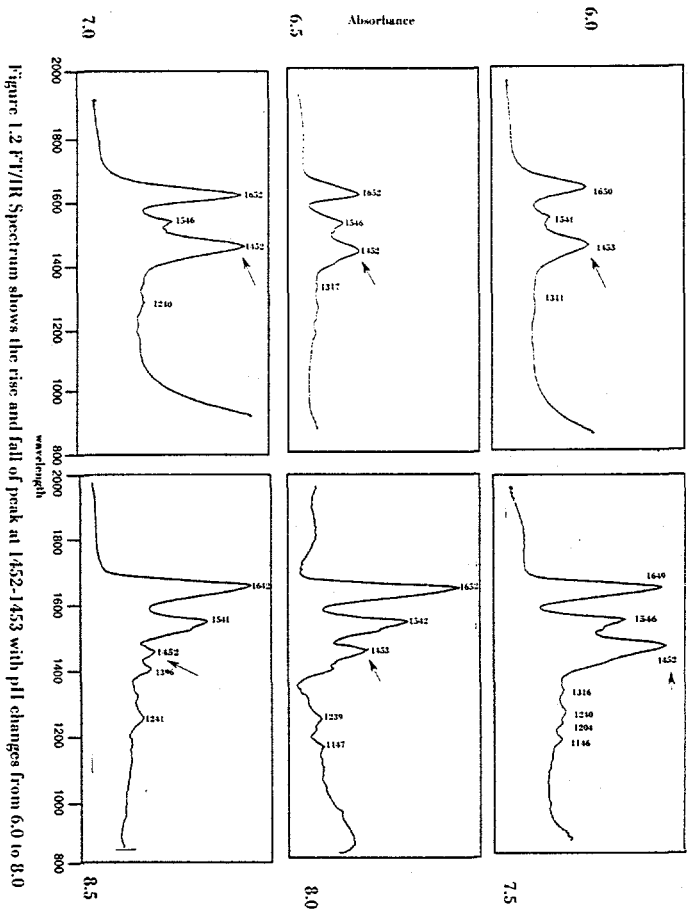


Figure 1.2 FT/IR Spectrum shows the rise and fall of peak at 1452-1453 with pH changes from 6.0 to 8.0

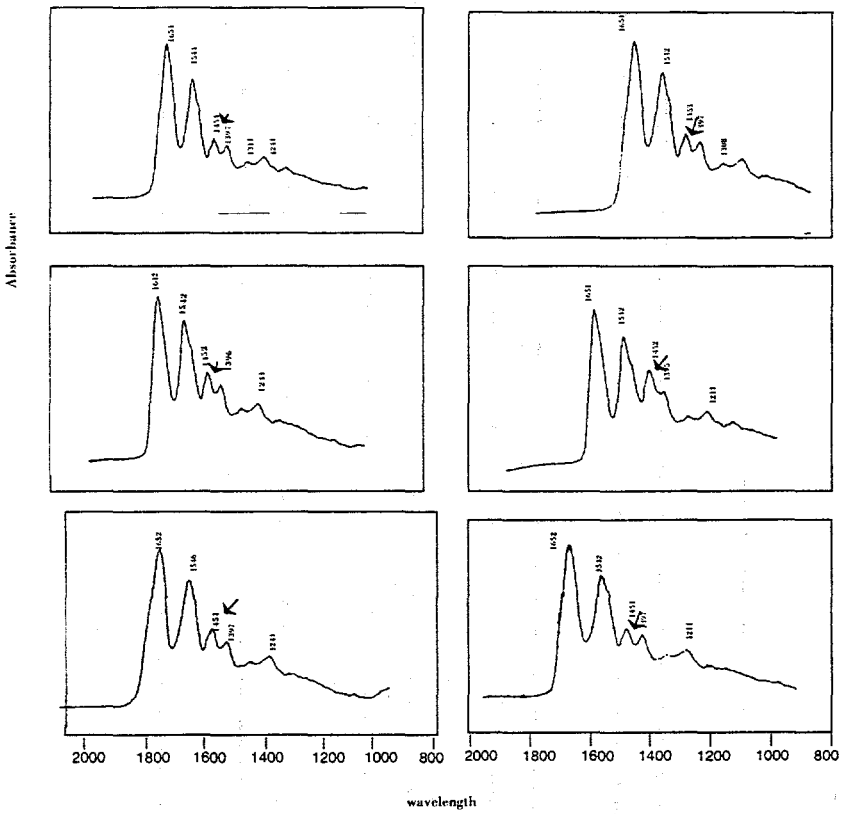


Figure 1.3 FT/IR Spectrum with inhibitor Oxindolyl-alanine added no changes occurred at the peak wich had a range of 1452-1453.

MOSSBAUER ANALYSIS OF BOG SOIL SAMPLES

John A. Jones

Department of Chemistry
Fayetteville State University
Fayetteville, NC 28301

Faculty Advisor:

Katherine M. Whatley

Department of Physics
UNC Asheville
Asheville, NC 28804-3299

INTRODUCTION

The mountain bogs of North Carolina are disappearing at an alarming rate. These ecosystems have not been studied in detail, despite the fact that many rare species of plants and animals inhabit them. An interdisciplinary study of mountain bogs is now underway at UNC Asheville, involving members of the Environmental Studies Program and the Physics and Chemistry Departments.

In the past, bogs were present in every mountain county in the South. Today, the known bogs in North Carolina are concentrated in a band from Henderson County west to Clay County in the southern mountains. More than fifty percent of mountain bogs are privately owned and are being altered from their natural state. Many bogs have been destroyed by grazing, loging, mining, and residential or commercial development.

The ecosystems of mountain bogs are quite diverse given the small amount of land they occupy. The hydrological needs of the bog systems include a clean, reliable, natural supply of ground water and uncontaminated surface water. Bogs in general receive hydrologic input primarily through precipitation, but mountain bogs also receive water from ground water seepage. Ground water comes from unconfined or confined aquifers. (Unconfined aquifers are sources of ground water not separated from the ground surface by a layer of a confining material such as clay. Confined aquifers may exist at a depth lower than unconfined aquifers and are separated from the surface by a layer of impenetrable material.)

The few studies that have considered bogs have concentrated on the vegetation or on the aquatic and terrestrial life that exist in bogs. Climate varies considerably among mountain bogs due to a wide range of elevations and latitudes. How differences in soil characteristics and climatic conditions affect the heterogeneity of bog vegetation has not yet been addressed. Soils play an important role in determining the composition and function of wetlands ecosystems. Current research underway at UNC Asheville will explore the soil characteristics of Southern Appalachian mountain bogs. Characteristics to be determined will include pH, texture, organic carbon content, and cation exchange capacity.

This paper represents a trial study of soils in one mountain bog using Mossbauer spectroscopy. The purpose was to determine if Mossbauer techniques were applicable to the study of these soils and to determine if dry studies of the soil samples would indicate differences in the soils sampled at the edge and the center of the bog.

Mossbauer spectroscopy is a nuclear technique involving the resonant absorption and emission of gamma rays by nuclei. Mossbauer spectroscopy is very sensitive to small changes in the atomic environment of particular elements, in this case iron. Information is generally obtained in the form of three main parameters: isomer shift, which is a measure of the electon charge density at the nucleus; quadrupole splitting, which is the result of an interaction between the quadrupole moment of

the nucleus and the electric field gradient created by the atomic electrons; and the magnetic hyperfine splitting, which is due to an interaction between the magnetic moment of the nucleus and the magnetic field created by the atomic electrons. In combination, these parameters can provide sufficient information to determine the oxidation state of iron in a given material.

METHODOLOGY

Soil core samples were taken at various depths at the edge (soil well E8) and at the center (soil well E14) of McClure's Bog, located in Henderson County, NC. The samples were oven dried and ground to a fine powder. They were then inserted into a Ranger 1200 Mossbauer spectrometer, at an approximate density of 0.17 g/cm2. Spectra were measured using a 57Co source, which decays into an excited state of 57Fe and then down to the ground state of 57Fe. After data collection, all spectra were fit using MOSFUN, a program which fits the data to Lorentzian peaks.

DATA

As can be seen in figures 1 and 2, the Mossbauer spectra of the samples from well E8 and well E14 are similar, but not identical. Table 1 lists the numerical data. Samples from both wells contain three distinct iron sites which each exhibit an isomer shift and a quadrupole splitting but no magnetic hyperfine interaction. Values of the isomer shift and quadrupole splitting for each site differ slightly between wells. This indicates a difference in the way iron is bound into the soils at the different wells. The relative intensities of the gamma ray absorption from each site are different in samples from the different wells and vary slightly with depth in the same well.

CONCLUSIONS

It is possible to collect meaningful Mossbauer data on samples of bog soils. Spectra of samples taken from the center of the bog are different from spectra taken at the edge of the bog, and the spectra of samples taken at each site vary with depth. Further analysis of the data should lead to the assignment of an oxidation state to each site, which will yield information about cation exchange in the soils. This study will be expanded to include other wells in McClure's bog.

ACKNOWLEDGEMENTS

The author would like to thank Dr. John Stevens, Dr. Kevin Moorhead, and Mr. Frank Cavadas, all of UNCA, for assistance with the project. Samples were provided by Dr. Moorhead.

REFERENCES

Mohan, J., Benjamin, S., and Sutter, R. "Site Design for McClure's Bog", report to the North Carolina Nature Conservancy, 1993.

Reberg-Horton, C. "Mountain Bog Management", report to the North Carolina Nature Conservancy, 1994.

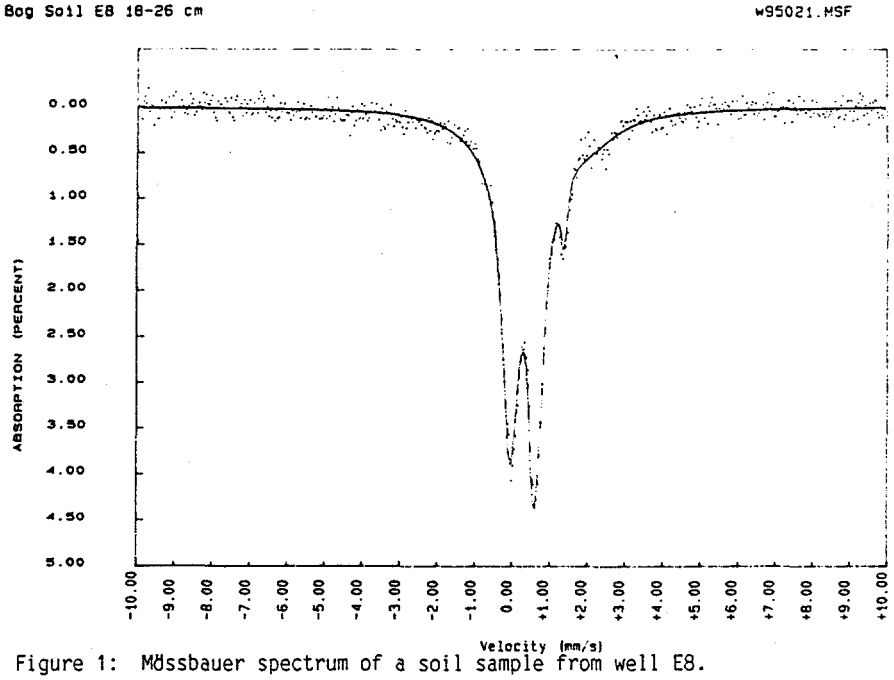


Figure 1: Mössbauer spectrum of a soil sample from well E8.

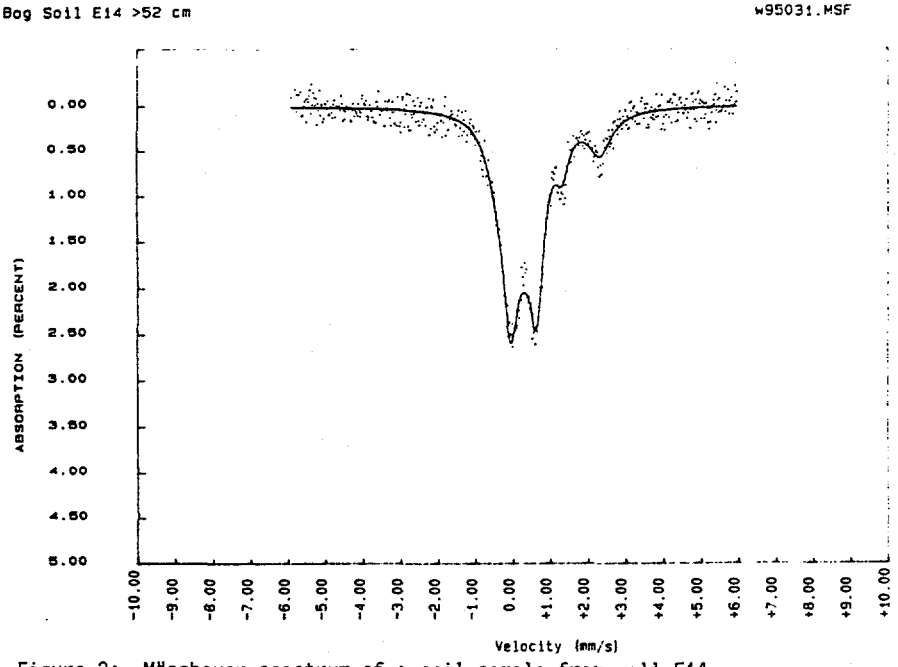


Figure 2: Mössbauer spectrum of a soil sample from well E14.

Table 1. Mossbauer data on samples from wells E8 and E14, McClure's Bog

Well	Depth	IS1	QS1	IS2	QS2	IS3	QS3
E8	0-18 cm	.285	.677	.923	.787	.790	2.40
E8	18-26 cm	.286	.701	.938	.814	.760	2.29
E8	>26 cm	.254	.701	.926	.761	1.07	2.56
E14	0-12 cm	.248	.683	.867	.819	.828	1.90
E14	12-38 cm	.262	.696	.830	.979	.796	2.95
E14	38-52 cm	.254	.651	.794	1.00	.911	2.74
E14	>52 cm	.248	.683	.750	1.08	.899	2.78

All isomer shift and quadrupole splitting data are given in units of mm/s. Errors are ± 0.01 mm/s except for QS3 which is ± 0.1 mm/s.

Analytical Spectroelectrochemistry of Selected Analytes

Sherry-Ann Callender

Department of Physical Science
Pembroke State University
Pembroke, NC 28372

Faculty Advisor:
Paul A. Flowers

Spectroelectrochemical (SEC) studies were performed on selected analytes in order to assess the feasibility of developing quantitative analysis schemes based on SEC techniques. Data from potential-step SEC experiments were used to derive calibration curves for each analyte examined by plotting change in absorbance versus concentration. Adherence to Beer's law was observed for aqueous o-tolidine and bilirubin ditaurate conjugate, while significant deviations were observed for aqueous ferricyanide and ascorbic acid.

INTRODUCTION

Many clinical techniques for determining substances in human body fluids (urine, plasma, serum, etc.) involve some or all of the following steps:

a) sample pretreatment, for example, analyte extraction, chromatographic separation, reconstitution;
b) chemical reaction after addition of reducing/oxidizing or chromogenic/fluorogenic complexing agents;
c) postreaction separation of components in the reaction mixture; and
d) spectroscopic analysis of a reaction product after transferring the sample to a suitable optical cuvette.

Ideally, an analytical method should include as few of these steps as is practical in order to minimize reagent consumption, sample transfer, and analysis time. Clinical analyses, however, often require several of the above steps because of the complex nature of the analyte matrix, i.e., the body fluid.[1]

Though often used for fundamental studies, spectroelectrochemical (SEC) methods have seen relatively little application for purely quantitative purposes.[2-6] Because they involve the simultaneous application of both spectroscopic and electroanalytical techniques, SEC methods may dramatically reduce analysis time, cost, complexity and interferences. In particular, many clinically significant analytes are well-suited for SEC determination because of their spectroscopic and electrochemical properties.

This research project investigates the SEC properties of selected compounds with the ultimate goal of developing clinical analysis schemes which offer advantages over those presently used for components of body fluids. Reported herein are data which address analytical aspects of the SEC behavior of aqueous ferricyanide, o-tolidine, ascorbic acid, and bilirubin ditaurate conjugate.

EXPERIMENTAL

Reagents. All reagents were obtained from commercial sources and used without further purification. Solutions were prepared using distilled/deionized water and were degassed prior to analysis.

Apparatus. The SEC cell employed is depicted in Figure 1. This cell was used in conjunction with a Hewlett-Packard 8452A diode array spectrometer and a BioAnalytical Systems CV-27 voltammograph to perform SEC experiments in the manner described below.

Procedure. The SEC cell was filled with the test solution, thumped to remove air bubbles from the RVC pores, placed in the spectrometer's sample chamber, and connected to the voltammograph. After recording a background spectrum, the RVC electrode potential was stepped to a value sufficient to bring about diffusion-controlled electrolysis of the analyte, and spectra were acquired as the electrolysis proceeded to completion. This procedure was repeated for test solutions of varying concentration, and the corresponding maximal absorbance changes were plotted versus analyte concentration.

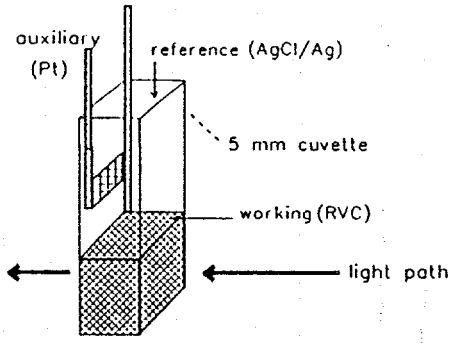


Figure 1. Schematic diagram of the SEC cell used in this work. The working electrode was 80 pores-per-inch reticulated vitreous carbon (RVC).

RESULTS AND DISCUSSION

Figure 2 shows potential difference spectra for the oxidative electrolysis of o-tolidine. The negative feature at 250 nm results from the disappearance of the o-tolidine as it is electrolyzed, while the positive feature at 440 nm is due to the appearance of the electrolysis product, o-tolidinium ion. A plot of absorbance at 440 nm versus time is shown in Figure 3. The concentration-dependence for the maximal absorabnce change, ΔA_{max}, was examined by

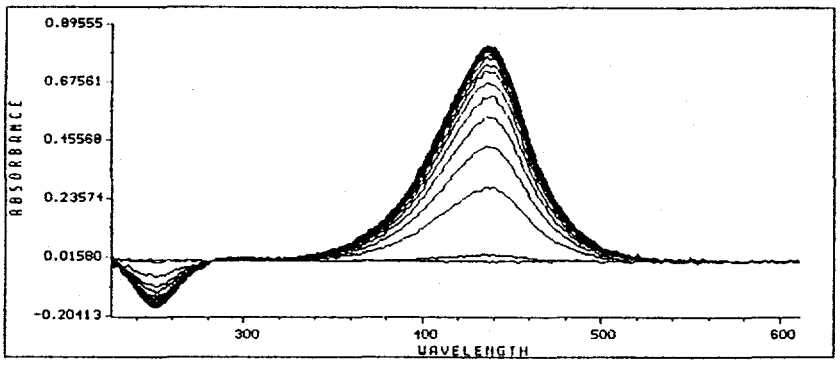


Figure 2. Potential difference spectra for 0.03 mM o-tolidine in 0.5 M acetic / perchloric acid. Spectra acquired every 2 s after a potential step from open circuit to +1.0 V vs. AgCl/Ag.

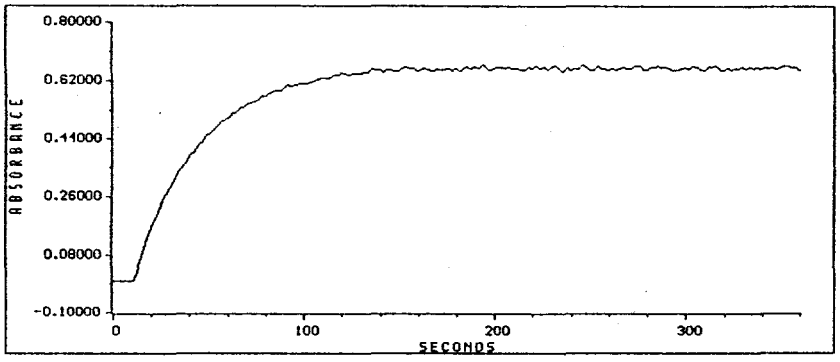


Figure 3. Absorbance at 440 nm versus time for the electrolysis of o-tolidine.

plotting this quantity versus concentration as shown in Figure 4.
For simple systems, the expected relation is analogous to Beer's law, i.e.

$$\Delta A_{max} = \Delta \epsilon bc$$

where $\Delta\epsilon$ is the difference in molar absorptivities for the analyte and its electrolysis product, b is the optical path length, and c is the analyte

concentration. For this system, as well as all others examined, a linear response was observed. However, calibration curves for ferricyanide, ascorbic acid, and uric acid showed significant negative intercepts, possibly due to pre-electrolysis adsorption of analyte on the RVC surface (data not shown). A new cell design which should overcome this problem has been constructed and is presently being characterized. Based on the calibration data, values for detection limit and sensitivity were computed for each analyte studied (see the Table).

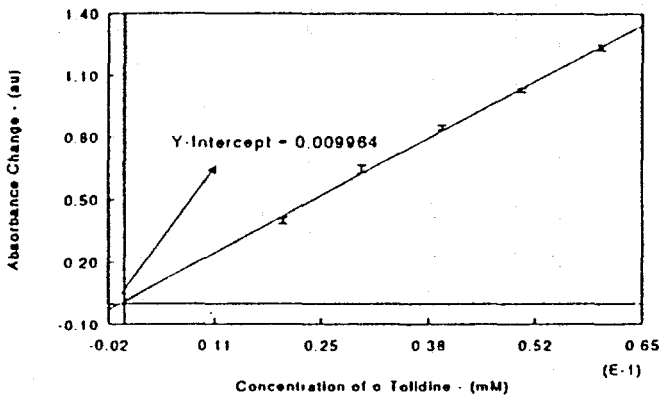


Figure 4. Calibration curve for the SEC determination of o-tolidine.

Table. Analytical figures of merit for the SEC determination of selected analytes.

analyte	*calibration sensitivity* (mM^{-1})	*peak-to-peak noise* (*mau*)	*detection limit* (μM)
ascorbic acid	7.44	4.7	0.38
bilirubin ditaurate	21.2	1.9	0.055
ferricyanide	0.498	2.0	2.4
o-tolidine	205	6.8	0.020

ACKNOWLEDGEMENTS

This work was supported in-part by an NSF grant to the North Carolina Consortium for Undergraduate Research. The supervision of Dr. Paul Flowers and the assistance of Tara Woods and Connie Polston is gratefully acknowledged.

LITERATURE CITED

1. Pesce, A.J.; Kaplan, L.A. "Methods in Clinical Chemistry"; Mosby Company: St. Louis, MO, 1987.
2. Xie, Q.; Kuang, W.; Nie, L.; Yao, S. Anal. Chimica Acta (1993) 276, 411-417.
3. Wei, W.; Xie, Q.; Yao, S. J. Electroanal. Chem. (1992) 328, 9-20.
4. Xie, Y.; Dong, S. J. Electroanal. Chem. (1990) 284, 279-288.
5. VanDyke, D.A.; Hung-Yuan, C. Anal. Chem. (1989) 61, 633-636.
6. Tyson, J. Talanta (1986) 33, 51-54.

Synthesis of the Acceptor Portion of a Molecular Triad for Artificial Photosynthesis

Tavia S. Boston
Aquita C. Robinson

Department of Chemistry/SOARS Program
North Carolina Central University

Durham, North Carolina 27707

Faculty Advisor: Dr. John A. Myers

ABSTRACT

Incorporation of an isoindolequinone into a molecular triad as the acceptor end of an electron transfer system is envisioned as a model system to observe artificial photosynthesis. In this project three new isoindolequinones were synthesized and characterized by ^{1}H-NMR spectroscopy. The two cyclopentadiene protected isoindolequinones appear to differ by a carbon-carbon double bond. Each compound has an ester functionality for covalently linking to an organo-ruthenium complex in formulating the desired molecular triad.

INTRODUCTION

A synthetic, five-part molecular device, or pentad, containing a carotene, zinc-porphyrin, free-base porphyrin, naphthoquinone, and a benzoquinone has been reported to convert light energy ($\Phi = 0.83$) to form a long-lived (55,000 ns), charge separation state (Gust, Moore, Lee, et. al., 1990). This energy transfer mimics an aspect of photosynthesis in plants.

Covalently bonding an isoindolequinone to an organo-ruthenium complex which is linked to an electron donor species is expected to yield a model system to artificially observe photosynthesis. In other words, the molecular triad might be expected to accept a photon of energy from sunlight which would cause one or more electron transfers. If the isoindolequinone portion, the acceptor end, gained a moving electron, it would become negatively charged. If the electron donor portion gave up an electron to the ruthenium complex in the middle which has passed an electron on to the isoindolequinone, then the donor end would become positively charged. The result of these photodriven electron transfer reactions would be a high energy, charge-separated state comparable to the initial step observed in natural photosynthesis in living plants.

In this research project, three protected isoindolequinones have been synthesized. Each isoindolequinone is diene-protected, and each has an ester functionality which may be exploited in later research to achieve covalent linkage to an organo-ruthenium complex. Proton nuclear magnetic resonance (^{1}H-NMR) spectra were recorded and are consistent with the structures assigned to the new isoindolequinone

SYNTHETIC DESIGN

Synthesis of a protected-isoindolequinone was envisioned to result from the 1,3-dipolar addition of an oxazolium 5-oxide to the C-C double bond of a protected 1,4-benzoquinone. After the cycloaddition, loss of carbon dioxide and two hydrogens would yield the desired compound. Generation of the unstable oxazolium 5-oxide could be accomplished by dehydrative cyclization of an acylated amino acid, N-ethyloxalylsarcosine. Protected -1,4-benzoquinones can be prepared by the Diels-Alder reaction of a diene with 1,4-benzoquinone. Only the unsubstituted double bond of a protected benzoquinone reacts with a diene. In this project, the protecting diene was not removed.

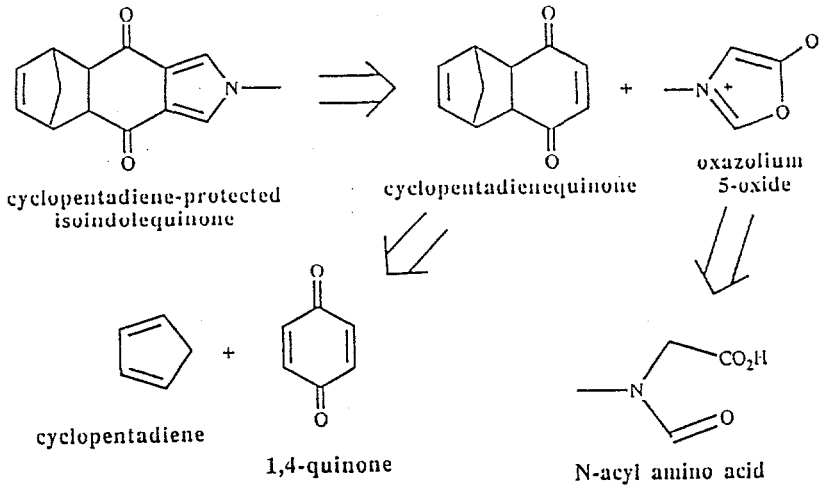


FIGURE 1: SYNTHETIC DESIGN

EXPERIMENTAL

Two protected 1,4-quinones were prepared for this study. Anthracene-quinone was prepared by heating anthracene with 1,4-benzoquinone in toluene to reflux for one hour (Clar, 1931). Cyclopentadiene-quinone was prepared in an analogous reaction of freshly-distilled cyclopentadiene with 1,4-benzoquinone in methanol at reflux (Albrecht, 1906).

An oxazolium 5-oxide was generated by reacting N-ethyoxalysarcosine (unpublished synthesis) with five equivalents of acetic anhydride in benzene at reflux for one hour under a stream of nitrogen. After cooling to room temperature, one equivalent of anthracene-quinone was added slowly. The reaction mixture was heated to reflux for four days. After cooling, the mixture was diluted with water and benzene, and sodium bicarbonate was added slowly to neutralize the acetic acid. After work-up, the crude product taken up in ethyl acetate was passed through a chromatography column consisting of 100-200 mesh silica gel. Cuts were monitored by TLC, and fractions containing the product were combined, rotary evaporated, and re-chromatographed over 230-400 mesh flash silica gel in hexane - ethyl acetate (5: 2). Approximately sixty 30-mL cuts were collected with a product isolated in cuts 14-25. A bright yellow solid was characterized by ^{1}H-NMR spectroscopy on a Varian EM-360L 60-MHz NMR spectrometer.

Reaction of N-ethyloxalylsarcosine with acetic anhydride, and then with cyclopentadiene-quinone for one day yielded a dark brown oil that was characterized by ^{1}H-NMR. The oil was isolated from column chromatography using 230-400 mesh flash silica gel developing with hexane-ethyl acetate (5: 1) and eluting with hexane-ethyl acetate (5: 2).

An equivalent reaction allowed to continue for four days yielded a bright yellow solid that was also characterized by ^{1}H-NMR. This product was isolated after column chromatography over 100-200 mesh silica gel eluting with hexane-ethyl acetate (5: 2). Solid precipitated in two of the fractions collected, and a yellow product was filtered and washed with hexane. The brown oil and yellow product revealed separate spots on TLC with different retention times.

RESULTS AND DISCUSSION

The anthracene-protected isoindolequinone (IIQ-1,see Figure 2) and the two cyclopentadiene-protected isoindolequinone products (IIQ-2 and IIQ-3, see Figure 3) revealed similar patterns in the ^{1}H-NMR spectra for the pyrrole ring substituents: pyrrole-H, N-CH_3, O-CH_2CH_3, and O-CH_2CH_3. The chemical shifts are shown in Table 1.

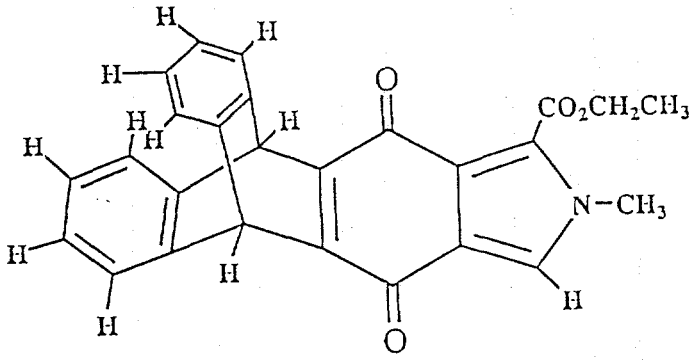
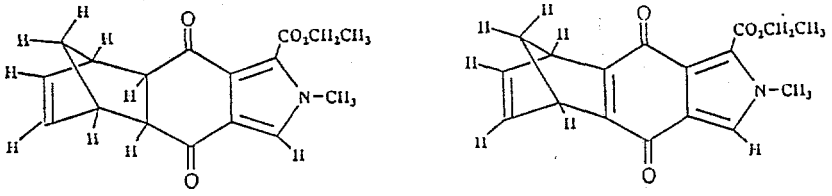


FIGURE 2. ANTHRACENE-PROTECTED ISOINDOLEQUINONE IIQ-1



IIQ - 2 (Short Term) IIQ - 3 (Long Term)

FIGURE 3. CYCLOPENTADIENE-PROTECED ISOINDOLEQUINONES

TABLE 1: ^{1}H-NMR CHEMICAL SHIFTS OF PYRROLE RING SUBSTITUENTS ON ISOINDOLEQUINONES

CHEMICAL SHIFTS OF PYRROLE RING SUBSTITUENTS ON ISOINDOLEQUINONES

SUBSTITUENT ISOINDOLEQUINONE	PYRROLE-H	N-CH_3	O-CH_2CH$_3$	O-CH_2CH_3
IIQ - 1	s, 7.3 ppm	s, 3.7 ppm	q, 4.3 ppm	t, 1.4 ppm
IIQ - 2	s, 7.3 ppm	s, 3.9 ppm	q, 4.4 ppm	t, 1.5 ppm
IIQ - 3	s, 7.2 ppm	s, 3.8 ppm	q, 4.3 ppm	t, 1.4 ppm

The NMR spectrum for the anthracene portion of IIQ-1 revealed eight aromatic hydrogens as a complex multiplet in the range 6.8-7.5 ppm downfield from TMS and two singlets for the two bridgehead benzylic hydrogens at 5.8 and 5.9 ppm.

The NMR specctrum for the cyclopentadiene-quinone portion of the dark brown oil IIQ-2 (short term product) revealed a multiplet centered at 6.08 ppm for the two vinylic hydrogens, a broad multiplet at 3.67 ppm for the two bridgehead hydrogens, a multiplet at 3.42 ppm for the two enolic quinone hydrogens, and a multiplet at 1.64 ppm for the bridging CH_2 group.

The NMR spectrum for the cyclopentadiene portion of the bright yellow solid IIQ-3 (long term product) was simpler revealing a multiplet for the vinylic hydrogens centered at 6.85 ppm, a multiplet at 4.09 ppm for the bridgehead allylic hydrogens, and a broadened singlet at 2.25 ppm for the bridging CH_2 group.

The anthracene or cyclopentadiene moiety used to protect one double bond of benzoquinone ensures that an unsubstituted C-C double bond is available in the isoindolequinones after covalent linkage to an organo-ruthenium complex using the ester group in each compound.

CONCLUSIONS

Three diene-protected isoindolequinones have been synthesized and the structures have been characterized by ^{1}H-NMR spectroscopy.

ACKNOWLEDGEMENTS

This research was supported by a grant from the Human Resources Division, NSF, to the Seizing Opportunities for Advancing Research Scholars (SOARS) Program of the North Carolina Consortium for Undergraduate Research (NCCUR). Special thanks are given to the University Undergraduate Research Program at North Carolina Central University and Marcus Brackeen of *Glaxo, Inc.* for encouragement and suggestions.

BIBLIOGRAPHY

Gust, D.; Moore, T.A.; Moore, A.L.; Lee, S.; Bittersman, E.: Luttrul, D.K.; Rehms, A.A.; Degrazino, J.M.; Ma, X.C.; Gao, F.; Belford, R.E.; Trier, T.T. *Science* **1990**, *248*, 199.

Clar, E. *Chemische Berichte* **1931**, *64*, 1676.

Albrecht, W. *Justis Liebigs Annalen der Chemie* **1906**, *34*, 348.

Unpublished synthesis from sarcosine and ethyloxalyl chloride.

STUDY OF SALT EFFECTS ON A HYDROPHOBICALLY ACCELERATED DIELS-ALDER REACTION

Jessica Speltz

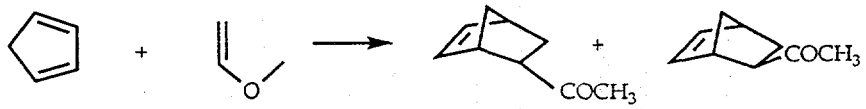
Department of Chemistry, Department of Physics
Guilford College
5800 W. Friendly Ave.
Greensboro, NC 27410

Faculty Advisor: Robert M. Whitnell

The Diels-Alder reaction is a pericyclic reaction whose rate constants are 30-5800 times larger in water than in organic solvents[1]. Salt effects and computer simulations are two tools that can be used to understand these rate accelerations. Rate constants were measured for the hydrophobically accelerated Diels-Alder reaction between cyclopentadiene and methyl vinyl ketone in varying concentrations of LiCl and GnCl. LiCl increased the reaction rate monotonically with the increase in concentration while GnCl decreased the reaction rate monotonically with the increase in concentration. These results indicate that the hydrophobic effect is one of the factors responsible for the rate increases. The molecular simulations done by Jorgenson, Blake and Lim of the reaction in water show that increased hydrogen bonding of water to the transition state maybe another cause of the rate increases[2].

INTRODUCTION

The Diels-Alder reaction, shown in Figure 1, is a pericyclic reaction between conjugated dienes to form a cyclic molecule[3]. It is often used in organic synthesis because it is one of the few ways known to form cyclic molecules and because it forms two carbon-carbon bonds in a single step[4].



cyclopentadiene methyl vinyl ketone endo-62% exo-38%

Figure 1: Diels-Alder reaction between cyclopentadiene and methyl vinyl ketone[5]

In 1980, Ronald Breslow and Darryl Rideout reported that when the Diels-Alder reaction was run in water instead of in organic solvents, a rate increase of 30-5800 fold was measured[6]. Since then, there have been several studies on various Diels-Alder reactions to look at why such large rate increases are seen in water[7].

One method used to examine the rate kinetics of accelerated Diels-Alder reactions is the addition of salts to the reaction system[8]. Some salts, such as LiCl and NaCl, are 'salting out' agents; they decrease the solubility of hydrocarbons in water. Other salts, such as GnCl and $LiClO_4$, are 'salting in' agents; they increase the solubility of hydrocarbons in water[9]. Results using these salts support the theory that rate increases are due, in part, to the inclination of nonpolar molecules to aggrate together in water, minimizing the water-hydrocarbon interactions. This behavior is known as the hydrophobic effect[10].

Recently, computer simulations have been used to look at the microscopic behavior of hydrophobically accelerated Diels-Alder reactions [11]. These simulations provide greater understanding of the microscopic interactions that lead to the observed rate increase because they allow a detailed examination of the dynamics of individual molecules[12].

EXPERIMENTAL SECTION

Cyclopentadiene was obtained immediately prior to its use in the reactions by distilling dicyclopentadiene[13]. The distilled cyclopentadiene was stored on ice in a

flask.

Reaction in 1-propanol:

Cyclopentadiene (1 x 10^{-4} M) was added to a methyl vinyl ketone (1 x 10^{-1} M)-1-propanol solution. The temperature of the reaction solution was kept at 25° C. Samples were taken from the reaction solution every 10 minutes and the disappearance of cyclopentadiene was monitored by recording the absorbance at 250 nm using a Hitachi U-2000 spectrophotometer.

Reaction In Water:

Cyclopentadiene (5 x 10^{-4} M) was added to a methyl vinyl ketone (9.85 x 10^{-3} M)-water solution whose temperature was kept at 25° C. The reaction mixture was placed in a UV cuvette and the disappearance of cyclopentadiene was monitored as described in the 1-propanol reaction.

Reactions in Salts:

The procedure is the same as that for water except LiCl (.998 M, 4.86 M, 7.5 M) was added to the MVK solution. This procedure was repeated for (.998 M, 4.86 M, 7.5 M) GnCl solutions.

All kinetic runs were performed at least three times. Pseudo first order kinetics were assumed and plots of ln (abs) vs. time was used to extract the rate constants. The pseudo first order rate constants were used to calculate the reported second order rate constants[14].

RESULTS

Table 1 shows the experimental second order rate constants for the water and salt solutions. Figure 2 shows examples of the plots used to calculate the rate constants. The rate constant in water increased almost 50 times compared to the rate constant in 1-propanol. LiCl, the salting out agent, increased the reaction rate while GnCl, the salting in agent, decreased the reaction rate. This is in agreement with the hydrophobic effect theory which assumes that a reagent that decreases the solubility of a hydrocarbon will increase the reaction rate and vice versa[15].

Table 1: Experimental Second Order Rate Constants

	1-Propanol* (x 10^{-2} L/ M s)	H_2O (x 10^{-2} L/M s)	LiCl (x 10^{-2} L/M s)	GnCl (x 10^{-2} L/M s)
Rate Constant	.20 ± .02	4.8 ± .5	.998 M: 6 ± 1 4.86 M: 8.8 ± .2 7.50 M: 10.1 ± .9	.998 M: 4.0 ± .1 4.86 M: 4.10 ± .08 7.50 M: 2.4 ± .8

* Only one experimentally accurate rate constant was calculated; published value[16] for rate constant: .912 x 10^{-3} L/M s

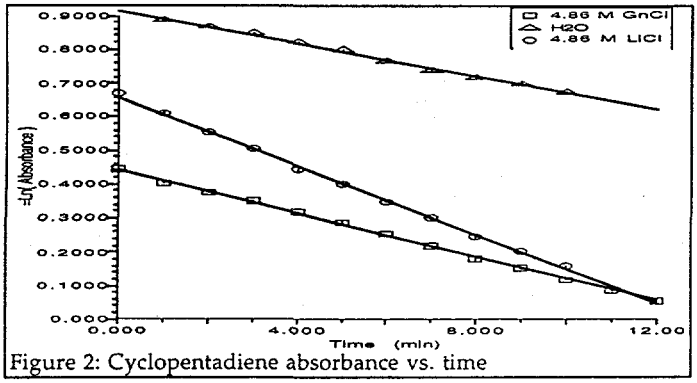


Figure 2: Cyclopentadiene absorbance vs. time

Figure 3 and 4 show the plots of molarity vs. rate constant for LiCl and GnCl respectively. The LiCl increased the reaction rate monotonically with the increase in concentration while the GnCl decreased the reaction rate monotonically with the increase in concentration.

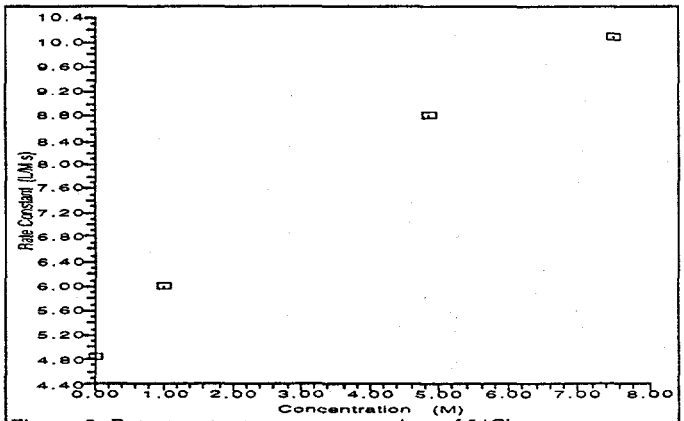


Figure 3: Rate constant vs. concentration of LiCl

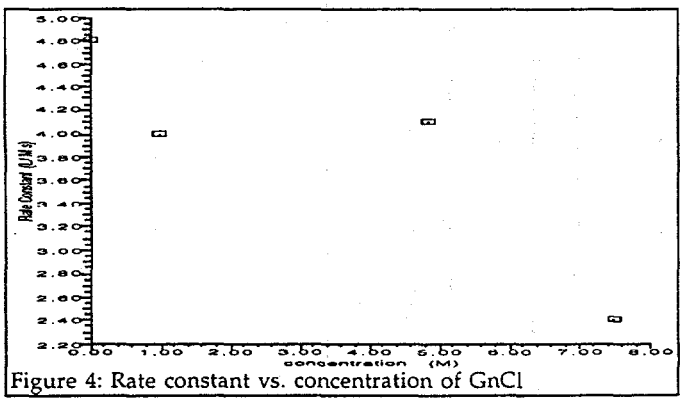


Figure 4: Rate constant vs. concentration of GnCl

The computer simulations done by Blake, Jorgenson, and Lim indicate that although the hydrophobic effect is responsible for some of the observed rate changes, it is not the primary cause of these changes[17]. Instead, the simulations have shown that there are water molecules hydrogen-bonded to the oxygen in the transition state of the reaction that lower the energy of activation and thus increase the rate of the reaction[18].

In conclusion, both the use of salts and the use of computer simulations have provided a basic understanding of why such dramatic rate increases are seen in Diels-Adler reactions in water. A questions of interest for future research is why the concentrations of LiCl and GnCl affect the rate constants the way shown in Figures 3 and 4. This question could be explored by constructing a molecular simulation of the experimental system described in this paper.

ACKNOWLEDGEMENTS

The author would like to thank Rob Whitnell for the time and information that he has donated to this project, the Guilford College Chemistry and Physics departments for their help, and the Jeiglinski family for the funding this project.

REFERENCES

1. Blokzijl, W.; Blandamer, M.; Engberts, J. *J. Am. Chem. Soc.* 1991, *113*, 4241-4246
2. Blake, J.; Lim, Dongchul.; Jorgenson, W. *J. Org. Chem.* 1994 *59*, 803-805
3. A pericyclic reaction occurs in a single step without intermediates
4. McMurry, John. Organic Chemistry, 3rd Edition. Brooks-Cole Publishing Co., Ca. 1992, 503
5. Fieser, L. Reagents for Organic Synthesis. New York: Wiley, 1986. 697
6. Breslow, R.; Rideout, D.; *J. Am. Chem. Soc.* 1990, *102*, 7817-7818
7. Blokzijl, W.; Blandamer, M.; Engberts, J. *J. Am. Chem. Soc.* 1991, *113*, 4241-4246, and references therein
8. Breslow, R.; Rizzo, C. *J. Am. Chem. Soc.* 1991, *113*, 4340-4341
9. Breslow, R.*Acc. Chem. Res.* 1991, *24*, ,
10. Breslow, R. *Acc. Chem. Res.* 1991, *24*, 164-170
11. Blake, J.; Dongchul, L.; Jorgensen, W. *J. Org. Chem.* 1994, *59*, 803-805
12. Whitnell, R.; Wilson, K. "Computational Molecular Dynamics of Chemical Reactions in Solution", Reviews in Computational Chemistry IV. New York: VCH Publishers , 1993
13. Pickett, L.; Paddock, E.; Sackter, E. *J. Am. Chem. Soc.* 1941. *63*. 1073
14. Cox, B. Modern Liquid Phase Kinetics. New York: Oxford Science Publications, 1994. 7
15. Breslow, R. *Acc. Chem. Res.* 1991, *24*, 164-170
16. Blokzijl, W.; Blandamer, M.; Engberts, J. *J. Am. Chem. Soc.* 1991, *113*, 4241-4246
17. Blake, J.; Lim, D.; Jorgenson, W. *J. Org. Chem.*, 1994, *59*, 803-805
18. Morrison, r.; Boyd, R. Organic Chemistry. Boston: Allyn and Bacon, 1983. 69

A Qualitative Analysis of Iron Carbonyls by Mössbauer Spectroscopy

Willie Randolph Hargrove Jr.

Department of Chemistry
North Carolina Central University
Durham, N.C. 27707

Faculty Advisors:

Dr. John G. Stevens and Dr. Kathy Whatley
Mössbauer Data Center
University of North Carolina at Asheville
One University Heights
Asheville, N.C. 28804-3299

Several iron carbonyl complexes were synthesized at Clemson University in Clemson, South Carolina in a dry box under argon gas. The structures of these complexes were determined by X-ray crystallography. Samples of these complexes were ground in boron nitride, sealed in epoxy and sent to the University of North Carolina at Asheville. Mössbauer Spectroscopy was performed on the complexes to determine the oxidation and spin state of each iron site. Also, the Mössbauer data were compared with the X-ray crystallography data to confirm the actual structure of each complex.

BACKGROUND

This research was a collaboration between the University of North Carolina in Asheville and Clemson University in Clemson, South Carolina. At Clemson University, several iron carbonyls were synthesized in a dry box under argon gas by Mr. Gregory Drake and Dr. Joseph Kolis. Also, X-ray crystallographic analysis was performed on the complexes to determine their structure. A sample of each complex was ground with boron nitride into a homogeneous mixture. Then the samples were placed in a sample holder and sealed in epoxy. These samples were sent to UNC-Asheville for further analysis. Mössbauer Spectroscopy was performed on these complexes to determine the oxidation state and spin state of each iron site. These iron carbonyls consist of a Fe atom bonded to a carbonyl and either a S, Se or Te atom. An interesting aspect of these complexes is that S, Se, or Te participates in polycation formation. The formula for these iron carbonyls complexes are as follows: $[Fe_3S_4(CO)_{10}][SbF_6]_2$ (I), $[Fe_3Se_3(CO)_{10}][SbF_6]_2$ (II), $Fe_3S_2(CO)_9$ (III), $[Ph_4P]_2[Fe_3Te(CO)_9]$ (IV), and $[Fe_6Te_8(CO)_{18}[AsF_6]_2$ (V). Except for the tellurium complex, $[Ph_4P]_2[Fe_3Te(CO)_9]$, none of these complexes have been made before.

Mössbauer Spectroscopy is a high-resolution nuclear technique that can be used to give specific information about the bonding, structural patterns and dynamical properties of various systems. Mössbauer Spectroscopy is based on the emission and absorption of gamma rays by nuclei in solids. Emission of gamma rays occurs when a nucleus decays from an excited state to a ground state, emitting a gamma ray. This gamma ray is absorbed by an identical nucleus, which travels from a ground state to an excited state. (Stevens and Ruiz, 1983)

Mössbauer allows one to observe various interactions and thus study the events affecting the nucleus and its immediate environment. The two interactions investigated in this project were the isomer shift (I.S.) and quadrupole splitting (QS). An isomer shift is the result of an electrostatic interaction between the nuclear charge and the electrons that penetrate to the nucleus. Isomer shifts are means by which atomic oxidation states can be directly investigated. Quadrupole splitting involves a splitting of nuclear energy levels corresponding to different alignments of the principal axis of the electric field gradient. Quadrupole Splitting data can give information relating to the electronic population of various orbitals, isomerization phenomena, ligand structure and defect structure of solids. By comparing the isomer shift and quadrupole splitting data of related materials to the data obtained by analyzing these iron carbonyl complexes, the oxidation and spin states of the Fe sites were determined. (Hoy, 1971)

The neutral sulfur complex, $Fe_3S_2(CO)_9$ has one kind of Fe site, according to data obtained from X-ray crystallography. This iron site consists of a Fe atom bonded to three carbonyls and two sulfur ligands. This is a seven-coordinate iron carbonyl complex. Seven-coordinate iron complexes have a quadrupole splitting that ranges from 0.4-1.4mm/s. A complex with the same

molecular formula as the neutral sulfur complex but having a different structure has been made in Italy (Aime; Milone; et al, 1980). This complex has two Fe atoms and two sulfur atoms at alternate corners of the base of a distorted tetragonal pyramid, whose apex is occupied by the third

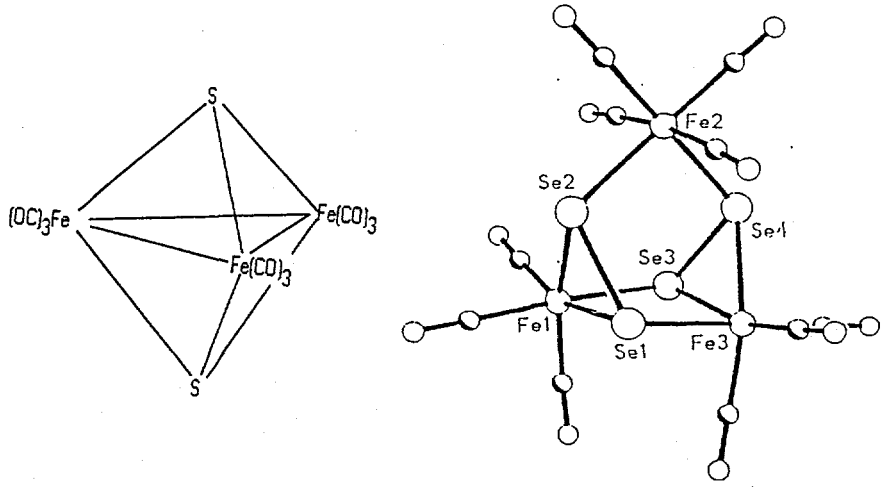


Figure 1: Structures of the neutral sulfur complex III and the selenium complex II.

iron atom. Three terminal carbonyls are bound to each iron atom. According to the solid-state structures, five resonances in the ^{13}C-NMR spectrum are expected. In this Italian experiment, only three or four resonances were discovered. The results are as follows:

Table I. ^{13}C-NMR Spectral Data for Complex: $[Fe_3(CO)_9S_2]$

	Fe(1)(CO)eq.	Fe(2)(CO)ax	Average(26°C)[a] Fe(2)(CO)ax	Fe(2)(CO)eq.
Chem. Shifts:	210ppm[b]	209.5ppm[b]	204.8ppm[a]	201.9ppm[b]
Relative Intensities	3	2		4

[b] The ^{13}C-NMR spectra were recorded at -85°C if not otherwise stated.

The resonance of intensity 3 was assigned to the carbonyls bound to the apical iron. The resonance of intensity 2 was assigned to apical carbonyls bound to the basal iron atoms, and that of intensity 4 to the remaining carbonyls. This data showed that the carbonyls are, therefore, in different environments.(Aime; Milone; et al, 1980).

RESULTS AND DISCUSSION

The neutral sulfur complex (III), which was analyzed by Mössbauer Spectroscopy has only one iron site. The Italian complex and the sulfur neutral complex are different compounds. The neutral sulfur complex had an isomer shift of -0.11mm/s and had a quadrupole splitting of 0.59mm/s. This is an Fe(II) low spin, an Fe(III) low spin, or a Fe(III) high spin site. There was not a large enough difference in the isomer shifts and quadrupole splittings to distinguish the oxidation states and spin states.

Another complex analyzed was the sulfur complex (I) $[Fe_3S_4(CO)_{10}][SbF_6]_2$. The data from X-ray crystallography showed that there are only two iron sites. This complex has two types of iron sites. The equivalent iron sites have an Fe atom bound to three carbonyls and three sulfur atoms. The unique iron site consists of an Fe atom bound to four carbonyls and two sulfur atoms. This is a six-coordinate iron complex. The quadrupole splitting is less than 0.6mm/s for six-coordinate iron complexes.(Gibb and Greenwood, 1984) The unique site in this complex has one more carbonyl than the iron site in the neutral sulfur complex. As the number of carbonyls

increases, the isomer shift increases because of significant sigma-donation capability of the carbonyl group. The carbonyl ligands cause a considerable increase in the isomer shift because the sigma-donation to the Fe 4s-orbital is reduced causing the s-electron density at the iron nucleus to decrease. The Mössbauer data shows three isomer shifts at velocities -0.11mm/s, 0.12mm/s, and 1.3mm/s. Also, there are three quadrupole splitting: 0.61mm/s, 1.08mm/s, and 2.76mm/s. This suggests that there may be three different iron sites present in the complex or an impurity due to decomposition. There was a 3:2:1 ratio of the intensities of the peaks in the Mössbauer spectrum. The iron site that consisted of an Fe atom bound to three carbonyls and three sulfur atoms has an isomer shift of -0.11mm/s and a quadrupole splitting of 0.61mm/s. This site is Fe(II) low spin,Fe(III) low spin, or Fe(III) high spin site. The other iron site is an Fe(II) high spin. Due to the fact that there was a low signal to noise ratio, it was difficult to determine the spin state of the unique iron site. Also, there was not a large enough difference between the isomer shifts and quadrupole splittings to distinguish between Fe(II) low spin and Fe(III) high or low spin..

The selenium complex (II) is quite similar to the sulfur complex (I). The sulfur atoms are replaced with selenium atoms. The molecular formula of the selenium complex is $[Fe_3Se_4(CO)_{10}][SbF_6]_2$. This also is a six-coordinate iron complex. The structure from X-ray crystallography suggest there are two iron sites. Furthermore, this complex also has two equivalent iron sites and one unique iron site. A few years ago a, tungsten-selenium carbonyl complex was characterized by X-ray crystallography. The molecular formula is $[W_2(CO)_{10}Se_4][AsF_6]_2$. This complex contains two $[W_2(CO)_5Se_2]^{2+}$ groups with a pentagonal-bipyramidal geometry. These groups are bridged by weak Se-Se bonds. The CO bond trans to Se_2 group (1.081Å) is the shortest of the CO bonds. The two axial CO groups have the longest bonds(1.153 and 1.142Å) while the other equatorial CO are immediate in length. The trans CO also has the longest W-C bond (2.094Å) while the axial CO's have the shortest W-C (2.032 and 2.047Å). The Se_2^+ ligand exerts a strong trans influence. This happens because Se_2^+ is a good sigma-donor as well as a good pi-acceptor (Collins; et al, 1986). The Se_2^+ ligands sigma-donation and pi-acceptor capabilities also affects the Mössbauer parameters. The partial isomer shift is increased both by sigma-donation and the pi-withdrawal of d-electron density. The partial quadrupole splitting becomes more negative as sigma-donation increases but more positive with an increase of metal to ligand bonding (Bancroft, 1973). The Mössbauer data showed three isomer shifts at -0.12mm/s, 0.14mm/s, and 1.3mm/s. Also, there were three quadrupole splittings at 0.58mm/s, 1.1mm/s, and 2.7mm/s. The iron site with an isomer shift of -0.12mm/s and quadrupole splitting of 0.58mm/s is Fe(II) low spin, Fe(III) low spin or high spin site. The iron site with a quadrupole splitting of 2.7mm/s and an isomer shift of 1.3mm/s is Fe(II) high spin. The signal to noise ratio made it difficult to determine the spin state. Furthermore there was not a large enough difference between the isomer shifts and quadrupole splittings to distinguish between the spin states. The other iron site may also be an impurity due to decomposition or another actual iron site.

The molecular formula for the tellurium (IV) complex is$[(Ph)_4P]_2[Fe_3Te(CO)_9]$. Each Fe atom is bound to three carbonyls, two other Fe atoms, and a Te atom. According to the structure given from X-ray crystallography this structure has only one kind of iron site. A similar complex $[W(CO)_4Te_3][SbF_6]_2$, contains a three-membered tellurium ring co-ordinated in a pi-fashion to the tungsten carbonyl fragment. This complex consists of the cationic cluster $[W(CO)_4Te_3]^{2+}$ and

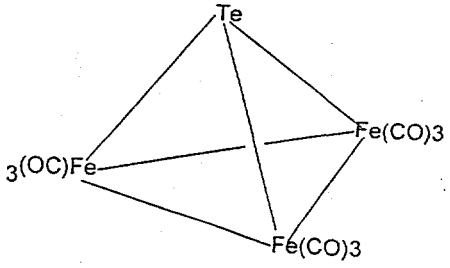


Figure 2: Structure of the tellurium complex IV.

two well separated counterions. The tungsten atom and one tellurium atom lie on a crystallographic mirror plane which bisects the molecule. The W-Te distances are 2.802, 2.802(1), and 2.187Å which are very close to the sum of the metallic radii (Å). The Te-Te distances are similar but not equivalent [2.718(1) and 2.736(1)Å] and not substantially different from those in elemental tellurium (2.74Å) or typical Te-Te single bonds [2.712(2)Å and 2.736(1)Å in PhTe-TePh]. However, they are substantially longer than in Te_4^{2-}, where it is probable that there is some multiple bonding. Because the W-Te and the Te-Te bonds coincidentally have almost the same bond lengths, the complex forms an almost perfect tetrahedron with angles near 60^0 (Te-W-Te 57.9^0 and 60.4^0 Te-Te-Te). This complex has only one tungsten site. All Te atom are in the same environment. Also the carbonyls are in the same environment (Faggiani; Gillespie, et al, 1987). The structure of $[(Ph)_4P]_2[Fe(CO)_6Te]$ has been determined by X-ray crystallography. This complex consist of 2 well separated tetraphenylphosphonium cations and a $[Fe_3(CO)_9Te]^{2-}$ dianion containing a $Fe_3(CO)_9$ fragment capped by a telluride. The Te^{2-} ion donates an electron pair to each $Fe(CO)_3$ fragment and the Te^{2-} ion retains one lone pair of electrons. The Fe-Fe bonds range from 2.612(4)Å to 2.634(4)Å which are considered normal, as are the Te-Fe bonds which range from 2.495(3)Å to 2.501(3)Å. The similarity of the Fe-Fe bonds makes the molecule nearly a perfect tetrahedron, with the Fe-Te-Fe angles averaging to 63.4^0(1), whereas the Fe-Fe-Fe angles average to 60.0^0. Each iron contains three terminal carbonyl ligands, with Fe-C-O angles averaging to 177^0(2) and C-Fe-C angles averaging to 101^0(9). The Fe-C and C-O bond are typical, averaging to 1.75(2)Å and 1.16(3)Å, respectively.(Roof; Smith; et al, unpublished) This complex has only one iron site. The Mössbauer data show 2 isomer shifts of -0.26mm/s and 0.23mm/s. This data suggest that there are two iron sites. One site is a Fe(II) low spin, Fe(III) high spin, or Fe(III) low spin. This site consist of a Fe atom bound to three carbonyls, a tellurium atom and two other Fe atoms. The other site may be an actual iron or an impurity due decomposition. Due to low to signal ratio it was difficult to determine which case was true.

Another tellurium (IV) complex examined in this project was the iron-tellurium complex. This complex (V) has the molecular formula $[Fe_6Te_8(CO)_{18}][AsF_6]_2$. One iron site consist of a Fe atom bound to three carbonyls and three tellurium ligands. This iron site has two more tellurium atoms than the one in the tellurium (IV) complex. The other iron site present in the iron-telluruim complex consists of a Fe atom bound to two carbonyls and three tellurium ligands. These two iron sites are bridged by a Te-Te bond. The Mössbauer data show two isomer shifts and two quadrupole splittings. The isomer shifts have velocities of -0.12mm/s and 0.22mm/s. The quadrupole splittings have velocities of 0.58mm/s and 0.79mm/s. This iron site is a Fe(II) low spin, Fe(III) high spin or Fe(II) low spin. The iron site with a Fe atom bound to three carbonyls and three tellurium atoms is the Fe(II) high spin site.

CONCLUSIONS

Each iron carbonyl complex had a Fe(II) low spin, Fe(III) high spin or Fe(II) low spin site. The iron-tellurium (V), sulfur (I), neutral sulfur (III), and selenium (II) complexes had parameters that were almost identical. The sulfur (I) complex has an iron that had one more sulfur atom than the neutral sulfur (III) iron site. These sites were the Fe(II) low spin, Fe(III) high spin or Fe(III) low spin sites. The second isomer shifts of the sulfur and selenium complexes were higher than the first isomer shifts. This occurs because there is one more carbonyl ligands present in the unique iron site than the two equivalent iron site. There is not a molecule with a greater sigma-donation capability than a carbonyl. As the number of carbonyls increases the isomer shift

Table II. Mössbauer Spectral Data for Various Iron Carbonyl Complexes

Complex name	I.S.(mm/s)	QS(mm/s)	Rel. Int.	Area(mm^2)	Rel. Area
Tellurium(IV)	-0.26	0.45	4	0.48	2
	0.24	0.73	1	0.29	1
Iron-Tellurium(V)	-0.12	0.58	3	0.37	2
	0.22	0.79	1	0.14	1
Sulfur(I)	-0.11	0.58	3	0.64	5
	0.22	0.79	1	0.14	1
	1.3	2.8	1	0.23	2

Table II. Mössbauer Spectral Data for Various Iron Carbonyl Complexes (continued)

Neutral Sulfur(III)	-0.11	0.54	1	0.18	1
Selenium(II)	-0.12	0.59	3	0.77	5
	0.14	1.1	1	0.15	1
	1.3	2.9	1	0.18	2

increases. The carbonyl ligand causes a considerable increase in the isomer shift because of the sigma-donation to the s-electron density of the Fe 4s-orbital is reduced causing the s-electron density to decrease at the iron nucleus (Bancroft, 1973). The quadrupole splittings of the selenium (II) complex are slightly higher than the sulfur (I) complex. The partial quadrupole splitting becomes more positive with metal to ligand bonding. Selenium has 3d-orbitals and the sulfur atom has empty 2d-orbitals. The 3d-orbitals of selenium can overlap the 3d-orbitals of iron. This causes an increase in the partial quadrupole splitting. The tellurium (IV), iron-tellurium (V), sulfur (I) and selenium (II) complexes either had Fe(II) low spin or Fe(III) high or low spin site. There was not a difference between the isomer and quadrupole splittings, so it was difficult to distinguish between the spin states. The X-ray crystallography and Mössbauer data both show there is only one iron site in the neutral sulfur(III) complex. Also, the iron-tellurium (V) has two iron sites and both methods support this. However, they do not agree with respect to the sulfur (I), selenium (II), and tellurium (IV) complexes. The Mössbauer indicates three iron sites and the X-ray crystallography data shows two sites

ACKNOWLEDGEMENTS

Great thanks goes to the National Science Foundation for giving a grant to the Seizing Opportunities for Advancing Research Scholars (SOARS) Program which was developed by the North Carolina Consortium for Undergraduate Research. Special thank goes to Dr. Joseph W. Kolis and Gregory Drake in the Department of Chemistry at Clemson University. The advice and support of Dr. John G. Stevens, Dr. Kathy Whatley, and Mr. Frank Carvadas at the Mössbauer Spectroscopy Data Center at UNC-Asheville are gratefully acknowledged. Also, thanks goes to the North Carolina Central University Undergraduate Research Program for financial support at the National Conference of Undergraduate Research.

REFERENCES

Stevens, John G. and Ruiz, M.J. "Mössbauer Spectroscopy" in *Treatise on Analytical Chemistry*, Second Edition, Vol. 10, pp. 440-448 (1983).

Hoy, Gilbert R. "Mössbauer Spectroscopy" in *Encyclopedia of Physical Science and Technology*, Vol. 10, pp. 469-483 (1992).

Gillespie, Ronald J.; Passmore, Jack; "Polycations of Group VI" *Accounts of Chemical Research*, 4, 413-419 (1971).

Collins M.J.; Gillespie, R.J.; Kolis, J.W.; and Sawyer J.F. "Preparation and Structure of $[W_2(CO)_{10}Se_4][AsF_6]_2$ and Related Compounds" *Inorganic Chemistry*, 25(12), 2057-2061 (1986).

Aime, S.; Milone, L; Rossetti, R.; and Stanghellni, P.L.; "Dynamic Properties and Solution Structures of the Clusters $[Fe_3(CO)_9X_2]$(X= S, Se, Te, or NMe) and their Derivatives" *Journal of the Chemical Society, Dalton Transactions*, 46-51 (1980).

Roof, Lisa C.; Smith, Donna M.; Drake, Gregory W.; Pennington, William T.; Kolis, Joseph W. "Synthesis and Reactivity of $[Fe_3(CO)_9Te]^{2-}$" Clemson University, Clemson, S.C, unpublished results.

Gibb, T.C. and Greenwood, N.N. *Mössbauer Spectroscopy*, pp. 142-155, 162-165 (1984).

Bancroft, G.M. *Mössbauer Spectroscopy, An Introduction for Inorganic Chemists and GeoChemists*. Prentice-Hall, pp. 42-56 (1973).

Faggiani, Romolo; Gillespie, Ronald J.; Campana, Chuck; Kolis, Joseph W. "The Preparation and the Structure of $[W(CO)_4\eta^3\text{-}Te_3][SbF_6]_2$ Containing the First Three-membered Chalcogen Ring", *Journal of the Chemical Society, Chemical Communications*, pp. 485-489 (1987).

SUBSTRATE SPECIFICITY WITH REGARDS TO THE INHIBITORY CHARACTERISTICS OF CARBONIC ANHYDRASE

Joseph M. Wilson

Department of Chemistry
Seattle University
Broadway and Madison
Seattle, WA 98122

Faculty Advisor:
Dr. John Meany

Carbonic anhydrase is a versatile enzyme which catalyzes both the hydration of carbon dioxide and the hydrolysis of several esters. The reversible hydration of carbon dioxide to bicarbonate ion by bovine carbonic anhydrase (BCA) was monitored using a stop-flow spectrometer and also by a pH indicator technique developed in this laboratory. These two methods were shown to give parallel results for both inhibited and uninhibited kinetic runs. The enzymatic hydrolysis of p-nitrophenylacetate by BCA was also followed using standard spectroscopic techniques.

The two enzymatic reactions were studied using a variety of inhibitors including saccharin. The product of the hydrolytic ring opening of saccharin, 2-carboxybenzene-sulfonamide, and its para isomer, 4-carboxybenzenesulfonamide, were also used as inhibitors. Results from these studies suggest that steric factors affect the extent of BCA inhibition. For example, 4-carboxybenzenesulfonamide is approximately ten thousand times more effective as an inhibitor than its ortho isomer or the saccharin. It was further shown that the relative extent of enzyme inhibition is independent of which substrate of BCA is used in the enzymatic assay.

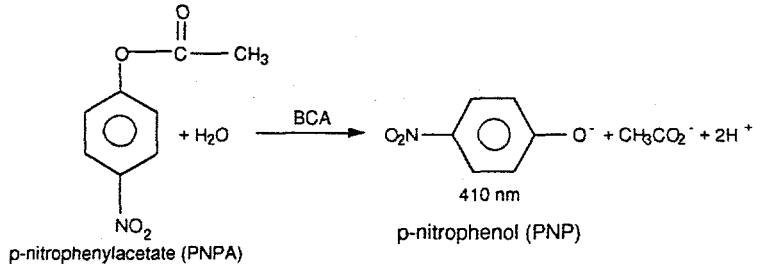
INTRODUCTION

Carbonic Anhydrase is the enzyme responsible for the catalysis of the reversible hydration of carbon dioxide to the bicarbonate ion. This reaction is essential for the transport of metabolically produced carbon dioxide from respiratory tissues (Lehninger, 1993).

$$CO_2 + H_2O \underset{}{\overset{BCA}{\rightleftharpoons}} HCO_3^- + H^+ \qquad (1)$$

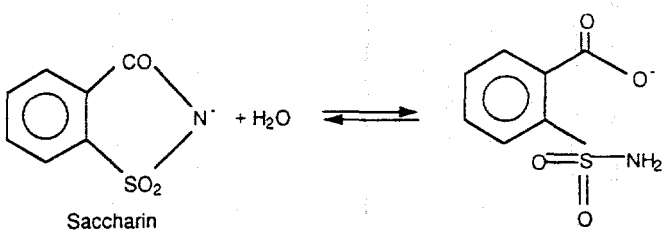
Carbonic Anhydrase is a zinc metallo enzyme which exhibits a rich chemistry. The catalytic site of the enzyme consists of a zinc atom surrounded by three histidine groups. The water molecule which serves as the nucleophile is bound to this zinc atom (Pocker and Meany, 1967). It is probable that inhibition of carbonic anhydrase by sulfonamides involves their binding directly to the zinc ion (Fersht, 1985).

Our earlier studies determined that saccharin is a weak inhibitor of the carbonic anhydrase catalyzed hydrolysis of p-nitrophenylacetate (PNPA). The rate of this reaction was measured using standard spectroscopic techniques (Spiridis et al, 1985).



(2)

Primary sulfonamides are known to powerfully inhibit BCA catalysis (Pocker and Stone, 1967). Thus, after it was found that Saccharin is a weak inhibitor of BCA, it was proposed that the hydrolysis and ring opening of Saccharin to form 2-carboxybenzene-sulfonamide was possibly occurring.



Saccharin

2-carboxybenzenesulfonamide

(3)

To test this hypothesis we studied the BCA inhibitory properties of 2-carboxybenzene-sulfonamide to determine if trace amounts of this compound could account for the observed inhibition.

We also studied the effects of 4-carboxybenzenesulfonamide on BCA to determine what steric factors, if any, would be required to achieve maximum binding of the inhibitor to the catalytic site of the enzyme.

Furthermore, to discover if the nature of carbonic anhydrase was substrate specific, the three inhibitors were also studied using carbon dioxide as the substrate and results were compared to the data obtained with PNPA.

EXPERIMENTAL

All buffers were made at 0.04M. Hepes (N-[2-Hydroxyethyl] piperazine-N'-[2-ethane-sulfonic acid]) buffer was made 6.9 pH for PNPA experiments and carbon dioxide experiments using the stop-flow spectrometer. Further carbon dioxide work was done at 8.2 pH for runs monitored using a variation of the Wilbur-Anderson method (Wilbur and Anderson, 1948).

The spectrometer analysis of the PNPA catalyzed reaction was measured by detecting the increase in absorbance at 410 nm which accompanies product formation. The absorbances of known amounts of PNP were used to create a plot which related absorbance and product concentration.

The uninhibited reaction of PNPA was monitored in the presence and absence of the catalytic carbonic anhydrase and the velocity of the enzyme was calculated.

$$v_{enzyme} = v_{total} - v_{buffer} \qquad (4)$$

Two methods were used to determine the effects of the earlier mentioned inhibitors on the BCA catalyzed hydration of carbon dioxide. Water which had been distilled, degassed, and deionized was saturated with carbon dioxide gas at 30.0°C to produce a substrate solution with a constant and known carbon dioxide concentration (Harned & Davis, 1943). The carbon dioxide hydration reaction could be followed by measuring the change in proton concentration. Both methods incorporated pH color indicators to follow the rate of reaction (PNP for the stop-flow spectrometer and Bromothymol Blue for the Wilbur-Anderson method).

Through the use of a stop-flow spectrometer we were able to follow the reaction for such a short time that the pH change was minimal and its effect on the reaction could be ignored. The enzyme velocity was calculated using the buffer coefficient (Q):

$$Q = \frac{[B]_t K_a^{B}(K_a^{In} + [H_3O^+])^2}{L\Delta\varepsilon[In]_t K_a^{In}(K_a^{B} + [H_3O^+])^2} \qquad (5)$$

Where $[B]_t$ is the total buffer concentration, K_a^B is the K_a value of the buffer, K_a^{In} is the K_a value of the indicator, L is the path length (in centimeters) of the cuvette used, and $\Delta\varepsilon$ is the difference in molar extinction coefficients between the acid and base forms of the indicator (Pocker & Deits, 1982).

Q relates a change in absorbance versus time to a change in proton concentration versus time.

$$v = \frac{d[H^+]}{dt} = \frac{dA}{dt} * Q = \frac{dA}{dt} * \frac{d[H^+]}{dA} \qquad (6)$$

Our modification of the Wilbur-Anderson technique involved following the reaction from an initial pH of 8.2 to a final pH of 6.35 (Wilbur & Anderson, 1948). By following the reaction between a constant beginning and end point, we were able to calculate the specific activity of our enzyme using the equation:

$$V = \frac{10(T_b / T_c) - 1}{\text{mg protein}} \qquad (7)$$

Where V is the reaction velocity, T_b is the rate of the buffer reaction (no BCA), T_c is the time for the enzyme catalyzed reaction, and 'mg protein' is the amount of active protein in the final solution.

By comparing the specific activity achieved for reactions containing varying amounts of an inhibitor with uninhibited rate data, we were able to find the degree of inhibition brought about by specific amounts of each of the inhibitors tested.

Furthermore, by maintaining constant initial pH for all of our runs, it is possible to factor in the effects of pH change on the velocity of the reaction and by doing so achieve a linear initial velocity which corresponds to that obtained with the stop-flow spectrometer.

The reaction was followed using a pH meter, color standards, and with a spectrophotometer (by measuring the maximum absorbance of the protonated pH indicator at 433 nm) and all three techniques were shown to give analogous results.

A series of runs with varying concentrations of the inhibitors were conducted with each of the previously mentioned methods to determine the ratio of inhibitor concentration to enzyme concentration which resulted in a fifty percent reduction in catalytic activity for each inhibitor. This concentration ratio is denoted as the IC_{50} value.

RESULTS

By plotting the ratio of enzyme concentration to inhibitor concentration versus percent activity for each of the three methods, it was shown that the extent of inhibition of carbonic anhydrase is not substrate specific. This implies that it is probable that both the hydration of carbon dioxide and the hydrolysis of PNPA are catalyzed by the same active site on the carbonic anhydrase. Furthermore, it was shown that the stop-flow spectrometer and Wilbur-Anderson methods give parallel results for the inhibition of carbonic anhydrase.

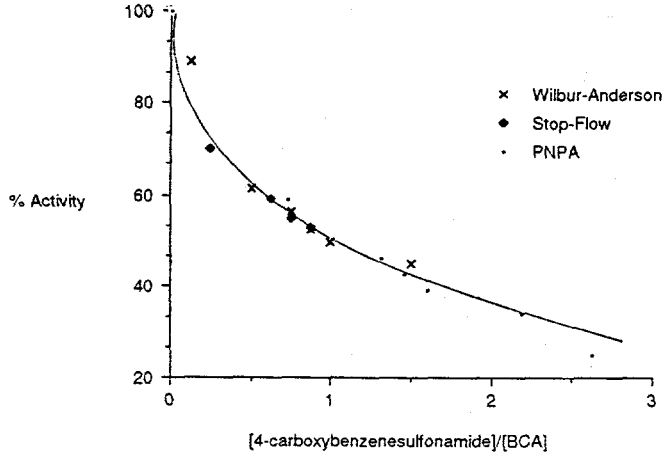


Figure 1: Comparison of the concentration of 4-carboxybenzenesulfonamide versus percent activity for the three experimental methods used.

This study also reflects the strong role molecular structure plays upon the extent of inhibition with regards to carbonic anhydrase. It was found that the 4-carboxybenzene-sulfonamide was approximately 10,000 times more effective as an inhibitor than either its ortho isomer or the saccharin. The method of plotting all data points on the same axis for the different reaction conditions that is described above was incorporated to find the relative effectiveness of each inhibitor tested.

CHART 1: IC_{50} VALUE COMPARISON

Inhibitor	IC_{50}
4-Carboxybenzenesulfonamide	9.9e-1
2-Carboxybenzenesulfonamide	3.0e3
Saccharin	1.1e4

One might expect that the capacity of 2-carboxybenzenesulfonamide to serve as a bidentate ligand would render it a substantially more powerful inhibitor than the Saccharin. However, kinetic data actually demonstrated that 2-carboxybenzenesulfonamide is only a slightly more powerful inhibitor than Saccharin.

Even though 4-carboxybenzenesulfonamide lacks the bidentate ligand structure of its nucleophylic groups which is present in the ortho isomer, its more linear shape makes it a significantly more effective inhibitor for both the PNPA and the carbon dioxide reaction. This shows that steric interactions are greatly responsible for determining the effectiveness of a possible inhibitor.

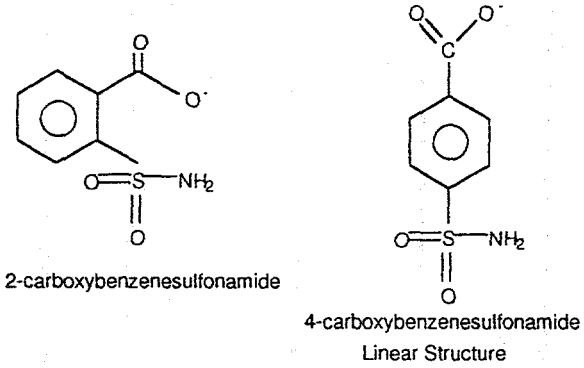


Figure 2: Structure of inhibitor isomers used

Previous studies have shown that sulfonamide drugs are capable of reducing the severity of seizures produced by electroshocks in test animals (Tanimuka *et al*, 1965). Structures where sulfonamide groups were arranged para to other groups on the benzene ring showed much stronger effects than those with the ortho orientation. In the literature, one explanation for the anti epileptic properties of these structures is their ability to inhibit carbonic anhydrase in the brain. The present study is consistent with this proposal by showing that greater carbonic anhydrase inhibition is indeed caused by 4-carboxybenzenesulfonamide in comparison with its ortho isomer.

Earlier studies have been conducted to determine the possible carcenogenic properties of Saccharin in laboratory test animals. Although we find that Saccharin is not a powerful inhibitor of carbonic anhydrase, we note that blood serum levels of Saccharin often exceeded 0.25M in these studies (Daun, 1971). The present study demonstrates that such a concentration would cause approximately fifty percent inhibition of the carbonic anhydrase *in vivo* and would result in extreme respiratory problems for the test animals.

BIBLIOGRAPHY

Daun, R.J. (1971) *J. Ass. Off. Anal. Chem.* 54, 1140-1145.

Fersht, Alan. Enzyme Structure and Mechanism. New York, NY: W. H. Freeman and Company, 1985.

Lehninger, Albert L. Principles of Biochemistry. New York, NY: Worth Publishers, Inc., 1993.

Pocker, Y. and Meany, J.E. (1967) *Biochem.* 6, 239.

Pocker, Y. and Stone, J. T. (1967) *Biochem.* 6, 668.

Spiridis, Greg, Meany, J. E. and Pocker, Y. (1985) *J. Chem. Ed.* 62, 1224.

Tanimuka, H. Inui, M., Hariguchi, S. and Kaneko, Z. (1965) *Biochemical Pharmacology* 14, 961-970.

Wilbur, K. M., & Anderson, N. G. (1948) *J. Biol. Chem.* 178, 147-151.

Thermodynamic Studies of the Enolization of Pyruvic Acid and Pyruvate Anions

Anthony P. Esposito

Department of Chemistry
Seattle University
Broadway and Madison
Seattle, WA 98122

Faculty Advisor:

John E. Meany

The present work describes the positions of equilibrium for the reversible enolization of pyruvic acid and pyruvate anion which have been determined using a spectrophotometric method involving the iodination of the pyruvate system. When equilibrated aqueous solutions of purified pyruvic acid or sodium pyruvate are treated with aqueous triiodide, an initial burst in the decrease of absorbance occurs at 353 nm, which is followed by a slower zero-order decrease due to the production of new enol pyruvate molecules. Thus, the first rapid phase of the spectrophotometric trace represents the reaction of the existing equilibrium concentration of enol pyruvate with triiodide. Equilibrium constants for the enolization of pyruvate have been determined as a function of temperature. The thermodynamic constants ΔG, ΔH, and ΔS have been calculated and are compared with those associated with the reversible hydration of pyruvate.

INTRODUCTION

Pyruvate is one of many carbonyl compounds that exists as an equilibrated mixture of enol, keto, and hydrated forms in aqueous solution (Damitio, Smith, Meany, and Pocker, 1992).

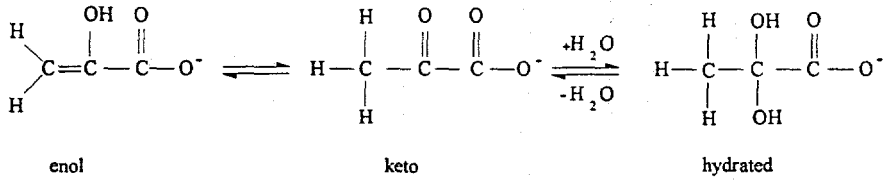


Figure 1: Three Predominant Forms of Pyruvate Anion in Aqueous Solution

Pyruvate is also a molecule inseparably linked to many biochemical processes regulated by enzymes (Lehninger, Nelson, and Cox, 1993). Enzymes perform highly specialized tasks in biological systems, operating on specific compounds while disregarding others. Knowledge of enzyme specificity enables one to identify compounds that may enhance or inhibit the action of certain enzymes. Such information may give clues as to the mechanism of action of the enzyme or may provide new compounds for medicinal purposes.

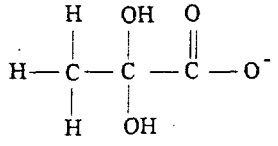
Often enzymes are inhibited by compounds that closely resemble compounds the enzyme prefers as its substrate. A number of oxioreductase enzymes are subject to "substrate" inhibition. Thus two questions arise regarding the enzymatic reactions of such systems: 1) Which structure serves as the substrate? 2)Which structure serves as the inhibitor?

One of the many biochemical fates of pyruvate involving enzymes is the anaerobic regeneration of nicotinamide adenine dinucleotide (NAD^+) from its reduced form (NADH) in the presence of the enzyme lactate dehydrogenase (LDH). The simultaneous reduction of pyruvate to lactate allows for this oxidation to occur (Lehninger et al, 1993).

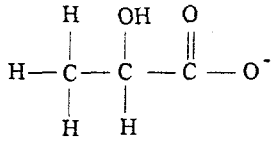
$$\text{pyruvate} + \text{NADH} \xrightleftharpoons{\text{LDH}} \text{lactate} + \text{NAD}^+ \qquad (1)$$

It is known that LDH is subject to "substrate inhibition" at high pyruvate concentrations (Hochachka and Somero, 1973). The keto form of pyruvate serves as the preferential substrate in the reaction involving NADH described above (Tienhaara and Meany, 1973). It has been suggested that both enol pyruvate and hydrated pyruvate serve as the inhibitor of LDH (Damitio et al, 1992). However, it is essential to know the relative concentrations of all three forms of pyruvate present in order to assess the level of inhibition due to either enol or hydrated pyruvate.

Some evidence points to hydrated pyruvate as the principal inhibitor of LDH (Waddington and Meany, 1981). It should be noted that the shape of hydrated pyruvate more closely resembles the shape of lactate than does enol pyruvate.



hydrated pyruvate



lactate

Figure 2: Comparison of Hydrated Pyruvate Anion and Lactate Anion

Lactate serves as the substrate of LDH in the reduction of NAD^+ to NADH (equation (1) above). Since hydrated pyruvate is more structurally and chemically similar to lactate than enol pyruvate, it is reasonable to suggest that it is a more likely inhibitor of LDH.

It is also known that the inhibition of LDH increases greatly as temperatures decrease (Hochachka and Somero, 1973). At the same time, it is known that the fraction of hydrated pyruvate increases as temperatures decrease. Additional research under isothermal conditions has shown that inhibition of LDH at a given temperature depends on the fraction of hydrated pyruvate present (Waddington and Meany, 1981). This is consistent with the hypothesis that hydrated pyruvate causes the LDH inhibition at colder temperatures.

The equilibrium constants of the keto-hydrate equilibrium are accurately known (Waddington and Meany, 1981). However, the fraction of enol pyruvate present at a given temperature is not accurately known. This paper outlines a thermodynamic study of the enolization of pyruvate.

EXPERIMENTAL

The position of equilibrium for the reversible enolization of pyruvic acid and pyruvate anion was determined using a spectrophotometric method that traced the two-step iodination of the pyruvate molecule.

$$CH_3COCO_2^- \underset{\text{slow}}{\rightleftharpoons} CH_2{=}C(OH)CO_2^- \qquad (2)$$

$$CH_2{=}C(OH)CO_2^- + I_3^- \underset{\text{fast}}{\rightleftharpoons} ICH_2COCO_2^- + H^+ + 2I^- \qquad (3)$$

The triiodide ion (I_3^-) absorbs strongly in the near-ultraviolet spectrum, with maximum absorbance at 353 nm. This allows one to track the reaction of enol pyruvate with I_3^-. Kinetic studies at various temperatures were carried out in buffered aqueous solutions of sodium pyruvate and pyruvic acid, prepared from distilled, deionized water. Kinetic runs were monitored by a Shimadzu UV-2101PC scanning spectrophotometer, and temperatures were maintained by a VWR 1160 thermostat bath and circulator.

The methodology used followed earlier work (Damitio et al, 1992). All components used were reagent-grade quality. Pyruvate solutions were prepared right before each set of runs, and sodium pyruvate was buffered at pH = 6.7 with a phosphate buffer. Ionic strength was maintained at $\mu = 0.35$ M, using appropriate quantities of NaCl. Sodium pyruvate was purified of I_3^- scavenging impurities by incubation with 0.100 mL of the I_3^- solution per 3 mL of the pyruvate solution. The pyruvate was allowed at least one hour to reestablish its equilibrium enol concentration.

The purification step is essential in order to achieve valid and reproducible results by this method. It is well known that aldehydic and ketonic compounds, including pyruvate, can combine in dilute acidic or basic solutions in the "aldol condensation." Furthermore, the β-hydroxy ketones that result when pyruvate aldolizes are easily dehydrated to give compounds containing carbon-carbon double bonds (Morrison and Boyd, 1992). These compounds would be suspected to readily take up I_3^-, and join the enol pyruvate in the uptake of I_3^-. Such unsaturated impurities result in the calculation of an invalidly high value of [enol].

To verify this conjecture, two other sets of pyruvate anion runs were conducted. The first set used 0.080 mL of the I_3^- solution for each 3 mL of pyruvate solution, to remove the impurities. The second set was a control group in which the pyruvate was not treated with any I_3^- before being reacted with the final 0.050 mL of I_3^- in the kinetic run. The resultant enolization equilibrium constants (K_{enol}) for these sets of runs are shown in Figure 3.

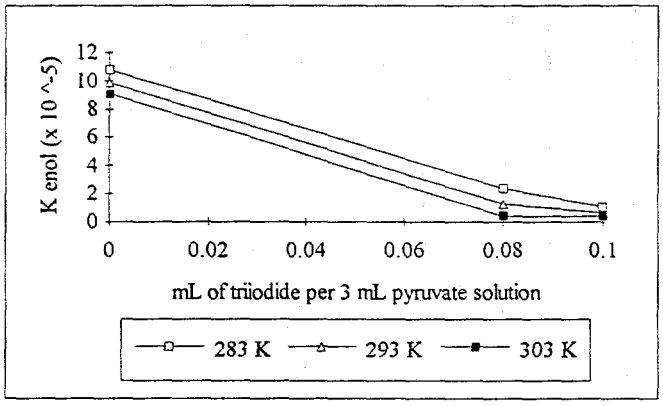


Figure 3: Variation of K_{enol} with Amount of Pretreatment I_3^- and With Absolute Temperature

Figure 3 indicates that the values for K_{enol} are an order of magnitude larger for the unpurified pyruvate than for the purified pyruvate. Preliminary research using volumes from 0.005 mL to 0.112 mL triiodide solution for this "incubation" indicated that 0.100 mL was a sufficient amount to remove all significant I_3^--scavenging impurities. The pyruvate anion values for K_{enol} reported below were obtained using the kinetic runs in which 0.100 mL of the I_3^- solution for each 3 mL of pyruvate solution was used to remove iodine-scavenging impurities.

After removal of the impurities, reactions were initiated by injecting 0.050 mL of a solution of 2.0×10^{-3} M I_2 and 1.0 M KI into the cuvette containing 3 mL of 0.10 M sodium pyruvate. The contents of the cuvette were mixed rapidly using a stirring paddle attached to the needle tip of the syringe used to inject the iodine solution.

As described above, the first few seconds of the spectrophotometric trace shows a rapid first order decay--the burst phase. Since this corresponds to the time of mixing of the components and closing of the compartment lid, it is difficult to extrapolate back to the start of the reaction for the initial absorbance, or A_0. However, since this A_0 value is due to the amount of I_3^- present at time t = 0 seconds, these conditions were exactly simulated in the absence of pyruvate. The A_0 values at various temperatures were obtained by injecting 0.050 mL of the same I_3^- solution into 3 mL of a solution with a composition closely resembling the incubated pyruvate solutions used. The same ionic strength, 0.35 M, was maintained by using the same phosphate buffer, NaCl, and KI concentrations; sodium acetate was used to simulate sodium pyruvate.

The equilibrium constant for the keto-enol equilibrium is defined as

$$K_{enol} = [enol] / [keto] \qquad (4)$$

where [enol] is the enol pyruvate concentration and [keto] is the keto pyruvate concentration at a given pH and temperature. Values for [keto] were calculated by subtracting the concentration of hydrated pyruvate from the total concentration of pyruvate (Waddington and Meany, 1981). Since [enol] is known to be very small (Damitio et al, 1992), it is not needed to calculate [keto].

Values for [enol] were calculated from the kinetic data, using the Lambert-Beer law,

$$A = \varepsilon bc \qquad (5)$$

where A is absorbance, ε is the extinction coefficient ($M^{-1}\,cm^{-1}$), b is the cell path length (cm) and c is the concentration of the absorbing species (M). The cuvettes used were of 1 cm path length. Average extinction coefficients were calculated at each temperature from the observed absorbance values and the calculated concentration of I_3^- (Hegazi, 1971). As noted above, the burst portion of the spectrophotometric trace is a rapid first-order decay, due to the reaction of I_3^- with the existing enol concentration. Figure 4 below is an example of a typical spectrophotometric trace obtained.

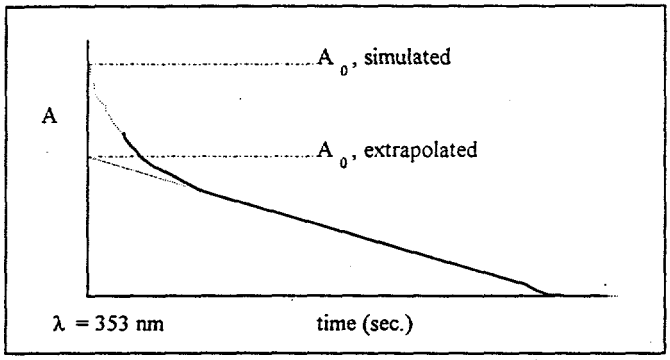


Figure 4: A Generalized Spectrophotometric Trace For The Iodination of Pyruvate

The value for A_0 of this portion ($A_{0,simulated}$) was obtained by the simulated pyruvate runs. The subsequent pseudo-zero order decay that followed this "burst" region is due to the loss of I_3^- to newly generated enol molecules. By extrapolating along this linear portion of the trace back to t = 0 sec., one obtains the absorbance due to the I_3^- not taken up in the burst region ($A_{0,extrapolated}$). The difference between $A_{0,simulated}$ and $A_{0,extrapolated}$ is the absorbance due to the I_3^- taken up by the equilibrium enol concentration. This concentration was determined as follows:

$$[enol] = (A_{0,simulated} - A_{0,extrapolated}) / \varepsilon \qquad (6)$$

RESULTS AND DISCUSSION

Values for the equilibrium constant, K_{enol}, have been calculated for various temperatures, and appear in Table 1 below.

Table 1: Keto-Enol Equilibrium Constants in Aqueous Solution

substrate	pH	temperature (°C)	K_{enol} (x 10^{-5})
pyruvic acid	1.2	25	6.4
pyruvate anion	6.7	10	1.04
pyruvate anion	6.7	20	0.613
pyruvate anion	6.7	30	0.394

Values for the K_{enol}, at 25 °C and pH near 7, have been previously reported as high as 6.54 x 10^{-3} (Chiang, Kresge, and Pruszynski, 1992), to as low as 8.2 x 10^{-6} (Damitio et al, 1992). The present data allow for a calculated value for K_{enol}, at 25 °C, of 5.17 x 10^{-6}. This is fairly consistent with the results of Damitio (1992), in which the equilibrium constant was approximated from the ratio of rate constants for enolization and ketonization respectively: $K_{enol} = k_{enol}/k_{keto}$. It is probable that the earlier literature values of K_{enol} are due to a disparity in the extent to which the pyruvate is purified before analysis.

The respective thermodynamic parameters ΔG, ΔH, and ΔS, for the enolization of keto pyruvate can be obtained using the equilibrium constants in Table 1. These parameters

appear in Table 2. The same parameters for the hydration of keto pyruvate appear as well, for the sake of comparison. These were obtained from the keto-hydrate equilibrium constants of previous work (Waddington and Meany, 1981).

Table 2: Thermodynamic Parameters for The Enolization and Hydration of Keto Pyruvate in Aqueous Solution, at 25 °C

reaction	ΔG (kJ mol^{-1})	ΔH (kJ mol^{-1})	ΔS (J K^{-1} mol^{-1})
enolization	+31.0	-27.6	-197
hydration	+7.05	-35.6	-143

These results indicate that, like the hydration, the enolization of pyruvate is an exothermic process. These results also indicate that the relative amount of enol pyruvate is small from 10 °C to 30 °C. Table 3 summarizes the relative amounts of each of the three types of pyruvate present.

Table 3: Fractions of the Three Forms of Pyruvate in Aqueous Solution

		fractions present		
pH	temperature (° C)	enol (x 10^{-5})	keto	hydrated
1.2 (pyruvic acid)	25	2.4	0.37	0.73
6.7 (pyruvate anion)	10	0.93	0.89	0.11
6.7 (pyruvate anion)	20	0.59	0.93	0.07
6.7 (pyruvate anion)	30	0.38	0.96	0.04

These results show that the amount of enol pyruvate present relative to either keto or hydrated pyruvate is 1 part in 10,000. Furthermore, as physiological pyruvate concentrations tend to be as low as 10^{-4} M, the concentration of enol present in biological systems can be as low as 10^{-8} M. By extrapolating from the thermodynamic data in table 1, the value obtained for K_{enol} at 37 °C, the body temperature of most warm-blooded animals, is 3.73×10^{-6}. This predicts an exceedingly small enol pyruvate concentration within the bodies of these organisms. These data are consistent with the argument that enol pyruvate is not a significant inhibitor in the LDH-NADH metabolic pathway.

REFERENCES

Chiang, Y., Kresge, A. J., and Pruszynski, P. Keto-Enol Equilibria in the Pyruvic Acid System: Determination of the Keto-Enol Equilibrium Constants of Pyruvic Acid and Pyruvate Anion and the Acidity Constant of Pyruvate Enol in Aqueous Solution. Journal of the American Chemical Society, 1992. vol. 114, pp. 3103-3107.

Damitio, J.; Smith, G.; Meany, J. E.; and Pocker, Y. A Comparative Study of the Enolization of Pyruvate and the Reversible Dehydration of Pyruvate Hydrate. Journal of the American Chemical Society, 1992. vol. 114, pp. 3081-3087..

Hegazi, Mohamed M. Fahmi. A Kinetic Analysis of the Iodination of Pyruvic Acid and Pyruvate Esters. pp. 24. master's thesis, Central Washington State College, 1971.

Hochachka, Peter W. and Somero, George N. Strategies of Biochemical Adaptation. pp. 58-59. Philadelphia: W. B. Saunders Co., 1973.

Lehninger, Albert L., Nelson, David L., and Cox, Michael M. Principles of Biochemistry, 2nd ed. pp. 413-419. New York: Worth Publishers, 1993.

Morrison, Robert Thornton and Boyd, Robert Neilson. Organic Chemistry, 6th ed. pp. 804-808. Englewood Cliffs, NJ: Prentice Hall. 1992.

Tienhaara, R. and Meany, J. E. The Lactate Dehydrogenase Catalyzed Reduction of Pyruvate. Active Substrate and Substrate Inhibition. Biochemistry, 1973. vol. 12, pp. 2067-2070.

Waddington, M. D. and Meany, J. E. The Inhibition of Lactate Dehydrogenase by Hydrated Pyruvate. Archives of Biochemistry and Biophysics, vol. 211, no. 1, Oct.1, 1981, pp. 447-453.

Large Zeolite Crystals: Environmental Applications and Heavy Metal Recovery

Richard O. Mikula

Department of Chemistry
Southern Oregon State College
1250 Siskiyou Boulevard
Ashland, Oregon 97520

Faculty Advisor:
Dr. Patricia Enzel

INTRODUCTION

There is a growing awareness of the necessity for finding methods to ensure the purity of water destined for human consumption. In addition, it is imperative to reduce the environmental degradation caused by the release of heavy metals into wastewater streams. Our studies provide basic data exploring the feasibility for the potential use of large zeolite crystals to extract these contaminants from water supplies via an ion-exchange process for heavy metals.

Zeolite crystals are aluminosilicate frameworks of uniform pore size, orientation and structure[1]. Zeolite crystals are naturally occurring minerals, and have been synthesized by chemists for decades[2]. The typical size of synthetic zeolite crystals has been in the order of one μm. Only as recently as the past several years, the synthesis of crystals in the order of 500 μm has been achieved, hence the name "large" zeolite crystals[3]. Large zeolite crystals must be investigated to compare their properties to those of smaller synthetic zeolites. The extended process of large crystal synthesis could introduce the possibility of defects in the crystal structure. These defects may block the access of ion-exchange solutions to the active sites contained within the crystal. Basic studies must be undertaken to determine the feasibility of industrial applications of large zeolite crystals. Uses in environmental monitoring are possible due to the inherent properties of the crystals for particular applications. Among these applications are ion-exchange, solid-acid catalysts, molecular sieves, and molecular sensors. Of particular interest is their capacity for ion-exchange of heavy metals (e.g., lead, cesium, strontium) to remove these contaminants from wastewaters.

There are many specific zeolite crystals, differing from one another by virtue of their framework, morphology and inclusion of various elements. Our study will focus exclusively on large crystals of aluminum-ferrierite, due to its potential for use in ion-exchange and other environmental applications[2].

SYNTHESIS OF ALUMINUM FERRIERITE CRYSTALS

The synthesis of large aluminum-ferrierite crystals was run at a temperature of 165° C for 14 days, under autogenous (high pressure) organothermal conditions. It was necessary to modify the literature procedure[3] due to environmental conditions at higher altitudes. Ashland, Oregon is located at about 2000 feet above sea level, thereby requiring adjustments in time and temperature that would be best suited to these local conditions. At higher altitudes, liquids boil at a lower temperature, thereby requiring a longer time to bring the reaction to completion. The synthesis was conducted in a Teflon lined, stainless steel reaction vessel that was sealed and left at constant temperature for the duration of the synthesis.

The use of an organic solvent, pyridine, enabled the rate of crystallization to be slower than a synthesis conducted in aqueous solution. The sources of aluminum and silica are highly soluble in aqueous solution. Therefore, the crystals being formed are in a dynamic equilibrium with those being redissolved into solution. Pyridine retards this tendency to return to solution, thereby encouraging the

crystallization to proceed at a slow rate. The size of the crystals can then be increased to the order of 500 μm.

The reaction mixture used in our synthesis was:[3]

reagent	molar ratio
• Pyridine	16.0
• HF/triethyl amine	2.0
• Alumina	0.18
• Fumed silica - "Cabosil"	2.0
• Propylamine	2.0
• reagent amounts of H_20	6.0
• Tetrapropylammonium-Bromide	0.5

WASHING AND CALCINATION OF CRYSTALS

After the required period for synthesis, the crystals were removed from the synthesis vessel and thoroughly washed. The washing process is necessary to remove any amorphous material from the crystal surface that exists as a residue from the synthesis. This amorphous material and other surface contaminants must be removed so that there is no blockage of the crystal pore openings prior to calcination. Any residue that would create a pore blockage would be responsible for the incomplete calcination of the organic template. In addition, the solution containing the cations available for ion-exchange will be unable to penetrate the blocked pore in order to reach the active sites within the crystal lattice. The crystals were washed with a 0.1 M HCl / methanol solution under mild agitation. It was necessary to try several different concentrations in the wash solution, and the effect of agitation was significant. Mild agitation was necessary because synthetic aluminum-ferrierite crystals are quite fragile. The crystals are easily shattered under excessive agitation during the wash phase.

After the washing process was completed, the crystals were ready for calcination. The zeolite crystal begins its growth at a nucleation point that is encouraged by the presence of organic molecules[1]. The crystal forms around these organic templates, thereby locking the organic template inside the crystal structure. In order to conduct ion-exchange within the crystals, the organic template needs to be removed from the zeolite. This is done through calcination. Calcination of aluminum-ferrierite is accomplished at 550° C. A constant flow of oxygen gas is necessary to facilitate oxidation and removal of the organic template.

ION-EXCHANGE

One of the most useful properties of zeolites is their ion-exchange capacity. The ion-exchange[4] capability of aluminum-ferrierite is possible due to the substitution of aluminum atoms in the framework of the silicate crystal lattice[5]. Silicon has a tetrahedral configuration, like carbon, and therefore has a tetravalent electronic structure. Aluminum, however, is trivalent and the substitution of aluminum for silicon creates a net negative ionic charge at the aluminum site[5] which must be balanced by positive counterions. This negative charge must be neutralized. Initially, this neutralization is satisfied by the inclusion, in the crystal pores, of a protonated organic template. The organic is subsequently removed through calcination, which restores the need to balance the net negative charge in the crystal lattice with another countercation. The cation is probably H^+, NH_4^+, or another residual fragment from the organic template. This residual organic can now be exchanged for another cation such as sodium. This was, in fact, the first ion-exchange that was initiated. After the successful exchange for Na^+, it was shown that we could substitute Pb^{2+} and Cs^+ in place of Na^+ (Figure 1). This was the result we had anticipated, proving the potential for ion-exchange of heavy metals in the large zeolite crystal.

$R_3Al_3Si_{33}O_{72}$
Aluminum-Ferrierite, (washed and calcined)
↓
ion-exchange with $Na^+(aq)$
↓
$Na_3Al_3Si_{33}O_{72}$ + 3 $R^+(aq)$
↓
ion-exchange with $Pb^{2+}(aq)$
↓
$Pb_{1.5}Al_3Si_{33}O_{72}$+ 3 $Na^+(aq)$

Figure 1: ION-EXCHANGE

CHARACTERIZATION OF CRYSTALS

Characterization of the aluminum-ferrierite crystals was conducted by the following techniques: IR spectroscopy (IR), powder X-Ray Diffraction (XRD), Scanning Electron Microscopy (SEM), and Energy Dispersive X-Rays (EDX). The use of IR provided evidence that the organic template was removed through calcination (Figure 2). XRD showed that the structure of the crystal was still intact after the calcination process. SEM indicated that our crystals were uniform in morphology and size, in the order of 500 μm. X-Ray mapping registered uniform distribution of aluminum in the crystal lattice, and subsequent uniform distribution of cations through the ion-exchange procedures. EDX provided a gross quantitative analysis of the relative amounts of cations in the crystal lattice, after ion-exchange (Figure 3). As a result of the findings from these characterization techniques, the feasibility for advanced applications of large zeolites is quite promising.

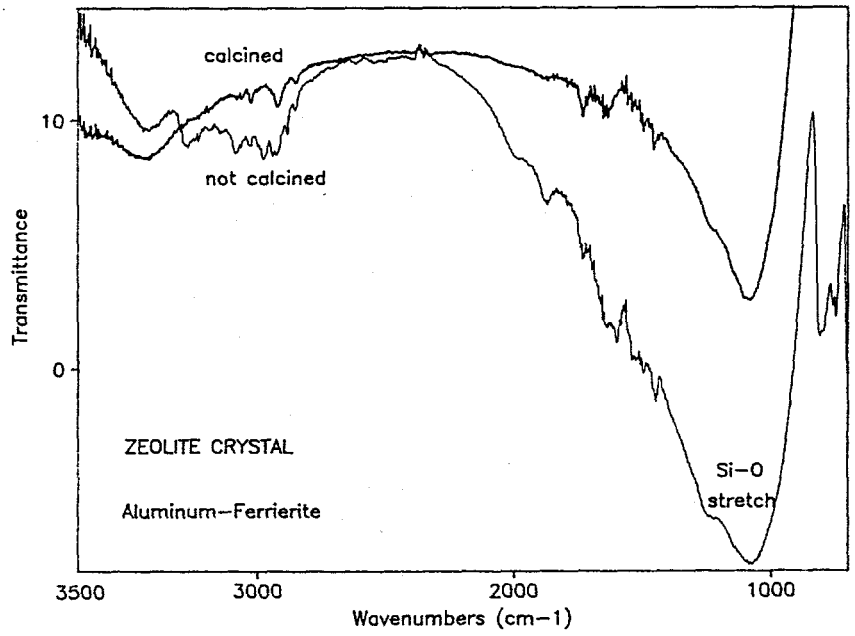


Figure 2: IR spectra indicating removal of organic template through calcination

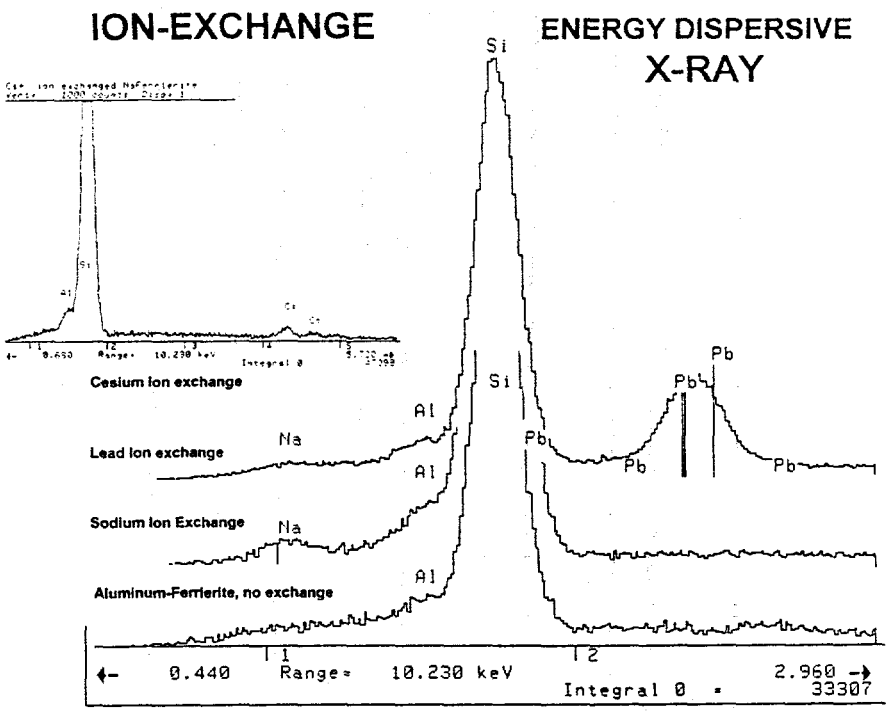


Figure 3: Energy Dispersive X-Rays, indicating the successful ion-exchange in the aluminum-ferrierite crystal lattice

CONCLUSIONS AND FURTHER STUDIES

We have proven that the property of ion-exchange that is present in small synthetic zeolite crystals of aluminum-ferrierite is also present in large crystals. This finding will enable chemists to explore the potential uses of large zeolites in all applications that have proven useful with small crystals. Further studies will focus on the reversibility of the ion-exchange process. This will be essential if the use of large zeolite crystals is to be economically feasible. After establishing the reversibility of the ion-exchange process, it will be important to conduct quantitative studies to determine the amount of heavy metals that can be recovered through the use of a certain amount of zeolite crystals. Our preliminary results are encouraging, and it remains to be seen whether or not this technology can be applied to the ever increasing need to provide clean water for the inhabitants of our planet.

REFERENCES

1-Dyer, A. (1988). An introduction to zeolite molecular sieves. New York: John Wiley and Sons.
2-Barrer, R. (1981). Zeolites and their synthesis. Zeolites, 1(3), 161-172.
3-Kuperman, A., Nadimi, S., Oliver, S., Ozin, G., Garces, J., & Olken, M. (1993, September 16). Non-aqueous synthesis of giant crystals of zeolites and molecular sieves. Nature, 365, 239-242.
4-Loizidou, M., & Townsend, R. (1987). Ion-exchange properties of natural clinoptilolite, ferrierite and mordenite: Part 2. Lead-sodium and lead-ammonium equilibria. Zeolites, 7, (2), 153-159.
5-Davis, M., & Lobo, R. (1992). Zeolite and molecular sieve synthesis. Chemical Materials, 4, 756-768.

EVALUATION OF SOIL-WASHING PROCESS FOR "UNWASHABLE" CLAYS AND SILTS FROM THE PALMERTON ZINC SITE

Brian M. Snyder

Department of Chemical Engineering and
Department of Civil & Environmental Engineering
Lafayette College - Easton, PA 18042

Faculty Advisors: Dr. Mary J.S. Roth and Dr. Ronald M. Dennis

INTRODUCTION

Many former and active mineral processing operations have resulted in areas of contaminated soil throughout the United States. The residues from these operations generally contain high concentrations of heavy metals and soils contaminated with these residues are considered toxic. If these metals are not removed from the soil, they can migrate away from the site and contaminate nearby surface water and groundwater.

The Palmerton Zinc Superfund Site in Palmerton, PA, is over 2,000 acres in size and was used to deposit residue from the production of zinc. Nearby wells and soils in residential areas of Palmerton have been found to be contaminated with zinc and cadmium. A preliminary analysis of soil and dust sampling conducted in May 1991 (CDM Federal Programs Corporation, 1991) has revealed that dust from the contaminated soils poses a potential threat to human health.

In a previous study (Tunnell et al., 1993), soils from Palmerton residential properties were evaluated using various soil classification tests. The results of these tests showed that the percentage of silt and clay varied from 42 to 74% by weight. Soils containing more than 30 to 50% of silt and clay are usually considered unsuitable for remediation using soil washing. In addition, the particle size distribution curves of the soils sampled were partially within the "difficult soil washing regime" as defined by the United States Environmental Protection Agency (U.S. Environmental Protection Agency, 1990). Therefore, based on the results of the previous study, it was concluded that soil washing is not likely to be a viable method to treat the soil and dust contamination in Palmerton.

Since the completion of the previously described study, Dr. Harry Parker at Texas Tech University has developed a soil washing process for "unwashable" clays and silts and called it the clay and silt washing(C&SW) process. It is claimed that this process effectively and economically scrubs contaminants from previously "unwashable" soils. According to Dr. Parker, its novel source of mechanical energy is far more effective than many conventional soil washing processes.

The C&SW process has been able to remove petroleum, diesel fuel, and unknown tars from a variety of soils containing large amounts of clay and silts to below 100 ppm total hydrocarbons (Parker, 1993). More recently, washing of pentachlorophenol from clays and silts has been demonstrated. These results will be presented at the Hazardous Waste Management VI meeting this September in Atlanta. Patent claims have now been allowed on the C&SW process. This paper will present the results of the application of Dr. Parker's C&SW process on residential soils contaminated with heavy metals from the Palmerton Zinc Site.

FIELD SAMPLING

Dr. Parker wanted to obtain at least two different soil samples from the Palmerton Zinc Site, one with high concentrations and the other with low concentrations of heavy metals. To determine representative sites for these samples, the Palmerton Zinc Pile Site Trip Report (CDM Federal Programs Corporation, 1991) and the Palmerton Zinc Off-Site Study Area Draft of Remedial Investigation and Risk Assessment (R.E. Wright Associates, Inc., 1988) were used. Three sites were selected based on the soil sample data for Palmerton residences contained in these reports.

Soil samples were collected from all sites during January, 1994. At each site, about 6 inches of snow were first removed from the surface of the soil. Soil samples were then collected using a shovel, spoon, and/or post-hole digger and were placed in stainless steel trays. The trays were covered with aluminum foil and brought to room temperature overnight. After the soils had thawed, the soils from each site were

thoroughly mixed, divided into either 3 or 4 equal portions, and placed in one-liter polyethylene jars. These jars were then stored at 4°C.

LABRATORY ANALYSES

The two most important soil parameters to be evaluated during the prescreening activities for soil washing treatability testing are the particle size distribution and clay content. Soil washing performance is closely tied to these parameters. Early characterization of these parameters and their variability throughout the site provides valuable information for the initial screening of soil washing as an alternative treatment technology.

Soils with relatively large percentages of sand and gravel respond better to soil washing than soils with small percentages of sand and gravel. Larger percentages of clay and silt reduce contaminant removal efficiency. In general, soil washing is most appropriate for soils that contain at least 50 percent sand/gravel. Soils rich in clay and silt normally tend to be poor candidates for soil washing. To determine the particle size distribution and clay content of the soil samples, ASTM D 422-63, Standard Method for Particle-Size Analysis of Soils, was used.

Moisture content and pH are two other soil parameters to be evaluated during prescreening activities for soil washing treatability testing. Moisture content affects pretreatment and transfer requirements, and pH may affect pretreatment requirements, compatibility with the processing equipment, and wash fluid compatibility. The appropriate ASTM and EPA methods were used.

BENCH-SCALE TESTING

For each site, two one-liter soil samples were sent from Lafayette College to Texas Tech University for bench-scale testing in Dr. Parker's soil washing process for "unwashable" clays and silts. The effectiveness of this process will be determined by a comparison of the heavy metals analysis of each sample before and after it is washed. To date, only samples from Site #1 have been used in Dr. Parker's process. The remaining samples may be used in this process in the near future.

Before any soil was washed using Dr. Parker's method, unwashed soil samples were analyzed for arsenic, cadmium, lead, and zinc. Samples were analyzed by Lubbock Christian University's Institute of Water Research, Lafayette College, and Benchmark Analytics in Hellertown, PA.

In Dr. Parker's soil washing process for "unwashable" silts and clays, water is added to the contaminated soil to make a slurry. A small amount of potassium carbonate is added to the soil to make it electrically conductive. The slurry is then sheared in a high speed mixer to make a homogeneous suspension. The soil slurry is then transferred to the Electrode Assisted Soil Washing(EASW) unit for treatment.

The novel design of the EASW cell facilitates an intense scrubbing of the contaminated soil particles. This action transfers the contaminants to the liquid phase of the soil-water slurry. The slurry is then fed to a centrifuge that separates the bulk of the water carrying the contaminants from the suspended solids. The treated soil is then reslurried with clean, recycled water in subsequent wash stages until the desired degree of decontamination is achieved.

The EASW process produces a clean, wet soil and a treatable wash-waste-water carrying the original soil contaminants. Even though the EASW process can be operated both as a batch and as a continuous process, it was operated as a batch process for bench-scale testing.

The sample from Site #1 was divided into four smaller samples. The first soil sample washed in the EASW process was slurried with water. The second soil sample washed in the EASW process had 15,000 ppm of crude oil added to it and the third sample had 15,000 ppm of vegetable oil added to it. The last soil sample washed in the EASW process had 150,000 ppm of vegetable oil added to it. This ten fold increase in vegetable oil gave a more distinct oil layer that could be analyzed and used to close the mass balance of heavy metals. In addition, the last soil sample substituted sodium acetate for potassium carbonate in the soil slurry.

All four washed soil samples were analyzed by Lubbock Christian University's Institute of Water Research for arsenic, cadmium, lead, and zinc. However, only one washed soil sample was analyzed by Benchmark Analytics for these heavy metals.

RESULTS

The particle size distributions for each site are shown in figure 1. These curves are compared with two of the three simplistic particle size distribution curves given in figure 2 that illustrate a general screening definition for soil washing technology(U.S. Environmental Protection Agency, 1991).

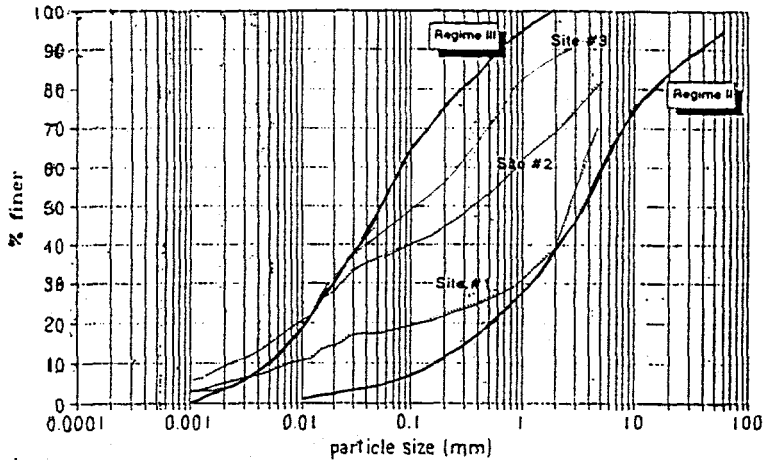


FIGURE 1. PARTICLE SIZE DISTRIBUTIONS FOR SITES 1, 2 & 3.

The results of the laboratory chemical analyses of unwashed soils are shown in Table 1. In this table, the soil samples from Site #1 had arsenic concentrations ranging from non-detectable to 24 ppm, cadmium concentrations ranging from 4 to 11 ppm, lead concentrations ranging from 28 to 115 ppm, and zinc concentrations ranging from 655 to 1,171 ppm. These concentration ranges were lower than the ones for the soil samples from Sites #2 and #3.

TABLE 1. RESULTS OF LABORATORY CHEMICAL ANALYSES OF UNWASHED SOILS

Site #	Sample No.	Arsenic (ppm)	Cadmium (ppm)	Lead (ppm)	Zinc (ppm)
1	1A[a]	24	11	115	960
	1C	ND[b]	4	28	
	1CT[c]				1,171
	1C-BA[d]	8.2	5.4	85	655
2	2C-1	ND[b]	29	170	
	2C-2	ND[b]	32	248	
	2CT[c]				3,843
	2C-BA[d]	13	24.6	134	2,330
3	3C-1	ND[b]	43	383	
	3C-2	ND[b]	37	393	
	3CT-D1[e]				2,024
	3CT-D2[e]				2,602
	3C-BA[d]	19	43.4	364	2,160

a Analysis performed by Lubbock Christian University's Institute of Water Research.
b Non-detectable
c Zinc Analysis required a separate acid digestion using trace metal nitric and hydrochloric acids.
d Analysis performed by Benchmark Analytics.
e Zinc analysis required a separate acid digestion using trace metal nitric and hydrochloric acids and two different dilutions.

For the most part, the chemical analyses summarized in Table 2 were performed by Lafayette College using acid digestion followed by analysis of the diluted extract using FLAA. However, the chemical analyses noted as being performed by either Lubbock Christian University's Institute of Water Research or by Benchmark Analytics utilized acid digestion followed by analysis of the extract using ICP.

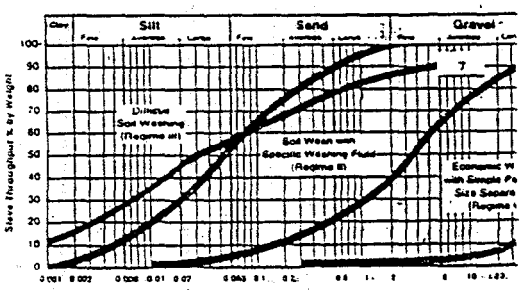


FIGURE 2. SOIL WASHING REGIMES

The results of the bench-scale testing with the EASW process show that, for the most part, the addition of either crude oil or vegetable oil did improve the removal of the heavy metals from the soil versus just washing with water alone. However, the removal efficiencies given in Table 2 are 55% or less except for arsenic removal with crude oil, which is greater than 79%. These removal efficiencies were calculated from the results of either Lubbock Christian University's Institute of Water Research's chemical analyses of unwashed and washed soils or Benchmark Analytics'.

TABLE 2. EASW PROCESS CONTAMINANT REMOVAL EFFICIENCIES - SAMPLES FROM SITE #1

Washed Soil	Arsenic (%)	Cadmium (%)	Lead (%)	Zinc (%)
Slurry with Water	25	18	6	13
Crude Oil @ 15,000 ppm	>79	45	35	34
Vegetable Oil @ 15,000 ppm	0	36	39	36
Vegetable Oil @ 150,000 ppm + Sodium Acetate	50	51	37	49
	55[a]	26[a]	38[a]	29[a]

a Removal efficiencies based on analysis performed by Benchmark Analytics.

DISCUSSION

The particle size distribution for all three samples showed that the percentage of silt and clay varied from 18 to 47% by weight. A high percentage of silt and clay (e.g., more than 30 to 50 percent) in the soil usually indicates that soil washing will be unfavorable due to the amount of time and money required to treat the contaminated soil (U.S. Environmental Protection Agency, 1991). Larger percentages of silt and clay also reduce contaminant removal efficiency. In general, soil washing is most appropriate for soils that contain at least 50% sand/gravel, e.g., coastal sandy soils and coarse-grained glacial deposits. Furthermore, the applicability of soil washing for silty/clay soils containing inorganic nonvolatile metals is moderate to marginal (U.S. Environmental Protection Agency, 1990). This is because metal species may be tightly bound and difficult to dislodge from clay-rich soils (U.S. Environmental Protection Agency, 1992).

The particle size distribution curves for each site fall within Regimes II and III as defined in Figure 2. Generally speaking, most contaminated soils will have a distribution that falls within Regime II. The types of contaminants found in the matrix will govern the composition of the washing fluid and the overall efficiency of the soil washing process. In Regime III, soils consisting largely of finer sand, silt, and clay fractions, and those with high humic content, tend to contain strongly adsorbed organics that generally do not respond favorably to systems that work by only dissolving or suspending contaminants in the wash solution. However, they may respond to soil washing systems that also incorporate a particle size separation step whereby contaminants can be concentrated into a smaller volume (U.S. Environmental Protection Agency, 1990).

Based on Table 1, it appears that soils from Site #1 would be more amenable to

soil washing with the appropriate washing fluid than those from Sites #2 and 3. However, except for arsenic removal with crude oil at 15,000 ppm, the results of the bench-scale testing of this sample were not very promising. The maximum removal efficiencies shown in Figure 4 for cadmium, lead, and zinc were 51%, 39%, and 49%, respectively. These efficiencies are low when compared to the 70% to greater than 90% removal efficiencies reported by the U.S. Environmental Protection Agency for heavy metals in pilot- and full-scale soil washing processes (U.S. Environmental Protection Agency, 1990).

Nevertheless, the criteria for contaminated soil cleanup is usually based on soil quality criteria concentrations on a case-by-case basis rather than removal efficiencies. For example, the Ontario Ministry of the Environment's (MOE's) cleanup guidelines for soils for residential/parkland use are 25 ppm, 4 ppm, 500 ppm, and 800 ppm for arsenic, cadmium, lead, and zinc, respectively (Fitchko, 1989). With respect to the sample from Site #1, the maximum arsenic and lead concentrations in the unwashed soil are already either near or below MOE's soil quality criteria concentrations for these heavy metals. On the other hand, the maximum cadmium and zinc concentrations in Site #1's unwashed soil are slightly above MOE's soil quality criteria concentrations for these metals and removal efficiencies around 50% may be all that is needed to meet these concentrations.

Therefore, the residential soils contaminated with heavy metals from the Palmerton Zinc Site may be good candidates for Dr. Parker's soil washing process for "unwashable" clays and silts. However, additional bench-scale testing of the remaining samples, which have higher levels of heavy metals, should be performed to further verify this.

CONCLUSION

Dr. Harry Parker's soil washing process for "unwashable" clays and silts was evaluated using residential soil contaminated with heavy metals from the Palmerton Zinc Site in Palmerton, PA. The results of this evaluation showed maximum removal efficiencies of >79%, 51%, 39%, and 49% for arsenic, cadmium, lead, and zinc, respectively, for soil containing 18% of silt and clay by weight. Based on these results, Dr. Parker's soil washing process for "unwashable" clays and silts may be a viable method to treat the soil and dust contamination in Palmerton depending on the soil quality criteria concentrations selected for site cleanup.

LITERATURE CITED

CDM Federal Programs Corporation. Palmerton Zinc Pile Site Trip Report; CDM Federal

Fitchko, J. Criteria for Contaminated Soil/Sediment Cleanup; Pudvan Publishing Company: Northbrook, IL, 1989.

Parker, H.W. "Soil Washing Process for 'Unwashable' Clays and Silts," Waste Stream Minimization and Utilization Technology Fair, Inventions and Technology Division of DOE, Austin, TX, April 22-23, 1993.

R.E. Wright Associates, Inc. Palmerton Zinc Off-Site Study Area Draft of Remedial Investigation and Risk Assessment, REWAI Project 8498; R.E. Wright Associates, Inc.: Middletown, PA, January 27, 1988.

Tunnell, D.M., Dennis, R.M., and Roth, M.J.S., "Soil Washing Evaluation Program for Palmerton Zinc Site," Presented at Emerging Technologies in Hazardous Waste Management V, Atlanta, GA, September 27, 1993.

U.S. Environmental Protection Agency. Engineering Bulletin of Soil Washing Treatment; U.S. Environmental Protection Agency: Cincinnati, OH, 1990; EPA/540/2-90/017.

U.S. Environmental Protection Agency. Guide for Conducting Treatability Studies under CERCLA: Soil Washing Interim Guidance; U.S. Environmental Protection Agency: Washington, DC, 1991; EPA/540/2-91/020A.

U.S. Environmental Protection Agency. Guide to Site and Soil Description for Hazardous Waste Site Characterization Volume 1: Metals; U.S. Environmental Protection Agency: Washington, DC, 1992; EPA/600/4-91/029.

SORPTION VERSUS COAGULATION IN THE TREATMENT OF HYDROCARBON CONTAMINATED WATERS

James L. Eifert

Civil/Environmental Engineering
Florida International University
University Park Campus
VH 151
Miami, Florida 33199

Faculty Advisor: Dr. Berrin Tansel

Coagulation, the process describing the aggregation of particles, involves the reduction of the electrostatic repulsion between the adsorbed-ion and counter-ion layers of colloidal particles. It is the reduction between layers that allows the coagulant to bridge with compounds in solution; i.e. contaminants. Similarly, clay has a strong tendency to sorb and immobilize dissolved chemical species in water. Clay minerals are an effective method of contaminant removal due to their structure and high surface area per unit weight. This study focuses on contaminant structure of mixed fuels in a brackish water sample in an effort to determine which method of removal, coagulation or sorption, is most effective. Mass spectrometric analysis of the contaminated water sample indicates the removal of higher molecular weight alkanes, those with a carbon number greater than ten, via coagulation. Knowing that coagulation has a positive affect on the removal of hydrocarbons with carbon numbers greater than ten, the focus was shifted to removing hydrocarbons of low molecular weight, those with carbon numbers lower than ten. Analysis of the clay treated samples shows little affect on such molecules.

INTRODUCTION

Every year major oil spills from ocean going tankers make headlines across the world. The fact is, more than half of the petroleum products that reach the oceans originate from land based and not ocean based sources. Most petroleum products, dumped on land or in the water by cities, industry, and individuals, make their way into the ocean via streams and surface runoff (Miller, 1991). Because of the wide spread environmental damage observed in the past, it is apparent that petroleum hydrocarbons (PHCs) and their derivatives be removed from contaminated waters. Many methods of improving the quality of such waters have proven to be effective, coagulation being one of them. This process involves the aggregation of particles by the addition of a chemical agent or "coagulant" (Manahan, 1991). The process of sorption by clay is also a method of removal for organic compounds that must be explored as a possible treatment for hydrocarbon contaminated waters. Clay, a group of microcrystalline secondary minerals consisting of hydrous aluminum silicates with sheet like structures, is abundant in natural aquatic systems as suspended colloidal particles or sedimentary matter (Manahan, 1991). It may be possible for PHCs to be trapped in the colloidal masses of clay. This study is an attempt to determine, through the use of mass spectrometry, which PHCs are more likely to be affected by coagulation, using a man made coagulant, or sorption, using clay; a product of the environment.

BACKGROUND

The coagulation process involves the addition of a coagulant, followed by rapid mixing, in order to destabilize colloidal particles and other organic pollutants in a contaminated water sample. The mixing acts to reduce the zeta potential of the particles. The zeta potential is a measure of the charge of the colloidal particles which depends on the distance through which the charge is effective (Regula, 1993). The higher the zeta potential, the greater the repulsive forces between colloidal particles. Coagulation acts to reduce these electrostatic repulsion forces between the ionic layers (adsorbed-ion layer and counter-ion layer) of the particles. Because of the double layer of electrical charge surrounding charged particles, this mechanism of aggregation is often called electric double layer (EDL) compression (Manahan, 1991). The aggregation of the destabilized particles is a function of the agitation caused by mixing and Van der Waals attractive forces. Continued aggregation results in the formation of larger particles which can be removed by filtration and settling. The removal of organic contaminants by coagulation depends on the ability of the contaminants to adsorb to other particles through chemical complexation, electrostatic attraction, or other means (Randtke, 1988).

When using coagulation as a water treatment process, one must consider the physical and chemical properties of both the coagulant and the contaminants. Such important characteristics of coagulants include charge density, molecular weight, and degree of cross-linkage (Dentel, 1991). Polymer coagulants destabilize colloids by neutralizing particle charge and interparticle bridging. These type of coagulants used in water treatment are composed of specific monomers linked in either linear or branched configurations containing specific functional groups. Polymer coagulants can be charged (polyelectrolytes) or neutral.

In much the same way, the process of sorption by clay can remove organic compounds suspended in water. Sorption can occur several ways: van der Waals forces arising from dipole-dipole interactions, ion exchange, and hydrogen bonding. Clay minerals can attain a net negative

charge by ion replacement, in which Si(IV) and Al(III) ions are replaced by metal ions of as similar size but lesser charge. The compensation for this net negative charge is achieved by the association of cations with the clay surface. This adjustment gives clay its cation-exchange capacity (CEC). CEC is defined as the amount of exchangeable cations expressed in milliequivalents per 100 g of dry clay (Manahan, 1991). The charge attained by ion replacement may act in a similar way as the dimethyl diallyl ammonium chloride functional group of the chosen coagulant.

In order to determine the effectiveness of a removal process at the chemical level, one must look at the structure of the contaminant. The most often studied characteristics of contaminants concerning the treatment of water are molecular weight, solubility, hydrophobicity, and functionality (Randtke, 1988). Past researchers have agreed that coagulation removes those contaminants that are acidic, hydrophobic, and of a higher molecular weight. Similarly, the degree of sorption of organic compounds by clays is influenced by such factors as solubility, volatility, charge, polarity, and molecular structure and size of the contaminant (Manahan, 1991). Most synthetic organic chemicals (SOCs), such as those found in synthesized petroleum products, can be removed by coagulants containing acidic functional groups that can attach to metals such as iron and aluminum, forming hydrophobic complexes (Randtke, 1988). Because clays also have the ability to form complexes with metals, it may be possible for the clay to act as a coagulant in treating PHC contaminated water.

METHODS AND MATERIALS

Experimental Design: The effect of coagulation and sorption on a contaminated water sample was studied by analyzing the removal or rejection of PHCs. Table 1 summarizes the experimental variables and settings involved.

Table 1. Experimental variables and settings

Variables	Settings
Source water	Brackish water (TDS=10000 ppm)
Coagulant type and dosage	Cat floc K-10 (0.5%) at 8.0 ml/L
Clay type and dosage	Bentonite at 0.50 g/L
Contaminant concentration	3000 ppm (1:1:1 mixture of jet fuel, diesel and unleaded gasoline)

Source water: The experiment was conducted using only brackish water. Brackish water (TDS=10,000) was prepared using distilled water and 10 g/L of NaCl.

Contaminant: The contaminant used in the experiment consisted of a 1:1:1 mixture of unleaded gasoline, diesel and jet fuel. The brackish water sample was prepared with a contaminant concentration of 3000 ppm (3 ml/L) in a 1 liter bottle and mixed for a 24 hour period at 22° C (room temperature) to achieve a homogeneous mixture and allow for the dissolution of the PHCs.

Coagulant: The coagulant used in this experiment was Cat floc K-10 manufactured by the Calgon Corporation, Pittsburgh, Pennsylvania. K-10 was chosen on the basis of past results from experiments run in the same laboratory under similar conditions. Properties of Cat floc K-10 are provided in Table 2.

Table 2. Properties of the Cat floc K-10 coagulant*

Coagulant	Chemical description	Specific gravity	pH	% Volatile (v/v)	% Volatile (w/w)
Cat floc K-10	Cationic polymer**	1.2-1.3	1.0-2.8	56	41

* Values adapted from Material Safety Data Sheets provided by Calgon Corp., Pittsburgh, PA.
** The polymer is composed of poly Dimethyl Diallyl Ammonium Chloride (DMDAAC).

Clay: The clay used in this experiment was a bentonite clay manufactured by American Colloid Company, Arlington Heights, Illinois. Bentonite clay was chosen on the basis of past research performed in the same laboratory. No properties of this compound could be provided.

Analytical analysis: Analysis was done at the Drinking Water Research Center, located on the campus of Florida International University, Miami, Florida. The experimental samples were analyzed for PHCs using a mass spectrometer.

Experimental procedure: After the brackish water solution was prepared and the contaminant added, it was mixed for 24 hours before undergoing the jar test. The jar test begins by pouring the 1 liter water-fuel mix into a 1000 ml (1 liter) beaker and allowing it to stand for 20 minutes before taking the initial 200 ml sample. Sampling of the experimental solution was done using a pipet, making sure the water extracted was from the bottom of the beaker to assure no direct contamination from the floating fuel mixture. The water-fuel mix is then pre-stirred for 15 minutes at 100+ (150-170) rpm. Next, the mixing is slowed to exactly 100 rpm and the chosen treatment media and dosage is added, 8 ml of Cat floc K-10 coagulant, or 0.50 g of bentonite clay. Mixing

should continue at 100 rpm for 2 minutes after the addition of the treatment media. The mixing of the experimental solution is then slowed as follows: 80 rpm for 2 minutes, 60 rpm for 2 minutes, 20 rpm for 2 minutes, and 0 rpm for 30 minutes to let the precipitate settle. After settling, the final 200 ml sample of the now treated solution should be extracted making sure no contaminant, flocs or colloidal particles are removed. Both samples should be refrigerated until the time in which they are prepared for analysis. In this experiment, the samples were prepared for mass spectrometric analysis by liquid-liquid extraction using pentane. The extracted samples were then placed in a 2 ml autosampler vial for injection into the mass spectrometer.

RESULTS AND DISCUSSION

Each compound's individual spectrum from the Total Ionic Chromatograms (TICs) was analyzed using the mass spectrometer's computer library. Each spectra was subjected to a computer search using a library of known PHCs and the best matches, if any, were displayed according to the percent match between the experimental and known compounds. The TICs from the before and after treatment analyses are shown in Figure 1, for the coagulant, and Figure 2, for the clay. Table 4 (next page) summarizes the compounds found in both the untreated and coagulant treated sample TICs.

When comparing the before and after TICs for the treatment using the coagulant, it is easy to see that a substantial number of contaminants were removed. Initially, the brackish water sample contained approximately 25 PHC compounds in ample concentrations. After the coagulation procedure, the TIC revealed approximately 11 PHC compounds. Those compounds not removed by coagulation were found in a lesser concentration in the treated sample. Analysis of the peak areas of each contaminant compound in the TICs shows an increase in the percent of contaminant removed as carbon number increases (Table 3).

Table 3. Percent of contaminants removed from brackish sample

Carbon Number	Percent Removed
C_7	10.4
C_8	21.7
C_9	74.7
C_{10}	69.5
$> C_{10}$	100.0

The analysis of the experimental results using the mass spectrum suggests that PHCs with carbon numbers between 10 and 35 (Naphthalene and Pentatriacotane), and possibly higher, were removed from the brackish water solution by simple coagulation. This observation follows previously accepted data relating the removal of a compound to its molecular weight. The higher the molecular weight of the compound, the more likely it will be removed by coagulation processes.

Figure 1. Total Ion Chromatograms for coagulant treated brackish sample

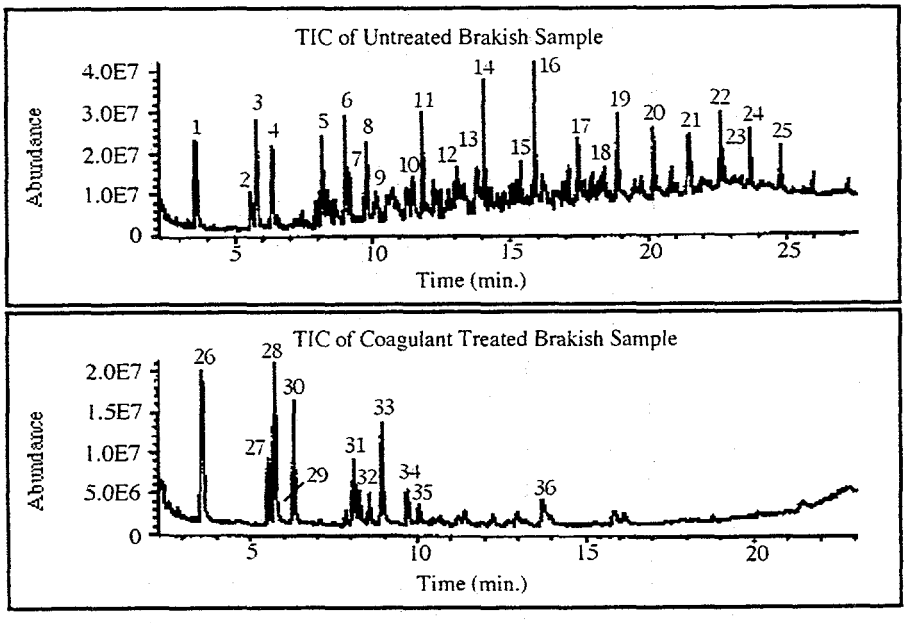


Table 4. Mass spectra data for TICs of coagulant treated sample

Formula	Compound	TIC Peak # "Before"	TIC Peak # "After"	%Match B/A*
C_7H_8	Benzene, methyl	1	26	94/89
C_7H_{10}	Benzene, ethyl	-	27	81
C_8H_{10}	Benzene, 1,2-dimethyl	2	29	67/74
C_8H_{10}	Benzene, 1,3-dimethyl	3	28	97/97
C_8H_{10}	Benzene, 1,4-dimethyl	4	30	89/74
C_9H_{12}	Benzene, 1-ethyl-3-methyl	5	34	96/54
C_9H_{12}	Benzene, 1,3,5-trimethyl	6	32	88/82
C_9H_{12}	Benzene, 1,2,3-trimethyl	-	33	83
$C_{10}H_{22}$	Decane	7	-	65
C_9H_{12}	Benzene, 1-ethyl-2-methyl	8	31	65/96
C_9H_8	1H-Indene, 2,3-dihydro-	9	35	73/55
$C_{10}H_8$	Naphthalene	13	36	89/83
$C_{10}H_{13}$	Benzene,methyl (1-methylethyl)	10	-	75
$C_{11}H_{24}$	Undecane	11	-	81
$C_{10}H_{14}$	Benzene, 1,2,4,5-tetramethyl	12	-	50
$C_{12}H_{26}$	Dodecane	14	-	87
$C_{10}H_{22}$	Heptane, 3-ethyl-5-methyl	15	-	67
$C_{13}H_{28}$	Tridecane	16	-	72
$C_{15}H_{32}$	Pentadecane	17	-	81
$C_{12}H_{12}$	Naphthalene, 1,4-dimethyl	18	-	94
$C_{14}H_{30}$	Tetradecane	19	-	74
$C_{16}H_{34}$	Hexadecane	20	-	96
$C_{17}H_{36}$	Heptadecane	21	-	95
$C_{18}H_{38}$	Octadecane	22	-	97
$C_{21}H_{44}$	Eicosane, 10-methyl	23	-	77
$C_{25}H_{52}$	Heptadecane, 9-octyl	24	-	89
$C_{35}H_{72}$	Pentatriacotane	25	-	85

* Mass spectrum library cross reference for the TIC peaks before and after coagulation

The compounds found in the initial brackish water sample varied from simple compounds such as toluene (methylbenzene) to larger, more complex compounds like 1,4-dimethylnaphthalene. The compounds remaining in solution after coagulation were almost exclusively derivatives of the aromatic compound benzene (C_6H_8). Table 4 (above) lists the specific compounds found both prior to and after coagulation.

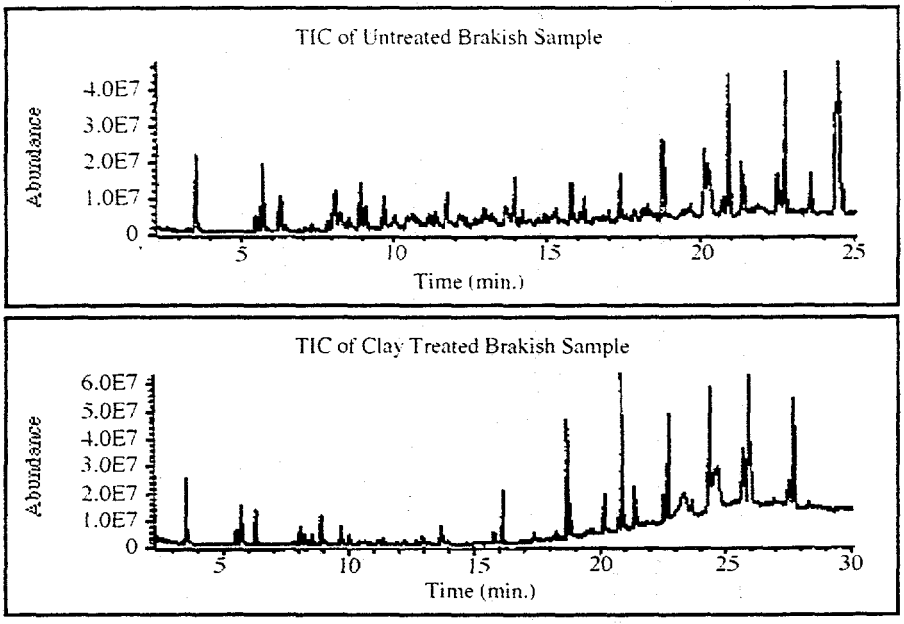
The inability of the smaller carbon number (C_7-C_9) benzene derivatives to coagulate can be postulated by the relatively unreactive structure of benzene itself. Benzene's symmetrical, aromatic structure gives it a unique stability. The conjugated system provides benzene with a dense cloud of π-electrons making it difficult for other compounds to penetrate and react. The stability of aromatic, cyclic compounds may decrease the chances of such compounds forming floc networks and coagulating.

Most of the compounds removed from solution were long chain alkanes with carbon numbers higher than 10. The coagulation of these compounds may be explained by their structure and size. Simple alkanes are generally more reactive than aromatic, cyclic compounds. The number of reaction sites (i.e. flocculation sites) increases with an increase in the size of the alkane chain. The physical increase in carbon number increases the probability of the alkane coagulating and the number of compounds it coagulates with, hence more compounds are removed from the contaminated solution.

Looking at the TICs for the before and after treatment with clay, it is obvious that the desired result was not achieved. Mass spectrum analysis of both brackish samples shows that the majority of the compounds found in the one TIC are found in the other, confirming the visual peak by peak comparison. Although the clay was unsuccessful in removing certain compounds, all compounds experienced a decrease in concentration after treatment. A table for the mass spectrum analysis for the clay treated samples is not included. Essentially all compounds in the untreated sample of Figure 1 are present in the untreated and treated samples of Figure 2 (next page).

The factors contributing to the inability of the bentonite clay to remove the PHCs can only be postulated. It is possible that the bentonite structure and surface area do not favor the sorption of organic chemicals such as PHCs. The bentonite type of clay may not be as efficient in absorbing large quantities of water between its alternating unit layers of silicon oxide and aluminum oxide as other clay types.

Figure 2. Total Ion Chromatograms for clay treated brackish sample



The structure of the PHC contaminants may also contribute to the results obtained from treatment with clay. Hydrocarbons, such as those found to exist in mixed fuel, do not posses any net charge. Clays often interact with suspended organic compounds utilizing their CEC. Because the contaminants used in this research are neutral, cyclic and long chain alkane structures, they could not bind to the clay surface in this way.

CONCLUSION

The analysis of the proposed compounds using the mass spectrometer indicates the removal of higher molecular weight alkanes as opposed to lower molecular weight, aromatic compounds via coagulation. Mass spectrometric analysis of the clay treated sample indicates a small decrease in contaminant concentration but, no substantial contaminant removal. Additional research will be needed in order to predict the eradication of compounds on a per molecule basis when using coagulation or clay as a primary treatment process.

Future research may include the use of one or more different coagulants or clay types in an effort to remove the lower carbon number (lower molecular weight) compounds ($< C_{10}$). In addition, other experimental variables such as different source waters, clay dosages and PHC contaminants should be studied, along with the possibility of using clay in conjunction with the coagulant.

ACKNOWLEDGMENTS

This project was funded by the United States Army Belvoir Research, Development, and Engineering Center (contract no. DAAK70-91-K-004). Special thanks to Dr. Mehrzad Mehran and the Drinking Water Research Center for their valuable assistance with the mass spectrometer.

REFERENCES

Dentel, S.K. 1991. "Coagulant Control in Water Treatment." Critical Reviews in Environmental Control. 21(1): 41-135.

Manahan, S.E. 1991. Environmental Chemistry, 5th ed. Lewis Publishers Inc. Chelsea, Michigan.

Miller, G.T. 1991. Environmental Science, 3rd ed. Wadsworth Publishing Inc. Belmont, California.

Randtke, S.J. 1988. "Organic Contaminant Removal by Coagulation and Related Process Combinations." Journal American Water Works Association. 80(5): 50-56.

Regula, J. 1993. "Coagulation Pretreatment for Ultrafiltration of Petroleum Hydrocarbon Contaminated Waters." Purdue University, Indiana. May 10-12.

Chronic and Acute Dioxin Exposures and Their Impacts on Human Populations

Deborah Feder

Department of Geography
Colgate University Hamilton, NY 13346

Faculty Advisors:

Susan Craddock and David Lighthall

Dioxin is a chemical contaminant. It is ubiquitous, is a modern day issue, and is linked to environmental and health ramifications. Regardless of these properties though, it is important to understand the leap from dioxin production to dioxin consumption. Exposure can occur via three major pathways: environmental, accidental, or occupational. Environmental exposure is chronic and accounts for daily contact with dioxin through food processing, the food chain, and through land, air, and water sources. Accidental and occupational exposure, on the other hand, qualify as acute due to their intensity. For example, the Vietnam War and its usage of Agent Orange, the BASF chemical production facility and its dioxin leak, and the high dose occupational interaction and contact that chemical workers receive daily are all acute exposures. Chronic and acute dioxin exposures are explored in this paper in order to evaluate dioxin's toxicity and pervasiveness.

CHRONIC DIOXIN EXPOSURE

The dioxin contamination of air supplies is of concern to human populations because of its implications for soils, surface waters, plant surfaces, and ultimately food. In today's industrial society dioxins are released into the environment from smokestacks where they are henceforth dispersed by physical processes such as evaporation, rainfall, and wind to places far from their original sources (Schneider Sept. 14, 1994: A5; Dickson 1993: 70). It is estimated that concentrations of dioxin in urban air from industrialized countries range from 1.3-9.6 pg/m^3, noting that a picogram is a trillionth of a gram (Travis 1989: 1061). Air thus contributes to the ubiquitous distribution of dioxins, as populations and habitats worldwide breath in, eat, and absorb dioxin.

Dioxin translocation has been seen on Isle Royale in northern Lake Superior National Park. Isle Royale is an entirely natural environment which has not had automobiles since 1940 (Gough 1986: 40). Therefore, any industrial chemicals that have reached the island have been borne by air. Nonetheless, scientists from Indiana University examining sediment from the island found dioxin in its upper most soil layers in levels closely parallel to those measured in air samples taken in Washington D.C. and St. Louis, Missouri (Gough 1986: 40). Soil samples were found to have 38 parts per trillion (ppt) of dioxin, with OCDD being the most abundant dioxin (Science Nov. 10, 1984). Furthermore, dioxin levels were found to be steadily decreasing in layers deposited before 1940 (Gough 1986: 40). Based on this information, scientists concluded that dioxin originated from far-off sources and was transported by wind to the island.

Moreover, the rate of airborne deposition of dioxin has additional implications in terms of the food chain. Dioxins which are deposited on plant foliage form a dioxin-vegetative-animal-human linkage. This is demonstrated by the fact that animals, including humans, eat leaves. Leaves of terrestrial plants are covered with a lipid cuticle layer which forms a sink for lipophilic chemicals such as dioxin (McCrady 1993: 343). Dioxin is also absorbed in plants via their roots and particle deposition. Nevertheless, it can not be denied that vapor mass transfer is the primary source of dioxin exposure for vegetation, accounting for 56% of absorption (McCrady 1993: 343). Particle deposition is responsible for 37% of exposure and root uptake accounts for 7% (McCrady 1993: 343). Inevitably though, exposure levels, bioconcentration factors, and bioaccumulation values are dependent on variables such as plant species, plant age, change in air concentrations, and photodegradation. In sum, dioxin circulates widely in the atmosphere depositing itself in places far from original sources. Air is the vehicle by which this distribution occurs. The inhalation of dioxin contaminated air accounts for 2% of daily dioxin intake for humans (Travis 1989: 1062).

Likewise, dioxin exposure on land occurs through the food chain, for dioxin magnifies at successive tiers of the ecosystem. Bioaccumulation is a major source of chronic low dose dioxin exposure (ATSDR 1993). Studies done in West Germany, Canada, and Japan have shown mean dietary background intake of dioxins in industrialized countries to be about 98 pg/kg per day, with meat and dairy products accounting for the majority of dioxin exposure (Travis 1989 1062). It has been calculated that the concentration of dioxin in the fat of Americans and Canadians averages between 5 and 10 ppt (Begley 1994: 57; Schneider, Sept 14, 1994: A5; Bukro Sept 14, 1994: 3). This has implications on human populations, for it has been shown that the average person is exposed to approximately 1 picogram of TCDD per kg body weight per day, 90% of which comes through dietary exposure in the form of meat, poultry, fish, dairy products (5-30% of total exposure), and eggs (Dickson 1993: 70; Dioxin Contamination of Milk 1989: 3). Small amounts of dioxin are considered

hazardous as demonstrated by the fact that the U.S. EPA has set acceptable limits of dioxin at .006 pg/kg, which is a minute quantity (Gough 1986: 242; Roberts 1991b: 624).

Furthermore, dioxin exposure through food also occurs from processing procedures such as packaging or bleaching. Dioxins have been detected in paper pulp, milk and orange juice cartons, coffee filters, tea bags, disposable diapers, tampons, facial and toilet tissue, paper towels, and microwave dinner trays (Dioxin Contamination of Milk 1993: 3). The U.S. Committee of Energy and Commerce in 1989 reviewed evidence concerning dioxin contamination of milk during its processing procedures (Travis 1989: 1061). Specifically, Mr. James S. Benson, Acting Deputy Commissioner of the Food and Drug Administration, testified before the House of Representatives about dioxin migration from paperboard cartons, since paperboard cartons manufactured and processed with chlorine bleaching chemicals allow for the leaching of dioxin from cardboard packaging materials into the inner contents of containers-be it milk, orange juice, or other foods (Science News Sept 9, 1989). Benson examined 15 milk packaging plants in the U.S. and found TCDD, the most toxic dioxin in 4 of 15 milk carton samples and TCDF in 7 of 15 (Dioxin Contamination of Milk 1989: 3). These dioxin values were not measured at the same levels in unpackaged milk collected at the plants, even though as denoted before much milk is already somewhat contaminated with dioxin due to its prior food chain exposure (Dioxin Contamination of Milk 1989: 3).

Thus, it is this dioxin migration in milk which has implications on human health. As estimated by Mr. Robert Scheuplein, Director of the Office of Toxicological Science, 5 out of 1 million are at risk of cancer from drinking milk laden with dioxin. This is computed on the basis of average consumption which assumes that children drink more milk than adults on a body weight basis (Dioxin Contamination of Food 1989: 7). Scheuplein estimates that young children getting all their milk from contaminated cartons might double their dietary dioxin intake to a level of 2 pg/kg a day which is far above the EPA's .006 pg/kg acceptable level (Raloff Feb. 18, 1989: 105). Moreover, in agreement with these findings Mark Floegal of Greenpeace maintains that these dioxin levels show that children drinking even a single half pint of milk per day are encountering more dioxin than the EPA has deemed acceptable to avoid risk. Floegal says a kindergartner who drinks a one half pint carton of milk per day is drinking 78 times the EPA's risk specific dose of TCDD, which is estimated to result in a lifetime cancer risk of one in a million (Dioxin Contamination of Milk 1989: 13). To him this is dairy roulette (Dioxin Contamination of Milk 1989: 13).

Additionally, coffee filters and frozen dinners have been found to be sources of dioxin exposure. It is estimated that heavy coffee drinkers consuming coffee from bleached paper filters might increase their daily dioxin intake 5-10% above the U.S average level due to dioxin migration from filters, and similarly this migration can occur when frozen dinners are cooked (Raloff Feb. 18, 1989: 105). Roberta Baskin, a consumer affairs reporter found meat cooked on microwave dinner trays increased in dioxin content by 1.7 parts per trillion (ppt) due to migration of dioxins from paper trays to meat during cooking (Raloff Feb. 18, 1989: 105).

Moreover, although dioxin is not water soluble, water still serves as a vector through which populations are exposed to dioxin. Dioxin deposited on surface waters is absorbed onto suspended sediments which in turn settle to the floor of water bodies where they contaminate plant and animal life (Dickson 1993: 70). Once dioxin is bound to soil and sediment it is essentially fixed except for bulk transport due to flooding, dredging, or erosion (Dickson 1993: 70). It is estimated that the levels of dioxin in the Great Lakes range from 300-2,000 ppt on a dry weight basis, shifting with industrial activity, waste disposal, and human activity (Dickson 1993 70).

Fish living in contaminated environments take in dioxin from water that flows across their gills, from ingested organic material, and from food. Internal physiological processes such as lipid metabolism and biotransformation control an aquatic organism's ability to metabolize dioxin (Porte 1993: 273). For example, certain marine biota, such as fish crabs, are not capable of metabolizing dioxin and therefore leave dioxin preserved in their tissues (Oehme 1990: 1836). Dioxin thus becomes concentrated in their fats and thereby magnifies in the food chain (Health and Environment Dec. 1992: 1). The EPA has estimated that fish concentrate dioxin in their lipid tissues by a factor of 5000. Therefore, it is this as well as dioxin's low water solubility and high affinity for organic matter which accounts for dioxin's relatively high concentration levels in fish as opposed to their surrounding waters (Gough 1986: 243). The U.S. FDA postulates bottom living fish such as carp and catfish are more likely to carry dioxin because of their feeding habits, which characteristically involve sucking up sediment particles. Higher living fish are not as acutely exposed to dioxin in their respective surface waters (Gough 1986: 238).

Dioxin's hydrophobic and lipophilic nature accounts for its behavior in water bodies. In regard to water contamination different precautions have been taken. Maine, for instance, is in the process of establishing state water quality criteria for TCDD in surface waters because of recent tests which found the 1984 EPA bioconcentration value of 5000 for dioxin accumulation in fish to be too low (Frakes 1993: 244). A bioaccumulation factor in the range of 15,000-25,000 is seen as more appropriate (Frakes 1993: 244). However, researchers still fear that this 3 to 5 fold increase may greatly underestimate concentration levels among some bottom feeding aquatic life, such as white suckers (Frakes 1993: 244). Many fish can

bioconcentrate dioxins up to 100,000 times in their tissues depending on water concentrations (Dioxin Contamination of Food and Water 1988: 5). The FDA considered these issues in its 1980 Great Lakes study. The FDA sampled about 250 edible fish for their accumulation of chlorinated chemicals, particularly dioxin (Raloff Feb. 18, 1989: 105). One species, the fathead minnow, accumulated dioxin at levels 159,000 times greater than levels present in its surrounding sediment and water (Raloff Feb. 18, 1989: 105). Unexpectedly high levels of chemical contaminants were also found in walleye, pike, bass, catfish, carp, and other fish downstream from paper and pulp processing mills (Raloff Feb 18, 1989: 105). Hence, it is evident that many components factor into the bioaccumulation equation. Among these are dispersion, water contamination, dioxin's hydrophobic and lipophilic nature, aquatic metabolism, bioaccumulation, and processing procedures.

ACUTE EXPOSURE

Vietnam

Between 1962 and 1970 the U.S. air force sprayed nearly 19 million gallons of herbicides, 11.2 of which were Agent Orange over 3.6 million acres of Vietnam (Veterans and Agent Orange 1994: 1). This area was roughly the size of Rhode Island and Connecticut combined (Gough 1986: 49). Agent Orange, a defoliant used to strip jungle canopies and clear tall grass and bushes, was used in order to reveal enemy troops. Ninety percent of all Agent Orange was sprayed on jungles, 8% was used against enemy crops, and 2% was used by the military for special purposes (Gough 1986: 52). Hence, the Agent Orange spraying program, encoded Operation Ranch Hands, contaminated South Vietnam's land, soil, water, and food sources. The use of Agent Orange stopped in 1970 when it was found to cause birth defects in laboratory animals (Veterans and Agent Orange 1994: 1). Thus, due to the toxicity of Agent Orange and allegations of Vietnam veterans who have fathered handicapped children, developed cancer, or suffered from a variety of other ailments associated with their occupational and environmental exposure to dioxin, much research has been done on Agent Orange and its health implications.

In regard to this research it is widely agreed that Ranch Hands, those pilots, co-pilots, spray operators, and ground crew who handled dioxin, were more heavily exposed to Agent Orange than other veteran groups. Ranch Hands which handled Agent Orange have been measured with dioxin concentrations at least three times higher than other Vietnam veterans and veterans who never served in Vietnam (Gough 1986: 251). For example, six sprayers who were measured for dioxin contamination 20 years after Agent Orange exposure were found to have levels of TCDD between 17-55 ppt in their lipid tissue, and it was estimated that their levels of TCDD may have been between 140 and 610 ppt at the time of contact, taking into account dioxin's half-life and the US EPA's present .006 pg/kg acceptable intake level (Schecter 1994: 191).

Agent Orange not only impacted Ranch Hands but it effected other veterans and the local Vietnamese population as well. Those who worked in defoliated areas, who were situated near spray areas, who had Agent Orange sprayed on them, who drank water in which Agent Orange had accumulated, or who ate fruit from Agent Orange sprayed trees were likewise exposed to dioxin (Gough 1986: 60). Dr. Arnold Schecter, a doctor of preventative medicine at the State University of New York at Binghamton claims that dioxin has persisted in the soil and plants of South Vietnam for 14 years now (Joyce 1986). Schecter substantiates the environmental-food chain-human linkage in his analysis of adipose tissue from people's stomachs in North Vietnam and South Vietnam. He found the South Vietnamese to have a net mean of 22.1 ppt of dioxin in their fat tissue, while the North Vietnamese to have negligible amounts (Joyce 1986). Furthermore, dioxin concentrations measured in South Vietnam were three times the values evidenced in the United States (Raloff 1985: 27).

Occupational Dioxin Exposure

As elaborated on above, acute exposure to dioxin can be related to warfare as well as to unintended accidents. However, it can also be related to occupational exposure. To elucidate this, two case studies and their health ramifications are presented below.

On November 17, 1953 an uncontrolled decomposition reaction occurred at BASF Aktiengesellschahaft in Germany (Zorber 1990: 139). The BASF plant had been producing 2,4,5 trichlorophenol. However by accident, on the seventeenth of November it produced 2,3,7,8 tetrachlorodibenzodioxin instead (Zorber 1990: 139). This unintentionally produced TCDD vapor then leaked into a BASF production building, exposing BASF employees to dioxin. Four BASF workers ended up dying from this exposure while other BASF employees tested 34-36 years after the incident still had dioxin concentrations in blood, adipose tissue, liver, kidney, bone marrow, and biopsy material 40-100 times higher than the average background concentrations of unexposed individuals (Reggiani 1994: 1830). Schecter found similar results in his study of six German workers at this facility who were measured 32 years after their initial exposure for the level of dioxin remaining in their adipose tissues (Schecter 1994: 138). In Schecter's analysis, workers had 11 to 141 ppt of TCDD in their lipid tissues (Schecter 1994: 138). From this it was estimated that exposure levels may have been between 917 and 11,750 ppt in 1953 (Schecter 1994: 138). Additionally, Friedemann Rohleder, a West German epidemiologist, measured a standardized mortality ratio

of 2.66 at BASF, finding that neoplasms of the larynx, trachea, bronchi, lungs, and respiratory organs resulted in 8 deaths instead of the expected 3.01 after the accident (Yanchinski Oct. 1989). Rohleder found identical ratios for cancers of the digestive tract.

In conjunction with these findings, Marilyn Fingerhut of the National Institute for Occupational Safety and Health examined the mortality records of all U.S. chemical workers exposed to occupational dioxin from 1942-1984. This survey consisted of a total of 5,172 workers from 12 different plants (Roberts 1991c: 8). Fingerhut found a 15% excess of all cancers (Fingerhut, 1992: 72). More specifically though, she accounted for the fact that blood serum levels correspond with how long an employee worked in a dioxin contaminated job. She measured a 46% excess of all cancers in a subcohort with more than 1 year of exposure and over 20 years of latency, with 42% of these cancers being respiratory (Fingerhut, 1992: 72). Among this subcohort a ninefold excess of soft tissue sarcomas was measured. A 50% excess risk of dying of cancer was measured among highly exposed workers who receive dioxin doses 500 times higher than the level of general populations (Roberts 1991c).

In regard to these issues, differences between acute and chronic exposure to dioxin are evident. Chronic exposure occurs in low doses, is often undetectable, and is difficult to measure. Conversely, acute exposure is intense, is finite, and is less difficult to detect. Chronic exposure encompasses land, water, and air contamination while acute exposure can be traced to definite sources, afflicts certain populations, and appears to be more drastic in its health effects. It is these factors as well as the mass transfer of dioxin within the ecosystem which have health implications for humans and the environment alike.

ATSDR. "Dioxin Toxicity." American Family Physician. March 1993. pp. 855-859.
Begley, Sharon, Hager, Mary. "Don't Drink the Dioxin." Newsweek. Sept 19, 1994. p.57.
Bukro, Casey. "Burning Issue of Dioxin Risks" Chicago Tribune. September 14, 1994. pp.1-3.
Dickson, LC, Buzik, SC. "Health Risks of Dioxins: A Review of Environmental and Toxicological Considerations." Vetinary Human Toxicology. Vol. 35. no. 1. February 1993.
"Dioxin Contamination of Milk." Hearing Before the Subcommittee on Health and the Environment. September 8, 1989. pp.1-31.
"Dioxin Contamination of Food and Water." Hearing Before the Subcommittee on Health and the Environment. December 8, 1988. pp.1-210.
"Dioxin Deposits far from the Source." Science-News. Vol. 126. November 10, 1984. p.297.
"Dioxin Toxicity." American Family Physician. Vol. 47. March 1993. pp.855-861.
Fingerhut, Marilyn, Steenland, Kyle, Sweeney Marie, Halperin, William, Piacitelli, Laurie, Marlow, David. "Old and New Reflections on Dioxin." Epidemiology. Vol. 3. no. 1. 1992.
Frakes, Robert, Zeeman, Catherine, Mower, Barry. "Bioaccumulation of 2,3,7,8 Tetrachlorodibenzo-p- dioxin (TCDD) by Fish Downstream of Pulp and Paper Mills in Maine." Ecotoxicology and Environmental Safety. Vol. 25. 1993. pp.244-252.
Gough, Michael. Dioxin, Agent Orange the Facts. Plenum Press. 1986.
Joyce, Christopher. "How toxic is dioxin? The mystery deepens." New Scientist. Vol 110. 1986.
McCrady, Joel, Maggard, Sharon. "Uptake and Photodegradation of 2,3,7,8 tetrachlorodibenzo-p-dioxin absorbed to grass foliage." Environmental Science and Technology. Vol. 27. 1993.
"Modeling Bioaccumulation." Health and Environment Digest. Vol. 6. no. 8. December 1992.
Oehme, Michael, Bartonova, Alena, Knutzen, Jon. "Estimation of polychlorinated Dibenzofuran and dibenzo-p-dioxin contamination of a coastal region using isomer profiles in crabs." Environmental Science and Technology. Vol. 24. Dec. 1990. p. 1836-1841.
Porte, C., Albaiges, J. "Bioaccumulation Patterns of Hydrocarbons and Polychlorinated Biphenyls in Bivalves, Crustaceans, and Fishes." Archives of Environmental Contamination and Toxicology. Vol. 26. 1993. pp.273-281.
Raloff, Janet. "How much Dioxin Did You Consume Today?" Science News. Vol. 135. 1989.
Raloff, Janet. "Dioxin Migrates out of Milk Cartons?" Science News. Vol. 134. Oct. 29, 1988.
Raloff, Janet. "Dioxin: Is Everyone Contaminated?" Science News. Vol.128. July 13, 1985.
Reggiani, G.M. "Dioxin Effects." Science. Vol. 264. June 24, 1994. p.1829.
Roberts, Leslie. "More Pieces in the Dioxin Puzzle." Science. Vol. 254. October 15, 1991a.
Roberts, Leslie. "Dioxin Risks Revisited." Science. Vol. 251. February 8, 1991b. pp.624-626.
Roberts, Leslie. "High Dioxin Dose Linked to Cancer." Science. Vol. 251. February 8, 1991c.
Schecter, Arnold, Ryan, John, Masuda, Yoshito, Brandt-Rauf, Paul, Constable, John, Dinh Cau, Hoang, Dai, Le Cao, Hoang, Tri Quynh, Ngoc, Nguyen. Phiet, Pham. "Chlorinated and Brominated Dioxins and Dibenzofurans in Human Tissue Following Exposure."

Environmental Health Perspectives. Vol. 102. 1994. 135-147.
Schmidt, Karen. "Puzzling over A Poison." U.S. News and World Report. April 6, 1992.
Schneider, Keith. "EPA Moves to Reduce Health Risks From Dioxin." New York Times. 1994.
Travis, Curtis, Hattemer-Frey, Holly, Silbergeld, Ellen. "Dioxin, dioxin everywhere." Environmental Science and Technology. Vol. 23. no. 9, 1989. pp.1061-1063.
Veterans and Agent Orange. Institute of Medicine. 1994.
Yanchinski, Stephanie."New Analysis Links Dioxin to Cancer." New Scientist. Vol. 124. 1989.
Zorber, Andreas, Messerer, Peter, Huber, Peter. "Thirty-four year mortality follow up of BASF employees exposed to TCDD after the 1953 accident." Occupation Environmental Health. Vol. 62.

Comparison of Endomycorrhizal Fungi of Organically and Conventionally Grown Crops

Kelley McMurray Sarkis

Department of Environmental Science
Nazareth College of Rochester
4245 East Avenue
Rochester, NY 14618-3790

Faculty Advisor:

Dr. Christine Gruhn

The presence of mycorrhizae in conventional and organic farms was assessed. Correlations between the percentage of mycorrhizal colonization and soil phosphorus concentrations and soil pH levels were compared. A significant relationship exists between mycorrhizal colonization and pH levels during the total sampling time for the comparison of conventionally grown corn and organically grown corn as well as in the comparison between the total sum of the crops sampled. Mycorrhizal colonization is also significantly affected by available soil phosphorus levels in organically grown corn and conventionally grown corn. The relationship between the total sum of the crops sampled and the potato crop implies a significant correlation between available phosphorus concentrations and pH levels. According to the results, mycorrhizal colonization decreases with increasing pH levels and increasing available phosphorus concentration in the majority of the sampled crops. There is also a significant relationship between increased phosphorus concentration and increased pH levels. The results from this research imply a mycorrhizae-phosphorus-pH cycle with each of the variables incumbent on the other.

INTRODUCTION:

Endomycorrhizal fungi, also known as vesicular-arbuscular mycorrhizae (VAM), form important symbiotic relationships with a diversity of plants, including many agricultural crops. The mycorrhizal fungus invades root cortical cells and makes nutrients, especially phosphorus, more accessible for absorption by the host plant (Raven, Evert and Eichhorn, 1992). The plant in turn provides the fungus with photosynthetically produced glucose. This relationship may be especially crucial in organic farming when synthetic fertilizers are not used.

Most farmers in developed countries forgo organic agricultural processes in which the reliance upon the mycorrhizal-plant symbiosis is crucial. Instead, these farmers choose to increase the health of their plants through phosphorus additions. Phosphorus fertilization at moderate levels does not interfere with mycorrhizal colonization, but at high levels it may inhibit mycorrhizal colonization, decrease spore production, decrease extra radical hyphal formation and decrease plant weight (Maartensson and Calgren, 1994).

The effectivity of the mycorrhizae is influenced by the fungal strains, and may range from mutualistic to parasitic (Johnson, 1993). Fertilizing crops may select for VAM fungal strains that are inferior mutualists or even parasites (Johnson, 1993). Mildly nutrient-stressed plants tend to release higher levels of soluble carbohydrate in root exudates which tend to select more mutualistic VAM fungi (Johnson, 1993). In response to fertilization, the abundance of VAM fungal strains that most aggressively acquire host carbohydrate will increase when fertilization causes host plants to allocate less carbohydrates to root exudates (Johnson, 1993). Fertilization may change species composition, whereby a mutually beneficial relationship may be replaced by a parasitic one (Johnson, 1993). Under high levels of phosphorus fertilization, a successful fungus could acquire carbohydrates that the host plant had not allocated to it, and thus, parasitically provision its own growth without contributing to the health of the host plant (Johhnson, 1993). In this type of situation, a less beneficial, or even detrimental, mycorrhizal fungus could be selected in fertilized soils (Johnson, 1993).

Organic farming does not rely on pesticides or synthetic fertilizers. Instead, it utilizes composts and manures to improve soil quality, controls pests naturally, rotates crops frequently and maintains diversified crops (Reganold et al., 1993). Organic farms have soils with greater biological and physical quality: significantly higher organic litter and microbial activity, more earthworms, improved soil structure, easier penetrability and thicker topsoil (Reganold et al., 1993). These properties may eliminate some of the erosion problems created by conventional farming methods by continuously improving soil structure.

Conversely, conventional farming usually involves little or no crop rotation between fields, virtually no variation in the types of crops grown and severe tillage treatments. These practices ignore the benefits supplied by the mycorrhizae, allow for plant pathogens to build up, and result in soil nutrients rapid depletion. Hence, conventional farming has created a environmentally destructive cycle which may only be controlled through the use of pesticides and synthetic fertilization.

The importance of organic farming methods, which rely on mycorrhizal technology , may not become fully realized until the world phosphate reserves near depletion, when there are more attempts to establish plants on devastated soils, and when there is a critical need to decrease fertilizer pollution in the environment (Janerette, 1991).

This study compares the concentration of available phosphorus and pH in the rhizosphere of plants grown on an organic farm with the percentage of mycorrhizal colonization. Along with this analysis, we will be assessing soil phosphorus availability which may have a direct impact on mycorrhizal colonization and thus impinge on soil pH levels. The purpose of this study was to determine the factors which limit the growth of endomycorrhizal fungi, as these variables would have a direct impact on the health of organic crops which rely on mycorrhizal colonization for their phosphorus supply.

METHODS:

A variety of root and soil samples were collected from both organic and conventionally grown crops. Three samples were taken from each field studied. The samples were placed in paper bags and labeled according to field, crop and placement. The placement of the samples was based on the collection of the roots and soil in three locations along the same row of one crop. Approximately 120 samples were collected from the Rose Valley Farm and a conventional corn field, both located in Wayne County, New York.

The sampled roots were washed in tap water and placed in plastic staining containers, in which they were stained (Kormanik and McGraw, 1992). The containers, with the roots, were placed in a glass beaker and covered with a 10% KOH solution. The specimens were placed in the autoclave for 10 min. The KOH solution cleared the host cytoplasm and nuclei and readily allowed for stain penetration. Next, the capsules were covered with alkaline hydrogen peroxide for 10 min. The capsules were rinsed at least three times with tap water. Then, the capsules were covered with 1% HCl and soaked for 4 min., after which the solution was poured off. The capsules were covered with 0.01% acid fucsin-lactic acid staining solution and autoclaved for 10 min. After removing the capsules from the autoclave, the roots were taken out of their containers and prepared for destaining with a solution composed of lactic acid, glycerol and water. After destaining, roots were placed in petri dishes and separated manually with dissecting needles. Petri dishes were set on a grid and placed under a dissecting microscope for counting. The threadlike hyphal projections of the fungus, which invade the cortical cells, were stained pink allowing for visual counting. The number of colonized root sections were compared for the percentage of mycorrhizal colonization.

Phosphorus was extracted from the soil and the level of phosphorus was determined (Olsen and Sommers, 1982). This method for available phosphorus analysis involves several steps. First, 12.0g of ammonium paramolybdate was dissolved in 250mL of distilled water. Then, 0.2908g of potassium antimony tartrate was dissolved in 100mL of distilled water. These dissolved reagents were added to 1.0L of 5N sulfuric acid, mixed thoroughly, and diluted with 2L of distilled water (reagent A). Next, 1.056g of ascorbic acid was dissolved in 200mL of reagent A, and mixed (reagent B).

5g of air dry soil which was added to a flask containing reagent was shaken in an acid solution for 5 minutes to extract the phosphorus and then the solution was centrifuged. Clear extracts were obtained and phosphorus was determined by the method of Olsen and Sommers, (1982). The 5g of air dried soil was mixed with 50 mL of distilled water and shaken for 5 minutes prior to pH testing.

RESULTS

The average percentage of mycorrhizal colonization, soil phosphorus and pH levels for individual crops, crops regardless of field and sampling time and the statistical anaylisis from two-way ANOVA tests from the sampled crop values are summarized in Table 1, Table 2 and Table 3, respectively.

Table 1. Average percentage of mycorrhizal colonization, soil phosphorus levels in parts per million, P (ppm) and average pH levels of individual crops, in each field during the three sampling times.

	Sampling Times									
	August 2			September 19			October 21			
Field and Crop	% mycorrhizal colonization	P (ppm)	pH	% mycorrhizal colonization	P (ppm)	pH	% mycorrhizal colonization	P (ppm)	pH	
6 Asparagus	47	3.7	7.0	--	--	--	--	--	--	
3c Broccoli	--	--	--	0	1.39	7.3	--	--	--	
2a Buckwheat	0	0.78	6.5	--	--	--	--	--	--	1b
Carrot	24	2.17	6.8	--	--	--	--	1.63	7.3	
5b Carrot	--	--	--	--	--	--	--	0.99	7.3	
3c Crimson Clover	--	--	--	--	--	--	35	0.89	7.0	
3c Mammoth Clover	--	--	--	--	--	--	42	0.55	7.0	
2b Corn	51	2.48	7.1	55	2.40	7.0	29	1.30	7.0	
3b1 Corn	45	1.30	7.1	--	--	--	--	--	--	
Burry Corn	50	1.33	6.2	29	1.35	6.6	--	--	--	
Burry Corn Post Harvest	--	--	--	--	--	--	36	1.00	6.3	
Conventional Corn	12	13.1	7.1	19	1.33	7.9	--	--	--	
3a Garlic	28	2.82	7.2	--	--	--	--	--	--	
Burry Green Beans	71	1.17	6.6	--	--	--	--	--	--	
Burry Lambsquarter	--	2.42	7.0	--	--	--	--	--	--	
3b Leek	--	--	--	--	--	--	14	1.74	6.9	
2b Bib Lettuce	--	--	--	--	--	--	16	0.23	7.1	
3b Red Lettuce	--	--	--	--	--	--	14	1.27	6.9	
3b Romaine Lettuce	--	--	--	--	--	--	25	0.54	6.8	
Burry Potato	76	1.90	6.6	60	0.78	6.5	22	2.79	6.3	
Burry Potato with Weeds	--	--	--	--	--	--	36	0.47	6.4	
Burry Red Beans	45	1.13	6.6	46	3.30	6.9	--	--	--	
3b1 Swiss Chard	--	--	--	0	1.44	7.3	--	--	--	

Table 2. Average percentage of mycorrhizal colonization, available phosphorus (ppm) and pH levels for each crop regardless of field and sampling time.

Crop	Average Mycorrhizal Colonization	Average pH Levels	Average Available Phosphorus Levels (ppm)
Asparagus	47	7.0	3.70
Broccoli	0	7.3	1.39
Buckwheat	0	6.5	0.78
Carrot	18	7.2	1.60
Crimson Clover	36	7.0	0.89
Mammoth Clover	43	7.0	0.55
Post-Harvest Corn	37	6.3	1.00
Organic Corn*	43	6.7	1.62
Conventional Corn	15	7.4	8.37
Garlic	28	7.2	2.82
Green Beans	71	6.6	1.17
Lambsquarter	--	7.0	2.42
Leek	14	6.9	1.74
Bib Lettuce	16	7.1	0.23
Red Lettuce	14	6.9	1.27
Romaine Lettuce	25	6.8	0.54
Burry Potato	67	6.6	1.28
Burry Potato No Weeds	22	6.3	0.28
Burry Potato with Weeds	36	6.4	0.47
Burry Red Beans	45	6.8	2.22
Swiss Chard	0	7.3	1.44

*Organic corn includes all of the corn sampled from Rose Valley Farm, except the corn sampled after harvesting.

Table 3. Correlation coefficient squared from two-way ANOVA tests of phosphorus and pH levels and vesicular arbuscular mycorrhizal (VAM) colonization.

	Source of Variance		
Response Variable	Mycorrhizal Colonization and Phosphorous Concentration	Mycorrhizal Colonization and pH Levels	pH Levels and Phosphorus Concentration
Carrots	0.09	0.82	0.05
Conventional Corn	0.03	0.01	0.01
Organic Corn	0.01	0.00	0.09
Potatoes	0.19	0.12	0.62*
Red Beans	0.37	0.48	0.79
Potatoes with weeds and Potatoes with no weeds	0.21	0.01	0.12
Organic Corn and Conventional Corn	0.13*	0.17*	0.07
Total of All Crops Sampled	0.02	0.13*	0.07*

* indicates that correlation coefficient squared was significant at $P < 0.05$.

DISCUSSION:

Mycorrhizal colonization decreases with increasing pH levels and increasing available phosphorus concentrations in the majority of the sampled crops. There is also a significant relationship between increased phosphorus concentration and increased pH levels. The results from our research imply a mycorrhizae-phosphorus-pH cycle with each of the variables incumbent on the other.

The majority of the sampled crops involved corn. When a comparison was made between organically and conventionally grown corn, we observed higher levels of available phosphorus associated with decreased percentages of mycorrhizal colonization. Maartensson and Calgren (1994), have also demonstrated that high levels of phosphorus fertilization inhibit mycorrhizal colonization. High soil phosphorus concentrations produce less extraradical hyphae and thus the fungi are less beneficial to the plant. Parasitism can occur when the available phosphorus levels in the soil are such that the fungi cannot extract extra phosphorus, and no benefit accrues to the plant in return for the carbohydrates supplied to the fungus (Paul and Clark, 1989). The fertilization of low nutrient soils favors the proliferation of parasitic associations between the mycorrhizae (Johnson, 1993). Once the plants have been fertilized they decrease the carbohydrate apportions to the roots (Johnson, 1993). The decreased nutrient supply selects for more aggressive fungal species which would attach the plant for their carbohydrate sources, thus producing an environment suitable for parasitic associations.

Rhizosphere acidification is a typically exhibited by roots in low nutrient environments (Marschner, 1992). The roots induce the excretion of organic acids, thus decreasing the pH of the soil. The increased acidity of the soil contributes to the solubility and thus acquisition of available phosphorus to the mycorrhizae (Marschner, 1992). These data correlate with our results regarding increased available phosphorus concentration and their impact on increased soil pH levels. Once the host plant's environment is lacking the nutrients critical for its survival, it may excrete organic acids creating a decrease in soil pH (Marschner, 1992). This function may be critical to the mycorrhizal-plant symbiosis, whereby the plant roots make the environment more suitable for mycorrhizal colonization by excreting organic acids. This association may have a direct effect on mycorrhizal species composition, whereby a once mutually beneficial interaction may be replaced by a parasitic one (Maartensson and Calgren, 1994). The mycorrhizal species itself may become parasitic or a different mycorrhizal fungus, which thrives at higher pH levels and phosphorus concentrations, may have a competitive advantage and take over, thus supporting a parasitic role in the plant-mycorrhizal symbiosis. This association may decrease the health of the host plant and thus decrease the yield of an agricultural crop which is dependent on mycorrhizal infection.

Mycorrhizae are important to many agricultural crops in maintaining the health of the individual plants. Implementing processes which utilize the benefits of mycorrhizal-plant symbiosis may have reaching effects on the health of the entire ecosystem. Decreasing the use of synthetic phosphorus fertilizers through the use of organic farming methods may decrease soil erosion, decrease the dependence on pesticides as well as decrease the pollution of streams and other waterways.

REFERENCES

Kormanik, P.P. and A.C. McGraw. 1992. Methods and Principles of Mycorrhizal Research, Quantification of Vesicular Arbuscular Mycorrhizae in Plant Roots, American Phytopathological Society, pp. 37-45.

Maartensson, A.M. and K. Calgren. 1994. Agriculture, Impact of Phosphorus Fertilization on VAM Diaspores in Two Swedish Long-Term Field Experiments, 47:327-334.

Marschner, H. 1992. Mycorrhizas in Ecosystems, Nutrient Dynamics at the Soil-Root Interface (Rhyzosphere). CAB International, pp. 3-4.

McGonigle, T.P. and M.H. Miller. 1993. Soil Science Society, Mycorrhizal Development and Phosphorus Absorption in Maize Under Conventional and Reduced Tillage, 57:1002-1006.

Miller, R.M. and J.D. Jawstrow. 1992. Mycorrhizal Functioning: An Integrated Plant-Fungal Process, The Application of VA Mycorrhizae to Ecosystem Restoration and Reclamation. Chapman and Hall, pp. 438-467.

Oslen, S.R. and L.E. Sommers. 1982. Methods of Soil Analysis, Phosphorus Soluble in Water. American Society of Agronomy, Inc., pp. 400-420.

Paul, E.A. and F.E. Clark. 1989. Soil Microbiology and Biochemistry, Academic Press, Inc., pp. 211-230.

Peterson, R.L. and M.L. Farquhar. 1994. Mycologia, Mycorrhizas-Integrated Development Between Roots and Fungi. 86:311-326.

Raven, P., R. Evert and S. Eichhorn. 1992. The Biology of Plants, Worth, pp. 239-240.

Reganold, J.P., A.S. Palmer, J.C. Lockhart and A.N. MacGregor. 1993. Science, Soil Quality and Financial Performance of Biodynamic and Conventional Farms in New Zealand, 260:344- 349.

Safir, G.R. and J.M. Duniway. 1982. Methods of Soil Analysis, Evaluation of Plant Response to Colonization by Vesicular-Arbuscular Mycorrhizal Fungi, American Society of Agronomy, Inc., pp. 77-80.

Wilson, J.M. and I.C. Tommerup. 1992. Mycorrhizal Functioning: An Integrated Plant-Fungal Process, Interactions Between Fungal Symbionts: VA Mycorrhizae, Chapman and Hall, pp. 199-248.

Wood, T. and B. Cummings. 1992. Mycorrhizal Functioning: An Integrated Plant-Fungal Process, Biotechnology and the Future of VAM Commercialization, Chapman and Hall, pp. 468-487.

Institutional Implications of Ecosystem Management: Perspectives of Innovative Natural Resource Managers

Patricia Bungert
International Relations Department
University of Minnesota
c/o 1992 Folwell Avenue
St. Paul, MN 55108

Faculty Advisors:
David N. Bengston
and Vernon W. Ruttan

Interviews with public natural resource managers revealed that institutions are challenged to respond in a variety of ways to ecosystem management, a new way to holistically manage natural resources that considers both biological and social definitions of natural resources and the environment. New institutional arrangements are necessary to accommodate ecosystem management.

INTRODUCTION

Natural resource management agencies in the United States are beginning to adjust to a new environmental paradigm that includes themes such as sustainable development, harmony with nature, skepticism toward scientific and technological solutions, finite natural resources, and a distinct emphasis on public involvement in decision-making. As a result, there is a sense that some natural resource management agencies are beginning the somewhat tumultuous process of institutional transformation. For example, USDA Forest Service Chief Dale Robertson declared that ecosystem management is now the "Forest Service way," and that "the Forest Service is committed to using an ecological approach in the future management of national forests and grasslands". While ecosystem management is not a new concept (Caldwell 1970), it has rapidly gained prominence in the natural resource community.

BACKGROUND

Despite this interest and activity, the natural resource management community is not in agreement about what this new holistic ecosystem management approach should entail. Ecosystem management is often viewed as either primarily an ecologically-based approach or as primarily a socially-based approach to resource management (Clark and Stankey 1991). This range of characterizations is summarized by Grumbine (1994) to include such things as data collection and monitoring, and adaptive management. Gerlach and Bengston (1994) identified 11 tasks for ecosystem management and summarized it as institutionalizing ecological and economic interdependence democratically. Moote (1994) summarized five main components of ecosystem management that include integrated holistic science, and socially defined goals and management objectives. Each of these characterizations of ecosystem management are summarized in Table 1.

Table 1: Principles of the Emerging Concept of Ecosystem Management

Grumbine (1994)	Gerlach and Bengston (1994)	Moote, et al (1994)
Hierarchical Context	Coordinate across established political borders	Socially defined goals and management objectives
Monitoring		
Ecological Boundaries	Coordinate across time horizons	Integrated, holistic science
Viable Populations	Holistic coordination of solutions to reduce likelihood that solutions cause new problems	Broad spatial and temporal scales
Ecosystem Patterns and Processes	Decisions based on ambiguous and uncertain information	Collaborative decision-building
Species Reintroduction	Public support to manage the "tragedy of the commons"	Adaptable institutions
Data Collection	Changes in rights and duties regarding natural resources	
Values	Fairness in distribution of costs and benefits of natural resource use	
Interagency Cooperation	Sustainable development	
Organizational Change	Institutionalize interdependence democratically	
Adaptive Management	Conflict management	
Humans as Part of Nature	Integration of human and biophysical factors	

METHODOLOGY

This study reports on intensive interviews conducted with 8 natural resource managers who are implementing ecosystem management. Figure 1 presents the interview questions. In designing the six questions, it was assumed that change results initially via the actions of natural resource managers who are the most innovative. Therefore, candidates for interviews were chosen based on their reputation for being innovative. Their activities are considered innovative by other natural resource professional outside their geographic region. Knowledge of participants' innovative activities initially arose from earlier research by or contacts of Professors Luther P. Gerlach and David N. Bengston at the University Minnesota. Data were obtained by conducting one-on-one interviews with the 8 governmental natural resource managers, generally of 1 to 2 hours duration. The timeliness of the topic necessitated that one-on-one interview methodology be utilized. The research objective was to determine how ideas embodied in the new ecosystem management concept are diffused through institutions and actually put into practice. The primary goal was to draw conclusions about the process of negotiating agreements for natural resource management among diverse participants (public, private, and unaffiliated sectors), and develop recommendations about how best to enhance the process.

1. *Is institutional change occurring in your organization right now? What is the nature of this change?*

2. *What is driving these changes?*
   - *Pressure from outside groups?*
   - *Structural support for change?*
   - *Legislation?*
   - *Diversity of values/backgrounds in the agency?*
   - *Innovative programs?*
   - *Communications/training?*
   - *Anything else?*

3. *How do you define ecosystem management?*

4. *What is the long-term objective of ecosystem management?*
   - *Respond to/incorporate changing social values into management?*
   - *To affect a shift in your institution's philosophy?*
   - *To encourage integration of new knowledge into management?*
   - *To deflect criticism without really changing?*
   - *To stimulate internal discussion about mission/values?*
   - *To reinforce basic tenets of management?*
   - *To open up the management process?*
   - *Anything else?*

5. *How are innovations such as ecosystem management diffused through your institution?*

6. *What are the processes through which agreements are negotiated and management of natural resources is coordinated among diverse participants? What can enhance this process?*

Figure 1: Interview Questions

RESULTS

Institutional change is occurring in natural resource agencies on two levels:

- An institutional level — the rules of a society or organization; and
- An organizational level — that reflects, and carries out, and makes, the rules.

Pressure from outside groups drives institutions to change. For example, the deputy commissioner of the Minnesota Department of Natural Resources (DNR) contends:

> The public is not content. A new fundamental difference is that the public is constantly saying that they are not content. The public is more demanding, has a better education with more information, and is more confident about its ability to draw conclusions. In the old days, the agency's word would have been good enough. Not anymore. The agency has to change.

A wetlands program manager said, "society as a whole has changed the way [natural resource management agencies] make decisions; the citizenry calls for more involvement in decision-making." This is a popular idea, that society is changing. A state forester in Illinois stated, "if agencies don't do what society wants, agencies won't be around." A Michigan DNR planner acknowledges various driving forces but proclaims: "Change is driven basically by a paradigm shift in society as a whole, at least on the order of the progressive movement of 100 years ago — or maybe a shift of even greater magnitude. This paradigm shift manifests itself in new philosophies and new theories" such as ecosystem management. One formal definition is:

> Ecosystem management is equally managing on a biophysical basis the way nature works and equally citizen participation in decision-making. The second component of the definition has to be present, or else it's not management, it's just allowing nature to take its course. Nature is perfectly capable of managing ecosystems all by herself. We are managing because we have needs and we place our values on ecosystems, we could just leave it alone.

Other natural resource managers provide definitions that are succinct, and similar because they all mention humans. For example, on the Wasatch-Cache National Forest in Utah, ecosystem management involves "humans recognizing the capability of our environment to support us and other life, and modifying our own behavior" and at the International Joint Commission, it means the "manipulation of human activities and endeavors to bring about a desired set of relationships." Most commonly, the long-term objective is to sustain the natural processes that occur in forests, prairie, and wetlands. However, the Michigan planner put the long-term objective into philosophical terms: "In the long term, ecosystem management is an opportunity to ask the question 'why?' Why are we here? This makes us deal with the meaning of our material existence on this earth."

When discussing how innovations such as ecosystem management are diffused through institutions, each resource manager eventually declared ecosystem management is not a new concept. After contending "this is not new" a district ranger in Utah commented:

> I see pockets of experimentation, and the majority of innovations are diffused informally rather than formally. People who are keen on a particular idea or experiment are talking to each other and calling each other up and sharing, and in this way they are picking things up from each other.

A ranger in Idaho tells a story about what it takes to be innovative that involves a local hot springs that was being overused (drinking, nudity, even shootings). The most extreme people were quoted in the paper as saying that the best solution would be to blow it up. The district ranger indicated:

> The agency was able to work with the community to come up with a solution for this hot springs. The agency engaged even the most extreme people who said to blow it up. Okay, there is some reluctance to bring in those people on the real extremes — it is a learning curve. Because the reality is, if you bring in the most extreme people, they actually bring along with them a lot of other supporters. If you can work with people at each of the extremes.

Admittedly, working with the most extreme people is difficult for natural resource managers trained in the traditional sciences. One state forester in Illinois mentioned the difficulty of working with extremists who chain themselves to trees or bury themselves up to their necks in logging trails. For the innovative district ranger in Idaho, there are no excuses:

> If you won't deal with the extremists, then you are not really doing your job. And if you blame your position within your agency or use it as an excuse to continue to work only with those people in the middle, then it is just an excuse. Even if you are constrained by your role in the agency, you have to be willing to try to work with all the people, and that includes the extremists.

Natural resource managers need not only scientific skills, they need leadership skills. They also need public relations skills and a commitment to civil rights. What could enhance the process of negotiating agreement for the management of natural resources among diverse participants, such as public, private, and unaffiliated sectors? A ranger in Utah contends: "One thing that can enhance this process is having more employees who enjoy interaction with people. Lots of agency employees didn't hire on at the Forest Service to interact with people, and don't enjoy it at all." Respondents repeatedly mentioned the social sciences as an important mechanism to enhance the

process of negotiating agreements for natural resource management. Most of the comments were about agencies' tendency to be very scientific and systematic about gathering information about specific types of wildlife and vegetation, but failing to research and understand humans. One comment is:

> What we really don't understand is working with people to come up with decisions. The Forest Service is not very good at listening to what people are saying. The agency should be hiring more anthropologists, more sociologists, and more psychologists to be line officers and decision-makers.

CONCLUSIONS

The coordination of natural resource management among diverse participants is a process that is artistic as well as analytical. It involves consensus building. The way to build consensus is to get diverse groups of people together. Some natural resource managers warned that the make-up of the groups depends on the project. Other natural resource managers see the process as one where natural resource managers must seek out extremists. The process would be greatly enhanced if agencies made an internal change in employees' background and education. For example, agencies should hire employees with more knowledge of humans — how they interact and how they communicate, and hire fewer employees who possess single-species or single-discipline knowledge. External details that could enhance the process of negotiating agreement among diverse participants include universities that teach the art of social discourse, and public participants with improved communication skills and less distrust toward public toward natural resource managers.

REFERENCES

Caldwell, Lynton K. 1970. The Ecosystem as a Criterion for Public Land Policy. Natural Resources Journal, Volume 10, No. 2:203-221.

Clark, Roger N. and George H. Stankey. 1991. New Forestry or New Perspectives: The Implications of Asking the Right Questions. Forest Perspectives 1(1):9-13.

Gerlach, Luther P. and David N. Bengston. 1994. If Ecosystem Management is the Solution, What's the Problem? Journal of Forestry, 92(8):18-21.

Moote, Margaret A., et al. 1994. **Principles of Ecosystem Management.** Water Resources Research Center, College of Agriculture, The University of Arizona. 14 p.

PROPOSED WILDERNESS AREAS OF THE DIXIE NATIONAL FOREST USING A GIS

D. Craig and Mitzi R. Nyborg

Department of Geography
Weber State University
Ogden, UT 84408

Faculty Advisor: Danny M. Vaughn, Ph.D.

The wise-use of our land's resources has given rise to a move to reserve selected land as wilderness. The purpose of our study was to demonstrate a method for evaluating roadless units as potential wilderness in the Dixie National Forest (DNF), using a GIS as a modeling instrument.

INTRODUCTION & PROBLEM STATEMENT

An issue of preserving wilderness areas for the wise use of our land's resources is at the forefront of controversy today. In some areas human activity has been so intense that it has prompted a call to arms by conservationists with the intent to reserve selected land parcels as wilderness.

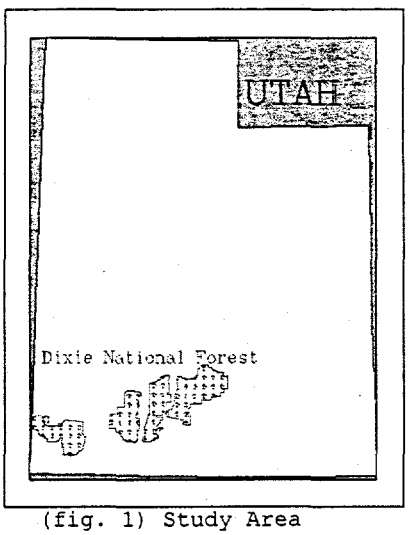
In 1964 the government took action implementing the Wilderness Act. The Secretary of Interior was given the responsibility of reviewing all roadless areas of 2,024 hectares or more within the National Parks System (16 USCS, 1983).

In the early 70s, under the Carter administration, the U.S. Forest Service (USFS) conducted a roadless study called RARE I and recommended 4,857,000 hectares for wilderness designation. After backing down from a law suit filed by the Sierra Club, the Administration agreed to a new study named RARE II, proposing 22,665,000 hectares as wilderness, and another 4,047,000 hectares for further evaluation (Arrandale, 1983).

In the mid to late 1980's, two actions were taken by Congress with the intent of laying to rest the controversies involving the wilderness areas within the State of Utah. The first was the 1984 Utah Wilderness Act UWA) which stated that "the RARE II recommendations regarding suitability of lands for wilderness is considered adequate." The act also stipulated that all national forest areas not designated wilderness be released for multiple use (Public Law 98-428, 1984). The second action was taken by Congressman Wayne Owens who requested that the RARE II areas in the State of Utah be re-evaluated. The Owens study has recently been concluded for the Dixie National Forest. The results of that study is the focus of our research. We will demonstrate a method for evaluating roadless units as potential wilderness areas, using a GIS as a modeling instrument.

DESCRIPTION OF STUDY AREA

The Dixie National Forest (DNF) extends 274 kilometers across southwestern Utah, covering approximately 809,375 hectares. It is the largest national forest within the state. Elevations range from 853 meters to 3,450 meters. Temperatures can range from 38° C near St. George to -1° C on the high plateaus. The forest has many climatic extremes with annual precipitation ranging from 25 centimeters in the desert to 101 centimeters in the highlands. The forest is comprised of five ranger districts with the Teasdale and Escalante districts being treated as one boundary (figure 1).



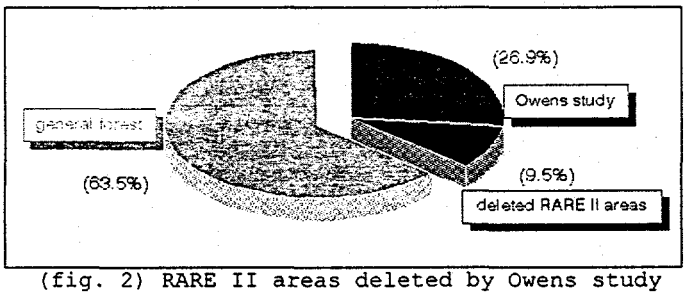
(fig. 1) Study Area

METHODOLOGY

We obtained 1:127,000 scale maps from the Forest Service delineating the roadless units, and digitized them into layers using an integrated raster/vector image processing program entitled Advanced Geographic Information Systems (AGIS). Vector files from other USFS maps showing area-use restrictions and general management plans for the forest were also obtained. A 1:500,000 USGS map was used to digitize the energy resources within the study area. The intent was to assess change in area, shape, and land-use of the roadless units over time; and to detect eminent threat of human development, and it's possible source such as timber harvest, mining, and vegetative manipulation.

DISCUSSION

The original RARE II inventory (shown as Owens and deleted Rare II) showed 36.4% of the forest as roadless. The Wayne Owens study reduced that inventory by 9.5%, leaving only 26.9% of the forest as roadless. There has been approximately a 1/4 reduction of the roadless area over the period between the two studies (figure 2).

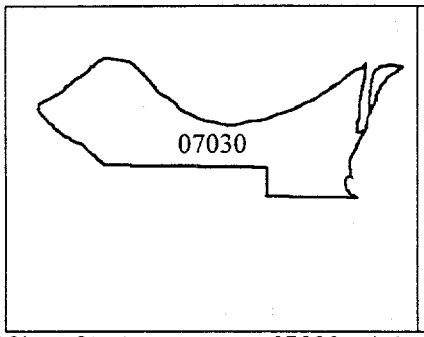


(fig. 2) RARE II areas deleted by Owens study

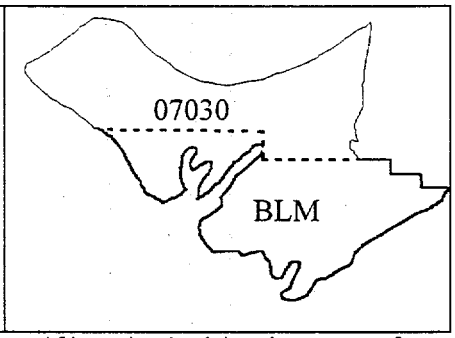
According to the criteria set by Federal Law, selected parcels must 1. be roadless and devoid of any human impact, 2. be a size equal to or greater than 2024 hectares, 3. provide opportunity for primitive recreation, and 4. have scenic, scientific, educational, or historical value. There are now 24 units remaining, from the original 43 RARE II units. These units meet both roadless and size qualifications as listed above. All the units have been assessed by the USFS for their ability to provide primitive recreation and scenic quality (Forest Service 1989).

We discovered an overall tendency by the USFS to rate desert areas much lower in scenic quality than alpine areas. However, rather than dispute these low ratings, there are still three other categories they can be evaluated for; historical, educational or scientific value. One of these units has already been established as having scientific value.

Many of the areas are characterized as having unmanageable boundaries. The forest service has stated that they will eliminate areas that have less than 402 meters between boundaries (Malyneux,1994). To determine if these boundaries were under their specifications, we ran a 201 meter buffer around the inside of the units. All areas that touched or were outside the range were eliminated (figure 3). There are four units within the DNF that adjoin Bureau of Land Management (BLM) wilderness proposals. When these areas are considered together, the boundaries become more manageable both in size and shape. Buffers were also run on the BLM units and the resulting narrow areas eliminated. The contiguous Owens and BLM units where then combined (figure 4).



(fig. 3) Owens area 07030 with $^1/_8$ mile buffer around inside perimeter

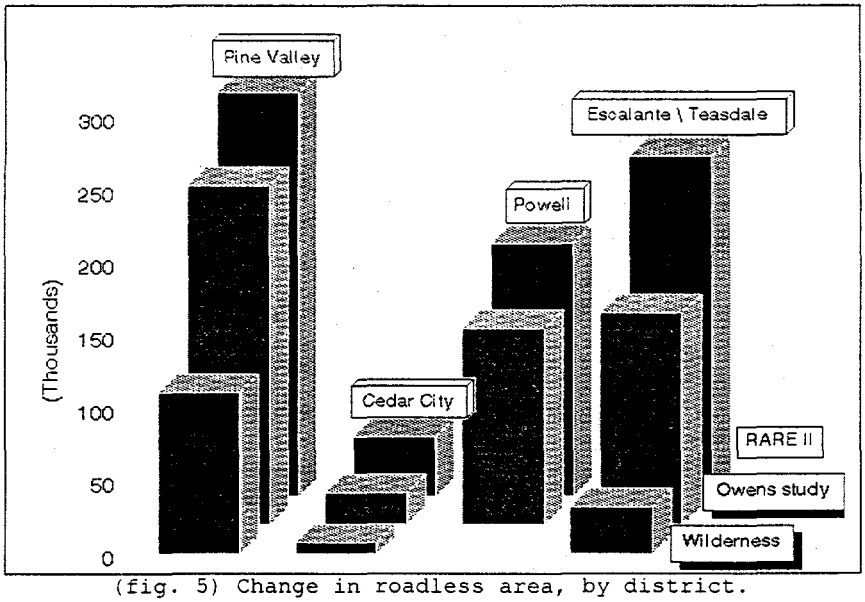


(fig. 4) Combined areas of Owens 07030 and BLM land

All of the roadless units were modeled with the current forest management plan and summary material of each unit, to determine eminent threat. The results showed the xeraphitic units of the Pine Valley District to be threatened mostly by vegetative manipulation for the purpose of improving grazing for livestock and game animals. Another potential threat to these western units is the damage done from development of hydrothermic power. This should be done with minimal environmental degradation.

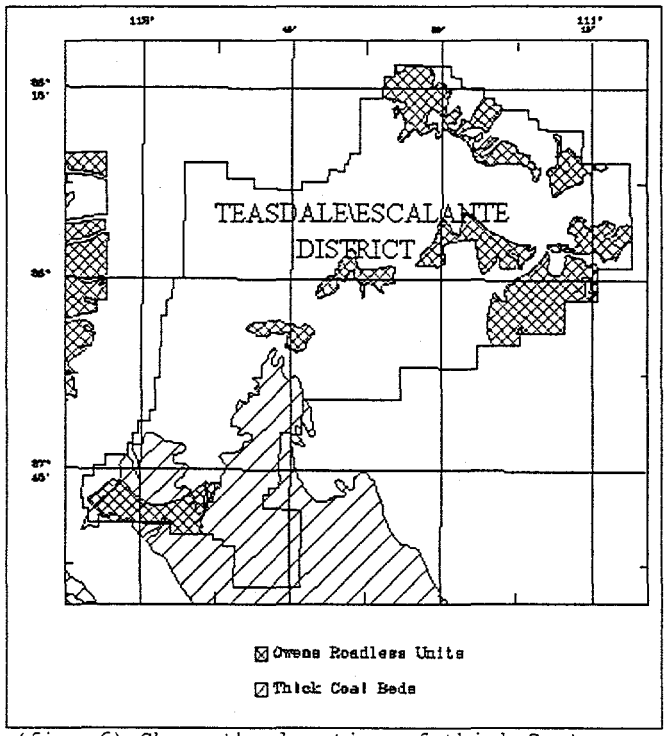
The Cedar City District of the DNF contains the least roadless area, yet has sustained a 47% loss from the RARE II to the Owens study. The Escalante/Teasdale districts have also had significant loss. The fact that so little exists in the Cedar City district gives a picture of urgency for it's two remaining units (figure 5). One of the two areas has already been established as a scientific study area. The other is stated to have timber stand with commercial value and "harvest could continue where feasible" (Forest Service, 1989).

The Powell Ranger District has a roadless unit that is protected due to several threatened and endangered plant species located within its boundaries. The other units within this district are threatened mostly by timber harvest. The entire southern half of this district has been impacted by logging and the necessary roads needed to support it. All of the remaining roadless units are now found only in the northern half of the district.



(fig. 5) Change in roadless area, by district.

In the USFS papers discussing the Teasdale and Escalante districts, there is coal and oil exploration reported, with more expected (Forest Service, 1989). When modeled for energy resources, it was found that part of this district including one of its roadless units, is underlain with thick Cretaceous coal deposits (figure 6). This is also the well known Boulder Mountain area which has been impacted by timber harvest and recreation access.



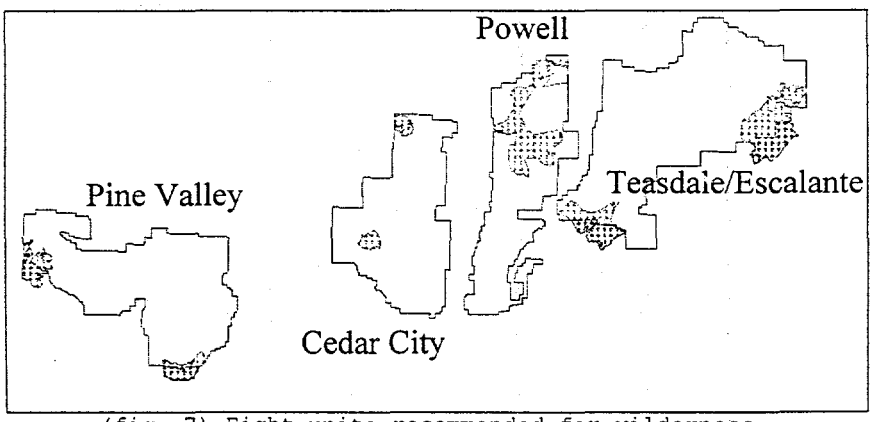
(fig. 6) Shows the location of thick Cretaceous coal beds in the Teasdale/Escalante District

As a whole the travel restrictions imposed by the forest service to protect the units from intrusion by vehicles is virtually non-existent in the Pine Valley District. The remaining two units of the Cedar City district are adequately protected, as are most of the units of the Powell district. Only about half of the Teasdale/Escalante roadless units are protected by any type of travel restrictions.

SUMMARY

Roadless units can be assessed by use of a GIS modeling system to determine compliance with the requirements for wilderness before the time and money is spent for lobbying. Unfortunately, this may serve to eliminate some units, but by the same argument it will serve to speed up the process for other units. The results of this paper show that the roadless units are continually being depleted under the pressures of multiple-use management. Without the roadless units being designated as wilderness this will continue. It is imperative that we move towards designating the units that meet wilderness regulations. At the same time, work on wilderness compliance should continue on the remaining roadless units.

We have modeled eight units that should be considered for permanent protection as wilderness as soon as possible. There are four of these that have contiguous BLM roadless units that should be incorporated into the wilderness boundaries. These units are also distributed across the breadth of the forest in a manner that will preserve the variety in habitat found within it. They contain a total of 320,997 hectares, and designating them wilderness will increase the total percent wilderness within the forest from 7.5% current, to 16% (figure 7).



(fig. 7) Eight units recommended for wilderness

We realize the need for resources in our society today and for the rights of others to enjoy the forest without having to do it in a primitive fashion, but we also feel that multiple use not result in permanent scars on every acre of public land.

REFERENCES

Arrandale, Tom; 1983; The Battle for Natural Resources; Congressional Quarterly; pp. 148-151.

Forest Service. Roadless area evaluation; 1989.

Malyneux, Max; 1994; Personal interview; Dixie National Forest; Cedar City, Utah.

Public Law 98-428; Utah Wilderness Act Of 1984.

16 USCS-1131; 1983; National Wilderness Preservation System. pp.371-376.

Soil Characteristics of McClure's Bog, Henderson County, North Carolina

Rachel E. Moynihan

Environmental Studies Program
University of North Carolina at Asheville
One University Heights
Asheville, NC 28804-3299

Faculty Advisor: Dr. Kevin K. Moorhead

INTRODUCTION

Very few wetlands are located in the Southern Appalachian region. Bogs and fens are among the rarest communities in the Southern Appalachians (Smith 1991). Prior to human disturbance, mountain bogs were probably present in every mountain county of the South (Richardson and Gibbons 1993). Currently there are an estimated 115 bogs and fens in Western North Carolina covering approximately 500 acres (Weakley and Moorhead, unpublished data). However, the threat to these ecosystems is growing: livestock grazing, logging, road construction, mining, residential development and politics are all activities that destroy these systems.

Mountain wetlands provide an impressive amount of biodiversity for occupying such a small amount of land. Southern Appalachian bogs support a wealth of rare and unique life forms, many of which are exclusive to these habitats. Over eighty species of endangered, threatened and otherwise rare plants and animals are found in Southern Appalachian bogs of North Carolina (Murdock 1994). Examples of endangered species found in these systems are: Clemmys mulhenbergii (bog turtle), Sarracenia jonesii (mountain sweet pitcher plant), and Helonias bullata (swamp pink).

McClure's bog is located in Henderson County, North Carolina on the French Broad River drainage. This bog is among the best remaining examples of the Southern Appalachian bog community type. It has been altered by human activity, but does provide an excellent example of a bog to learn more about this community type.

There is very little information available on mountain bogs. The studies done on these systems have concentrated on vegetation, aquatic or terrestrial life. Little research has been conducted on the soils of Southern Appalachian bogs. Soils play an important role in determining the composition and function of all ecosystems, especially wetlands.

The objectives of this study were to examine the following soil characteristics of McClure's bog: pH, texture, cation exchange capacity (CEC), organic carbon and exchangeable cations. These characteristics provide a foundation for further research on soil/plant relationships in Southern Appalachian bogs.

METHODS

Field Collection- Using the existing water monitoring wells established by The Nature Conservancy, ten collection sites were identified. These sites were located along horizontal and vertical transects that intersected in the interior of the bog. Each site was approximately two meters off the transect. At each site a one-meter dutch augar was used to collect five to six core samples for each horizon. Horizons were determined in the field based on physical differences in the soil cores. Each site had an A1 horizon, A2 horizon, B1 horizon, and two sites had a B2 horizon. The depth of the horizon was recorded at each site.

Laboratory- Moisture content was determined using 15-g samples that were oven dried at 95° C. The remaining soil samples were air dried, ground and sieved through a two-mm sieve to remove any organic debris and stones. The pH was tested using a 1:1 soil weight/water volume slurry and tested with an ion analyzer/combination electrode. Texture was determined with a hydrometer after

removing organic matter with H_2O_2 and dispersion of the sample with sodium-hexametaphosphate (Gee and Bauder 1982). Organic carbon was determined using the Walkley-Black method (Nelson and Sommers 1982).

Exchangeable cations (Ca, Mg, K) were replaced with NH_4 by using 1-N NH_4OAc (Buffered at pH 7) in a modified procedure similar to Thomas (1982) and Plumb (1981). Duplicate one-gram samples were placed in 15-ml centrifuge tubes. The tubes were filled with 1-N NH_4OAc and were shaken and allowed to equilibrate for thirty minutes. They were then centrifuged at 2000 rpm for ten minutes and the supernate was transferred to a 50-ml volumetric flask. The procedure was repeated three times. The supernate was filtered through a Whatman 42 filter paper with a Buchner funnel and a 125-ml suction flask. The filtered supernate was used to determine the cations on a Smith-Hieftje 12 atomic absorption spectrophotometer (Thermo-Jerrell-Ash Corp., Franklin, MA).

To determine CEC, the samples used for the exchangeable cations were washed and centrifuged three times with isopropyl alcohol to remove excess NH_4OAc. They were then washed with 10% NaCl three times and the supernate collected in 50-ml volumetric flasks. The supernate was used to determine CEC with an NH_4 electrode and an Orion expandable EA 920 ion analyzer (Orion Research Inc., Cambridge, MA). This procedure was similar to Plumb (1982).

The soil parameters were statistically analyzed using GLM procedures of SAS 6.0 (SAS Institute, Cary, N.C.). Statistical differences were determined for soil parameters within a specific horizon across the elevational gradient of the bog and between soil horizons.

RESULTS AND DISCUSSION

The average depth of the A1 horizon was 16cm and the depth ranged from 12-20cm. In the A2 horizon the average depth was 16 to 50cm with the range from 12 to 65cm. The B1 horizon was 13cm to 100cm. The A2 horizon was typically shallower at the sites that were near Gash Creek, which runs adjacent to the bog. The B1 horizon became progressively deeper in the interior of the bog.

The pH of southern Appalachian mountain bogs is typically acidic with pH ranging from 2.6-3.3 (Richardson 1993). In McClure's bog the average pH of the A1 horizon was 4.51 (Table 1). The A2 horizon had an average pH of 4.78, and the average pH of the B1 horizon was 4.63. Similar pH data were found in the surface layer of two of the bogs studied by Stewart and Neilson, pH's of 4.7 and 4.0. The three other bogs sampled by them had lower pH's of 3.6, 3.7, and 3.9 (Stewart and Neilson 1993). The pH is important because of the effect of acidity on plant growth. For example, the sweet water pitcher plant, Sarracenia jonesii, has evolved in nutrient poor soils, such as those that are highly saturated and acidic (Schwartz 1974). The pH was statistically significant between horizons, but was not at any horizon across the elevational gradient.

Texture is the relative proportion of sand, silt and clay in the soil. The texture of soils has a direct effect on the hydrology of the soil by influencing water movement within the soil. In the A1 horizon, the average texture was 68.2% sand, 23.4% silt and 8.4% clay (Table 1). For the A2 horizon, sand was still the predominant particle size (74.8%), silt averaged 17.3% and clay averaged 8.0%. Clay increased in the B1 horizon to 12.9% as did silt to 27.0%, and sand decreased accordingly to 60.1%. The B2 horizon was 68.4% sand, 22.7% silt and 8.9% clay. As anticipated, clay increased in the lower horizons. The silt content of samples was highest (>30%) at sites located near Gash Creek. Clay and sand were statistically different between the horizons, but silt was not. In the A1 horizon silt was the only particle size that was statistically different across the elevational gradient of the bog. In the A2 horizon both sand and silt were statistically different across the elevational gradient. None of the particle sizes were statistically different in the B1 horizon.

Organic carbon is the measure of organic matter in the soil. The percent carbon decreased with soil horizons. In the A1 horizon the average organic carbon content was 5.13% (Table 2). In the A2 horizon it decreased to 3.44%. It decreased to 1.30% in the B1 horizon and 0.67% in the B2 horizon. There was an inverse relationship with clay increasing and organic carbon decreasing with soil depth which is important because of the influence of carbon and clay on CEC. Organic carbon was not statistically different across the elevational gradient of the bog in any

horizon, but it was statistically different between horizons.

Table 1: Average pH and texture of soil samples found at McClure's bog

HORIZONS	pH	TEXTURE sand	silt	clay
		----------%----------		
A1	4.51 (0.31)	68.2 (8.0)	23.4 (7.0)	8.4 (1.8)
A2	4.78 (0.28)	74.8 (8.6)	17.3 (7.4)	8.0 (2.0)
B1	4.63 (0.30)	60.1 (8.7)	27.0 (8.3)	12.9 (3.3)
B2	4.58 (0.13)	68.4 (19.8)	22.7 (15.3)	8.9 (4.5)

Cation exchange capacity (CEC) is the total amount of cations that can be held by a given mass of soil at a specific pH. The CEC is influenced primarily by the amount of clay and organic carbon. The average CEC in McClure's bog ranged from 16.4 cmol/kg for the A1 horizon, 10.9 cmol/kg for the A2 horizon, 10.3 cmol/kg for the B1 horizon and 6.0 cmol/kg for the B2 horizon (Table 2). The CEC decreased in lower soil horizons as percent carbon decreased. The CEC was not statistically different in any of the horizons across the elevational gradient. CEC was statistically different between horizons.

Table 2: Organic carbon, CEC, and exchangeable cations at McClure's bog

HORIZONS	organic carbon %	CEC	Ca	Mg	K	base saturation %
		----------cmol/kg----------				
A1	5.13 (1.9)	16.4 (4.7)	0.96 (0.62)	0.44 (0.29)	0.20 (0.06)	10.6 (5.6)
A2	3.44 (1.5)	10.9 (1.9)	0.72 (0.42)	0.23 (0.16)	0.08 (0.03)	9.7 (5.6)
B1	1.30 (0.52)	10.3 (2.6)	0.42 (0.4)	0.14 (0.09)	0.12 (0.06)	7.5 (7.4)
B2	0.67 (0.21)	6.0 (3.1)	0.05 (0.06)	0.04 (<0.01)	0.04 (<0.01)	2.7 (2.3)

Exchangeable cations are the cations attracted and retained by the negative charge of exchange sites. Exchangeable Ca and Mg both decreased in the lower soil horizons. Exchangeable Ca ranged from 0.96 cmol/kg in the A1 horizon, to 0.05 cmol/kg in the B2 horizon (Table 2). Exchangeable Mg ranged from 0.44 cmol/kg in the A1 horizon to 0.04 cmol/kg in the B2 horizon. Exchangeable K was more irregular. In the A1 horizon exchangeable K was 0.20 cmol/kg, in the A2 horizon it was 0.08 cmol/kg, to 0.12 cmol/kg in the B1 horizon and then decreased in the B2 horizon to 0.04 cmol/kg. Exchangeable Ca, K, and Mg were statistically different between horizons. In the B1 horizon, K was statistically different across the elevational gradient.

Base saturation is the percent of exchangeable Ca, Mg and K relative to

CEC. It decreased in lower horizons. Base saturation in the A1 horizon was 10.6% compared to 2.7% in the B2 horizon (Table 2). There was no statistical difference in base saturation between horizons and across the elevational gradient except in the B1 horizon. The statistical results are summarized in Table 3. Data are given for statistical differences between soil horizons and within soil horizons across the elevational gradient.

Table 3: Statistical data for McClure's Bog

Soil property	statistical differece			
	between horizons	across elevational gradient		
		A1	A2	B1
pH	**	*	NS	NS
%sand	*	NS	*	NS
%silt	NS	***	*	NS
%clay	*	NS	NS	NS
Organic carbon	***	NS	NS	NS
CEC	***	NS	NS	NS
exchangeable Ca	*	NS	NS	*
exchangeable Mg	**	NS	NS	NS
exchangeable K	***	NS	NS	*
%base saturation	NS	NS	NS	*

* indicates significant difference at $p<0.05$
** indicates significant difference at $p<0.01$
*** indicates significant difference at $p<0.001$

CONCLUSIONS

This study is a small step in the attempt to understand soil characteristics of a rare ecosystem--Southern Appalachian mountain bogs. The data represents spatial characteristics of soils for one bog. Understanding these systems is important for their protection. These unique habitats are being lost at an astounding rate. Southern Appalachian mountain bogs support a multitude of rare, threatened and endangered species of plants and animals. Proper management of mountain bogs will require more information on their soils and hydrology.

REFERENCES

Caudle, Melanie A. 1994. Nutrient status of Etowah Bog in relation to Sarracenia rubra var. jonesii. Senior thesis, University of North Carolina at Chapel Hill, Environmental Science Program.

Gee, G.W. and J.W. Bauder. 1982. Particle-size analysis. In A. Klute (ed.). Methods of Soil Analysis, Part 1, 2nd ed. Agron. Monogr. 9. American Society of Agronomy, Madison, WI.

Murdock, Nora. 1994. Rare and Endangered Plants and Animals of Southern Appalachian Wetlands. Water, Air and Soil Pollution 77:385-405.

Nelson, D.W. and L.E. Sommers. 1982. Total carbon, organic carbon, and organic matter. p. 539-579. In A.L. Page et al (ed.) Methods of Soil Analysis, Part 2, 2nd ed. Agron. 9. American Society of Agronomy, Madison, WI.

Plumb, R.H., Jr. 1981. Procedures for handling and chemical analysis of sediment and water samples. Environmental Laboratoriy, Vicksburg, MS.

sediment and water samples. Environmental Laboratoriy, Vicksburg, MS.

Richardson, C.J. and J.W. Gibbons. 1993. Pocosins, Carolina bays and mountain bogs. 257-310. In W.H. Martin, et al. (ed.). Biodiversity of the Southeastern United States/Lowland Terristrial Communities. John Wiley & Sons, New York, NY.

Schwartz, Randell. Carnivorous Plants. Deborah Leavy, ed. Praeger Publishers; NY, 1974.

Smith, Alan B. 1991. Rare Plants of Southern Appalachian bogs and fens. Symposium on Southern Appalachian Mountain Bogs and Fens. Annual Meeting of the Association of Southeastern Biologists, Boone NC.

Stewart, C. Neal Jr. and Erik T. Nilsen. 1993. Association of edaphic factors and vegetation in several isolated Appalachian peat bogs. Bulletin of the Torrey Botanical Club 120: 128-135.

Thomas, G.T. 1982. Exchangeable cations. p.159-165. In A.L. Page et al (ed.) Methods of Soil Analysis, Part 2, 2nd ed. Agron. Monogr. 9. American Society of Agronomy, Madison, WI.

Water Efficiency at the University of North Carolina at Asheville

Wendy L. Mackin

Department of Environmental Studies
University of North Carolina at Asheville
One University Heights
Asheville, NC 28804-3299

Faculty Advisor:

Richard P. Maas

Water use patterns, existing system shortcomings and the community attitude toward efficiency must be understood in order to implement a comprehensive water efficiency program. Students working to initiate water efficiency measures at UNC-Asheville found a wealth of published studies dealing with residential water use, but little information about water consumption habits, program acceptance or effectiveness on college campuses. Interns studied water consumption patterns at UNC-Asheville and conducted an inventory of the general campus water outlets. This, combined with information gathered during three on-campus surveys, from utility records, and a study available technology led to a successful pilot efficiency project involving ultra-low flow toilets, faucet aerators and showerheads.

BACKGROUND

Water is necessary for human existence and, fortunately, Americans have been blessed with a relative abundance of it. Even the most arid regions of our country receive fresh water through an intricate system of pipes and valves. Over the last twenty years, Americans have begun to realize that the marvels of advanced technology have led us to wasteful attitudes and practices. Now, efficiency must prevail when utilizing remaining fresh water sources.

Legislation such as the Clean Water Act proves that maintaining the quality of fresh water as a non-renewable resource is not a passing fancy with the public. Local water source and quality protection have been on the agenda for some time in Buncombe County, North Carolina. The Asheville Buncombe Water Authority, the county's main drinking water distributor, has recently embarked a water efficiency plan that is expected to include every home and business subscribing to their service. In the early 1990's, the University of North Carolina at Asheville, an ABWA subscriber, was faced with a unique opportunity to become a leader and trend setter in the plan to use Western North Carolina's clean mountain water in the most efficient manner. Not only could the University use water more efficiently, thus saving one of the finest fresh water sources in the country, but, could set an example for thousands of people involved with the University each school year.

WATER USE STUDY

This project, intended for completion during the summer of 1993, relied heavily on the reorganization of utility data and on the construction of a computer program to analyze the information. Originally, this project was expected to familiarize student interns with water uses and the volume of consumption at UNCA. However, a program that would manipulate the data for the project remains on the worktable at UNCA's physical plant.

Since the project could not be completed, an effort was made to organize all of the information that would be needed when the program was realized. Preliminary work included gathering files and obtaining additional water consumption records from the Asheville Buncombe Water Authority, and offered a basis for the completion of a faucet aerator replacement project, and pilot ultra-low-flow toilet and showerhead replacement projects. Once computerized, the Water Study might readily justify further water efficiency programs on campus.

LOW FLOW AERATORS AT UNCA

As of October, 1993, all general campus buildings (non-housing) were retrofitted with low-flow aerators. A spreadsheet was designed as a quick, easy to use reference with a complete inventory of the bathrooms, sinks and aerators on campus. This spreadsheet includes a detailed description of the bathrooms in each building, including: room number, number and location of sinks, along with the aerator size and type.

It was estimated that 127 aerators were replaced on campus. This accounts for every sink on the general campus, except for the sinks in Ramsay Library and Karpen Hall. These buildings were equipped with 0.5 gpm aerators when they were built, and thus were not in need of a retrofit. However, the figure does include seven aerators which were installed in Ramsay and Karpen buildings due to theft or damage of the low-flow originals.

In all cases, one of two aerators was used. Both designed by Omni, the aerators possess either a soft laminar flow, rated at 1.5 gallons per minute (gpm), or a sprinkler type rosetta flow, rated at 0.5 gpm. Micro-screens within the laminar flow fixture align water molecules into a parallel flow pattern that makes the water to 'feel' wetter to human hands. Laminar flow screens prevent excess splashing by reducing the intensity of the water stream. Omni's laminar flow aerator is also equipped with a variable orifice to eliminate fluctuations in pressure. The rosetta flow aerator does not incorporate the laminar flow pattern but, does have the pressure compensation feature. Rosetta flow aerators have a sprinkler type flow pattern, much like the sprayer nozzle that is common in kitchens. When tested, both aerators were operating within their expected ranges and were compensating for sudden changes in water pressure.

The average cost of the laminar flow aerators is $5.16. Rosetta flow aerators were priced at $4.50. At the onset of the retrofits, adapters were used to fit the new aerators on old fixtures. In later orders, interns specified that a dual threaded aerator be purchased to avoid the extra expense (about $2.44 per aerator) of installation. The dual threaded aerators also minimize inventory and confusion. The rosetta flow aerator provided the highest level of water savings and had the shortest pay off time.

The age and inefficiency of campus aerators ensured the success of the low flow aerator project, although a formal pay-off time and justification were not calculated at the onset. A calculation of the projected savings was done before completion, however, placing water and sewer cost savings at an estimated $902.69 per year. A two semester year was assumed for this figure, since the Summer term population in general campus buildings is significantly lower than at other times during the year, and restrooms may go completely unused for days on end. This two semester assumption is a conservative estimate of the savings which could be realized. In addition, untold savings will be found in the reduced volume of water that is heated for hand washing. It is estimated that the laminar and rosetta aerators would pay for themselves in water savings alone after 319 days.

The figures are not as cut and dry as they may seem. In addition to inaccurate inventory records, the physical plant had not recorded the number of aerators which had been lost or stolen for the first year of the project. According to the University's plumber, after the original installation, a rash of theft occurred. The plumber contended that aerators disappeared as campus employees found that the new aerators meant it took longer to fill a coffee pot. When the project was first reviewed, in June, 1993, it was found that at least four of the missing aerators were likely the victims of "coffee pot fillers." An additional twelve aerators were missing after the replacement of handicapped sinks, when the low flow aerator retrofit project was not coordinated with other physical plant projects. In both cases, the losses were unnecessary, as theft could have been curtailed with appropriate publicity and leadership. Since the discovery of the original thefts, the aerators were replaced and informal contact was made with employees to inform them of the water efficiency project. These aerators were still in place when checked in November, 1993. The entire project, including the costs of theft and loss, would pay for itself after just 1.21 years, or 442 days.

To ensure no further thefts, both a vandal resistant aerator and a publicity campaign were considered. After some investigation, it was found that the vandal proof aerators could be removed with two ballpoint pens. With this in mind, the significantly greater cost of vandal proof aerators could not be justified. After the replacement of the missing aerators, an attempt was made to publicize the project and raise support from the Administration on campus for preservation of the aerators. It was hoped that a campus wide notice of water efficiency efforts from the Chancellors office would curtail theft of the aerators and promote positive attitudes toward efficiency projects. A letter, from the student interns, was submitted for approval through the ranks, but later returned with an explanation that notice to all employees and students through the Chancellors office was not necessary. The issue has not been pursued

further.

ULTRA-LOW FLOW WATER CLOSETS AT UNCA

In June, 1993, the physical plant undertook UNCA's first ultra-low flow toilet project. The project served as an excellent example for future projects involving the ultra-low flow technology both on and off campus.

Site selection was imperative for this project. Originally, the pilot was scheduled for a restroom which frequently had little traffic and a near-level sewer pipe slope. The 6" sewer pipe was known to clog occasionally and it was feared that reduced flow would aggravate the problem. The project was subsequently relocated to Zagier Hall, a classroom building, which receives significantly more traffic and has a sewer discharge route set on a steeper slope.

Eight bowls were installed (three in each of the two women's restrooms and one in each of the two men's restrooms) in Zagier Hall, along with four urinals. The water closet bowls, urinal bowls and urinal flush valves were manufactured by Mansfield Plumbing Corporation. Flush valves for half the water closets were manufactured by Sloan Royal, while the other half were manufactured by Zurn Plumbing. The Torpedo Urinal Flushmeter valves installed are rated at 0.75 gallons per flush and worked flawlessly. In contrast, all eight water closets were defective.

The Mansfield bowls were designed for use with a 1.6 flush valve, and manufacturer claims said the bowls were compatible with the Sloan and Zurn 1.6 gallon per flush valves that were installed. However, when flushed, a "fountain" of water rose in the center of the bowl, splashing over the seat and rim, and onto the floor. The bowls rarely cleared with less that two flushes.

To remedy the problem a number of solutions were considered. First, the water pressure in the building was checked. It had been set at the standard 60 pounds per square inch (psi), the pressure used in all the buildings on campus. When the pressure was eliminated as a factor, an adjustment was made on the valves. The stop valve, located to the right side of the valve, is normally used to control the volume and velocity of water entering the bowl. The valve adjustment screw can be turned all the way down to shut off water to the valve, when maintenance requires removal of the diaphragm. During normal operation, the screw is turned completely open. Slight variances made in the position of the screw can alter the inflow of water to the valve and bowl without disturbing the outflow of wastes into the sewer. Drastic changes often result in more frequent clogs and less bowl clearance. To reduce the force with which water entered the bowl and the spill-over effect, the screw was adjusted closer to the off position. This curtailed the problem but, did not offer a final solution. After several conversations with the manufacturer, who ran tests simulating the conditions at Zagier Hall in their factory, it was determined that the bowl was of a bad design and must be redesigned. For the next five months, Mansfield Plumbing worked on a redesign of the bowl. Once a satisfactory design was found, the bowls were shipped to us at no charge. During the 1993 Winter break, the new bowls were installed and have been operating problem-free.

During Fall, 1994, a survey of student toilet use was conducted. Of approximately 700 surveys sent out, 405 were returned. The average number of flushes, per person (student, faculty or staff) was calculated at 2.6, with answers ranging from never to 20 times per day. The standard deviation between answers was 2.49. A separate survey of Zagier Hall was used to justify the replacement of fixtures in that building. Twenty surveys were returned in that building and the average number of flushes per day remained at 2.6.

The retrofit in Zagier Hall was found to offer a 51 percent water savings. However, since the installation of new bowls was contracted to a local plumbing firm, the cost of the pilot project was much higher than if it had been an in-house effort. The initial cost of the contracted job was $5282.40 which included the installation of twelve fixtures, of which the contractor supplied half of the fixtures. The additional fixtures were taken from stock which the University had purchased in a previous year. The project is expected to pay for itself in 4.74 years.

Substantial savings could be had if the retrofit were done as an in-house project. Currently, an ultra-low flow bowl and flush valve would cost about $200. With labor performed by University employees or interns as an in-house project, the Zagier retrofit would have only cost the University $2400, a 55 percent reduction in the cost of materials and labor. As an in-house project, the pay off time could be reduced to 2.15 years.

During the disassembly of the old fixtures in Zagier Hall, a restricting device was found in the flush valves. It was later learned that the restrictor, called a Water Warden, had been placed in all of the water closets and urinals in Zagier Hall, and then forgotten. Records indicate that the University purchased 16 Water Wardens in January 1992 and Plant employees recalled their installation. Although some flush valve malfunctions had been reported when the Wardens were initially installed, they had been operating without problem for several years.

Flow measurements indicated that the restrictors would consistently cut a gallon of water from each flush. The Water Wardens were purchased for $3.89 each and were found to have a pay off time of just 12 days.

In future campus construction, ultra-low flow toilets and urinals should be installed to meet Federal regulations. Hopefully, the University will utilize the advanced technology for replacement of broken fixture also. As for retrofitting general campus buildings, the new technology has proven to be costly but, has a relatively short pay off time. Retrofits with the Water Warden might be the least expensive way to reduce consumption in a short period of time but, certainly the age and maintenance demands of older fixtures should be considered. In some cases, fixtures are so old that they may not operate effectively with a one gallon reduction in water use, making the Warden a poor choice. Quite possibly, there is not an across the board answer, and each building should be studied for retrofit on an individual basis.

LOW FLOW SHOWERHEADS AT UNCA

While retrofitting sinks across campus, it was noted that the showers in Justice Gym appeared to be extremely wasteful. In fact, after measuring the flow with a graduated metal bucket, it was found that these showers use water at a fate of four gallons per minute although they are rated for three gallons per minute.

To justify the expense of replacing the showerheads at Justice Gym, a survey was sent to all teachers in the Athletic Department. Professors were asked to distribute the survey to students and then return them to the athletics office or the physical plant. Of 200 surveys, 12 were returned. In an effort to obtain more data on which to base average shower use figures, a walk-through poll of the gym was taken. Interns polled athletes in the gym and attended several classes to poll students, professors and faculty at random. It was determined that the overwhelming majority of people in the gym don't even use the showers. Of approximately 80 people surveyed, only 13 used the showers. A record of the actual number of people polled who did not use the showers at Justice Gym was not kept. Of those polled who did use the gym showers, an average frequency of 1.32 times per week and 7.4 minutes per use was reported. It was also noted that the gym is `rented' to community organizations for athletic activities and that an accurate count of shower users was not possible.

Due to the wastefulness and high maintenance requirements of the current showerheads, a pilot project was designed despite use patterns. Four different shower heads were tested before a replacement shower head was selected. These included: two styles of Omni 2 gpm, Omni 2.75 and 1.5 gpm, and a showerhead distributed in the ABWA home water efficiency kit. The Omni 2.75 gpm replacement was selected for the replacement since it offered a compromise between water savings and comfort. The part was placed on order and was installed by campus employees sometime during Fall, 1994. The retrofit is expected to offer a 69 percent reduction in water use attributed to the gym showers. Interns estimated that the showers at Justice Gym were used sporadically. Certainly early morning, lunch and evening hours were peak. Assuming that 50 people each day showered at the gym for an average of 7.4 minutes per use, the project would pay for itself in 1.47 years, based on water and sewer savings alone. The project will save approximately $491.40 per semester in water and sewer savings, not to mention the huge amounts of energy savings that will be accrued from heating 69 percent less water.

FEMININE HYGIENE PRODUCT DISPOSAL AT UNCA

Ultra low flow water closets and sinks offer substantial water savings but, along with this are a whole new realm of repair problems inherent to the design. In fact, these reduced flow models have a steadfast reputation for clogs. In an effort to avoid regular clogs and maintenance problems, feminine hygiene product disposal was studied.

Initially, signs were printed for each low flow stall and hung conspicuously on the back of the door. This ensured that virtually every

one using that restroom would see the sign and hopefully be moved not to flush hygiene products for fear of an overflow.

To understand feminine hygiene product disposal, a survey of women's restrooms was conducted. Results showed that 73 percent of women on campus use the product disposal bins in each stall. Of the women surveyed though, 26 percent still flush the products. Results also showed that 45 percent would use the bin because they know flushing the products would clog the toilet. Another 41 percent might be compelled to use another means of disposal.

It was determined that the bins in the stalls were messy to use and often missing from the stall. A recommendation was made to the housekeeping staff that all bathrooms be equipped with the disposal bins. After seeing the different types of disposal bins that were available to the University, it was recommended that a normal, home-type bathrooms waste bin be utilized as a standard replacement for missing bins. This bin was the least expensive of the three options. It was easy to line with an inexpensive plastic liner and was by far the easiest for housekeeping staffers to clean. In addition, the bin offered no messy lids for women to touch.

CONCLUSIONS AND RECOMMENDATIONS

Meaningful work has begun in the area of water efficiency at UNCA but, this is only a beginning. The University has yet to establish a campus policy on water, electric, natural gas or any other sort of efficiency. A general policy statement would serve to establish a mission for the course of future projects and should be established immediately.

Beyond policy, the practicality of a course in which students would research and implement efficiency projects, should be investigated. Courses such as this have been offered at other Universities and have been shown to benefit the students, employees of the physical plant and the University as a whole. Some of the projects undertaken by students in such a course might include:

1. An analysis of the past five years of water use should be completed. This organization of data would allow for some priorities to be set within the heading of water efficiency on campus.
2. Water use in the cooling towers should be studied. Preliminary studies have shown that these towers should be fitted with sand filters to prevent clogging. However, their overall use of water and chemicals has never been evaluated. In addition, a credit from the Water Authority should be sought for the amount of water lost to evaporation in these towers. This is water that never reached the sewer for treatment, although the University is billed for treatment of this water.
3. Water consumption in campus housing should be a top priority. This is possibly the University's largest source of waste and potential savings.
4. With improved landscaping at UNCA, the need for an updated irrigation system has become apparent. A variety of irrigation systems should be researched and a design submitted for implementation. As an interim measure, an exception from sewer fees should be sought for water used as irrigation water on campus.
5. An education campaign, promoting efficiency use of water among the campus population should be designed including signage, participation in festivals and promotion through the campus newspaper. As a larger issue, the campus policy could be spread to the community through publicity of the campus' efforts.
6. It has been said that natural wells exist below the ball field at UNCA. The existence of these wells should be researched. These wells could serve as an excellent source of irrigation water, another use for which the University charged for sewer treatment that is never used.

The water efficiency program at the University is young, but shows incredible potential. With the right energy and promotion, future projects have to potential to be more successful than the initial efforts described here. With this UNCA has yet another opportunity to establish itself as a leader among Southeastern Universities and to further diversify its liberal arts focus.

ACKNOWLEDGEMENTS

The author is grateful to the following for their advice and encouragement: Paul Braese, Bobby Buckner, Richard P. Maas, Robert Yearout, and (referee) 3J04.

Radial Relief Displacement in Vertical Aerial Photographs

Jason D. Wolfe

Department of Geography
Remote Sensing and Geographic Information Systems Laboratory
Weber State University
Ogden, UT 84408

Faculty Advisor:
Danny M. Vaughn, Ph.D.

Changes in topographic relief and distance from photographic nadir have a direct effect on scale variation and radial relief displacement within a vertical aerial photograph. It is known that relief displacement will increase with an increase in relief and distance from the photographic nadir, yet the rates of increase with regard to these variables is not consistent. This research seeks to illustrate the varied changes in relief displacement by examining these two variables in low, high, and mixed relief aerial photographs. Fifteen control points are used as a basis for measurement of these variables in each photograph. Linear and multiple regression analyses were conducted using a SPSS statistical program. Relief displacement was found to increase in the high relief photograph with values ranging from 114.0 to 322.7 feet, compared with 0.02 to 6.5 feet in the low relief photograph and 0.9 to 366.0 feet in the mixed relief photograph (Table 1) as was hypothesized, and distance from nadir and elevation change exhibited a direct relationship with scale change.

INTRODUCTION

Aerial photographs provide a visual means of assessing regions in preparation for initial field reconnaissance. Unlike a map with an established coordinate system, a vertical aerial photograph presents geometric discrepancies of the earth's surface, which can be assessed through quantitative measurements extracted from the photograph. A vertical aerial photograph represents a selected region of the earth's surface; however, scale varies with changes in terrain elevation. Equation 1 shows scale as a function of altitude and focal length. When the altitude between the photographic platform and the datum plane decreases (as with high relief terrain), scale increases. This assumes a constant focal length.

$$\text{Scale} = \frac{\text{Focal length}}{\text{Altitude above datum plane}} \qquad (1)$$

A map represents an orthographic projection which displays earth surface features in their correct horizontal positions. Thus, scale remains constant throughout a map. Scale changes are related to the degree of change in relief, and become more pronounced with an increase in high relief terrain. Since a vertical photograph represents a central projection, in which objects are positioned as though they were being viewed from the principal point (or ground nadir), it follows, features on aerial photographs almost always occupy positions other than their true relative map positions (Wolf, 1983). Objects located further from the nadir will display a greater amount of geometric displacement relative to their actual position at the surface (Avery, 1992). Since a disparity exists between the actual (map) location and the location on an aerial photograph, it is desirable that scale variation throughout a vertical aerial photograph be understood so that an analyst may establish the true variance in dimensional errors propagated throughout the photograph being studied.

The most significant source of deviation of earth surface features from correct ground positions within a vertical aerial photograph is *radial relief displacement*. Wolf (1983) states radial relief displacement is the "shift or displacement in the photographic position of an image feature caused by the relief

of the object." The subject of radial relief displacement is well documented in photogrammetry. Wolf (1983) explains that relief displacement increases with an increase in relief, and as the distance of an object increases from the nadir. Furthermore, he explains that scale will increase with increasing terrain elevation, and decrease with decreasing terrain elevation (1983). This relationship is expressed as focal length/flight height (Equation 1).

In order for one to interpret the underlying characteristics within a vertical photograph, one must first understand the mechanics of radial relief displacement. Given a specified horizontal datum plane, an object observed on a vertial aerial photograph will be displaced *inward*, or toward the photographic nadir, if it lies at an elevation below the datum plane (Figure 1). Conversely, the object will be displaced *outward* from the photographic center, if its position lies above the given datum plane (Wolf, 1983). Implicit within these statements is the premise that any point (surface feature) within a specified area of terrain will be displaced outward relative to any lower point (Wolf, 1983).

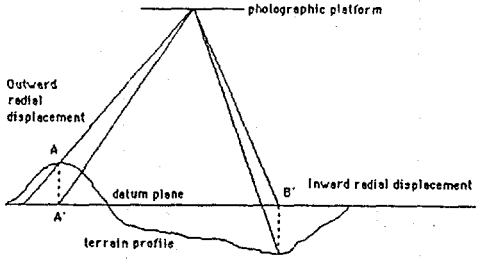


Figure 1: Inward and outward radial relief displacement

Avery (1992) describes several rules which apply to the amount of displacement due to relief, two of which apply to this particular study. First, radial displacement will be greater for a point farther from the principal point, given two points of the same elevation. Second, for points of different elevation, but equally distant from the principal point, displacement will be greater for a point of higher elevation (Figure 2).

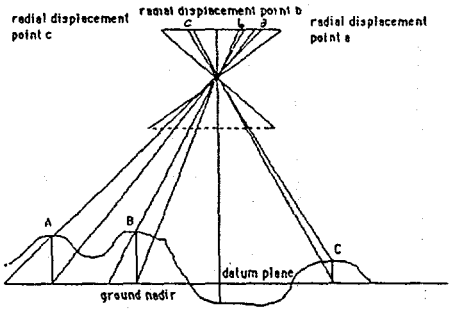


Figure 2: Reference points from photographic platform

The validity of these statements, along with the relationships between changes in topographic relief, distance from nadir, and radial relief displacement, with respect to scale variation, will be assessed through quantitative methods. Because scale differences are a function of differential displacement of features about an image, it follows that distance from a photographic nadir will contribute to scale variation, with the nadir representing the only point on the aerial photograph that exhibits no radial relief displacement, since it is the only point that is truly vertical with reference to the horizontal datum. Other factors contribute to the deviation from true geometric accuracy. Shrinkage or expansion of photographic film, radial lens distortion, atmospheric refraction, and distribution due to earth curvature will not be considered in this research (Wolf, 1983). Factors directly related to scale variance throughout a vertical aerial photograph are the primary focus of this research.

PROBLEM STATEMENT

The purpose of this research is to determine what extent changes in topographic relief and distance from the photographic nadir have on variations in relief displacement. Three vertical aerial photographs with varied relief were analyzed, to determine how much relief displacement occurs in each. A photograph exhibiting low relief, high relief, and mixed relief, was examined.

HYPOTHESIS

Radial relief displacement will increase more in photographs displaying high relief. Variations in elevation and distance from a photographic nadir will contribute to a greater degree of scale variation in a photograph displaying high relief, as compared with a low relief photograph.

METHODOLOGY

Three 9 X 9 inch USDA aerial photographs, dated 7-16-92, were used to determine fifteen control points. The first photograph was of Huntsville, Utah--a low relief area comprised of residential land use and a marsh/fringe area immediately east of Pineview reservoir. The second photograph displayed a high relief area with mountainous terrain located north of Huntsville, and east of North Ogden, Utah. The third photograph displayed a combination of low and high relief, with the image captured from the south end of Huntsville. All three photographs were taken along the same flight path, with the same focal length (153.46 millimeters), and at the same flight altitude.

U.S. Geological Survey 7.5 minute quadrangle maps were used to establish control points for the areas displayed in the photographs. The Huntsville 7.5' quadrangle was used as a reference for the high and low relief photographs, and the Snow Basin 7.5' quadrangle was used with the mixed relief photograph. The elevation of the ground nadir was established for each photograph by determining the principal point, referencing that same point on its associated map, and determining the elevation from contour lines. Elevations were interpolated by assuming a linear change in slope between contours. Fifteen points were selected on each photograph such that each point could easily be referenced on the associated map. This included primarily road intersections, stream confluences, and trail intersections.

The most crucial task in the procedures involved the actual photogrammetric measurements. The following summarizes the values to be calculated for each point.

(A). Distance from nadir (photo): The measured distance (inches) from the principal point of the photograph, and each of the fifteen points on the photograph.

(B). Representative Fraction (RF): A relationship between distance on a photograph and the corresponding distance on the ground. Calculated by the equation:

$$RF = \frac{\text{Photo distance between two points (photo)}}{\text{Ground distance between two points (map)}} \quad (2)$$

(C). Computed distance (photo): Represents the linear distance (feet) on the ground between the ground nadir and each of the points on the photograph.

(D). Elevation: The elevation in feet, derived from the topographic map.

(E). Δ Elevation: The amount of elevation change (feet) between the elevation at the nadir and each point as it is located on the map. An absolute value was computed for this figure.

(F). Height above selected datum plane (h): In order to compute this figure, a datum plane was first selected for each photograph. The lowest elevation (above sea level) represented in each photograph was used as the datum plane, and was derived from the associated topographic map. The h value was then computed by noting the difference between the elevation of each point and that of the datum plane for that particular photograph.

(G). Altitude (flight height): Represents the altitude (inches) of the photographic platform above each point. It is calculated by the following equation:

Altitude = [(RF denominator)(focal length in inches)] - [(12)(elevation above sea level of each point in feet)] (3)

(H). Relief displacement: Represents the amount of differential displacement between each point on the photograph and the same point as it is known to be located on the ground. It is calculated by the following equation, with the resulting value in inches (Wolf, 1983):

$$\text{Relief displacement} = \frac{(h \text{ in feet})(\text{distance from nadir (photo) in inches})}{\text{Altitude}} \quad (4)$$

The resulting value is then converted to feet by multiplying it by 12.
A summary of these measurements is given in Table 1. After the data were collected for each photograph, the next step involved statistical analyses. A linear regression analysis was conducted between the following variables for all three photographs:
(1) Computed distance from nadir (photo) as an independent variable and Relief displacement (dependent variable).
(2) Δ Elevation (independent variable) and Relief displacement (dependent variable).
A multiple regresssion test was also conducted between the following variables for all three photographs:
(1) Relief displacement (dependent variable) vs. Δ Elevation, and Computed distance from nadir (independent variables).

DISCUSSION

An interesting relationship exists between relief displacement and distance from nadir in a low relief photograph. For example, point 13 exhibits .02 feet of relief displacement, and is 800 feet from the nadir (Table 1). When the distance from nadir increases to 4,781 feet, relief displacement increases only 2.9 feet (point 15). In the high relief photograph, there is also a direct relationship between these two variables. Point 7 exhibits 154.5 feet of relief displacement within 600 feet from the nadir (Table 1). When the distance from nadir increases to 4,500 feet, relief displacement increases to 262.9 feet (point 5). This relationship does not exist, however, in the mixed relief photograph. For example, point 8 exhibits 3.8 feet of relief displacement and is 980 feet from the nadir. As distance from nadir increases to 5,080 feet (point 1), relief displacement decreases to 1.1 feet (Table 1). The influencing factor here is the relief of the feature which is 4,930 feet.

Another relationship exists between relief displacement and elevation change in a low relief photograph. For example, point 13 exhibits only 0.02 feet of relief displacement and 14 feet of elevation change, however, the distance from nadir is only 800 feet. When relief displacement increases to 6.5 feet as with point 14, the change in elevation is 30 feet (Table 1). In the high relief photograph, this relationship is also apparent, as point 13 exhibits 114.2 feet of relief displacement and 360 feet of elevation change. When relief displacement increases to 322.7 feet as with point 1 (Table 1), the change in elevation is 1,100 feet. Finally, a relationship exists between these two variables in the mixed relief photograph, as point 5 exhibits 0.91 feet of relief displacement and 310 feet of elevation change. When relief displacement increases to 365.7 feet as in point 13, the change in elevation is 650 feet (Table 1).

Distance from nadir and relief displacement show a correlation of 0.653 in the low relief photograph, for a linear regression model. Elevation change and relief displacement show a correlation of 0.609 in the low relief photograph. In a multiple regression model, elevation change is entered as a second independent variable with distance from nadir yielding a multiple R-value of 0.775.

In the high relief photograph, elevation change and distance from nadir are correlated with relief displacement with correlations of 0.514 and 0.694, respectively in a linear regression model. Distance from nadir has the higher correlation with relief displacement (0.694) in the linear regression test, and is

entered as the first step in a multiple regression test, with an R-value of 0.695. Relief displacement has increased dramatically in the photograph displaying high relief, with measurements ranging from 114.2 to 322.7 feet.

In the mixed relief photograph, there is a good correlation between elevation change and relief displacement (0.776), but not between distance from nadir and relief displacement (0.391). Elevation change is also entered as a second independent variable, against relief displacement in a multiple regression test, and results in a correlation of 0.772. Relief displacement in the photograph displaying mixed relief varies widely, with measurements ranging from 0.9 to 365.7 feet. However, 13 of the 15 control points in this photograph present values of relief displacement less than 100 feet.

Table 1: Comparisons of measurements between different photographs

	Pt.	Comp. Dist. (photo)	Elev. change	Rel. Disp.
Low relief	13	800	14	0.02
	14	6,382	30	6.5
	15	4,780	12	3.0
High relief	1	4.001	1,100	323.0
	5	4,500	640	262.9
	7	600	1,320	154.5
	13	1,920	360	114.0
Mixed relief	1	5,079	310	1.0
	5	4,041	310	0.9
	8	980	130	4.0
	13	6,478	650	366.0

CONCLUSION

Relief displacement increased significantly in the high relief photogaph, and ranged from 114.2 feet to 322.7 feet. The mean value was 183.5 feet. Relief displacement was low in the low relief photograph, and ranged from 0.02 feet to 6.5 feet. The mean value was 1.7 feet. The range of relief displacement in the mixed photograph was from 0.9 feet to 365.7 feet. The mean value for relief displacement was 60.45 feet, which is greater than that of the low relief photograph, but less than that of the high relief photograph.

Based upon the results of the linear and multiple regression models, it is apparent that elevation change and distance from nadir both exhibit a direct relationship with relief displacement. Since the control points used in the photograph do not change consistently with respect to relief and distance from nadir, the correlations between the variables are somewhat lower than expected. However, when distance from nadir increases and relief increases, the relief displacement increases. The amount of increase in relief displacement in high relief areas has been computed in this example and compared to low relief and mixed relief areas. This quantitative assessment provides some quantitative limits with which to evaluate photogrammetric errors propagated in varied relief terrain. As exemplified in the low relief example, relief displacement is relatively low when compared to the higher relief photographs. Clearly, distance from nadir does not play as significant a role in the low relief photograph as in the high relief example. Since these aerial photographs have not been georeferenced to accurately coincide with the earth's geometry, it will be necessary to next evaluate these factors that contribute to relief displacement to determine limits of accuracy in scale and distance measurements. This study contributes to a better understanding of the dominant factors associated with these errors.

REFERENCES

Avery, Thomas E. Fundamentals of Remote Sensing and Airphoto Interpretation, 5th ed., 1992, pp. 74-76.

Wolf, P.R. Elements of Photogrammetry, 2nd ed., 1983, pp. 58-61.

ACKNOWLEDGEMENT

The Editors and the University of North Carolina at Asheville express their appreciation to:

USDA, Forest Service, Southeastern Forest Experiment Station

Glaxo, Inc.

as the sponsers of the **Proceedings of the Ninth National Conference on Undergraduate Research.**

The Ninth National Conference on Undergraduate Research (NCUR 95) gratefully acknowledges the generous financial support of the following organizations:

AT&T FOUNDATION

THE CAMILLE AND HENRY DREYFUS FOUNDATION, INC.

RESEARCH CORPORATION

GENERAL ELECTRIC FUND

COUNCIL ON UNDERGRADUATE RESEARCH

DR. ROBERT I. PANOFF

SIGMA Xi-SCIENTIFIC RESEARCH SOCIETY

AMERICAN CHEMICAL SOCIETY-EASTERN NEW YORK SECTION

NATIONAL SCIENCE FOUNDATION

UNITED STATES DEPARTMENT OF ENERGY